

THE MECHANICS OF POWER HACKSAWING AND
THE CUTTING ACTION OF BLUNT TOOLS

by

MOHAMMED SARWAR, BSc(Eng), MSc, CEng, MIMechE, AMIST

A Thesis Submitted to the Council for National
Academic Awards in Partial Fulfilment for the Degree of
Doctor of Philosophy

Department of Mechanical and Production Engineering
Sheffield City Polytechnic

April 1982

Collaborating Establishment

James Neill (Services) Ltd
Napier Street
Sheffield

THE MECHANICS OF POWER HACKSAWING
AND THE CUTTING ACTION OF BLUNT TOOLS

by

MOHAMMED SARWAR

SUMMARY

The work presented in this thesis is part of and continuation of the work carried out by the author on the Mechanics of Power Hacksawing, on behalf of a hacksaw blade manufacturer.

Process parameters which influence the metal removal rate during power hacksawing have been identified and thus a detailed explanation of the basic sawing mechanism suggested. Power hacksaw machine characteristics have also been investigated.

The problem of blade testing is discussed. A method for assessing the blade performance is proposed which is based on metal removal rate but is independent of the machine characteristics. This could be used as a quality index for power hacksaw blades. This performance index is found to vary with workpiece breadth and tooth pitch. A theoretical model is used to give some explanation of this variation. However, there is evidence that the gullet size and geometry are more significant factors influencing the variation in blade performance with changes in the breadth of the workpiece and pitch of the blade teeth.

Examinations of saw blade teeth have revealed that they have large cutting edge radii compared to the layer of metal removed, indicating that saw blades are basically blunt tools. The cutting action of tools with large cutting edge radii has been investigated and extensive simulation tests have been undertaken. From the observations of the chip formation mechanism and measurements of the relative position of the tool and machined surface during cutting, some new light is thrown upon the ploughing process.

A slip-line field is proposed which qualitatively represents the assumed chip formation mechanism under steady state cutting conditions. The application of an empirical relationship between the chip tool contact length and the undeformed chip thickness in conjunction with the slipline field, provides quantitative correlation with the test results of a single point tool and qualitative correlation with a hacksaw blade.

DECLARATION

The candidate has not been registered for another award of the CNAA or of a University during the research programme.

Work on the Mechanics of Power Hacksawing has been undertaken continuously at Sheffield City Polytechnic since 1970. The Candidate was employed as a full-time Technical Officer to work under the direction of Professor P J Thompson on the Mechanics of Power Hacksawing from September 1971 to August 1973. The Candidate was then appointed as a Lecturer at Sheffield City Polytechnic in September 1973. Since the date of this appointment, the Candidate has worked part-time on the Mechanics of Power Sawing and associated work. A project on the Mechanics of Sawing was devised and an application to register the Candidate for the award of a Doctor of Philosophy degree was approved by the Council. Since the date of registration the Candidate has been supervised jointly by Professor P J Thompson and Professor D S Dugdale. The present title of the thesis: 'The Mechanics of Power Hacksawing and the Cutting Action of Blunt Tools' was defined and based on the work undertaken prior to the submission of the thesis for examination in 1982.

A scientific study of Power Hacksawing had not been undertaken prior to the work initiated at Sheffield City Polytechnic in 1970. The work reported in Chapter 2: Characteristics of Power Hacksaw Machines and Blades and in Chapter 3: Performance Testing of Hacksaw Blades was undertaken during the period September 1971 to the date of the Candidate's registration. The Candidate, therefore, made significant contributions to the work reported in these chapters prior to his registration. The work on the Cutting Action of Blunt Tools arose from the earlier work on Power Hacksawing and from the fact that the cutting edges of saw blades are blunt. All the work on the cutting action of blunt tools and its relationships with the cutting characteristics of saw blades contained in Chapters 4, 5 and 6 has been undertaken by the Candidate since registration.

The work presented by the Candidate has not been submitted for any other academic award.

CONTENTS

ACKNOWLEDGEMENTS	(i)
SUMMARY	(ii)
NOMENCLATURE	(iv)

PAGE

CHAPTER 1 - INTRODUCTION	1
1.1 Sawing	4
1.1.1 Power Hacksawing	5
1.1.2 Hacksawing Machines	6
1.1.2.1 Gravity Feed Machines	7
1.1.2.2 Hydraulic Machines	8
1.1.2.3 Positive Displacement Machines	9
1.1.3 Bandsawing	9
1.1.4 Circular Sawing	11
1.1.5 Relative merits and requirements of sawing operations	13
1.1.6 Factors for consideration when selecting cut-off method	16
1.2 Alternative cut-off methods	17
1.2.1 Friction sawing	17
1.2.2 Abrasive cut-off	18
1.2.3 Single point cut-off and shearing	20
1.3 Survey of previous work	21

1.3.1	Sawing	21
1.3.2	The cutting action of blunt tools	24
CHAPTER 2 - CHARACTERISTICS OF POWER HACKSAW MACHINES AND BLADES		30
2.1	Power Hacksaw Machines	30
2.1.1	Instrumentation	32
2.1.2	Observations of the load characteristics	33
2.1.3	Load developed by hydraulic machines	35
2.1.4	Results from the machine survey	38
2.1.5	Stroke of the saw	39
2.1.5.1	The equivalent number of teeth	40
2.1.5.2	Requirements of the saw stroke	44
2.2	Power Hacksaw Blades	46
2.2.1	Hacksaw Blade Material	47
2.2.2	Hacksaw blade specifications	48
2.2.3	Cutting edge geometry	50
2.2.4	Slot width	52
CHAPTER 3 - PERFORMANCE TESTING OF HACKSAW BLADES		53
3.1	Introduction	55
3.2	Formulation of a cutting test to assess the performance of a blade	57
3.2.1	A method for assessing the blade performance	58
3.2.2	Determination of the average depth of cut per tooth	58

3.2.3	Determination of the mean thrust load per tooth	62
3.2.4	The establishment of a cutting efficiency parameter	64
3.3	Instrumentation and Testing Procedures for Hacksaw blades	65
3.4	Processing of cutting test results to determine the average depth of cut, and the mean thrust force per tooth per unit blade thickness	66
3.5	Experimental Results - Performance testing of hacksaw blades	68
3.5.1	The cutting action of new blades	68
3.5.2	Comparison of blade performance of different pitches	69
3.5.3	Comparison of the performance of different manufacturers blades	71
3.6	Some factors influencing the cutting performance of power hacksaw blades	74
3.6.1	Teeth spacing	74
3.6.2	Cutting edge geometry	75
3.6.3	Slot width	77
3.6.4	Effect of blade width on the cutting performance of power hacksaw blades	78
3.6.5	Effect of blade tension	82
3.6.6	Blade wear and its effects on blade performance	85
3.7	Variation of blade performance with blades of different pitch and workpieces of different breadth	93
3.7.1	Introduction	93

3.7.2	Theory	96
3.7.3	Explanation of the variation of the cutting constant	102
3.8	Economics of hacksawing	104
3.8.1	Process costs and the machine	104
3.8.2	Estimating blade life, cutting rate and cost	106
CHAPTER 4 - CUTTING ACTION OF BLUNT TOOLS		110
4.1	Introduction	110
4.1.1	Material behaviour near the tool point	111
4.2	Experimental approach	113
4.2.1	Experimental apparatus	115
4.2.2	Preparation of tools and cutting tool geometry	117
4.2.3	Workpiece material specifications and cutting conditions	120
4.2.4	Measurement of nominal and true depths of cut	120
4.2.5	Relationship between the base of the tool and the machined surface	124
4.3	Procedure for cutting tests	126
4.3.1	Analysis of overcutting and undercutting	128
4.3.2	Chip-tool contact length measurements	134
4.3.3	Nature of the chip and the dead metal zone	135
4.3.4	Photomicrographs	137

4.4	Discussion of Results	139
4.4.1	Cutting Test Results	139
4.4.2	Ploughing, dead metal zone and the chip mechanics	144
4.4.3	Steady state cutting forces	148
CHAPTER 5 - SLIP-LINE FIELD MODEL		152
5.1	Review of slip-line field theory applied to metal cutting	152
5.2	Development of the slip-line field for cutting with a blunt tool	162
5.2.1	Stress fields	167
5.2.2	Calculation of cutting forces from the model	169
5.2.3	Discussion of results	171
CHAPTER 6 - PREDICTING THE PERFORMANCE OF SAW BLADES DERIVED FROM THE SIMULATION TESTS AND THE SLIP-LINE FIELD MODEL		
6.1	Predicting forces and specific cutting energy in sawing	
6.2	Comparison of a Single Point Tool and Blade Performance	179
6.3	Examination of the Pitch Effect	180
6.4	Gullet Size and Geometry	181
6.5	Discussion of Results	183
CHAPTER 7 - GENERAL CONCLUSIONS		187
SUGGESTIONS FOR FUTURE WORK		191
APPENDIX		193
REFERENCES		
LIST OF FIGURES		
FIGURES		

ACKNOWLEDGEMENTS

The author wishes to express his most sincere gratitude to his supervisors Professor P J Thompson, BSc, MSc, DTech, CEng, FIMechE, FIProdE, of Trent Polytechnic, and Professor D S Dugdale, PhD, DSc of Sheffield University.

Thanks are due to Mr O Bardsley, Head of Mechanical and Production Engineering, and the authorities of Sheffield City Polytechnic for permission to undertake the work.

The author is extremely grateful to Mr D Taylor, Director of Research and the authorities of James Neill (Services) Limited, for their interest, co-operation and support in the earlier parts of the project on sawing.

Particular thanks go to my colleagues, Dr B Worthington and Dr D Gillibrand for their valuable discussions and encouragement in the latter part of the project.

Thanks are due to Mr S Leigh, Mr J Taylor, Mr R Wilkinson, Mr R Roddis and all other technician staff for their help and co-operation in the experimental work.

Last, but not least, thanks to my wife for her moral support and patience.

SUMMARY

The work presented in this thesis is part of and continuation of the work carried out by the author on the Mechanics of Power Hacksawing, on behalf of a hacksaw blade manufacturer.

Process parameters which influence the metal removal rate during power hacksawing have been identified and thus a detailed explanation of the basic sawing mechanism suggested. Power hacksaw machine characteristics have also been investigated.

The problem of blade testing is discussed. A method for assessing the blade performance is proposed which is based on metal removal rate but is independent of the machine characteristics. This could be used as a quality index for power hacksaw blades. This performance index is found to vary with workpiece breadth and tooth pitch. A theoretical model is used to give some explanation of this variation. However, there is evidence that the gullet size and geometry are more significant factors influencing the variation in blade performance with changes in the breadth of the workpiece and pitch of the blade teeth.

Examinations of saw blade teeth have revealed that they have large cutting edge radii compared to the layer of metal removed, indicating that saw blades are basically blunt tools. The cutting action of tools with large cutting edge

radii has been investigated and extensive simulation tests have been undertaken. From the observations of the chip formation mechanism and measurements of the relative position of the tool and machined surface during cutting, some new light is thrown upon the ploughing process.

A slip-line field is proposed which qualitatively represents the assumed chip formation mechanism under steady state cutting conditions. The application of an empirical relationship between the chip tool contact length and the undeformed chip thickness in conjunction with the slip-line field, provides quantitative correlation with the test results of a single point tool and qualitative correlation with a hacksaw blade.

Nomenclature

<u>Symbol</u>	<u>Definition</u>
a	material constant for a particular blade type
b	material constant for a particular blade type
B	breadth of a rectangular workpiece
C	material constant for a particular blade type
D	depth of a rectangular workpiece (3.7)
F_c	instantaneous cutting force component (3.16)
F_c	cutting force component (5.4)
F_{cm}	mean total cutting force acting during the cutting
F_t	instantaneous thrust force component (3.16)
F_t	thrust force component (5.5)
F_{tm}	mean total thrust force acting during the cutting stroke (3.12)
f_c	instantaneous cutting force per unit thickness per tooth

f_t	instantaneous thrust force per unit thickness per tooth (3.8.1)
f_{ta}	average instantaneous thrust force per unit thickness per tooth (3.8.9)
f_{tm}	mean thrust force per unit thickness per tooth during the cutting stroke (3.12)
i	tooth number, taken from the tooth just beginning its cut
K	cutting constant
k	specific cutting energy (3.18)
k	shear yield stress = $\frac{Y}{\sqrt{3}}$ (5.4)
ℓ	length of blade in contact with the workpiece
L	effective length of the blade
M	cutting constant for a fully established chip
n	number of teeth per unit distance (section 2.1.5.1)

Symbol	Definition
n	cutting force index (3.8.1)
n_c	number of teeth in contact with the workpiece = B.p. for broad workpieces
n_t	number of teeth having a partly formed deformation zone (3.8.6)
N	number of cutting strokes required to saw through a rectangular workpiece
N_c	number of teeth which make contact during the cutting stroke
N_e	equivalent number of teeth
p	pitch of the blade teeth (3.5)
p	hydrostatic stress (5.2)
R	cutting edge radius
S	stroke of the saw

Symbol	Definition
t	blade thickness
w	width of the slot produced (3.6)
W	width of the tool (5.4)
y	length of cut made by a tooth
y_c	critical length of cut made by a tooth to fully establish a deformation zone
Y	flow stress of the material
$z = \frac{W}{t}$	thickness ratio
δ	instantaneous depth of cut per tooth
$\delta_s = \frac{D}{N}$	increase in slot depth produced per cutting stroke
δ_a	average depth of cut per tooth measured over one stroke
Δ	undeformed chip thickness (5.8)
\overline{PQ}	chip-tool contact length (5.4)

Symbol	Definition
--------	------------

$\overline{UP} = R$	workpiece-tool contact at the flank (5.4)
---------------------	---

α	rake angle
----------	------------

λ	friction angle = $\tan^{-1} \mu_A$ (3.8.3)
-----------	--

μ_A	apparent coefficient of friction
---------	----------------------------------

ϕ	shear plane angle
--------	-------------------

ϕ	angle of rotation of the slip lines (5.2)
--------	---

ψ	chip factor (3.8.11)
--------	----------------------

$\eta = \frac{S}{B}$	stroke efficiency
----------------------	-------------------

η	angle of the fan field in the slip line field (5.4)
--------	--

Brand 'X'	Refers to the 4, 6 and 10 TPI blades
-----------	--------------------------------------

Brand 'Z'	Refers to the 3 TPI blades
-----------	----------------------------

... CHAPTER 1

INTRODUCTION

The problem of cutting-off material to size is common to practically every industry. Often, sawing is the first operation carried out on bar stock. Therefore, it is surprising that so little work has been done to understand the problems of this common operation. Many reasons have been given for this lack of interest, such as that it is a routine operation and that there is no need to consider better methods. Often the foreman will assign a new trainee to a sawing task, on the principle that it is easy to learn and difficult to foul up. Furthermore,, cut-off machines are frequently housed in stores away from the main production areas and the operation of the sawing machines appears to be simple. The fact remains that cutting-off operations can account for a significant part of the cost per piece(3).

The reason for carrying out the present work is the growing realisation, on the part of manufacturers of both blades and machines, that the factors which control the mechanics and economics of power hacksawing are complex. Also, power hacksawing has been receiving increased competition from

other cutting off processes, such as band and circular sawing.

Whilst the British Standard BS 1919:1974 gives specifications for hacksaw blades regarding dimensions etc, the standard relates to testing of hacksaw blades for hand use only and does not include power hacksaw blade testing. Thus, both manufacturers of hacksaw blades and users have experienced considerable difficulty in establishing standard testing procedures and in obtaining consistency in test data using power hacksaw machines. Preliminary investigations by the author have revealed that existing blade testing methods were not independent of the machine characteristics, which could contribute to one of the reasons for the inconsistency in the test data. Hence, there has been a requirement to identify the machine characteristics under normal working conditions and to investigate the mechanics of the sawing process and the variables affecting metal removal rate.

Most of the early published work on cutting-off has been primarily concerned with circular and band sawing and cost comparisons between alternative processes. Whilst these alternative processes are

frequently quicker than power hacksawing their costs (3, 4) are in many applications higher. Whilst the impact of these alternative processes on the application of power hacksawing cannot be denied, there remains a significant field of application for power hacksawing which is likely to remain unchallenged^(4,12). A factor of prime interest to manufacturers is that, if the costs of power hacksawing can be reduced by developing the blade and the saw machine, the potential field of application will be widened.

During the past fifty years very little attention has been devoted to developing the geometry of the hacksaw blade or the machine, although some improvements in the blade material, together with methods of applying the load and mechanised work handling, have been achieved.

The present work critically examines the metal removal process, both the saw blade and machine characteristics. The factors controlling metal removal rate are outlined, and some improvements in both the blade and saw machine are proposed, which can lead to a reduction in the cost of power hacksawing.

Examinations of the blade teeth have shown them to have a large cutting edge radii compared with uncut chip thickness. Thus extensive simulation tests with single point blunt tools have been carried out to investigate the mechanics of the metal removal process.

1.1 SAWING

If all raw stock was delivered in ready-to-machine shapes and sizes, there would be no need for sawing machines in a metal working shop. Machine operators could merely go over to the stock, select the suitable workpiece, and perform the necessary finishing operations. Such a situation rarely exists, due to the fact that the majority of the stock requires to be cut in some way prior to starting a machining schedule. The alternative to this primary operation of sawing is to buy-in prepared lengths and shapes; this however introduces a service which the company has to pay for and, in the majority of the cases, it is simpler and more economical to carry out the basic cutting-to-size operation in house.

One of the major advantages of sawing over all other kinds of machining is the narrowness of cut, in both cutting-off and cutting-out operations. Most sawing

machines perform the cut-off operation, where a piece of stock is cut to a workable length prior to subsequent machining operations. Machines that accomplish this job include hacksaws, bandsaws and circular saws. Cutting-out operations, where large pieces of material are removed, rather than tiny chips, are carried out on vertical contouring bandsaws and holesaws.

1.1.1 Power Hacksawing

The simple back-and-forth motion of the blade made the hacksaw one of the first types of sawing machines designed for power. The simplicity in the blade motion has kept the price of the saw machine relatively cheaper than other types of sawing machines. The low initial cost, coupled with the flexibility and adaptability, has enabled the hacksaw to remain popular in industry.

In hacksawing, a single blade is tensioned in the bow, and reciprocated back and forth over the workpiece. The cutting action is achieved only during half of the cycle of operation. During the second half of the cycle, the return stroke, the blade is lifted clear of the workpiece, giving a discontinuous cutting action, which is considered to be one of the drawbacks of the operation. Despite this

disadvantage, as compared to the continuous cutting action of the bandsaw, hacksaws remain equally or even more popular alternative machines. As with many other basic processes, hacksawing is a tried and tested method, reliable, consistently accurate, quick and easy to repair, is less dependent on correct blade tension and less likely to run-out. Furthermore, power hacksaws can be left unattended for long periods when cutting large diameter bar and require minimum operator skill. Blade replacement is relatively cheap and simple.

1.1.2 Hacksawing Machines

For a given blade and workpiece the material removal rates achieved by hydraulic and gravity fed machines are controlled solely by the thrust loads developed. Therefore, hacksawing may be said to be a process in which the material removal rate is force controlled, unlike most other material removal processes.

The machines available can be divided into two broad categories, according to the method used to develop the load between the blade and the workpiece, namely, gravity feed machines and hydraulic machines. A third, but not common, machine is the positive displacement machine.

Power hacksaw machines are used mainly for cutting-off operations.

1.1.2.1 Gravity Feed Machines

In this type of machine, which is usually of light construction for general duty, the thrust load is developed by the gravity feed of the saw bow. In many of these machines the magnitude of the thrust load is fixed, although some machines are provided with adjustable masses on the over-arm for thrust load adjustment. The thrust load varies throughout the cutting stroke (Figure 2G), due to the reciprocating displacement of the over arm mass and the action of the cam operated lift-off device which acts at the beginning and the end of the stroke. This type of machine generally has a workpiece capacity between 150 - 200 mm (6 and 8 inches) diameter and is ideal for the small workshop where the cutting requirement is only occasional and the configuration of workpieces to be cut ranges from mild steel flat complex shaped sections and tubular sections up to 6 inches diameter. Due to the light construction and gravity feed the applications for this type of machine are limited.

1.1.2.2 Hydraulic Machines

The thrust force between the blade and the workpiece in this type of machine is developed by a hydraulic device. Pressure may be developed in the load cylinder by either a restricted back-flow system, or the pressure may be supplied from a separate pump. In some of these machines, greater flexibility of control has been introduced by means of an arc cutting action combined with a universally controlled hydraulic system which allows better performance from the saw blade. The advanced types of heavy duty electro-hydraulic hacksaws have a very wide range of operation and are available in semi-automatic or fully automatic form, with provisions for automatic feeding of bar stock, cutting-off to predetermined sizes and unloading etc. The feature of power down-feed to the saw bow incorporated in these machines makes the machine suitable for cutting the tougher steels and alloys. These machines are the most common and develop greater thrust loads than machines of other type and have a reputation for sawing without problems and requiring minimum operator skill.

1.1.2.3 Positive Displacement Machines

Whilst these machines are not as popular as the gravity feed or hydraulic machines, a few machines are available where the feed rate of the blade, and, hence, the metal removal rate is directly controlled by a mechanical screw device, giving a positive feed. This type of machine can lead to overloading of the blade giving premature blade failure, particularly when the blade is worn. Positive displacement machines are not prone to variation in thrust loads during the cutting stroke since the thrust loads directly arise as a result of the constant rate of penetration of the blade teeth.

1.1.3 Bandsawing

Bandsawing, unlike hacksawing, is a continuous cutting operation. An endless blade, the band, is tensioned between two shrouded, rotating wheels, and part of the band is exposed to carry out the cutting operation of the workpiece. The band travels in a continuous motion, with the teeth fed against the workpiece.

Whilst earlier metal sawing bands were wide (over 25 mm), and were used strictly for cut off methods, narrow blades, introduced about 50 years ago, brought contouring capabilities. Furthermore, due to the small throat clearance of

the early bandsaws, they were limited in use by the basic design, thus the length of the workpiece could only be as long as the machine throat. However modern machines have been modified, to give adequate throat clearance, by intentionally twisting the blade so that the toothed face is in line with the machine throat.

As with hacksaw machines, bandsaws can be divided into two broad categories. A general purpose bandsaw, having a gravity fed system, controlled by a dash-pot and using a 25 mm (1 inch) deep blade, is the most popular machine available. This machine is suitable for general fabrication work and accurate cutting of solid bars. This type of machine is limited to about 175 mm (7 inches) diameter for mild steel.

In order to meet the present day requirements for high volume production, cutting all grades of steel and to introduce high accuracy and reliability, it has been necessary for the bandsaw machine manufacturers to incorporate in the design not only heavy duty construction having capacities up to 450 mm (18 inches) diameters, but also innovations in the hydraulic power down-feed, to allow the cutting of difficult alloys, such as nimonics and titanium.

1.1.4 Circular Sawing

Circular saws have a continuous cutting action, use blades having many teeth, and a large range of rotational speeds. This operation is similar to a milling operation. The machines available range from the earlier, inexpensive, hand-loaded models to the very large, power loaded type and incorporate material handling devices for semi and then fully automatic operations.

Modern production circular saws are built with several alternate basic feed mechanisms ie horizontal, vertical, rocking head and variations of these. The choice of the most suitable type of machine depends on the particular application and the size and shape of component. With vertical feed, the rotating blade travels downwards in a straight line to engage the workpiece. On machines designed for horizontal feed the blade is fed into the workpiece from the back. A third basic feeding arrangement is a pivot motion or rocking head system, this is as efficient as a vertical feed system and is a rugged arrangement.

The bench, or floor mounted, manual-feed circular saw, when installed together with a general duty bandsaw or hacksaw in a small workshop, provides a complete cutting facility

for the small fabricator. Fully automatic circular saws, having features such as dial-in component length, in-process gauging, choice of loading magazines, etc, are widely used where high quality production is required and often present the production engineer with a difficult choice to make between circular sawing and bandsawing. The deciding factor is usually the length of the component. If the cut length is in excess of 150 mm (6 inches), the bandsaw will not show any significant savings in material and will require reloading very quickly(15).

Compared with other types of cut-off saws, the circular saw is a heavier machine for similar capacity, mainly because the blade width requires considerably more power than a hacksaw or bandsaw of similar capacity. Although circular saws can be used reasonably economically for work up to 400 mm (15 inches) diameter and have a high metal removal rate, the lower capital cost of the bandsaw and hacksaw is often a dominant factor. If, however, account is taken of the kerf loss (loss due to the thickness of the blade), circular sawing becomes a more expensive method of cutting.

1.1.5 Relative merits and requirements of sawing operations

The simplicity of design and operation, coupled with the low initial cost, has made the hacksaw grow in popularity. Its limitations are due to its mode of operation, ie cutting only on half of the stroke, the slow cutting speed, and the fact that not all the length of the blade is utilised. Some of the features in a modern hacksaw which achieve improved performance are:-

- (i) A range of cutting speeds, uniform over the cutting stroke, and a fast return stroke.
- (ii) Means to regulate and monitor the cutting pressure.
- (iii) Adjustable stroke.
- (iv) Automatic relief of the blade on the return stroke.
- (v) Some means of indicating and correcting blade tension.
- (vi) Automatic stopping device when the cut is complete.

Power hacksawing is generally thought of as a low cost, low cutting rate operation.

With the developments of bandsaw blade materials, tooth forms and machines, the metal removal rates in bandsawing are more comparable with modern circular saws. Although the cutting rate of a high efficiency circular saw may be 30-40% greater than a bandsaw, the kerf loss in a circular saw is far greater, which is a critical factor with expensive materials. Due to the essential differences in blade thicknesses, the kerf losses per cut are: for circular saws 3.5 to 10 or even 20 mm; hacksaws 2.0 to 4.0 mm; and bandsaws 1.0 to 2.5 mm. At times there may be a need to compromise, between increased blade thickness, to provide the rigidity for higher production rates at the required accuracy, at the cost of the kerf loss.

In addition to low kerf loss with bandsawing, a wide variety of materials and shapes can be cut and the desired finish obtained. The maximum diameter of section cut on a bandsaw is limited to about 750 mm (30 inches), above this size the blade guides are so far apart that the blade lacks rigidity.

Some of the features to be considered when selecting a

bandsawing machine are:-

- (i). A range of band speeds suitable for cutting different materials and able to use the newer types of blades available.
- (ii) The machine should be rigid and have adequate power available for high metal removal rates.
- (iii) Blade tensioning devices.
- (iv) Rigid and wear resistant blade guides.
- (v) Controlled feed force application.
- (vi) Adequate vices and clamping fixtures necessary for angle sawing etc.

Circular sawing can be cost effective, with a high metal removal rate, when sawing limited types of metals in a small range of sections; however, when taking account of kerf loss and variety of work, it may be a more expensive method. Some of the reasons are:-

- (i) Initial cost of blade is high and must be designed for size of work and workpiece material. Sharpening, re-tensioning (by peening) and

rebalancing add to the cost.

- (ii) Blade change time is greater than in hacksawing or bandsawing.
- (iii) Blade damage from hard spots, scale etc, can be a problem, and if damage is frequent, then it is cheaper to use a hacksaw or bandsaw.

The performance of the circular saw blade is limited by clogging of teeth spaces by swarf, an important limiting practical factor, and by the highest feed per tooth which is usable(19).

1.1.6 Factors for Consideration when Selecting cut-off Method

- (i) Machinability of the workpiece material.
- (ii) Dimensions of the workpiece.
- (iii) Accuracy of cut - run out.
- (iv) Kerf loss.
- (v) Metal removal rate.

- (vi) Cost of band or saw blade.
- (vii) Blade or band teeth pitch.
- (viii) Transmission of thrust load.
- (ix) Cost of machine.

The above list is by no means comprehensive, neither is the list in order of importance. Furthermore, the above parameters may be inter-related, eg increasing the beam strength of the blade introduces an increase in kerf loss or increase in blade cost, or both.

1.2 ALTERNATIVE CUT-OFF METHODS

Sawing is only one of a number of methods for cutting-off material. There are alternative cut-off methods which are generally not classed as sawing. Some of these alternative methods are outlined below:-

1.2.1 Friction Sawing

The work expended between a fast moving blade or band and a stationary workpiece is sufficient to create enough heat to soften the workpiece material near to the edge of the blade. Under certain conditions this may be used

to remove metal faster than by conventional sawing. Under some conditions blades need not have teeth, but they can be an advantage to carry away the softened metal.

A comprehensive range of steels can be cut by friction sawing, and the process is particularly useful for cutting hardened steel, stainless steel and other similar materials. The method is not suitable for cast irons, due to the breakdown of the grain structure which occurs prior to softening of the material; or for non-ferrous materials, since they do not reach a suitably softened state without melting and adhering to the blade.

In order for the process to be successfully carried out, the blade speed must be high, 40-80 m/sec, and the machine power should be sufficient to maintain the high blade speed. The thickness of the material being cut in friction bandsawing is limited to approximately 12 to 25 mm. If an attempt is made to cut a workpiece of greater thickness, the blade overheats, which, in turn, leads to excessive blade wear.

1.2.2 Abrasive Cut-Off

Abrasive cut-off machines use a grinding action and when thin bonded abrasive wheels are used a wide range of

materials can be cut, especially those with high strength and hardness. The peripheral speeds of the abrasive wheels are very high and, hence, the operator requires the same safety precautions as are taken when grinding.

The process is extremely fast and achieves cutting times of 5 secs for 25 mm diameter HSS round solid sections, and 2 seconds for 40 mm diameter brass pipe.

Whilst the initial capital cost of an abrasive machine is low compared to a sawing machine of similar capacity, the power required is far higher and, furthermore, the annual costs of the abrasive wheels can be equal to the cost of the machine itself.

Simple downstroke, pivoted head abrasive machines are the most commonly used for high volume production and may be used for cutting bars or tubes up to about 100 mm diameter. To cut-off more massive sections, large machines with special coolant systems and complex materials handling systems are used. Some of the machines have oscillating-heads which simulate a sawing action, and lead to improved cutting rates. There are also horizontal-traversing machines for use on plates and slabs.

1.2.3 Single point cut-off machines and shearing

Since lathes are the primary machine tools, single point cut-off on a lathe is one of the basic cut-off methods. Traditionally, cut-off lathe tools are narrow, flat, and take a plunge cut. When the cut is near the outside diameter, favourable results are obtained, but, as the tool tip approaches the centre of the workpiece, cutting conditions get less favourable. The loss of cutting speed can produce unfavourable cutting conditions and there is a tendency for the tool to jam as it progresses its cut towards the centre of the workpiece. Furthermore, the possibility of the tool flexing, wandering, cutting over, or cutting under centre, can all occur during this cut-off operation.

Shearing is a typical sheet metal process and it is relatively seldom used in general workshops. However, it is probably the most common cut-off method employed in bar rolling mills. Incidentally, shearing is the only process which involves hardly any loss of material.

1.3 SURVEY OF PREVIOUS WORK

1.3.1 Sawing

Although the popular cutting-off process of sawing is frequent in practically all industries, relatively little attention has been given to understanding the process or the behaviour of the machine. Whilst some developments have taken place on the materials used for the cutting media, ie the blade, the geometry of the cutting edge has remained unaltered in the majority of cases.

Most of the earlier published work on sawing (1, 2, 4, 5, 6, 7, 9, 12, 14) has mainly been concerned with general descriptions, principles and relative merits of hacksawing, bandsawing, circular sawing and alternative cut-off methods, with particular emphasis on applications of each operation. Some of the previous work has been extended to include cost comparisons between these alternative cut-off processes (3, 8, 10).

Some of the variables affecting the choice to be made when selecting either a hacksawing or bandsawing operation have been outlined by Nelson (4). Some suggested cutting conditions for bandsawing are given in Table 1, (Appendix A), together with comparative cutting times and blade cost per cut for both this and the hacksaw operation

figure 1 (Appendix A). The results show that, although a bandsaw will cut faster (on a basis of square inches cut-off per minute) than a hacksaw, the total cost per square inch cut may be greater for the bandsaw operation due mainly to the high cost of the band. Tests carried out by Nelson (4) have shown that bandsawing is limited to an area of cut of 50 square inches as compared to 140 square inches for hacksawing. The feed force that can be applied by a bandsawing machine is limited by the beam strength of the sawband. The larger the workpiece, the further apart the band guides must be placed, and hence, the lower the feed force which may be applied. Thus for larger workpieces, the power hacksaw is more practical and economical than the bandsaw; furthermore, for harder-to-cut materials, the hacksaw becomes almost essential.

More recently several articles on sawing have appeared in Metalworking Production (13, 15, 18, 19) stressing the importance of this 'cutting-off' method which has become a part of an integrated production operation. These articles make general qualitative assessments of hacksawing, bandsawing and circular sawing, with some guidelines (Table 2, Appendix A) as to the proper selection of the appropriate sawing machine for a particular application.

They indicate some of the problems encountered and their possible solutions with the power hacksaw machines (Table 3, Appendix A). Some of the basic requirements for better performance of bandsaws has been discussed in (20), and some relative comparisons of the performance of different hacksaw blades has been discussed in Metalworking Production (20) and made by Soderberg (18). He has shown that bimetal blades are better value, giving longer life, for a relatively minimal price difference, to all hard blades. However, the criteria used for assessing the performance of the blades, ie $\text{Capacity} = \text{Service life} \times \text{Average metal removal rate}$, does not take into account the width of cut, the teeth setting, or geometry of the teeth. Furthermore, the results do not indicate whether the thrust force was accurately controlled throughout the tests.

It is apparent from this information that the material removal rate in sawing is dependent on several of the variables of both the machine and blade. In both hacksawing and bandsawing the metal removal is achieved by forcing the teeth of the blade into the workpiece during the motion of the blade and the load required to achieve adequate penetration and, hence, cutting rate is based on the

machinability of the metal being cut. The ability of either a hacksaw or bandsaw to make a cut accurately and efficiently depends on how well the blade or band transmits the applied load to the workpiece without distortion.

The literature survey showed that, whilst some effort has been made to produce a code of practice for particular applications and to highlight some relative cost differences, taking into consideration the costs of the machine and the blades, the survey indicated that a detailed study of the machine characteristics, the blade geometry and the process parameters controlling the metal removal rate had not been undertaken.

More recently extensive work has been carried out at Sheffield City Polytechnic on Hacksawing, Bandsawing and Circular sawing by Thompson, Sarwar, Taylor et al, see references 21-31. This work investigated machine characteristics, the process parameters controlling metal removal, the effects of blade geometry and dimensions using a more scientific approach.

1.3.2 The cutting action of blunt tools

On examination of the geometry of hacksaw blade teeth it was found that their cutting edges consisted of large

radii which were extremely large compared with conventional, nominally sharp, single point cutting tools. The hacksaw blade has, as a consequence, been classified as a blunt tool.

In conventional metal cutting, during such operations as turning, milling etc, the lack of sharpness of a tool is associated with tool wear, ie if the flank or crater wear is at an advanced stage, the tool is considered to be blunt. In the present study blunt tools refer to the large cutting edge radii which have been defined (32) to be the cylindrical surfaces connecting the tool flank and tool face surfaces.

The significance of a tool edge radius on conventional single point cutting tools has received considerable attention from many research workers. In addition to the conventional force diagram (33), Albrecht (32) and others (34, 35) have developed a more complete force diagram which separates the chip-rake force from the forces induced by the edge radius of the tool and have shown that material is displaced or ploughed around and under such a cutting edge. Rubenstein et al (36) have shown that ploughing occurs when the rake angle is negative and coincides with the shear plane angle. Connolly and Rubenstein (35)

proposed a theory which related to tools of finite sharpness by considering the extreme cutting edge radius of a tool to form a rake face with a large negative rake angle. They showed that there existed a critical rake angle, such that at any rake angle greater than, or equal to, this angle, the workpiece material was always ploughed around the tool. During ploughing part of the material in front of the cutting tool is compressed under the flank face and elastically recovers behind the tool and part is plastically deformed to spread sideways without separating from the bulk, so that this is not a two-dimensional process. Palmer and Yeo (37) and other researchers (38, 39, 40, 41) have carried out investigations into the characteristics of the metal flow near the tool point using artificially blunt tools with the implications of establishing the relevance to the action of nominally sharp tools. The results reported (37) implied that a small, active, unstable, dead-metal zone existed near the tool tip, and appeared to exist even with materials that did not tend to exhibit large active built-up edges, as described by Heginbotham and Gogia (42). Kregelski (43), in his work on abrasive wear, considered the transition between different modes of deformation of a surface loaded by a

spherical sliding indenter. The depth of indentation was small compared with the radius of the indenter and Kregelski concluded that for most surfaces, plastic conditions were established under light loads. He furthermore discussed the transition from plastic indentation to a process involving 'piling up' in front of a spherical indenter virtually cutting or tearing the surface.

Previous work has established the material behaviour in the region of the cutting edge and the influence of cutting edge configuration to clarify some of the unexplained phenomena which existed in previous conventional metal cutting theories (33), and has led to the conclusion that under normal cutting conditions with nominally sharp tools, where the undeformed chip thickness is far greater than the cutting edge radius, the ploughing force is insignificant. However, the concept of ploughing is valid or more appropriate to cutting conditions where the undeformed chip thickness is relatively small compared to the cutting edge radius. The cutting edge radius of nominally sharp tools has been estimated (32) to be in the order of $7\text{ }\mu\text{m}$ (0.0003 inch) and cutting conditions are such that the undeformed chip thickness is many times greater than the cutting edge radius.

In Fig 23 presented here, also in paper (21) it has been shown that the depth of cut achieved per tooth during sawing was small compared with the cutting edge radius even when the blade was new and the load applied to the blade was high. The cutting edge radii were found to be in the range 20 μm - 76 μm for blades of various pitch teeth, whilst the average depth of cut per tooth achieved was found to be 2 - 30 μm , depending on the thrust load applied to the blade.

Preliminary experimental work carried out by Sarwar and Thompson (23) showed that under orthogonal cutting conditions where the depth of cut was less than the cutting edge radius, a complex combination of modes of chip formation were produced. Furthermore, the induced cutting forces exhibited a transient behaviour during the initial stages of the cut, which reflected the geometry of the chip produced.

Previous experimental work on metal cutting has not dealt with the situation where the depth of cut is far less than the cutting edge radius; as is known to exist in the metal cutting process of hacksawing. This has led to a further interest in the cutting action of blunt tools. Whereas

most previous studies have been concerned with the cutting edge radii relating to sharp tools and have been either of an experimental nature, or led to empirical models, in the present work extensive tests have been carried out with blunt tools and the various phenomena previously reported have been related to this mode of cutting.

CHAPTER 2

2.0 CHARACTERISTICS OF POWER HACKSAW MACHINES AND BLADES

2.1 POWER HACKSAW MACHINES

As previously discussed, the metal removal rate in power hacksawing is basically thrust force controlled and the machines are classified according to the methods used to develop the loads between the blades and the workpieces during the cutting strokes. In all types of machines this load should be removed on the return or idle stroke, as hacksaw blades are not designed to cut on the return stroke.

The performance characteristics of the power hacksaw machines used were investigated. The principal reasons for this were:-

- (i) Wear tests carried out by various hacksaw blade manufacturers have shown wide variation in results when using similar blades, test bars and machines. It was suggested that this variation could possibly be accounted for partly by different machine characteristics when operating under apparently identical

settings and conditions.

- (ii) Traditionally, the thrust force developed by a power saw, particularly the gravity fed type, has been measured when the saw was in its mid-cutting stroke position and at the mid-point of the blade. This single force measurement has been taken as that applied by the machine throughout the cutting stroke. This assumption required detailed examination.
- (iii) A more appropriate thrust load parameter which could be used during research work on the performance of saw blades needed to be defined.
- (iv) There was a need to verify whether it was possible to eliminate completely the effects of the sawing machine characteristics when undertaking performance tests on hacksaw blades.

With the above objectives in mind and by using the portable instrumentation described below, performance tests on a selection of power sawing machines were carried out. The machines covered in the survey were those available at Sheffield City Polytechnic, at the testing laboratory of James Neill Limited and those

supplied by Wickstead Limited.

2.1.1 Instrumentation

The basic requirement of the instrumentation was to enable the load developed between the blade and the workpiece and the other components of the cutting force, to be measured continuously, against the position in the stroke and to be easily adaptable to the various hacksawing machines.

The components of the cutting force were measured, via the workpiece, by a Kistler piezoelectric, three force component dynamometer, clamped on a special base in the workpiece vice of the machine. The position of the blade was measured using a linear displacement transducer. The output signals from the dynamometer and the transducer, at slow reciprocating speeds of the saw, were displayed via charge amplifiers on to an x-y plotter to record loads against blade displacement. At high reciprocating speeds the output signals were displayed on a multi-channel oscilloscope and the results recorded with a camera. Figure 1 gives a schematic diagram of the power hacksaw and associated instrumentation.

The list below gives some details of the power hacksaws tested.

<u>Saw Machines</u>	<u>Type or Number</u>	<u>Principle of Operation</u>
Kasto	UBS 240R	Hydraulic feed
Kasto	VBS 221	Hydraulic -
Wickstead	Hydromatic	Hydraulic
Wickstead	ACME	Hydraulic
Wickstead	Hydromatic	Hydraulic
Marvel	No 9	Positive feed
Rapidor		Gravity fed, cam lift

In order to show the thrust load characteristics of these machines, a thrust force - crank angle diagram has been produced for each machine. These diagrams for the above machines are shown in Figure 2 and obtained using the arrangement shown in Figure 1.

2.1.2 Observations of the load characteristics

- (i) All machines developed thrust loads which under-

went considerable variation during the cutting cycle. The position of the developed thrust load 'loop' can be changed relative to the crank angle position by dashpot adjustment and load setting, on most of the machines tested. The Marvel No 9 saw developed the most constant form of thrust force characteristics.

- (ii) Most machines developed some thrust load on the return or idle stroke which was impossible to eliminate by the adjustment available.
- (iii) The Kasto UBS 240R saw developed a reduction in thrust force at a crank angle of 51 degrees. The reason for this characteristic has not been found but it obviously must be connected with the hydraulic mechanism which develops the thrust. A similar effect was seen on setting No 2 with the Wickstead Hydromatic saw.
- (iv) The load adjustment when provided was not always linear and, in the case of the Wickstead Hydromatic, was not progressive.

2.1.3 Load Developed by Hydraulic Machines

The force between the blade and the workpiece, the thrust force, is developed in this type of machine by a hydraulic device. Pressure may be developed in the loading cylinder by a restricted back-flow system, Figure 3, or the pressure may be supplied from a separate pump. These machines are the most common, and develop greater thrust loads than machines of other types. The thrust load developed by any hydraulic machine varies considerably throughout the cutting stroke, Figure 4, and the variation is characteristic of the hydraulic system used.

Figure 5, (21) shows a simplified diagram of the principal mechanical and hydraulic arrangements of a typical hydraulic machine, operating on the restricted back-flow principle. The saw bow is carried in a slideway, housed in the swing-arm assembly. This assembly rotates about the pivot shown. The slideway in the swing-arm assembly, and the fixing points for the blade on the saw bow, are arranged so that a small taper exists between the cutting edge of the blade and the swing-arm slideway. The effect of this taper is such that, during the inward cutting stroke, the blade and the swing-arm assembly rotate clockwise about the pivot point. This motion

causes the piston in the hydraulic cylinder to rise, and displaces oil through the flow control valve. The back-flow develops pressure in the cylinder and a torque about the pivot point which opposes the motion of the swing-arm. It is this torque which develops the thrust load between the workpiece and the blade.

An analysis of the above mechanism has shown (21) that the general shape of the thrust load curve, Figure 5, is such that no load is developed by the machine at the beginning or the end of the cutting stroke. Whilst this makes it easy to engage and disengage the blade without suddenly loading or unloading the blade teeth, it does mean that for part of the stroke the blade is only lightly loaded and, as a consequence, the material removed during this part of the stroke is small. The analysis also shows that the maximum load is developed at the mid-stroke position. Whilst the general shape of the curve predicted by the above analysis is typical of those measured experimentally when the blade is loaded lightly, see Figure 7, high loads cause considerable blade deflection and high material removal rates, which cause large variation in the effective wedge angle throughout the cutting stroke, Figure 6. The effect of blade deflection and material

removal rate is to displace the point of maximum load from the mid-stroke position, usually towards the end of the cutting stroke, Figure 7, and to affect the magnitude of the loads developed. These effects in particular make this mechanism prone to strong interaction between the characteristics of the blade and the cutting action, and the load developed by the machine for a given flow control valve setting.

The only way in which the load developed can be controlled by the operator for a given set of conditions is by adjustment of the flow control valve, which is a crude method for load adjustment and it cannot be assumed that doubling the load setting in the machine doubles the mean load acting between the blade and the workpiece.

Despite the large difference in the machine characteristics, an attempt has been made to devise a thrust load parameter which enables the characteristics of the machine to be eliminated from the performance of the blade. To do this a mean thrust load parameter has been defined and is given in the section 'Assessing the performance of a blade' (3.2.3). This parameter enables any load variation during the cutting stroke to be taken into account. However, the parameter does ignore the effects of thrust load applied

on the return stroke. The success of this parameter may be seen in Figure 9.

This graph shows the number of strokes required to cut through a standard mild steel test bar against the mean thrust force. It can be seen that results obtained on the different machines agree reasonably well with the general trend. This curve represents the performance of the Brand 'X' 6TPI blade, used throughout the machine survey, with the machine characteristics eliminated as far as possible.

2.1.4 Results from the Machine Survey

- (i) Saw machines do have widely different thrust force characteristics and some apply partial thrust load during the return or idle stroke. This latter characteristic must have some effect on the wear induced during normal use. Since normal blades are not designed to cut on the return stroke, it is probable that considerable wear in relation to the material removed would occur on the return stroke. This could go some way to explain the variations observed by various hacksaw blade testers.

- (ii) The results clearly show that the method of measuring the thrust load when the saw is at mid-stroke position and at mid-point along the blade, is not an accurate way of measuring the effective thrust load, Figure 4. The method tends to over-estimate the thrust load and give considerable variation from one machine to another.
- (iii) The mean thrust load gives a much improved estimate of the effective thrust load and provides a method of eliminating much of the machine's individual characteristics. If the order of accuracy in Figure 9 is acceptable, then any production saw may be used for assessing the material removal performance of blades, providing the mean thrust load is measured.

2.1.5 Stroke of the Saw

A feature which was common between the Wickstead Hydraulic saw and many others was that the stroke was fixed. Some important relationships between the breadth of the work-piece, stroke of the saw machine and the effective blade length are derived below.

If length ' ℓ ' of the blade makes contact with the workpiece;

From Figure 10 it can be seen that,

$$\ell = S + B$$

or
$$\left(\frac{\ell}{L}\right) = \left(\frac{S}{L}\right) + \left(\frac{B}{L}\right)$$

and
$$\left(\frac{\ell}{L}\right)_{\max} = 1 = \left(\frac{S}{L}\right) + \left(\frac{B}{L}\right)$$

The final expression enables the limiting breadth of the workpiece to be determined for a given blade length and saw stroke. Note the length of blade in contact at any time is always (B).

2.1.5.1 The equivalent number of teeth (N_e)

For the purpose of determining this number, any tooth which traverses only a fraction of the workpiece breadth contributes the same fraction to the equivalent number of teeth, ie a tooth which traversed one half of the workpiece breadth contributes one half of a tooth to the equivalent number.

Thus the volume of metal removed during a stroke of the saw can be determined from a knowledge of the equivalent number of teeth, the common depth of penetration made by all teeth and the width of the cutting edge of the blade teeth.

To calculate the equivalent number of teeth the fraction of the breadth traversed by each tooth which makes contact with the workpiece is determined, the variation

in this tooth factor is shown in Figure 10. The equivalent number of teeth is the sum of these fractions or the area under the graphs shown in Figure 10 divided by the pitch of the teeth.

When $S \geq B$ (See Figure 10 (a))

When the stroke is larger than the breadth of the workpiece all teeth are clear of the workpiece slot at some time during the stroke so that normal chip and debris clearance can take place.

$$N_e = (\frac{1}{2}B + (S - B) + \frac{1}{2}B)n = Sn$$

when n = number of teeth per unit distance.

This is the most efficient geometric situation for hack-sawing.

When $S < B$ (See Figure 10 (b))

When the stroke is smaller than the breadth of the workpiece some of the teeth at the centre of the blade remain completely enclosed within the workpiece slot. Over this centre section the normal process of chip and debris clearance cannot take place and some reduction in cutting efficiency is most likely to occur.

$$N_e = \left\{ \frac{1}{2}S \left(\frac{S}{B} \right) + \frac{S}{B} (B - S) + \frac{1}{2}S \left(\frac{S}{B} \right) \right\} n$$

$$= Sn \left\{ \frac{S}{B} + 1 - \frac{S}{B} \right\}$$

or $N_e = Sn$

It is seen that this is the same result as in the previous geometric case. However, it may be more appropriate to ignore the effect of the teeth in the centre section since they are likely to become filled and 'clog'.

Hence,

$$N_e = \left\{ \frac{1}{2}S \left(\frac{S}{B} \right) + \frac{1}{2}S \left(\frac{S}{B} \right) \right\} n$$

or $N_e = Sn \left\{ \frac{S}{B} \right\}$

Hence $N_e = S.n.n$ where $n = \text{efficiency} = \frac{S}{B}$

All these geometric relationships have been incorporated in the graphs shown in Figure 11, in which the ratios of workpiece breadth to the effective blade length $\left(\frac{B}{L} \right)$ is shown against the ratio of the saw stroke to the effective blade length $\left(\frac{S}{L} \right)$.

Use of Figure 11

The following data relate to the two power hacksawing machines in use at Sheffield City Polytechnic.

Make	Stroke S (in)	Maximum Workpiece Breadth B_{\max} (in)	Effective Blade Length L (in)	$\frac{B_{\max}}{L}$	$\frac{S}{L}$
Kasto (A)	5.25	9.50	16.56	.575	.318
Wickstead (B)	5.50	8.00	15.22	.525	.361

The maximum workpiece breadth has been taken to be that quoted by the manufacturer. These two machines are shown on the graphs in Figure 11, points A and B. Other data obtained from the graphs are as follows:

	Kasto	Wickstead
1 Percentage of blade length which makes contact with the workpiece	88%	87%
2 Percentage of blade length enclosed by the workpiece	26%	16%
3 Stroke efficiency	57%	68%
4 Reduced equivalent number of teeth (assuming 10 TPI)	30	38
5 Equivalent number of teeth (assuming 100% efficiency and 10 TPI)	52	55

2.1.5.2 Requirements of the Saw Stroke

- a. Figure 11 clearly shows that for a fixed stroke machine and maximum cutting efficiency over the full capacity of the machine, the stroke should be one half of the effective blade length, ie $(\frac{S}{L}) = 0.5$, both the Kasto and Wickstead machines are below this limit.
- b. Another general conclusion which may be drawn from Figure 11, is that, if full utilisation of the blade is to be obtained for all sizes of workpiece within the capacity of the machine, the stroke should be adjustable. A machine with such a facility would have a greatly improved overall metal removal efficiency. For optimum efficiency, the largest possible stroke should be used that is consistent with the effective blade length and workpiece breadth, eg

$$S_{\max} = L - B$$

- c. The data obtained from Figure 11, indicate that the Wickstead machine is likely to be more efficient, ie requires fewer strokes per cut, with larger sizes of workpiece for a given thrust load than the Kasto

machine.

From the analysis given in Chapter 3, it is shown that for a given workpiece

$$N F_{tm} S = \text{constant}$$

where N = number of strokes needed to cut through the workpiece

F_{tm} = mean thrust force developed

S = stroke of the saw

This shows that the number of strokes required to cut through a given workpiece may be reduced by either increasing the thrust load or the stroke of the saw. The thrust load could be varied on the hydraulic saws tested but the stroke was fixed. The reason for this is presumably because of the additional cost in providing such adjustment.

However, the above shows that this is just as important as load adjustment. If the stroke could be adjusted then not only would the number of strokes be reduced, but also, the blade wear would be more uniformly distributed along the blade.

This would lead to improved blade life.

2.1.6 Rotational speed of the sawing machine

The major influence of the rotational speed of the saw is the required cutting time. An increase in the speed would reduce this cutting time, and, therefore, the direct labour costs. There is, therefore, much benefit in operating a sawing machine at the highest speed compatible with the work being done. Some preliminary tests have been carried out on the Wickstead Hydraulic sawing machine to look at any changes in performance at high speeds. Figures 12a and 12b show thrust load variations for the above machine at two different speeds under otherwise identical conditions. It was seen that, at high speeds, the load developed exhibited variations of a cyclic nature which was most probably due to dynamic instability in the machine. The instability and its limiting effect on speed, is another factor which is worthy of some further consideration.

2.2 POWER HACKSAW BLADES

Although the basic operating motion of the hacksaw is different from that of other sawing machines, the material

from which the blade is constructed is similar to bandsaw blades.

2.2.1 Hacksaw Blade Material

Power hacksaw blades are available in two different materials:-

- a. All-hard, one-piece blade made of high speed steel. Tungsten steel is sometimes used if the workpiece is a hard alloy or a stainless; more often the blade will be made of molybdenum steel, which provides better toughness, wear resistance, and heat resistance. Standard tool-steel blades are sometimes used for soft metals, and often for 'one-of-a-kind' cut off jobs. The all-hard molybdenum HSS blade is the more commonly used and least expensive of all power hacksaw blade.
- b. A welded edge blade consisting of a high-speed - steel cutting edge electron-beam welded to a carbon alloy back. The high speed cutting edge delivers equal or better cutting performance compared to the all-hard blade while the alloy steel back is less prone to breakage, especially shatter, than the all-hard blade, if it is suddenly dropped on the work,

bends in the cut, or is fed at too high rates etc, creating a hazard for the operator and nearby personnel. Furthermore, the bi-metal blade permits greater tensioning for higher feed loads.

2.2.2 Hacksaw Blade Specification

Hacksaw blades are usually classified according to their principal overall dimensions, teeth pitch, the teeth set pattern and the material from which they are made. Details of the nomenclature and definitions can be found in the British Standards Institution publication BS 1919 (48). Figure 13 shows the terminology and nomenclature used for saw blades. The principal overall dimensions and the teeth pitch (number of teeth per 25 mm) are always expressed in this order, shown as follows:

length of blade between centres of the pin holes, (mm)	x overall blade width, (mm)	x blade thickness, (mm)	x pitch (number of teeth per 25 mm)
---	--------------------------------	-------------------------------	--

eg 250 x 13 x 0.65 x 1.4

or 250 x 13 x 0.65 x 1.4 (18)

Saw blade teeth vary in shape depending on the work characteristics for which the blade was designed. The regular tooth form Figure 14b (i) (49), is the one most

commonly used. Faces of the cutting teeth are perpendicular to the back of the blade, and the gullets are full and rounded to promote good chip curl. The skip tooth form Figure 14b (ii) makes for a much wider gullet, which is relatively flatter, and this tends to break up very ductile material. This makes the skip tooth ideal for aluminium, copper, magnesium, soft brass etc, and similar metals which can clog a standard blade, especially when cutting large solids.

The hook tooth form Figure 14b (iii) is similar to the skip tooth, except that it has a slight positive rake, to provide a better bite with lighter feed rates. The gullet is more rounded to promote chip curl. This form is used to cut harder materials with thick cross sections.

Some of the teeth which make up the cutting edge of the blade are bent laterally, or set, during manufacture, so that clearance is achieved between the blade and the slot produced, which would otherwise generate high frictional heat and bind in the slot cut by the blade. It also determines the width of the slot, or kerf, cut in the work. The following set patterns are common, Figure 14a,

- (i) Alternate set.
- (ii) Raker set.
- (iii) Wavy set.

In the alternate raker the teeth are set left and right. The raker set is a general purpose pattern, consisting of right, left, straight tooth sequence. The straight (unset) tooth serving as a chip clearing function, suitable for solid uniform work.

Wavy set consists of three teeth set to the right, one unset tooth and three set to the left, the wavy set teeth forming a sine wave.

2.2.3 Cutting Edge Geometry

Examinations of the cutting edges of hacksaw blade teeth have shown them to be inconsistent. This is due to the traditional method of manufacture in which the tooth profile is produced by gang-milling followed by heat treatment and the milling and heat treatment processes produce badly formed cutting edges. The actual profile of the cutting edge differs considerably from one tooth to the next. For most blades the major cutting angles are as shown in Figure 15.

By describing the cutting edge profile as a radius, some measure of the magnitude and variation of the tooth profile has been made. The influence of this radii is discussed later. These measurements were carried out on an optical projector which gave a magnification of 50, and a master transparent template was produced which enabled radii less than 0.0003 inches ($7\text{ }\mu\text{m}$) to be measured. To check cutting edge radii six blades each of 4, 6 and 10 teeth per 25 mm (TPI), were subjected to cutting edge profile measurements. All the teeth in line with the body of the blade, approximately one third of the total number of teeth on the blade, were subjected to measurement. Because of the inconsistent nature of the cutting edge-profile Figure 16, the curvature of the extreme edge of the teeth was measured in these early tests. The results of these tests are shown in tabulated form in Appendix B, Table 1. They show that considerable differences occur in the cutting edge radii of teeth on the same blade, giving a range of approximately 0.02 mm (0.0008 in) to 0.07 mm (0.003 in). The average of all the teeth measured on a blade was considered representative of the whole blade. The results shown in Appendix B indicate that some variation was recorded between one blade and another having

the same pitch, but, more significantly, the averages for blades 4, 6 and 10 teeth per 25 mm did differ.

2.2.4 Slot Width

Another geometric variation, introduced during manufacture, which produces changes in the metal removal rate of the blade is the variation in the overall thickness of the blade after setting. The overall thickness is measured across the set teeth from the extreme edge on one side of the blade to the extreme edge on the other.

A random sample of blades having the three teeth pitches considered above were used to produce a slot in the mild steel test bar. The slot widths were then measured using a travelling microscope and the results compared. Table 2 Appendix B shows the results of these tests. It was seen that up to 7% variation was occurring in the slot width to blade thickness ratio, a parameter which is used in the future for assessing blade performance.

CHAPTER 3

3.0 PERFORMANCE TESTING OF HACKSAW BLADES

3.1 INTRODUCTION

Although a British Standard BS 1919 (48) exists for specifications, which provides details of dimensions, tooth configurations, metallurgical properties such as composition, grain size, hardness etc, of both power and hand hacksaw blades, the above standard relates to testing of only hand hacksaw blades.

A considerable amount of testing of power-hacksaw blades has been, and is still being undertaken, by both individual manufacturers and users. The British Hacksaw Manufacturers' Association (BHMA) sub-committee, have performed tests under fixed, standardised conditions in their search for a performance test for HSS power-hacksaw blades (56), and similar work has in the past also been undertaken by HM Dockyard in connection with the Admiralty Specifications (51). The results of these tests show the great difficulty in establishing adequate reproducibility over an indefinite period of the behaviour of the test material, the saw machine characteristics and the sawing conditions not

only in the individual company but in a number of companies, ensuring that the results are a true indication of the performance of the power-hacksaw blade, independent from these extraneous effects.

Many manufacturers and users are engaged in a continuous programme of cutting tests on power-hacksaw blades under arbitrarily chosen conditions in which they compare the performance of their product with that of their competitors or to their own standards.

The criteria used for assessing blade performance and the conditions under which the tests are carried out differ from firm to firm and the test conditions used within a firm usually differ from time to time. This has eliminated the possibility of collecting useful, consistent, reproduceable data from the different testing procedures and obtaining an absolute value of blade performance.

Each blade manufacturer or user appears to place a different value on the relative importance of the many different variables which could affect the performance of the blade during a sawing test, or the condition of the end product. The criterion used for performance testing by the majority of users appears to be qualitative

more than quantitative. Some users base their choice on a general impression, gained over a period of time, of the relative performance of a number of brands in different operations on the shop floor; others would purchase a brand of blade purely on a cost basis. However, there are some specifications for power hacksaw blade testing in the United Kingdom (51, 57) and abroad (52, 53, 54, 55), which, whilst they are based upon tests carried out under standardised conditions, use various criteria to assess the blade performance, eg

- (i) Test blade shall cut satisfactorily 'n' sections from the standard test bar.
- (ii) Test blade shall cut satisfactorily 'm' sections and the time taken for the 'mth' section will not exceed 'x' minutes.
- (iii) Number of strokes required to cut a specified section exceeds the stated number of strokes, the number of strokes being different, for different pitch teeth.

- (iv) Each sample blade, in accordance with its type and number of teeth/25 mm, shall completely cut through the number of sections specified, and the time for the final cut section is less than a maximum value stated.

Although the criterion preferred by most foreign specifications appears to be the specific number of cuts required to be made by a blade, and the time taken to make the final cut to be less than a specified amount, there appears to be little attempt to standardise test conditions. Some tests specify the cutting speeds, others carry out tests at various speeds according to the blade geometry and dimensions. Similarly the load of the hacksaw blade when the machine is at mid-stroke varies with the size of blade and has a large range from one tester to another. Most testers stipulate the length of the stroke and the relief on the return stroke, but the blade tension is rarely specified. Tests are carried out both dry cutting and with lubricants, but the quantity and type of cutting fluid is not specified.

It is not surprising from the above, that, due to the lack of control of the test conditions, and the variables which

influence the metal removal in the sawing operation, the BHMA and other organisations testing blades have experienced difficulty in formulating a test which would quantitatively characterise a blade, so that the results would be consistent.

The BHMA (56) and NEL (50), have both pointed out, without quantifying, that the machine characteristics are a major factor and a large contributor to the inconsistency in the test results previously obtained.

This is not at all surprising considering the results obtained by the author in the previous chapter on power hacksaw machine characteristics.

3.2 Formulation of a Cutting Test to Assess the Performance of a Blade

It is clear, from the difficulties encountered by the hacksaw blade manufacturers and users and the findings discussed in the previous chapters, that the best test of the performance of a power-hacksaw blade is to quantitatively measure the cutting efficiency of the blade whilst identifying and controlling the process variables. It has also been shown (Figure 17) that the measured load

applied to the saw frame at mid-stroke is not an accurate measure of the dynamic thrust load acting during the stroke, especially when hydraulic hacksaws are used. Thus, it is essential that the thrust load be measured during operating conditions, in order to obtain a mean thrust load parameter.

3.2.1 A method for assessing the blade performance

In this method, regard is taken of the fact that the depth of cut achieved by a particular blade is dependent on the thrust force component generated by the sawing machine. Test results have shown (Figure 18), that, for a 6 TPI blade and various sawing machines, the average depth of cut per tooth is directly proportional to the mean thrust force component, thus,

$$\delta_a = K f_{tm} \dots\dots\dots (3.1)$$

where K is a constant for a given workpiece material and teeth spacing.

3.2.2 Determination of the average depth of cut per tooth

Consider the blade to be initially displaced by an amount x from its position at the beginning of the cutting stroke.

The volume of material removed as the blade is further displaced by an amount Δx from this position (Figure 19) is

$$\Delta(\text{vol}) = t n_c \delta \Delta x \quad \dots\dots\dots (3.2)$$

Where

$\Delta(\text{vol})$ = Volume of material removed during the small displacement of the blade Δx

t = thickness of the blade

n_c = number of teeth in contact with the workpiece
 $= Bp$ for broad workpieces

B = breadth of the workpiece

p = pitch of the blade teeth

δ = instantaneous depth of cut achieved per tooth

As the thrust load varies during the cutting stroke, the instantaneous depth of cut achieved per tooth also varies. Hence, the volume of material removed during one cutting stroke becomes

$$(\text{Vol})_s = t n_c \int_0^s \delta dx \quad \dots\dots\dots (3.3)$$

As the instantaneous depth of cut is difficult to measure experimentally, it is convenient to introduce the average depth of cut achieved during the cutting stroke per tooth,

defined as

$$\delta_a = \frac{1}{S} \int_0^S \delta \, dx \quad \dots\dots\dots (3.4)$$

Where

δ_a = average depth of cut per tooth

Combining these expressions, when the workpiece is broad compared with the pitch of the blade teeth, gives

$$(\text{Vol})_s = t \, B \, p \, \delta_a \, S \quad \dots\dots\dots (3.5)$$

The volume of the material removed during the cutting stroke may also be found from the loss in volume of the workpiece. For a rectangular workpiece this becomes

$$(\text{Vol})_s = w \cdot B \cdot \delta_s \quad \dots\dots\dots (3.6)$$

Where

w = width of the slot produced

δ_s = increase in the slot depth produced per cutting stroke = D/N

D = depth of a rectangular workpiece

N = number of strokes required to cut through the rectangular workpiece

Combining these expressions gives

$$\delta_a = \left(\frac{w}{t} \right) \cdot \frac{D}{N} \cdot \frac{1}{S.p} \quad \dots\dots\dots (3.7)$$

The ratio (w/t) is the ratio of the slot width, or the thickness of the blade measured from the outside edges of the set teeth, to the thickness of the blade material, and is known as the thickness ratio, z.

The number of teeth which make contact with the workpiece during the cutting stroke, N_c , is

$$N_c = (S + B)p \quad \dots\dots\dots (3.8)$$

However, the teeth which are in contact with the workpiece at the beginning and at the end of the cutting stroke do not travel across the full breadth of the workpiece. The equivalent number of teeth which may be said to make one complete traverse of the workpiece, N_e , may be shown to be

$$N_e = S.p. \quad \dots\dots\dots (3.9)$$

Therefore, the expression for the average depth of the cut per tooth may be written

$$\delta_a = \frac{D}{N} \cdot \frac{z}{N_e}$$

$$z = w/t \quad \dots\dots\dots (3.10)$$

3.2.3 Determination of the mean thrust load per tooth per unit thickness

The mean thrust load per tooth per unit thickness may be defined as the mean load acting between the blade and the workpiece during the cutting stroke per tooth per unit blade thickness, assuming that each tooth in contact carries equal load.

The mean total thrust load (F_{tm}) acting between the blade and the workpiece is given by

$$F_{tm} = \frac{1}{S} \int_0^S F_t dx \quad \dots\dots\dots (3.11)$$

Where

F_t = instantaneous thrust load after a displacement x of the blade from the beginning of the cutting stroke

The mean thrust load per tooth per unit blade thickness

f_{tm} , is obtained from

$$F_{tm} = f_{tm} \cdot n_c \cdot t \quad \dots\dots\dots (3.12)$$

For broad workpieces this may be written

$$f_{tm} = \frac{F_{tm}}{B.p.t} \dots\dots\dots (3.13)$$

As the load developed between the blade and the workpiece, and its variation during the cutting stroke, depends on the type and characteristics of the sawing machine, the mean thrust load per tooth per unit blade thickness is a machine parameter which is controlled by the machine setting etc. Combining the following equations

$$\delta_a = K f_{tm} \dots\dots\dots (3.1)$$

$$\delta_a = \frac{w}{t} \cdot \frac{D}{N} \cdot \frac{1}{S.p} \dots\dots\dots (3.7)$$

$$f_{tm} = \frac{F_{tm}}{B.p.t} \dots\dots\dots (3.13)$$

gives the number of cutting strokes, N, required to cut through a rectangular workpiece

$$N = \frac{D.w.B.}{K.S.} \cdot \frac{1}{F_{tm}} \dots\dots\dots (3.14)$$

$$\text{or } N.F_{tm}.S = \frac{D.w.B}{K} = \text{constant} \dots\dots\dots (3.15)$$

In equation (3.1) the parameters δ_a , the average depth of cut achieved during the cutting stroke and f_{tm} , the mean thrust force per tooth, can be measured, thus giving a method for determining the constant K.

Further cutting tests using Brand 'X' blades have shown that during the cutting stroke the thrust (F_t) and cutting force (F_c) components are directly proportional to each other, see Figure 20 giving

$$F_c = C \cdot F_t \quad \dots\dots\dots (3.16)$$

and $F_{cm} = CF_{tm}$

or $(f_c)_{\text{mean}} = C \cdot (f_t)_{\text{mean}} \quad \dots\dots\dots (3.17)$

From the empirical relationships of equation (3.1) and equation (3.17) it is possible to determine the specific cutting energy of material removed, and thus assess the performance of a blade.

3.2.4 The Establishment of a Cutting Efficiency Parameter

The specific cutting energy (Energy per unit Volume, k) for a given material is a measure of the efficiency of the cutting process, the lower the specific cutting energy value the more efficient the cutting process.

The specific cutting energy k is

$$k = \frac{f_{cm} \cdot t \cdot B + f_{tm} \cdot t \cdot \delta_a}{t \cdot B \cdot \delta_a} \approx \frac{f_{cm}}{\delta_a} = \frac{f_{cm}}{f_{tm}} \cdot \frac{f_{tm}}{\delta_a} \text{ since } \delta_a \ll B.$$

$$\text{or } k = \frac{C}{K} \dots\dots\dots (3.18)$$

A convenient method for assessing the relative cutting efficiencies of blades is by means of a graph showing the average depth of cut per tooth against the mean thrust force component per tooth/mm. The higher the blade efficiency the greater the slope of the graph, K .

The above parameter K , referred to as the cutting constant, is used throughout the present work for assessing the blade performance.

3.3 Instrumentation and Testing Procedure for Hacksaw Blades

Figure 21, shows the power hacksaw with the instrumentation which has been previously described in Chapter 2. Prior to placing the blade in position, the dimensions, ie blade width and thickness, were measured using a micrometer. When the blade was in position, it was tensioned by initially 'finger' tightening the hexagonal nut, and finally giving the nut specified turns with a spanner, simulating current

industrial practice. The workpiece was fastened at mid-stroke to the top of the dynamometer, which in turn was secured in the vice of the saw. The operation of the saw was checked to ensure that it did not cut on the return stroke.

The outputs from the dynamometer, the thrust force and cutting force components were recorded on an X-Y plotter, against the position in the stroke of the saw. The time required to cut through the specimen was recorded for a particular load setting.

The experiment was repeated for various machine hydraulic settings and the results tabulated as shown in Table 3, (Appendix B).

3.4 Processing of Cutting Test Results to Determine the Average depth of Cut per Tooth, δ_a , and the Mean Thrust Force per Tooth per Unit Blade Thickness

A typical thrust load developed during the cutting stroke between the blade and the workpiece for a particular load setting is shown in Figure 22.

Consider the column in Table 3 (Appendix B) relevant to machine setting (2).

Using a planimeter the

Area under the curve $= 92 \text{ cm}^2$

Length of base of curve $= 16 \text{ cms}$

Mean height $= 5.75 \text{ cms}$

Mean thrust force during
the cutting stroke (F_{tm}) $= 129.26 \text{ lbf}$

From equation (3.13) $f_{tm} = \frac{F_{tm}}{B.p.t.} = \frac{F_{tm}}{n_c t}$

$$= \frac{129.26}{6 \times 2}$$

$\therefore f_{tm} = 10.77 \text{ lbf/mm/Tooth}$

NOTE: The load in the above case has been expressed in lbf, due to the instrumentation being calibrated at the time being in imperial units.

The average depth of cut per tooth δ_a , has been determined using equation (3.10), thus

$$\delta_a = \frac{D}{N} \cdot \frac{z}{N_e}$$

Using the results again from Table 3 machine setting (2)

$N = 91.2$ and $N_e = S.p. = 5.5 \times 6 = 33$

and from cutting tests $z = \frac{w}{t} = 1.362$

$$\therefore \delta_a = \frac{25}{91.2} \cdot \frac{1.362}{33}$$

$$\delta_a = 11.32 \times 10^{-3} \text{ mm}$$

The values of δ_a and f_{tm} are shown tabulated in Table 3, for various machine settings.

3.5 EXPERIMENTAL RESULTS - PERFORMANCE TESTING OF HACKSAW BLADES

3.5.1 The Cutting Action of New Blades

Cutting tests have shown (Figure 23) that the average depth of cut achieved per tooth, δ_a , is very small in most applications. Calculations of δ_a and the measurements of the cutting edge radius of the saw teeth, show that, in the majority of applications, the depth of cut is less than the cutting edge radius. Thus, the hacksaw blade may be classified as a blunt cutting tool. The significance of this is discussed in Chapter 4.

Observations of steel chips, produced by hacksawing under the action of light thrust loads, confirm that the chips are produced by a shear type mode of deformation. The chips and debris vary considerably in size. Microscopic examinations of these chips show evidence of surface shear

lines, produced as the material 'piles-up' in front of the blunt cutting edges. Frequently the chips show evidence of surface oxidation, indicating high temperatures. When cutting soft material, under the action of a large thrust load, the chips produced are continuous curls of material similar to chips produced by a sharp tool. This change in chip formation is brought about by the depth of cut achieved being significantly larger than the cutting edge profile radius on the blade teeth.

3.5.2 Comparison of Blade Performance of Different Pitches

Figure 23 shows the variation in the average depth of cut per tooth against the mean thrust load per tooth per unit blade thickness for En 1a workpiece and blades of different pitch. It can be seen that these parameters are directly proportional to each other for a given blade pitch. This result may be written for a given workpiece material, workpiece size and blade pitch thus

$$\delta_a = K.f_{tm}$$

Figure 23 thus indicates that the 4 TPI blade performs better than the 6 TPI, which performs better than the 10 TPI.

It should be noted that the values of the constant K for a given tooth spacing will vary with the design of the blade and the values obtained from Figure 23 should only be used with the existing blade design. Blades of other manufacturers will most probably have different K values.

The repeatability of this test has been found to be very good, provided every test includes load measurement and the slot width is measured for each blade tested.

Figure 24 shows the variation in the cutting constant against the reciprocal of the number of teeth in contact with the workpiece. Each point on this graph has been obtained by carrying out cutting tests and producing curves similar to Figure 23 and determining the value of the constant K from the slope of the individual curves. The results in Figure 24 show a significant size effect. These effects may be summarized as follows:

When $B \geq 25$ mm for En 1a

$$K \approx a + b.p. \text{ (for a particular blade)}$$

When $2p < B < 25$ mm for En 1a

$$K.n_c = c$$

Where B = breadth of the workpiece

n_c = number of teeth in contact with the workpiece

p = pitch of the blade teeth

a, b, c = material constants for a particular blade type

3.5.3 Comparison of the Performance of Different Manufacturer's Blades

The method previously outlined has been used to compare the performances of several Brand 'X' blades from one manufacturer and Brand 'Z' blades from another manufacturer. The results of this comparison are shown in Figures 25 and 26. In Figure 25, which shows the average depth of cut against the mean thrust force component, a result obtained with a lathe parting-off tool has been included. Since the parting-off tool was ground with a sharp cutting edge and was used at comparatively large depths of cut, the result shown indicates the upper boundary possible for the performance of hacksaw blades.

The results from these tests can be summarised as follows:

- (i) Both Figures 25 and 26 indicate a superior performance by the Brand 'Z' blade compared with the Brand 'X' blades. Figure 26 gives some manufacturer's details of the Brand 'Z' blades.

- (ii) By inspection of the cutting edge of the blades under a microscope the Brand'Z' blade has a much sharper cutting edge, ie the cutting edge radius is smaller than those on Brand'X' blades.
- (iii) From observations of the chips produced by the Brand'Z' and Brand'X' blades, see Figures 28 and 29, it is clear that the Brand'Z' blade is achieving a much superior cutting action at all applied loads and an action similar to a lathe single point cutting tool. The cutting action of the Brand'X' blades results in many irregular chips compatible with their 'blunt' cutting edges.
- (iv) The tooth design of the Brand'Z' gives much more support to the cutting edge and enables more heat to be conducted away from the cutting edge than is possible with the Brand'X' design. This means that the Brand'Z' cutting edge will operate at a lower working temperature and should, therefore, be more resistant to wear.
- (v) Figure 25 compares the performance of Brand'X' blades having 4, 6 and 10 TPI. It is seen that the cutting edge performance of these blades is

improved as the number of teeth per inch decreases.
 Extrapolating these trends, however, to 3 TPI
 does not account for the differing performance
 between the Brand 'X' blades and the Brand 'Z' 3 TPI
 blades.

It can also be shown that the specific cutting energy
 required for the Brand 'Z' blades is far less than the
 Brand 'X' blades:

ie for Brand 'X' blades:

From Figures 18 and 20 we have

$$C = 1.20 \text{ and } K = 0.00144 \text{ mm}^2/\text{lbf}$$

∴ the specific cutting energy $k = \frac{C}{K}$

$$= \frac{1.2 \times 4.448 \times 10^6}{0.00144}$$

giving $k = 3.71 \times 10^9 \frac{\text{Nm}}{\text{m}^3}$ (or Joules/m³)

For Brand 'Z' blades, from Figures 25 and 26 we have

$$C = 2.2 \text{ and } K = 0.0055 \text{ mm}^2/\text{lbf}$$

∴ The specific cutting energy $k = \frac{C}{K}$

$$= \frac{2.2 \times 4.448 \times 10^6}{0.0055}$$

giving $k = 1.78 \times 10^9$ Joules/m³

Comparing these energy values, the low value obtained with the Brand 'Z' blade is also consistent with its superior cutting action.

3.6 SOME FACTORS INFLUENCING THE CUTTING PERFORMANCE OF POWER HACKSAW BLADES

A number of different tests have been carried out on standard Brand 'X' power hacksaw blades with a view to assessing the influence of some geometric design parameters on the cutting performances of the blades.

3.6.1 Teeth Spacing

A random sample of Brand 'X' blades with 4, 6 and 10 teeth per inch were subjected to the cutting performance tests previously described. The results obtained are shown in Figure 30. This figures shows the cutting performance reduced to that of a single tooth in the blade.

These results show that the cutting performance of the 4, 6 and 10 teeth per inch blades differ considerably, a

conclusion which has been confirmed by earlier tests. Also, they show that a variation of about 10% can be obtained between blades having the same teeth spacing. In obtaining the last result an average slot width was taken for all blades having the same teeth spacing. However, different average slot widths were taken for blades having different teeth spacings. Variation in slot width does not, therefore, explain the differences in cutting performance shown between blades of different teeth spacing. Figure 30 shows that the teeth on a blade having 4 teeth per inch appear to be 150% more efficient than the teeth on a blade having 10 teeth per inch, a surprising result which needs explanation. This variation in performance is discussed in Section 3.7.

3.6.2 Cutting Edge Geometry

As a result of the above tests it was decided to look for geometric differences in the cutting edges of the 4, 6 and 10 teeth per inch.

As stated earlier, it was considered that the cutting edge radius was an important geometric parameter and, since the depth of cut per tooth achieved with the mild steel test piece was less than 0.050 mm (0.002 inches), the radius which

was important was confined to the extreme edge of the blade. To check cutting edge radii, six blades of 4, 6 and 10 teeth per inch, 36 blades in total, were subjected to cutting edge profile measurement on an optical projector. All the teeth in line with the body of the blade, approximately one third of the total number of teeth on the blade, were subject to measurement. Because of the irregular nature of the cutting edge profile, the curvature of the very tip of the teeth was measured, rather than the mean radius of the cutting edge. The results of these tests are given in Appendix B, Table 1.

It is seen that some variation was recorded between one blade and another having the same teeth spacing but, more significantly, the averages for blades of 4, 6 and 10 teeth per inch did differ. These measurements confirmed an earlier result that the depth of cut achieved is less than the cutting edge profile radius, a fact which explains much of which has been observed in the cutting action of a blade. From subsequent cutting tests carried out on these blades it appears that the average cutting edge radius did not explain the difference in the cutting performances of blades having the same teeth spacing.

The trends shown in these measurements were not considered conclusive. It may well be that the shape of the cutting edge profile was only one of a number of differences between blades of different teeth spacing. Another difference which was difficult to quantify was that the side angle due to the setting of the teeth differs considerably with the overall size of the teeth and, therefore, with the spacing. This was also true of the distortion that was produced by the setting operations.

In conclusion, a number of small but important geometric differences have been observed between blades having different teeth spacing. As a result the teeth of Brand 'X' blades having different pitch are not geometrically consistent; a fact which may lead to their differences in cutting performance.

3.6.3 Slot Width

The slot width was controlled by the dimension across the blade from the edge of the set teeth on one side of the blade to the set teeth on the opposite side. Any variation in this dimension led to variation in the volume of materials which must be removed to achieve the cut. In the cutting performance test previously described, the ratio of the

slot width to the blade thickness was a factor in the calculated average depth of cut per tooth. An average value of this ratio was taken when calculating the data shown in Figure 30. It was considered possible that the slot width produced by Brand 'X' blades may vary sufficiently to cause the apparent differences in performance of blades having the same teeth spacing. To verify this, a random sample of blades, having the three teeth pitches considered, were used to produce a slot in the mild steel test bar. The slot widths were then measured and the results compared. Table 2, Appendix B shows the results of these tests. It was seen that up to 7% variation was occurring in the slot width to blade thickness ratio. The results show that it was important that the slot width be measured for every blade tested and that the use of an average or representative value was not sufficiently accurate. It was believed that the variation was the major explanation of the differences in the cutting performance between blades of the same teeth spacing shown in Figure 30. However, it does not explain the differences in performance between blades of different teeth spacing, as the slot width variation was taken into account in these comparisons.

As a result of these tests it was suggested that the accuracy of the setting operation in the manufacture of the blades be looked into, as it was causing up to 7% variation in the cutting performance of the blades produced.

3.6.4 Effect of Blade Width on the Cutting Performance Of Power Hacksaw Blades

The blade width is a major design parameter and controls the beam strength of the blade, for a given blade thickness. By reducing the width of the blade it is made more flexible and the deflection produced under the action of the cutting loads is increased. With large blade deflection the teeth, and therefore, the cutting edges are presented to the workpiece in a different geometric relationship. The purpose of these tests was to investigate whether these changes alter the cutting performance.

Prior to these tests it was thought that the effects of blade width on the cutting performance may also be affected by blade wear, thus, tests were carried out on both new and worn blades.

The tests on a new blade consisted of taking a standard 6 TPI production blade 400 mm long x 40 mm wide and subjecting it to the cutting performance tests previously described. The back of the blade was then ground to give a reduced width of 17.5 mm over a central section, 340 mm long, and the modified blade re-subjected to the cutting performance tests. This procedure eliminated any difference due to the cutting edge variations.

The procedure adopted for the worn blades was similar to that described above. The cutting performance tests were carried out on a new 6 TPI blade, 400 mm long x 40 mm wide. It was then subjected to the standard wear tests procedure as described in section 3.6.6, and its cutting performance re-assessed. Figure 31 shows the reduction in cutting performance due to the wear that had taken place. The back of the blade was then ground to give a new width of 19 mm over a central section 340 mm long and the cutting performance test repeated. Figure 32 shows the comparisons of the cutting performances of both the new and worn blades before and after the reduction in width.

The reduction of the blade width to approximately 50% of its standard value, reducing its stiffness by approximately eight times, did not produce any measurable change in the cutting performance of either new or worn blades, despite the large differences in deflections produced. However, the following points should be noted when considering the results produced:

- (i) The effect of reduced width on the wear resistance of the blades was not measured.
- (ii) Reducing the blade width obviously limits the maximum thrust load that may be applied, although this was not measured and, therefore, reduces the maximum metal removal rate of the blade.
- (iii) Reducing the blade width may lower the fatigue life of the blade to an extent that this becomes a limit to blade life.
- (iv) Reducing the blade width affects the load characteristics of the Wickstead saw, see Figure 8.

3.6.5 Effect of Blade Tension

The principal effect of applying tension to a hacksaw blade is to stiffen the blade to minimise the deflection produced by the action of externally applied cutting forces. The important forces to be considered are the thrust component of the cutting force and the lateral loads applied by the engagement and disengagement of the set teeth. The effects of these forces are as follows:-

a. The Thrust Component of the Cutting Force

This force undergoes cyclic variation during the stroke and reaches high magnitudes. As the frequency of this variation is small and the vertical stiffness of the blade is much greater than the lateral stiffness, vertical vibrational instability in the blade is unlikely. However, the thrust component of the cutting force will produce significant blade deflections in the vertical plane which may affect the life of the blade. The effect of applying blade tension is to increase the vertical stiffness of the blade and thus reduce this deflection.

b. Lateral Forces Applied by the Set Teeth

As each tooth in the set pattern that is bent to the right or the left engages and disengages the workpiece, lateral force variations occur.

Whilst it is believed that these forces are small compared with the components of the cutting forces, they may combine to give lateral force excitation to the blade which, if the set pattern is regular, will resonate or set up chatter in the blade, in a lateral mode of vibration.

This would lead to large lateral deflections, poor surface finish and even blade fracture.

The effect of blade tension is to considerably increase the lateral stiffness and, therefore, increase the natural frequency of the blade.

In doing so a more dynamically stable set of operating conditions may be achieved.

The analysis in Appendix C, shows some of the effects of the above forces acting on a hacksaw blade.

The most important effect of applying blade tension is to increase both the vertical and

lateral stiffnesses of the blade. The lateral stiffness is increased considerably more than the vertical stiffness for a given tension. The effects of these increases is to reduce deflections for a given load and to increase the natural frequency of vibration.

The engagement and disengagement of the set teeth apply a lateral load to the blade of such a frequency that chatter is possible, particularly when the tooth pitch and the set pattern are regular. The balanced set pattern helps to overcome these difficulties.

Further work in the above area has been carried out by Thompson and Taylor (26). The theoretical model proposed by the above for the lateral displacement of the cutting edge shows that lateral equilibrium of the blade can be achieved in a number of ways, namely,

- (i) By the cutting edge adopting a large angle to the vertical such that the components of the cutting force acting on the set teeth are self balancing in the lateral

direction and that little or no restraint is needed due to the elastic distortion of the blade.

- (ii) For the lateral force to be opposed by the restraint due to the elastic distortion of the blade.

The analysis (26) shows that the tendency of the cutting edge to wander is due to variances in the cutting efficiency and setting angles of the set teeth. Thompson and Taylor (26) have pointed out that the variation in the elastic restraint imposed by a blade during power hack-sawing not only depends on the geometry of the blade but it also depends on the blade tensioning force and the position of the workpiece relative to the blade.

3.6.6 Blade Wear and its Effects on Blade Performance

The geometric shape of many partly worn blades was examined to determine suitable wear parameters. As a result of this work it was decided to measure the reduction in saw tooth height of those teeth that are in line with the body of the blade and the shape of the cutting edge

profile. These measurements were carried out on a optical projector using a magnification of 50:1.

Initial wear tests were carried out using a gravity fed power hacksaw and 300 x 25 x 1.25 x 6 TPI blades.

The teeth are worn in such a way that a wear flat is produced at the tip of each tooth, and the outer corners of the set tooth are rounded. The effect of this wear is to increase the thrust load needed to achieve a given depth of cut.

Figure 40 shows the loss in tooth height with the increase in the number of cuts made. The shape of this graph is similar to that obtained by measuring flank wear on a single point cutting tool, and it shows secondary and tertiary regions. A primary region is produced by the rounding of the profile, produced during manufacture. During the earlier part of the blade life, the loss in height is proportional to the number of cuts made; this is the secondary region. The tertiary region is associated with rapid increase in wear. Wear can become so pronounced that under normal applied thrust loads, the blades ceases to cut.

Further wear tests were carried out on 400 x 40 x 2 x 6 TPI blades to assess the change in the metal removal capability of the blade as wear takes place.

Wear on the blade teeth was produced using the standard test bar adopted by some hacksaw blade testers; ie a 36 mm diameter En 44E bar. As this test bar was circular, the method for assessing the blade performance, previously described was not possible. Therefore, the procedure was adopted in which a number of cuts were taken, using the circular En 44E bar, followed by measurement of the wear produced and the assessment procedure previously proposed, using a square 25 x 25 mm mild steel test piece. Figure 41 shows the variation between the average depth of cut per tooth and the mean thrust load per tooth per unit thickness, for a blade in three stages of wear. It can be seen that wear reduces the cutting constant and shifts the curve along the thrust force axis. This indicates that some initial load is needed before material is removed, when the blade is worn.

In the graphical results shown in Figures 42 and 43 the cutting force components and the average depth of cut were those achieved whilst cutting mild steel, however, the wear produced between the tests shown had been

produced whilst cutting the En 44E bar material. It was assumed that the number of cuts made using the mild steel bar produced negligible wear and they are not included in the number of cuts shown on the wear graph, Figure 42. The initial loss in height due to manufacture has not been included in the measurements. The wear graph, therefore, represents the secondary wear stage. The loss in tooth height produced by the wear tests, Figure 43, was a linear function of the number of sections cut. It required 36 cuts to double the cutting time, a criterion used by some hacksaw blade testers, producing a loss in tooth height of 0.25 mm (0.010 in).

The principal effects of blade wear were to decrease the average depth of cut and increase the cutting force component for a given applied thrust load, see Figure 42. The result of these changes is to considerably increase the specific cutting energy:

No of cuts	$K = \frac{\delta a}{f_{tm}}$ mm ² lbf ⁻¹ mild steel	$C = \frac{F_{cm}}{F_{tm}}$ mild steel	$k_a = \frac{C}{K}$ G Joules/m ³ mild steel
En 44E			
0	0.0017	0.85	2.21
36	0.00133	1.20	4.02

The above results show that the specific cutting energy has been doubled during the test.

The wear flat produced in the above results was similar to that produced in many other metal removal processes. The presence of the wear flat means that the applied thrust load, which governs the blade penetration and the depth of cut, was divided into two components. The first component generates a contact pressure over the area of the wear flat, this was a redundant use of the applied load and did not by itself achieve a useful effect. In fact, it led to considerable dissipation of energy, due to the sliding of the wear flat over the cut surface, which generated considerable heat, and hence, accelerated the rate of wear. The second component was due to the normal cutting action and was present no matter what degree of wear had been achieved. The applied thrust load may, therefore, be considered to be made up of these two components.

The presence of the wear flat implies that a certain load must be applied to the blade before any material is removed. The wear test results of Figure 41 show the movement of the cutting performance curves to the right as the blade wears. The other effect, as previously reported, is a reduction in the slope, and therefore, in the performance of the blade. In the terms used in the above expression, 'b' increased with wear as the cutting edge deteriorated.

Whilst these were the effects of wear on the cutting performance of the blade, little has been done to relate them to specific geometric changes in the teeth profile.

One important effect, in addition to the production of the wear flat, was the considerable rounding of the corner of the teeth, due probably to the high temperatures obtained in these regions by the side cutting action of the teeth.

- It should be noted that in the design of the Brand 'X' previously mentioned these corners were given special

treatment by grinding on each tooth a corner cutting edge. This may go some way to explain the better performance of the Brand 'Z' blade previously experienced.

Thompson and Taylor (25) have studied some of the factors influencing the wear rate of power hacksaw blades and have attempted to identify the wear mechanisms involved in blade wear. They adapted a method based on dimensional analysis (57) which relates some of the engineering parameters associated with power hacksaw operations to the wear rate of blades. Some attempt has also been made by the above (25) to identify the fundamental wear mechanisms involved, using the system of classification proposed by Wright and Trent (58).

Some of the features of power hacksaw operations which influence blade wear have been identified (25), as follows:

- (i) the surface against which the blade is rubbing is newly cut from the work material and there is little time for oxide films to form.
- (ii) the surface on which the blade is rubbing has been severely work hardened in the plastic processes involved in forming the chip.

- (iii) the temperature and pressure at the sliding interface can be exceptionally high, and the specific cutting energy could be in the order of $5-6 \text{ GJ/m}^3$.
- (iv) due to sawing being an intermittent cutting action, the time the teeth are in actual contact with the workpiece can vary between 10-30 percent.
- (v) as the blade teeth wear during the sawing operation, the depth of cut achieved per tooth decreases, and hence the geometry of chip formation varies throughout the blade life. This variation of chip geometry has been confirmed in tests carried out by the Author.
- (vi) the cutting speed during a power hacksaw operation varies approximately sinusoidally during each cutting stroke; typical variation of speed at 76 strokes per minute is from zero to a maximum of 72 metres per minute.
- (vii) the thrust load acting per tooth per unit blade thickness also varies throughout the cutting stroke. The variation observed was from zero to a maximum of 140 Nm^{-1} at a cutting rate of 76 strokes per minute.

Microscopic examinations of the sections of teeth during the secondary stage of the wear (linear phase) process have been undertaken (25), and Figure 44 has been compiled from the above observations. Thompson and Taylor have suggested that hacksaw blade wear has been produced by the following two main processes:-

- (i) superficial plastic deformation by shear at high temperatures.
- (ii) plastic deformation of the cutting edge.

3.7 THE VARIATION OF BLADE PERFORMANCE WITH BLADES OF DIFFERENT PITCH AND WORKPIECES OF DIFFERENT BREADTH

3.7.1 Introduction

From the test results obtained with blades of different tooth pitch and on workpieces of different breadth, it has been found that the cutting constant, which has been defined as a measure of the efficiency of the blade, varies with the pitch of the teeth, Figure 23, and the workpiece breadth, Figure 24.

Initially it was thought that this variation was due to two possible causes:-

- (i) blade deflection and the relative movement such deflection produced between individual teeth in contact with the workpiece. However any effects of blade deflection on the cutting constant have been checked, Figure 32 (b), and it has been shown that blade deflection performs a minor role in determining the metal removal rate of the blade, and the overall effect of blade deflection is small when considering one complete cutting stroke of the saw.
- (ii) the second possible cause investigated was due to some feature of the mode of chip formation. During the cutting stroke some metal removed 'piles up' in front of each tooth, some is 'ploughed' around the tooth and some breaks away from the main chip forming small pieces of debris. The author has previously established (23), (Appendix D), that a deformation zone is produced in front of each tooth which once fully established is unaffected by further metal removal. The deformation zone associated with this steady state is large and not instantaneously established when the tooth first makes contact with the workpiece.

During the earlier stage of chip formation, when the size of the deformation zone is increasing, it is known (23) that both the components of the cutting force acting on the tooth gradually increase until a final steady state is achieved, corresponding to the fully established deformation zone.

According to this model of chip formation some of the teeth in contact with the workpiece will be acted on by a constant thrust force, whilst those teeth which have just commenced their cutting action will be acted on by a thrust force which increases with the movement of the teeth along the cut. It has also been shown by the author (23) that the length of cut a tooth must make, before the cutting force components acting on it reach a steady value, is approximately constant for a given workpiece material, Figure 49, for a particular tooth geometry, and does not vary with the depth of cut.

The model presented below helps to explain the variation in the cutting performance of power hacksaw blades with changes in the breadth of the workpiece and the pitch of the blade teeth.

From a simulation of the cutting action of a single tooth (23) the author shows that the thrust load increases with the length of cut in the period prior to the fully established deformation zone. Once the deformation zone is established the thrust load is considered to remain constant.

From the results obtained by the author, Thompson (24) presented the following model.

3.7.2 Theory

If y = length of cut made by a tooth
 and y_c = critical length of cut made by a tooth to
 fully establish a deformation zone

thus

$$\text{when } y \leq y_c \quad f_t = M \cdot \delta \cdot \left(\frac{y}{y_c} \right)^n \quad \dots\dots\dots (3.8.1)$$

and once steady state is established

$$\text{ie when } y \geq y_c \quad f_t = M \delta \quad \dots\dots\dots (3.8.2)$$

where M is the cutting constant for a fully established chip.

(a) Chip Formation Once the Deformation is Fully Established

The model figure 50(a), proposed by Thompson (24)

and based on the Lee-Shaffer model (59), shows the fully established deformation zone. The workpiece is separated from the chip by a shear plane AB and the chip makes contact with the saw tooth along the plane AC, a wedge of material surrounds the cutting edge, forming a chip. Figure 50(b) shows the corresponding Mohrs stress diagram from which:-

$$\phi + \lambda - \alpha = \frac{\pi}{4} \quad \dots\dots\dots (3.8.3)$$

The thrust component of the cutting force can be determined by considering the forces acting on the shear plane A'B in Figure 50(a), giving:-

$$f_t = k \delta (\cot \phi - 1) \quad \dots\dots\dots (3.8.4)$$

Comparing this with equation (3.8.2) gives

$$M = k (\cot \phi - 1) \quad \dots\dots\dots (3.8.5)$$

Equations (3.8.3) and (3.8.5) enable the cutting constant M for a fully established chip to be determined for a given apparent coefficient of friction and material, Figure 51.

(b) The Average Thrust Load Per Tooth Per Unit Thickness

The tooth loading and chip size for individual

teeth in contact is shown in Figure 52, when n_c , the number of teeth in contact, is 6 and n_t , the number of teeth having a partly formed deformation zone is 5 and when one tooth is about to begin its cut.

The equation (3.8.1), the tooth loading per unit thickness, can be written

$$f_{ti} = M \cdot \delta \cdot \left(\frac{i}{n_t} \right)^n \dots\dots\dots (3.8.6)$$

$$\text{since } y = ip \dots\dots\dots (3.8.7)$$

$$\text{and } y_c = n_t \cdot p.$$

Thus the total thrust load acting is given by

$$F_t = t \left[\sum_{i=n_t}^{i=n_c} f_{ti} + \sum_{i=0}^{i=n_t} f_{ti} \right]$$

or

$$F_t = M \delta t \left[n_c - n_t + \sum_{i=0}^{i=n_t} \left(\frac{i}{n_t} \right)^n \right] \dots\dots (3.8.8)$$

due to the difficulty in experimentally measuring the individual loads, an average tooth load per unit blade thickness is used and is given by

$$f_{ta} = \frac{F_t}{n_c \cdot t} \dots\dots\dots (3.8.9)$$

By combining the above equations

$$f_{ta} = M \cdot \delta \cdot \psi \dots\dots\dots (3.8.10)$$

Where

$$n_c \geq n_t; \quad \psi = \frac{1}{n_c} \left[n_c - n_t + \sum_{i=0}^{i=n_t} \left(\frac{i}{n_t} \right)^n \right] \dots (3.8.11)$$

and

$$n_c \leq n_t; \quad \psi = \frac{1}{n_c} \sum_{i=0}^{i=n_c} \left(\frac{i}{n_t} \right)^n \dots\dots\dots (3.8.12)$$

(c) The Cutting Constant

Previous experimental work, Figure 23, has shown that a linear relationship exists between the average depth of cut per tooth and the mean thrust load per tooth per unit thickness.

$$\text{ie } \delta_a = K f_{tm} \dots\dots\dots (3.1)$$

where

$$f_{tm} = \frac{F_{tm}}{n_c t} \dots\dots\dots (3.12)$$

$$\text{and } \delta_a = \frac{W}{t} \cdot \frac{D}{N} \cdot \frac{1}{S.P} \dots\dots\dots (3.7)$$

The average depth of cut achieved per tooth during one complete stroke has been defined as

$$\delta_a = \frac{1}{s} \int_0^s \delta \, dx \dots\dots\dots (3.3)$$

Combining this with equation 3.8.10

$$\delta_a = \frac{1}{M \psi s} \int_0^s f_{ta} \, dx$$

by definition

$$f_{tm} = \frac{1}{s} \int_0^s f_{ta} \, dx$$

$$\therefore \delta_a = \frac{1}{M \psi} \cdot f_{tm}$$

Combining this with equation 3.1

$$K = \frac{1}{M \psi} \dots\dots\dots (3.8.13)$$

The above expression enables the cutting constant to be related to the characteristics of the chip formation and variations in the cutting constant to be investigated.

The above analysis has shown that, as the number of teeth in contact with the workpiece increases, the cutting constant approaches the value associated with a fully established chip, thus

$$\text{When } n_c \rightarrow \infty, K \rightarrow \frac{1}{M}$$

The values for each tooth pitch may be obtained from Figure 24, and the corresponding apparent coefficient of friction obtained from Figure 51. Theoretical values of apparent coefficient of friction using the above model, obtained from Figure 51, gave a good agreement with experimental results obtained from cutting tests (61), see Table 3(a), Appendix B.

From equation 3.8.13

$$\frac{1}{\psi} = M.K.$$

$$\text{but } M = \frac{1}{(K) n_c \rightarrow \infty}$$

therefore

$$\psi^{-1} = \frac{K}{(K) n_c + \infty}$$

Experimental values of the chip factor (ψ), were obtained using equation (3.8.13), as above. Figure 53 shows the computed values of the reciprocal of the chip factor for various values of the cutting force index with a blade having 10 teeth per 25 mm. The results of Figure 53 indicate that a cutting force index $n = 1.0$ is required for close agreement. Figure 54, shows computed values of the reciprocal of the chip factor for a force index of $n = 1.0$ together with the experimental values obtained with blades of different pitch. From the above results Thompson (24) calculated that the average critical length of cut (y_c) made by a tooth to fully establish a deformation zone is 14.8 mm.

3.7.3 Explanation of the Variation in the Cutting Constant

Substitution of differing values of workpiece breadth and tooth pitch into the proposed model demonstrates trends similar to the results obtained experimentally. It is suggested (24) that, for workpieces of small breadths, a high proportion of the teeth in contact will have a partly established deformation

zone. Thus, the applied thrust load appears more effective, because, for a given applied load, larger depths of cut are possible. This condition leads to a high cutting constant, indicating an apparently improved blade cutting performance. When the breadth of the workpiece is large a high proportion of the teeth in contact have a fully established deformation zone and the cutting constant will be to a large extent dependent on the thrust load produced by the fully established deformation zone. This situation leads to a low cutting constant and, thus, an apparent reduction in the cutting efficiency of the blade. For a given workpiece breadth, the cutting performance of a blade is influenced by the pitch of the teeth, figure 24. The length of cut needed to fully establish the deformation zone has been shown by simulation tests (23) not to be dependent on the depth of cut per tooth, or the pitch of the teeth (24). However the pitch of the teeth controls the number of teeth in contact with the workpiece and the number of teeth associated with a partly formed deformation zone. These factors affect the total thrust load required to achieve a given depth of cut per tooth and, therefore, the average tooth loading.

The cutting constant and, thus, the cutting efficiency of the blade, increases with an increase in the tooth pitch (Figure 23), due to these effects.

3.8 ECONOMICS OF HACKSAWING

3.8.1 Process Costs and the Machine

Considerable cost data is available (3, 4, 8) for power hacksawing, band sawing and circular sawing. However, in many cases, the method of arriving at the cost figures quoted is not stated fully, and the data used are not given in sufficient detail to enable a breakdown of cost to be undertaken. The author (21) has undertaken two cost analyses based on present day costs and typical operating conditions for workpiece materials which are known to be difficult to cut. It is concluded that, for the occasional user whose time utilization is low, the predominant cost is the time cost; this is because the cost rate is very high. The change most likely to benefit this type of user is to reduce the cutting time. For the frequent user whose time utilization is high, the predominant cost is the total blade cost with the cutting time cost also significant; this situation offers more scope for change. It would be possible to increase the cost

of the machine to this type of user and still produce an overall cost benefit which could be significant, provided the higher cost machine could reduce the cutting time and increase the blade life.

The cutting time can be reduced by either reducing the number of cutting strokes needed to saw through the workpiece or by increasing the rate of cutting strokes. Equation (3.15) shows that the number of strokes needed to cut through the workpiece can be reduced by either increasing the mean thrust load or by increasing the length of the stroke.

The maximum load that can be satisfactorily used depends ultimately on the breaking strength of the blade.

However, the thrust load has been shown to undergo considerable variation and the mean thrust load is considerably less than the maximum thrust load developed. For a given blade strength, the number of cutting strokes needed could be reduced if the mean thrust load were increased relative to the maximum thrust load. To achieve this, the thrust load would need to be uniform throughout the cutting stroke.

The other possible way to reduce the number of cutting strokes would be to increase the machine stroke for any

workpiece size. Most existing machines operate with a fixed stroke, the size of which is determined by the blade size and the maximum workpiece size to be accommodated. In use, such a machine would only rarely cut workpieces as large as the maximum machine capacity. For small workpieces, say 75 mm diameter being a reasonable average, and a blade of usable length 375 mm with a machine of 150 mm stroke, the length of blade used would only be 225 mm. The blade would be discarded with the remaining length unused.

Another way to reduce the cutting time is to increase the cutting speed, ie by increasing the stroke rate; 70-120 strokes per minute is typical of present machines. However, it has been found that at the higher stroke rates the saw machine becomes dynamically unstable.

3.8.2 Estimating Blade Life, Cutting Rate and Cost

Thompson and Taylor (27) combined their earlier work on blade wear (25), and developed a computer programme to simulate the power hacksaw operation and used the programme to investigate the effects of some of the machine and blade parameters previously discussed. The method enables laboratory test data to be converted to

cutting rates and cost, thus providing an assessment of a particular combination of workpiece material and blade to be made in terms of realistic criteria which can be understood and used by those intending to utilise the hacksaw operation.

Although the data used by the above relates to unusual and difficult to cut materials, many of the trends obtained are believed to be typical of those which would be obtained with the more common workpiece materials.

Figures 45, 46, 47 and 48 show the influence of the stroke rate, thrust force, stroke and the breadth of the workpiece respectively on the three performance criteria.

The results, Figure 45, show that the most economical stroke rate is much smaller than the rate which produces the greatest average cutting rate for each material. Thus, when choosing optimum conditions for the power hacksaw operation, a choice must be made as to whether cost or cutting rate is to be optimised. The results also show that high cutting rates can only be obtained by incurring high cost, and low cost can only be achieved at low cutting rates. Thompson and Taylor (27) concluded that the power hacksaw operation is a low cost, low cutting rate operation.

Figure 46 shows that, over the typical range of thrust force developed by a hydraulic sawing machine, the average cutting rate increases and the blade life is reduced as the thrust load increases. The cost of cut reaches a minimum value at a load approximately in the middle of the range. It is possible that the cutting rate could be further increased by developing a machine having an extended load range. However, at the higher load range existing blades would be prone to fracture at these high loads.

Figure 46 shows that, within the range of stroke considered, the cost reaches minimum values for both materials considered and the average cutting rate reaches a maximum for En 44E. The results also show that the average output rate could be increased by combining the development of a machine with an adjustable stroke, with the development of blades which are longer than those presently available.

The combined effects of the pitch of the teeth and the breadth of the workpiece on the three performance criteria are shown in Figure 48. They show that, as the number of teeth per inch is increased, the blade life is increased, the cost per cut is reduced and the average cutting rate is little affected. It has been suggested (27) that the

trends in the predicted performance shown in Figure 48 are sensitive to the workpiece material.

CHAPTER 4

4.0 INVESTIGATION INTO THE CUTTING ACTION OF BLUNT TOOLS

4.1 INTRODUCTION

The hacksaw blade tooth has been classified as basically a blunt tool, due to its large cutting edge radius.

Furthermore, experimental work on hacksawing has shown (21) that the ratio of the depth of cut achieved per tooth to the cutting edge radius, under normal operating conditions, is approximately one third. Under the above cutting conditions, simulating the saw tooth cutting action (23), the tests revealed a complex combination of modes of chip formation, which were similar to those produced during hacksawing. Whilst the initial work (23) revealed some interesting results, which went a long way to explain some of the phenomena observed in the sawing tests, the work was in no way exhaustive.

This has led to further interest in examining the cutting action of blunt tools under conditions where the undeformed chip thickness, or the layer of material removed, is equal to, or less than, the cutting edge radius. This is a cutting condition which exists when removing material by sawing.

In the present work great emphasis has been placed on the accuracy of tests with regard to the actual layer of material removed, under the above conditions. The relevant nature of the chips and the forces produced have been examined.

It was anticipated that the above combination of results would give a clearer picture of the chip formation mechanism during the metal removal process in the sawing action, and possibly go some way to highlight the so called 'ploughing' action.

It was also thought relevant to determine experimentally the effect of the undeformed chip thickness: cutting edge radius ratio on the cutting performance for a single tooth in order that the possible benefits to a hacksaw blade could be quantified and considered when examining blade manufacturing methods.

A slip-line field model has been developed to enable the effect of edge sharpness on performance to be predicted and is described in Chapter 5.

4.1.1 Material Behaviour Near the Tool Point

Figure 55 shows various schematic diagrams proposed by researchers (32, 35, 37) showing the material behaviour in the region of the cutting radius. Whilst the diagrams are not to scale Figure 55(a) shows a small portion of material accumulated in front of the rounded portion of the tool edge. As the tool progresses

all material above the horizontal dashed line is removed in the form of a chip, including the small portion of the metal in front of the cutting edge, which is pressed into and becomes part of the chip. Albrecht (32) described this action as ploughing. Furthermore, it was assumed that a small portion of the ploughed metal would be pressed into the workpiece surface. In Figure 55(b) and 55(c) it was assumed that if flow was possible round the edge without the formation of a built-up edge, then all material above the point 'D' known as the stagnation point will be removed in the form of a chip, and all the material below this point will be compressed underneath the tool and elastically recover, thus remaining part of the workpiece. Rubenstein (35), Figure 55(c) suggested that the height of material recovery $h = R(1 - \sin \gamma_c)$ where R is the cutting edge radius and γ_c is the critical rake angle as shown in the diagram. This suggests that with nominally sharp tools with an estimated (32) cutting edge radius of the order $7 \mu\text{m}$ and a critical rake angle of 70° (36), the height of material recovery would be $h \approx 0.5 \mu\text{m}$, which would be very small compared with the undeformed chip thickness in conventional metal cutting tests. Whilst the above suggested ploughing height is very small it suggests that the new machined surface does not coincide with the base of the tool.

If, however, the cutting edge radius of the tool was considerably larger (0.56 mm), as in the present tests, then according

to the model suggested by Rubenstein (35), the height of recovery would be considerable (0.034 mm). It was found in the present tests that there was no evidence of material recovering behind the tool, but, on the contrary, that the machined surface was in line with the base of the tool.

4.2 Experimental Approach

The general experimental aim was to measure the magnitude of the forces and observe the nature of the chip during orthogonal cutting under cutting conditions where the undeformed chip thickness was equal to or less than the cutting edge radius of the tool. The two main features of these tests which are distinct from conventional cutting tests are:-

- (i) The depth of cut or undeformed chip thickness is very small.
- (ii) The cutting edge radius is large, giving the cutting point an initial, relatively large negative rake which would vary from -90° to zero rake.

Figure 56 shows schematic diagrams of the possibilities of the cutting process occurring with a tool of finite cutting edge radius, assuming no build up of material to occur immediately in front of the tool. One of the difficulties in cutting tests of this nature is establishing the true depth of cut as compared with the nominal depth

of cut and, furthermore, establishing the position of the base of the tool as compared with the machined surface. It has been previously suggested (35, 36) that Figure 56(c) is representative of the cutting process when cutting with tools of a finite radius. Whilst other researchers have suggested that a combination of several of the models shown in Figure 56, represents the cutting process.

It is of interest to establish which of the models represents the cutting action and, in particular, the proportion of material going into the chip compared with elsewhere..

With a view to investigating the above, a series of tests have been conducted with copper and steel workpieces, using single point HSS tools which had a radius ground on the cutting edge. It was hoped that the low yield strength of copper might permit cutting on a larger scale while still retaining manageable forces. Furthermore, cold-rolled copper is fairly well behaved, producing a continuous chip and little work hardening.

4.2.1 Experimental Apparatus

Cutting tests were carried out on a universal milling machine as shown in Figure 57, suitably modified to hold a single point tool in a planing operation. A ground steel plate was secured to the top of a Kistler, three force component dynamometer which was in turn fastened to the work table of the milling machine, Figure 58. The workpiece material was bolted to the top of the steel ground plate, which was used as a datum for carrying out measurements of nominal depth of cut, Figure 59(a) and for locating a dial indicator bridge set-up, Figure 59(b) used for measuring the layer of material removed.

The output signals from the dynamometer were displayed on an ultra violet recorder. Incorporated in the tool holder, immediately behind the tool cutting edge, was an air gauge transducer which allowed the vertical movement of the tool, relative to the machined surface, to be monitored during the cutting processes. A second dial indicator, fastened to the tool holder in line with the tool and located on the ground steel plate, allowed nominal depths of cut to be applied accurately.

Initial tests with the cutting tool wider than the workpiece (≈ 6.00 mm wide), having a cutting edge radius of 0.56 mm, under planing conditions produced random, inconsistent results. The nominal set depth was kept low (≈ 0.05 mm) because the high forces produced were beyond the range of the dynamometer.

With the width of the copper specimen reduced to approximately 3.5 mm, the results were still inconsistent and unrepeatable. These variations were attributed to:-

- (i) Machine tool deflection due to the high thrust loads causing the nominal set depth to change during cutting. Figure 60 shows the Parkson Miller stiffness measurements at the position of the tool holder. The results showed that under the test conditions, at a nominal depth setting of 0.04 mm, a thrust load of ≈ 2.2 kN was produced, which could cause a machine tool deflection of ≈ 0.04 mm.
- (ii) Considerable spreading of the workpiece material, which altered the geometry of the workpiece specimen, thus giving a false impression of the undeformed chip thickness and the quantity of material going

into the chip. Figure 61 shows a cross-section of an initially 3.55 mm wide copper specimen machined with eight consecutive cuts at a nominal set depth of 0.25 mm, under orthogonal cutting conditions using a tool of cutting edge radius 0.56 mm, with the tool wider than the workpiece. Calculations showed that the total volume of material in the side spread, plus the chip, was equal to the volume contained in the undeformed chip thickness.

During the above tests, chips of varying geometry and shape were obtained, Figure 62, under identical cutting conditions.

In order to eliminate sidespread, all subsequent tests were carried out with the tool cutting in a groove, which is more realistic of plane strain conditions.

4.2.2 Preparation of Tools and Cutting Tool Geometry

The tools used for the simulating tests were standard high speed steel orthogonal tools of 15 mm square section.

For groove cutting tests, the cutting portion of the tool was ground to approximately 3.5 mm width with one degree

side clearances, which was to prevent the tool binding in the grooves.

A machine vice, which was capable of swivelling in two planes, was used to hold the tool blank for grinding the rake and clearance faces. The final stage in grinding the tools was the production of the cutting edge radius. It was essential that this radius should be accurately ground and the rake and clearance faces blended into the radius uniformly.

The radii were ground using a jig, as shown in Figures 63(a), 63(b) and the procedure adopted was as follows:-

- (i) The tool was set to the centre line of the jig pivot point. This was accomplished using a peg, relieved to half its diameter and set vertically in a bore, concentric with the axis of the jig.
- (ii) The machine slide was advanced so that the tool tip 'just' touched the side of the wheel. The slide was backed-off to the value of the approximate desired cutting edge radius and the machine handwheel set to zero.

- (iii) The tool was rotated to the position shown in Figure 63(c) and the machine slide advanced again to the desired value of the radius.
- (iv) By means of the adjustable packing and jack screws, the tool could be advanced until the side of the tool just touched the side of the wheel squarely.
- (v) The machine slide was withdrawn to just beyond the zero reference set in (ii).
- (vi) The tool was advanced slowly towards the rotating grinding wheel until the value of the radius was reached. The tool holder was rotated about the axis until the wheel touched squarely on both faces of the tool, while advancing the tool to the wheel, as shown in Figure 64(a) and 64(b).

Finally the rake face, cutting edge radius, and the clearance faces were lapped gently to remove any scratches, burrs etc.

The actual size and profile of the resulting tool tips were checked by means of a shadow

graph by comparing the magnified image on the ground glass screen with a series of radii drawn on a transparent sheet to the same magnification as the projector lens, (x 50), see Figures 65(a), 65(b) showing shadowgraphs of the cutting edge radius profile and Figure 65(c) showing the specified cutting edge geometry.

4.2.3 Workpiece Material Specifications and Cutting Conditions

Copper:- Electrolytic Copper 99.807% Cu,
0.03% Fe, 0.013% P, 0.05% As, 0.1% Ni.
Density of Copper: $8.96 \times 10^3 \text{ Kg/m}^3$
Cold rolled to 115 HV.

Free Cutting Steel:- 89.196%Fe, 0.11%C, 1.1% Mn, 9.02%Si,
0.043% P, 0.18% Ni, 0.13% Cr, 0.06% Mo,
0.16% Pb, 0.001% Al, 212 HV.

Cutting Speed:- 95 mm/min.

4.2.4 Measurements of Nominal and True Depths of Cut

The nominal depths of cut used during the cutting tests were varied from 0.05 mm to ≈ 0.5 mm ie equal to, or less

than the cutting edge radius of the tools.

During preliminary groove cutting tests the undeformed chip thickness (depth of cut) was determined in three ways:-

- (i) By weighing the chip.
- (ii) Using a dial indicator bridge reading.
- (iii) The nominal set depth, as applied by advancing the knee of the milling machine using a DTI.

The results showed discrepancies, the reasons for which were not easily determined due to the small depths of cut at which the cutting tests were carried out. Table 5, (Appendix B), shows results obtained while groove cutting with a tool having a cutting edge radius of 0.50 mm.

First, for each cut, the results obtained showed that the nominal set depth, the actual depth obtained by weighing a chip did not agree. Furthermore the repeated tests did not show agreement. A variation of 10-20% discrepancies occurred between the nominal set depth and the actual layer of material removed, as determined by the other two methods. This was also reflected in the magnitude of the forces obtained, Figure 66, although the magnitude of the

forces did not necessarily follow the trend of the magnitude of the layer of material removed. On examining the chips, they appeared to be of a consistent shape and nature. Although the discrepancies obtained in the above cutting tests were not as severe as those obtained previously, where considerable spreading of the workpiece material was noted, nevertheless, this variation in results had to be eliminated.

By carrying out further tests, similar to those above and placing dial gauges at various points on the machine, some of the problems were identified, and the conditions contributing to the above discrepancies were due to:-

- (i) The dial indicator used for measuring the nominal depth of cut applied, was approximately 100 mm away from the tool tip, thus, any movement of the machine table, when advancing the knee of the milling machine could contribute to the error obtained in the depth of cut applied. For this reason, the particular dial gauge used for measuring the nominal depth of cut was fastened to the tool holder in line and as close as possible to the tool, see Figure 59(a).

- (ii) On the first cut taken, it was understandable that the actual layer of material removed would be the nominal set depth minus the corresponding machine deflection, caused by the thrust load.
- (iii) In order to improve the accuracy of the results the layer of material removed, as measured by the dial indicator bridge set-up, was carried out along three positions of the workpiece and the average readings taken, see Figure 59(b).
- (iv) The variation in the magnitude of the steady state forces obtained under identical cutting conditions, was reflected by the variable geometry along the length of the chips obtained.

Further tests carried out during groove cutting, using the blunt tool (0.5 mm radius) with the dial indicator for applying the nominal depth of cut moved to the position described in (i) above, produced more consistent results, see Table 6 and Figure 67(a) and 67(b). There was a good agreement between the nominal set depth, average depth of cut measured by the bridge readings, and the depth of cut obtained by weighing the chip. The trends of the forces were also found to be similar, except for the first cut,

Test R1, which did not reach steady state conditions, this is reflected in the geometry of the chip produced, see photographs of chip corresponding to Test R1, Figure 67(a).

The chip (R1) is far more heavily compressed than R2, R3, R4 or R5, and the chip R1 has maintained contact with the tool face throughout the cut, hence, both the cutting force component and the thrust force component have continued to rise. This situation is discussed in detail later under 'discussion of results' (section 4.4).

From the experience gained in the preliminary cutting tests, a procedure for carrying out the tests was adopted (see Section 4.3) which minimised the errors and discrepancies in results obtained.

4.2.5 Relationship Between the Base of the Tool and the Machined Surface

In order to establish the conditions under which cutting is carried out (Figure 56) the air gauge transducer (Figure 68) allowed the distance between the base of the tool and the generated surface to be measured during cutting. Furthermore by initially setting the tool and air gauge to the same height, using slip gauges, the air

gauge could be used for establishing the tool-workpiece contact. From the experimental results (Table 7) there was no evidence of material recovering behind the tool, although the air-gauge readings fluctuated between $\pm 0.0002''$ (0.005 mm) and ± 0.0003 (0.0075 mm), which could be attributed to changes in the surface finish and displacement of the cutting fluid in the air gauge path. There was also the possibility of the tool fixture misaligning, to give this small air-gauge reading, but this was checked by applying a normal and horizontal load of the magnitude encountered during the cutting tests, at the cutting edge of the tool, and the air-gauge did not show any change in reading.

The full scale deflection on the air gauge meter was capable of monitoring $\pm 0.002''$ (± 0.05 mm). According to the model presented by Connolly and Rubenstein (35) and results obtained by Rubenstein et al (36), the critical rake angle γ_c has been estimated to be in the order of $50-55^\circ$, and others (44) have estimated it to be $\approx 70^\circ$, thus, the height of material recovery as postulated (Figure 56) by Rubenstein (35), is given by $h = R(1 - \sin \gamma_c)$, where R is the cutting edge radius and γ_c is the critical rake angle, providing there is no side spread of the

material. According to the above model proposed the height of material recovery behind the tool using a tool of cutting edge radius 0.5 mm as in the present tests would be expected to be in the order of 0.034 mm to 0.13 mm, which would have shown large readings on the air transducer. Further cutting tests during groove cutting with blunt tools confirmed that the base of the tool coincided with the generated surface.

4.3 PROCEDURE FOR CUTTING TESTS

The set-up of the equipment and instrumentation was as shown in Figures 58 and 59, and as previously described. A slip gauge was wrung on to the ground steel plate below the position of the tool holder. The tool was placed loosely in the tool holder and the tool tip allowed to rest on the slip gauge. The tool was then clamped in the tool holder by means of screws located in both the front and the side of the tool holder, ensuring that the tool was seated squarely. The machine table was then moved so that the air gauge occupied the same position on the slip gauge as vacated by the tool tip, and the air gauge meter adjusted to give a zero reading (Figure 68 (b)).

A cleaning cut was first taken with a sharp tool. It was then replaced with the appropriate blunt tool and re-set to the same height, using the air gauge transducer.

The tool workpiece contact was established using the air gauge and the tool cleared of the workpiece to the beginning of the cut. Dial-indicator bridge readings were taken at three points along the length of the workpiece specimen. The table was traversed across, moving the workpiece past the tool and air gauge, to ensure that the tool was running parallel to the unmachined surface, giving a zero reading on the air-gauge meter. The appropriate nominal cut was applied and measured using the front mounted dial indicator with 0.002 mm increments (Figure 59 (a)), and cutting commenced. In order to give uniform cutting conditions and reduce the irregularity of results, cutting fluid (sulphurised oil) was used during the cutting operation. During cutting the air gauge reading was observed, the forces recorded and, at the end of each cut, the chips were collected. Prior to weighing, the chips they were cleaned in a solvent to remove any cutting oil present. The tool was cleared of the workpiece and returned to its original starting position. Final bridge readings were taken again at the same three points along the length of the workpiece specimen, enabling the layer of material removed to be measured. Using this procedure several cuts were taken at the same nominal depth setting. Further results obtained (Table 7 and Figure 69) by the

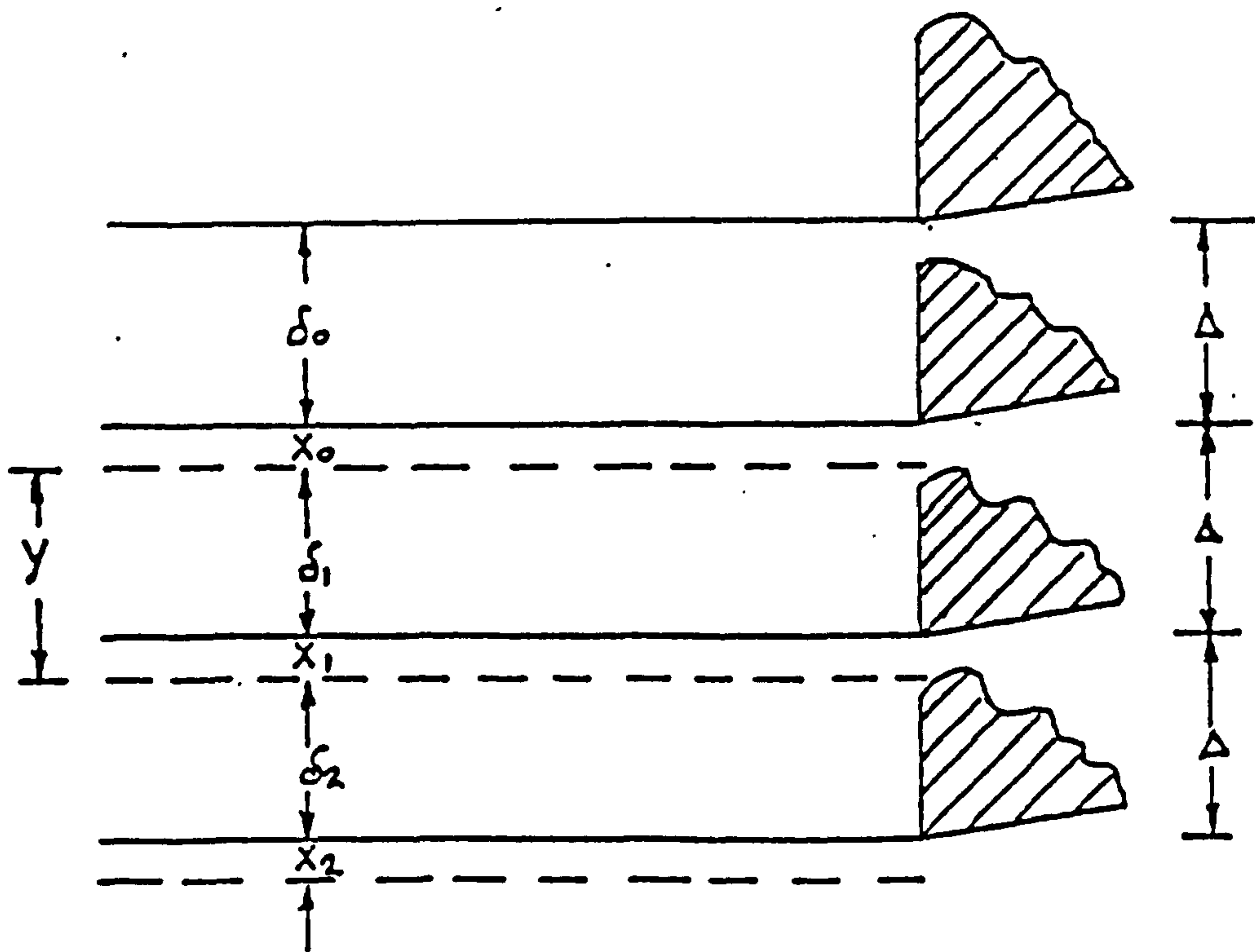
above procedure showed that the undeformed chip thickness, defined as the depth from the uncut surface to the cut surface, as measured by the bridge readings and by weighing of the chips, were in good agreement. Also the nominal set depth, defined as the depth from the uncut surface to the base of the tool, was in disagreement with these results on the first cut; this effect was due to the machine tool deflection. However, on subsequent cuts the results were in better agreement.

The above results showed that, providing the nominal depth of cut was applied accurately and measured as close as possible to the cutting tool, the layer of material removed after two to three subsequent cuts was equal to the nominal set depth.

The simple analysis below shows this to be true:-

4.3.1 Analysis of Overcutting and Undercutting

(a) Consider Case I - Tool Overcutting



Let Δ = Displacement of Tool and Workpiece (vertically)

δ = Distance between machined surface and the tool

x = Amount of overcut

y = Total slot depth achieved = $\delta + x$ = Bridge reading

Let $x = k\delta$ where k = constant

For 1st cut $\delta_0 = \Delta$ $\therefore x_0 = k\Delta$

$$y_0 = \delta_0 + x_0$$

$$y_0 = \Delta + \Delta k$$

$$y_0 = \Delta (1 + k)$$

For 2nd cut $\delta_1 = \Delta - x_0$

$$\delta_1 = \Delta - k\Delta$$

$$\delta_1 = \Delta(1 - k)$$

$$\therefore x_1 = k\delta_1 = k\Delta(1 - k) = \Delta(k - k^2)$$

$$\therefore y_1 = \delta_1 + x_1 = \Delta(1 - k) + k\Delta(1 - k)$$

$$y_1 = \Delta(1 - k^2)$$

For 3rd cut $\delta_2 = \Delta - x_1$

$$= \Delta - k\delta_1$$

$$= \Delta - k(\Delta - \Delta k)$$

$$\delta_2 = \Delta(1 - k + k^2)$$

$$x_2 = k\delta_2$$

$$= k(\Delta - \Delta k + \Delta k^2)$$

$$x_2 = \Delta(k - k^2 + k^3)$$

$$\therefore y_2 = \delta_2 + x_2 = \Delta(1 + k^3)$$

For 4th cut $\delta_3 = \Delta - x_2$

$$= \Delta - k(\Delta - \Delta k + \Delta k^2)$$

$$\delta^3 = \Delta(1 - k + k^2 - k^3)$$

$$x_3 = k\delta_3$$

$$= k\Delta(1 - k + k^2 - k^3)$$

$$\therefore y_3 = \delta_3 + x_3$$

$$= \Delta(1 - k + k^2 - k^3) + \Delta(k - k^2 + k^3 - k^4)$$

$$y_3 = \Delta(1 - k^4)$$

$$\therefore \delta_n = \Delta(1 - k + k^2 - k^3 \dots \pm k^n)$$

$$x_n = \Delta(k - k^2 + k^3 - \dots \pm k^{n+1})$$

$$y_n = \Delta(1 \pm k^{n+1})$$

Example:

Say tool overcuts by 20% of the applied cut

$$y_0 = \Delta(1 + 0.2) = 1.2\Delta$$

$$y_1 = \Delta(1 - 0.2^2) = 0.96\Delta$$

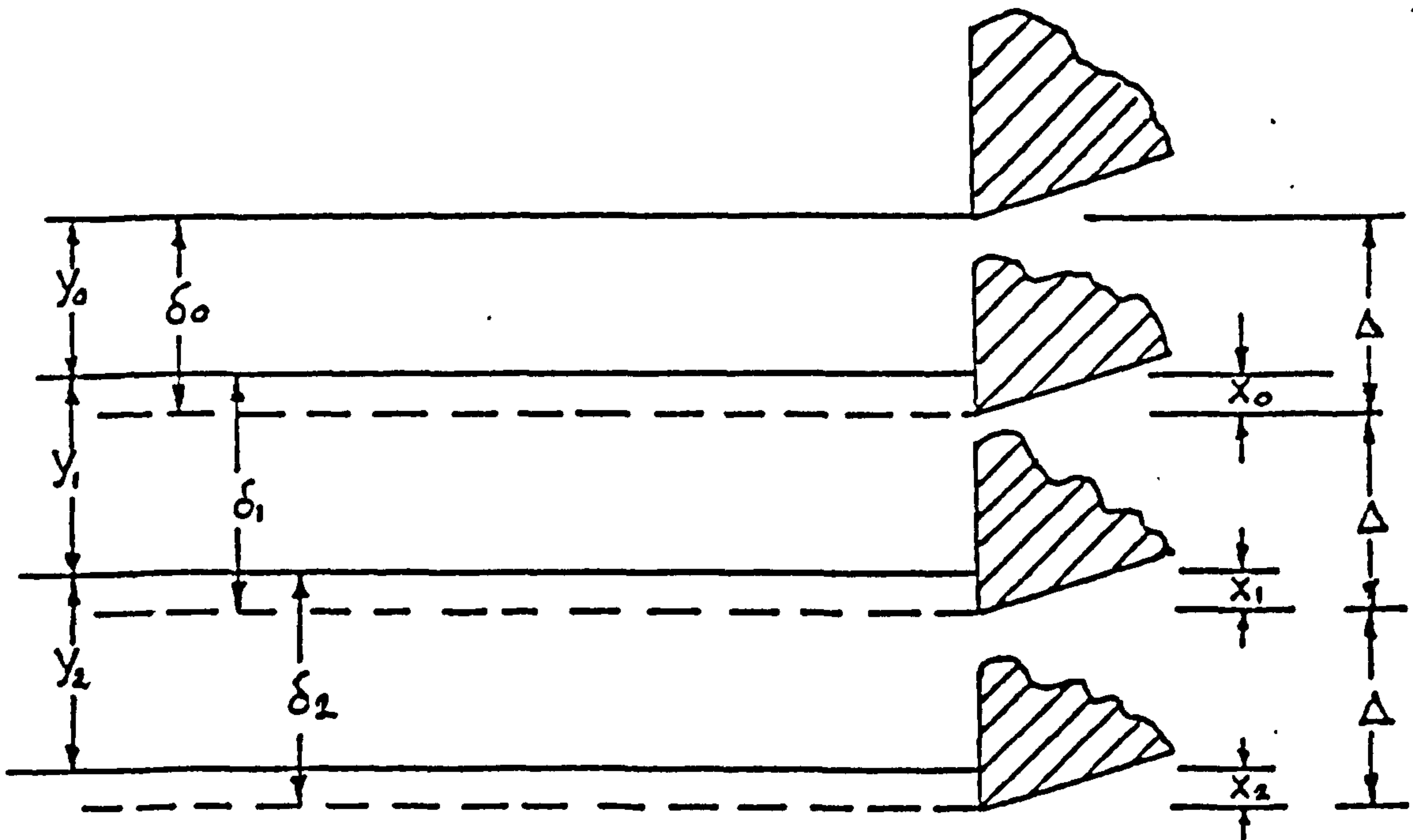
$$y_2 = \Delta(1 + 0.2^3) = 1.008\Delta$$

•
•
•

$$y_5 = \Delta(1 - k^6) = 0.999936\Delta$$

This shows that the slot depth achieved, y , very rapidly approaches the nominal set depth, Δ .

4.3.1 (b) Consider Case II - Tool Undercutting



Initial cut $\delta_0 = \Delta$

$$x_0 = k\delta_0 = k\Delta$$

y_0 = initial bridge reading after the first cut

$$y_0 = \delta_0 - x_0$$

$$= \Delta - k\Delta$$

$$y_0 = \Delta(1 - k)$$

$$\text{Second cut } x_1 = k\delta_1 \quad \delta_1 = \Delta + x_0$$

$$= \Delta + k\Delta$$

$$\delta_1 = (1 + k)\Delta$$

$$\therefore x_1 = k\Delta(1 + k)$$

$$x_1 = \Delta(k + k^2)$$

$$y_1 = \delta_1 - x_1$$

$$= \Delta(1 + k) - \Delta(k + k^2)$$

$$y_1 = \Delta(1 - k^2)$$

$$\text{Third cut } x_2 = k\delta_2 \quad \delta_2 = \Delta + x_1$$

$$= \Delta + k\Delta + k^2\Delta$$

$$\delta_2 = \Delta(1 + k + k^2)$$

$$y_2 = \delta_2 - x_2$$

$$= \Delta(1 + k + k^2) - \Delta(k + k^2 + k^3)$$

$$= \Delta - \Delta k^3$$

$$y_2 = \Delta(1 - k^3)$$

These results also show that the layer of material removed 'y' as measured by the Bridge readings, very quickly approach the nominal set depth ' Δ '.

4.3.2 Chip-Tool Contact Length Measurements

Chip-tool contact length measurements were carried out during groove cutting for tools having a radius of 0.56 mm, 0.81 mm and a nominally sharp tool using copper and leaded steel workpiece specimens.

Prior to starting the cut, the face of the tool was coated with black felt tip ink. The low cutting speeds and, hence, the low temperatures, did not affect the ink coating used. The experimental procedure previously described was followed.

In addition to measuring the depths of cut and recording the cutting force components, on completion of each cut the chip-tool contact length was measured using a graduated eye-piece.

Figure 70(a) shows the results of initial tests carried out, showing the variation of chip-tool contact length with increase in depth of cut. The graph shows the results to fall into two bands. On examination of the corresponding chips produced, the higher band, shown by the dotted

line, corresponds to the results produced by heavily compressed lumpy chips, as compared with the lower band indicated by the continuous line which are results of a continuous type chip reaching steady conditions as produced by the blunt tools. Further test results shown in Figure 70(b), for the cutting conditions stated, were obtained when the above, latter type of chip was produced, as shown in Figure 70(c).

Figure 70(b) shows also the results obtained by a blunt tool with a higher cutting edge radius (0.81 mm). The chip tool contact length does not appear to be influenced by the cutting edge radius, within the range tested. For comparison purposes, the results from a nominally sharp tool are also shown. The above results enable an empirical relationship to be established between the chip-tool contact length and the undeformed chip thickness. This relationship will be found useful in the slip-line field model proposed in the next chapter for predicting the forces during the cutting action of blunt tools.

4.3.3 Nature of the Chip and the Dead Metal Zone

In the previous experimental tests it has been shown that there is no evidence of material recovery behind

the tool. Furthermore, test results have shown various geometry of chips to have been produced under identical cutting conditions (Figure 62). Figure 71(a) and 71(b) show 'still' pictures taken during orthogonal cutting, machining copper, using a nominally sharp tool (cutting edge radius < 0.015 mm (0.0006")), and a blunt tool (cutting edge radius 0.56 mm), under otherwise identical cutting conditions. The corresponding chips obtained are shown in Figures 71(c) and 71(d). During the cutting tests it was observed that the approximate effective plane or zone of shear was far less for the blunt tool than the sharp tool. Furthermore the chip obtained using the blunt tool (Figure 71(d)), was very heavily compressed and shorter in length, as compared with a fairly conventional flat type of chip produced when using the sharp tool Figure 71(c).

Figure 72(a), (b), (c), and (d), show some features of the chips obtained whilst groove cutting, using a blunt tool, under identical cutting conditions. In most cases, when machining with blunt tools, the chip starts to form, with a fairly uniform rectangular cross-section, Figure 72(d), and increases in thickness steadily, until the steady state is reached, this steady state feature is

also reflected in the force traces obtained. When the steady state is reached, the chip is uniform in cross-section, but no longer rectangular. In the case of groove cutting, the typical steady state cross-section of the chip obtained was as shown in Figure 72(d), with the sides of the chip being restrained by the walls of the groove. Figure 72(c) shows a sketch of a chip which has continued to build up without reaching steady state conditions.

Due to some of the above variations observed in the mode of chip formation it was decided to examine the chip-root area and the behaviour of the workpiece material in the region of the cutting edge radius, by taking photomicrographs of sections of 'frozen' cuts.

4.3.4 Photomicrographs

When machining copper with blunt tools, the cutting action was quickly stopped by reversing the milling machine table in the direction of cutting. This procedure of 'freezing' the cut was repeated several times. The measured time to reverse the milling machine table and interrupt the cut was less than 0.05 seconds. It was considered that, at the low cutting speed used (95 mm/min), this procedure was adequate to give a satisfactory result (See Appendix F).

Specimens were cut out from the workpiece, encompassing the chip and root area, approximately 12 mm square, and set in conducting bakelite. The mounted specimens were then polished using 120 grit down to 600 grit wheels, thoroughly washing the specimens with soap and water regularly. Finally the specimens were polished on 6 micron pads down to 1 micron and etched using Alcoholic Ferric Chloride. Some difficulty was initially experienced when mechanically polishing the specimens because the surface of the copper specimens became deformed. This was overcome mainly by experience, and by examining the specimen continuously under a microscope.

Figures 73 and 74 show photomicrographs of the relevant areas of the specimens, under the cutting conditions stated, taken with the aid of a projection microscope, whilst Figure 75 shows a picture of the chip root area taken on a scanning electron-microscope.

The above results clearly show evidence of a metal cap to exist between the envelope enclosed by the cutting edge radius extending from the base of the tool and the machined surface. The implications of this metal-cap are discussed in detail in the next section.

4.4 DISCUSSION OF RESULTS

4.4.1 Cutting Tests

The discrepancies in the results obtained during the initial tests, with regard to establishing the relationship between the nominal depth of cut and the layer of material removed, could be attributed to two major causes:-

- (i) The stiffness of the machine tool system, effects of which can be overcome by repeated cuts. It has been shown that after the third consecutive cut the layer of material removed was within 1% of the nominal set depth, defined as the depth from the uncut surface to the base of the tool.
- (ii) The side spread of the material which was reported earlier, Figure 61, which occurred whilst carrying out cutting tests with the tool wider than the workpiece, gave false impressions of the relative position between the base of the tool and the machined surface. It was initially postulated by Rubenstein (35) that this material was actually going beneath the cutting edge and recovering behind the tool. Explanation of the phenomenon of

workpiece material spread has been given by Form and Bellinger (62). Under cutting conditions, where the tool is wider than the workpiece, plane strain conditions are applicable only at the centre of the specimen. Figure 76 illustrates what happens near the centre of the workpiece. Owing to the vertical force component, the material immediately on top of the tool face is being compressed in the z and expanded along the x and y directions; the material adjacent to the relief face, on the other hand, is compressed in the x and expanded along the y and z directions. Near the centre of the workpiece, the material in the vicinity of the tool tip is thus subjected to a tri-axial stress and a bi-axial strain state. Towards the edges of the workpiece, on the other hand, the stress state changes gradually to bi-axial and the strain state to tri-axial, because the material becomes free to bulge out, causing spreading of the workpiece material. This is more pronounced with blunt tools due to the higher forces than with nominally sharp tools, although formations of burrs occurs during the above cutting conditions when machining with sharp tools.

The model presented by Connolly and Rubenstein (35), Figure 55 (c) would suggest that some material would be compressed below the tool and would recover behind the flank face. However, the results of the experiments, carried out both with the tools wider than the workpiece and during groove cutting, gave no evidence of this occurring and, in fact, the machined surface was in line with the base of the tool as represented by Figures 56(b) and (d).

During the orthogonal groove cutting tests, the thrust and cutting force components were recorded against time. As the cutting speed was constant, the time axis was proportional to the workpiece displacement. Figure 77 shows some of the force variations recorded during the displacement of the workpiece. The relevant chips formed are also shown. The results show a variety of chip shapes formed under similar cutting conditions. The geometry of the chip is reflected in the corresponding force trace obtained.

In the results obtained, shown in Figure 77(a) and (b), the steady state conditions have not been reached. Figure 77(a) shows that the initial stages of the chip

have an apparently conventional form, starting with a thin section but then gradually building up to a lumpy, heavily deformed section, followed by a very short section which is thinner and finally building up to a heavily deformed chip. The chip shown in Figure 77(b) is of gradually increasing thickness and does not achieve steady state conditions; the force trace varies similarly. Figure 77(c) shows results obtained from cutting conditions identical to those of Figure 77(b) and yet the chip obtained in the former case is a fairly long thin chip. The increased efficiency in this case is reflected in the lower more stable cutting force components and higher chip thickness ratio. .

Figure 77(d) shows an apparently conventional type of flat chip, produced at a low depth of cut (0.15 mm), which has reached steady state conditions, although it is still very heavily compressed. Figure 77(e) shows the results obtained at a nominal set depth of 0.5 mm under otherwise identical cutting conditions to Figure 77(d).

The differing geometry of the chips produced above and their characteristics confirm the earlier results obtained

in simulation tests by the Author (23). Furthermore, all the test results display the transient forces which have also been reported earlier. The effects of these transient forces have been used in an earlier chapter to explain the performance of hacksaw blades of various pitch with workpieces of different breadth.

The test results indicate that, under the cutting conditions stated, three basic types of chips are produced when cutting with blunt tools:-

- a. A heavily deformed lumpy chip which increases in thickness as the cut progresses.
- b. A chip which is initially thin and forms in a conventional manner, increases in thickness as the cut progresses and then reaches a steady state condition. This is reflected by the uniform thickness of the chip and fairly constant cutting forces (Figure 78).
- c. A combination of (a) and (b) and a continuous or segmented chip, (more pronounced at very low depths of cut).

4.4.2 Ploughing, Dead Metal Zone and the Chip Mechanics

Ploughing of the material, which occurs when machining with highly negative rake angled tools, certainly appears to exist under the conditions described above when using blunt tools. However, there has been no evidence of material flow beneath the tool and recovery of same as has been suggested (35, 37). Furthermore, under the conditions of groove cutting, material is restrained at the sides to prevent it from spreading sideways, a condition which is more realistic of plane strain conditions.

In the present context, the phenomenon of ploughing is explained as follows. Owing to the very high negative rake at the extreme cutting edge radius, some material ahead of the tool is heavily deformed and piles up ahead of the tool without leaving the bulk of the material.

This condition occurs when the shear plane angle coincides with the high effective negative rake angle, as suggested by Koenigsberger et al (36). Under this condition no material is available to go into the chip and, thus, the material ahead of the tool is ploughed.

From the photomicrographs (Figures 74, 75) there is evidence of a metal cap ahead of the tool. This cap of material develops within a very short time after the commencement of the cut. The development of the 'cap' results in the primary transient cutting force components shown in Figure 78. The active geometry of the tool cutting edge thus changes to that shown in Figure 56(d). Further material accumulates in front of the tool, giving a steady rise of forces, as shown by the force traces, until the steady state conditions are reached, when the chip begins to leave the rake face of the tool. Any subsequent chip produced after this stage is of a fairly uniform thickness, although very heavily compressed (Figure 79 (a)). This type of chip was commonly produced during the cutting tests. If the friction conditions were severe between the 'cap' and the chip, tool rake face and the chip, a severely 'piled-up' chip was produced which did not reach steady state conditions.

It will be appreciated that 'quick-stops' for studying the area around the chip root only represent the cutting conditions at a particular instant. To study the gradual building up of the stagnant zone would require a large number of quick-stops. Under cutting conditions, the size

and geometry of the cap may vary and, furthermore the 'cap' may be unstable. Earlier it was mentioned that in some cases, under identical cutting conditions, random geometry of chip formation occurred and, furthermore, the thickness of the chip changed during the length of cut.

The changes in chip thickness could be attributed to the metal cap being of an unstable nature, thereby altering the friction conditions at the 'cap-chip' interface. Thus, the metal cap grows very rapidly at the initial stages of the cut and is wedged between the cutting edge radius of the tool and the machined surface, altering the active geometry of the tool. Friction conditions on the rake face of the tool are increased to give metal to metal contact in the 'cap' region; furthermore, the base of the 'cap' will have a tendency to cause increased shear drag on the machined surface, sufficient to cause surface deformation. Evidence of the above two situations were present in the photomicrographs obtained (Figures 73 and 74), which showed a secondary deformation on the rake face and some deformation on the machined surface. Under the conditions previously described, whilst the metal cap stays intact with the tool, a chip of increasing thickness is formed and finally reaches steady state. The situation is reflected in the

force traces obtained during the cutting operation, Figure 78. There is also the possibility that, once the metal cap is established, with further cutting the structure of the cap is unable to support the required forces and consequently collapses with pieces of the cap being carried away with the chip or the workpiece. Workpiece material subsequently entering the vacated cap space is extruded into the chip, Figure 79(b), changing the mode of deformation and, hence altering the geometry of chip formation. The formation of the 'metal cap' could then re-establish itself.

Other factors which can contribute to the random type of chip geometry is the influence of the grain size and anisotropy of workpiece material. Measurements of the grain size of the copper workpiece give a mean linear intercept size, $\bar{d} = 131 \mu\text{m}$ which gives a true grain diameter, $\bar{D} = 231 \mu\text{m}$. This relatively high value of the grain size of the workpiece material, compared with a tool cutting edge radius of $558 \mu\text{m}$ and low depths of cut, could possibly lead to inhomogeneous deformation in some part of the cutting process. The copper workpiece used for the tests was a single phase material with a face centred, cubic lattice structure. This lattice

structure could give rise to anisotropic effects, ie adjacent grains of copper may have a Young's modulus of 28×10^6 lbf/in² in (111) directions and 10×10^6 lbf/in² in (100) direction (63). Furthermore, it has been reported (64) for high purity copper that the variations in hardness can be as much as 64%.

4.4.3 Steady State Cutting Forces

The graphs of steady state cutting forces, (Figure 80, 81 and 82) against the undeformed chip thickness, (layer of material removed), are approximately straight lines up to 0.3 mm undeformed chip thickness using blunt tools (0.56 mm and 0.8 mm radii) whilst machining a copper workpiece. Beyond 0.3 mm and up to 0.5 mm undeformed chip thickness the slopes of the curves tend to decrease slightly. This decrease is possibly due to the decreasing influence of the cutting edge radius and it would be reduced in proportion to the overall cutting forces. This increase in efficiency of the process as the depth of cut is increased is also reflected in the specific cutting energy curves, Figures 84 and 85, where the specific cutting energy tends to level off beyond 0.3 mm undeformed chip thickness. For the leaded steel workpiece, using blunt tools, the cutting force components are straight-lines,

within the range of the depths of cut tested. As with the copper workpiece, Figure 84, the leaded steel also shows a dramatic decrease in specific cutting energy, Figure 85, from 0.05 mm to 0.3 mm undeformed chip thickness. The high specific cutting energy values experienced above, at the very low depths of cut, are not at all surprising. Figures 80, 81 and 82 all indicate that, when cutting with blunt tools, approaching zero depth of cut, cutting forces are considerably higher than with sharp tools (Figure 83). The above force, in previous metal cutting research, has been identified as the ploughing force (35, 36, 65, 66, 67, 68). It has been considered that, at large values of undeformed chip thickness, the force acting on the tool cutting edge forms only a small proportion of the cutting force and has thus been neglected in the past. However, at small values of undeformed chip thickness, the force that acts on the tool edge is proportionally larger, and significant, particularly if the cutting edge radius is large.

Furthermore, due to the high stresses acting near the tool cutting edge, some deformation of the tool material may occur, which leads to increased contact between the tool and the machined surface over an area

at the base of the cutting edge radius. This contact area would be further increased in the present cutting tests where a metal cap has been reported (Figure 74), which would make the situation even more severe. Thus, when cutting under the conditions of small depths of cut and a tool having a large cutting radius, a substantial frictional force may act in the tool cutting edge region. This force will form a large proportion of the total cutting force at small depths of cut.

The above mentioned, redundant force does not contribute to removal of the chip, but forms part of the overall cutting force. The existence of this redundant force results in some important effects and can explain the so called 'size effect', (69), which refers to the increase in specific cutting energy at low values of undeformed chip thickness (Figures 84, 85). It has been suggested (69) that the rapid increase in specific cutting energy at low values of undeformed chip thickness is due to the redundant force being constant and thus forming a greater proportion of the total cutting force. The specific cutting energy is proportional to the cutting force and inversely proportional to the undeformed chip cross-sectional area, thus, the portion of specific cutting energy resulting from

the redundant force will increase as the chip thickness decreases.

CHAPTER 5

5.1 REVIEW OF SLIP-LINE FIELD THEORY APPLIED TO METAL CUTTING

The shear plane, or shear zone models, form the basis for the analysis of chip formation mechanism today, despite their shortcomings. Practically all the models are centred around the calculation of the stress fields in the so called shear plane or primary shear zone. Some of the assumptions on which such calculations are based include:-

- (i) Chip formation occurs with regular continuity, and, thus the analysis is carried out by steady state mechanics.
- (ii) Chip formation takes place in a plane, the so called shear plane, or in a triangular plastic field passing through the cutting edge.
- (iii) The stress state on the shear plane is uniform.
- (iv) Chip separation can be described by an angle which fixes the orientation of the shear plane at which chip formation is assumed to take place.
- (v) The deformation is under plane strain.

- (vi) The forces acting on the tool surfaces can be represented by a single force passing through the cutting edge.

Furthermore, the workpiece material for simplicity has been generally treated as isotropic, homogeneous and ideally plastic or strain hardens at a constant rate.

Ernst's (71) observations from photomicrographs and films, show that deformation occurs in a fairly narrow zone, and he assumed that this zone could be idealised as a simple shear plane (figure 86) which extends from the tool tip to the free surface. Merchant (33) developed an analysis based on the thin shear model under the following assumptions:-

- (i) the tool tip is sharp and no rubbing or ploughing occurs between the tool and the workpiece;
- (ii) the deformation is two-dimensional;
- (iii) the stresses on the shear plane are uniformly distributed;
- (iv) the resultant force on the chip applied at the shear plane is equal and opposite to the force applied to the chip at the chip tool interface.

From these conditions and assuming that the minimum energy principle applied in metal cutting, Merchant obtained a solution for the inclination ϕ of the shear plane in terms of the rake angle α and the mean angle of friction λ between the tool and chip, so

$$\phi = \frac{\pi}{4} + \frac{\alpha}{2} - \frac{\lambda}{2}$$

Experimental tests carried out by Merchant on plastics and steels showed agreement with theory when cutting plastic materials only. The results for steel were only brought into agreement with the theoretical relationship by assuming that the value of the yield stress was some function of the normal stress on the shear plane.

Ernst and Merchant's analysis deals only with the forces on the chip and makes no statement about the stress distribution. Lee and Shaffer (60), while retaining the assumption of a single shear plane, applied slip-line field theory and thereby ensured that the yield stress of the material was not exceeded in at least part of the chip. By considering a uniform triangular field above the shear plane with slip lines parallel to and perpendicular to the shear plane, Figure 87, they

derived a similar expression for the inclination of the shear plane, that is

$$\phi = \frac{\pi}{4} + \alpha - \lambda$$

In the above solution, figure 87, flow occurs entirely across the shear line ST, the triangle RST being a fictitious plastic field which is the limit of the rigid region. The reason for the consideration of the slip line field in RST is associated with the need to examine the transmission of the machining force between the tool face and the shearing surface ST. The direction of AC being chosen to give the minimum machining force.

In the above process the use of the concept of the rigid-perfectly plastic material is said to be justified because:-

- (i) for most metals the work-hardening rate falls to small values for large strains and so reaches a near constant stress.
- (ii) the high strain rates which occur during machining operations are said to raise the yield strength of the material and to make it approach the ideally plastic.

Lee and Schaffer's solution was found not to be acceptable for certain values of the parameters α and λ .

The above solution was extended to cover the case of cutting with a continuous chip and built-up nose and the conditions under which these processes would arise were considered. The slip line field and hodograph associated with the built-up nose with friction between the tool and sliding material is shown in figure 88.

The predictions of the above theories have been compared with experimental results and the disagreement between them is quite marked. This has been confirmed by several independent workers (82,83). These discrepancies appear to stem from:-

- (i) the assumptions of plane strain conditions in experiments, zero strain hardening, the absence of any effects due to temperature on the material properties and lubrication.
- (ii) the fact that the slip line field solution is only an upper bound solution for the particular configuration chosen. It is thus quite possible that at some parts of the stress field the stress boundary conditions are violated.
- (iii) a complex friction situation on the rake face.

Permissible stress conditions at the end of the shear plane, implied by the shear plane type of solutions, have been examined by Hill (72), in which he showed that if the yield criterion were not to be violated, the position of the shear plane was limited to a certain range. Hill suggested that a unique solution of cutting in terms of the depth of cut, the rake angle and the coefficient of friction may not be possible and the final stable cutting depends upon the initial condition. Similar conclusions have been reached from results obtained from experimental tests conducted by Low (72) and Low and Wilkinson (73).

Christopherson, Palmer and Oxley (75), (76), examined the previous assumptions that deformation takes place on a shear plane by developing an experimental technique of taking Cine films of the process. Subsequently the mechanics of machining were investigated as a problem in plane plasticity. Estimates of cutting force etc, were made, using modified Hencky equations, to allow for strain-hardening, ie for values of k that vary with strain. In the slow speed experiments, the deformation zone observed from the Cine films record enabled the

individual crystals to be followed to ascertain the slip lines. From the results it was possible to construct a slip-line field to which the modified Hencky equations could be applied. The picture which emerged from their work is shown in figure 89. The correlation of theory and experiment was improved by including the effect of work-hardening. They concluded that:-

- (i) the plastic zone was of a considerable width and the streamlines of flow were smooth curves passing from the work to the chip;
- (ii) the chip curved in the plastic zone and contact between the chip and tool occurred in a zone some distance up the tool face, where the deformation was elastic;
- (iii) tensile stresses occur near the tool tip and compressive stresses at the free surface.

When examining the mechanics of the orthogonal cutting using a tool which has a rake face of infinite length, ie the length of contact between the chip and tool is unknown and not well defined, the question arises as to the length of region where the shear stress is acting, and its distribution over the contact length.

Bhattacharyya (78) showed that it is common to divide the contact length into two regions, that is, a region over which the shear stress is constant and an upper contact region over which the stress decreases following a power law.

When machining with a tool of restricted length of contact between the chip and rake face, a constant frictional stress can be assumed which eliminates the complications of the presence of the second zone. Johnson (77) (79), has presented slip line fields for restricted contact tools, for various conditions of cutting tool geometry, figure 90, together with the expressions for the horizontal component of the cutting force and the coefficient of friction at the chip tool interface. The hodographs in the above show the chip to be directed along a direction which is more oblique to the vertical than the rake face, so that, if the tool was not cut back, the chip would tend to rub the tool face.

Usui et al (81) have presented plastic fields associated with cut-away tools, similar to those proposed by Johnson (77), for various contact lengths. They

(81) have used cutting data obtained from conventional tools to set the angles η and θ (figure 91), knowing the chip tool contact length for various values of undeformed chip thickness and tool rake angle. The stress field above is composed of one centred fan and two straight slip-line fields. Based upon the above proposed stress field and quantitative treatment for variation of coefficient of friction at the rake face with artificial restriction of the tool-chip contact length, the model provided close correlation with experimental results.

Kudo (82) has further explored the slip-line fields for restricted tool-contact and has presented modified fields of Johnson-Usui as shown in figure 92. Kudo (82) further modified the slip-line fields for unrestricted tools, as shown in figure 93 and 94, and has shown from the models presented that the natural contact length for the unrestricted tool face is about 2.6 times the depth of cut. Furthermore, Kudo's solution as compared to Johnson-Usui solution, gave lower cutting resistance. Whilst slip-line solutions, resulting in lower cutting resistance, cannot necessarily be regarded as more realistic, a steady deformation mode, associated with smaller cutting

resistance, appears more realistic than those with higher resistance. Kudo's solution showed a constant cutting resistance for lengths of tool face larger than a certain limit, Figure 94(c). His investigations revealed that any rigid-perfectly plastic solution with a built-up-edge was unlikely for zero or positive rake angles, but such solutions for negative rake angles were feasible. The results of his study, however, revealed that some phenomena observed in actual cutting could be explained qualitatively with the rigid-perfectly plastic model.

Johnson (79) has presented slip-line field solutions for restricted tool contact, for orthogonal machining, where the tool cutting edge radius or nose has been approximated by straight edges, figures 95(a) and (b). In these models, it is assumed that only part of the undeformed chip thickness is removed in the form of a chip. The remainder of the material is assumed to be compressed underneath the tool and recovers behind the flank face. Johnson has, however, only explained his results qualitatively.

5.2 DEVELOPMENT OF THE SLIP-LINE FIELD FOR CUTTING WITH A BLUNT TOOL

Initially, it was postulated that, when cutting with a blunt tool, part of the undeformed chip thickness was removed in the form of a chip and part was compressed below the tool, to recover behind the flank face, as has been previously suggested (35,41). Figure 96 shows a slip-line field which would fit the above situation, on the assumption that only part of the undeformed chip thickness (δ), goes into chip. The above stress field and hodograph satisfy continuity and the stress boundary conditions, provided the point 'P' can be considered as a singular point. The point 'T' is at the same level as point 'P'. The dimensions of the metal cap and the chip tool contact length are unspecified and have not been drawn to scale. A stress field of this nature gives a thrust force which is greater than the horizontal force, since the hydrostatic stress on face UP is dependent on the angle ψ which has a minimum value of 135 degrees. Under this condition points 'T' and 'P' would be on the same horizontal line, coincident with the machined surface, and the undeformed chip thickness ' Δ ' would completely be going into chip.

If the undeformed chip thickness ' Δ ' completely goes into chip and material does not flow below the tool, then the slip-field below the tool does not exist and the field is invalid.

From the experimental work carried out with blunt tools (Chapter 4), there was no evidence of material being compressed underneath the tool. On the contrary, the evidence suggested that the base of the tool coincided with the machined surface and that the layer of material removed was equal to the nominal set depth, once steady state conditions were reached.

Some preliminary work on simulating the cutting action of blunt tools (21), using a perspex model of a tool and striped plasticine, showed that a metal cap developed in front of the cutting edge radius, figures 97(a) and (b). Further experimental work confirmed the above and showed evidence (figure 74) that a dead metal cap existed at the extreme cutting edge radius, giving the tool the geometry shown in figure 98. The cap has been approximated by 'UPQ' and became an integral part of the tool once steady state conditions have been reached. It is the steady

state forces which the proposed model predicts. The situation considered here is one of orthogonal machining and the deformation occurs in plane strain, allowing the theory of plastic flow in plane strain to be applied.

The theory assumes a rigid, ideally-plastic material which does not work harden, so the material is assumed to flow at a constant yield stress. In applying plastic deformation theory to the problem of metal cutting, the stress must satisfy the equilibrium equations and stress boundary conditions and nowhere violate the yield criterion. A complete solution satisfies the stress and velocity equations, the boundary conditions in stress and velocities, and the condition that stresses transmitted from the plastic region must be capable of being withstood by the rigid regions without producing large plastic flow.

Figure 98 shows the mode of deformation ahead of the tool represented by the general steady state slip-line field, which is similar to the slip-line fields suggested by Johnson (47), for cutting with a tool of restricted contact length.

Consider the tool to be stationary and the workpiece to be approaching the tool with unit velocity, under steady state conditions, ie when the chip is fully developed. Near the cutting tool, plastic flow occurs and the material particles enter a highly stressed region. Subsequently the state of stress remains at the yield stress value until finally the material leaves the plastic region as a rigid and stress free body. The stress field is shown in Figure 98 and consists of a uniform triangular stress field PQR, connected to the tool face by a fan field, PQS. The triangular field consisting of an orthogonal family of straight lines is rigid and stressed up to the yield point of the material. These straight lines intersect the stress free boundary QR at an angle of 45° , separating the stressed and unstressed regions. Each element with surface on the boundary, QR, such as abc, is in equilibrium under the action of the normal and shear stresses acting on the surfaces 'a' and 'c' only, since surface 'b' is stress free. Thus, the normal and shear stress on each element along QR is equal to the shear yield stress k .

In the plastic region PQS, the lines normal to PS are also lines of maximum shear stress. The arc PS, which is normal to QS and continuation of RS, is also a curve of maximum shear stress, separating the uncut workpiece and the plastic region, which satisfies the yield condition on the boundary between the plastic region and the uncut workpiece. Due to the metal cap it is assumed that the tool chip contact surface will be perfectly rough so the frictional stress along the whole of the tool face is assumed to be 'k', whilst it is recognised that the friction conditions along the tool face QQ' will not be severe as those in the region PQ'. The hydrostatic stress P_c on the face of the tool PQ will vary as a function of the fan angle η in the non-uniform stress field PQS. The slip lines meet the tool face tangentially and normally as shown in the figure. The shear stress on the base of the tool UP is also k and, since the apex of the tool is 90° , the point P is a common point, indicating the hydrostatic stress on UP, $P_p = P_c$.

Figure 98(b), shows the hodograph appropriate to the suggested slip line field. Particular lines of tangential velocity discontinuity are conveniently defined by the

letters in the two regions which they separate;

oa = unit vector for the workpiece, while o is the origin of the hodograph and corresponds with the stationary tool.

The arc ob in the hodograph represents the changing direction of the absolute velocity of the workpiece material entering across the arc PS in the deformation zone QPS . The line ab in the hodograph represents the velocity discontinuity across the shear line SR and ob represents the exit velocity of the chip.

With a knowledge of the velocities from the hodograph and applying continuity of material flow the suggested slip line field satisfies the velocity boundary conditions.

5.2.1 Stress Fields

The region II in figure 98 is a uniform stress field of straight slip lines. Assuming the stresses on the plane QR are zero, the stress state is represented by the Mohr's Circle figure 99(a), which origin of stress is o . The principal stresses for an incompressible, ideally plastic material can be expressed in terms of the hydrostatic stress $-P$, equal to σ_2 , figure 99(b).

Thus:-

$$\begin{array}{lcl} \sigma_1 & = & -p - k \\ \sigma_2 & = & -p \\ \sigma_3 & = & -p + k \end{array} \left. \begin{array}{l}) \\) \\) \end{array} \right\} \dots\dots\dots 5.1$$

where $\sigma_3 > \sigma_2 > \sigma_1$

According to Hencky's theorem of ideal plasticity, the following equations hold along slip lines:-

$$\begin{array}{lcl} p + 2k\phi & = & \text{constant, along an } \alpha\text{-line} \\ p - 2k\phi & = & \text{constant, along a } \beta\text{-line} \end{array} \left. \begin{array}{l}) \\) \end{array} \right\} \dots\dots\dots 5.2$$

where ϕ is the angle of rotation of the slip line.

Considering stress field II, $a' \sim b'$ - α line, since surface QR is stress free, $\sigma_3 = 0$.

$$P_{a'} = k = p_{b'}, \text{ since slip line is straight.}$$

Considering stress field I, $b' \sim c'$ - α line

$$\therefore P_{c'} = k(1 + 2\eta)$$

The hydrostatic stress on the tool flank UP is

$$p_p = k(1 + 2\eta) = p_{c'} \dots\dots\dots 5.3$$

since UP is a continuation of the slip line RSP.

The same Mohr's circle that was used for the region II can be used for region I provided the ' τ ' axis is shifted

in proportion to the angle η turned through in going from point to point. Thus the stresses along PQ are given by the circle if the τ axis is shifted to O_1 , figure 99(a).

The slip line field proposed gives a qualitative answer to the cutting action under consideration. From the slip line field the hydrostatic stress and hence the principal stresses can be calculated in terms of the angle η . However, in order to quantify the results, the chip-tool contact length has to be determined. The angle η will then be a function of the chip-tool contact length, and the undeformed chip thickness. An empirical relationship between the chip-tool contact length and the undeformed chip thickness has been established from cutting tests (figure 70(b)).

5.2.2. Calculation of cutting forces from the model

The cutting force component for a tool of width W is given by:-

$$F_c = (P_c \times \overline{PQ} \times W) + (k \times \overline{UP} \times W)$$

$$F_c = [k(1 + 2\eta) \times \overline{PQ} + k \times \overline{UP}]W$$

$$F_c = [(1 + 2\eta) \times \overline{PQ} + \overline{UP}]kW \dots\dots\dots 5.4$$

The thrust force component is given by:-

$$F_T = [(P_p \times \overline{UP}) + (k \times \overline{PQ})W$$

$$F_T = [(1 + 2\eta)\overline{UP} + \overline{PQ}]kW \dots\dots\dots 5.5$$

\overline{UP} = Cutting edge radius R.

So equation 5.4 becomes

$$F_c = [(1 + 2\eta)\overline{PQ} + R]kW \dots\dots\dots 5.6$$

and equation 5.5 becomes

$$F_T = [(1 + 2\eta)R + \overline{PQ}]kW \dots\dots\dots 5.7$$

Equations 5.6 and 5.7 give the cutting force and thrust force components in terms of the angle η , the angle of the fan field, R the cutting edge radius, \overline{PQ} the chip tool contact length, the shear yield stress k and the width of the tool W.

From the geometry of the slip-line field figure 98,

$$\sin \eta = \frac{x}{RS}$$

where $x = \Delta - x'$

and $x' = RS - RS \cos \eta$

also $RS = QS = \overline{PQ}$

$$\therefore \sin \eta = \frac{\Delta - x'}{\overline{PQ}}$$

$$\sin \eta = \frac{\Delta - \overline{PQ} + \overline{PQ} \cos \eta}{\overline{PQ}}$$

$$\therefore \cos \eta - \sin \eta = 1 - \frac{\Delta}{\overline{PQ}} \dots\dots\dots 5.8$$

Equation 5.8 enables the angle η to be determined using the empirical law relating chip-tool contact length and undeformed chip thickness.

5.2.3 Discussion of Results

To compare the experimental results with the calculated theoretical values of the forces, the workpiece material yield stress Y was determined from a compression test. The shear yield stress k for the copper workpiece using the Von Mises relationship was found to be 230 MN/m^2 and for the leaded steel workpiece 404 MN/m^2 , (figure 100). Due to the low cutting speeds under which tests were carried out, the effects of strain rate and temperature on the material properties have not been taken into account. Figures 101 and 102 show the variation of the experimental and theoretical steady state cutting forces for tools of nominal zero rake and a cutting edge radius of 0.56 mm and 0.81 mm during groove cutting, using copper workpiece material. Although the analysis proposed is based

upon ideal plastic theory, the above results show fairly good agreement, especially the thrust force values. It should be pointed out that the value of the angle η , which is the basis of the calculations, is obtained from the chip tool contact length measurements from the experimental results. The predicted thrust force (F_T) is in good agreement with the experimental results over the whole range of depths of cut, whilst the cutting force (F_C) is in good agreement at low depths of cut, but is under-estimated as the depth of cut increases. It should be further pointed out that, whilst the results are of interest at the higher depths of cut, the results directly relevant to the work of the Author are in the range where the ratio $\frac{A}{R}$ is approximately up to 0.3, which is the situation arising during the sawing process [21]. The results for the cutting force component within the range as predicted by the analysis are under-estimated by 15-20%, whilst the thrust forces are in good agreement.

The experimental ratio of the two components of the cutting force F_C/F_T increases from 1.1 to 1.4 within the range tested, whereas the ratio predicted by the analysis increases from approximately 1 to 1.15, in the same range. Further experimental tests showed good

repeatability and correlation with the analytical results. For comparison purposes Figure 102 shows the experimental results obtained for the force components when machining with a nominally sharp tool under identical cutting conditions. The analytical results for the leaded steel, figure 103, are in fairly good agreement with those obtained from experiments.

On examining the model proposed, for cutting conditions when the chip-tool contact length is equal to the cutting edge radius, the force ratio will be equal to unity, and for chip-tool contact length less than the cutting edge radius, the force ratio is less than unity. From the chip-tool contact length curve figure 70(b) (leaded steel), the undeformed chip thickness value giving a chip tool contact length equal to the radius of the tool, is approximately 0.125 mm, whilst experimental results, figure 103, give this value to be approximately 0.20 mm.

Figure 104 shows the slip-line field model drawn to scale for the cutting conditions stated. The chip ratios obtained from the model ($r_c = 0.08$), as compared to the practical test results ($r_c = 0.1$) are in fairly good agreement.

Figures 105(a) and (b) show the specific cutting energy curves for the cutting conditions stated. As expected, the specific cutting energy is higher for the blunt tools as compared with the nominal sharp tools; furthermore, the specific cutting energy rapidly increases at small depths of cut for the blunt tools. Various explanations for this rapid increase in specific cutting energy at low depths of cut have been previously reported. Backer et al (84), explained the phenomenon with the concept of size effect, ie smaller specimens having a higher yield stress. An alternative explanation by Nakayama and Tamura (85) was the increase in the shear plane length at smaller depths of cut. Whilst recognising these possibilities the situation of the high effective negative rake angle of the tool due to the high cutting edge radius, further accompanied by the high shear drag at the flank of the tool caused by the metal cap previously described, are additional factors to be considered. From the results of high speed films and examination of the chips produced, the Author observed that the shear-plane zone was of a dynamic nature during the initial stages of the cutting

action, with the shear angle decreasing as the cut progressed until steady state conditions were reached.

The model proposed in its present state has certain weaknesses. Although the thrust force predictions are in good agreement, the ratio of the force components are under-estimations. It is worth examining the model presented to consider the reasons why the difference between analytical and practical results occurs. First, for simplicity of the model, maximum friction has been assumed along the length of the rake face of the tool where the chip-tool contact occurs, ie the shear stress is assumed to be k , although this friction value is only valid in the metal cap region. Beyond this, friction is decreasing to the point where the chip eventually leaves the rake face of the tool. The effect of the above assumption would be to theoretically over-estimate the thrust force. In reality therefore, force ratio would be greater which would give closer agreement with the force ratio obtained in the practical test results. Another point in question is the value of the shear yield stress of the material calculated from the compression test of the workpiece specimen. The value of the yield stress taken

was at a strain of approximately 1.1, although the true stress-strain curve indicated possibly an increase in the yield stress at strains greater than the above value. From the shear strain calculations using chip measurements, the shear strains indicated were in excess of 3. Hardness tests on the copper compression test specimen, and from Merchants force balance equations, gave shear yield stress values of 266 MN/m² and 320 MN/m² respectively. This would indicate that the value of the shear yield stress taken from the compression test results is probably an under-estimation and an increase in the value of k , the shear yield stress, would have increased the theoretical forces by 20-30%, whilst not altering the force ratio.

CHAPTER 6

PREDICTING THE PERFORMANCE OF SAW BLADES DERIVED FROM THE SIMULATION TESTS AND THE SLIP-LINE FIELD MODEL

6.1 Predicting Forces and Specific Cutting Energy in Sawing

The slip line field model enables the single point tool performance to be satisfactorily predicted.

The thrust force component F_T can be predicted from the model in chapter 5;

$$F_T = \left[(1 + 2\eta)R + \overline{PQ} \right] \text{ kW} \text{-----} (5.7)$$

Divided through by R

$$\frac{F_T}{R} = \left[(1 + 2\eta) + \frac{\overline{PQ}}{R} \right] \text{ kW} \text{-----} (6.1)$$

The fan angle η in the slip line field model may be determined from the following equation derived in chapter 5,

$$\cos \eta - \sin \eta = 1 - \frac{\Delta}{\overline{PQ}} \text{-----} (5.8)$$

provided the chip tool contact length \overline{PQ} is known.

To obtain this, Figure 70 (b)(c) was replotted in the form shown in figure 106.

From figure 106, for steel workpiece

$$\frac{\overline{PQ}}{R} = 3.8 \frac{\Delta}{R} \text{-----} (6.2)$$

Combining 6.1 and 6.2 gives:-

$$\frac{F_T}{R} = \left[(1 + 2\eta) + 3.8 \frac{\Delta}{R} \right] \text{ kW} \text{-----} (6.3)$$

By combining equations 6.3 and 5.8

$$F_T = [1.48R + 3.8\Delta] \text{ kW}$$

The mean thrust force per tooth per unit thickness f_{tm} , used in the sawing calculation is given by

$$f_{tm} = \frac{F_T}{W} = (1.48R + 3.8 \delta_a) k \text{ -----6.4}$$

since $\Delta = \delta_a$ for comparison with saw blade performance.

Substituting shear yield stress for steel,

$k = 404 \text{ MNM}^{-2}$ and an average cutting edge radius of sawblades

$R = 27\mu\text{m}$ into equation 6.4 gives the following derived expression for the mean thrust force per tooth per unit thickness:

$$f_{tm} = [16.14 + 1535\delta_a] \text{ Nmm}^{-1} \text{ -----6.5}$$

This expression allows the results obtained with the model of the single point cutting tool to be compared with results obtained from sawing tests.

Similarly, an expression for the specific cutting energy can be obtained, using the expression for cutting force component:

$$F_C = [(1 + 2\eta) \overline{PQ} + R] \text{ kW} \text{ -----5.6}$$

Specific cutting energy,

$$Esp = \frac{F_C}{W\Delta}$$

$$\therefore Esp = \frac{f_C}{\Delta} = [(1 + 2\eta) \overline{PQ} + R] \frac{k}{\Delta}$$

Combining this expression with equation 5.8 and 6.2 gives:-

$$E_{sp} = \left[5.61 + \frac{R}{\delta_a} \right] k \quad \text{-----} \quad 6.6$$

The above expression allows the specific cutting energy to be calculated for different values of cutting edge radius R and material shear yield stress k .

6.2 Comparison of a Single Point Tool and Blade Performance

Figure 107 compares the results obtained from the model for values of δ_a within the range of power hacksawing with those obtained from the saw blade tests, Figure 23.

The model predicts the forces for steady state conditions, that is, when the chip is fully established. The model does not include parameters which provide differences in blade performance due to changes in workpiece breadth and varying pitch. The slope of the curves in figure 107 appears to depend on geometric factors, a problem which has been previously noted in Chapter 3.

Although some attempt has been made previously(24)

to explain the effect of workpiece breadth and pitch on blade performance, the explanations have been unsatisfactory.

The slope of the curves in figure 107, defined as the cutting constant K , has been shown to be a performance parameter in power hacksawing. This has been plotted for various blades of different pitch, figure 108, together with the results obtained from the slipline model obtained from the simulation tests. This figure confirms that there is a geometric factor influencing saw blade performance and that the results obtained from the model analysis for a single tooth agrees with the trends of the results obtained from the sawing tests.

6.3 Examination of the Pitch Effect

Performance Tests were carried out on a standard 4 T.P.I. blade (88). The same blade was then modified to an apparently 2 T.P.I. blade by relieving the tip of every other tooth. The set pattern, which was repeated in sets of three teeth, was not appreciably altered by this modification. The performance of the modified blade did not show any change in cutting performance, figure 109. The results of these tests clearly showed that the pitch of the teeth was not the geometrical factor causing change in performance.

A further series of tests were carried out on standard 4 and 6 T.P.I. blades. The blades in their new condition were subjected to the cutting performance tests. The blade teeth were then modified by completely

removing every other tooth, thus increasing the gullet size. The blades were again subjected to the performance tests. The 6 T.P.I. blade was subsequently further modified by increasing the gullet depth. Figure 110 shows the results of these tests for the standard and modified blades.

6.4 Gullet Size and Geometry

Standard hacksaw blades are designed so that the pitch of the teeth, gullet radius and depth are all geometrically similar. There was a possibility that for broad workpieces the gullet size was inadequate to accommodate the chip produced. This would make the gullet ineffective by chip crowding. Some dimensions of the gullet geometry for standard blades are shown below.

Blade	Root-tip height (mm)	Root radius (mm)	Pitch (mm)
4 T.P.I.	3.3	1.14	6.35
6 T.P.I.	2.28	0.69	4.1
10 T.P.I.	1.4	0.43	2.54

Preliminary calculations showed that under normal hacksaw operating conditions when cutting steel workpieces of 50 mm breadth, the volume of metal removed was far less than the gullet volume. So the difference in blade performance was not due to chip crowding as such.

Observations of the chip formation in hacksawing have revealed the production of various chip forms, figure 111.

Condition I - When the breadth of the workpiece is small, the chip travels up the rake face of the tooth and does not reach the root of the gullet. Under these conditions the blade appears to perform at maximum efficiency.

Condition II - For a broader workpiece the chip is formed, travels up the rake face of the tooth and is obstructed at the root, causing the base of the chip to spread. Any further metal removal is made increasingly difficult owing to the back pressure applied by the obstruction.

Condition III - Under these conditions extra energy is expended in the chip travelling around the root radius. The chip continues to travel around the gullet until it hits the workpiece where it can either break or become locked into this position.

In the above three conditions the gullet radius and the gullet perimeter are of paramount importance.

Condition IV - Finally, in some cases, chip curl occurs. However, even in this situation, back pressure is caused by the chip curling.

Figure 112: shows the limiting length of workpiece that can be cut efficiently for various pitch blades. The calculations are based on the criteria of condition II and III above and the size of gullet for geometrically similar blades (Appendix E).

The above observations confirm that, when sawing broad workpieces, the chips are obstructed in the gullet space. The obstruction thus modifies the chip mechanism. Since the resistance offered to the chip by the gullet shape applies a back pressure to the deformation zone, the stress field is altered.

6.5 Discussion of Results

The cutting constant K , calculated from the test results of the standard and modified blades, is compared (figure 108) with the single point tool performance obtained from the model. The model results agree well with the hacksaw blade test results. There appears to be a geometric factor, in that the shape and size of the tooth gullet influences the blade performance.

In the model presented, Figure 98, it is assumed that the region QR is stress free. This assumption is valid, provided the chip is allowed to flow freely without any obstruction, as was the case in the single point simulation tests. However, an additional back

pressure can be applied on QR owing to the obstruction of the chip in the gullet. The effect of this additional pressure is to increase both the thrust and cutting force components for the same undeformed chip thickness. The model suggests that if the thrust force F_T and hence f_{tm} is increased for the same value of δa , the slopes of the curves in figure 23 will decrease. This will have the effect of lowering the cutting constant K and thus increasing the specific cutting energy.

It is believed that what appears to be a pitch effect is in fact a 'cavity' or gullet effect. This explains the difference in blade performance obtained in Figure 108. Further confirmation exists in the results of figure 110(a), where the blade showed improvement in performance when gullet size was increased without altering the pitch of the teeth.

The 4, 6 and 10 T.P.I. blades tested were geometrically similar and the performance curves (figure 23) refer to a single tooth. The overall differences in the blades are the size of the gullet with respect to the root radius, root to tip height and the perimeter of the gullet, all of which contribute to the blade performance. It is believed that the above differences contribute to the change in blade performance with the variation in blade pitch.

The results of Figure 112 confirm the trend of the results obtained in figure 24 where, as the work-piece breadth increased for a particular blade pitch, the cutting constant decreased, indicating a decline in blade performance. This explanation of workpiece breadth effect is an alternative to the explanation based on transient forces. In power hacksaw cutting of steel, it has been observed that the chip remains of fairly constant thickness as it travels up the tooth face, up to the point when it impinges on the gullet root. Single-point tool cutting of steel certainly gives chips of uniform thickness. This suggests that the increase in cutting force with distance of tooth travel is not the dominant factor and interaction of chip with gullet root is more significant.

The specific cutting energy obtained from the model, correlates well with the test results of the blades, figure 113. The figure also shows the effect of increasing the edge radius of the blade tooth, confirming the single point tool simulation tests. The edge radius of 70 μm compared with the average measured values for the blades is perhaps a little high, but it has been used as an indicator of the extreme condition.

This discussion is now summarized :-

The single point tool study confirms the mechanism of chip formation under free chip flow conditions. There

is evidence that the gullet geometry and size are a deciding factor in blade performance. The value of specific cutting energy in the saw blade tests is higher than that in the model results. This is explained as follows :-

The single point tool study does not take into consideration the effect of gullet size or geometry. The effect of any additional forces, due to chip obstruction or frictional forces on the walls of the blade or gullet, is clearly to increase the specific cutting energy. When specific cutting energy, as obtained in the saw blade tests, is compared with that obtained from the model, the deviations can be explained by constraint of the chip in the saw gullet. Investigations of detailed explanations would seem to be a fruitful topic for future work.

The results presented above refer only to the steel workpiece. Whilst adequate single point cutting test data was available for the copper workpiece (chapter 4), insufficient sawing test data on the copper did not allow the comparison of blade performance to be made.

CHAPTER 7

GENERAL CONCLUSIONS

1. The thrust load characteristics of the power hacksaw machines vary dramatically. At high reciprocation speeds, the effective thrust load is reduced, due to the instability in the power hacksaw machines.
2. A method of assessing the blade performance, based on the metal removal rate and independent of the saw machine characteristics, is proposed (3.2), which could be used as a quality control test. The repeatability of this test has been found to be very good, and the tests could be carried out on a commercial saw provided every test includes load measurements.
3. Cutting tests have shown that the average depth of cut achieved per tooth is very small in most applications of power hacksawing. These measurements together with the cutting edge radius of the saw teeth show that, in the majority of applications, the depth of cut is less than the cutting edge radius. Therefore, the hacksaw blade may be classified as a blunt cutting tool. Under these cutting conditions, metal removal takes place with a complex combination of chip formation.

4. The specific cutting energy in the hacksawing operation has been shown to be three to four times greater than that usually obtained when cutting with nominally sharp tools (turning) thus indicating the relatively inefficient cutting action of a hacksaw blade.
5. The cutting constant, which has been used as a measure of the blade performance, varies with both blades of different teeth pitch and workpieces of different breadths.
6. From the experimental observations when machining with tools having a large cutting edge radius as compared to the undeformed chip thickness, there was no evidence of material flowing beneath the tool and recovering behind the flank as has been previously suggested.
7. When cutting with blunt tools, a stationary metal cap enveloped between the cutting edge radius and machined surface, appears to exist, which could be unstable in nature. It is believed that this instability contributes to the variation in the type of chips produced.

8. The efficiency of the cutting process when machining with blunt tools, decreases as the length of cut is progressed causing transient build up forces, which confirms previous results obtained by the author.
9. A useful empirical relationship between the chip-tool contact length and the undeformed chip thickness has been presented which does not appear to be influenced by the cutting edge radius within the range tested.
10. By applying the theory of plasticity, the plastic field is found to be composed of one centred fan and one straight slip-line field. The associated fields of stress and velocity with slip-line construction are found to satisfy all boundary conditions.
11. The simple, slip-line field model presented has its weaknesses but gives a qualitative and fairly good quantitative agreement (Figures 101 - 105) with the single point experimental results. Both experimental and analytical results have shown that at very low depths of cut, as compared with the cutting edge radius, the force ratio $\frac{F_c}{F_T} < 1$, a situation which could arise in processes such as sawing, grinding

and broaching. The model presented can be used to study the effects of different tooth configuration on the tooth performance.

12. The results predicted by the theoretical model for a hacksaw blade tooth and results from experimental blade tests (Figure 107 and 108) fall into a simple pattern.

The cutting edge radius effect on blade performance can be satisfactorily predicted by the model which shows close correlation with blade tests, figure 113.

13. The model assists the explanation of the workpiece breadth and blade pitch effect in conjunction with the influence of the gullet.

The work undertaken demonstrates that there is a geometric factor due to gullet shape and size affecting the blade performance.

The model and single point tool study qualitatively relates to the blade performance. In order to quantify the results the analysis has to be modified to take into consideration the above geometrical aspects.

SUGGESTIONS FOR FUTURE WORK

1. Saw Machine

A feasibility study and investigations should be carried out to improve the performance of the power hacksaw machine. These improvements should include some of the following:-

- (i) a variable stroke saw machine
- (ii) dynamic stability at the higher available reciprocation speeds of the saw machine
- (iii) the mean thrust force during the cutting cycle to be closer to the maximum thrust force
- (iv) a thrust load measuring system built into the saw machine, with feedback facilities to the load applying system, which would enable the thrust force per tooth to be monitored and maintained to a pre-determined value. This would be particularly useful when cutting workpieces of varying cross-section
- (v) a blade tensioning and measuring system
- (vi) a quick return mechanism on the idle/return stroke

2. Saw Blade

Assuming that the blade material and its heat treatment at present are as good as can be achieved, then further work is required in improving the efficiency and life of the cutting edge, which can be improved by:-

- (i) increasing the sharpness of the cutting edge, and maintaining the sharpness
- (ii) geometry of the blade teeth (rake and clearance angles)
- (iii) reducing the thickness of the blade in order to reduce the kerf loss

3. Simulation Tests

To carry out simulation tests using different workpiece materials and cutting tools having a larger range of cutting edge radii. This would provide comprehensive data for more effective use of the slip-line field model. The single point tool study should be extended to include the effect of gullet size and geometry when machining different materials.

4. Sawing Tests

Blade performance tests should be carried out using different workpiece materials. This would provide more comprehensive data for the blade user and designer.

APPENDIX

Appendix A

- (i) Suggested conditions for Bandsawing
- (ii) Comparative cutting times and blade costs
- (iii) How to choose the most universal sawing machine
for your application
- (iv) Power Hacksaw Blades - some of the problems
and their solutions

Appendix B

- Table 1 Tooth radii measurement - results
- Table 2 Measurement of slot width
- Table 3 Performance testing of Blades - Data Sheet
- Table 4 Cost data for a hydraulic Power Hacksaw
- Table 5 Cutting test results for Blunt Tools
- Table 6 Cutting test results for Blunt Tools
- Table 7 Cutting test results for Blunt Tools
- Table 8 Computer programme - slip line field
- Table 9 Theoretical results from slip line field

Appendix C

Analysis of the effects of Blade tension

Appendix D

Simulating the cutting action of a single Hacksaw Blade Tooth

Appendix E

Predicting the Limiting Length of Cut for Blades of Various Pitch

Appendix A

SUGGESTED CONDITIONS FOR BANDSAWING [4]					
Material	Work size and blade teeth per inch			Feed pressure (lb)	Saw band velocity (fpm)
	Under 3 in	3 to 6 in	Over 6 in		
SAE steels					
1020	8 or 6	6 or 4	4 or 3	75 to 200	225
1050	8 or 6	6 or 4	4 or 3	75 to 200	200
1110	8 or 6	6 or 4	4 or 3	75 to 200	250
1120	8 or 6	6 or 4	4 or 3	75 to 200	200
1320	8 or 6	6 or 4	4 or 3	75 to 200	175
2340	8 or 6	6 or 4	4 or 3	75 to 200	165
3135	8 or 6	6 or 4	4 or 3	75 to 200	150
4140	8 or 6	6 or 4	4 or 3	75 to 200	140
5140	8 or 6	6 or 4	4 or 3	75 to 200	130
52100	8 or 6	6 or 4	4 or 3	75 to 200	125
9260	8 or 6	6 or 4	4 or 3	75 to 200	100
Other metals					
High speed steel	8	6	4	75 to 200	75
Tubing or channels (thin wall)	10	10	10	75 to 100	225
Tubing or channels (heavy wall)	8 or 6	6	6 or 4	75 to 200	225
Brass: SAE 72	8 or 6	6 or 4	4 or 3	75 to 200	250
Bronze: SAE 73	8 or 6	6 or 4	4 or 3	75 to 200	225
Aluminum alloys	8 or 6	4 or 3	3	75 to 175	300

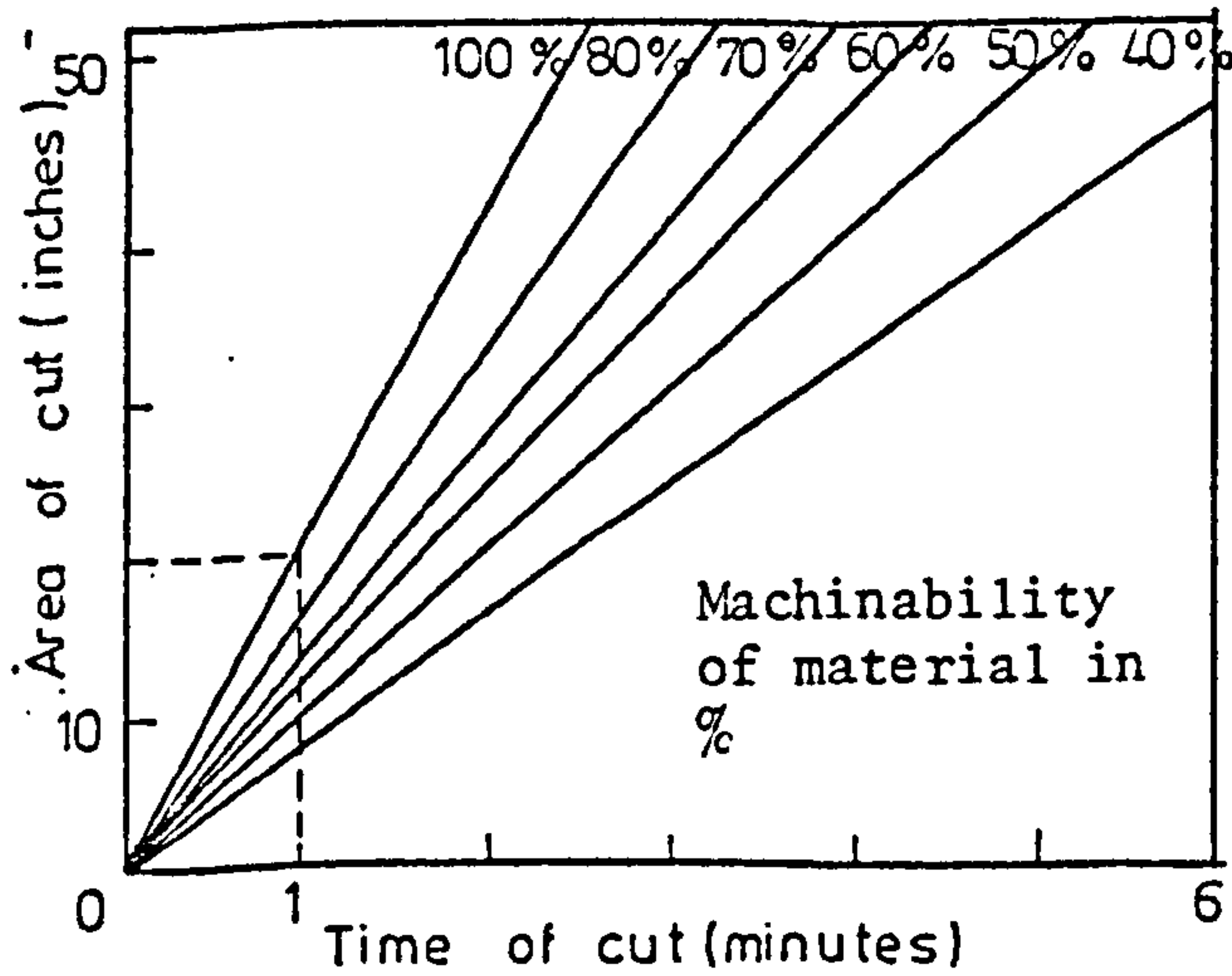
A1

TABLE 1 SUGGESTED CONDITIONS FOR BANDSAWING [4]

APPENDIX A

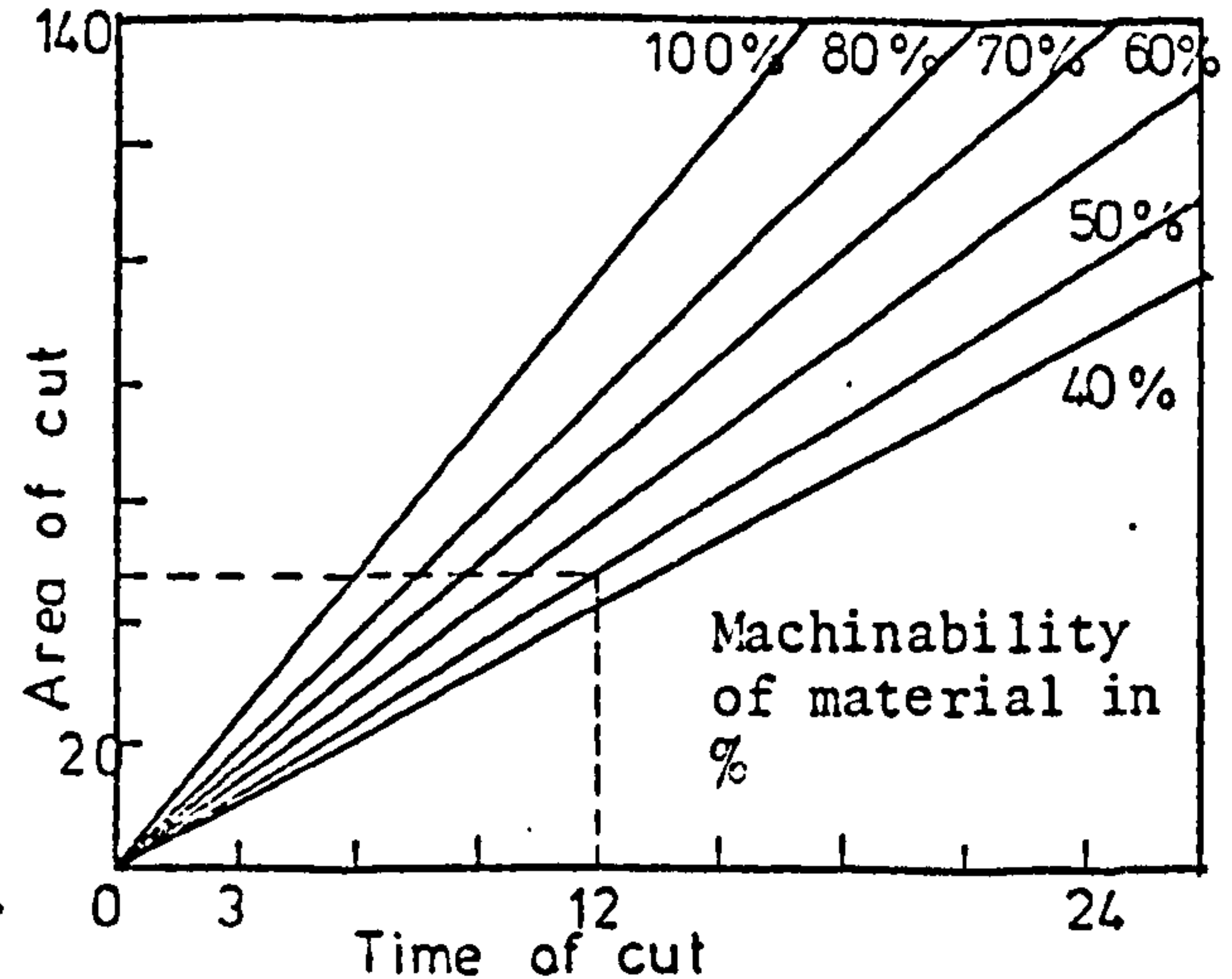
Figure 1 Comparative cutting times, blade costs per workpiece [4]

- (a) Cutting time for bandsawing depends on material machinability, and beam strength of the saw blade



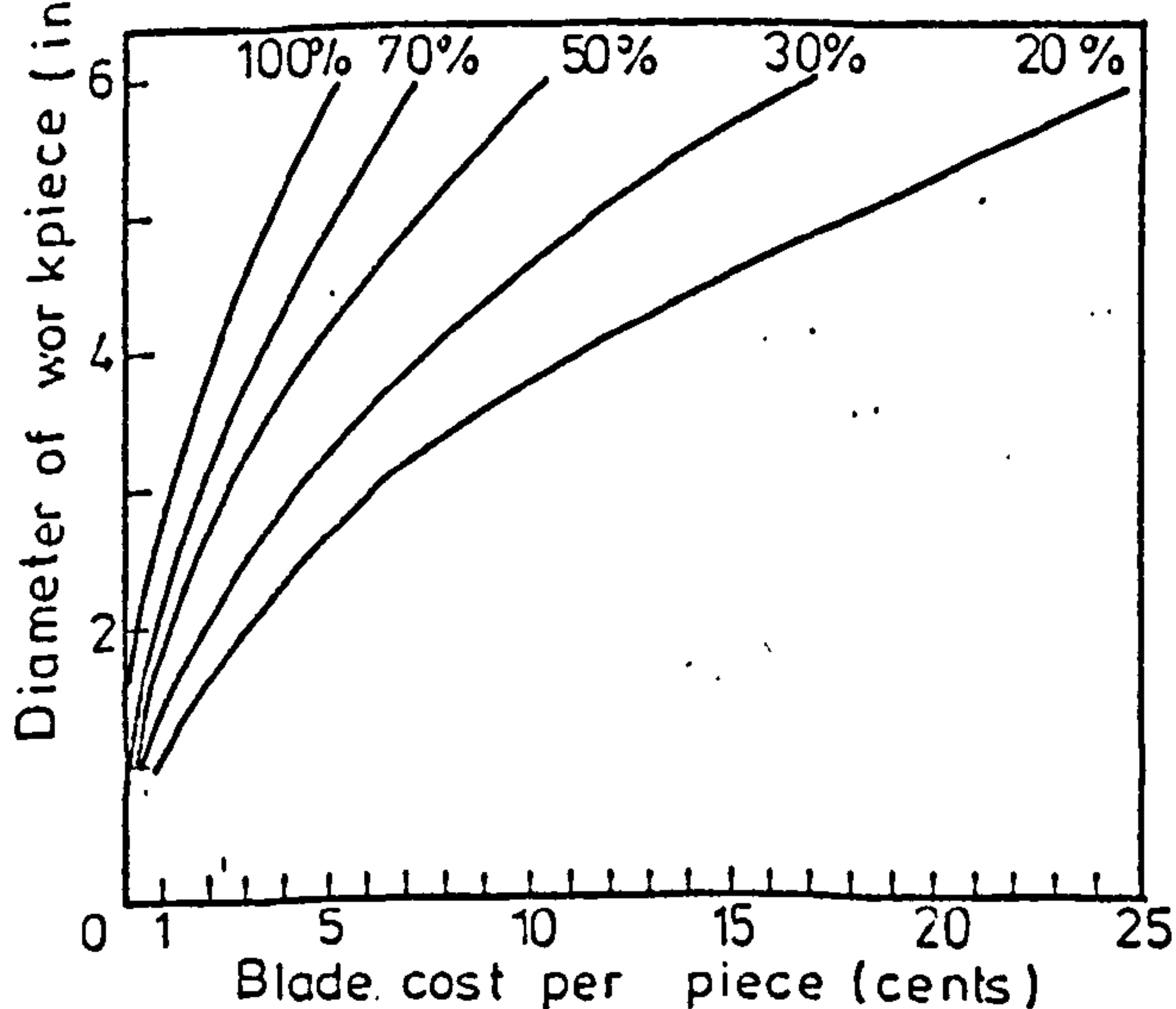
Example: Given 20 sq inches 100% machinability then time = 1 min

- (b) Power hacksaws can apply adjustable feed pressures to tensioned hss blades supported by backup blades

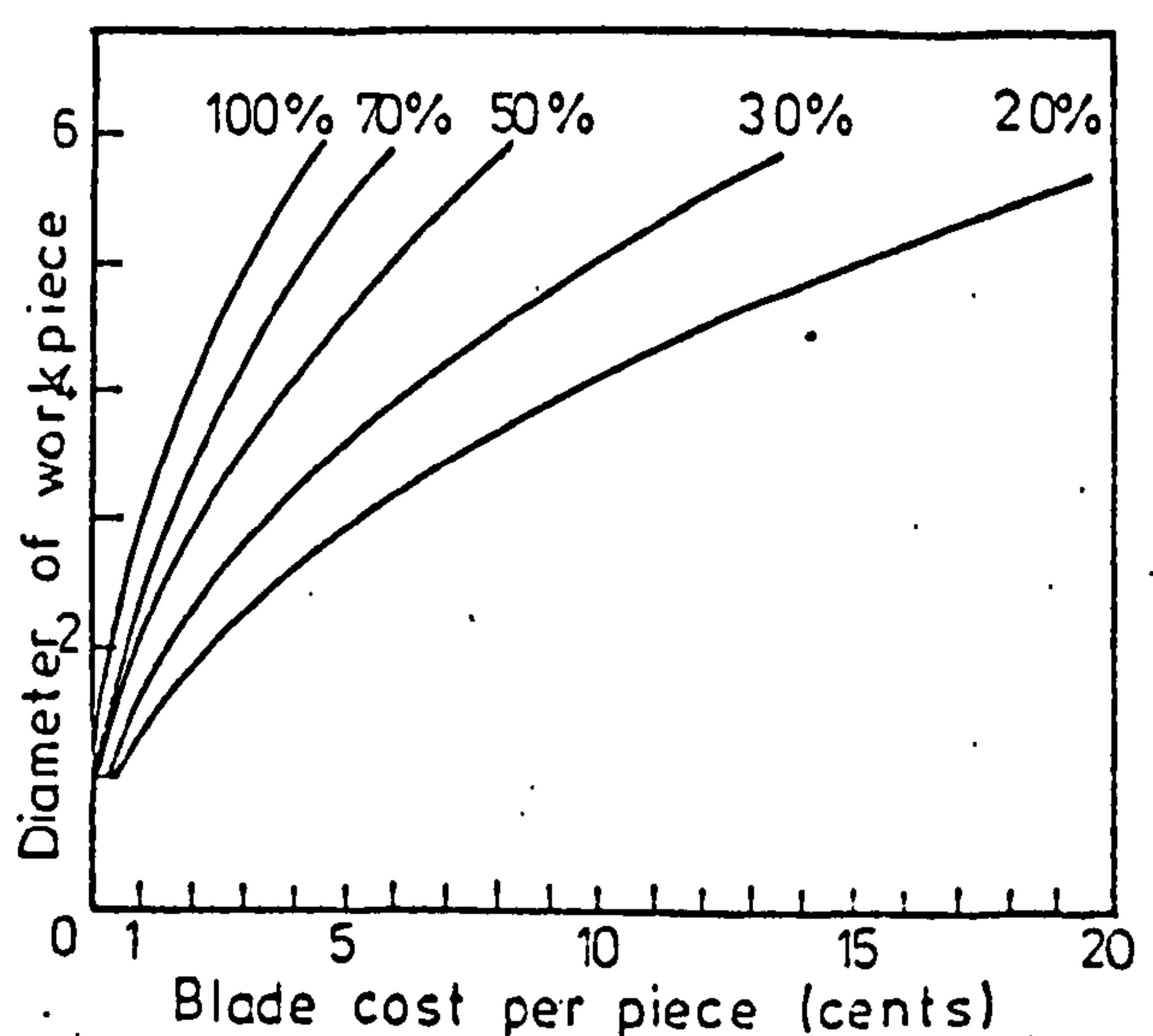


Example: Given 48 sq inches 50% machinability then time = 12 min

- (c) Blade cost per workpiece cut off with bandsaw varies with diameter and machinability, at \$18.55 a blade



- (d) Blade cost per workpiece cut off with power hacksaw is based on tungsten hss blades at \$4.22 a blade



Appendix A - Table 2

HOW TO CHOOSE THE BEST UNIVERSAL SAWING MACHINE FOR YOUR APPLICATIONS [15]

Material to be cut		Gravity feed hacksaw	Gravity feed Bandsaw	Hyd feed hacksaw	Hyd feed Bandsaw	Good quality production Circular saw	Large capacity Circular saw	Light duty Circular saw	Small capacity Circular saw
Solids	Small dia (below 5in) mild steel	++	++	++	+++ short cuts	+++ long cuts	+	++ semi-auto	† small solids
	Bundle or multi-cutting	-	+	+	+++	-	-	-	-
	High strength steels and tool steels	-	-	++	+++ short cuts	+	+++ long cuts	-	-
	Stainless steels also ni-mo and titanium	-	-	++	+++	+	++ at high blade cost	-	-
	Large diameter solids	-	-	+++	++	-	+++ at high blade cost	-	-
Profiles and tubes	Small - L section - I section - T section - U section - tube	-	+	-	++ bundle cutting	+++ tube cutting	-	+++	+++
	Large - L section - I section - T section - U section - tube	+	++ large tube	+	++	-	+++	-	-
	Non ferrous - profiles and solids	-	-	-	-	+++ high speed for solid	-	+++ high speed	+++ high speed
Length of cut	Short	+	+++	+	+++	-	-	-	+
	Long	++	+	++	+	+++	++	++	++
No of cut pieces required	Low quantity	++	++	++	-	-	-	++	++
	Large quantity short	-	-	+	+++	+	-	-	-
	Large quantity long	-	-	++	+	+++	+++	-	-
Accuracy and angularity of cut		+	+	++	+++	+++	+++	+	+
Running costs (blades and the like)		low	low	low	med	high	very high	med	med
Floor area occupied by machine		low	low	low	med	med	high	low	low
Capital investment		low	low	med	high	high	very high	med	low
Flexibility of machine		+	+	+++	++	+	+	++	++
Required operator skill		low	low	low	med	high	high	med	low

+++Ideal choice
 ++Good
 +Average
 -Not recommended

TABLE 3(a)
POWER HACKSAW BLADES: SOME OF THE PROBLEMS AND THEIR SOLUTIONS [13]

PROBLEM	CAUSES	SOLUTIONS
Blade breakage	<ol style="list-style-type: none"> 1 Blade contacting work before cutting 2 Cutting in the same slot with a new blade previously cut by worn blade 3 Insufficient tension 4 Excessive feed when cutting thin sections 5 Using a worn out blade 6 Material loose in vice 	<ol style="list-style-type: none"> 1 Start machine with blade above work and allow automatic feed to make contact 2 Always start a new cut with a new blade, or turn material over and saw to meet the old cut 3 Check the blade for tension after 3 or 4 cuts 4 Reduce the pressure 5 Fit new blade 6 Hold/Clamp material firmly. especially in multiple cutting
Blade not cutting straight	<ol style="list-style-type: none"> 1 Insufficient tension 2 Blade worn out 3 Excessively hard spot in material forcing blade off straight path 4 Excessive pressure 5 Saw frame worn in slide or out of perpendicular alignment 6 Excessive speed 7 Blade fails to lift on return stroke 	<ol style="list-style-type: none"> 1 Check blade for tension after 3 or 4 cuts 2 Replace with new blade - an over-dull blade is both a time and money waster 3 Turn material over and start a new cut. If set has become unevenly worn replace with new blade 4 Reduce the pressure and watch the improvement in alignment 5 Inspect adjustment of machine and adjust as necessary 6 Reduce to correct speed 7 Inspect machine for probable necessary adjustments

TABLE 3(b)

POWER HACKSAW BLADES: SOME OF THE PROBLEMS AND THEIR SOLUTIONS [13]

PROBLEM	CAUSES	SOLUTIONS
Premature wearing out of teeth	<ol style="list-style-type: none"> 1 Excessive pressure 2 Teeth facing wrong way 3 Incorrect pitch of teeth 4 Lack of or improper cutting compound or coolant 5 Excessive tension 	<ol style="list-style-type: none"> 1 Reduce pressure 2 Teeth should face towards the machine if drawcut type - away if push out machine 3 Replace with correct pitch 4 Use reliable cutting coolant with correct mixture for material being cut 5 Do not apply excessive pressure in tensioning blade
Blade breaking at pin hole	<ol style="list-style-type: none"> 1 Blade not correctly mounted 2 Worn pins or improper size 3 Too many teeth for large material 	<ol style="list-style-type: none"> 1 Make sure blade is flat against the holders and pins are drawn up to the end of eye before final clamping and tensioning of saw 2 Replace with new and correct pins 3 Select correct tooth pitch etc
Teeth ripping out	<ol style="list-style-type: none"> 1 Sawing against corner or a sharp edge 2 Material moving during cutting 	<ol style="list-style-type: none"> 1 Carry out 3 tooth rule on material being cut 2 Hold/Clamp material firmly especially when multiple cutting

APPENDIX B

Table 1(a)

RESULTS OF TEETH RADII

BLADE SPECIFICATION:- BRAND 'X' 400 x 40 x 2 x 4 TPI

Radius x 10⁻³ inches

BLADE						
TOOTH	No 1	No 2	No 3	No 4	No 5	No 6
1	1.1	1.6	3.0	-	-	0.7
2	2.5	1.2	0.9	1.5	1.6	0.8
3	-	1.0	1.4	1.5	0.6	1.4
4	1.0	1.4	1.0	1.1	1.1	1.2
5	0.5	0.6	1.1	1.2	1.9	1.0
6	0.5	0.8	1.4	0.6	0.6	1.1
7	0.5	1.4	0.8	1.1	1.1	0.8
8	0.8	0.7	1.0	0.7	1.2	1.0
9	1.4	1.4	0.8	0.55	1.4	0.6
10	0.9	0.8	0.8	0.6	1.2	0.9
11	1.4	1.0	1.2	0.8	0.4	1.4
12	0.7	1.2	1.5	1.1	1.0	1.2
13	0.8	0.9	0.9	1.2	1.2	0.5
14	1.2	0.7	1.1	1.1	0.9	1.5
15	0.8	1.4	1.6	1.2	1.1	0.9
16	0.8	0.9	-	1.2	1.1	0.8
17	0.7	1.0	1.2	1.4	1.0	0.9
18	0.6	1.1	1.6	1.2	1.1	1.5
19	1.2	0.8	1.1	1.4	0.5	1.5
20	0.9	1.2	1.0	1.5	0.8	1.4
21	1.0	1.2	1.5	-	1.1	1.2
22	0.8	-	1.5	1.6	-	-
Average Radii	0.957	1.100	1.257	1.1275	1.045	1.0619

Table 1 (b)

RESULTS OF TEETH RADII

BLADE SPECIFICATION:- BRAND 'X'400 x 40 x 2 x 6 TPI

Radius x 10⁻³ inches

BLADE TOOTH	No 1 Radius	No 2 Radius	No 3 Radius	No 4 Radius	No 5 Radius	No 6 Radius
1	2.6	2.8	1.5	2.6	1.4	1.4
2	2.6	1.1	1.6	1.8	1.5	1.5
3	1.8	1.1	1.8	2.2	1.5	1.8
4	0.9	1.2	1.9	0.9	1.2	1.8
5	1.5	1.1	1.4	1.4	1.5	1.2
6	1.6	1.5	1.6	1.1	1.4	1.5
7	1.8	2.2	1.2	1.4	0.9	1.1
8	1.0	1.8	1.5	0.9	1.1	1.2
9	1.6	1.2	1.2	1.9	1.6	1.4
10	1.1	1.2	1.0	1.5	1.2	1.0
11	1.2	1.4	1.2	1.8	1.8	1.2
12	1.4	1.4	0.6	1.0	1.4	0.9
13	1.1	1.2	1.6	1.4	1.2	1.1
14	1.5	1.2	1.0	1.5	0.55	0.8
15	1.6	1.5	1.5	0.8	-	0.7
16	1.5	1.2	1.6	1.9	1.2	1.2
17	1.1	0.4	1.6	1.4	0.6	0.6
18	0.9	1.8	1.1	1.5	1.2	0.6
19	2.4	1.9	1.0	0.7	0.8	0.55
20	0.9	1.4	1.5	0.8	1.4	0.6
21	1.2	1.5	1.6	0.9	1.4	0.8
22	1.2	1.4	0.8	1.6	0.5	0.7
23	1.8	1.6	0.9	1.8	1.4	0.9
24	1.9	1.5	1.6	0.9	1.4	1.2
25	1.4	1.1	1.9	1.5	1.5	0.6
26	1.9	1.0	1.1	1.6	0.8	1.1
27	2.4	1.6	1.6	-	1.2	1.0
28	1.4	1.2	1.0	1.1	1.2	0.9
29	1.0	1.5	1.4	1.8	1.4	1.5
30	0.8	1.2	1.5	1.6	1.6	1.4
31	1.4	1.2	1.5	1.4	0.9	2.6
32	1.6	2.5	1.5	-	1.2	1.1
33	1.0	4.0	1.6	1.0	-	1.5
Average Radii	1.4878	1.512	1.376	1.409	1.224	1.134

Table 1 (c)

RESULTS OF TEETH RADIIBLADE SPECIFICATION:- BRAND 'X' 400 x 32 x 1.6 x 10 TPIRadius x 10^{-3} ins

BLADE TOOTH	No 1 Radius	No 2 Radius	No 3 Radius	No 4 Radius	No 5 Radius	No 6 Radius
1	1.8	1.6	2.5	2.4	-	1.2
2	1.6	2.5	0.9	1.2	2.0	1.2
3	2.2	0.9	1.4	0.8	1.6	1.9
4	1.9	1.6	0.6	0.6	1.0	1.4
5	1.0	2.5	-	-	2.2	0.9
6	1.6	1.4	0.8	-	0.7	1.0
7	-	1.5	0.6	0.8	1.8	1.2
8	2.0	1.0	1.0	1.5	0.8	1.4
9	1.6	1.5	0.6	1.8	2.0	0.6
10	1.5	1.4	1.2	1.6	1.1	1.2
11	1.6	1.2	0.7	1.4	0.7	1.1
12	1.8	1.1	0.8	2.4	2.5	0.9
13	0.9	1.6	1.5	1.8	1.2	0.4
14	1.2	1.8	0.5	1.4	1.1	0.7
15	1.2	0.3	0.5	3.0	1.2	1.1
16	0.7	1.8	1.0	2.2	1.0	0.8
17	0.8	1.6	1.4	0.7	1.2	1.1
18	1.4	0.9	1.2	3.4	0.7	1.2
19	1.0	1.6	0.7	1.4	1.2	1.2
20	2.0	1.1	1.1	1.4	0.5	1.2
21	1.1	1.6	0.9	1.4	0.9	0.7
22	1.6	1.6	0.7	1.4	0.5	1.3
23	1.4	1.2	1.1	1.5	1.4	1.2
24	1.8	1.6	1.2	0.8	1.5	1.8
25	-	1.2	1.0	1.5	1.6	2.4
26	1.5	1.9	1.0	0.6	1.0	0.8
27	1.5	1.6	1.6	1.2	1.4	1.0
28	1.4	1.0	0.8	0.7	1.5	1.2
29	1.2	1.8	0.9	1.6	1.2	1.4
30	1.5	1.9	1.8	1.5	1.9	1.2

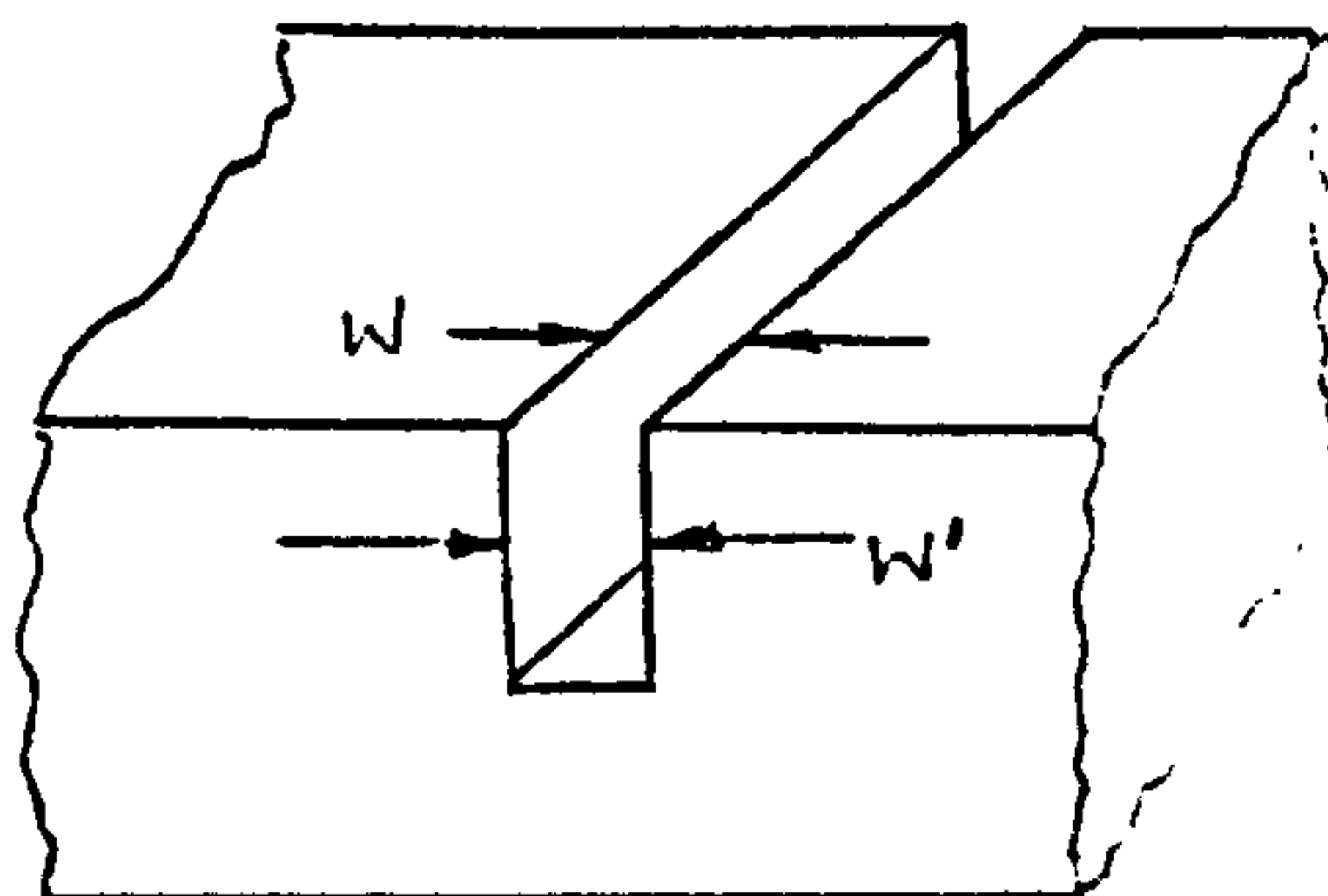
BLADE SPECIFICATION:- BRAND 'X' 400 x 32 x 1.6 x 10 TPI continued

Radius x 10⁻³ ins

BLADE TOOTH	No 1 Radius	No 2 Radius	No 3 Radius	No 4 Radius	No 5 Radius	No 6 Radius
31	1.8	1.4	2.4	1.6	1.0	1.4
32	0.7	-	0.9	1.6	1.4	0.7
33	0.7	2.0	1.6	1.1	1.1	0.9
34	0.8	1.1	1.5	1.2	1.2	0.9
35	1.0	1.6	2.4	1.6	1.0	1.1
36	1.2	1.5	1.6	1.6	1.1	1.2
37	1.5	2.0	0.9	1.4	1.2	1.1
38	1.2	2.6	1.0	2.5	0.8	0.8
39	1.0	1.6	2.4	2.4	0.9	1.5
40	1.6	-	1.2	1.8	0.9	1.4
41	0.9	2.6	1.4	1.9	1.2	0.8
42	1.5	1.5	1.6	1.9	1.4	1.0
43	1.4	2.0	0.8	1.9	1.5	-
44	1.5	2.6	1.4	1.1	0.7	0.4
45	0.6	-	1.5	1.8	0.9	0.6
46	1.1	1.4	1.8	2.5	1.4	0.7
47	1.9	1.4	1.1	1.8	1.8	0.8
48	1.6	1.2	0.7	1.2	1.4	1.2
49	1.6	1.5	1.4	-	1.1	0.6
50	0.6	1.5	1.1	0.7	0.9	1.1
51	1.5	1.5	1.6	0.7	0.55	1.4
52	1.6	1.6	1.8	1.9	1.1	-
53	1.2	-	1.9	1.4	1.4	2.0
54	1.6	1.5	1.6	1.4	-	0.7
55	1.6	1.4	1.0	0.9	1.2	-
56	1.6	2.2	2.0	2.0	1.4	1.0
57	2.0	1.5	1.6	2.8	0.9	0.7
58	2.6	2.2	0.9	-	0.9	-
59	3.4	-	-	-	-	-
Average Radii	1.440	1.587	1.247	1.598	1.2098	1.087

TABLE 2 (b)

MEASUREMENT OF SLOT WIDTH

400 x 32 x b x 10 TPI

Blade No	Width of Blade b mm	Width of Slot		$\frac{w}{z}$	$\frac{w^1}{z^1}$
		w mm	w ¹ mm		
1	1.52	2.0125	2.26		
1	1.515	2.1685	2.50		
1	1.475	2.280	2.585		
1	1.515	2.1825	2.045		
Mean	1.5062	2.1608	2.347	1.4346	1.5582
2	1.525	2.3675	2.180		
2	1.560	2.3475	2.170		
2	1.570	2.2550	2.6025		
			2.6675		
Mean	1.5516	2.3233	2.405	1.4973	1.550
3	1.605	2.2525	2.295		
3	1.665	2.255	2.825		
3	1.665	2.190	2.1485		
3			2.140		
Mean	1.645	2.2325	2.3521	1.3571	1.4298
4	1.555	2.555	2.3580		
4	1.590	2.485	2.5775		
4	1.585	2.400	2.245		
4	1.575	2.3875	2.292		
Mean	1.5762	2.4568	2.368	1.5586	1.502
5	1.595	2.2225	2.255		
5	1.570	2.2325	2.420		
5	1.570	2.3175	2.385		
5			2.4225		
Mean	1.5783	2.2883	2.370	1.4498	1.5016
6	1.60	2.340	2.4875		
6	1.61	2.335	2.710		
6	1.60	2.340	2.785		
			2.200		
Mean	1.6033	2.3383	2.5456	1.4584	1.5877
Mean				1.4593	1.5215

$$\Delta z \text{ max} = .1022 = 7\%$$

$$\Delta z \text{ min} = .0993 = 6.8\%$$

$$\Delta z^1 \text{ max} = .0917 = 6.38\%$$

$$\Delta z^1 \text{ min} = .0662 = 4.35\%$$

TABLE 2 (b)

MEASUREMENT OF SLOT WIDTH

400 x 40 x b x 6 TPI

Blade No	Width of Blade b mm	Width of Slot		$\frac{w}{z}$	$\frac{w^1}{z^1}$
		w mm	w ¹ mm		
1	1.910	2.715	3.02		
1	1.915	2.6765	3.020		
1	1.930	2.7475	3.040		
1			3.0025		
Mean	1.918	2.713	3.0206	1.4144	1.5748
2	2.02	2.9375	3.1475		
2	2.01	3.1625	3.165		
2	2.00	2.820	3.3275		
2	2.01	2.990	2.8875		
Mean	2.01	2.9775	3.1318	1.4813	1.558
3	1.77	2.645	2.500		
3	1.78	2.66	2.700		
3	1.76	2.535	3.145		
3		2.750	3.000		
Mean	1.77	2.6475	2.8365	1.4957	1.602
4	1.915	2.930	2.955		
4	1.91	3.1650	2.930		
4	1.90	2.705	2.965		
4			2.820		
Mean	1.908	2.9333	2.9175	1.5373	1.5290
5	1.94	2.992	2.915		
5	1.95	3.055	3.335		
5	1.98	3.090	3.165		
5			3.100		
Mean	1.9566	3.0456	3.1287	1.5565	1.599
6	1.885	2.650	2.8925		
6	1.900	2.865	3.2025		
6	1.875	2.7425	3.1975		
6			3.135		
Mean	1.8866	2.7525	3.1068	1.4589	1.664
Mean				1.4906	1.5878

$\Delta z \text{ max} = .0762 = 5.11\%$
 $\Delta z \text{ min} = .0659 = 4.42\%$

$\Delta z^1 \text{ min} = .0588 = 3.7\%$
 $\Delta z^1 \text{ max} = .0762 = 4.79\%$

TABLE 2(c)

MEASUREMENT OF SLOT WIDTH

400 x 40 x b x 4 TPI

Blade No	Width of Blade b mm	Width of Slot		$\frac{w}{z}$	$\frac{w^1}{z^1}$
		w mm	w ¹ mm		
1	1.885	2.6125	2.6125		
1	1.89	3.000	2.855		
1	1.94	3.0850	2.905		
1	1.88	2.7525	2.875		
Mean	1.89875	2.8625	2.8115	1.5075	1.4807
2	1.94	2.9875	2.8175		
2	1.96	3.015	2.8725		
2	1.94	2.995	2.875		
2	1.93	2.685	2.920		
Mean	1.9425	2.9206	2.87125	1.5035	1.4781
3	1.97	3.1275	3.127		
3	1.985	3.115	3.255		
3	2.01	3.515	3.125		
3	2.01	3.075	3.0925		
Mean	1.9937	3.2081	3.1498	1.609	1.5798
4	1.975	3.1425	3.0925		
4	1.97	3.305	3.1750		
4	1.99	3.035	3.2625		
4	2.01	3.07	3.150		
Mean	1.98625	3.1381	3.170	1.57991	1.5959
5	1.84	2.5425	2.7465		
5	1.83	2.3100	2.835		
5	1.86	2.865	2.740		
5	1.835	2.6775	2.545		
Mean	1.8412	2.5987	2.7166	1.4114	1.4754
6	2.02	2.825	2.955		
6	2.03	3.230	3.085		
6	2.02	3.390	3.100		
6	2.01	2.865	3.030		
Mean	2.02	3.0775	3.0425	1.52351	1.5061
Mean				1.52248	1.5193

$\Delta z \text{ max} = .11108 = 7.29\%$
 $\Delta z \text{ min} = .08652 = 5.68\%$

$\Delta z^1 \text{ max} = .0766 = 5\%$
 $\Delta z^1 \text{ min} = .0439 = 2.8\%$

TABLE 3

PERFORMANCE TESTING OF HACKSAW BLADES - DATA SHEET

SAW MACHINE: Wickstead 200 mm Hydraulic

CUTTING SPEED: 76 strokes/min

Dynamometer sensitivity
22.48 lbf/cm

BLADE SPECIFICATION: 400 x 40 x 2 x 6 Tpi

BLADE CONDITION: New

Saw stroke = 5.5 inches

CUTTING FLUID: Air

WORKPIECE MATERIAL: 25 x 25 mm, En 1a

Machine setting	(2)	(4)	(6)	(8)	(10)	(12)	
Area cm ²	92	89	105	127.15	163	213	
Mean height cm	5.75	5.56	6.56	7.96	10.18	14.59	
F _{Tm} lbf	129.26	124.98	147.46	178.94	228.8	327.96	
f _{Tm} lbf/mm/ tooth	10.77	10.415	12.28	14.91	19.06	27.33	
Time per cut secs	72	66	63	51	42	31	
N Strokes	91.2	83.6	79.8	64.6	53.2	39.3	
$\delta_a \times 10^{-3}$ mm	11.32	12.35	12.94	15.98	19.41	26.2	

Remarks:

TABLE 3a - APPENDIX B

	Number of blade teeth per 25 mm		
	10	6	4
The apparent coefficient of friction obtained from the model	0.77	0.70	0.67
The apparent coefficient of friction obtained from force measurement	0.77	0.73	0.72

THE APPARENT COEFFICIENT OF FRICTION OBTAINED FROM
THE MODEL AND FORCE MEASUREMENTS (24)

TABLE 4 - COST DATA FOR HYDRAULIC POWER HACKSAW

Cost per cut for a En 58J austenitic stainless steel workpiece,
75 mm diameter

Time utilization of the machine (%)	C ₁ (%)	C ₂ (%)	C ₃ (%)	C ₄ (%)	Total cost in pence per cut
20	4	61	18	17	39.0
40	3	45	27	25	26.2
60	2	36	32	30	22.0
80	2	30	35	33	19.9
100	1	26	38	35	18.6

Cost per cut for a En 44E steel workpiece, 75 mm diameter

Time utilization of the machine (%)	C ₁ (%)	C ₂ (%)	C ₃ (%)	C ₄ (%)	Total cost in pence per cut
20	6	69	20	5	24.2
40	5	56	31	8	15.0
60	4	47	39	10	12.0
80	3	40	46	11	10.5
100	3	35	50	12	9.5

C₁ = non-productive time cost per cut

C₂ = cutting time cost per cut

C₃ = total blade cost per cut

C₄ = scrap material cost per cut

COST DATA:

Cost of machine = £710

Cost of blade = £1.12

Cost of workpiece material

(i) En 44E = £145 per ton

(ii) En 58J = £790 per ton

Operators labour rate = 60p per hour

Annual weeks worked = 48

Hours worked by the plant = 40

Non-productive time = 30 sec

per cut

Cutting time per cut

(i) En 44E = 6 min

(ii) En 58J = 8.5 min

Time to change = 75 sec
blade

Width of cut = 2.35 mm

Blade life in
cuts

(i) En 44E = 24

(ii) En 58J = 16

The cost data shown in Table 4 above are based on a hydraulic power saw, a 400 mm x 40 mm x 2 mm x 4 TPI blade and two workpieces both 75 mm diameter, one is En 44E and the other is En 58J, austenitic stainless steel. The blade life and cutting time were obtained on a 6-7 load setting at a rotational speed of 104 strokes per minute.

It is assumed that the cost of the sawing machine is written-off over a period of 10 years and no interest is paid on the capital involved. The operators hourly labour rate is based on current semi-skilled rates, and it is assumed that he is operating two machines simultaneously; this assumption is believed to represent current trade practice. The workpiece is assumed to be manually clamped in the vice. All power and cutting fluid costs have been ignored.

WIDTH OF TOOL:- 3.385 mm

TOOL:- BLUNT (1A)

CUTTING SPEED:- 95 mm/min

CUTTING FLUID:- SULPHURISED OIL

WORKPIECE MATERIAL:- COPPER

LENGTH OF SPECIMEN:- 180 mm

CUTTING CONDITION:- GROOVE CUTTING

Test	Tool	Tool Radii mm	Nominal Set depth mm	Depth Measurement by Bridge Readings (mm)			Average Depth Bridge Readings (mm)	Mass of Chip (grms)	Depth Chip mass (mm)	F _c		F _T		Remarks
				A	B	C				mm	KN	mm	KN	
Q1	1A	0.51	0.1	0.076	0.078	0.076	0.0766	0.375	.068					
Q2	1A	0.51	0.1	0.104	0.108	0.108	0.1067	0.552	.100					
Q3	1A	0.51	0.1	0.116	0.123	0.122	0.120	0.638	0.115					
Q4	1A	0.51	0.1	0.116	0.117	0.118	0.117	0.587	0.106					
Q5	1A	0.51	0.1	0.118	0.110	0.110	0.113	0.593	0.107					
Q6	1A	0.51	0.1	0.12	0.115	0.116	0.117	0.623	0.113					
Q7	1A	0.51	0.1	0.12	0.12	0.118	0.119	0.604	0.109					
Q8	1A	0.51	0.1	0.113	0.113	0.116	0.114	0.595	0.108					

TABLE NO: 5 RESULTS OBTAINED FROM GROOVE CUTTING WITH A BLUNT TOOL (I)

WIDTH OF TOOL:- 3.385 mm

TOOL:- BLUNT (1A) CUTTING SPEED:- 95 mm/min CUTTING FLUID:- SULPHURISED OIL
WORKPIECE MATERIAL:- COPPER LENGTH OF SPECIMEN:- 180 mm CUTTING CONDITION:- GROOVE

Test	Tool	Tool Radii mm	Nominal Set depth mm	Depth Measurement by Bridge Readings (mm)			Average Depth Bridge Readings (mm)	Mass of Chip (grms)	Depth Chip mass (mm)	F _c		F _T		Remarks
				A	B	C				mm	KN	mm	KN	
R1	1A	0.51	0.25	0.258	0.262	0.258	0.259	1.313	0.24	STEADY NOT REACHED		STATE		SURFACE CUT Interesting chip*
R2	1A	0.51	0.25	0.25	0.25	0.252	0.251	1.346	0.246	28	2.8	22	2.2	
R3	1A	0.51	0.25	0.24	0.248	0.252	0.247	1.348	0.247	34	3.4	25.5	2.55	
R4	1A	0.51	0.25	0.265	0.255	0.258	0.259	1.386	0.254	34.53	3.45	26	2.6	
R5	1A	0.51	0.25	0.23	0.26	0.26	0.25	1.36	0.249	36.53	3.65	27	2.7	
	Total mass of workpiece before machining			= 948.8 grms										
	Total mass of workpiece after machining			= 940.75 grms										
	Total loss			= 8.05 grms										
	Total mass of chips			= 8.036 grms										
	Therefore Good Agreement													

TABLE NO: 6 RESULTS OBTAINED FROM GROOVE CUTTING WITH A BLUNT TOOL (II)

WIDTH OF TOOL:- 3.4 mm

TOOL:- 3A BLUNT

CUTTING SPEED:- 95 mm/min

CUTTING FLUID:- SULPHURISED OIL

GROOVE

WORKPIECE MATERIAL:- COPPER

LENGTH OF SPECIMEN:- 178 mm

CUTTING CONDITION:- CUTTINGS

Test	Tool	Tool Radii mm	Nominal Set depth mm	Depth Measurement by Bridge Readings (mm)			Average Depth Bridge Readings (mm)	Mass of Chip (grms)	Depth Chip mass (mm)	F _c		F _T		Remarks
				A	B	C				mm	KN	mm	KN	
V1	3A	0.56	0.2	0.16	0.169	0.166	0.165	0.878	0.161	SEE	Figure 69			Air gauge reading fluctuated ± 0.005 mm to ± 0.0075 mm
V2	3A	0.56	0.2	0.198	0.208	0.204	0.203	1.087	0.200					
V3	3A	0.56	0.2	0.216	0.216	0.215	0.215	1.128	0.208					
V4	3A	0.56	0.2	0.213	0.208	0.208	0.209	1.114	0.204					
V5	3A	0.56	0.2	0.206	0.211	0.21	0.209	1.075	0.205					
V6	3A	0.56	0.2	0.206	0.20	0.206	0.204	1.11	0.198					
						MEAN	0.201		0.196					

TABLE NO: 7 RESULTS OBTAINED FROM GROOVE CUTTING WITH A BLUNT TOOL (III)

```

DIMENSION MATERL(2)
C ** INPUT PROGRAM PARAMETERS
WRITE(6,98)
98 FORMAT(' TYPE WORKPIECE MATERIAL, <=8 CHARACTERS' )
99 READ(9,99)MATERL
FORMAT(2A4)
WRITE(6,100)
100 FORMAT('TYPE W,K,R,A0,A1,A2 IN FREE FORMAT' )
READ(9,*)W,XK,R,A0,A1,A2
C ** INITIALISE TEKTRONIX 4010 & CLEAR SCREEN
CALL T4010
CALL PICCLE
C ** PRINT PROGRAM PARAMETER SUMMARY
WRITE(6,110)
110 FORMAT(10X,'THEORETICAL RESULTS FROM SLIP LINE FIELD MODEL'
1/10X,46(' '))
WRITE(6,111)W,R,MATERL,XK
111 FORMAT(' TOOL WIDTH = ',F4.2,' MM TOOL RADIUS = ',F5.3,' MM'
1/' WORKPIECE MATERIAL = ',2A4,3X,'SHEAR YIELD STRESS = ',F4.0,
2' MN/M^2' )
WRITE(6,112)A0,A1,A2
112 FORMAT(' CHIP TOOL CONTACT LENGTH COEFFS:--'
1/' A0 = ',F7.3,5X,'A1 = ',F7.3,5X,'A2 = ',F7.3)
WRITE(6,101)
101 FORMAT(/3X,65(' ')/
13X,'* DELTA * PQ * ETA * FC *',
2' FT * FC/FT * ESP * ESR *',
3/3X,'*',25X,'(KN)',4X,'(KN)',11X,'(GN/M^2)',7X,'*')
4/3X,65(' '))
C ** CALCULATE & PRINT OUTPUT DATA
DO 1 I=1,10
DELTA=0.1*I*R
PQ=A0+A1*DELTA+A2*DELTA**2
A=1-DELTA/PQ

```



```

T=(-2+SQRT<4.-4.*(A**2-1.)>>)/(2.*(A+1.)>
ETA=2.*ATAN(T)
FC=((XK*(1.+2.*ETA))*PQ+(XK*R))*W/1000.
ET=((XK*(1.+2.*ETA))*R+(XK*PQ))*W/1000.
ETA=180./3.14159*ETA
RF=FC/FT
ESP=FC/(DELTA*W)
ESR=ESP/XK
WRITE(6,102)DELTA,PQ,ETA,FC,FT,RF,ESP,ESR
102  FORMAT(3X,'*',63X,'*',7(F6.3,2X),F6.3,1X,'*')
1  CONTINUE
WRITE(6,103)
103  FORMAT(3X,'*',63X,'*',3X,65('*'))
C ** WAIT FOR CHARACTER THEN RELEASE DEVICE & EXIT PROGRAM
CALL NPRMPT
READ(9,*)IQ
CALL DEVEND
CALL EXIT
END

```


THEORETICAL RESULTS FROM SLIP LINE FIELD MODEL

TOOL WIDTH = 3.40 MM TOOL RADIUS = 0.558 MM
WORKPIECE MATERIAL = COPPER SHEAR YIELD STRESS = 230. MM/M^2

CHIP TOOL CONTACT LENGTH COEFFS:-

A0 = 0.276 A1 = 14.132 A2 = -13.520

DELTA	PQ	ETA	FC	FT	FC/FT	ESP	ESR	(GN/M^2)	

0.055	1.023	3.046	1.321	1.283	1.030	6.964	0.030	*****	
0.112	1.685	3.679	1.923	1.810	1.063	5.069	0.022	*****	
0.167	2.263	4.095	2.459	2.268	1.084	4.321	0.019	*****	
0.223	2.757	4.469	2.929	2.660	1.101	3.859	0.017	*****	
0.279	3.167	4.849	3.332	2.987	1.116	3.512	0.015	*****	
0.335	3.492	5.259	3.669	3.247	1.130	3.223	0.014	*****	
0.391	3.734	5.719	3.939	3.443	1.144	2.966	0.013	*****	
0.446	3.891	6.246	4.142	3.574	1.159	2.729	0.012	*****	
0.502	3.964	6.865	4.279	3.640	1.175	2.506	0.011	*****	
0.558	3.952	7.607	4.348	3.643	1.193	2.292	0.010	*****	

THEORETICAL RESULTS FROM SLIP LINE FIELD MODEL

TOOL WIDTH = 3.40 MM TOOL RADIUS = 0.558 MM
 WORKPIECE MATERIAL = STEEL-PB SHEAR YIELD STRESS = 404. MN/M^2

CHIP TOOL CONTACT LENGTH COEFFS:-

A0 = 0.112 A1 = 3.995 A2 = -1.986

DELTA	PQ	ETA	FC	FT	FC/FT	ESP	ESR
			(KN)	(KN)	(GN/M^2)		
0.056	0.329	9.042	1.361	1.460	0.932	7.174	0.018
0.112	0.533	11.002	1.781	1.794	0.993	4.693	0.012
0.167	0.725	12.049	2.182	2.085	1.046	3.834	0.009
0.223	0.905	12.811	2.566	2.352	1.091	3.381	0.008
0.279	1.072	13.458	2.931	2.599	1.128	3.090	0.008
0.335	1.227	14.057	3.279	2.828	1.159	2.881	0.007
0.391	1.370	14.638	3.609	3.040	1.187	2.718	0.007
0.446	1.500	15.222	3.921	3.234	1.213	2.584	0.006
0.502	1.618	15.818	4.215	3.412	1.236	2.469	0.006
0.558	1.723	16.438	4.491	3.573	1.257	2.367	0.006

THEORETICAL RESULTS FROM SLIP LINE FIELD MODEL

TOOL WIDTH = 3.37 MM TOOL RADIUS = 0.812 MM
 WORKPIECE MATERIAL = COPPER SHEAR YIELD STRESS = 230. MN/M^2

CHIP TOOL CONTACT LENGTH COEFFS:-
 A0 = 0.039 A1 = 13.209 A2 = -10.602

* DELTA *	* PQ *	* ETA *	* FC *	* FT *	* FC/FT *	* ESP *	* ESR *
***** (GN/M^2) *****							
* 0.081	1.041	4.310	1.558	1.531	1.017	5.693	0.025
* 0.162	1.904	4.699	2.347	2.209	1.063	4.289	0.019
* 0.244	2.627	5.093	3.028	2.778	1.090	3.688	0.016
* 0.325	3.210	5.538	3.599	3.239	1.111	3.288	0.014
* 0.406	3.654	6.058	4.060	3.595	1.130	2.968	0.013
* 0.487	3.958	6.680	4.412	3.844	1.148	2.687	0.012
* 0.568	4.121	7.440	4.654	3.987	1.167	2.429	0.011
* 0.650	4.145	8.395	4.784	4.027	1.188	2.185	0.010
* 0.731	4.030	9.629	4.803	3.964	1.211	1.950	0.008
* 0.812	3.774	11.291	4.708	3.803	1.238	1.720	0.007

THEORETICAL RESULTS FROM SLIP LINE FIELD MODEL

TOOL WIDTH = 3.37 MM TOOL RADIUS = 0.812 MM
WORKPIECE MATERIAL = COPPER SHEAR YIELD STRESS = 230. MN/M^2

CHIP TOOL CONTACT LENGTH COEFFS:-

A0 = 0.091 A1 = 13.812 A2 = -11.859

*****											*****										
* DELTA * PQ * ETA * FC * FT * FC/FT * ESP * ESR *											* (GN/M^2) *										
*****											*****										
* 0.081	1.134	3.968	1.630	1.596	1.022	5.958	0.026					* 0.162	2.021	4.436	2.439	2.293	1.063	4.456	0.019		
* 0.244	2.752	4.871	3.125	2.869	1.089	3.807	0.017					* 0.325	3.326	5.353	3.689	3.325	1.110	3.370	0.015		
* 0.406	3.744	5.919	4.131	3.661	1.128	3.019	0.013					* 0.487	4.005	6.604	4.449	3.879	1.147	2.710	0.012		
* 0.568	4.110	7.460	4.645	3.979	1.167	2.425	0.011					* 0.650	4.059	8.563	4.716	3.964	1.190	2.154	0.009		
* 0.731	3.851	10.046	4.661	3.835	1.215	1.893	0.008					* 0.812	3.487	12.150	4.478	3.599	1.244	1.637	0.007		
*****											*****										

Appendix C

ANALYSIS OF THE EFFECTS OF BLADE TENSION

The distribution of stress in a hacksaw blade under the action of the cutting force components and the applied tensile load the cross-section of the blade is subjected to the combined action of a bending moment and a longitudinal load. The stress distributions due to these loads and their combinations is shown in figure 33.

Notation

- b = breadth of the blade
- d = effective depth of the blade, ie the actual depth minus the depth of the teeth
- E = Young's modulus
- e = displacement of the neutral axis of bending from the centre of the cross section of the blade.
- F_t = instantaneous thrust (or vertical) component of the cutting force
- f = frequency
- I = second moment of area
- L = effective length ie the free length between the blade end supports
- M = bending moment
- N = number of teeth in one set pattern
- n = number of teeth per unit length of the blade
- P = tensile load
- RPM = revolutions per minute of the sawing machine

S = stroke of the saw
 U = tensile factor, defined in the text
 V = cutting velocity
 W = applied load
 w = load per unit length of the blade
 y = vertical distance from the centre of the cross section of the blade
 δ = deflection
 ϕ = deflection factor, defined in the text
 σ = longitudinal stress

The longitudinal stress acting at any distance from the centre section of the blade is

$$\sigma = \frac{12 My}{bd^3} + \frac{P}{bd}$$

At the neutral axis of bending this stress is zero and hence

$$e = \frac{P}{M} \cdot \frac{d^2}{12}$$

This shows that the neutral axis of bending is displaced towards the cutting edge of the blade by an amount which depends on the ratio of the tensile load to the bending moment. A typical position of the neutral axis is shown in Fig 33(b).

(ii) Blade end supports

Before blade deflections and stiffnesses can be estimated it is necessary to know the method of holding the blade at its ends and the extent to which the holding device restrains blade movement.

It is normal for the blade to be held by a pin which passes through the end hole and for the blade to be clamped between side plates. The effect of this method of fixing is to give greater support to the blade in the lateral than the vertical direction. It will be assumed in what follows that the blade is simply supported in the vertical plane and built-in in the lateral plane.

(iii) Vertical Deflection and Stiffness of the Blade

For simplification it will be assumed that the thrust force component of the cutting force is concentrated and acts at the centre of the blade. This gives the most severe loading condition that the blade will experience. The ends will be assumed simply supported. Fig 34(a) shows this configuration together with the equations for central deflection (δ_{\max}). As the central deflection for a simply supported beam loaded at the centre but without longitudinal tension is:

$$\delta_{\max} = \frac{WL^3}{48EI} \quad \text{when } P = 0$$

the factor ϕ gives the reduction in deflection due to the application of tension. Fig 35 shows the variation of the deflection factor ϕ , against the tension factor U . The reason why deflection is reduced by the application of tension is that it introduces an additional bending moment which opposes these moments produced by the vertical loads. Fig 36 shows the determination of Young's Modulus for the M2 high speed steel used in the manufacture of Brand X saw blades. Fig 37 shows the tension induced in a Brand X

400 x 40 x 2 x 6 TPI blade against the turns of the tension nut for the Wicksteed Hydromatic machine.

The vertical stiffness of the blade is given by:

$$\text{Stiffness} = \frac{W}{\delta_{\max}} = \frac{48EI}{L^3 \phi_1}$$

Sample Calculations based on the Brand X 400 x 40 x 2 x 6 TPI blade and the Wicksteed power saw

Data: $d = 37.5 \text{ mm}$

$b = 2.0 \text{ mm}$

$L = 400 \text{ mm}$

$E = 198.7 \text{ GNm}^{-2}$ (M2, high speed steel)

$P = 7.5 \text{ kN}$, produced by approximately one turn of the tension nut

$$U = \sqrt{\frac{PL^2}{4EI}} \text{ when } I = \frac{bd^3}{12} = \frac{2 \times (37.5)^3 \times 10^{-12}}{12} = 8.78 \times 10^{-9} \text{ m}^2$$

$$\therefore U = \sqrt{\frac{7.5 \times 10^3 \times 0.4^2}{4 \times 198.7 \times 10^9 \times 8.78 \times 10^{-9}}} = 0.415$$

From Fig 35 $\phi = 0.88$ or 88%. This shows that under the tension used in the example the deflection is reduced to 88% of its un-tensioned value.

$$\text{Stiffness} = \frac{48 \times 198.7 \times 10^9 \times 8.78 \times 10^{-9}}{(0.4)^3 \times 0.88} = 1.487 \times 10^6 \frac{\text{N}}{\text{m}}$$

The mid-stroke thrust load produced by the Wicksteed power saw on load setting No 8 is 250 lbf (1112 N). The maximum deflection of the Brand X 6 TPI blade under the action of

this load is,

$$\delta_{\max} = \frac{W}{\text{Stiffness}} = \frac{1.112 \times 10^3}{1.487 \times 10^6} = 0.748 \text{ mm (0.0295 in)}$$

Experimentally determined vertical stiffnesses are shown in fig 38. These are smaller than those predicted by the above theory. The difference is believed to be due to movement of the blade ends under load. However, the change in stiffness due to increase in blade tension agrees well with the above theory.

- (iv) Lateral stiffness and natural frequency of the blade
- As the main use of the lateral stiffness will be in natural frequency calculations the load is considered uniformly distributed to simulate the distribution of mass along the length of the blade. The ends of the blade will be assumed to be built-in. Fig 34(b) shows this configuration together with the equations for the central deflection. The factor ϕ_2 again gives the reduction in deflection due to the application of tension and is shown in fig 35. The lateral stiffness will be taken to be,

$$\text{stiffness} = \frac{WL}{\delta_{\max}} = \frac{384EI}{L^3\phi_2}$$

The most convenient method for determining the natural frequency of lateral vibration is to consider the mass of the blade to be concentrated at its centre. The natural frequency is then given by,

$$f = \frac{1}{2\pi} \sqrt{\frac{\text{stiffness}}{\text{effective mass}}}$$

where the effective mass is one half of the actual mass of the blade.

Sample Calculations based on the Brand X 400 x 40 x 2 x 6 TPI blade and the Wicksteed power saw

Data: $d = 12 \text{ mm}$

$b = 37.5 \text{ mm}$

$L = 400 \text{ mm}$

$E = 198.7 \text{ GNm}^{-2}$ (M2, high speed steel)

$P = 7.5 \text{ kN}$, produced by approximately one turn of the tension nut

$$I = \frac{bd^3}{12} = \frac{37.5 \times (2)^3 \times 10^{-12}}{12} = 25 \times 10^{-12} \text{ m}^4$$

$$U = \sqrt{\frac{PL^2}{4EI}} = \sqrt{\frac{7.5 \times 10^3 \times (0.4)^2}{4 \times 198.7 \times 10^9 \times 25 \times 10^{-12}}} = 7.78$$

From fig 17 $\phi = 0.148$ or 14.8%

$$\text{Stiffness} = \frac{384 \times 198.7 \times 10^9 \times 25 \times 10^{-12}}{(0.4)^3 \times 0.148} = 201.38 \times 10^3 \frac{\text{N}}{\text{m}}$$

The mass of the Brand X 6 TPI blade is 0.236 kg, therefore,

$$f = \frac{1}{2\pi} \sqrt{\frac{201.38}{0.118}} = 208 \text{ cs}^{-1}$$

Fig 39 shows the experimentally determined natural frequency and its variation with blade tension. It is seen that at a tension of 7.5 kN the measured natural frequency is approximately 180 cs^{-1} .

- (v) Forcing frequency due to engagement and disengagement of the blade teeth

Suppose the set pattern given to the blade teeth was periodic along its length and the number of teeth in one complete pattern was N^1 , then the lateral forcing frequency due to engagement and disengagement of teeth becomes

$$f = \frac{Vn}{N^1}$$

Since the cutting velocity (V) undergoes variation in which the maximum value is

$$V_{\max} = \frac{\text{RPM}}{60} \cdot 2\pi R = \frac{\text{RPM}}{60} \cdot \pi S \therefore f_{\max} = \frac{V_{\max} \cdot n}{N^1}$$

Sample calculations for the Wicksteed Hydromatic

Data: RPM = 140

S = 140 mm

n = 240 teeth per metre (6 TPI)

$$\therefore f_{\max} = \frac{140 \times \pi \times .140 \times 240}{60 \times N^1} = \frac{242}{N^1} \text{ cs}^{-1}$$

- (a) Frequency due to the engagement and disengagement of individual teeth ie.

$N^1 = 1$ is

$$f_{\max} = 242 \text{ cs}^{-1}$$

- (b) Frequency due to alternate set eg right-left-right set, ie $N^1 = 2$ is

$$f_{\max} = 121 \text{ cs}^{-1}$$

- (c) Frequency due to the Raker set right-centre-left-centre set, ie $N^1 = 4$ is

$$f_{\max} = 60 \text{ cs}^{-1}$$

- (vi) Blade resonance or chatter due to engagement and disengagement of the blade teeth

A blade is not likely to vibrate with its fundamental lateral frequency as calculated above since the presence of the workpiece must establish a nodepoint somewhere along the blade length. With the workpiece at the centre of the blade a second node of vibration is possible having a frequency four times greater than the fundamental frequency shown in fig 39.

The frequency for this mode of vibration considering the Wicksteed machine, the Brand X 400 x 40 x 2 x 6 TPI blade and a tension of 5.0 kN becomes

$$f = 4 \times 140 = 560 \text{ cs}^{-1}$$

Assuming a blade with an alternative set pattern, ie $N = 2$ and of similar proportions to the Brand X 6 TPI blade, the rotational speed of the machine needed to achieve this frequency would be

$$\text{RPM} = \frac{560 \times 60 \times 2}{\pi \times 0.140 \times 240} = 631$$

As this rotational speed is large compared with the maximum used with commercial power hacksawing machines it is tempting to conclude that a hacksaw blade of the proportions considered would be dynamically stable at normal operating

speeds. However, work carried out on other types of machine tools show that chatter can be achieved at frequencies of $1/2$, $1/3$, $1/4$ etc of the fundamental frequency, hence at rotational speeds of 315, 210, 159 RPM etc.

A more extensive dynamic analysis would enable these chatter frequencies and their resulting amplitudes of vibration to be determined more accurately. Even if blade fracture was not produced by lateral blade chatter the surface finish of the cut would be badly affected.

APPENDIX D

Simulation of the cutting action of a single hacksaw blade tooth

M. Sarwar and P. J. Thompson

SUMMARY

The cutting action of tools with very large cutting edge radii has been investigated. These actions have been classified according to the types of chips formed and the variations in the thrust and cutting components of the cutting force obtained. The discussion includes a summary of the implications of the results obtained to the cutting action of power hacksaw blades.

Introduction

Rubenstein, Groszman and Koenigsberger¹ have shown that ploughing occurs when using a sharp single point orthogonal cutting tool when the rake angle is negative and coincides with the shear plane angle. During ploughing part of the material in front of the cutting tool is compressed and elastically recovers and part is plastically deformed to spread sideways without separating from the bulk. Thus no material is removed from the workpiece.

Other researchers^{2,3,4} have shown that some ploughing can take place when using a single point tool of finite sharpness. In this cutting action some of the material in front of the tool forms a chip and is removed, whilst some is compressed by the cutting edge radii to recover elastically as the tool passes. In addition to the conventional force diagram of the orthogonal cutting process these researchers have developed a more complete force diagram which separates the chip tool interface force, from the ploughing forces due to the radius of the tool. This work was carried out with large depths of cut compared with

the cutting edge radius of the tool. The cutting edge radius was estimated to be in the order $7.62\text{ }\mu\text{m}$ – $15.24\text{ }\mu\text{m}$ and the depths of cut greater than $127\text{ }\mu\text{m}$. Under these conditions it was concluded that the ploughing force due to the cutting edge radius was insignificant.

Kregelski⁵ in his work on abrasive wear has considered the transition between different deformation modes of a surface loaded by a spherical sliding indenter. The depth of indentation was small compared with the radius of the indenter and Kregelski concluded that for most surfaces, plastic conditions are established under light loads. He also discussed the transition from plastic indentation to a process involving 'piling up' in front of a spherical indenter being pushed along a surface, virtually 'cutting or tearing'.

Previous work on metal cutting has not dealt with the situation where the depth of cut is far less than the cutting edge radius, a situation known to exist in some metal cutting processes.

Current work on power hacksawing has shown that the depth of cut achieved per tooth is small compared with the cutting edge radius even when the blade is new. Fig. 1 shows the geometry of a single tooth in a power saw blade. The cutting edge radii have been found to be in the range $20\text{ }\mu\text{m}$ – $76\text{ }\mu\text{m}$ for blades of various pitch of teeth. The depth of cut achieved per tooth has been found to be $2\text{--}30\text{ }\mu\text{m}$, depending on the thrust load applied by the saw frame.

This has led to an interest in the cutting action of a tool



M. Sarwar studied mechanical engineering at the Thames Polytechnic (formerly Woolwich Polytechnic) London, and was awarded an honours degree at London University in 1968. In the same year he entered the machine tool engineering division of the Department of Mechanical Engineering UMIST for post-graduate studies. During this period he carried out research into problems associated with dynamic testing of machine tools. After completing his MSc in January 1970, he worked in manufacturing for International Harvester Company of Great Britain for approximately two years. In 1971, Mr Sarwar entered the Department of Mechanical and Production Engineering, Sheffield Polytechnic, as technical officer for James Neill (Services) Ltd, Sheffield, carrying out research into the mechanics of sawing. He was appointed to his present post as lecturer in production technology in 1973.



P. J. Thompson, commenced his engineering education in 1953 as an apprentice development engineer with Messrs Accles & Pollock Ltd. In 1956 he was awarded a Whitworth Society Prize on the results of the Ordinary National Certificate examinations, and a Tube Investments student apprenticeship. He studied mechanical engineering at the College of Advanced Technology, Birmingham, and was awarded a first class honours degree.

After completing four years as a lecturer at the Harris College, Preston, he joined the UKAEA as a senior scientific officer in 1965. Whilst at the UKAEA he worked on the development of hydrostatic extrusion, and obtained an MSc, by research, as an external student of the University of Aston in Birmingham. Following a further two-year period as a senior lecturer at the Harris College, Preston, he obtained his present post as principal lecturer in production technology at Sheffield Polytechnic. His main research interests are the mechanics of metal cutting during sawing operations, intermittent metal cutting and lubrication of wire drawing. He has been a consultant to James Neill (Services) Ltd, Sheffield, since 1970.

having a larger cutting edge radius than the depth of cut. It appears that with this geometric arrangement the action of 'ploughing' and 'piling up' combine to give an unusual cutting action. It is believed that this action can be applied to operations other than power hacksawing, such as filing, cold chiselling, scraping and possibly grinding.

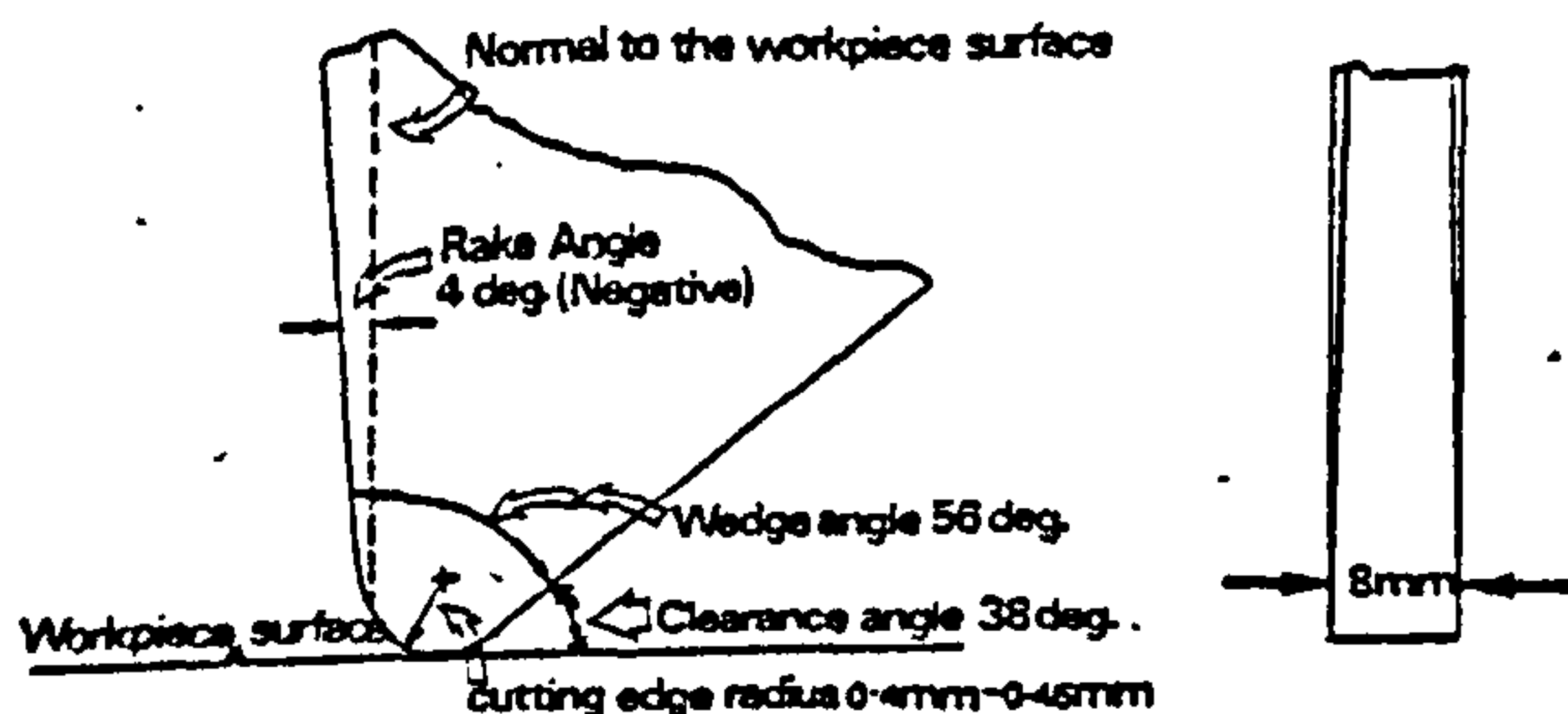


Fig. 1. Tool-cutting edge geometry.

Instrumentation and testing

The cutting tests were carried out on a universal milling machine suitably modified to hold the tool, in order to obtain steady-state orthogonal cutting conditions. The workpiece material was bolted to the top plate of a three component dynamometer which was secured to the worktable of the milling machine. Only two components of the dynamometer were used, namely the cutting force component F_c , and the thrust force component F_t . The two outputs from each channel of the dynamometer were simultaneously displaced via amplifiers on to an ultra-violet recorder.

Cutting tool

A standard orthogonal tool made from 18:4:1 high-speed steel and 15mm square was used. The geometry was (Fig. 1):

rake angle:	-4 deg.
wedge angle:	56 deg.
clearance angle:	38 deg.
cutting edge radius:	0.406mm.

A radius was ground on to the cutting edge and measured with an optical projector. Finally, in order to give the cutting tool the surface finish similar to that of a saw blade tooth, the surface of the cutting tool was oxidised by heat treatment.

Workpiece metals

- 1 **Aluminium:** HP 30M. As rolled condition
BS 1477, 0.7Mn, 1.0Si, 0.8mg.
85 VHN
 - 2 **Mild steel:** En1A type Bright drawn, 178-182 VHN
 - 3 **Copper sheet BS 1172** Cu: 99.85%
Fe: 0.03, P: 0.013, Pb: 0.01,
As: 0.05
Ni: 0.1, VHN: 64-68
 - 4 **Brass:** 60Cu-40Zn.
 - 5 **Lead:** Commercial, as received.
- Workpiece dimension: 145mm x 145mm x 15mm.

Cutting test results

Cutting tests were carried out using workpieces made from the metals listed above at depths of cut ranging from 0.02mm to 0.2mm and cutting speeds of 32mm/min and 3.34m/min. During each test the thrust and cutting components of the cutting force were recorded against time, as the cutting speed was constant the time axis was proportional to the cutting tool displacement. Some results

of these tests are shown in Figs. 2, 3, 4 and 5. It was found that cutting actions observed could be classified into three groups:

- a metal removal by a ploughing and 'piling up' action;
- b metal removal by ploughing and continuous or segmented chip formation; or
- c metal removal by a combination of a and b.

Metal removal by a combination of ploughing and 'piling up' was obtained when cutting the copper workpiece, Fig. 2 shows a result from these tests obtained at a depth of cut 0.12mm and at a speed of 3.34m/min. These tests show that, due to the very high negative rake at the extreme cutting edge radius workpiece material is initially heavily deformed and some is displaced sideways, indicating a ploughing action. As cutting begins there is an accumulation of material in the sector enclosed by the envelope of the cutting edge radius, the point of contact of the tool and the surface of the workpiece to form a built up edge effect. As cutting progresses metal 'piles up' as indicated

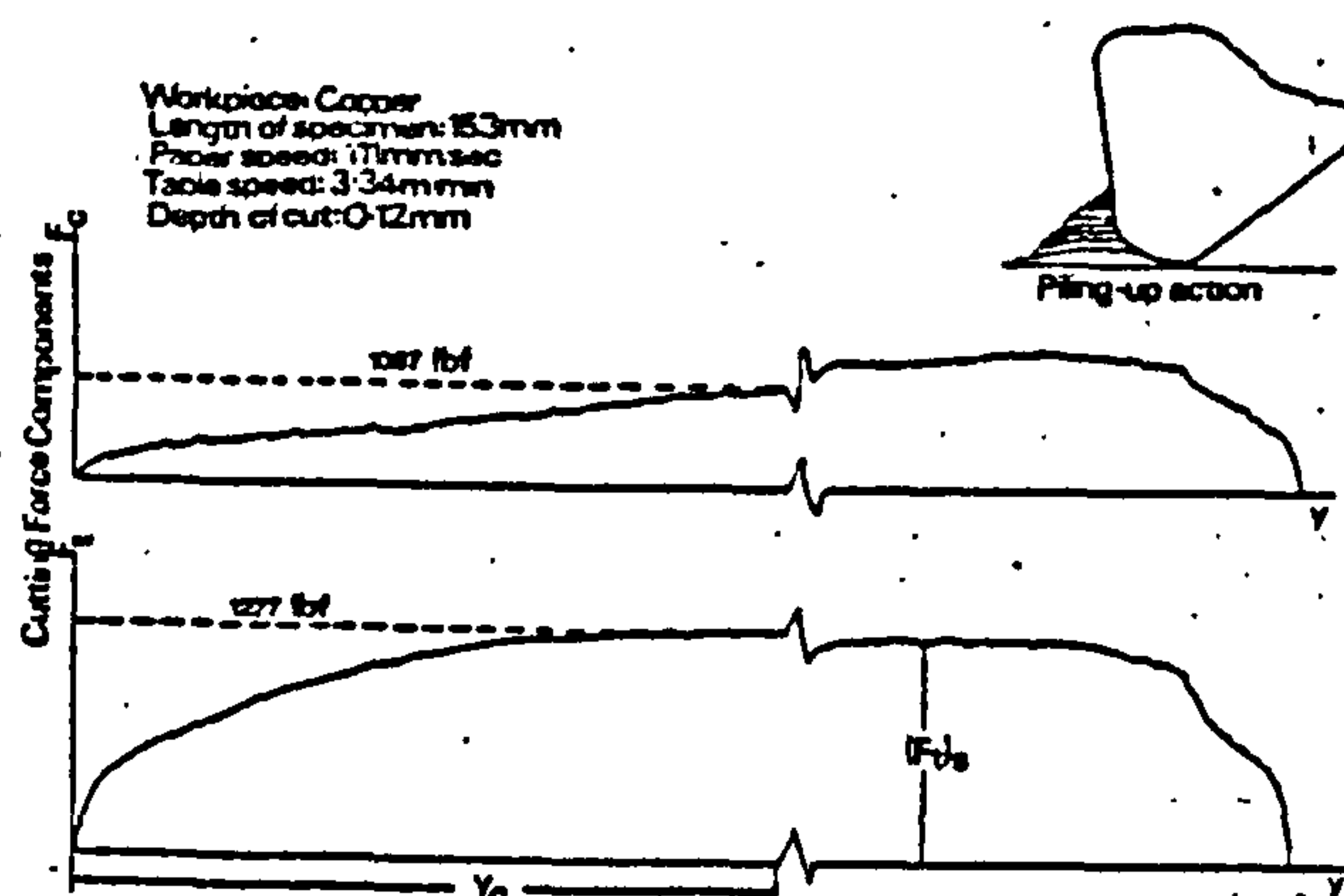


Fig. 2. Piling-up action.

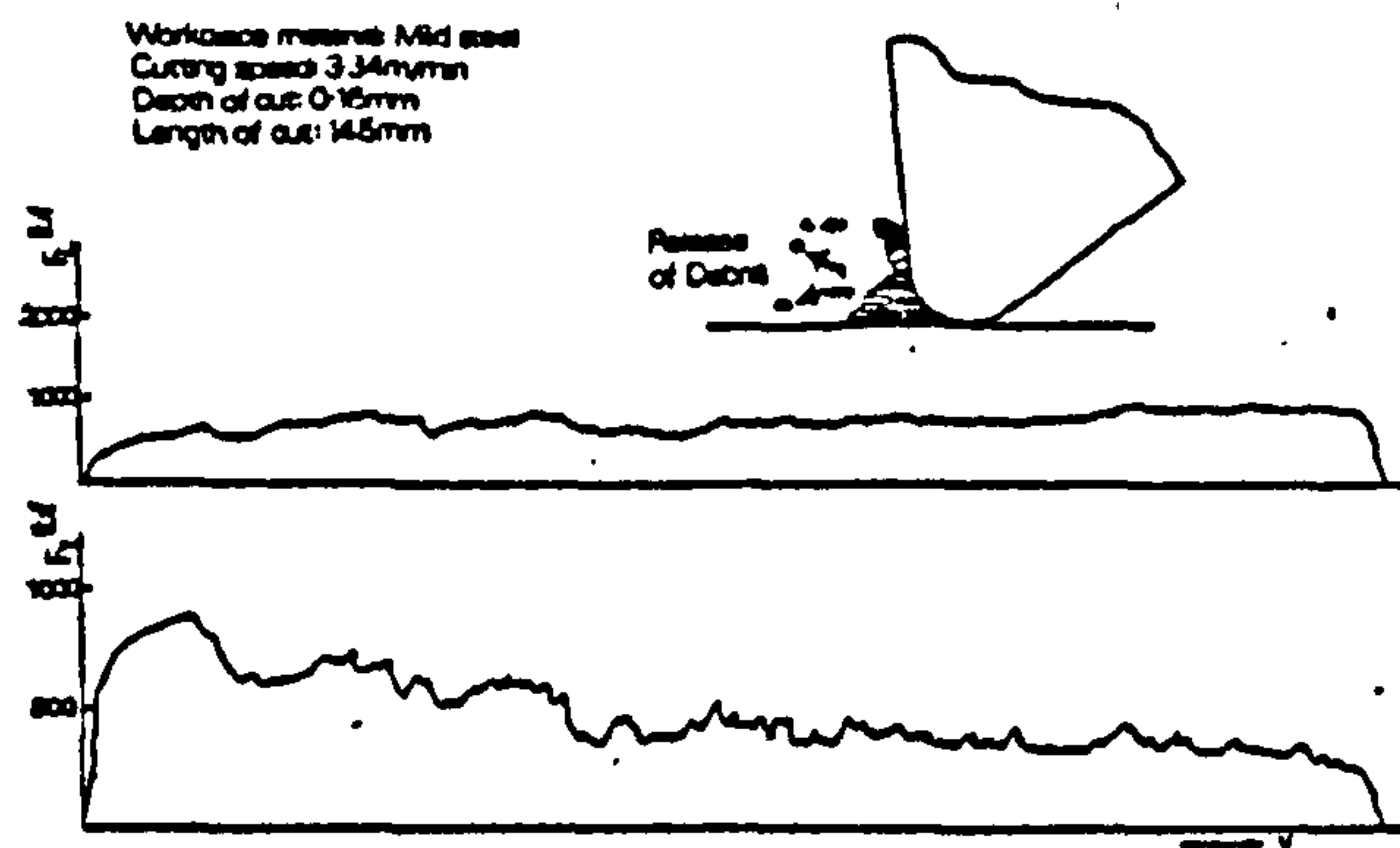


Fig. 3. Discontinuous piling-up action.

in Fig. 2, and also shown in Figs. 6 and 7. This piling-up action continues resulting in a very heavily compressed chip. Results of this type of action show that there exists transient build up of the thrust force over an initial distance y_0 corresponding to the formation of the chip by the 'piling up' action. When the chip is fully formed the thrust force reaches a steady value, which is then maintained for the remainder of the cut. Fig. 8 shows an analysis of the transient state of the build up of the thrust force component for various depths of cut. It can be seen that there exists a relationship between the instantaneous thrust force and steady state thrust force, for the transient state:

$$\frac{(F_T)_i}{(F_T)_s} = \left(\frac{y}{y_0}\right)^n \dots\dots\dots (1)$$

for $y \leq y_0$ and n from graph = 0.35.

Where $(F_T)_i$ = instantaneous thrust force at any point in the transient state; and y = corresponding distance travelled by the cutting tool.

$(F_T)_s$ = steady state value of the thrust force component; and y_0 = corresponding distance travelled by the cutting tool to produce a fully formed chip, i.e. when $y \geq y_0$ $(F_T)_i = (F_T)_s$.

The intercept at zero depth of cut (Fig. 9) gives the tool nose or ploughing force which confirms the results obtained by previous researchers^{6,7}. Although the magnitude of this force is relatively high, it may be explained to be due to the extremely large cutting edge radius.

Metal removal by a combination of ploughing and segmented chip formation was observed when cutting both mild steel and aluminium. This action was accompanied by the release of small particles of metal in the form of debris. The variation in the thrust force component showed a very

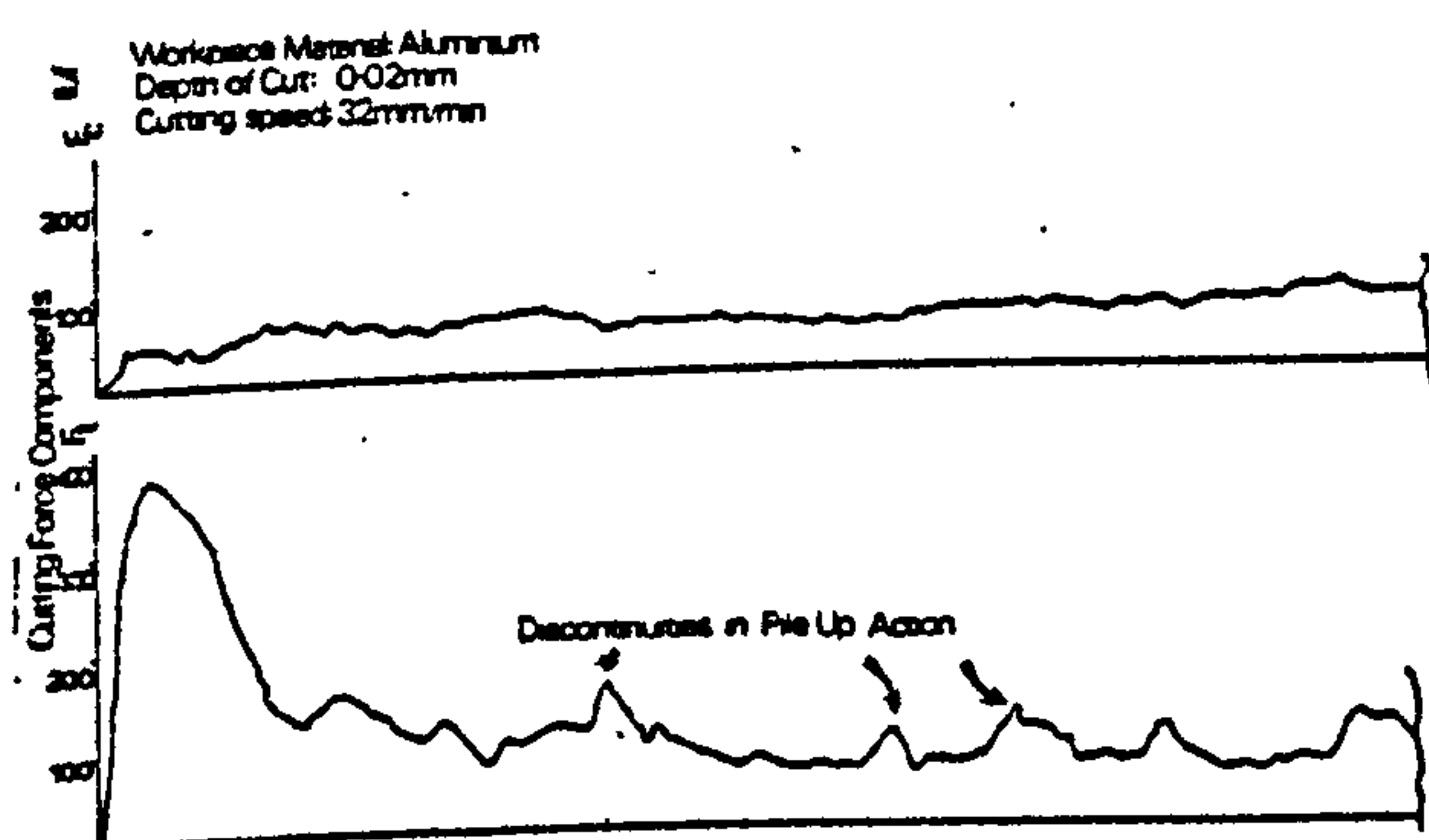


Fig. 4. Discontinuous piling-up action.

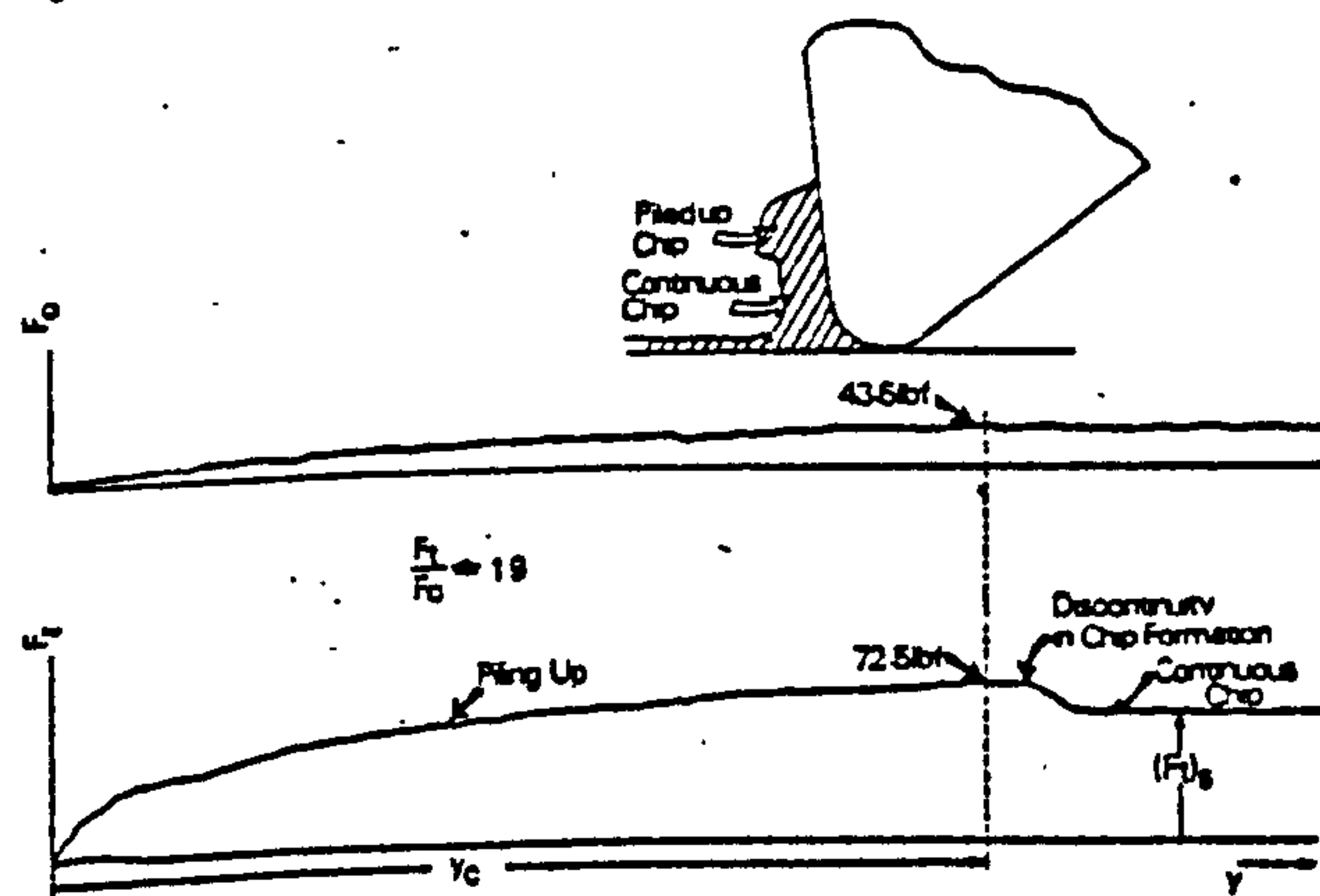
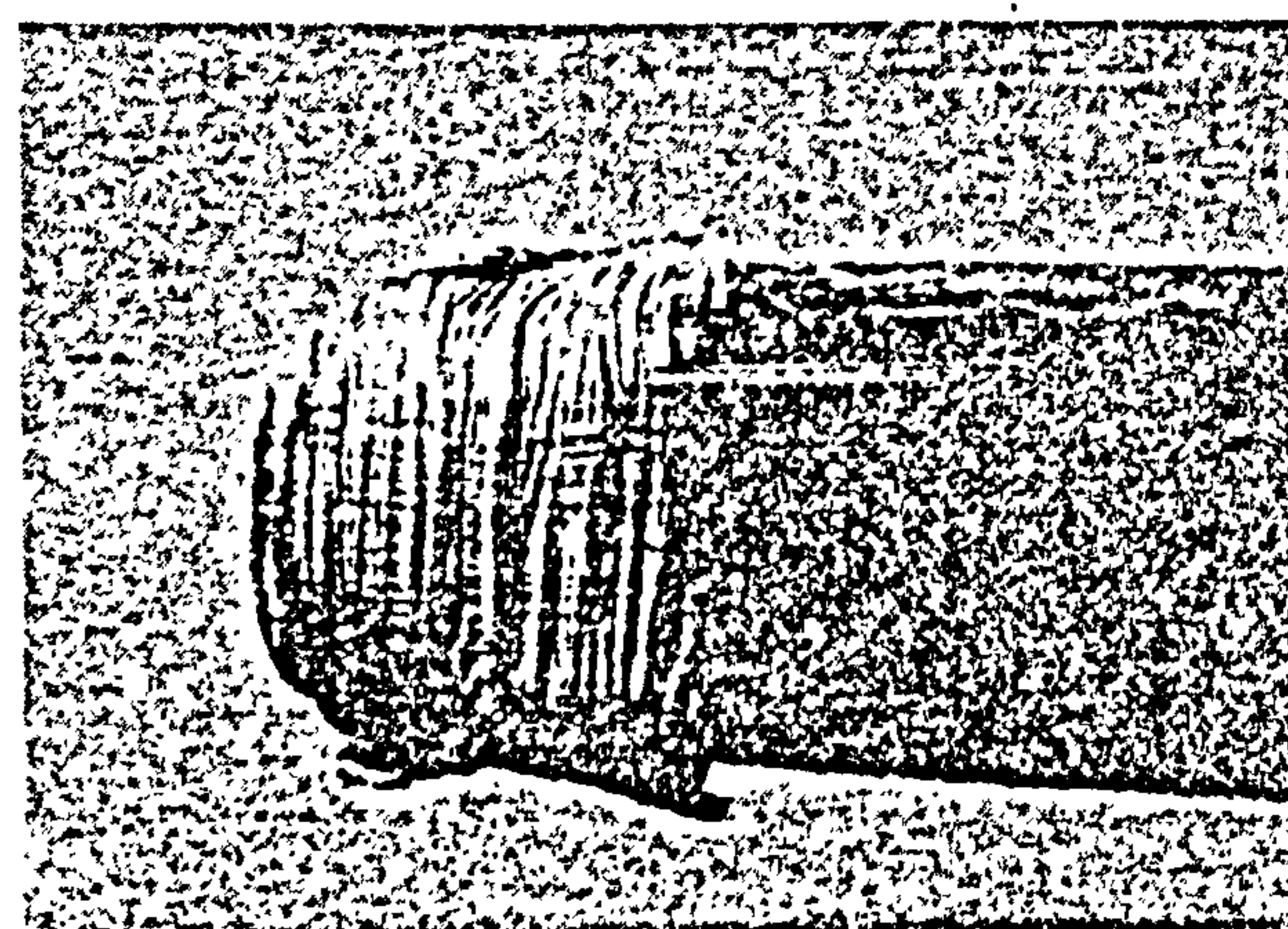
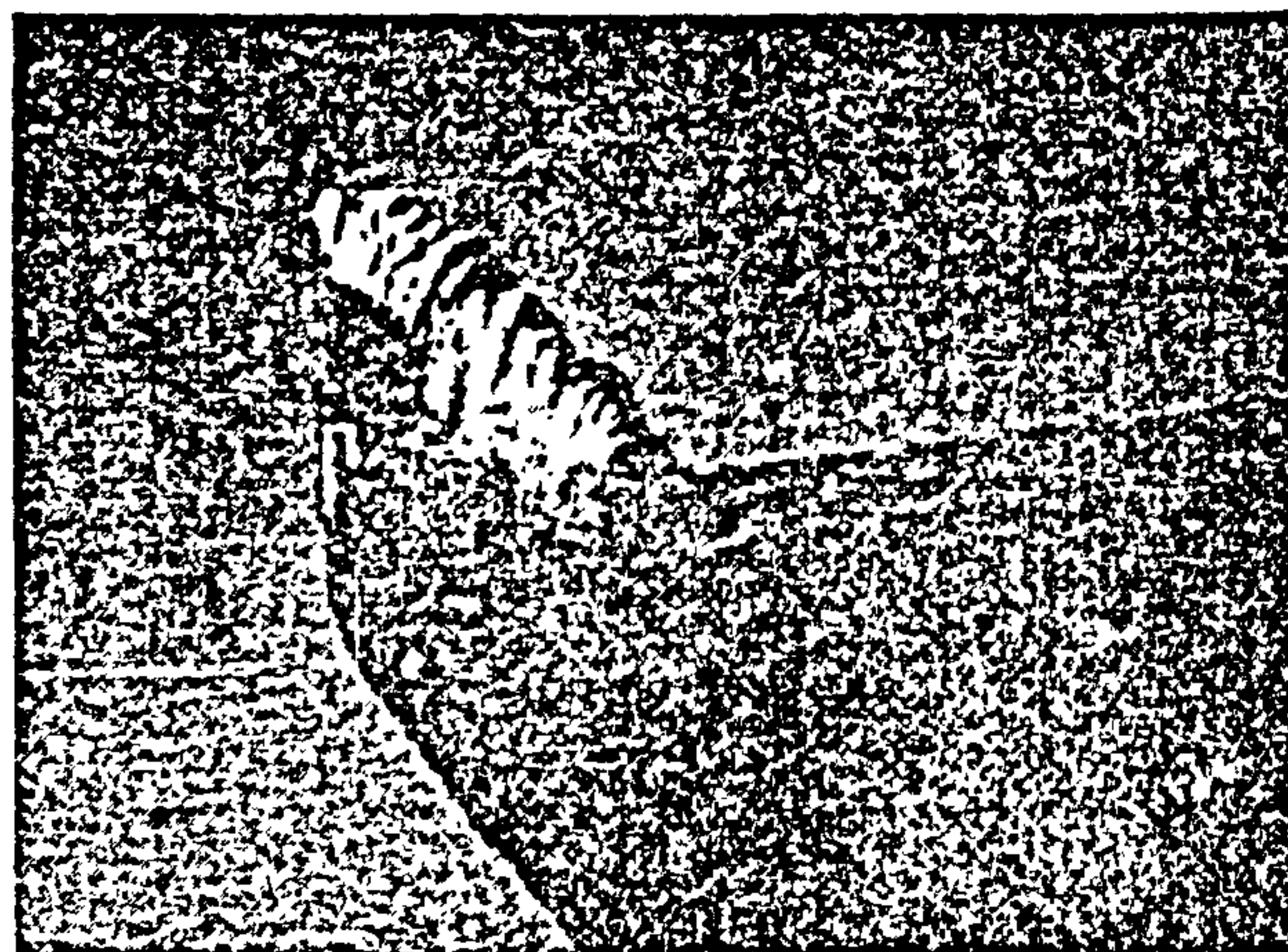


Fig. 5. Piling-up action leading to continuous chip formation. (Workpiece: lead; depth of cut: 0.12mm; cutting speed: 32mm/min.)

rapid initial increase followed by a gradual decay to an approximately steady value. The cutting force components, however, gradually increase throughout the cut, the total length of cut made was 145mm. The effects may be seen in Figs. 3 and 4. The surface finish produced by this cutting action was very poor.

Metal removed by a combination of ploughing, 'piling up' and a 'continuous' type of chip formation was obtained when cutting lead. The initial metal cutting action produced by the metal piling up in front of the tool, is similar to that obtained with copper. This piling up action abruptly ended and gave way to a conventional continuous chip formation. The rapid transition was associated with a fall in the thrust force component of the cutting force and a decrease



Figs. 6 and 7. Pile-up as cutting progresses.

in the chip thickness. These effects are shown in Fig. 5. During the early stages when piling up was occurring the thrust component of the cutting force gradually increased, in a similar manner to the increase obtained with copper.

Discussion

It has been shown that the cutting action of a tool having a large cutting edge radius involves complex combination of modes of chip formation previously observed with sharp cutting tools. Ploughing, as previously defined by Rubenstein, Grozman and Koenigsberger, plays an important role in the three cutting actions observed. The important difference between these actions and the action of sharp cutting tools lies in the way in which metal removal is achieved. The principal method is by an action which Kregelski called 'piling up'. This involves the gradual accumulation of material in front of the tool until a type of chip is formed. With metals which lack ductility the piling up action can lead to a form of segmented chip formation so that the metal is removed in the form of small chip segments and debris.

Another distinguishing feature of the type of cutting action investigated is the high value of the thrust component of the cutting force compared with the cutting component. In addition, considerable variation in the thrust component occurred at the beginning of each cut. In the piling-up action the thrust-load gradually increases until a steady state has been reached. This steady state is associated with the termination in growth of contact between the chip and the tool. The tool has to progress along the cut for a considerable distance compared with the depth of cut before the steady state condition is achieved.

This has a significant effect on the cutting action of a multi-point cutting tool such as a power hacksaw blade.

As previously described the geometry at the tip of each blade tooth is similar to that which gives rise to the complex metal cutting action observed in the tests. Metal removal by sawing is achieved by applying a thrust load to the blade, this is shared between all the teeth in contact with the workpiece. The actual depth of cut achieved depends on the metals involved and the geometries of both the blade and the workpiece, but is proportional to the applied thrust load and is equal for all the teeth in contact. The thrust load variations obtained during the tests when a 'pile-up' action was observed indicate that for the hacksaw blade teeth which have just commenced their cutting action, the thrust load per tooth will be small compared with the load acting on the teeth which have achieved a longer length of cut. It follows that the thrust load per hacksaw blade tooth is not uniform along the length of contact with the workpiece. This gives rise to the size effect observed when sawing workpieces of different widths. If the width of the workpiece is smaller than the distance needed for each tooth to fully establish a chip, the thrust-load per tooth will never obtain the relatively high steady state values observed in these tests and hence the depth of cut achieved will be larger for given applied load. As the width of the workpiece is increased the effect of this transient build up of thrust load becomes less significant since more teeth will be associated with a fully-developed chip and hence the depth of cut achieved will be small for a given applied thrust load.

REFERENCES

1. Rubenstein, C., Groszman, F. K., Koenigsber, F., *Proc., Int., Industrial Diamond Conf.*, Oxford, 1968. 'Force Measurements during cutting tests with single point tools simulating the action of a single abrasive grit.'
2. Albrecht, P., *Transactions of the ASME, Journal of Engineering for Industry*, 'New developments in the theory of Metal Cutting Part 1. The ploughing process in metal cutting,' p. 348, Nov. 1960.
3. Connolly, R., Rubenstein, C., *Inst. J. Mach. Tool. Des. Res.*, 'The Mechanics of Continuous chip formation in orthogonal cutting,' Vol. 8, pp. 159-187.
4. Masami Masuko, *Trans. Society of Mechanical Engineers (Japan)*, Vol. 19, 153, pp. 32-39. 'Fundamental Researches on the Metal Cutting. 1. A new Analysis of Cutting Force'.
5. Kregelski, X., *Friction and Wear*, London, Butterworth's Press, 1965.
6. Albrecht, P., *Transactions of the ASME*, p. 343, No. 1960. 'New developments in the theory of the Metal-Cutting Process. Part 1. The ploughing process in Metal cutting'.
7. Wallace, P. W. and Boothroyd, G., *Journal Mech. Eng. Science*, Vol. 6, No. 1, 1964. 'Tool Forces and Tool Chip Friction in orthogonal machining'.
8. Wallace, P. W., Boothroyd, G., *Journal Mech. Eng. Science*, Vol. 6, No. 1, 1964. 'Tool Forces and Tool Chip Friction in orthogonal machining'.
9. Zorev, N. N., *Proc. I. Mech. E. Conference on the Technology of Engineering Manufacture*, p. 255, 1958.

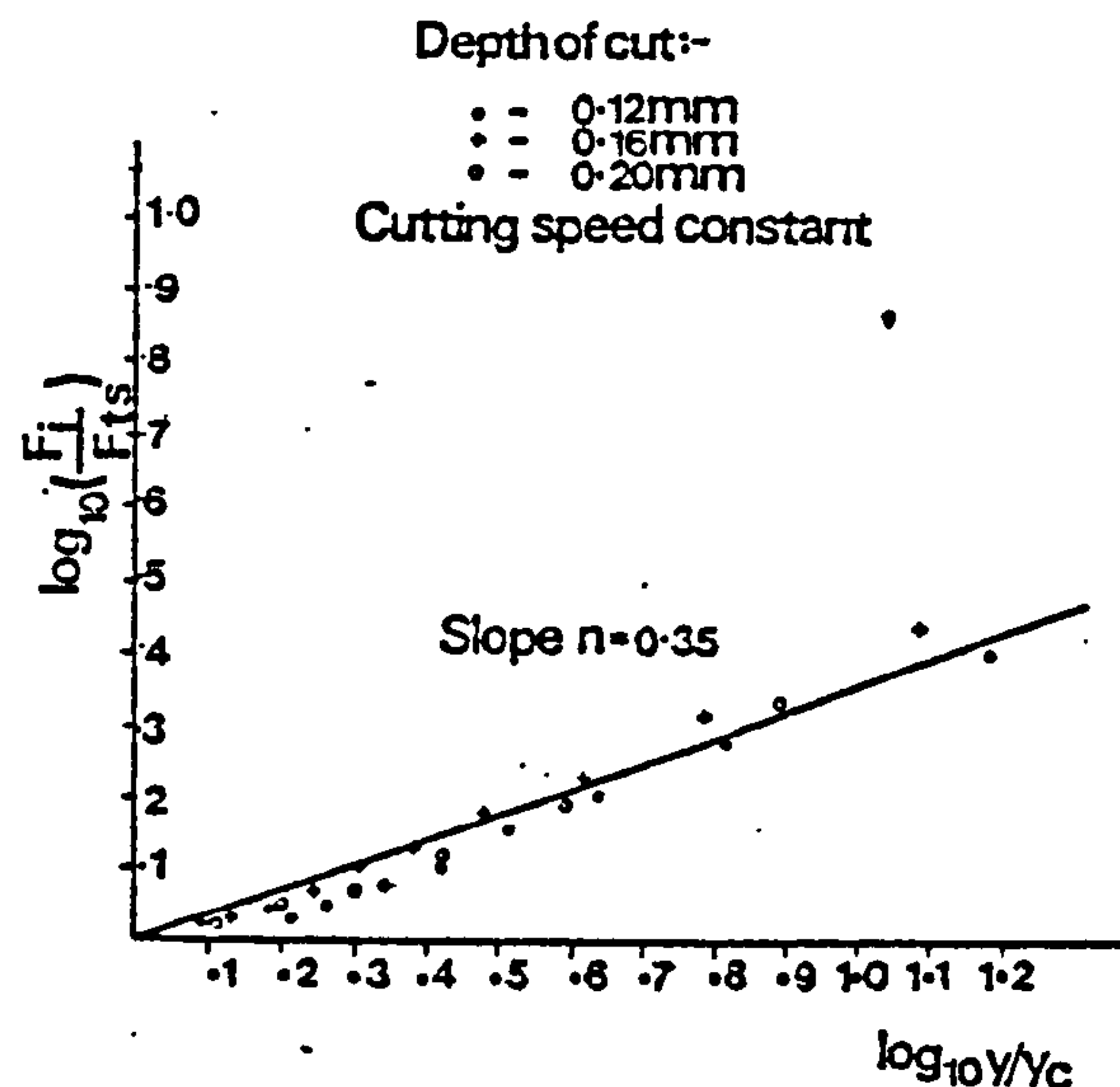


Fig. 8. Analysis of the transient zone (results taken from copper tests). (Depth of cut and cutting speed shown in figure.)

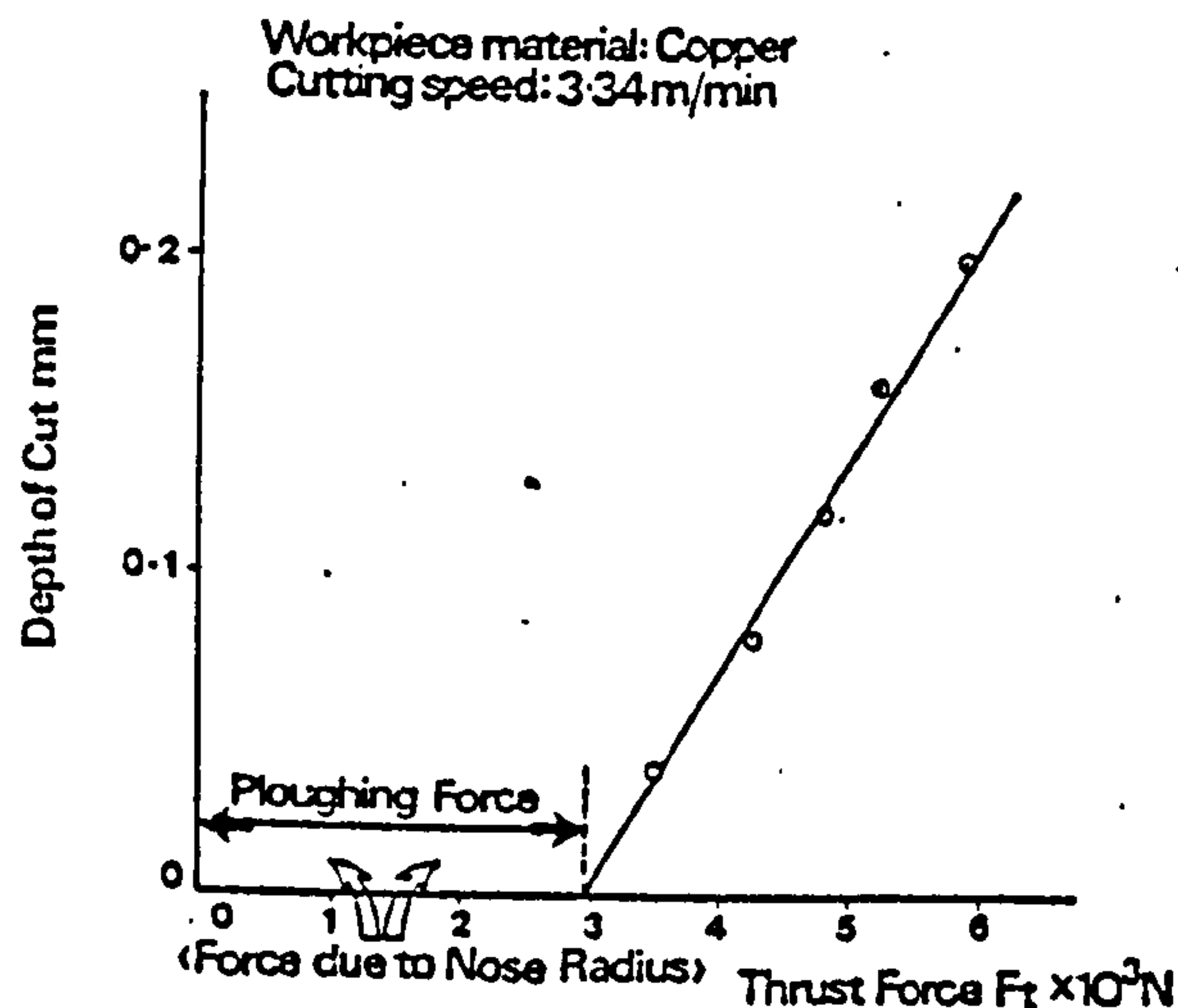


Fig. 9. Intercept at zero of cut showing the tool nose or ploughing force.

APPENDIX E

Predicting the Limiting Length of Cut for Blades of Various Pitch

The calculations below assume that the gullet performs with maximum efficiency until:

- (a) the limit of condition II (Gullet height), fig. 111 is reached, (length of cut B_1) or
- (b) the limit of condition III (Gullet perimeter) fig. 111 is reached, (length of cut B_2).

From a knowledge of the chip ratio ($C_h \approx 0.3$) for steel workpiece cutting with blunt tools, the limiting length of cut B_1 and B_2 can be calculated and is shown in the table below.

Blade T.P.I.	Pitch (mm)	Gullet height (mm)	Gullet Perimeter (mm)	Limiting length of cut	
				B_1 (mm)	B_2 (mm)
4	6.35	3.3	10.5	11	35
6	4.1	2.28	7.05	7.6	23
10	2.54	1.4	4.32	4.66	14
14*	1.79	0.94	3.00	3.14	9.7
18*	1.41	0.73	2.33	2.44	7.7

*These calculations have been based on the assumption that the blades were of the same type as 4, 6 and 10 T.P.I. and geometrically similar.

Calculations ignore the root radius and chip thickness but can be expected to have minor effect on Fig. 112

APPENDIX F

QUICK-STOP TESTS

In principle, the equipment used for interrupting the cutting action should function so quickly that a particle in the work-piece has no time to go through the shear zone during the time needed to stop the process. CIRP (62) have recommended that, to obtain satisfactory results, equipment should be used which has a stopping time less than the time needed for the chip to move ten per cent of the thickness of the shear zone. The above recommendations were intended to be applied in conventional high speed cutting tests (200 - 400 m/min). Owing to the complex deformation zone (Figures 73; 74) produced in the present tests, difficulty has been experienced in applying the above recommendations to the simulation tests.

The time required to reverse the milling machine table and interrupt the cut, as measured on an ultra violet recorder timer mechanism, was less than 0.05 seconds. It was considered that, at the low cutting speeds (95 mm/min) the normal problems associated with quick-stop techniques were much reduced and the procedure adopted for reversing the milling machine table was adequate to give a satisfactory result.

It would prove useful to carry out further work in this area to test the performance of the interrupted cutting action when machining at speeds comparable with that in the sawing process.

REFERENCES

- 1 EMERSON C How to cut-off metal
American Machinist Special Report 428 1956
- 2 ANDERSON R A Band machining and friction sawing
I. Mech. E. Proc. Conf. Tech. of Eng. Manufacture 1958
3. REMMERSWAAL J L, MATHYSEN M J C
Economics of the cutting-off of metals
Microtecnic, 1961 15(4) August, 140-150
- 4 NELSON R E Bandsawing or hacksawing?
Am. Mach. Volume 109 No 24. November 22 1965.
Pages 90-93
5. Sawing to Blueprint Tolerances
Machine and Tool Blue Book Volume 60 No 2. February 1965
Page 98-102
6. Carbide saw slices the superhard
The Iron Age June 16 1966. Page 82
- 7 Pushbutton bandsaw handles huge loads
The Iron Age August 11 1966. Page 56
- 8 CORKER J Fabrication Estimating
Welding and Metal Fabrication June 1966. Page 230
- 9 BILSTON S & L High speed hot sawing
Iron & Steel December 1967. Page 524
- 10 JOHNSTON C A Cutting the cost per cut
American machinist April 17 1972. Page 90
- 11 MORTIMER J Blade breakthrough to get the edge in
hacksaw exports
The Engineer 16 November 1972. Page 42
- 12 GREENSLADE A Metal sawing today
Sheet Metal Industries August 1976. Page 125

- 13 Sawing developments lift cut-offs status
Metalworking Production December 1975. Page 43
- 14 JABIONOWSKI J Fundamentals of Sawing
American Machinist April 15 1975. Page 54-68
- 15 HAYWARD J Compare the costs in cutting off
Metalworking production May 1977. Page 47
- 16 Trends in sawing
Tooling and Production January 1978. Page 70
- 17 RAKOWSKI R LEO Know your saw blades
Machine and Tool Blue Book July 1978. Page 84
- 18 Cutting survey tests hacksaw's bite
Metalworking production June 1979. Page 133
- 19 Sawing Sophistication comes in very slowly
Special Report Metalworking Production.
February 1980. Page 113
- 20 Get your basics right (Bandsawing)
Metalworking Production. November 1980. Page 149
- 21 THOMPSON P J & SARWAR M Power Hacksawing
Proceedings 15 MTDR. Conf 1974. Page 217
- 22 SARWAR M 'Hacksawing'
I. Mech. E. Lecture. G & S Section. North Midlands
Branch. November 1974. Sheffield City Polytechnic
- 23 SARWAR M & P J THOMPSON
Simulation of the cutting action of a single hacksaw
blade tooth
The Production Engineer. June 1974. Page 195
- 24 THOMPSON P J A theoretical study of the cutting
action of power hacksaw blades
Int. J. Mach. Tool Des. Res. Volume 14 1974.
Page 199

- 25 THOMPSON P J & TAYLOR R W
An Investigation into factors influencing the wear rate of power hacksaw blades using dimensional analysis
Blade Wear Testing 16 MTDR Conf 1975
- 26 THOMPSON P J & TAYLOR R W
An analysis of the lateral displacement of a power hacksaw blade and its influence on the quality of cut
16 MTDR Conf 1975
- 27 THOMPSON P J & TAYLOR R W
A computer simulation of the power hacksaw operation and its use in estimating blade life, cutting rate and cost
The Production Engineer. January 1976. Page 25.
Volume 55 No 1
- 28 THOMPSON P J
Factors influencing the sawing rate of hard ductile metals during power hacksaw and bandsaw operations metals technology. October 1974. Page 437
- 29 THOMPSON P J & MALIN R A
How angular motion of the workpiece reduces sawing time Welding and Metal Fabrication. July/August 1979
- 30 THOMPSON P J & HEAVER G R
Characteristics of saw operations when cutting circular sections
Metals Technology. November 1976 Page 522-28
- 31 TAYLOR R W & THOMPSON P J
A study of bandsaw blade wear and its effects on cutting rates and economics
17 MTDR Conf Birmingham 1976
- 32 ALBRECHT P The Ploughing process in metal cutting
Trans. Am. Soc. Mech. Engrs. Volume 82 (Series B) 1959. Page 263
- 33 MERCHANT M E Mechanics of the metal cutting process
J. Appl. Phys. Volume 16 1945. Page 267

- 34 MASAMI MASUKO "Fundamental researches on the metal cutting. A new analysis of cutting force"
Trans. Soc. of Mech. Engrs. (Japan). Volume 19
1953. Page 32-39.
- 35 CONNOLLY R & RUBENSTEIN C The mechanics of chip
formation in orthogonal cutting
Int. J. Mach. Tool Des. Res. Volume 8 1968.
Page 159-187
- 36 RUBENSTEIN C, GROSSMAN F K & KOENIGSBERGER F
Force measurements during cutting tests with single
point tools simulating the action of a single
abrasive grit
Proc. Int. Industrial Diamond Conf. Oxford 1966
- 37 PALMER W B & YEO R C K
Metal flow near the tool point during orthogonal
cutting with a blunt tool
MTDR Conf. 1963. Page 61-70
- 38 OKUSHIMA K & KAKINO Y
Study on the generating process of machined surfaces
Bull. JSME, Volume 12 (1969). Page 141-148
- 39 CUMMINES J D et al
A new analysis of the forces in orthogonal cutting
J. Eng. Ind. Volume 90 (1965). Page 480-486
- 40 BITANS K & BROWN R H
An investigation of the deformation in orthogonal
cutting
Int. J. Mach. Tool Des. Volume 5 (1965). Page 155-165
- 41 HASLAM D & RUBENSTEIN C
Surface and sub-surface work-hardening produced by
a planing operation
Annals of the CIRP Volume XVIII 1970. Page 369-381
- 42 HEGINBOTHAM W B & GOGIA S L
Metal cutting and the built-up nose
Proc. Inst. Mech. Engrs. Volume 175 (1961).
Page 892

- 43 KRAGELSKI
Friction and wear
London Butterworth's Press 1965
- 44 BUSURAY P K, MISRA B K & LAL G K
Transitions from ploughing to cutting during
machining with blunt tools
Wear, Volume 43 (1977). Page 341-349
- 45 BACKER W R, MARSHALL E R & SHAW M C
The size effect in metal cutting
Trans Am. Soc. Mech. Engrs. Volume 74 (1952).
Page 61-72
- 46 NAKAYAMA K & TAMURA K
Size effect in metal cutting force
J. Eng. Ind. Volume 90 (1968). Page 119-126
- 47 JOHNSON W & MAHTAB F U
Upper bounds for restricted edge machining
Advances in MTDR Proc. 6 Conf. (1965). Page 447-462
- 48 British Standards Institution BS 1919 1974
Specification for Hacksaw blades
- 49 Machine and Tool Blue Book, July 1978
- 50 NEL Divisional Report. A survey undertaken by NEL
to assess the feasibility of a cutting test for
Power Hacksaw Blades. 1969
- 51 Admiralty Specification No 1055B August 1964
- 52 American Specification GGG-B-451 d 1968
- 53 Canadian Government specification 46-GP-1
- 54 Australian Standard July 1968
- 55 USSR State Standards - Saw blades for metal cutting.
GOST 664

- 56 Testing carried out by BHMA Sub-Committee on testing in their search for "A Performance Test for HSS Power Hacksaw Blades".
Jan. 1969 (Confidential).
- 57 The Government Department Specification for General Stores No. TG81 1941. Hacksaw Blades for Hand Frames and Power Machines.
- 58 COLDING B N
A Three Dimensional Tool-Life Equation-Machining Economics.
Trans ASME 81, 1959 pp 239
- 59 WRIGHT P K & TRENT E M
Metallurgical Appraisal of Wear Mechanisms and Processes on High Speed Steel Cutting Tools.
Metal Technology Jan 1974
- 60 LEE E H & SHAFFER B W
The theory of plasticity applied to a problem of machining. J App Mech Eng; Trans ASME 1951, Vol 73, p 405.
- 61 THOMPSON P J & SARWAR M
Confidential Report on Power hacksawing to James Neill (Services) Ltd. Sheffield 1973
- 62 CIRP Group C Report on Terminology and procedures for turning research.
- 63 FORM G W & BELINGER H
Fundamental Considerations in Mechanical Chip formation
Annals of CIRP Vol XVIII pp 153-167. 1970
- 64 VAN VLACK L H
"Materials Science for Engineers"
Adison-Wesley Publishing Company (1975) p 198
- 65 MOTT B W
"Micro-Indentation Hardness Testing"
p 73, Butterworths Scientific Publications (1956)

- 66 HAHN R S
"On the Nature of the Grinding Process", Advances
in Machine Tool Design and Research, p 129,
Oxford: Pergamon Press Ltd, 1962
- 67 ARMAREGO E J A & BROWN R H
"On the Size Effect of Metal Cutting", Int J Prod
Res, Vol 1 (1962), p 75
- 68 WALLACE P W & BOOTHROYD G
Tool forces and tool-chip friction in orthogonal
machining, J Mech Engrg Sci, Vol 6, No 1, p 74,
1964
- 69 BOOTHROYD G
Fundamentals of Metal Machining and machine tools.
McGraw Hill Book Company, 1975, p 71
- 70 BACKER W R, MARSHALL E R & SHAW M C
The size effect in metal cutting
Trans Amer Soc Mech Engrs, Vol 74 (1952), 61
- 71 ERNST H
Trans Symposium on Machining of Metals I. Physics
of Metal Cutting, Trans Amer Soc Metals 1938
- 72 HILL R
"The Mechanics of Machining", a new approach,
J Mech Phys Solids, Vol 3, p 47, 1954
- 73 LOW A H
"Effects of initial conditions in metal cutting",
NEL Report No 49, 1962
- 74 LOW A H & WILKINSON P T
An investigation of non-steady state cutting,
NEL Report No 65
- 75 PALMER W B & OXLEY P L B
Mechanics of orthogonal machining, Proc Inst Mech
Engrs, Vol 173, No 24, 1959

- 76 CHRISTOPHERSON D G, OXLEY P L B & PALMER W B
Orthogonal Cutting of a work-hardening material,
Engineering Vol 186, p 113, 1958
- 77 JOHNSON W
"Some slip-line fields....Machining", Int J Mech Sci,
Vol 4, pp 323-347, 1962
- 78 BATTACHARYYA A
On the friction process in metal cutting, 6th MTDR
Conf, p 491, 1966
- 79 JOHNSON W
Cutting with tools having a rounded edge. Annals
of the CIRP Vol XIV, pp 315-319, 1967
- 80 JOHNSON W & MELLOR P B
Engineering Plasticity, Van Nostrand p 483-484, 1973
- 81 USUI E KIKUCHI K, HOSHI K
The theory of plasticity applied to machining with
cut-away tools, ASME paper No 63, Prod 5, 1963
- 82 KUDO H
Some slip-line solutions for two-dimensional steady
state machining. Int J Mech Sci, Pergamon Press,
Vol 7, pp 43-55, 1965
- 83 ROWE G W, SPICK P T
A new approach to determination of the shear-plane
angle in machining.
Trans ASME Jnl of Eng Ind, pp 530-538, 1967
- 84 PUGH H U D
"Mechanics of the cutting Process", The Institution
of Mech Engrs, London, England.
Conf on Tech of Engrg Manufacture, 1958
- 85 BACKER W R, MARSHALL E R, SHAW M C
The size effect in metal cutting, Trans Am Soc
Mech Engrs, Vol 74, 1952, p 61-72

- 86 NAKAYAMA L & TAMURA K
 Size effect in metal cutting force, J Eng Ind,
 Vol 90, p 119-126 (1968).

- 87 SARWAR M & THOMPSON P J
 Cutting Action of Blunt Tools.
 22nd Int MTDR Conf. 1981

- 88 SARWAR M and HALES W
 The Effect of gullet geometry on Blade
 Performance in Power Hacksawing
 (To be published).

- 89 ROWE G W
 Principles of Metalworking
 Processes, Arnold 1977,
 p 24-25

LIST OF FIGURES

CAPTION

Fig. No.

- 1 Method used to instrument a Power Hacksaw
- 2 Variation of thrust force against crank angle for various saw machines
- 3 Simplified hydraulic unit of the Wickstead hydraulic sawing machine
- 4 The load developed during the cutting stroke, between the blade and the workpiece by a hydraulic saw on various load settings
- 5 (a) Main features of the restricted 'back flow' method for a hydraulic machine
(b) A theoretical thrust load against blade displacement diagram for such a machine and a rigid, non-cutting blade
- 6 Factors influencing the effective wedge angle
- 7 Effect of blade deflection on the thrust load developed by the Wickstead hydramatic machine
- 8 Variation in thrust force developed by the Wickstead hydramatic saw on a common load setting with blades of different widths
- 9 The number of saw strokes to cut through a 25 mm x 25 mm mild steel bar using a Brand X 6 blade against the mean thrust force developed by various power hacksaw machines
- 10 Geometry of the sawing action showing variation in the tooth factor
- 11 Geometric relationship between the saw stroke, workpiece breadth and the effective blade length

- 12 Thrust load variations, slow and high speed, for the Wicksteed saw
- 13 Some features of power hacksaw blade, and its cutting action
- 14 Hacksaw blade teeth patterns
- 15 Cutting edge geometry of a hacksaw blade tooth
- 16 Saw tooth profile of a 6 TPI blade
- 17 Comparison between the mean thrust force and the static force at mid stroke position for various sawing machines
- 18 The depth of cut achieved by an Brand X blade 6 TPI cutting mild steel against the mean thrust force per tooth per unit thickness, by various power hacksaw machines
- 19 Paths followed by individual teeth through the workpiece
- 20 Instantaneous cutting force component against the instantaneous thrust force component for a Brand X 6 TPI blade cutting mild steel
- 21 Hacksaw machine and associated instrumentation for blade testing
- 22 Typical thrust loads developed between the blade and the workpiece, during the cutting stroke, for various machine load settings
- 23 The average depth of cut per tooth against the mean thrust load per tooth per unit thickness, for blades having different pitch teeth
- 24 The cutting constant against the reciprocal of the number of teeth in contact with the workpiece
- 25 Comparison of blade performances

- 26 Comparison between the Brand 'Z' 3 TPI blade and a Brand 'X' 6 TPI blade showing instantaneous cutting force components
- 27 Profile of the Brand 'Z' 3 TPI tooth
- 28 Samples of metal chips obtained when cutting with Brand 'X' 4 TPI blade, for various machine load settings
- 29 Samples of metal chips obtained when cutting with Brand 'Z' 3 TPI blade, for various machine load settings
- 30 The effect of tooth spacing and cutting edge radii, on the cutting performance of Brand 'X' blades
- 31 Effect of blade wear on the cutting performance
- 32 Effect of blade deflection on the performance of new and worn blades
- 33
 - (a) longitudinal stress distribution due to a bending moment, a tensile load and their combination
 - (b) Position of the neutral axis of bending due to a central load, for a hacksaw blade
- 34 Deflection models and equations for:-
 - (a) A simply supported blade with longitudinal tension
 - (b) A uniformly loaded blade with built in ends
- 35 Deflection factor against tension factor
- 36 Load/extension curve for High Speed Steel blade
- 37 Tensile load induced in a saw blade against the number of turns of the tension nut

- 38 The effect of blade tension on the vertical stiffness of the blade
- 39 Natural frequency of lateral vibration against the blade tension
- 40 (a) Blade tooth wear against the number of sections cut
(b) Tooth profile showing wear
- 41 The average depth of cut per tooth against the mean thrust load per tooth per unit thickness for a blade in three stages of wear
- 42 The effect of blade wear on its cutting performance
- 43 Loss in tooth height against the number of sections cut
- 44 Deformation occurring in both the blade and the workpiece, compiled from microscopic observations during wear tests
- 45 The effects of the cutting stroke rate on the blade life, average cutting rate and the cost factor
- 46 The effects of the thrust load on blade life, the average cutting rate, and the cost factor
- 47 The effects of the stroke of the saw on blade life, the average cutting rate, and the cost factor
- 48 The effects of the teeth pitch and the breadth of the workpiece on blade life, the average cutting rate, and the cost factor
- 49 Variation of the cutting force components with the increase in length of cut
- 50 (a) A fully established deformation zone
(b) Mohr's stress diagram for all points in the deformation zone

- 51 Predicted variation in the cutting constant against the apparent coefficient of friction for a fully established deformation zone
- 52 Thrust loads acting on the saw teeth
- 53 Comparison between the computed values of the reciprocal of the chip factor for various values of the cutting force index and experimental values
- 54 Comparison between the computed values of the reciprocal of the chip factor for cutting force index of one, and experimental data obtained with blades of various pitch
- 55 Diagramatic representation of the cutting process with a tool having a large cutting edge radius
- 56 Diagramatic representation of the relationship between the nominal set depth, layer of metal removed and the machined surface
- 57 Machine tool and the associated equipment used for simulation tests
- 58 View of the cutting tool workpiece set-up
- 59 Close-up of the bridge dial gauge arrangement
- 60 Machine tool (Parkinson Miller) stiffness measurements at the position of the tool holder
- 61 Cross-section of an initially 3.55 mm wide copper specimen, after machining, showing the side spread
- 62 Chips of varying geometry produced when machining copper workpiece with a blunt tool (0.56 mm radius) at 0.25 mm nominal depth of cut
- 63 (a) Tool radius grinding jig, set up on the surface grinding machine
(b) Essential features of radius grinding jig
(c)

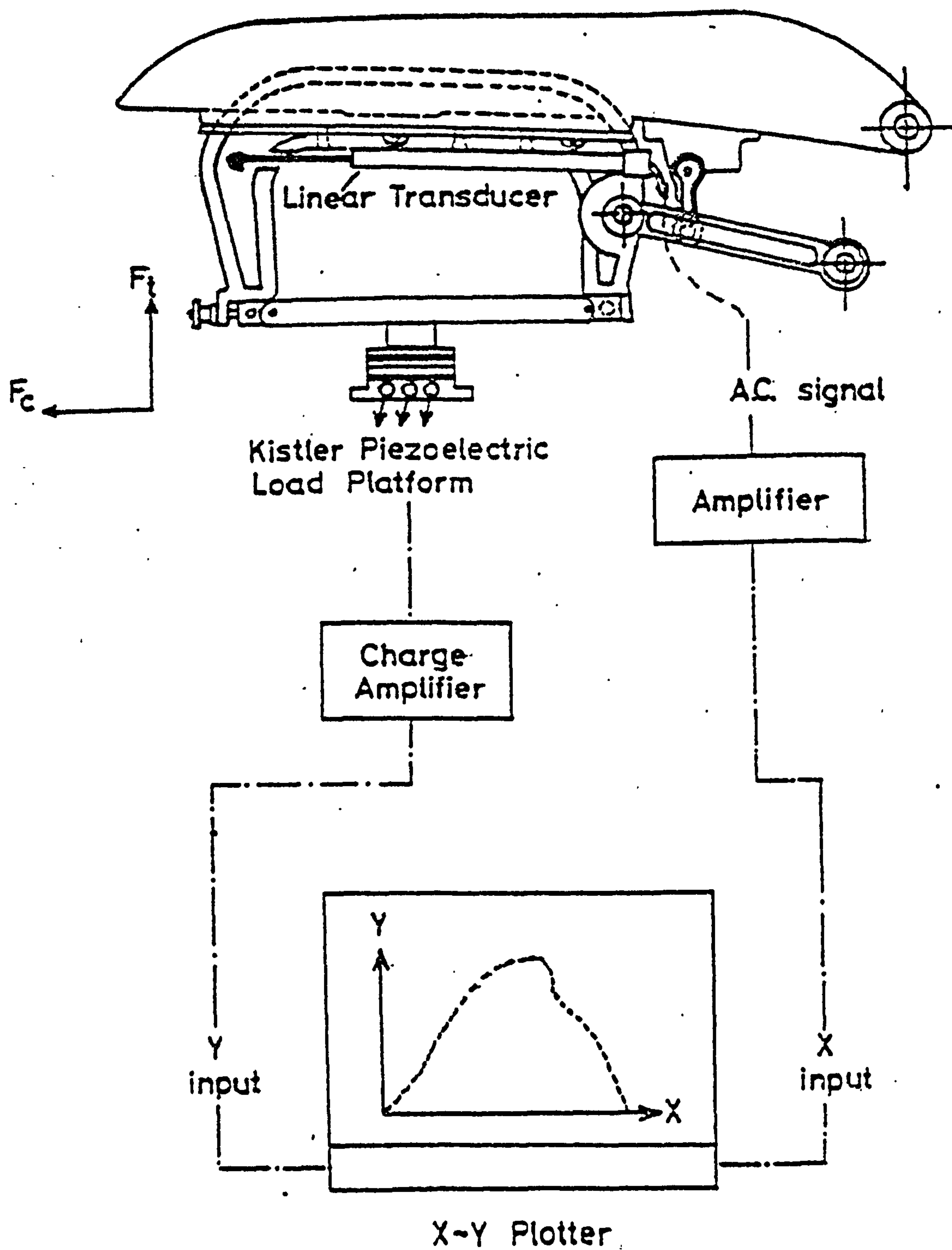
- 64 (a)(b) Close-up photographs when grinding the face and flank of the tool
- 65 (a)(b) Shadow graphs of the tool cutting edge profiles
 - (c) Tool cutting edge geometry
- 66 Forces obtained during groove cutting for a constant nominal depth of cut (0.1 mm) using a blunt tool (0.51 mm edge radius)
- 67 Cutting forces and the corresponding chips obtained when groove cutting, for a constant nominal depth of cut (0.25 mm), using a blunt tool (0.51 mm edge radius)
- 68 (a) Measurement of workpiece recovery
 - (b) Initial setting-up of the tool and air gauge
- 69 (a) Force traces obtained during groove cutting using a blunt tool at a constant nominal depth of cut
 - (b) Chips obtained corresponding to figure (69(a))
- 70 (a) Variation of chip-tool contact length with increase in depth of cut, for different type of chips
 - (b) Variation of chip-tool contact length with increase in depth of cut, for various tools, machining copper and steel
 - (c) Photograph of the chip-tool contact length and the appropriate chip
- 71 Photographs showing the chip formation at various positions along the length of cut
 - (a) Sharp tool

- (b) Blunt tool
 - (c) Chip produced when machining copper with a nominally sharp tool
 - (d) Chip produced when machining copper with a blunt tool
- 72 Some features of copper chips produced during groove cutting, using a blunt tool
- 73 Photomicrograph showing primary and secondary deformation zone when machining with a blunt tool
- 74 Photomicrographs showing the chip-root area
- 75 Electron-microscope picture of the chip-root area
- 76 Material behaviour at the centre of the workpiece
- 77 (a)(b)(c)(d)(e) Variation of the cutting forces during groove cutting, when cutting with a blunt tool and the appropriate chips
- 78 Variation of cutting forces during groove cutting showing, primary, secondary and steady state regions and the relevant chip
- 79 (a) Schematic diagram of the chip formation when machining with a blunt tool
- (b) Schematic diagram, showing layer of material being extruded around the chip root area
- 80 Variation of cutting forces and the corresponding chip tool contact length with the increase in depth of cut (0.56 mm cutting edge radius)
- 81 Variation of cutting forces and the corresponding chip tool contact length with the increase in depth of cut (0.81 mm cutting edge radius)

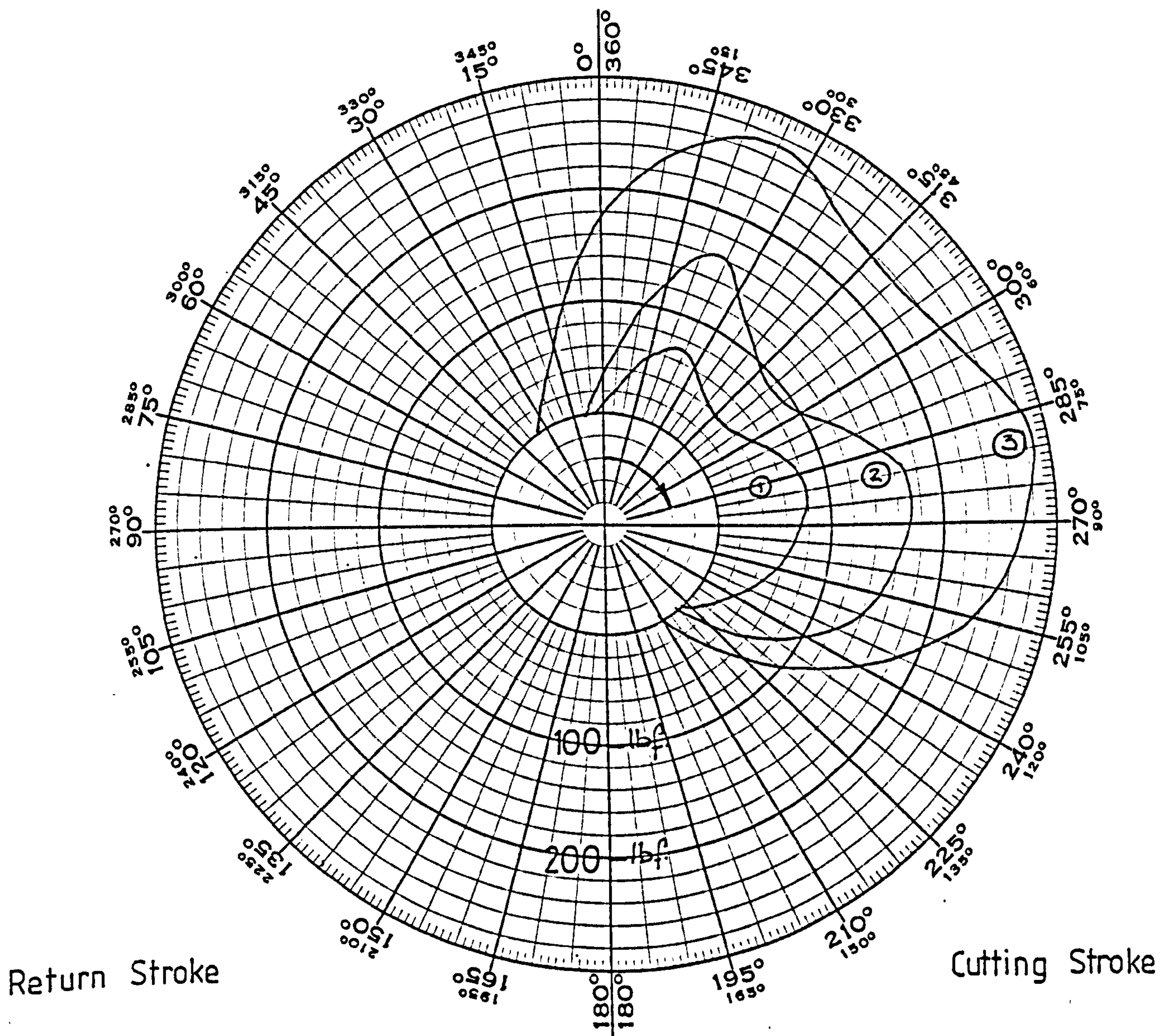
- 82 Variation of cutting forces and the corresponding chip tool contact length with the increase in depth of cut (0.56 mm cutting edge radius, workpiece - steel)
- 83 Comparison of thrust forces with increase in depth of cut, for a nominally sharp and blunt tool
- 84 Variation in specific cutting energy with increase in depth of cut, for blunt and sharp tools (workpiece - copper)
- 85 Variation in specific cutting energy with increase in depth of cut, using a blunt tool (workpiece - steel)
- 86 Single shear plane model
- 87 Lee and Schaffer's slip line field solution for a single shear plane
- 88 Slip-line field and hodograph for a built-up nose
- 89 Diagramatic sketch of suggested cutting process
- 90 Slip-line field solutions and hodographs for restricted tool contact
- 91 Slip-line field in machining with cut-away tool
- 92 Modified Johnson-Usui slip-line solution for
93 restricted and unrestricted chip-tool contact
- 94 Slip-line field solutions for restricted and unrestricted chip-tool contact
- 95 Slip-line field and hodograph for restricted tool contact, where cutting edge radius is approximated by straight edges
- 96 Slip-line field (invalid), where material is assumed to flow beneath the tool, when machining with blunt tool

- 97 Deformation patterns produced in horizontal and vertical layers of plasticine, when simulating the cutting action of blunt tools, using a perspex model tool.
- 98 Slip-line field in machining with a blunt tool and the corresponding hodograph.
- 99 Mohr's stress circles for figure 98.
- 100 True stress-strain curves from compression tests
 - (a) Copper
 - (b) Lead steel.
- 101 Experimental and theoretical forces - with increase in depth of cut.
- 102 Comparison of experimental and theoretical forces - sharp and blunt tools, machining copper.
- 103 Comparison of experimental and theoretical forces - blunt tool, machining lead steel.
- 104 Suggested slip-line field to scale, for particular cutting conditions.
- 105 Variation in Specific Cutting energy with depth of cut (copper and steel).
- 106 Chip Tool Contact Length/Edge radius vs Undeformed Chip thickness/Edge radius derived from simulation tests.
- 107 Comparison of single point performance and blades of different pitch.
- 108 Comparison of the performance of new and modified blades of different pitch.
- 109 Comparison of the performance of a standard and modified 4 T.P.I. Blade.
- 110 Comparison of the performance of standard and modified blades.
- 111 Schematic diagrams showing chip formation in the Gullet for various situations in sawing.
- 112 Influence of blade pitch on the limiting length of cut (steel workpiece).

FIG. 1: METHOD USED TO INSTRUMENT A POWER HACKSAW.



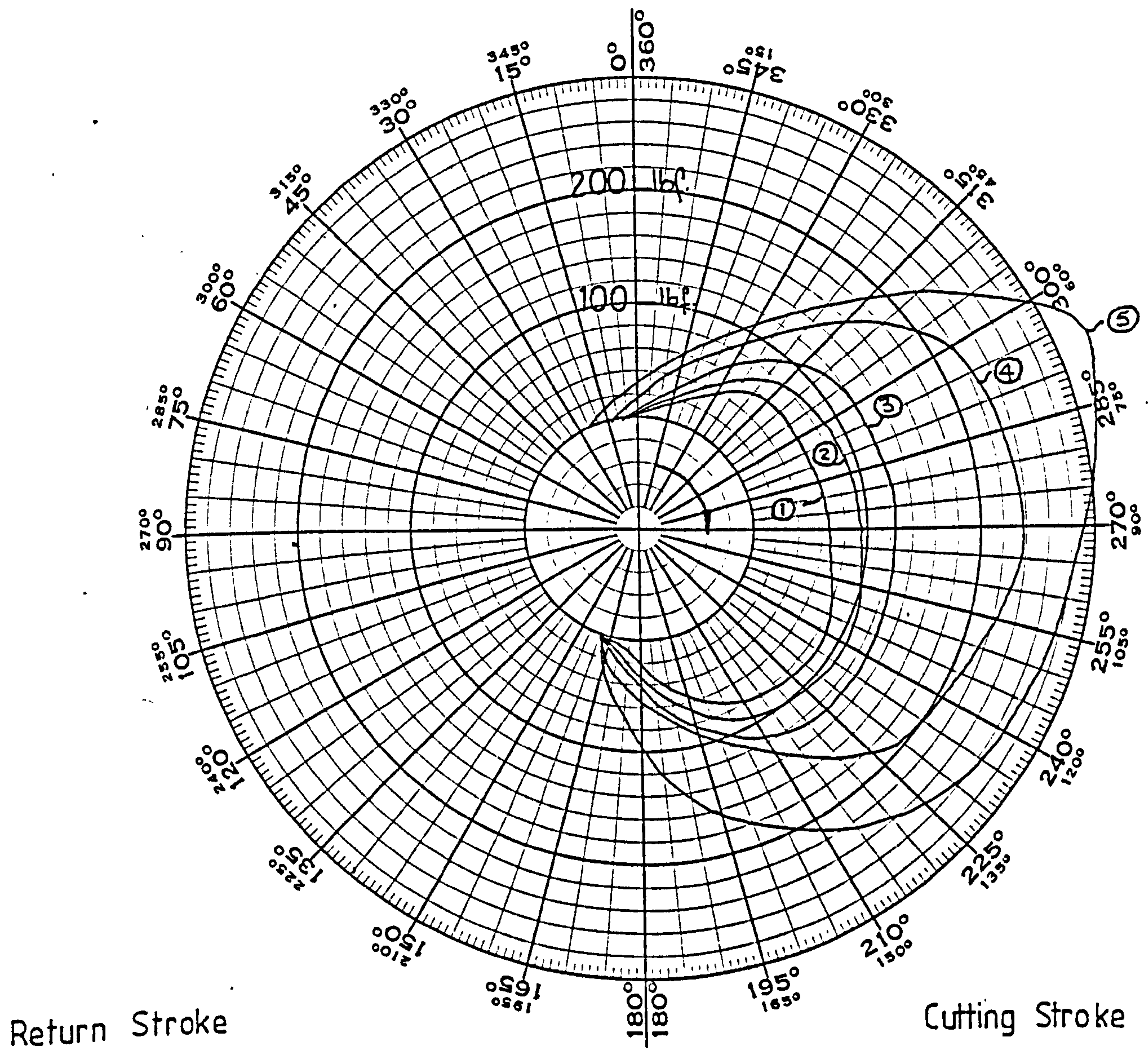
SPEED 64 STROKES/MIN



MACHINE SETTINGS SHOWN THUS (1)

FIG 2(A) VARIATION OF THRUST FORCE AGAINST CRANK ANGLE FOR A KASTO POWER SAW AND THREE MACHINE SETTINGS

SPEED 84 STROKES/MIN



MACHINE SETTINGS SHOWN THUS (1)

FIG 2(B) VARIATION OF THRUST FORCE AGAINST CRANK ANGLE FOR A KASTO VBS 221 POWER SAW AND FIVE MACHINE SETTINGS

SPEED - 120 STROKES/MIN

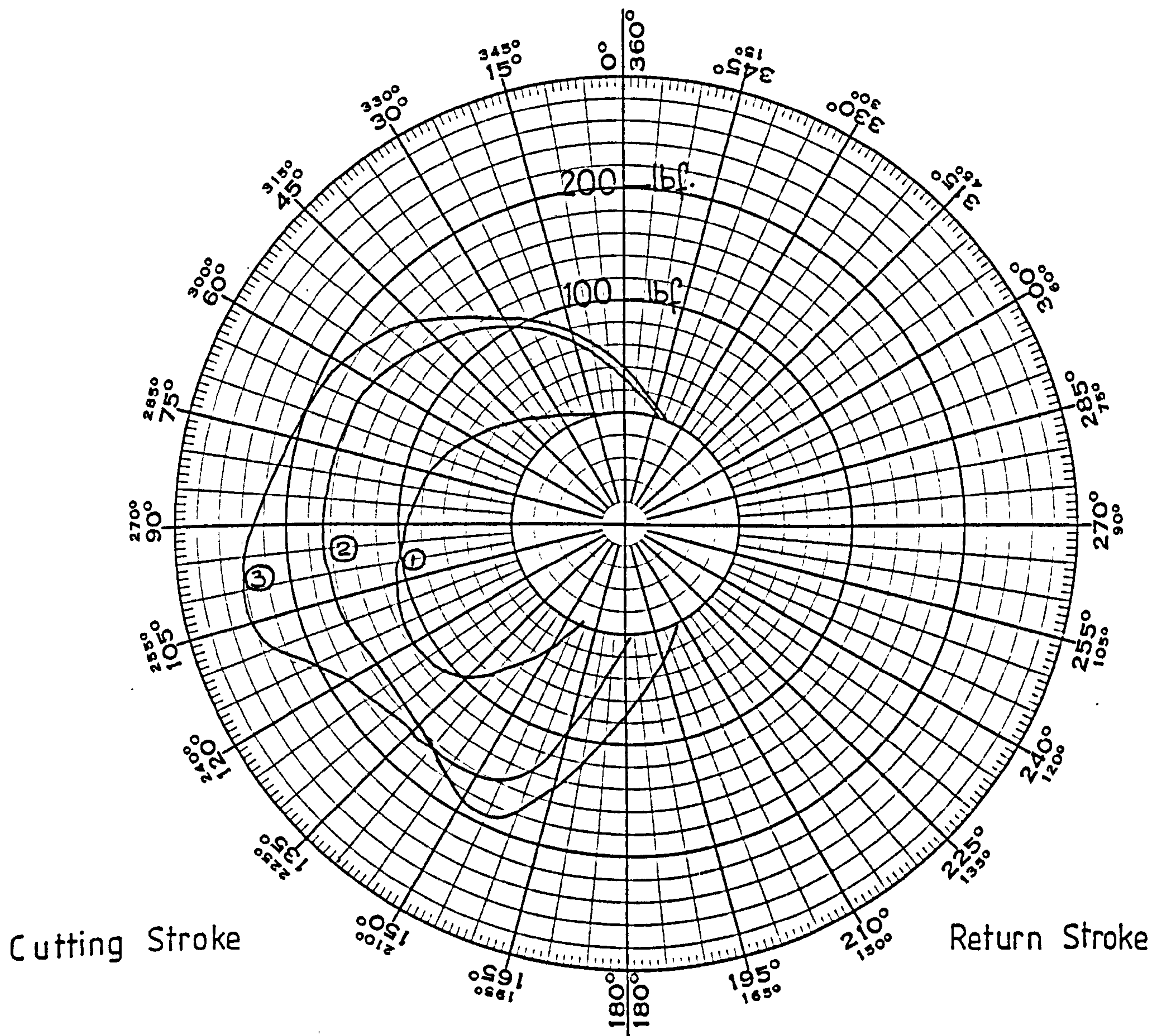


FIG 2(c) VARIATION OF THRUST FORCE AGAINST CRANK
ANGLE FOR A WICKSTEAD HYDROMATIC POWER SAW
AT THREE DIFFERENT SETTINGS

CUTTING SPEED - 120 STROKES/MIN

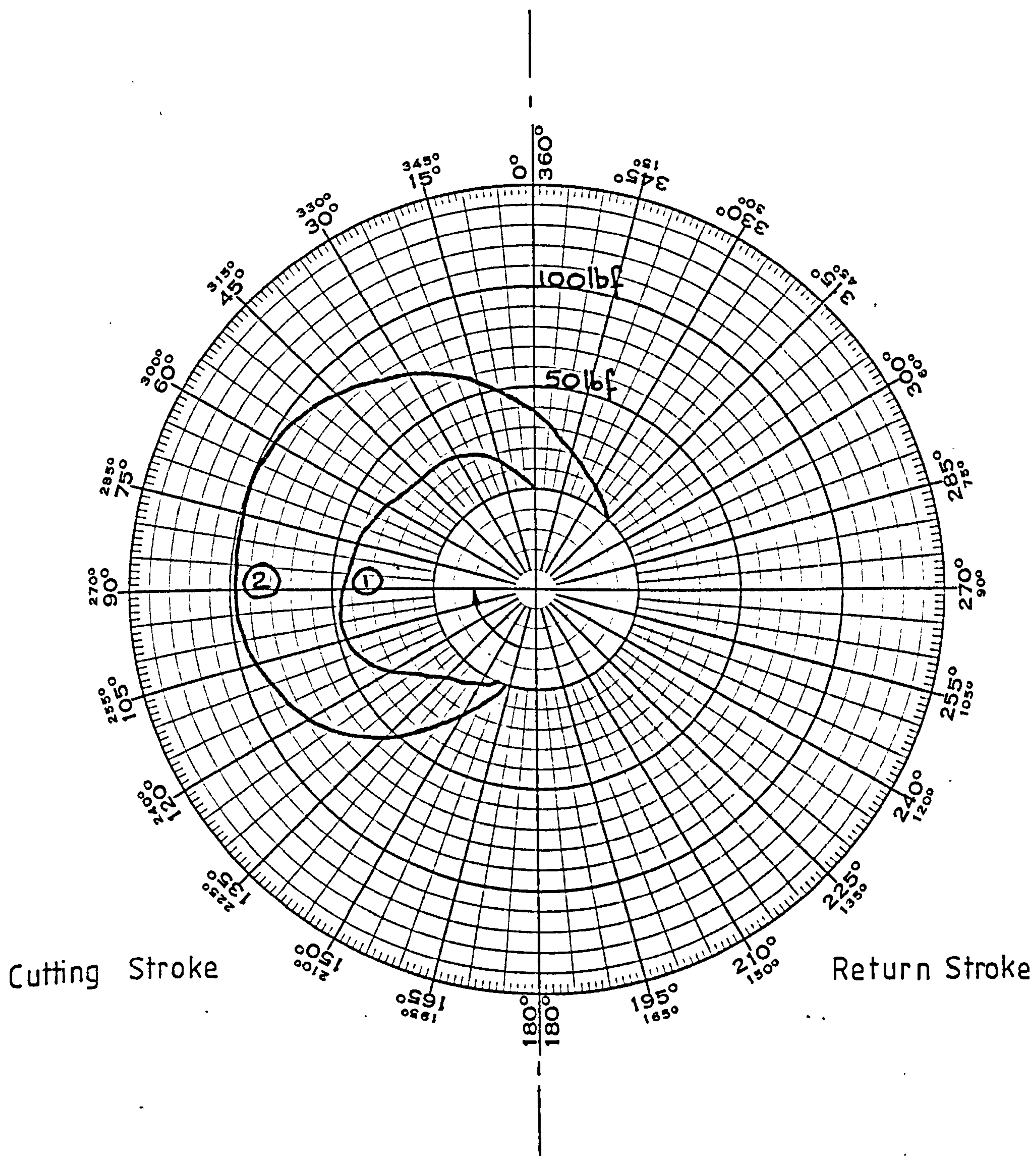


FIG 2 (D) VARIATION OF THRUST FORCE AGAINST CRANK
ANGLE FOR A WICKSTEAD ACME POWER
SAW WITH DIFFERENT THRUST LOAD SETTINGS

CUTTING SPEED 68 STROKES/MIN

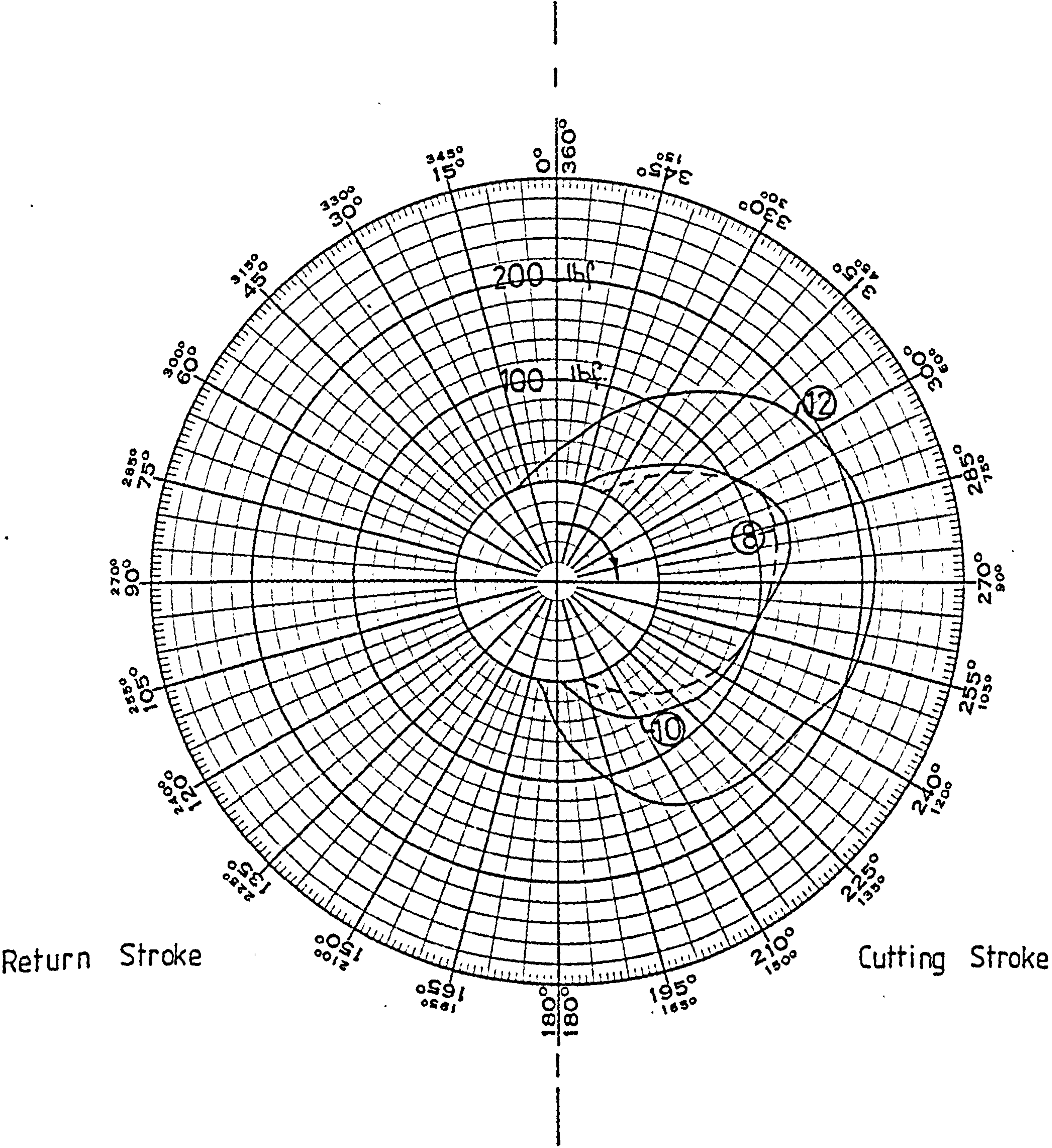


FIG 2 (E) VARIATION OF THRUST FORCE AGAINST
CRANK ANGLE FOR A WICKSTEAD POWER SAW (SHEFFIELD CITY
POLYTECHNIC)

SPEED 120 STROKES/MIN

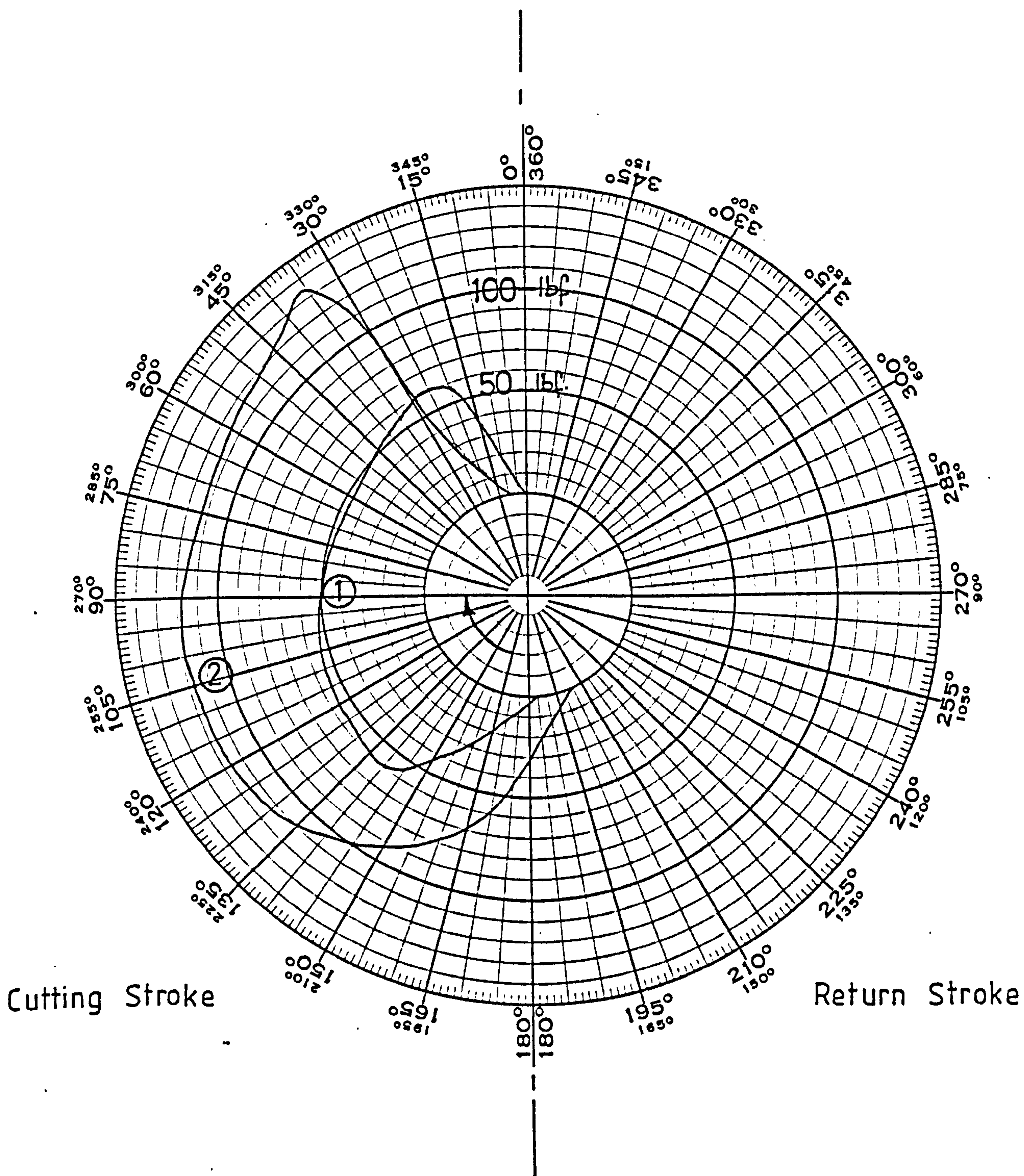
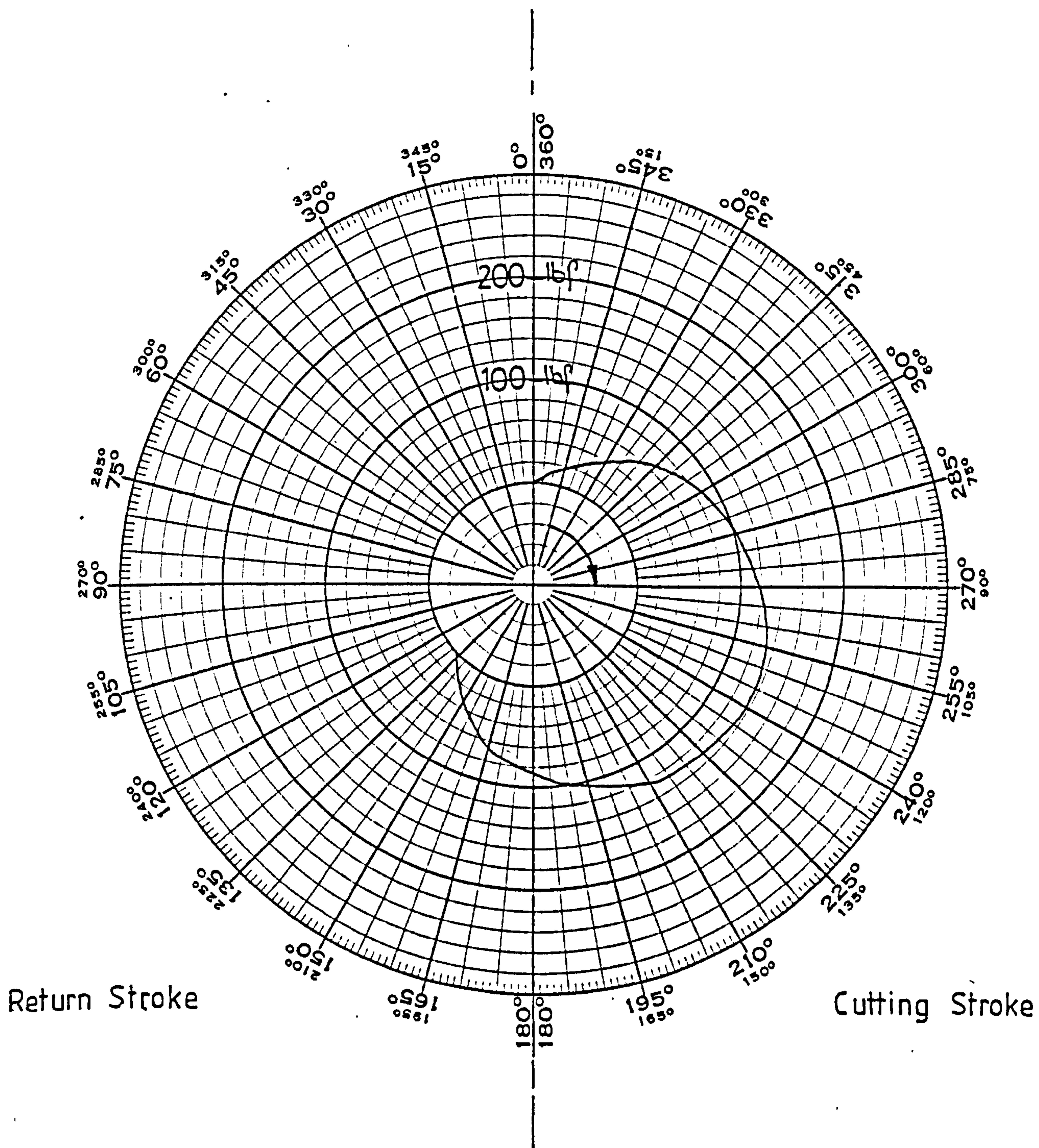


FIG 2 (F) VARIATION OF THRUST FORCE AGAINST CRANK
ANGLE FOR A MARVEL NO 9 POWER SAW
AT DIFFERENT FEED RATE SETTINGS



DASH-POT ADJUSTMENT IN MID-POSITION

FIG 2 (G) VARIATION OF THRUST FORCE AGAINST
CRANK ANGLE FOR A RAPIDER POWER SAW
SPEED 64 STROKES/MIN

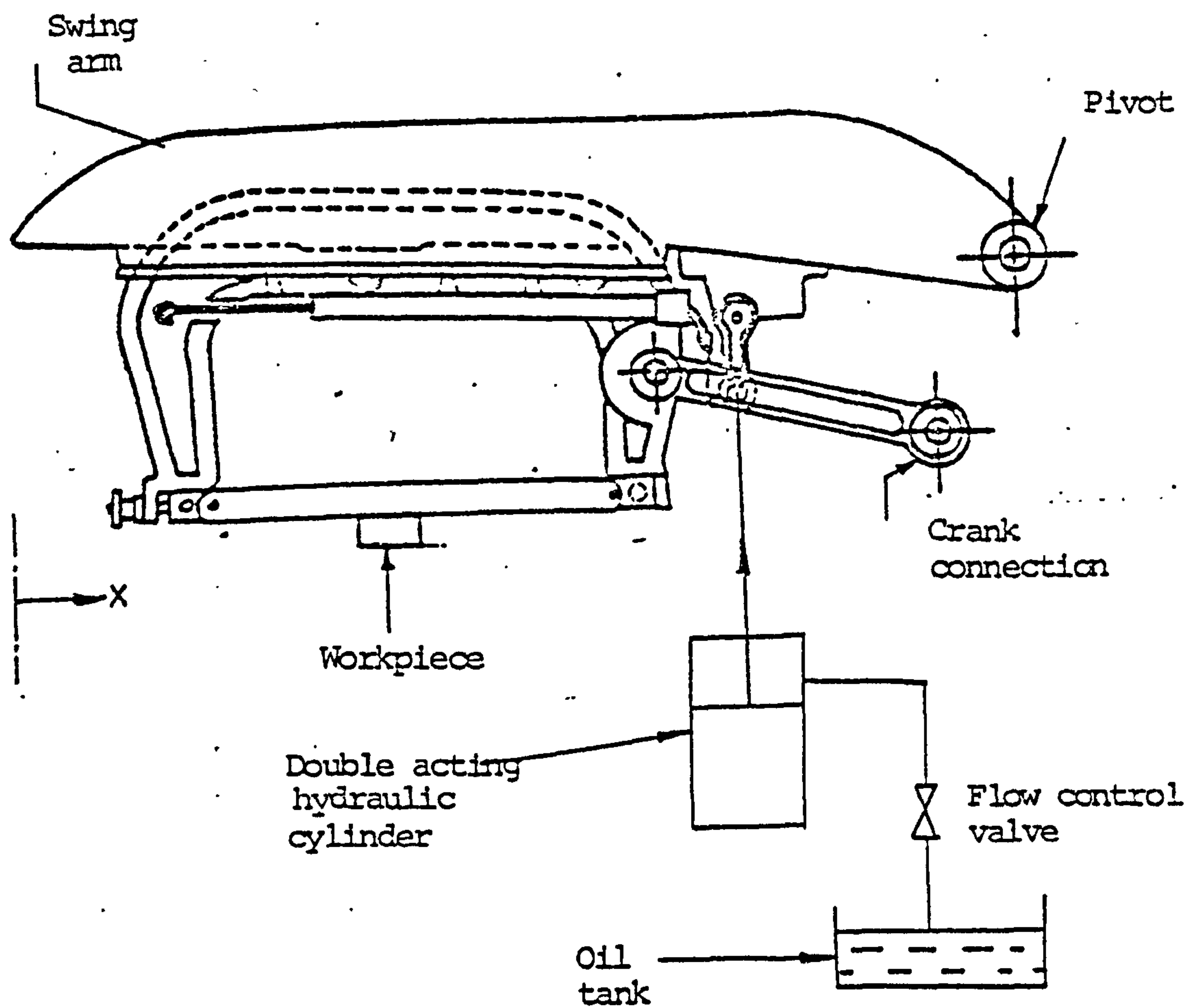


FIG. 3: Simplified hydraulic unit of the Wickstead hydraulic sawing machine

FIG. 4: The load developed during the cutting stroke between the blade and the workpiece by a 200mm hydraulic saw on various load settings

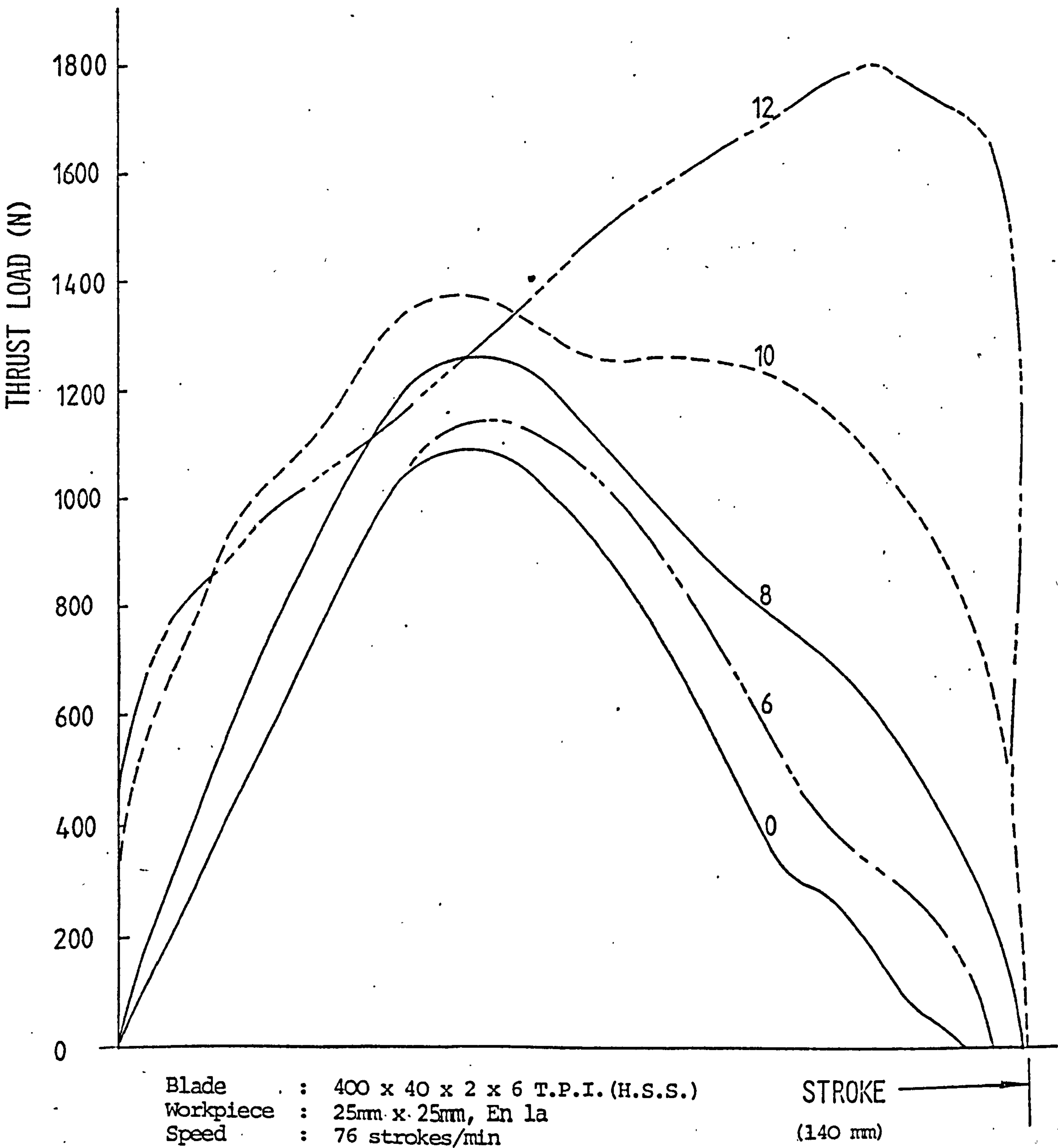
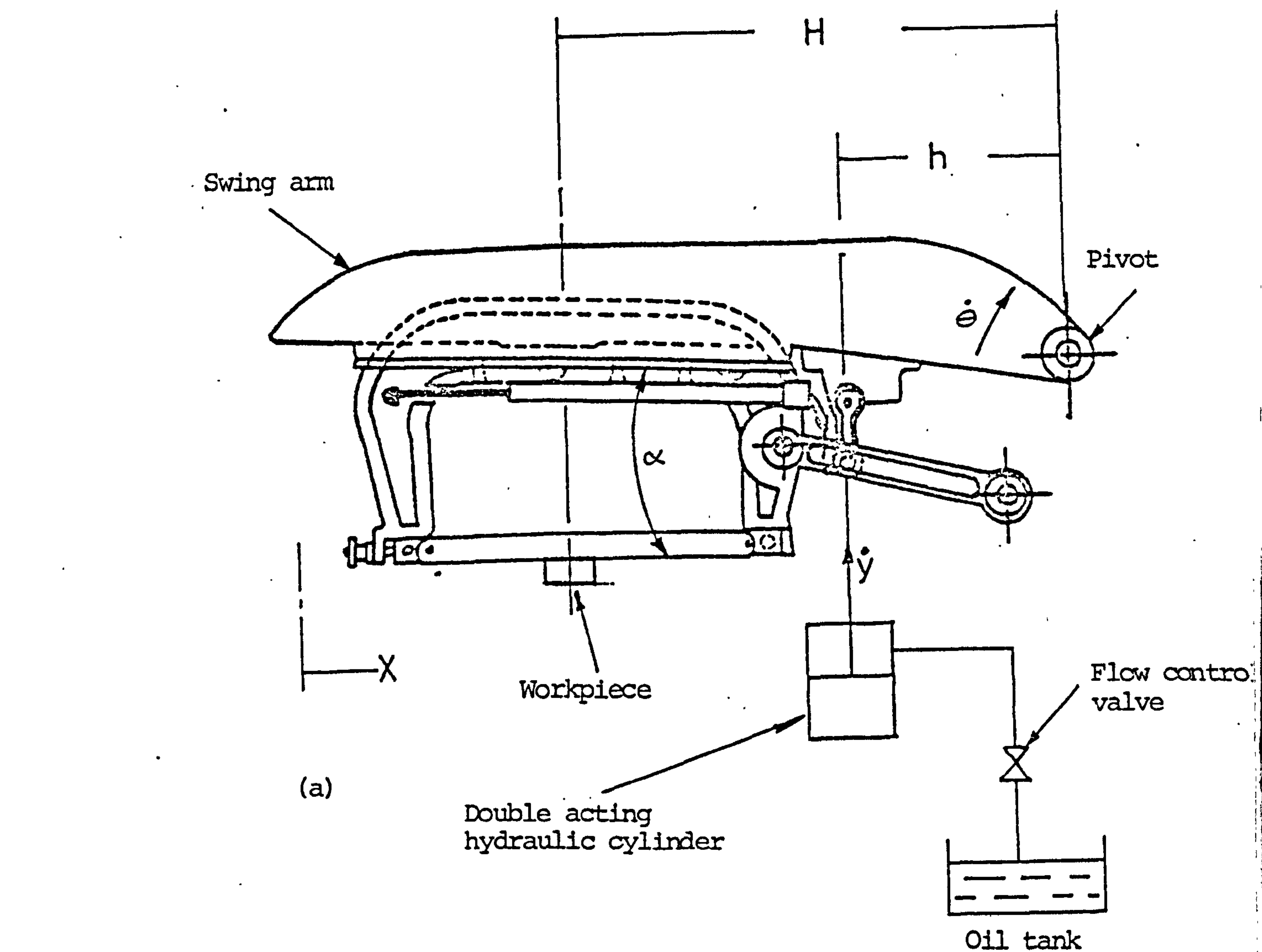


Fig.4



(b)

$\frac{X}{2R}$

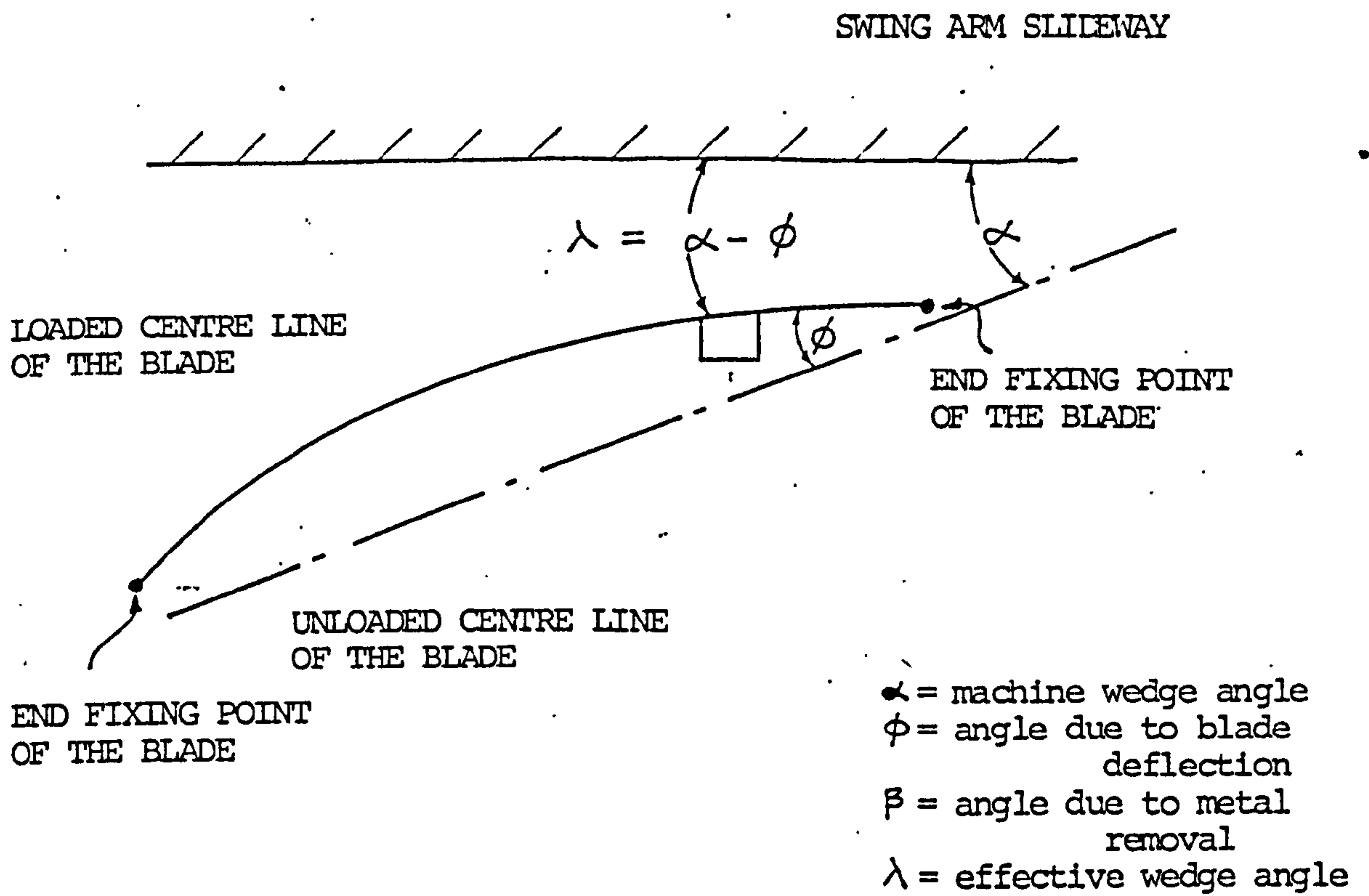
A = cross-section area of the hydraulic cylinder
 k = flow valve constant
 R = crank radius
 ω = angular velocity of the crank

FIG. 5(a): Main features of the restricted back flow method for a hydraulic machine

(b): A theoretical thrust load against blade displacement diagram for such a machine and rigid, non-cutting blade

FIG. 6: Factors influencing the effective wedge angle

(a) Angle due to blade deflection



(b) Angle due to metal removal

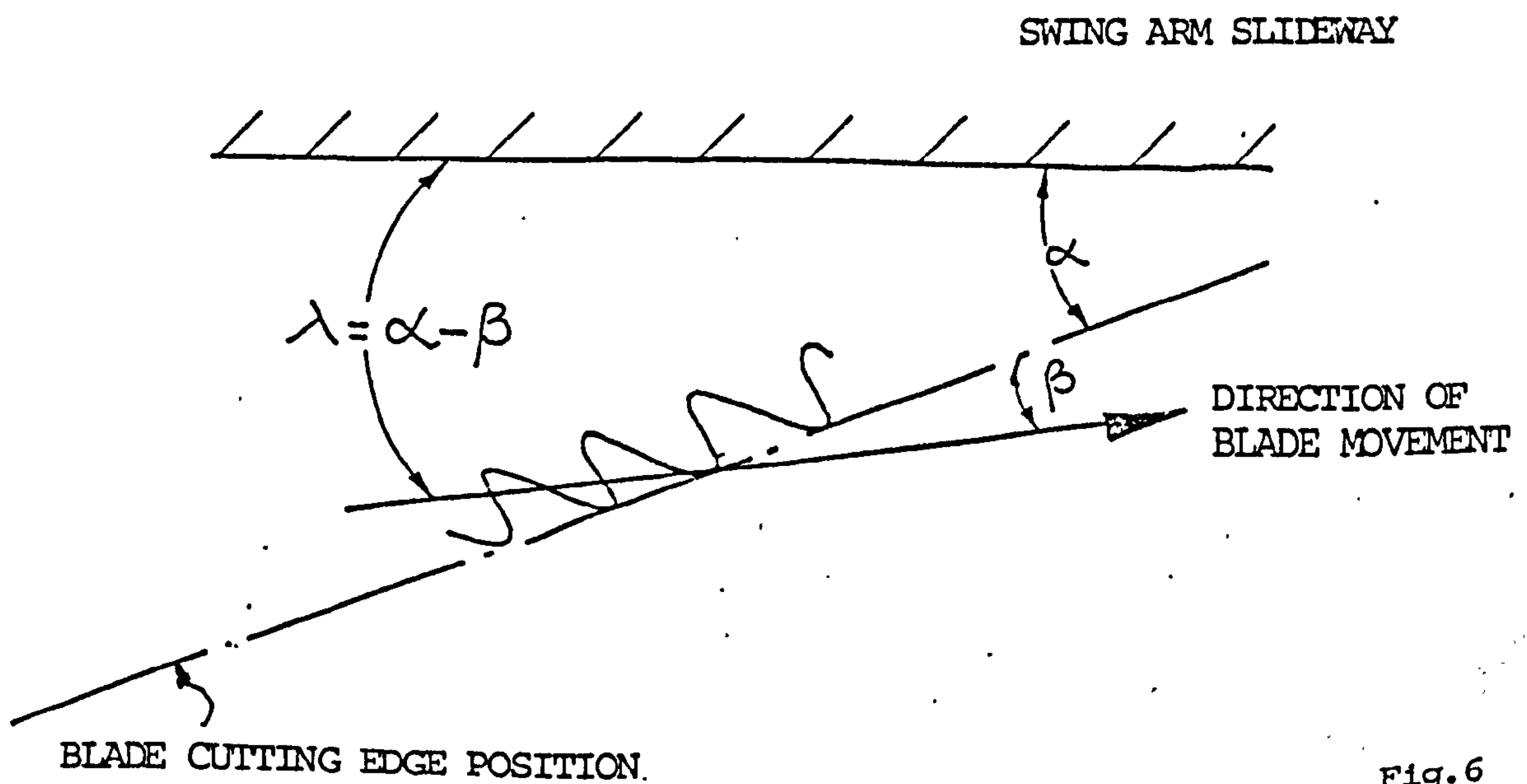


FIG. 7: Effect of deflection
on the thrust
load developed
by the
Wicksteed
Hydramatic
machine

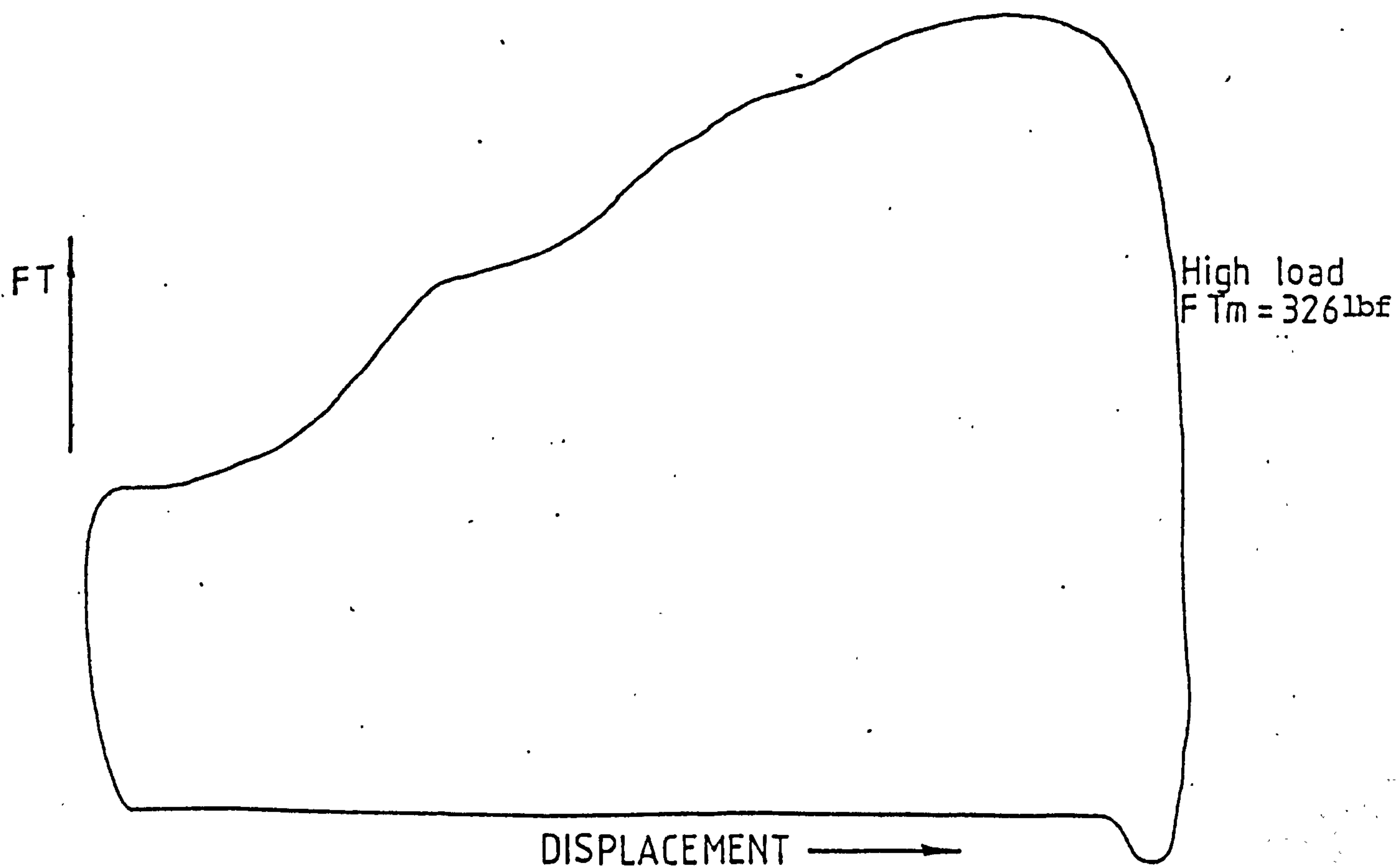
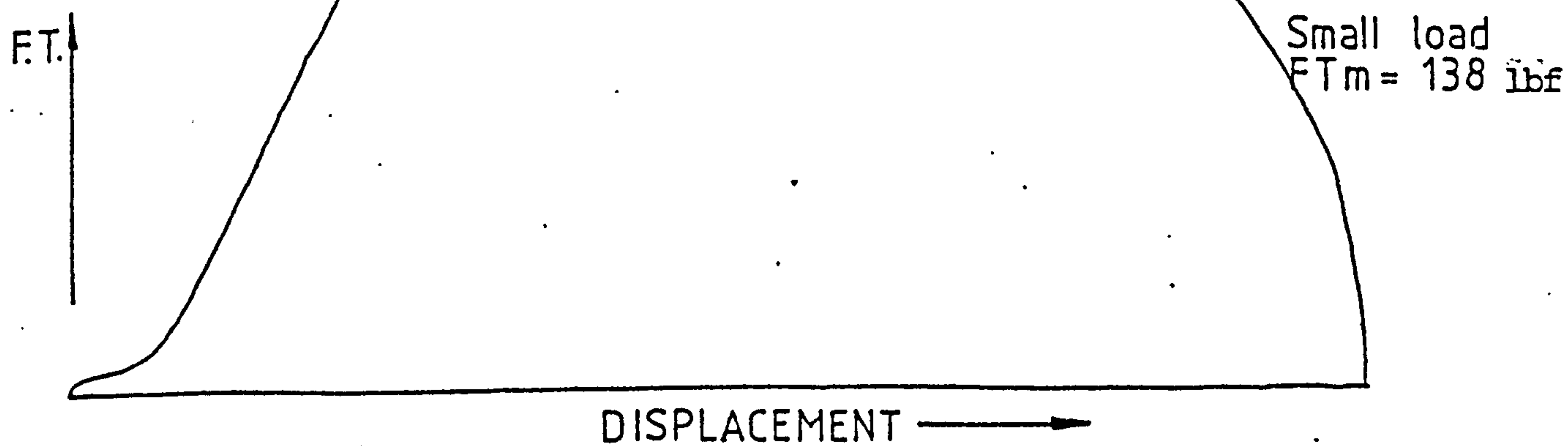


FIG. 8: Variations in thrust force developed by the Wicksteed Hydramatic saw on a common load setting with blades of different widths

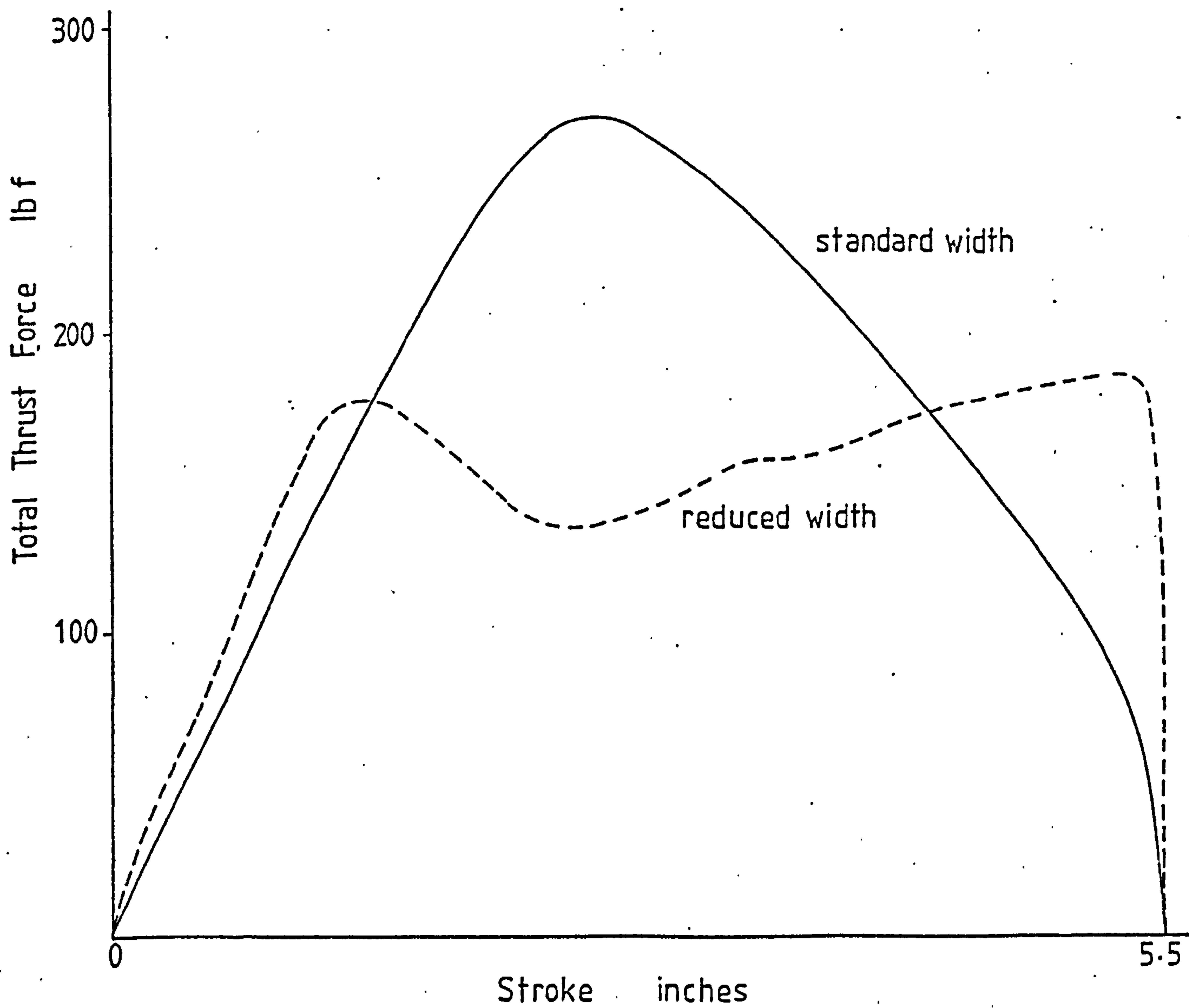


FIG. 9: The number of saw strokes to cut through a 25mm by 25mm mild steel bar using a Brand 'X' 6 T.P.I. blade against the mean thrust force developed by various power hacksawing machines

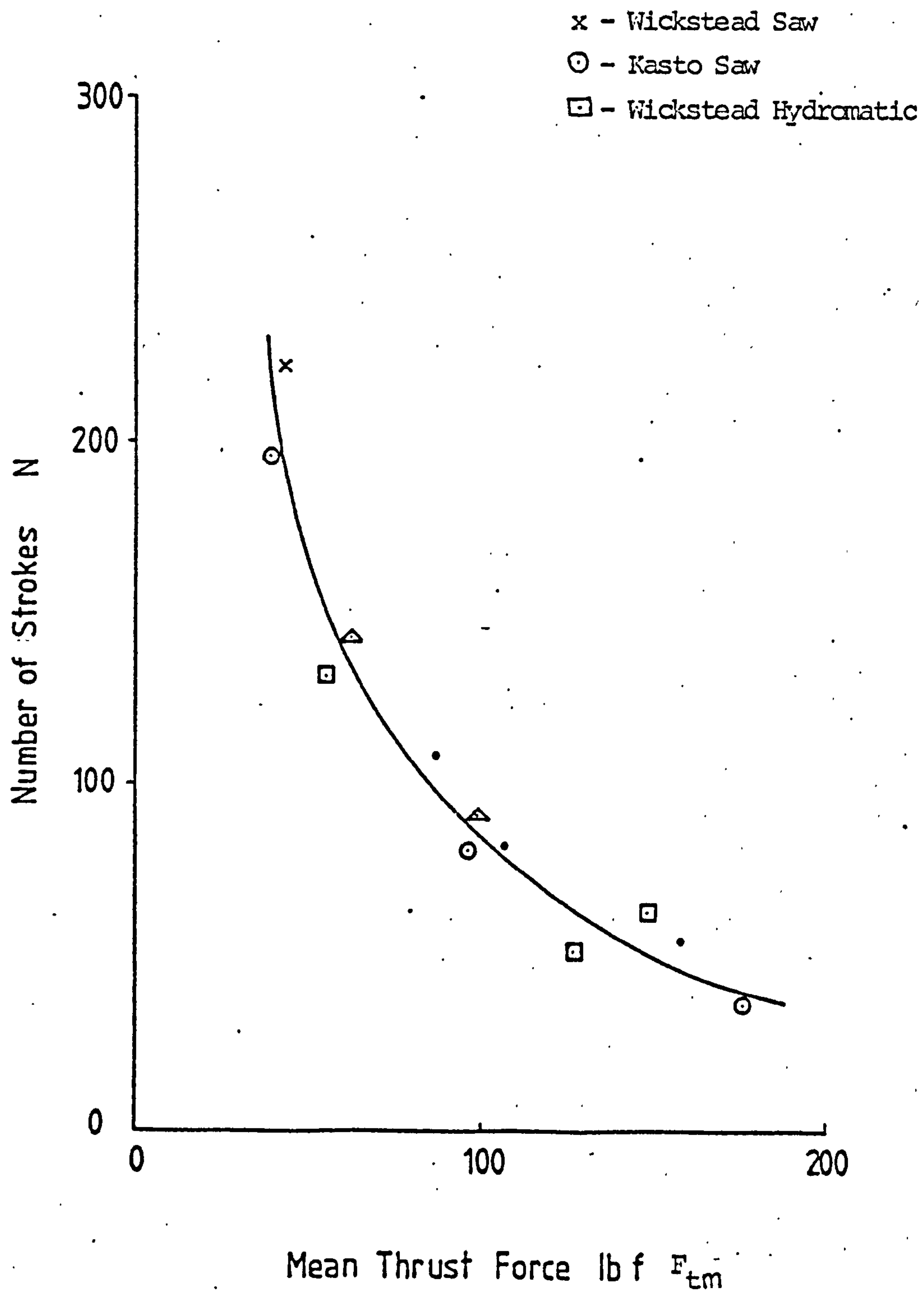


FIG. 9

FIG. 10: Geometry of the sawing action showing variations in the tooth factor

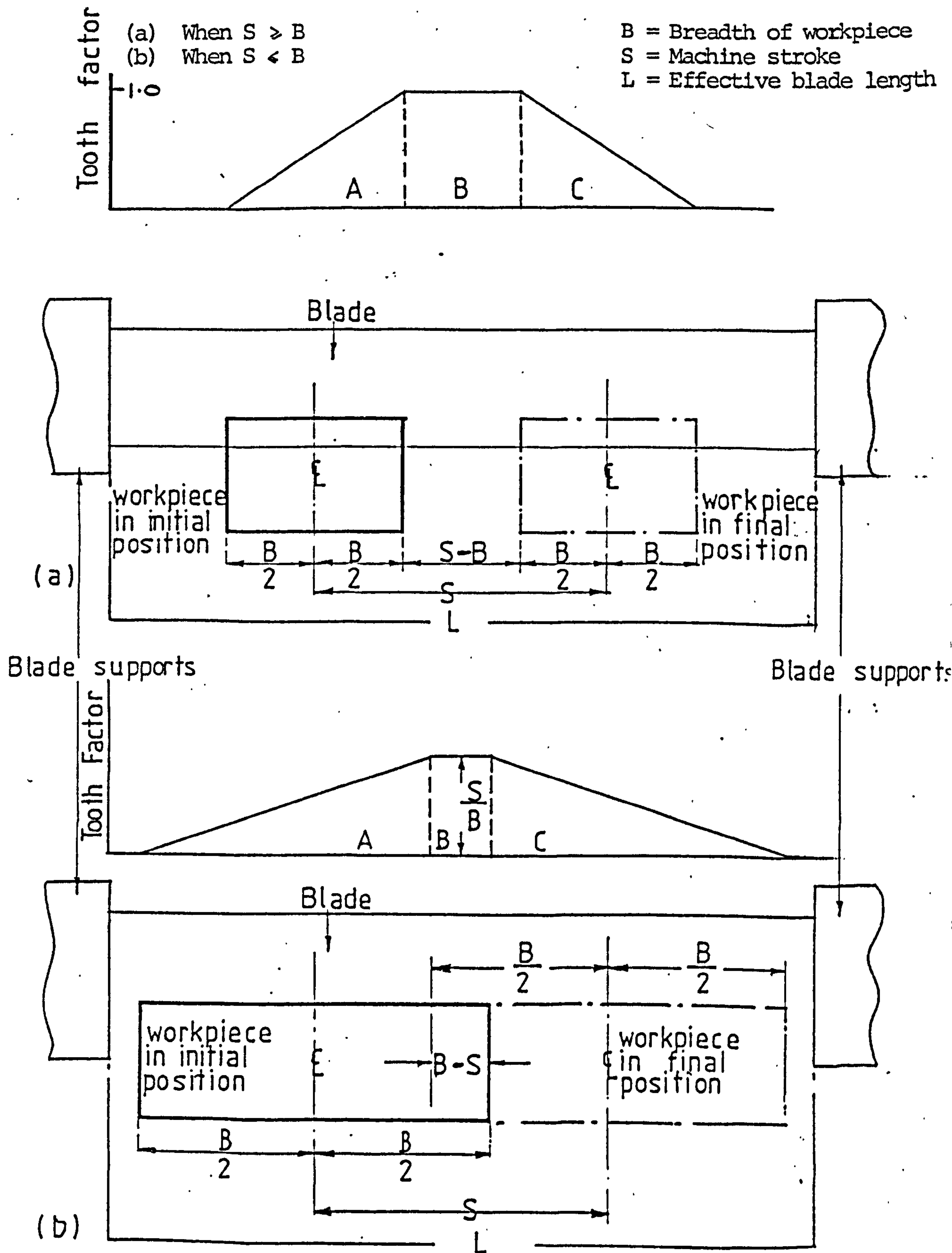
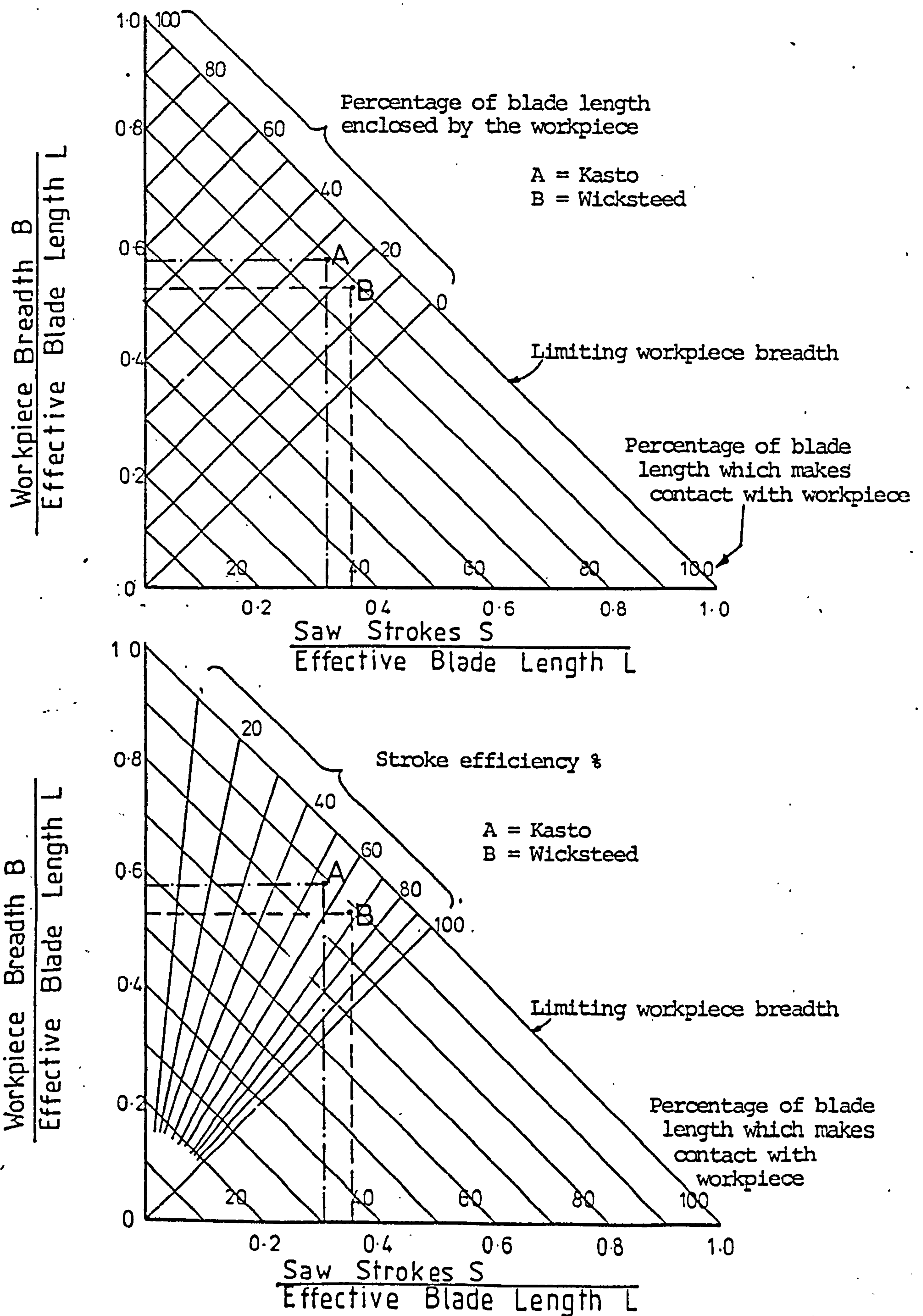
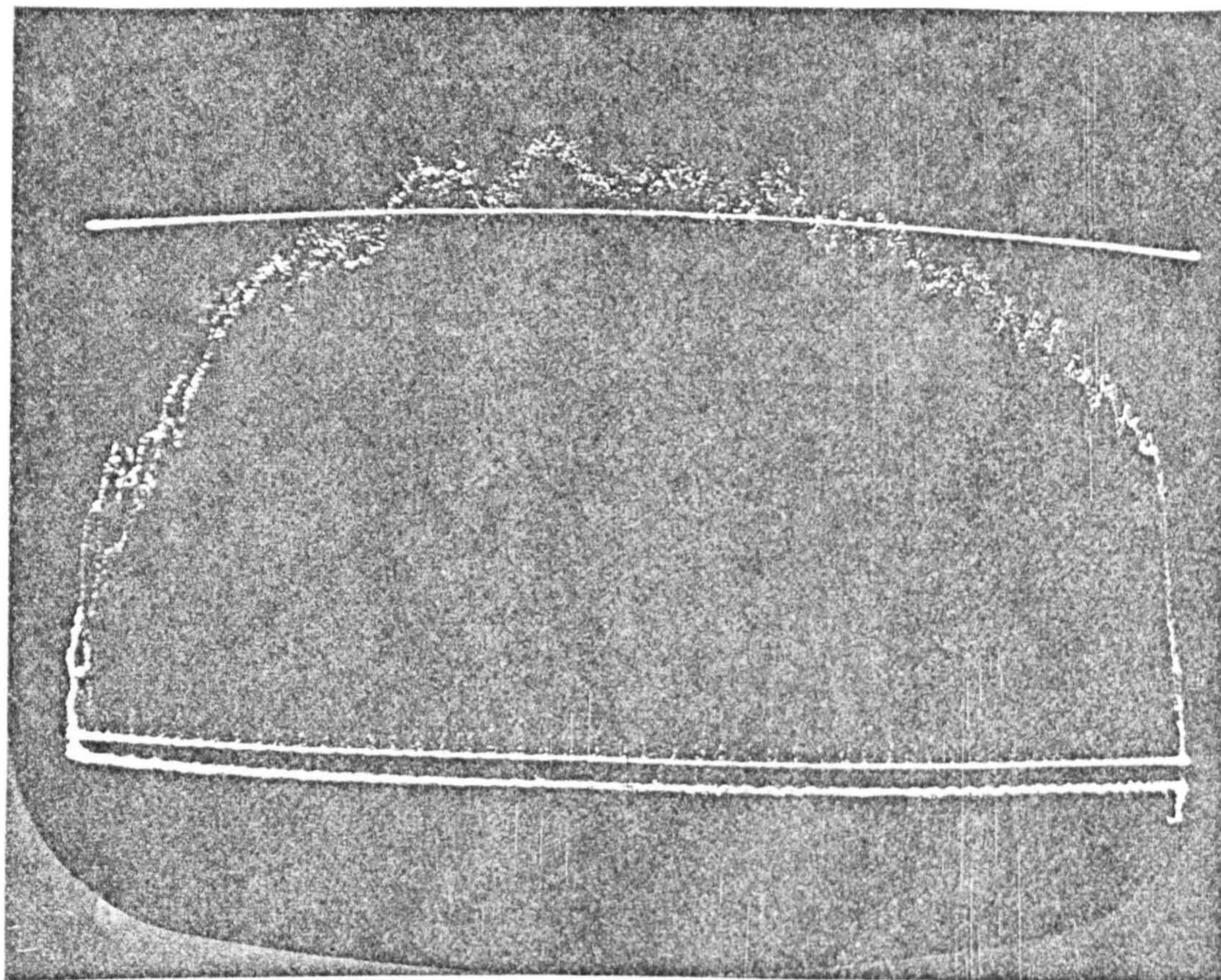


FIG. 11: Geometry relationships between saw stroke, workpiece breadth and the effective blade length



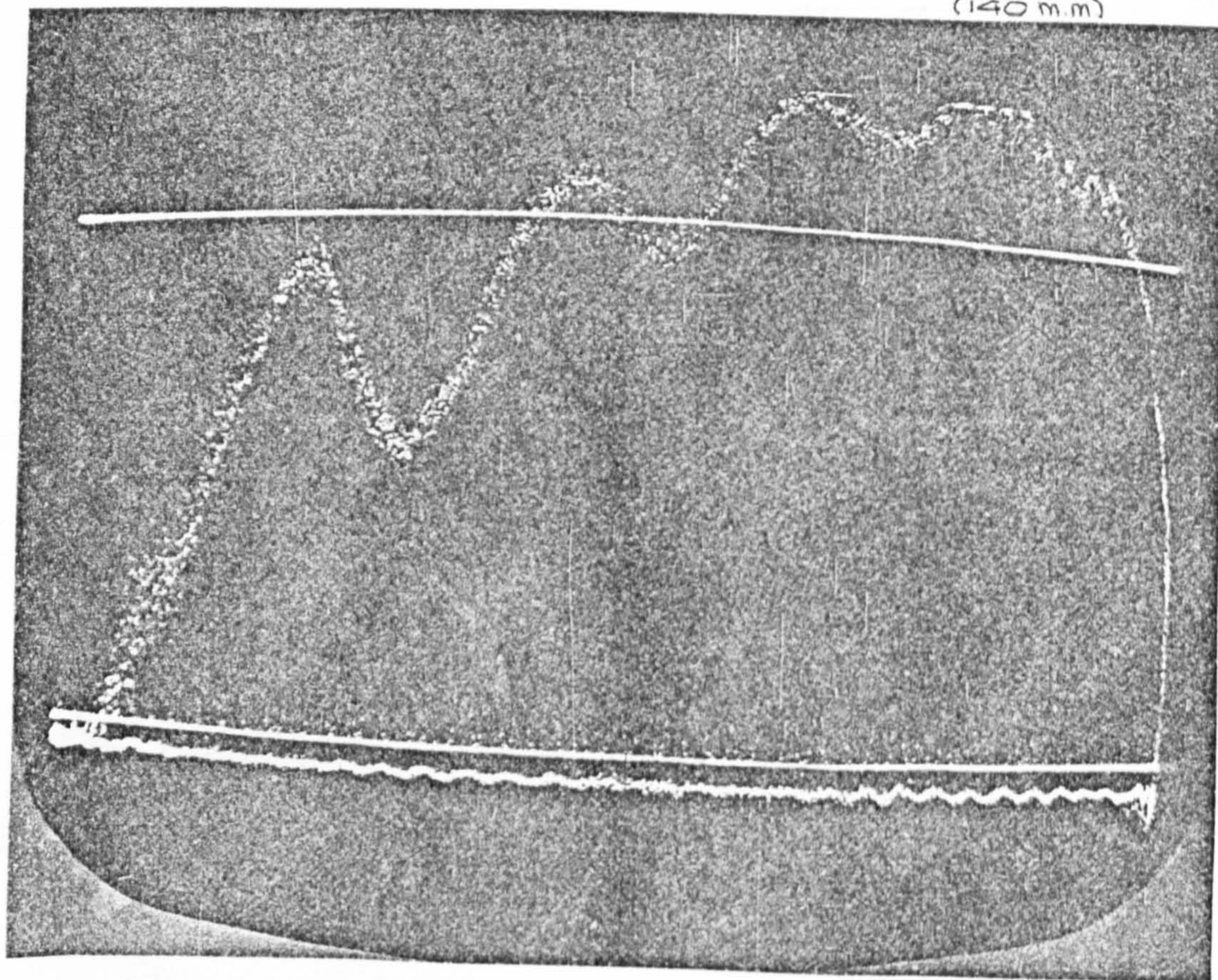
THRUST LOAD 1bf



(A) SLOW MACHINE SPEED (68 STROKES/MIN)

STROKE (140 mm)

THRUST LOAD 1bf



(B) HIGH MACHINE SPEED (120 STROKES/MIN)

STROKE (140 mm)

FIG.12 THRUST LOAD VARIATIONS DURING CUTTING STROKE FOR WICKSTEED HYDRAULIC SAW

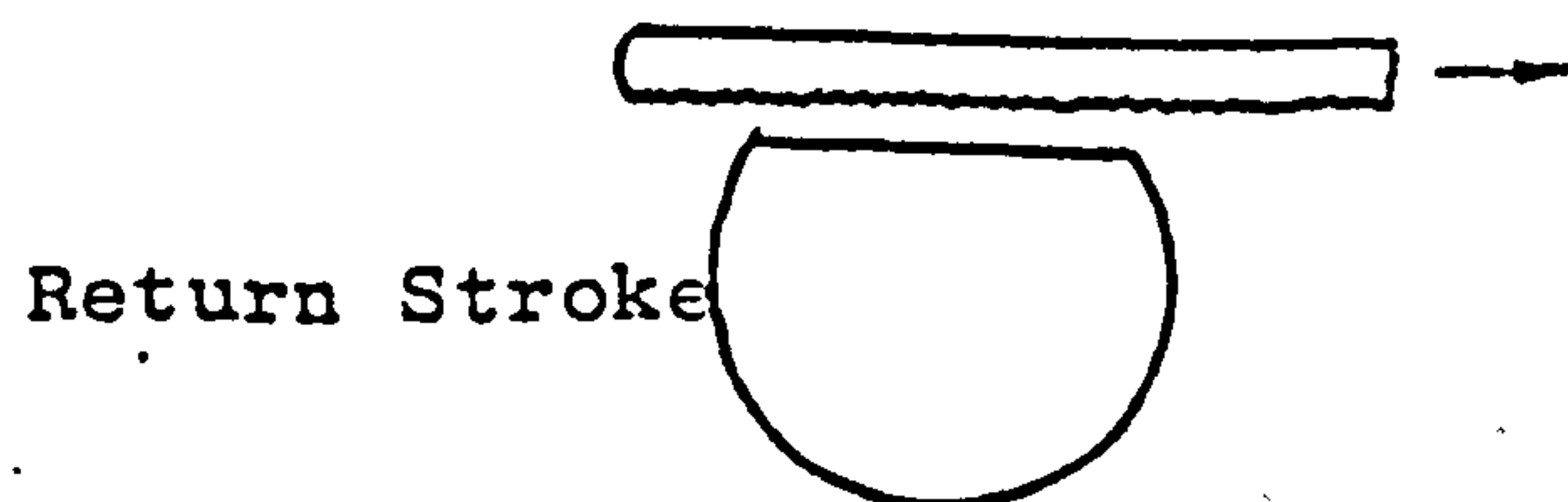
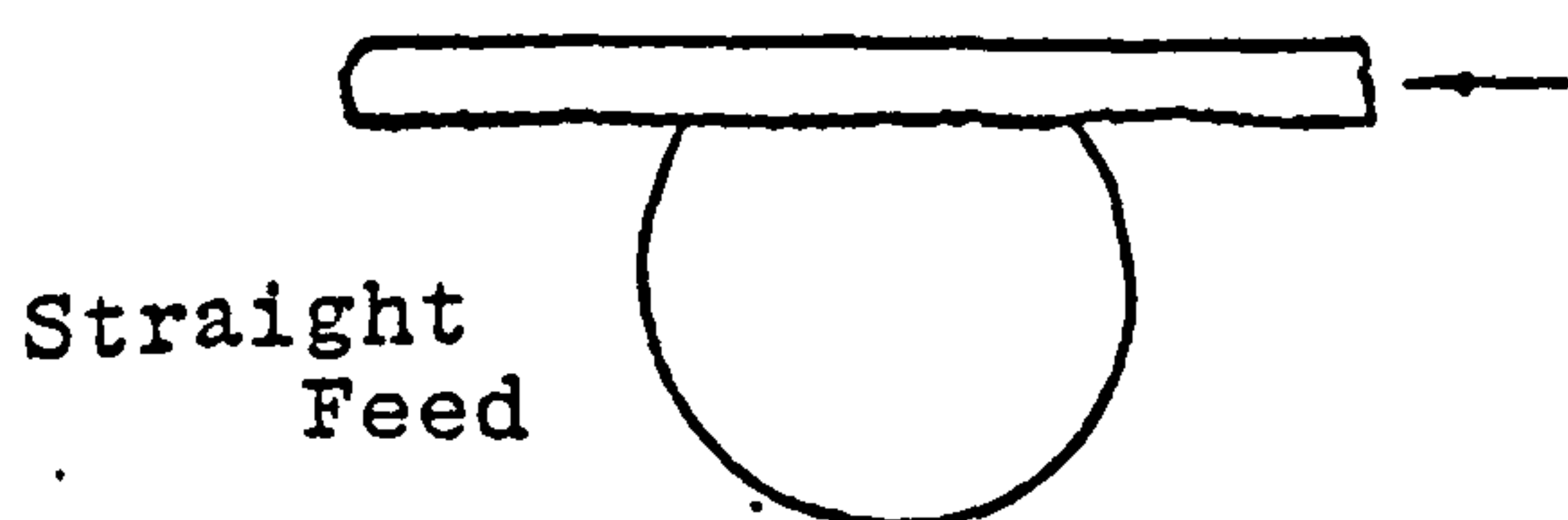
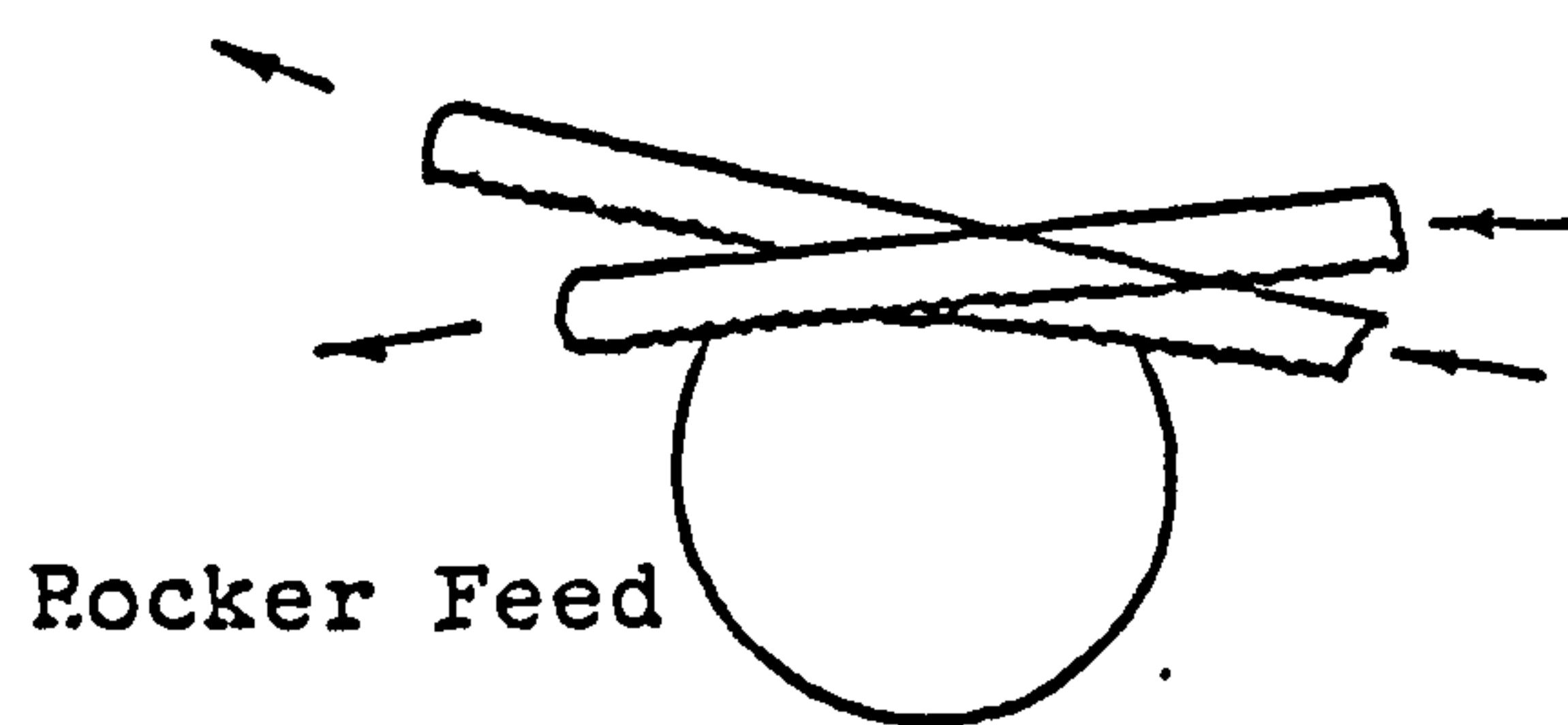
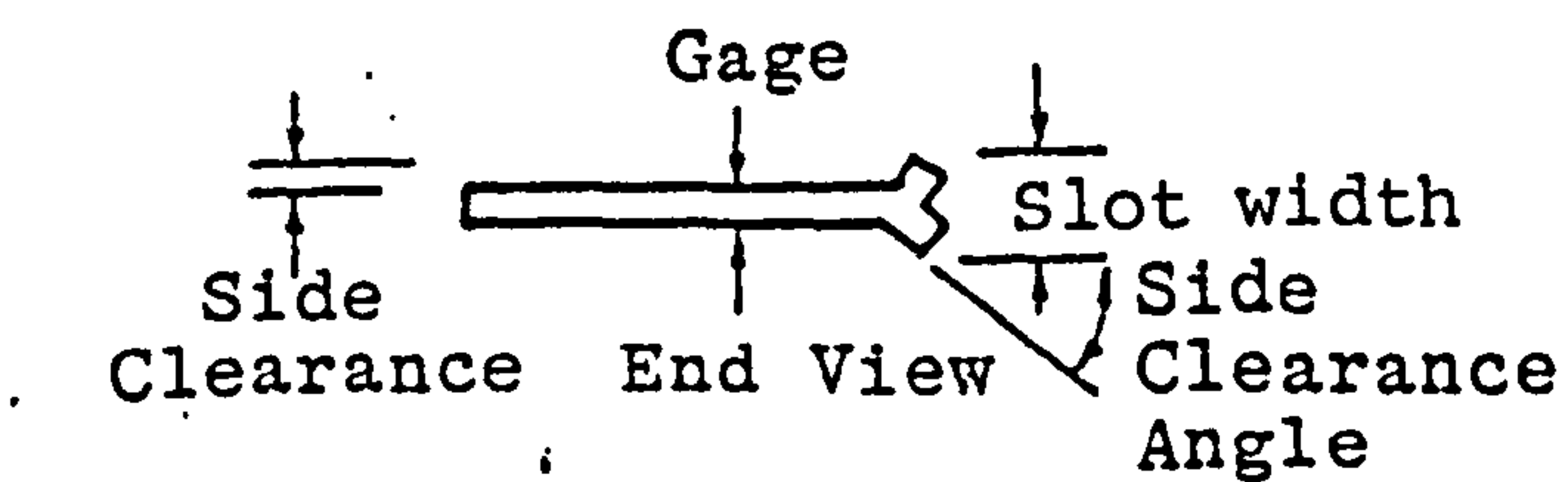
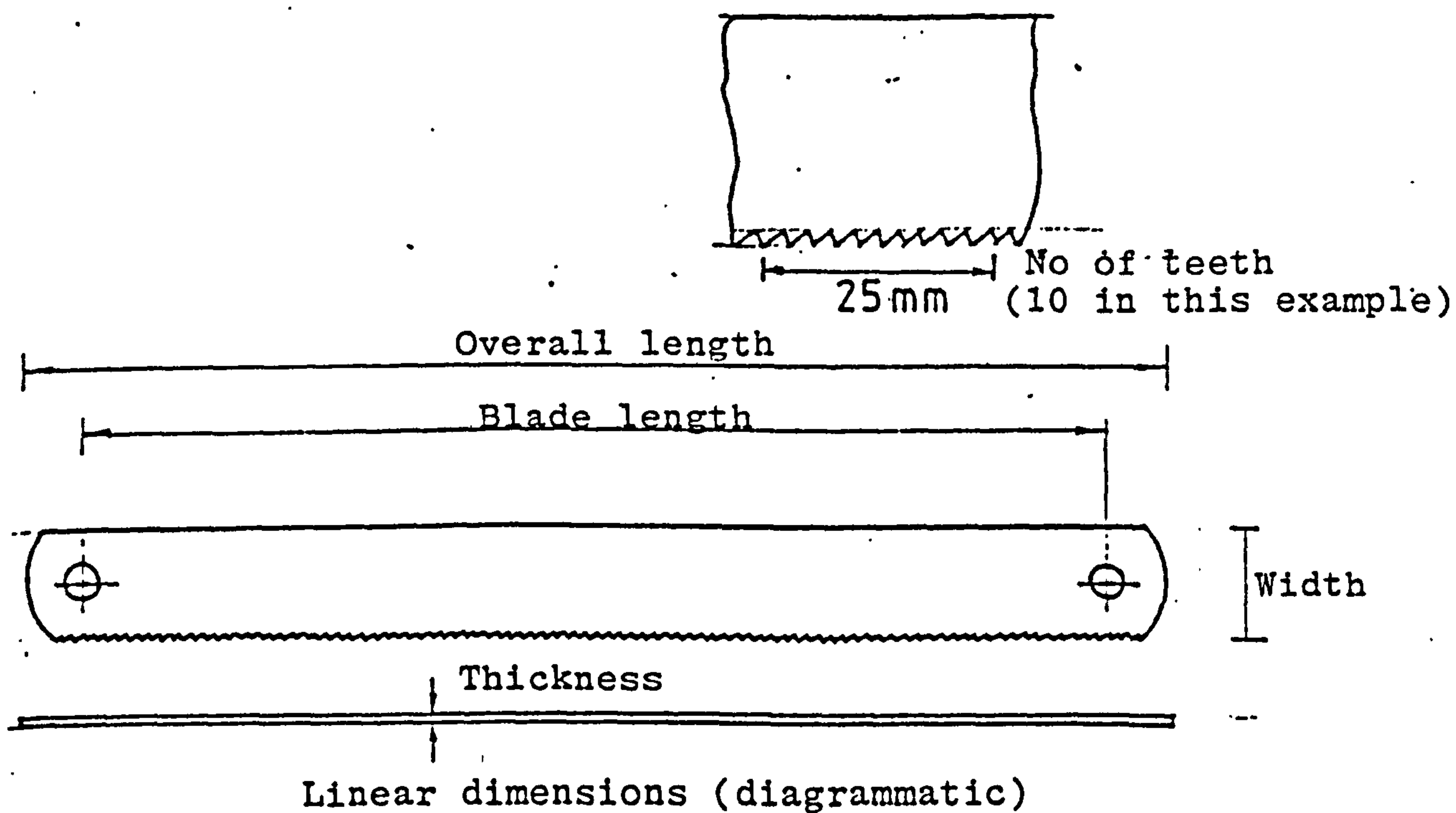
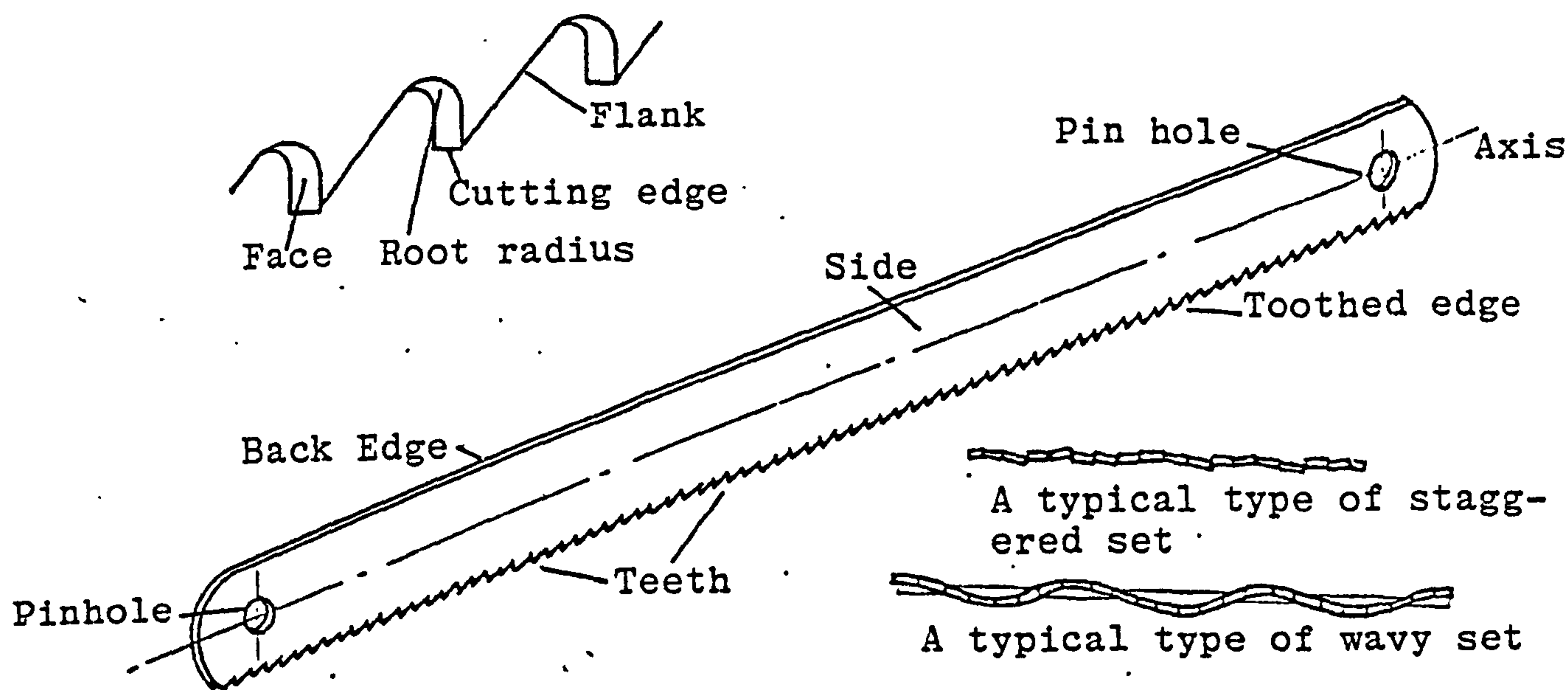


FIG.13 SOME FEATURES OF POWER HACKSAW BLADES AND THEIR CUTTING

FIG. 14: Hacksaw blade teeth patterns

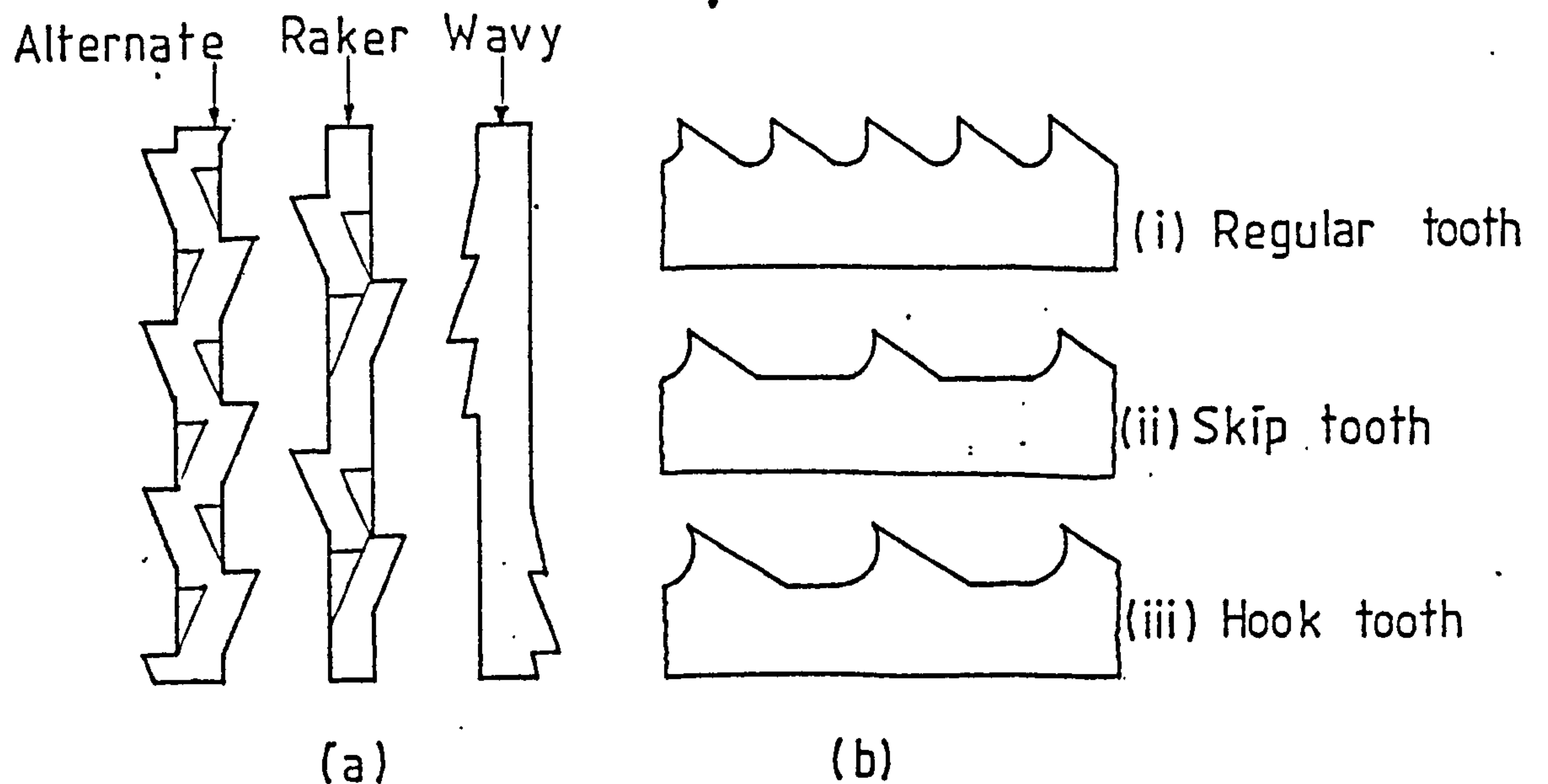
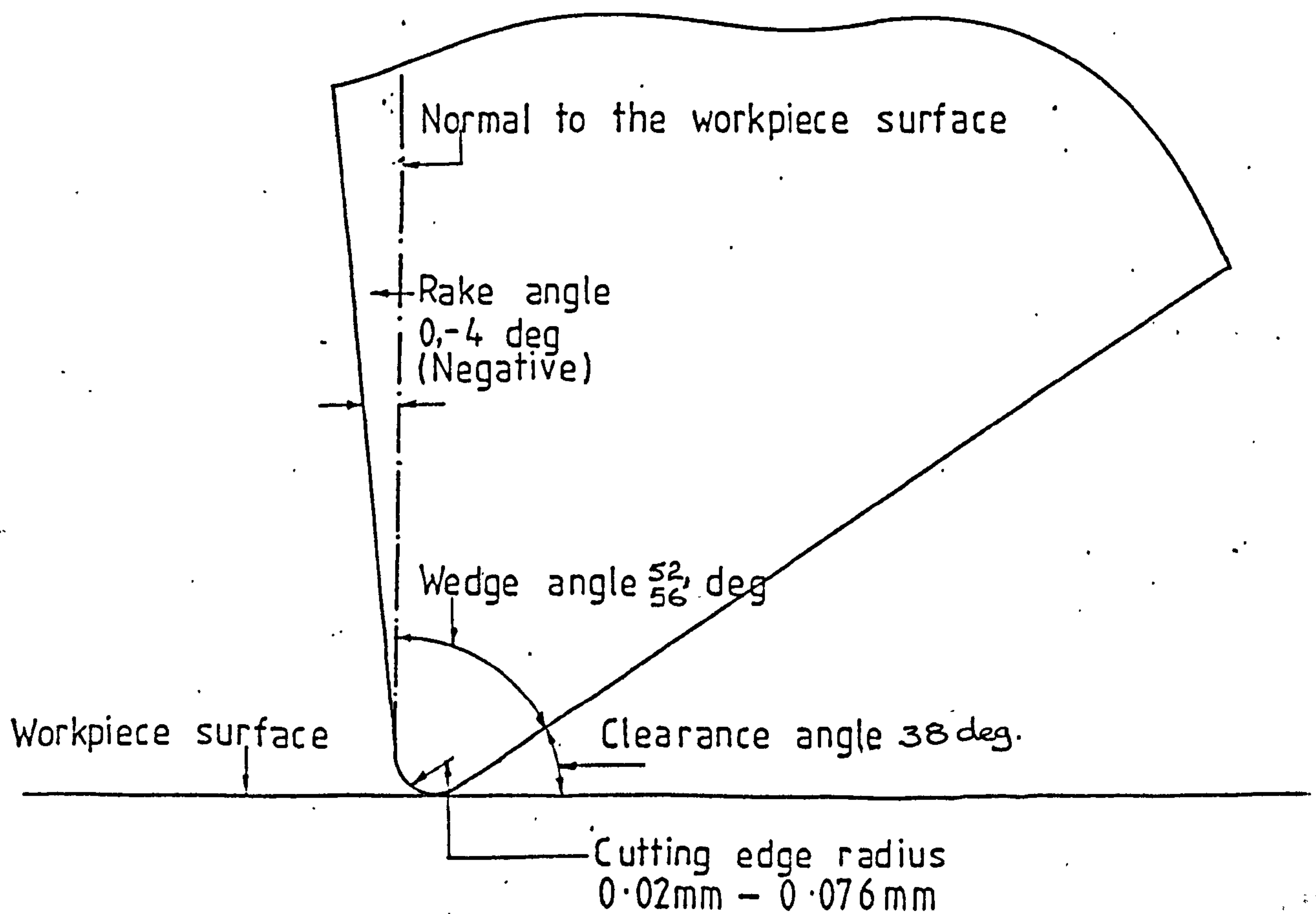


FIG. 15: Cutting edge geometry of a hacksaw blade tooth



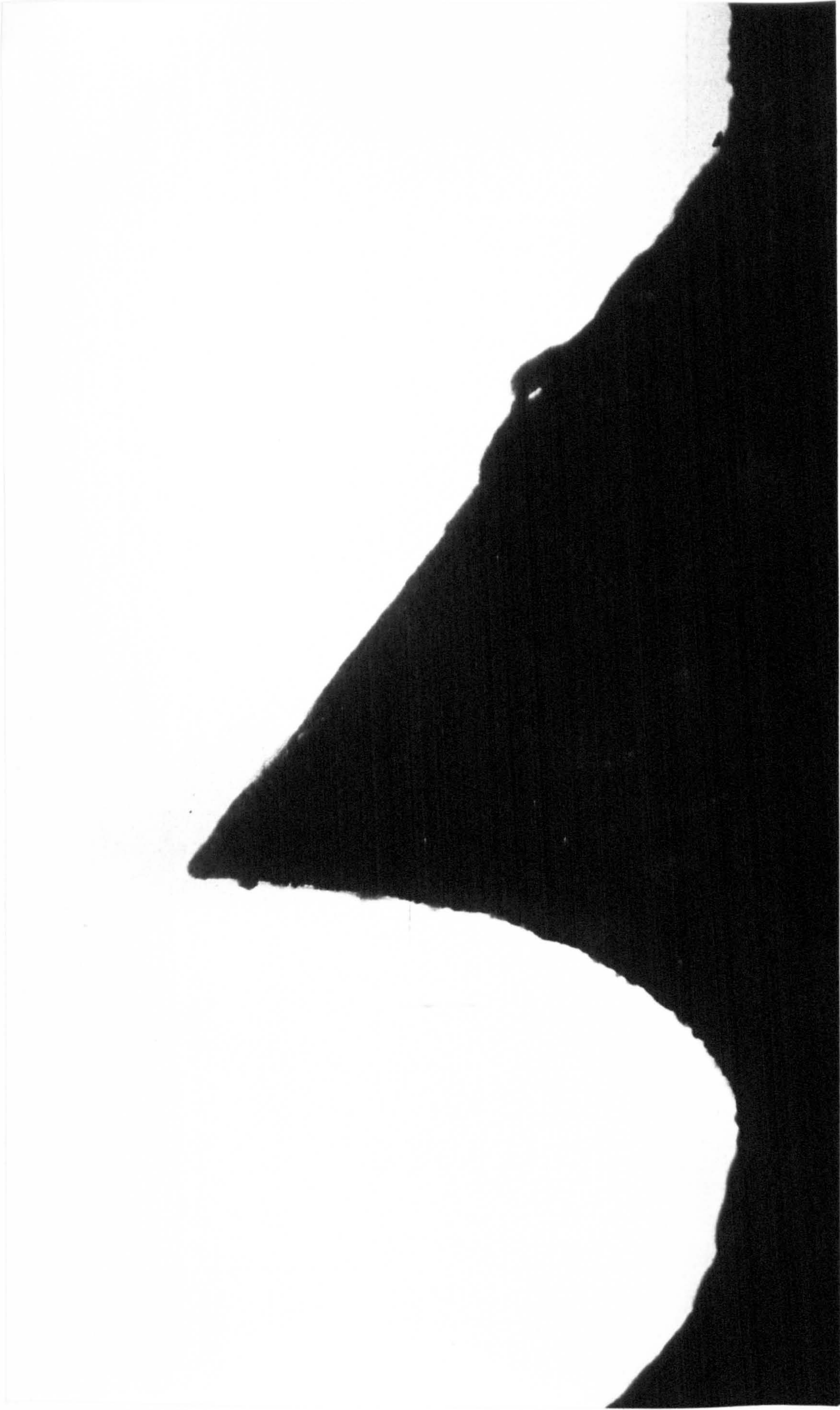


FIG.16. SAW TOOTH (NEW) PROFILE - SHADOGRAPH (x 50) 6 TPI BLADE

FIG. 17: Comparison between the mean thrust force and the force at mid-stroke position for various sawing machines

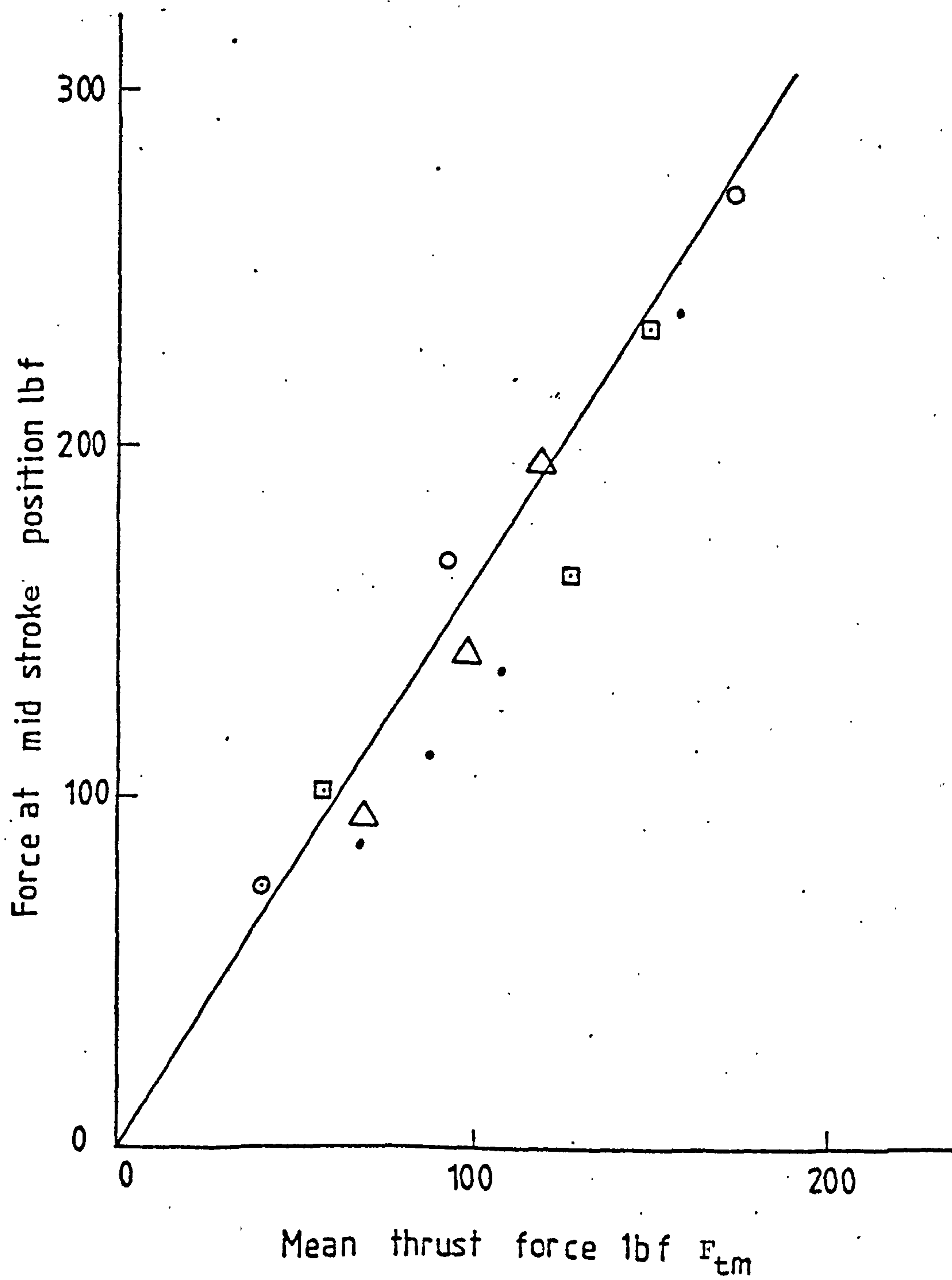


FIG. 17

FIG. 18: The depth of cut achieved by a Brand 'X' 6 T.P.I. blade cutting mild steel against the mean thrust force developed by various power hacksawing machines

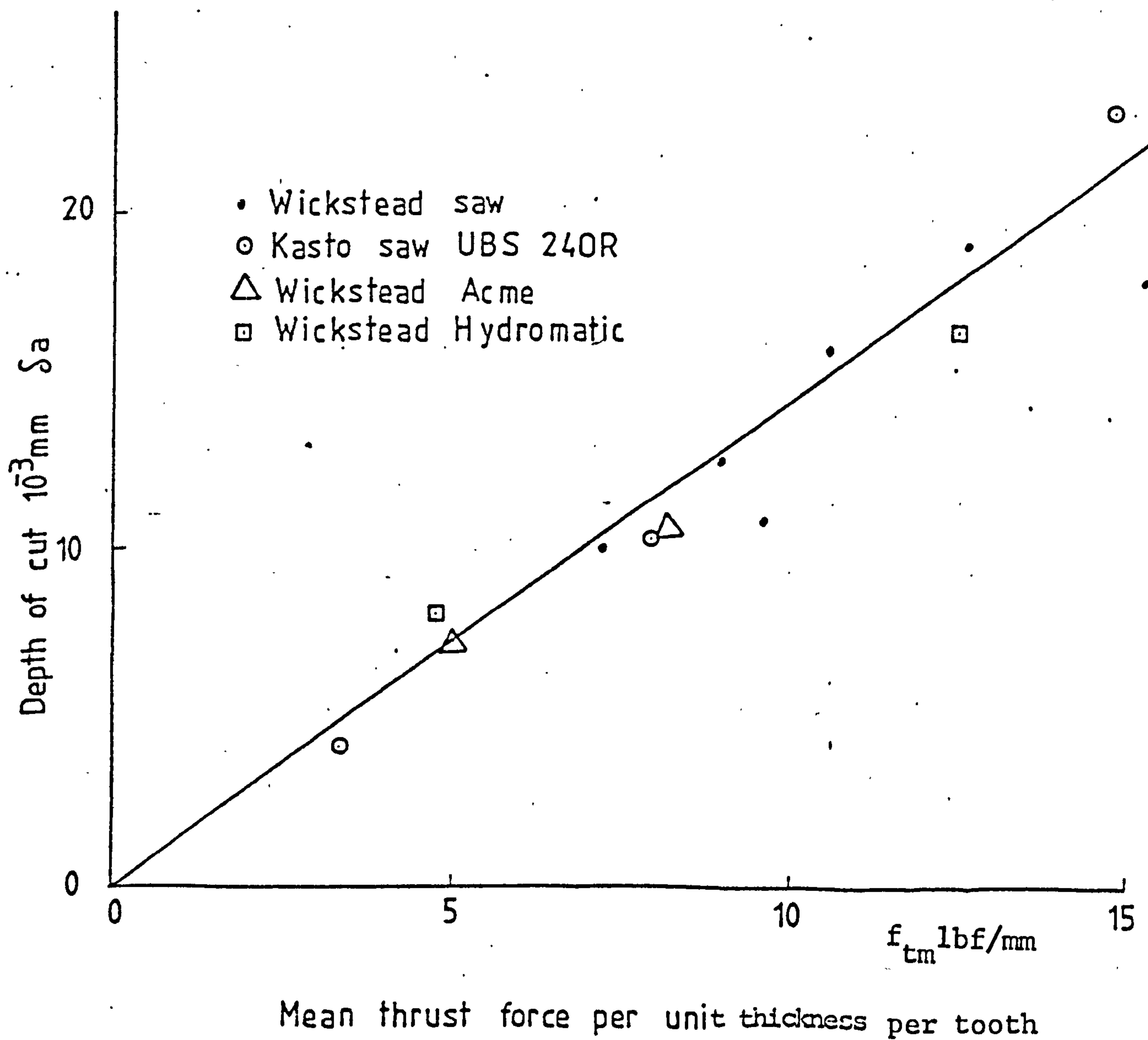


FIG. 18

FIG. 19: Diagrammatic representation of the paths followed by each tooth

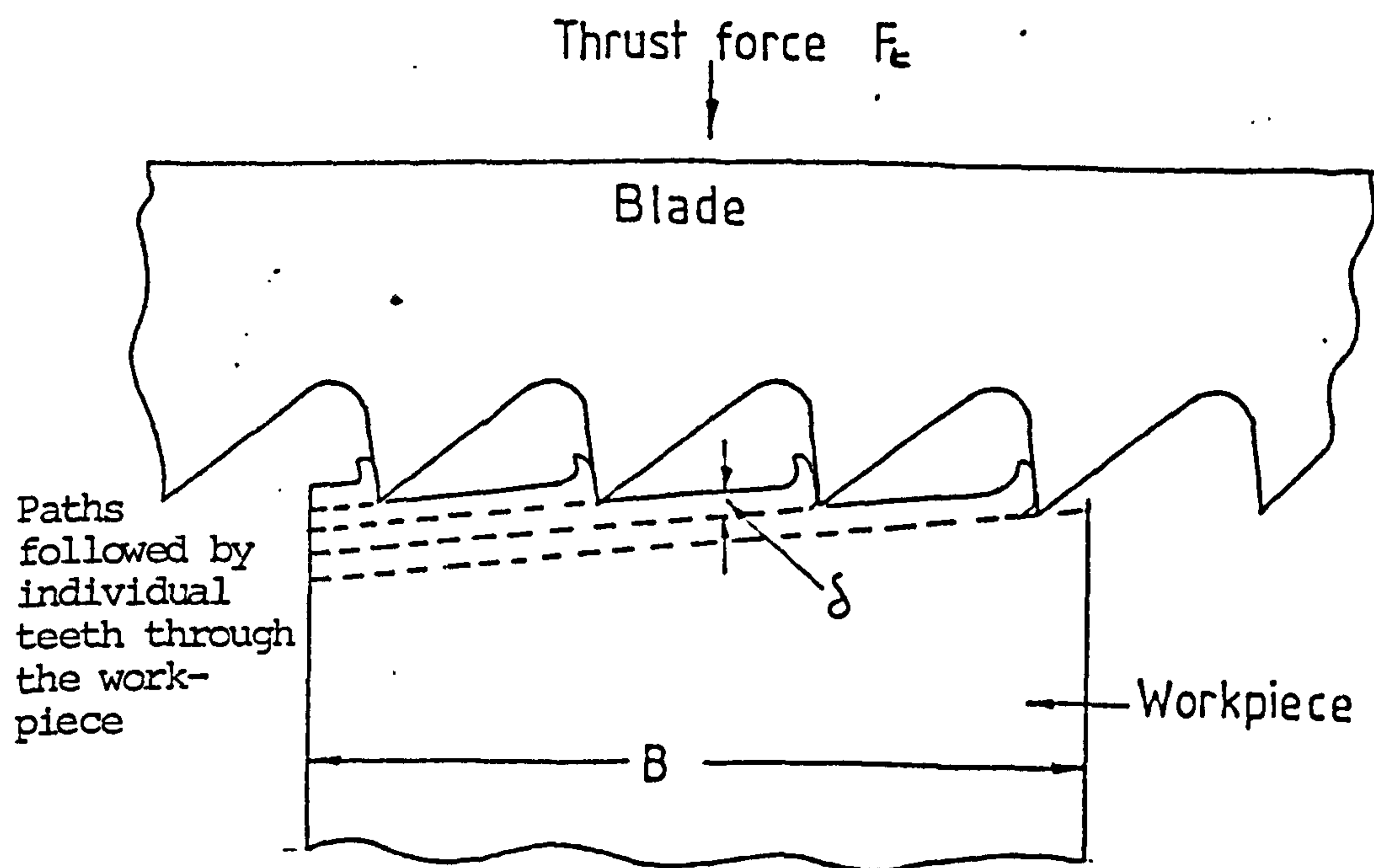


FIG. 20: Instantaneous cutting force component against the instantaneous thrust force component for a 6 T.P.I. blade cutting mild steel

Workpiece breadth: 25 mm

Blade: 400 x 40 x 2 x 6 T.P.I. (Raker Set)

Stroke: 5.5 inches

76 Strokes/min

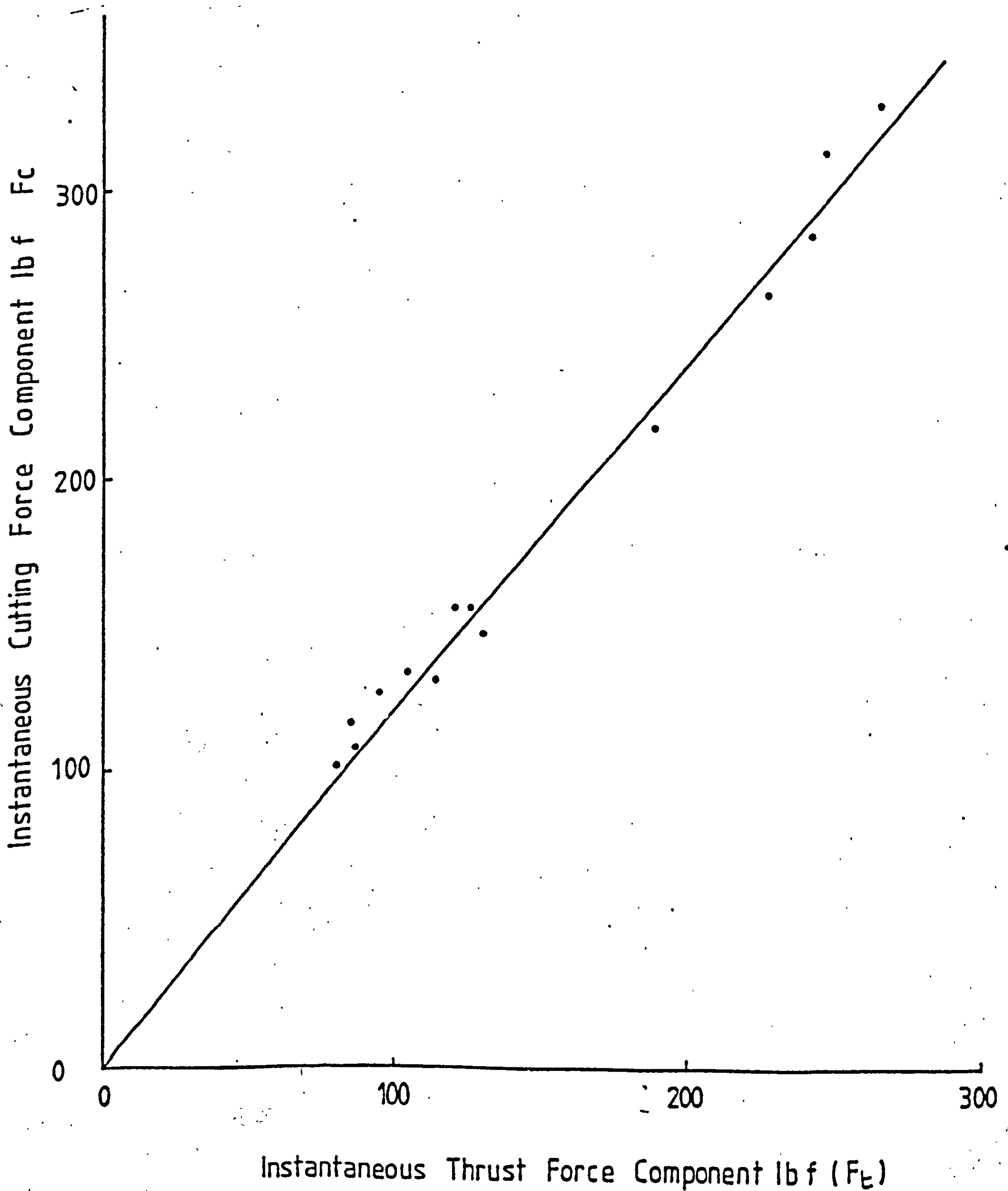


FIG. 20



FIG.21 HACKSAW MACHINE AND ASSOCIATED INSTRUMENTATION FOR
BLADE TESTING

FIG.22 THE LOAD DEVELOPED BETWEEN THE BLADE AND THE WORKPIECE DURING THE CUTTING STROKE ON VARIOUS LOAD SETTINGS

LOAD SETTINGS INDICATED BY (2)

NEW BLADE:- 400 x 40 x 2 x 6 TPI
76 STROKES/MIN
WORKPIECE:- ENI A 25 x 25 MM

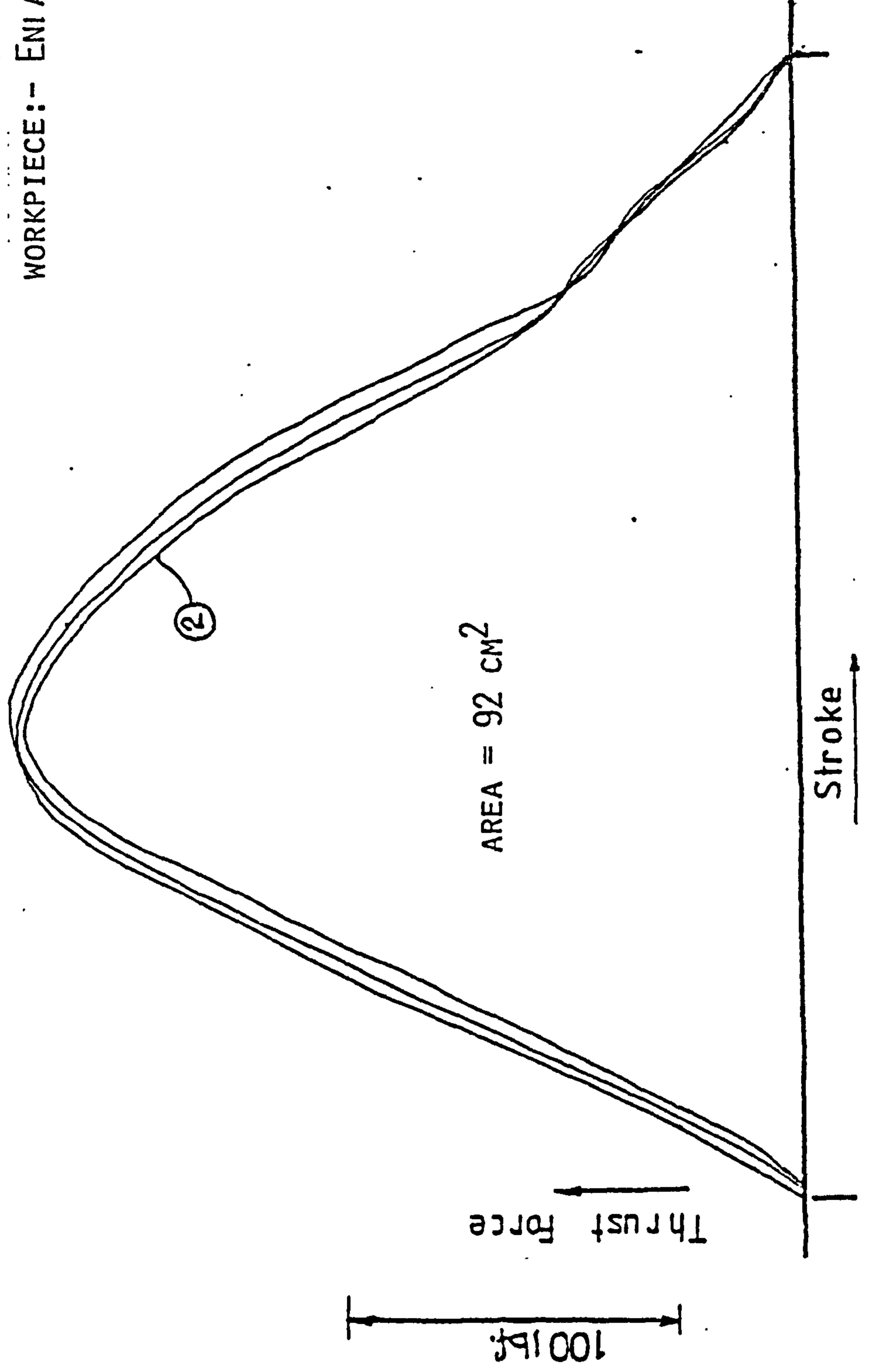


Fig.22(A)

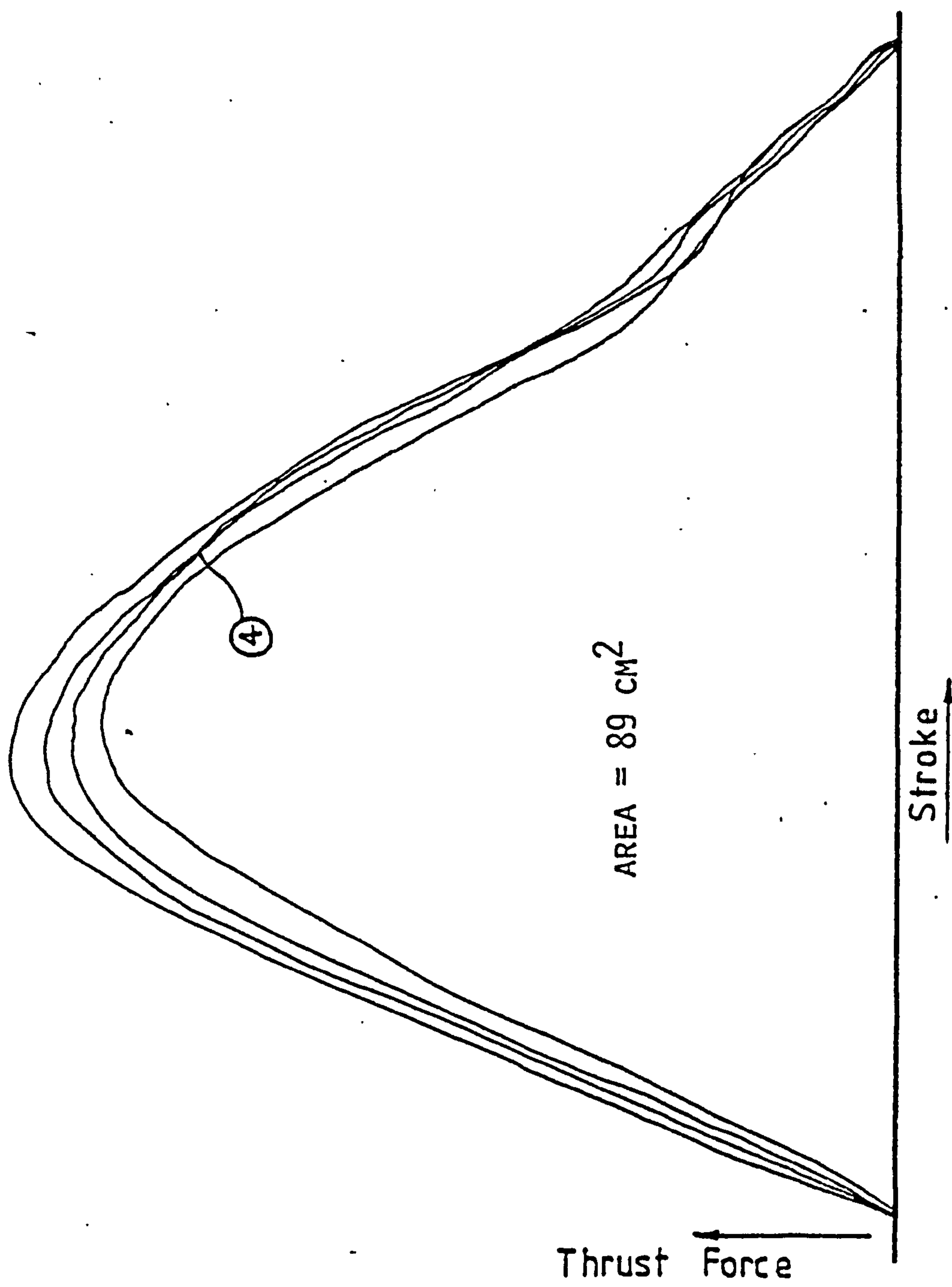


FIG.22(B)

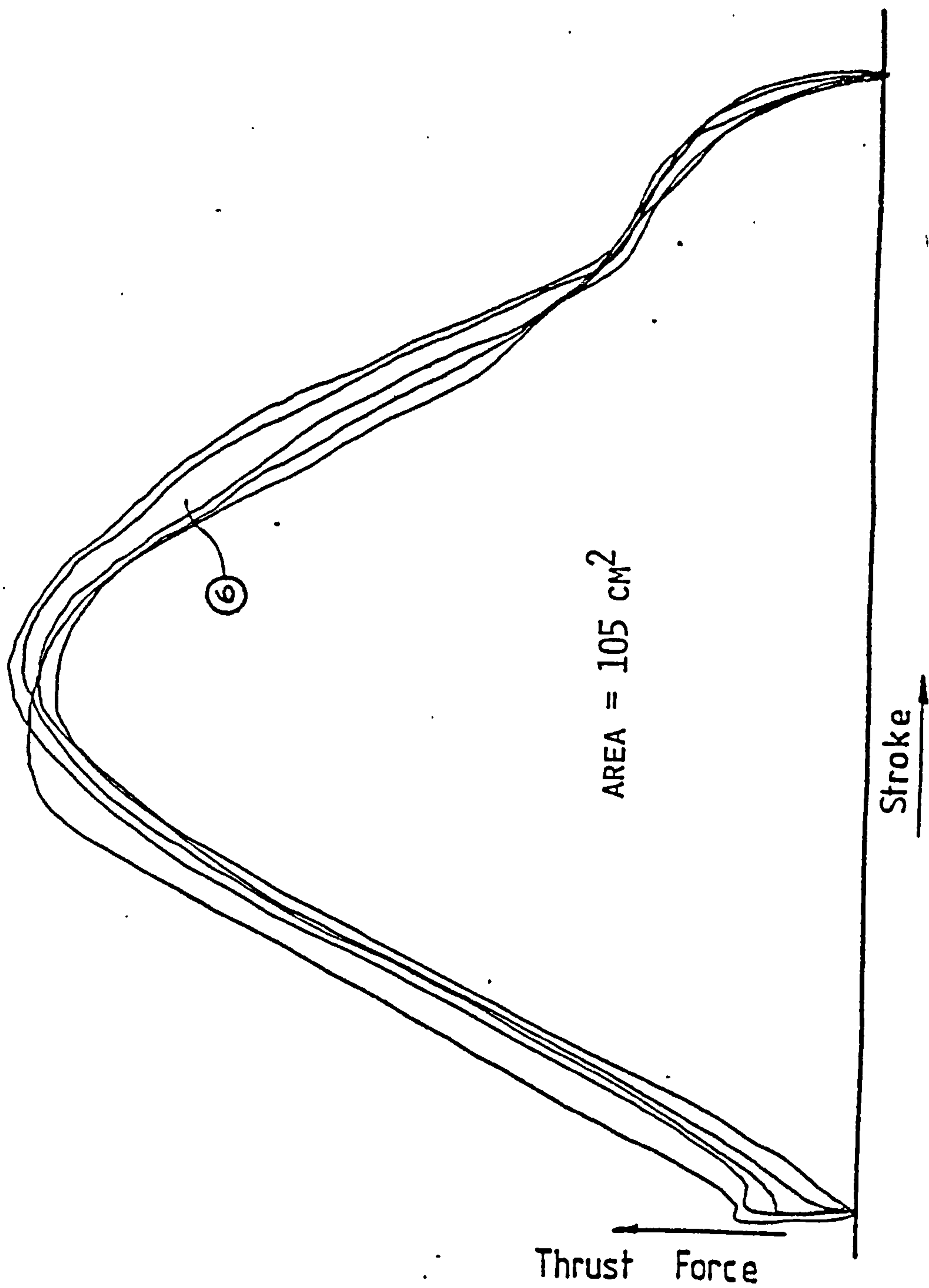


FIG.22(c)

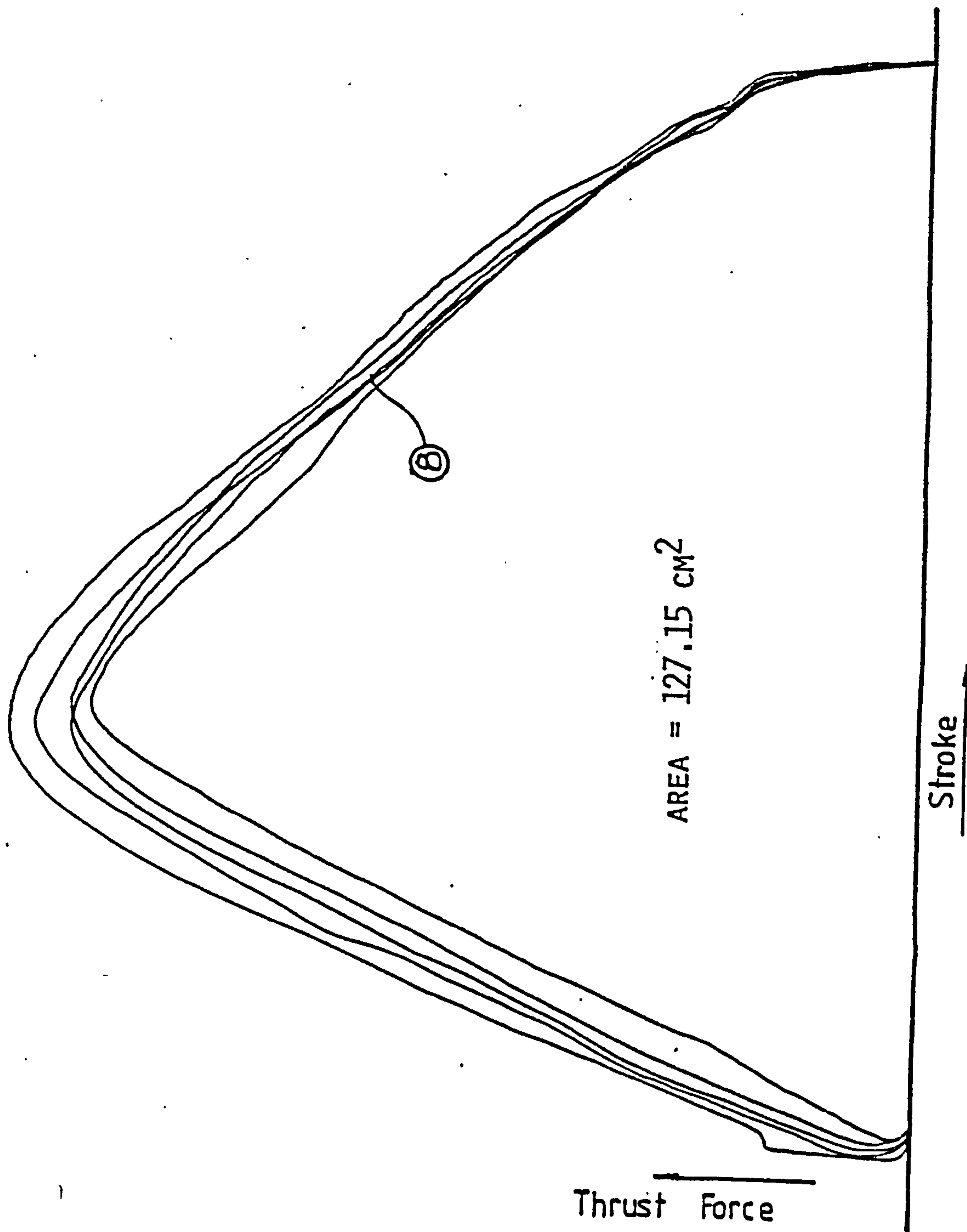


FIG.22(D)

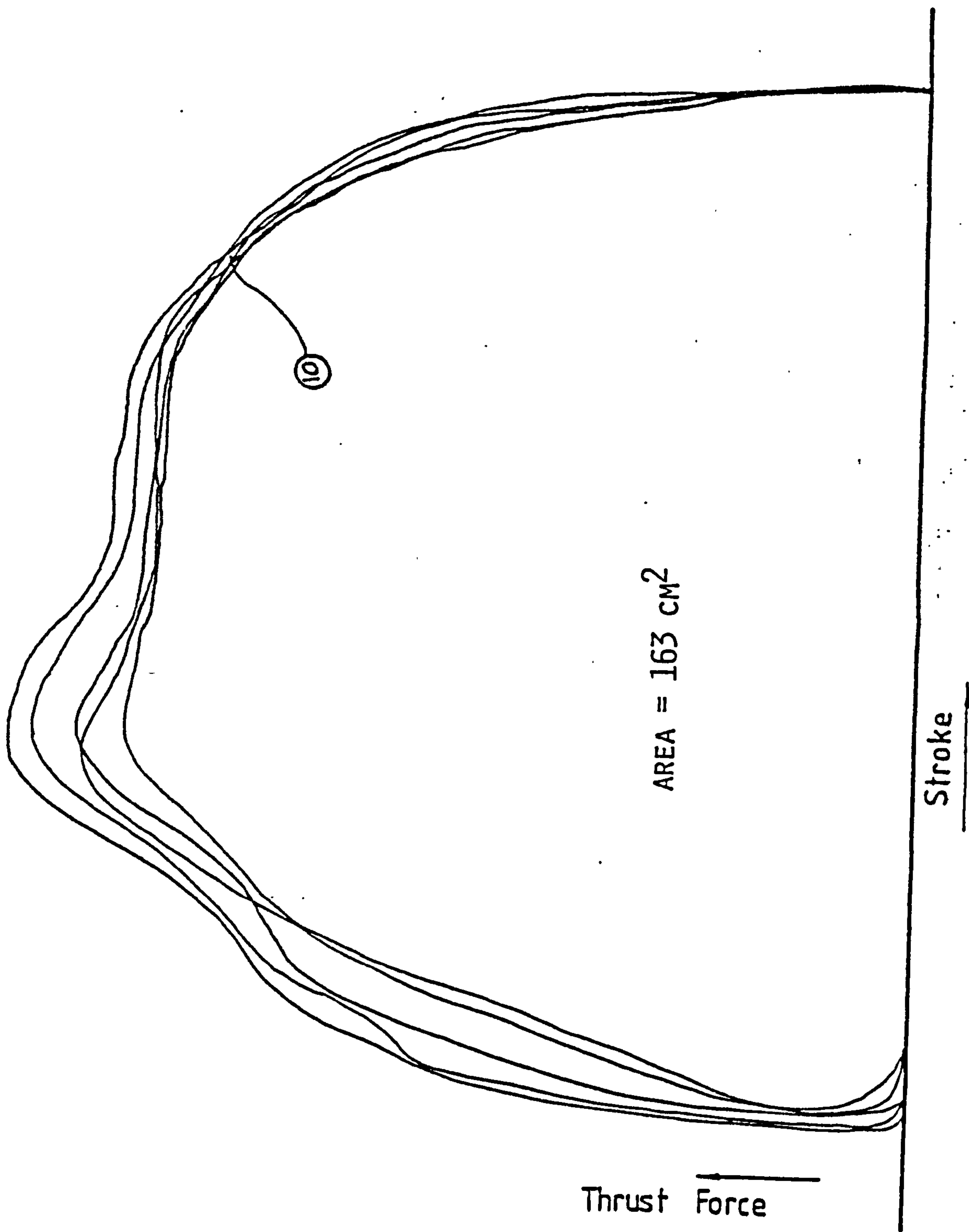


FIG.22(E)

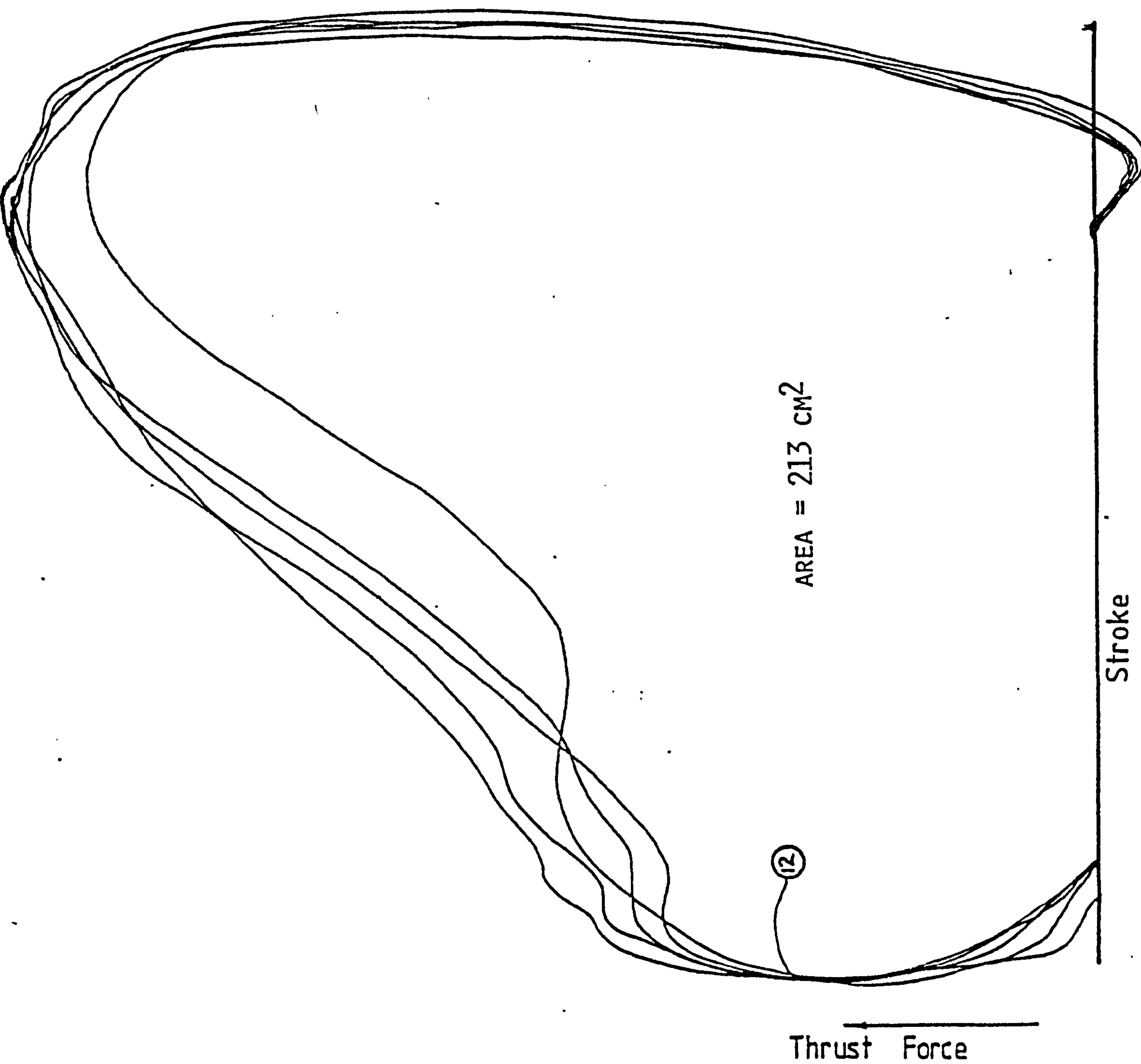


FIG.22(F)

FIG. 23: The average depth of cut per tooth against the thrust load per tooth per unit thickness for blades having different teeth pitch.

Cutting specimen: 25mm x 25mm, Enla
 Cutting fluid : Air
 Cutting speed : 76 strokes/min
 Machine : Wickstead 200mm Hydramatic Saw

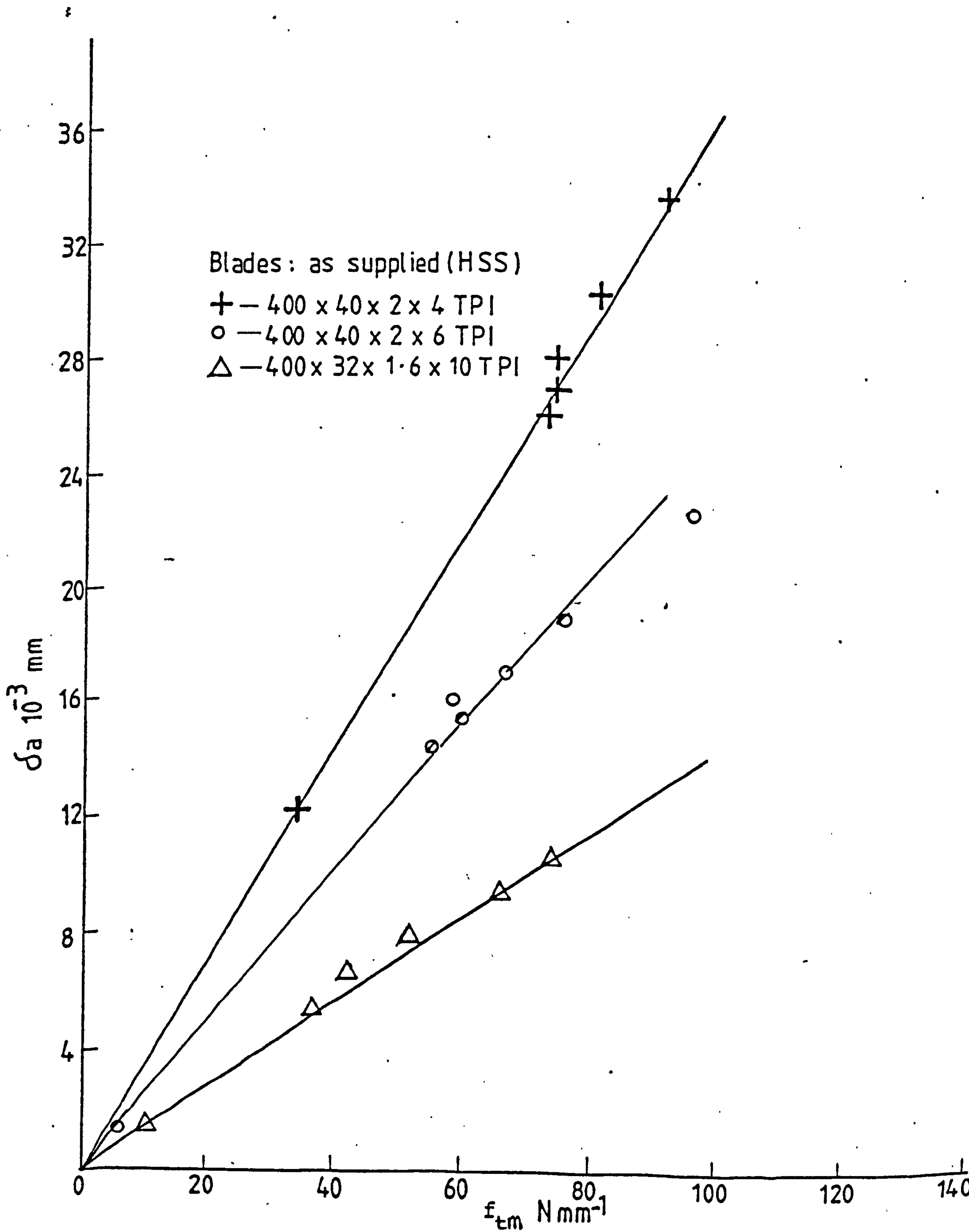


FIG. 23

FIG. 24: The cutting constant against the reciprocal of the number of teeth in contact with the workpiece

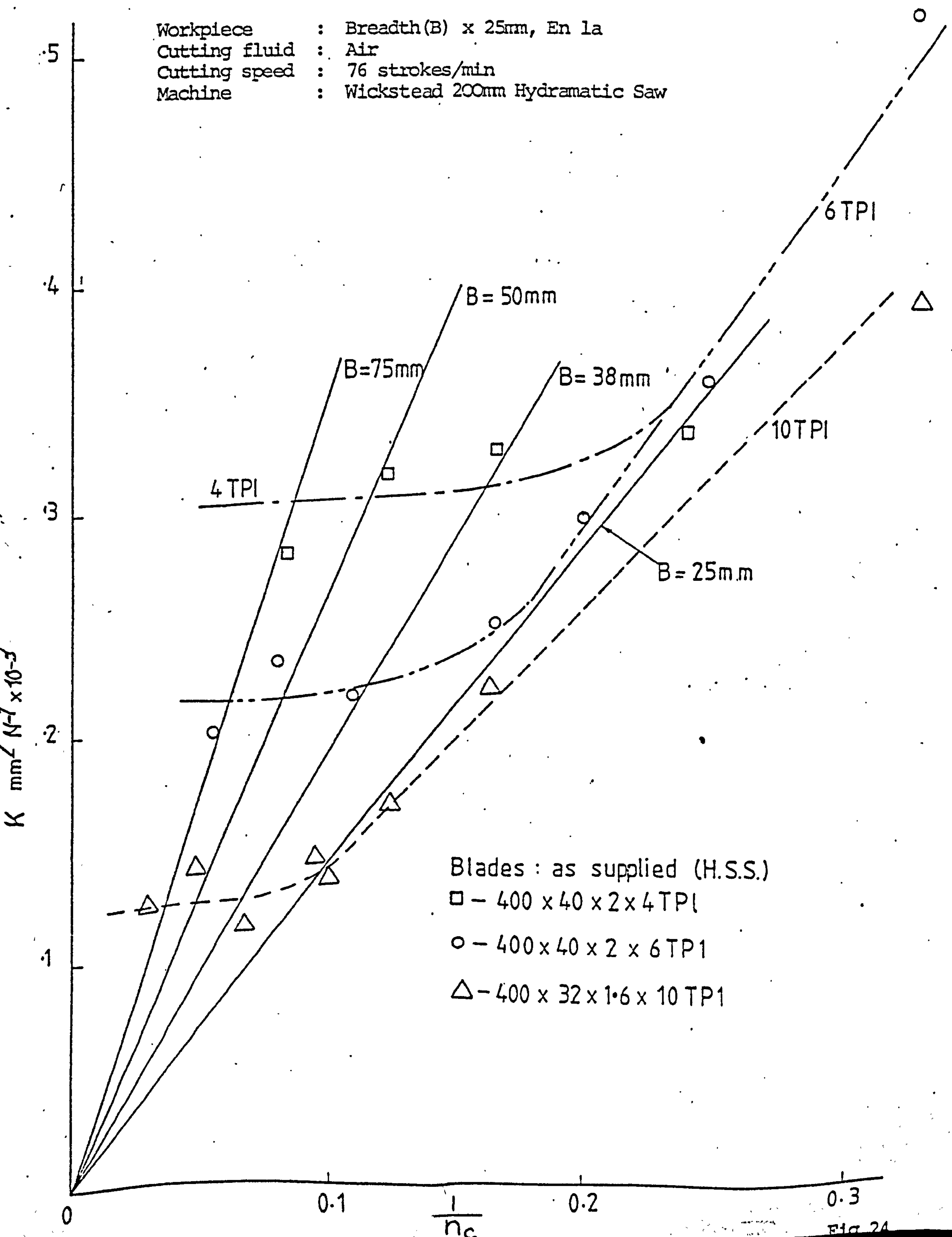


FIG. 25: Comparison of blade performances.

Machine: Kasto Power Saw

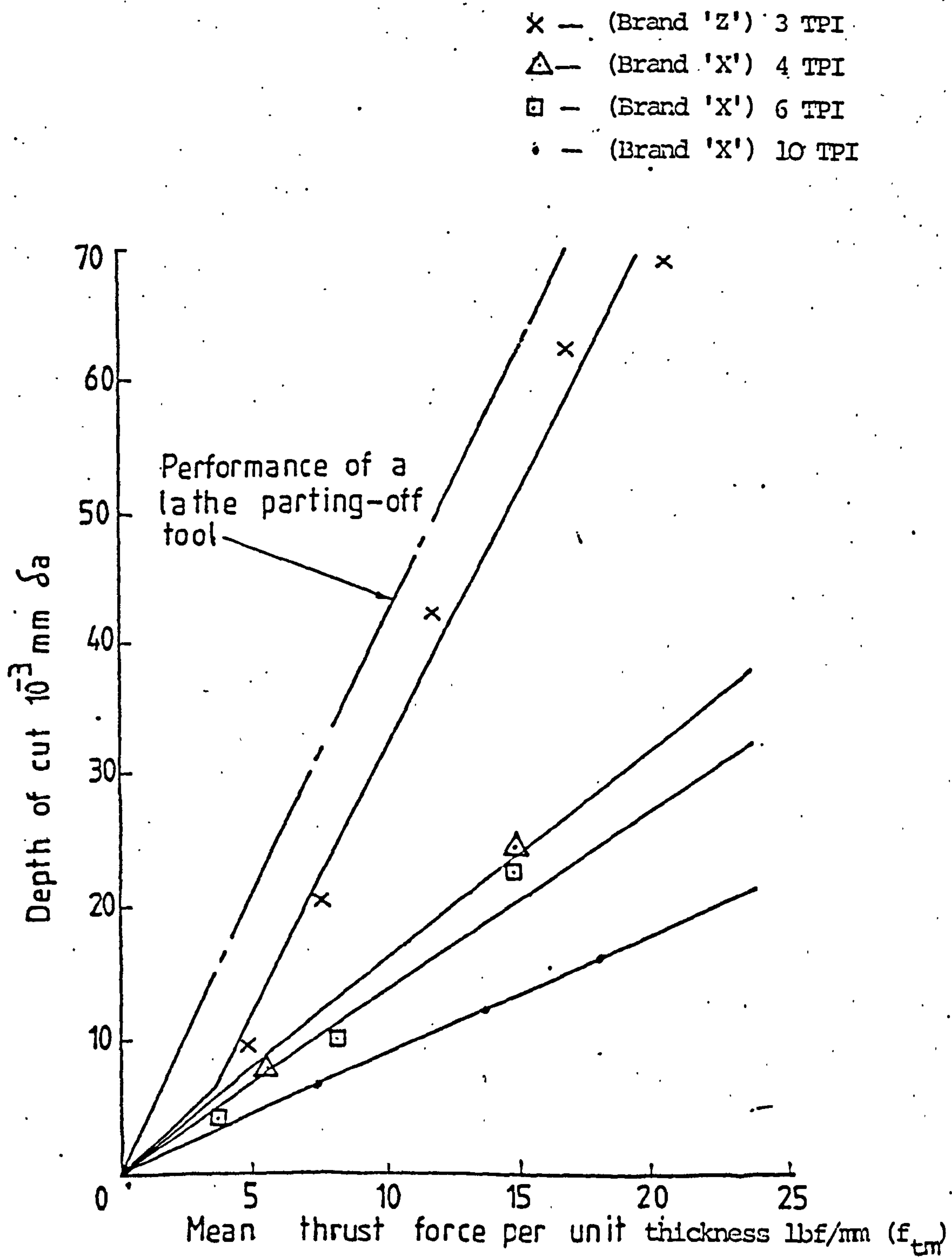


FIG. 25

FIG. 26: Instantaneous force components for
Brand 'X' 6TPI Blade

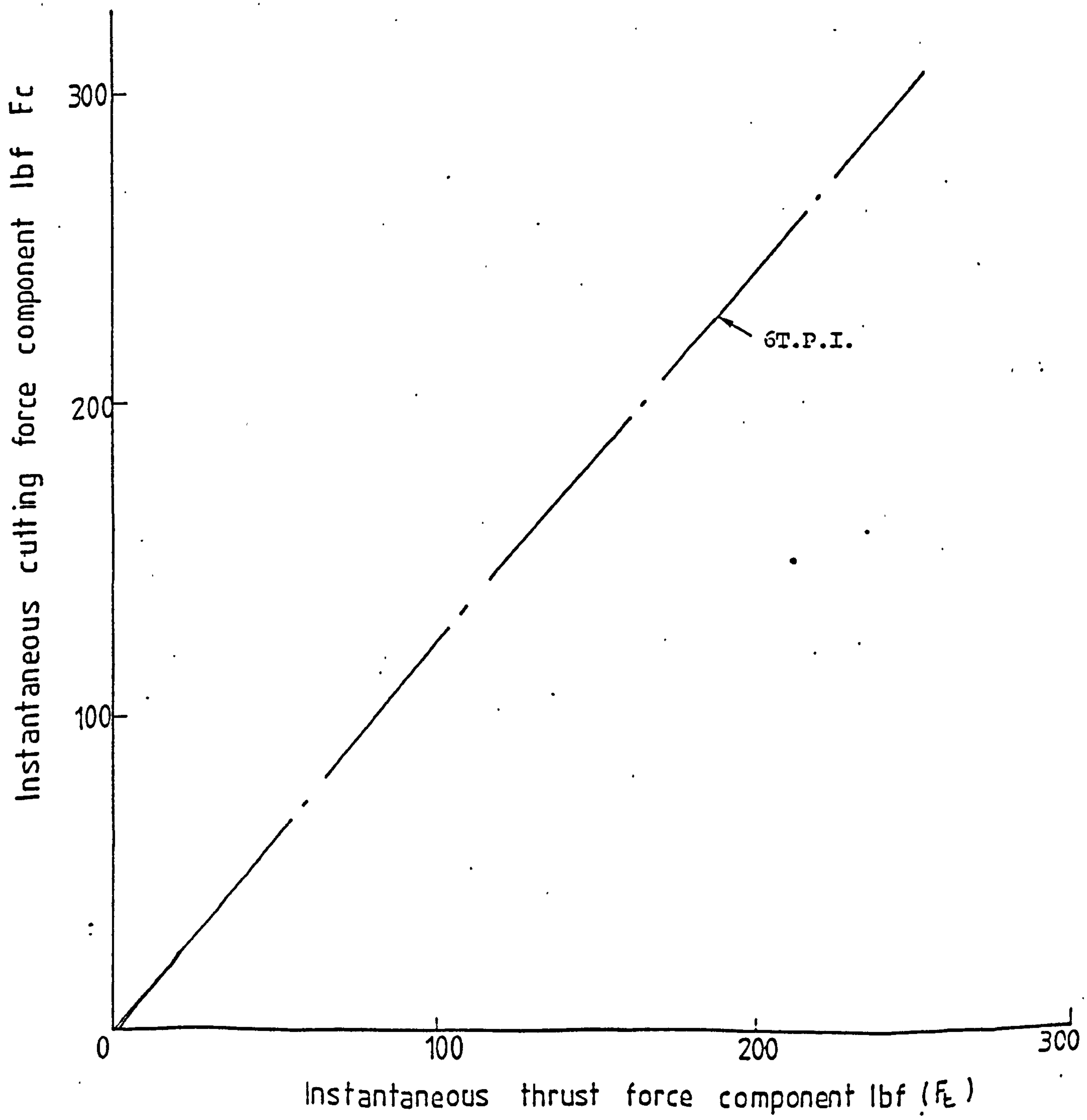


FIG. 26

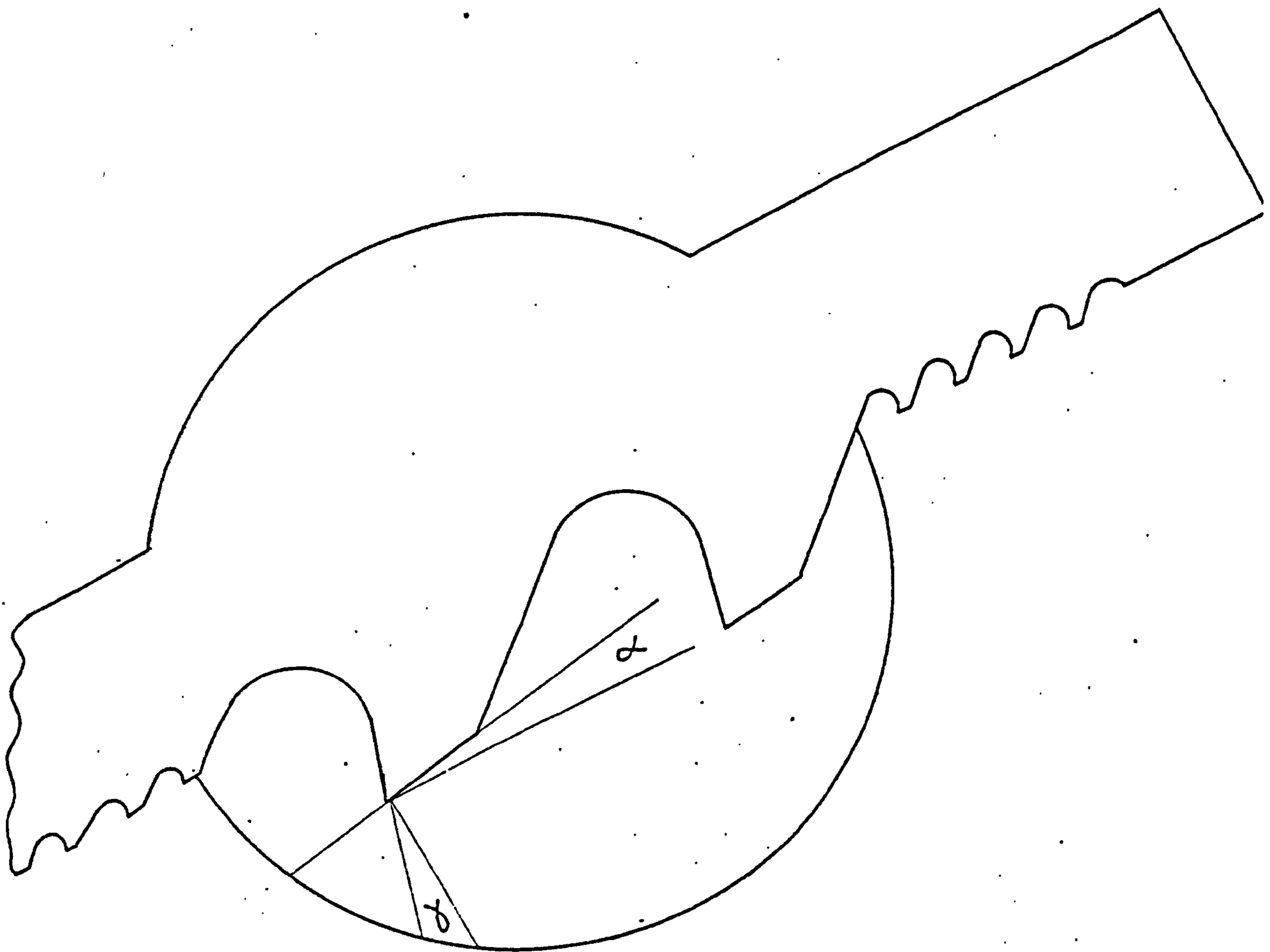


FIG.27 PROFILE OF THE BRAND 'Z' 3 T.P.I. BLADE



INCREASING
LOAD —————>

FIG.28 SAMPLES OF METAL CHIPS PRODUCED WHEN CUTTING MILD STEEL
(BRAND X 4 TPI BLADE, 64 STROKES/MIN)



FIG.29 SAMPLES OF METAL CHIPS, CUTTING MILD STEEL
(BRAND Z 3 TPI BLADE, 64 STROKES/MIN)

FIG. 30: The effect of tooth spacing and cutting edge radii on the cutting performance of blades

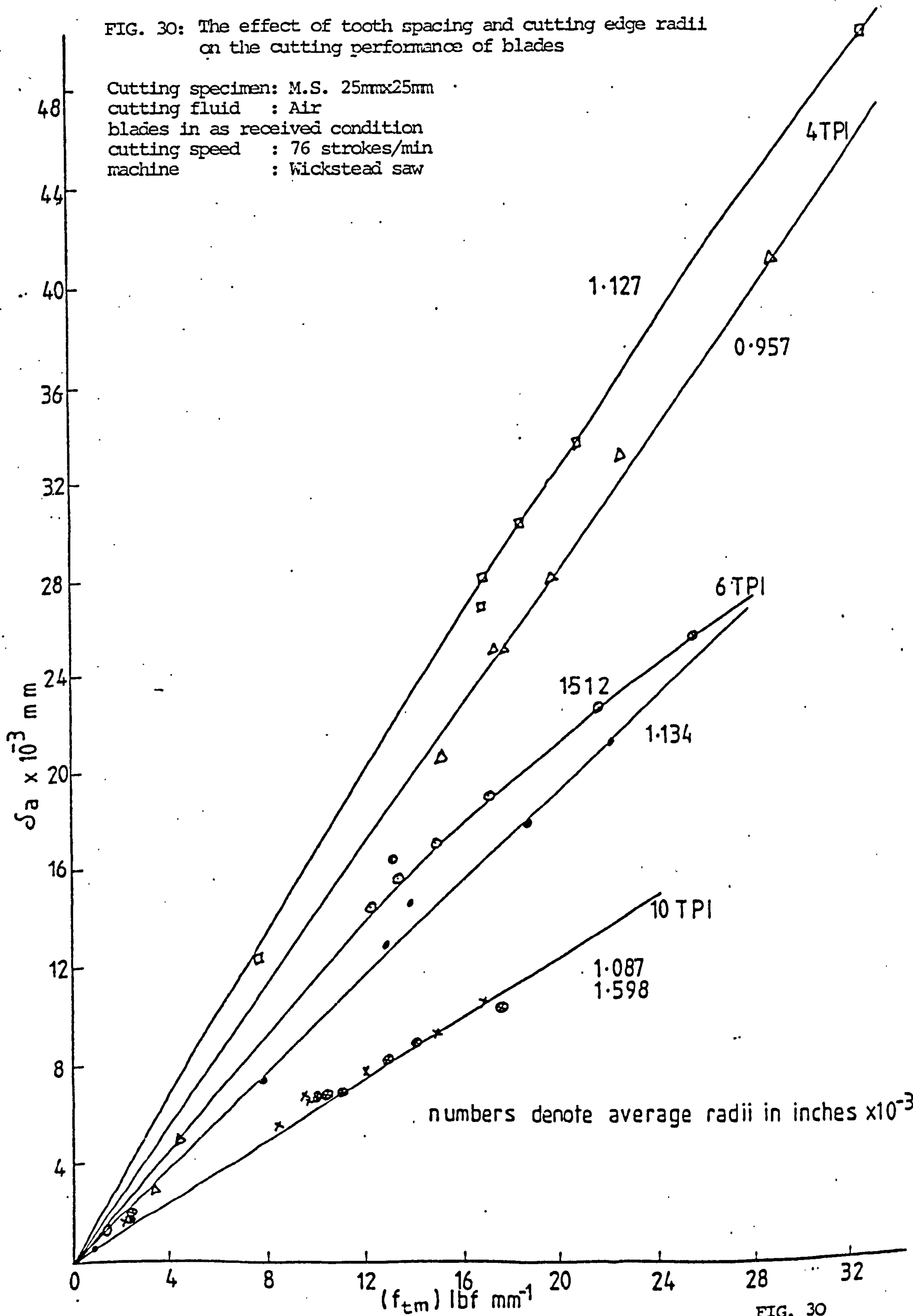


FIG. 30

FIG. 31: Effect of blade wear on the cutting performance

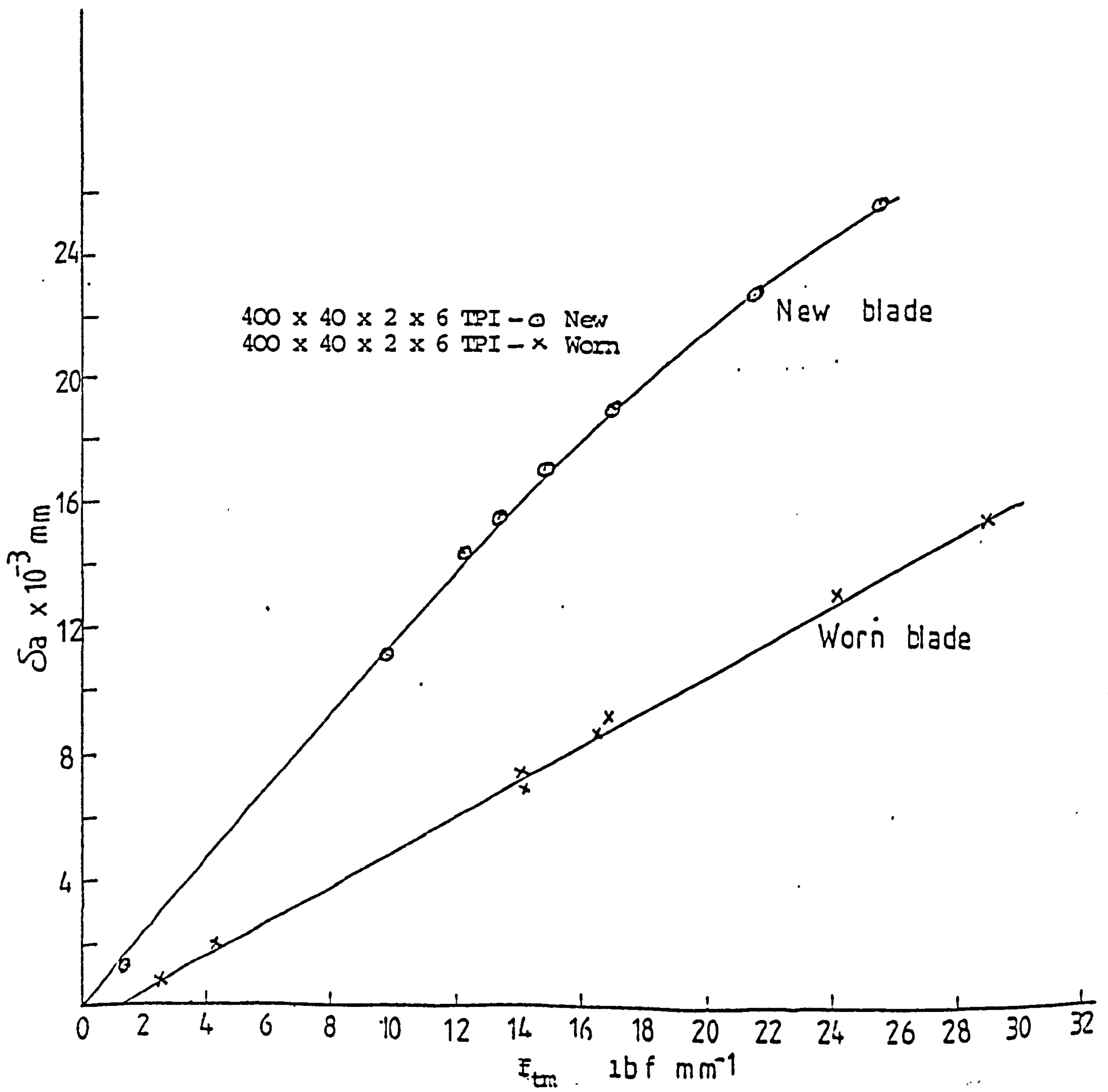
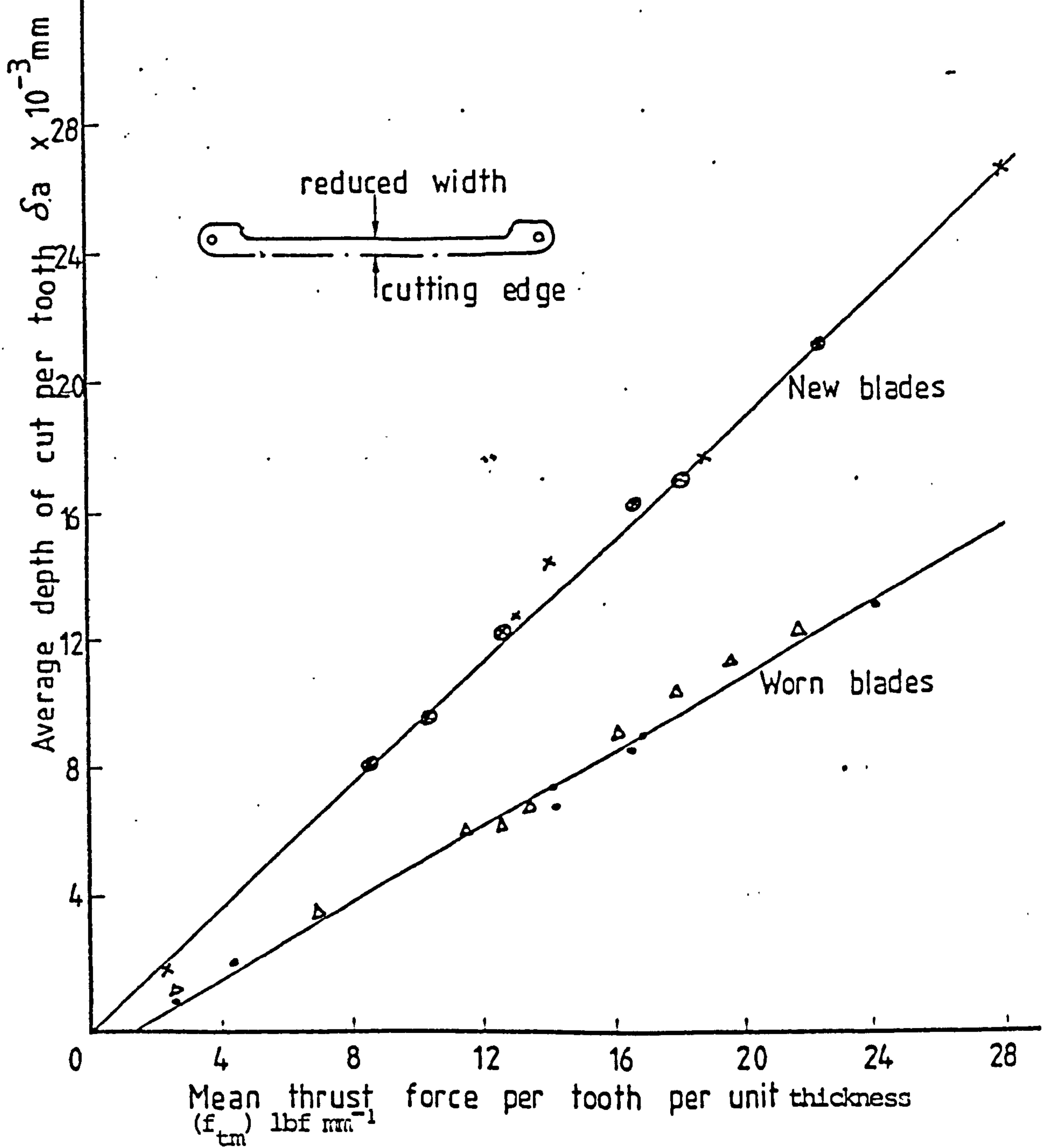


Fig.31

FIG.32: Effect of blade deflection on the performance of new and worn blades

Specimen : 25mm x 25mm Mild Steel
 Cutting fluid: Air
 Cutting speed: 76 strokes/min
 Machine : Wickstead Saw



400 x 40 x 2 x 6 T.P.I. Blade No. 6	New blade	x	Standard width
400 x 17.5 x 2 x 6 T.P.I. Blade No. 6	New blade	⊗	Reduced width
400 x 40 x 2 x 6 T.P.I. Blade No. 2	Worn blade	•	Standard width
400 x 19 x 2 x 6 T.P.I. Blade No. 2	Worn blade	Δ	Reduced width

FIG. 33 (a) Longitudinal stress distributions due to a bending moment, a tensile load and their combination

(b) Position of the neutral axis of bending due to a central load

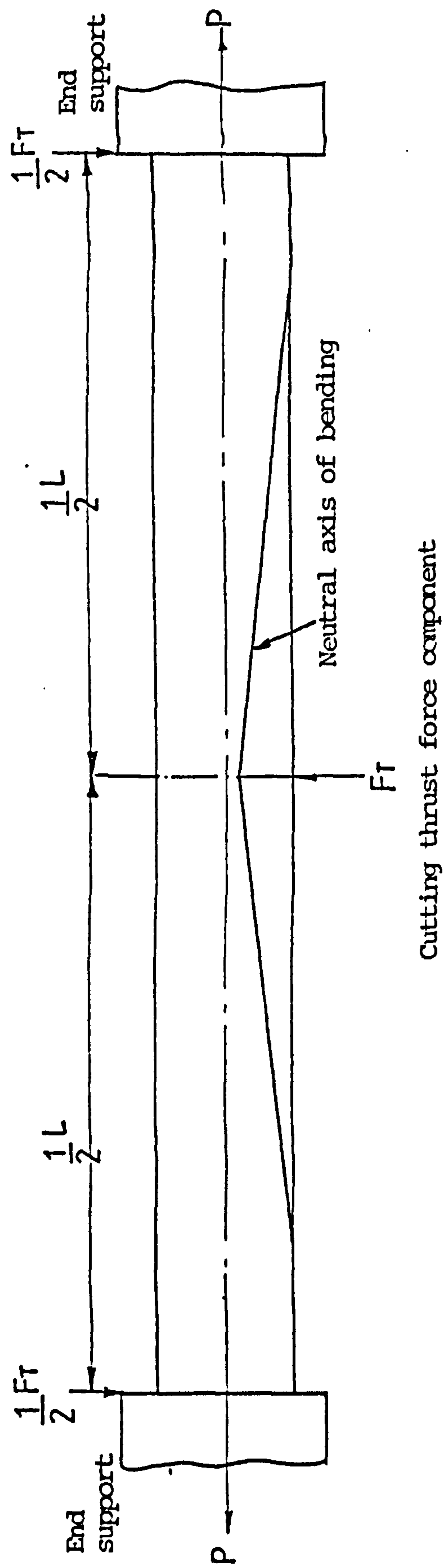
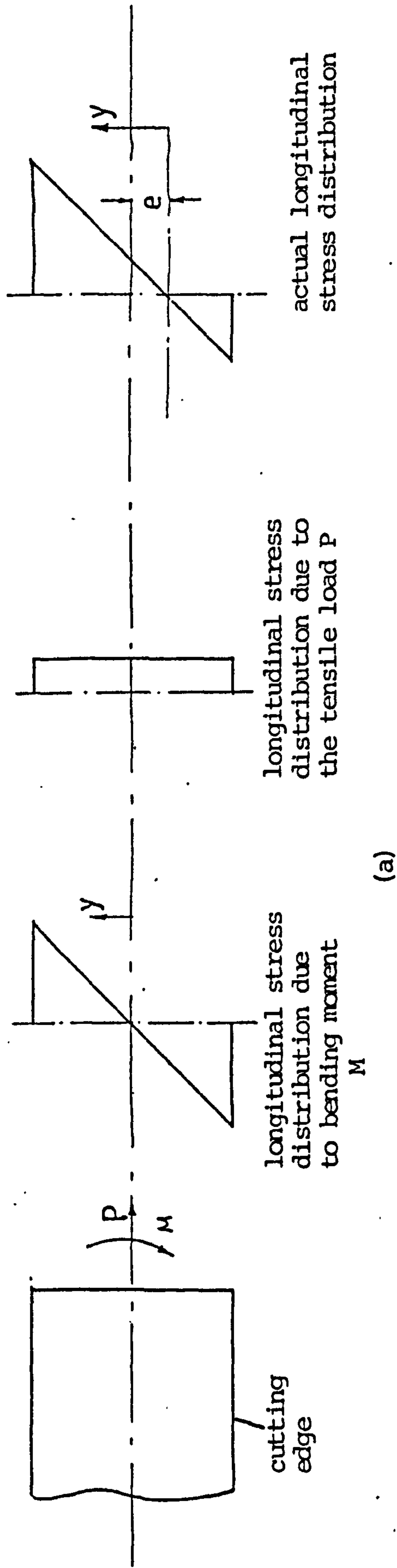
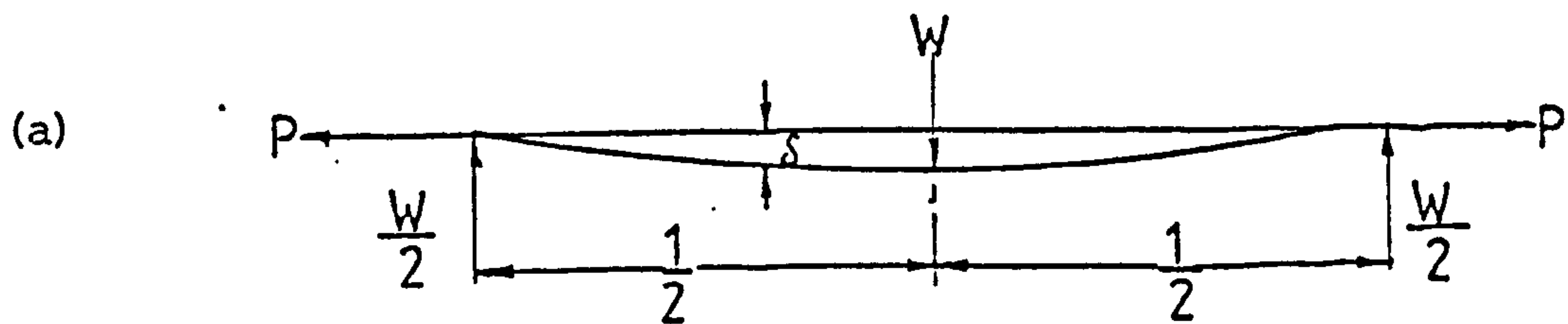


FIG. 34: Deflection models and equations



A simply supported blade with longitudinal tension

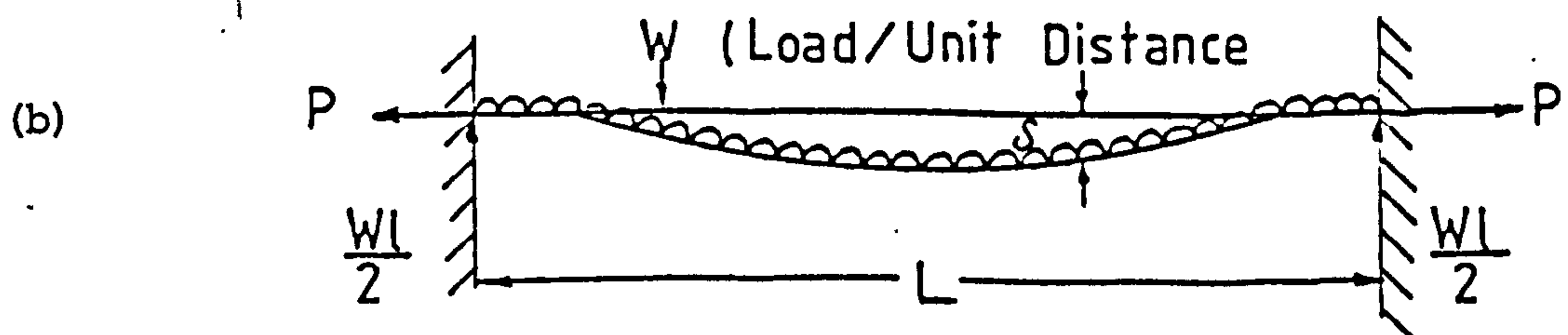
$$\delta_{\max} = \frac{WL^3}{48EI} \phi_1$$

where

$$\phi_1 = \frac{U - \tanh U}{1/3 U^3}$$

and

$$U = \sqrt{\frac{PL^2}{4EI}}$$



A uniformly loaded blade with built-in ends

$$\delta_{\max} = \frac{wL^4}{384EI} \phi_2$$

where

$$\phi_2 = \frac{24}{U^4} \left\{ \frac{U^2}{2} - \frac{U \cosh U - U}{\sinh U} \right\}$$

and

$$U = \sqrt{\frac{PL^2}{4EI}}$$

FIG. 35: Deflection factor against tension factor

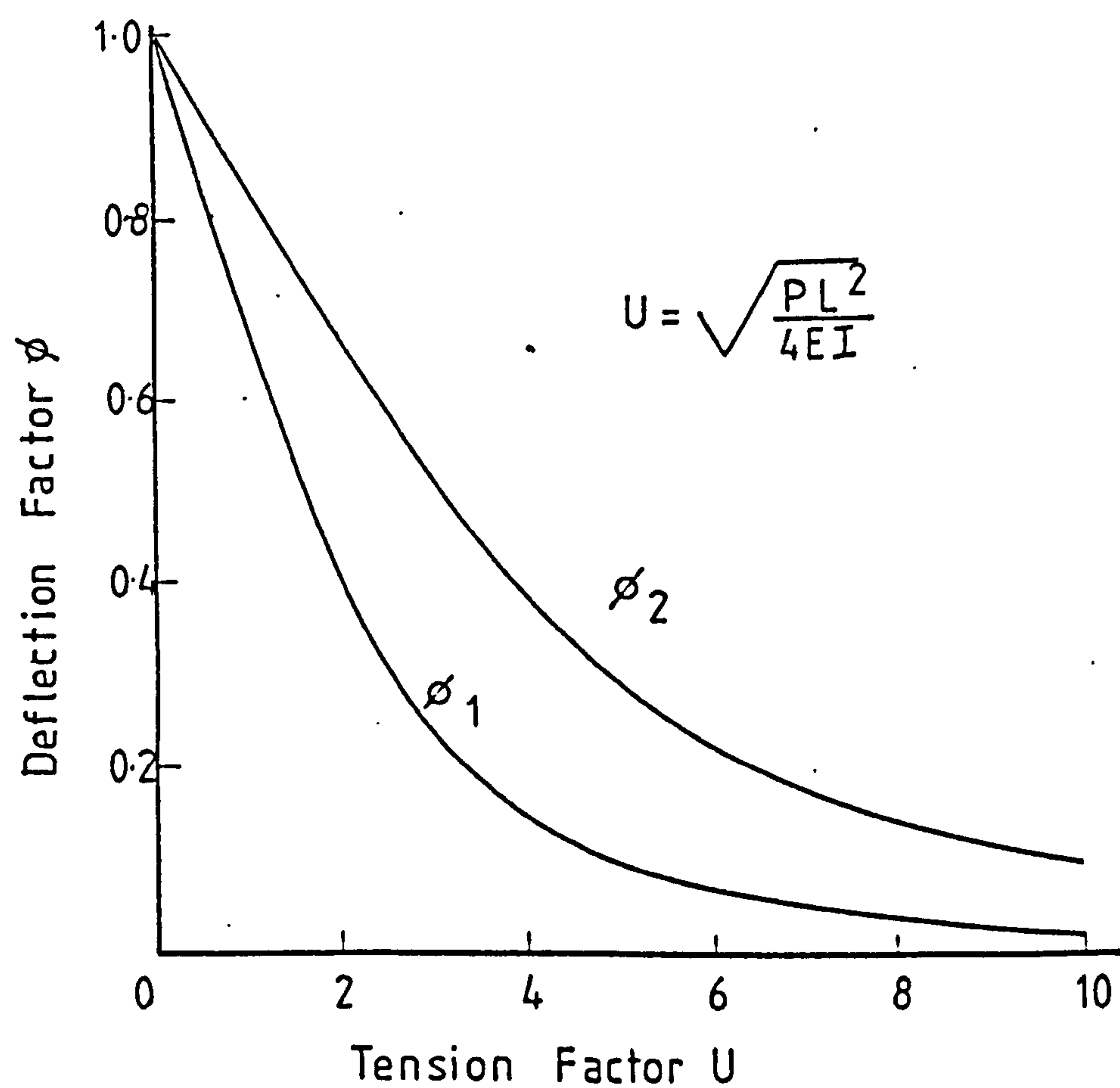


FIG. 36: Load/extension curve for H.S.S. blade (Brand 'X').

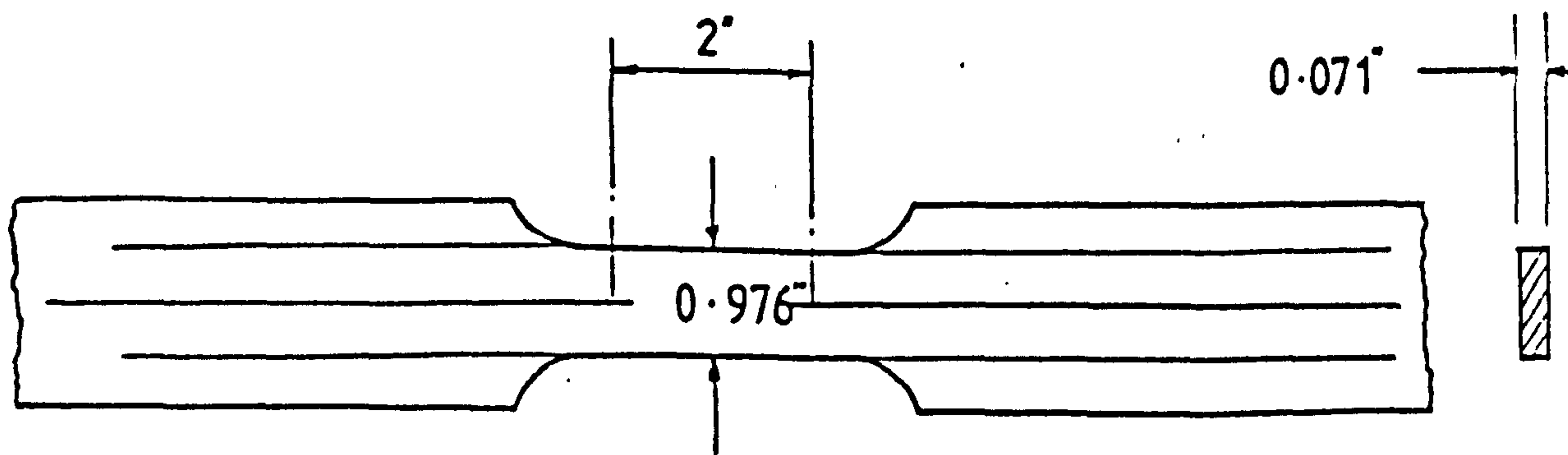
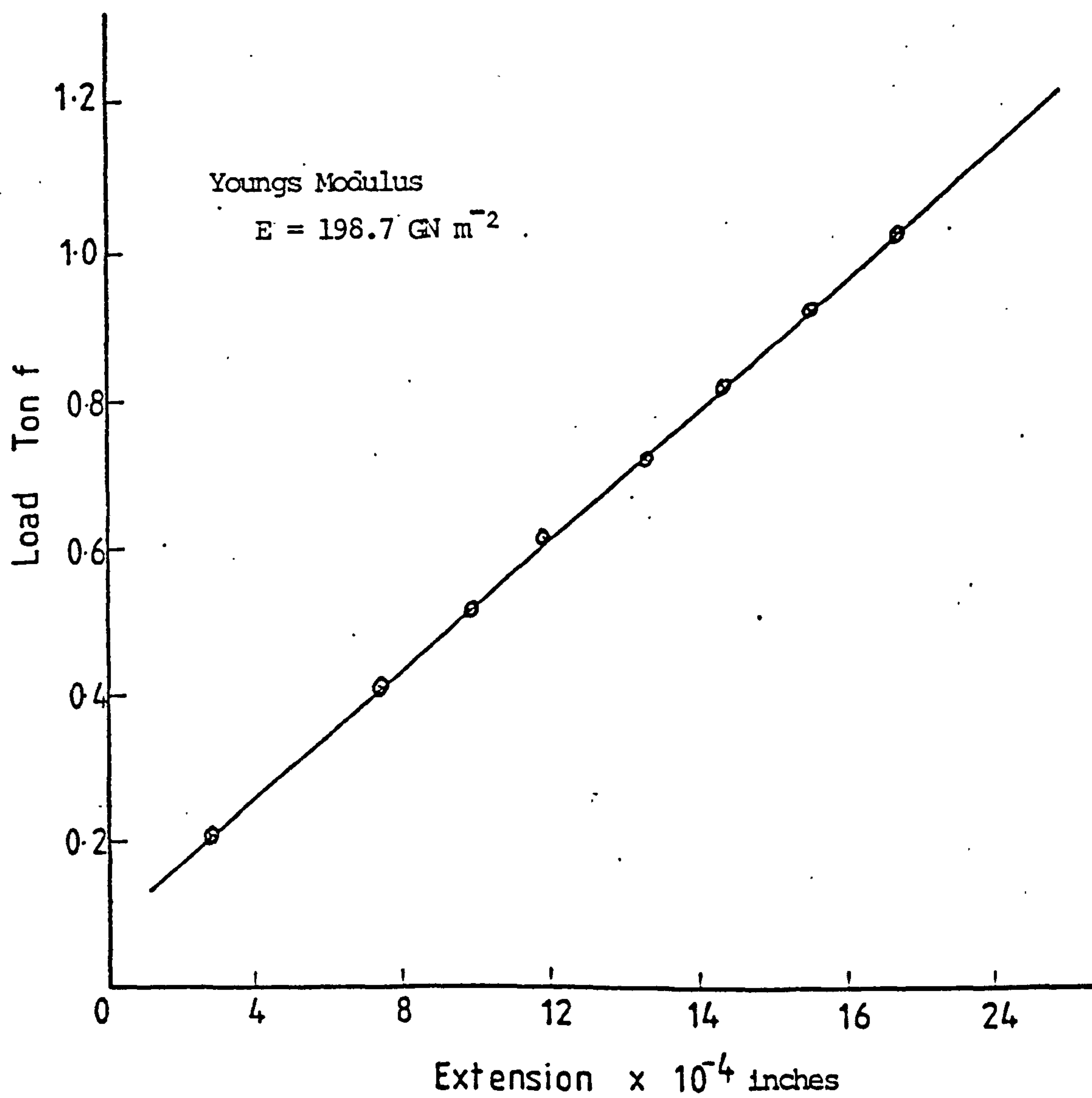
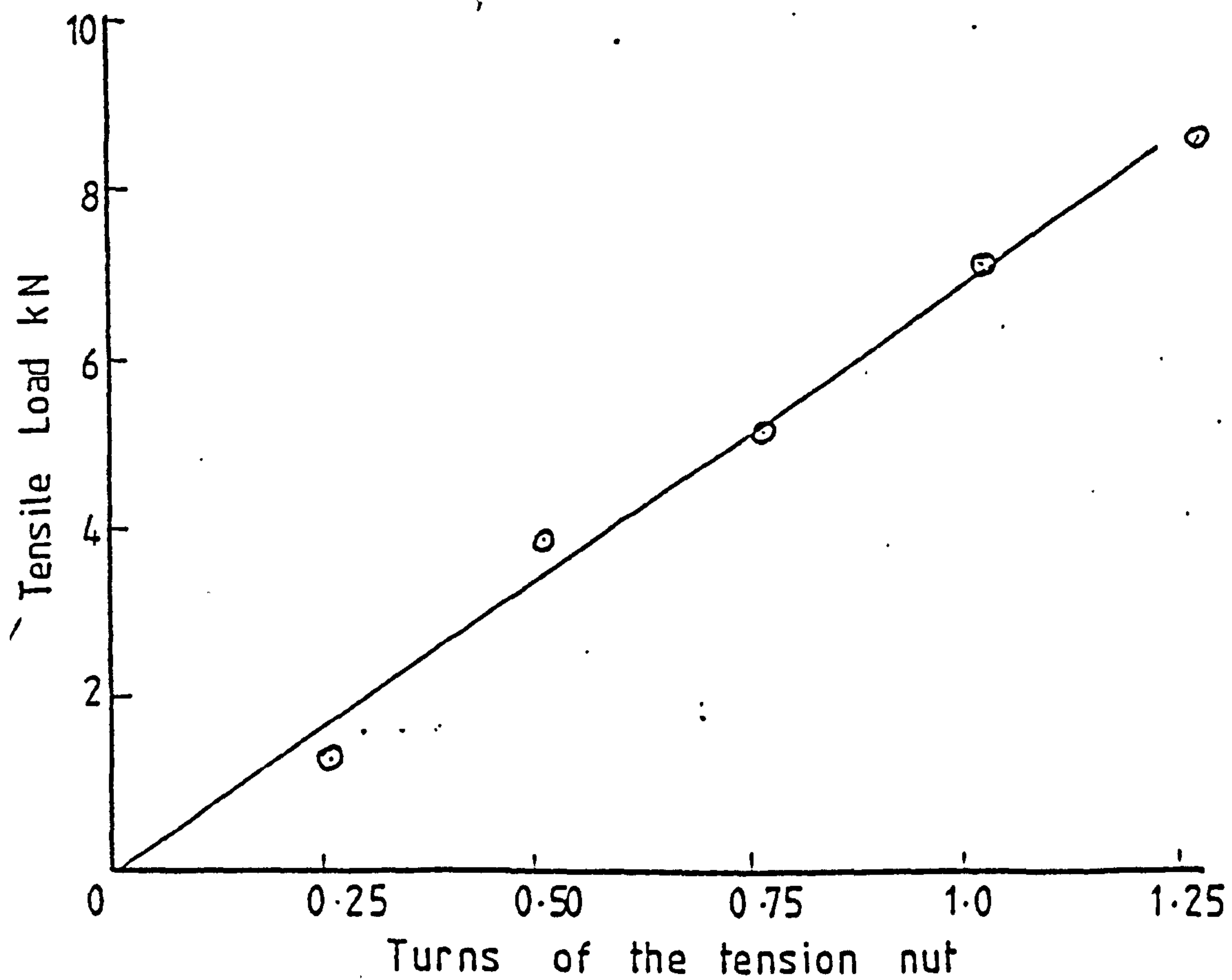
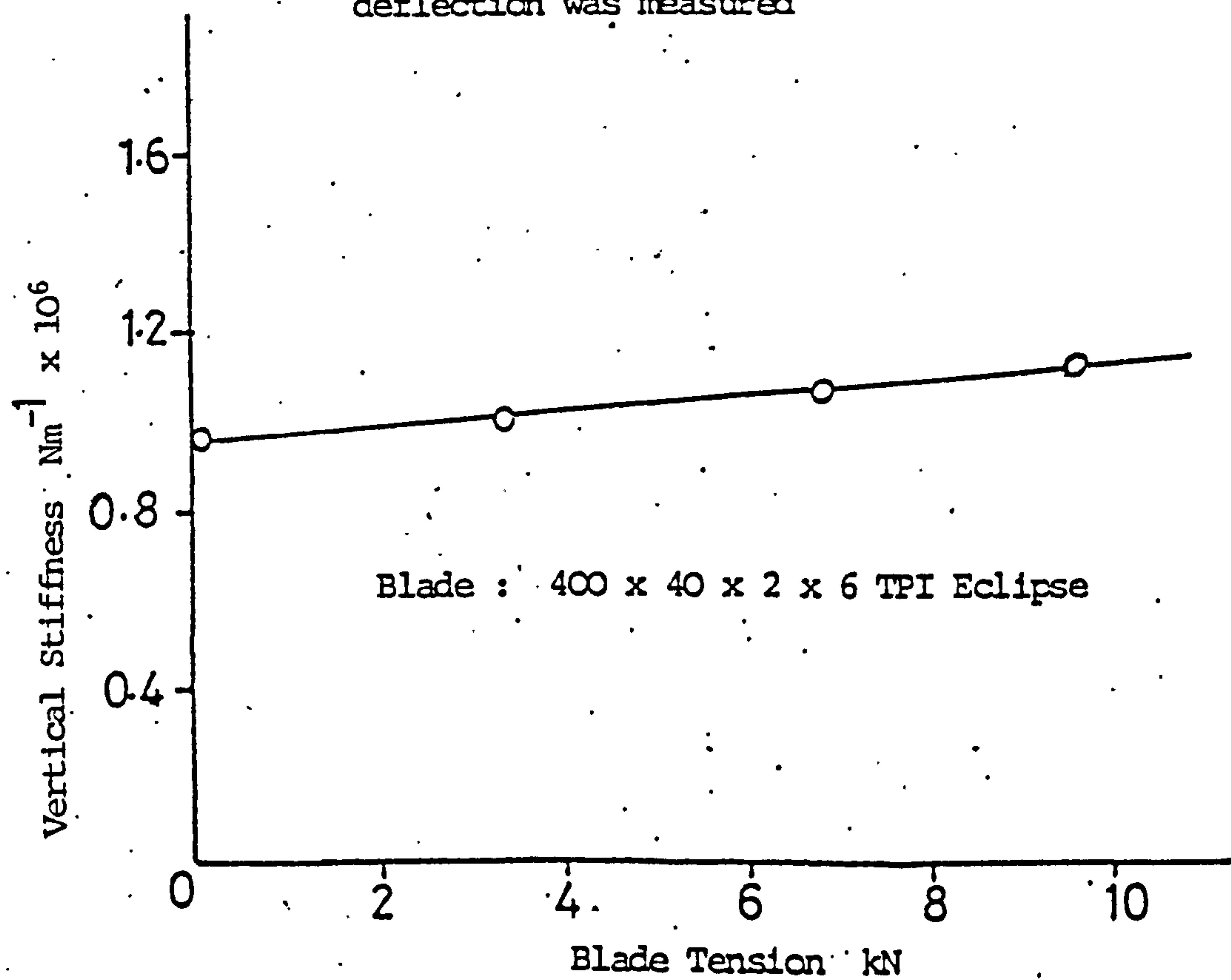
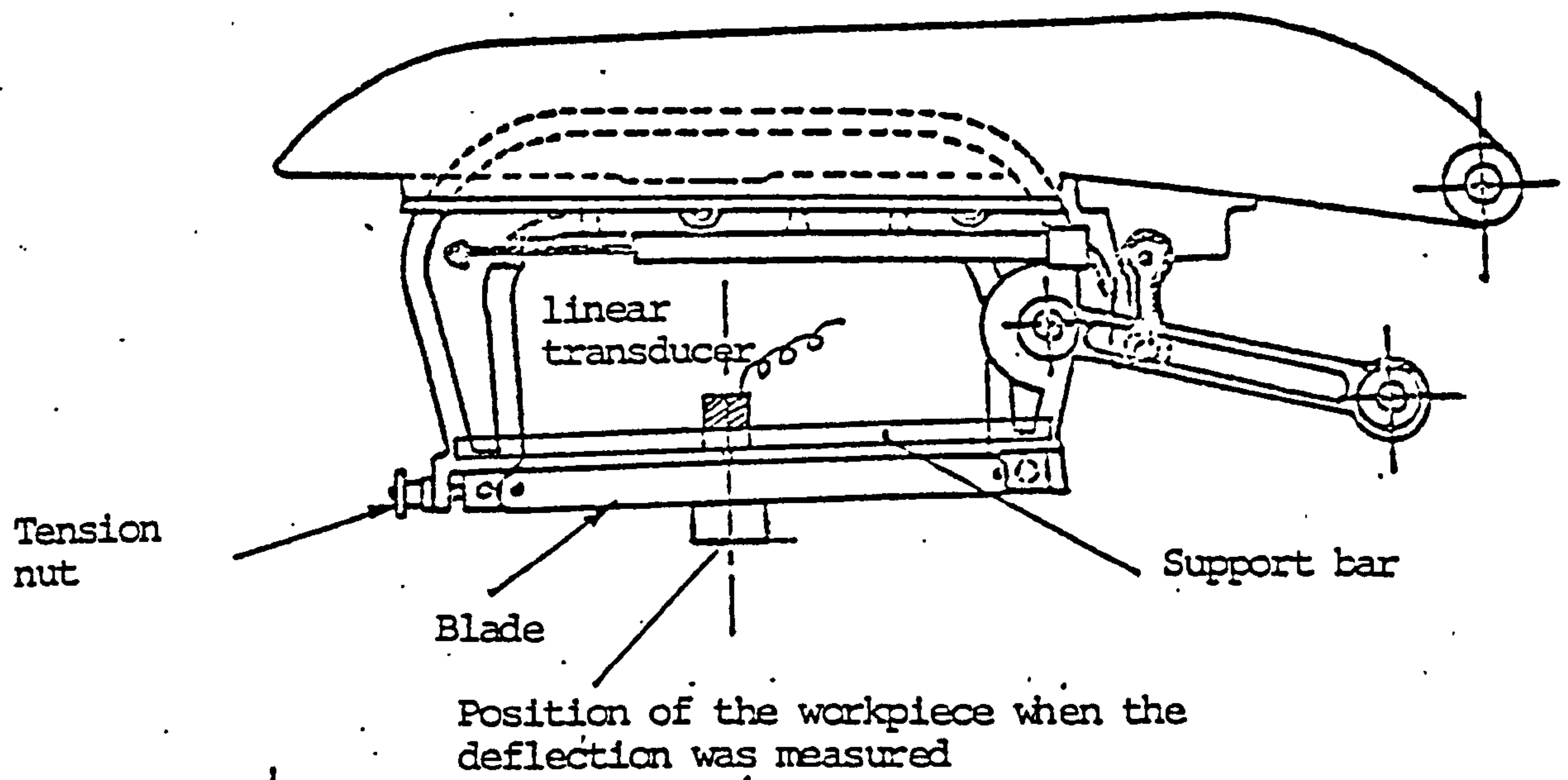


FIG. 36

FIG. 37: Tensile load induced in a
400 x 40 x 2 x 6 T.P.I. blade against the
number of turns of the tension nut

Machine : Wickstead Hydramatic 8" x 8"





(All measurements made during cutting)

FIG. 38: The effect of blade tension on the vertical stiffness of the blade.

FIG. 39: Natural frequency of lateral vibration against blade tension for a Brand 'X' 400 x 40 x 2 x 6 T.P.I. blade

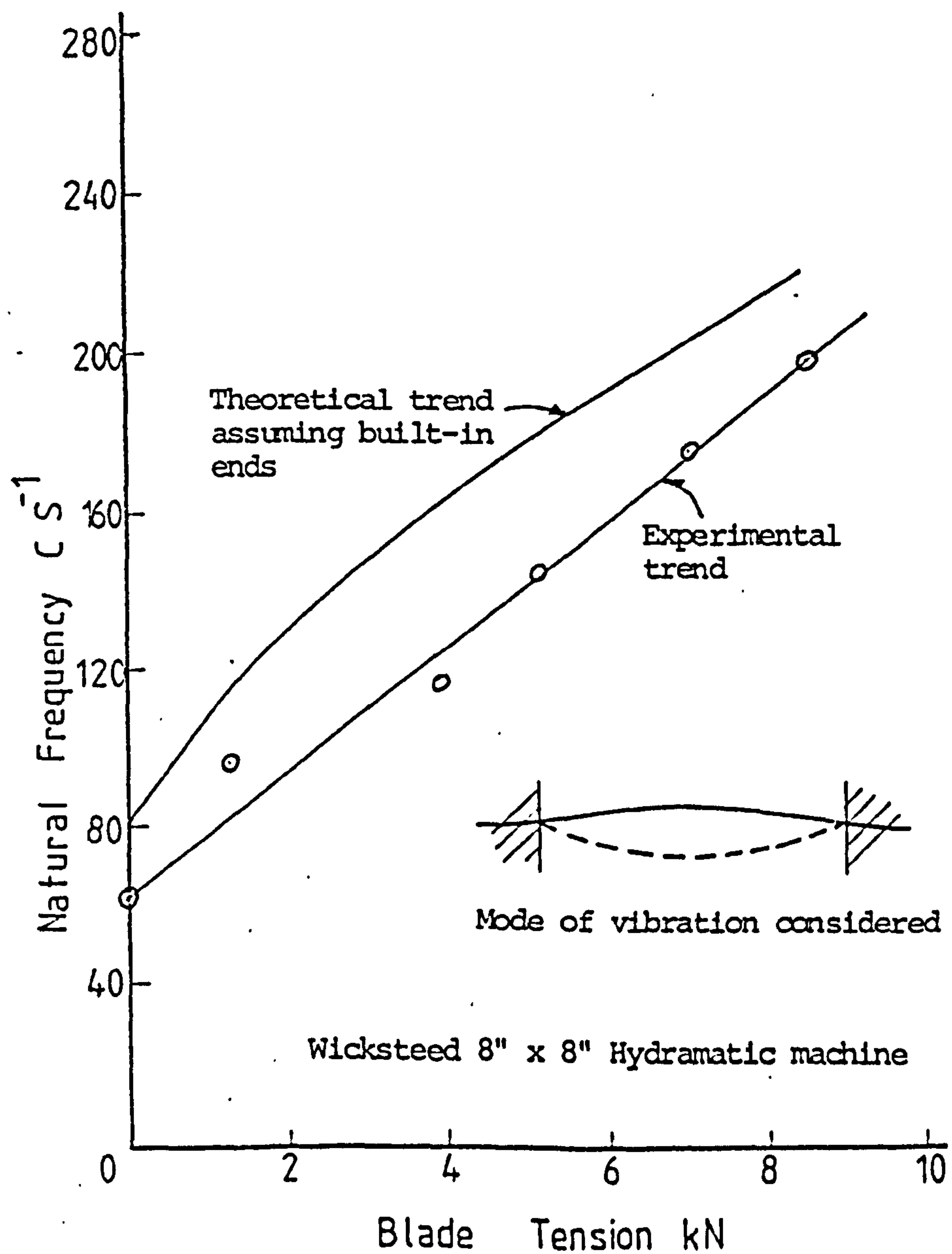


FIG. 40(a): The tooth wear against the number of sections cut

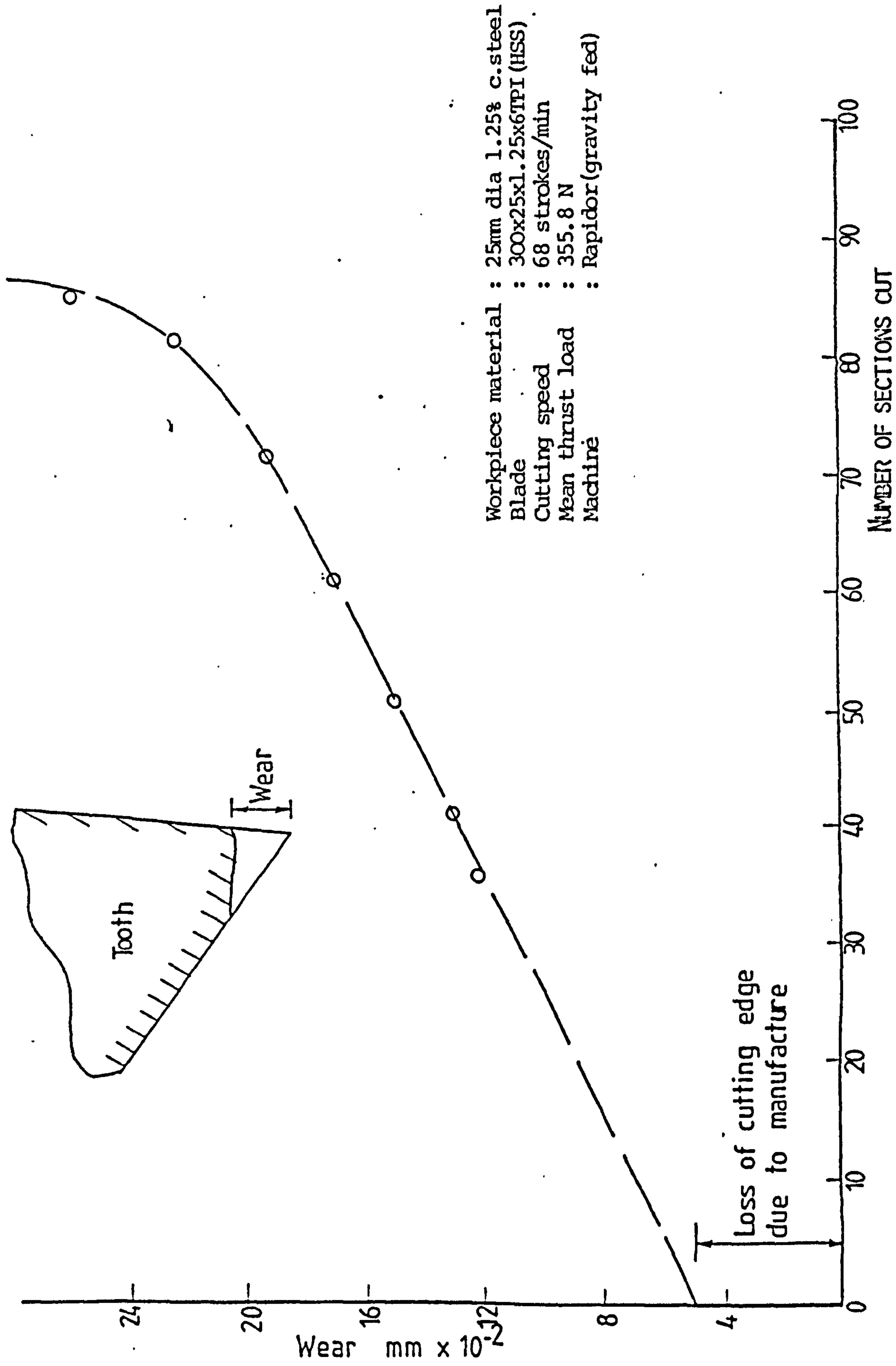


Fig. 40(a)

FIG. 40(b) Tooth profile - showing wear

Workpiece material: 1.25% carbon steel
Blade : Brand 'X' 6 T.P.I.
cutting speed : 68 strokes/min
thrust load : 355.8 N
magnification : X 50

Wear after
83 cuts

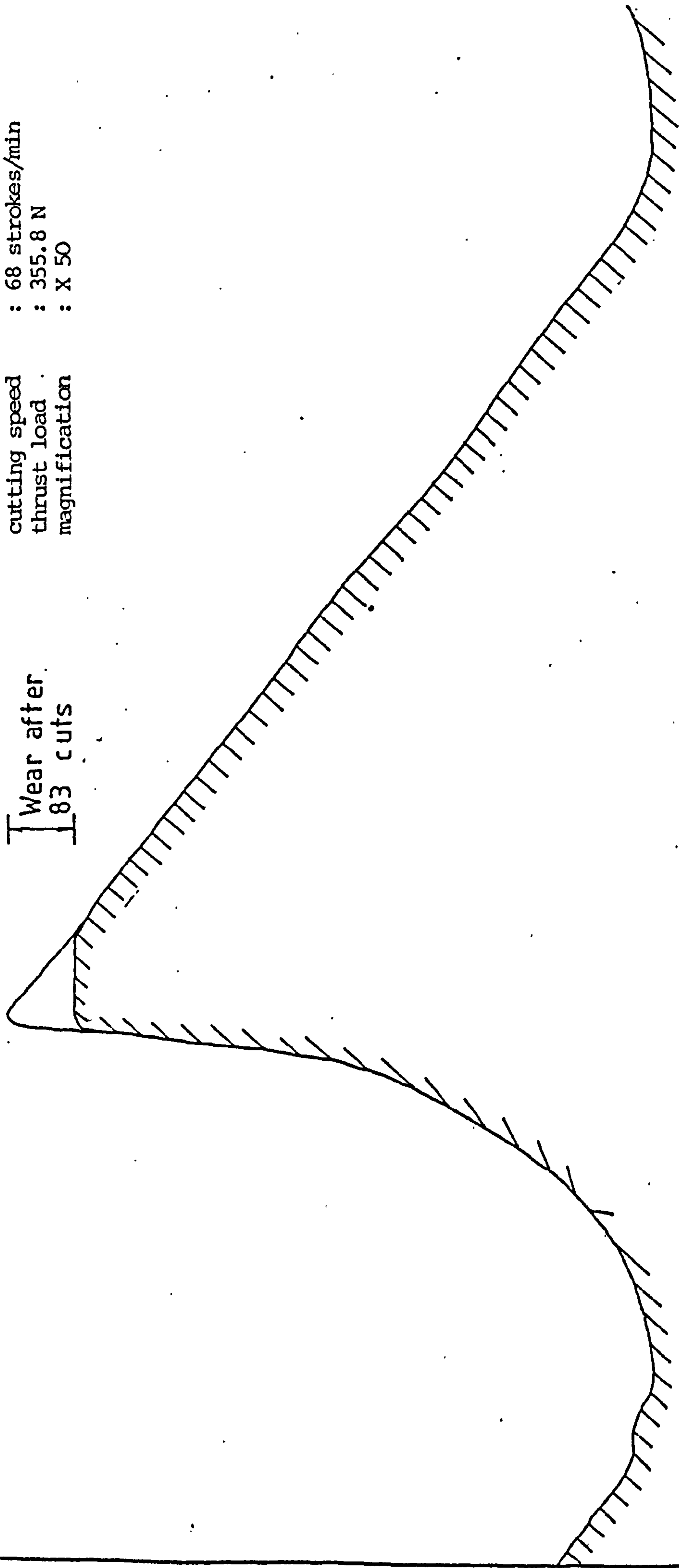


Fig. 40(b)

FIG. 41: The average depth of cut per tooth against the main thrust load per tooth per unit thickness for a blade in three states of wear

Workpiece : 25mm x 25mm En 1a
 Cutting speed : 120 strokes/min
 Blade : 400 x 40 x 2 x 6 T.P.I. (HSS)
 Machine : Wickstead 200mm Hydraratic saw

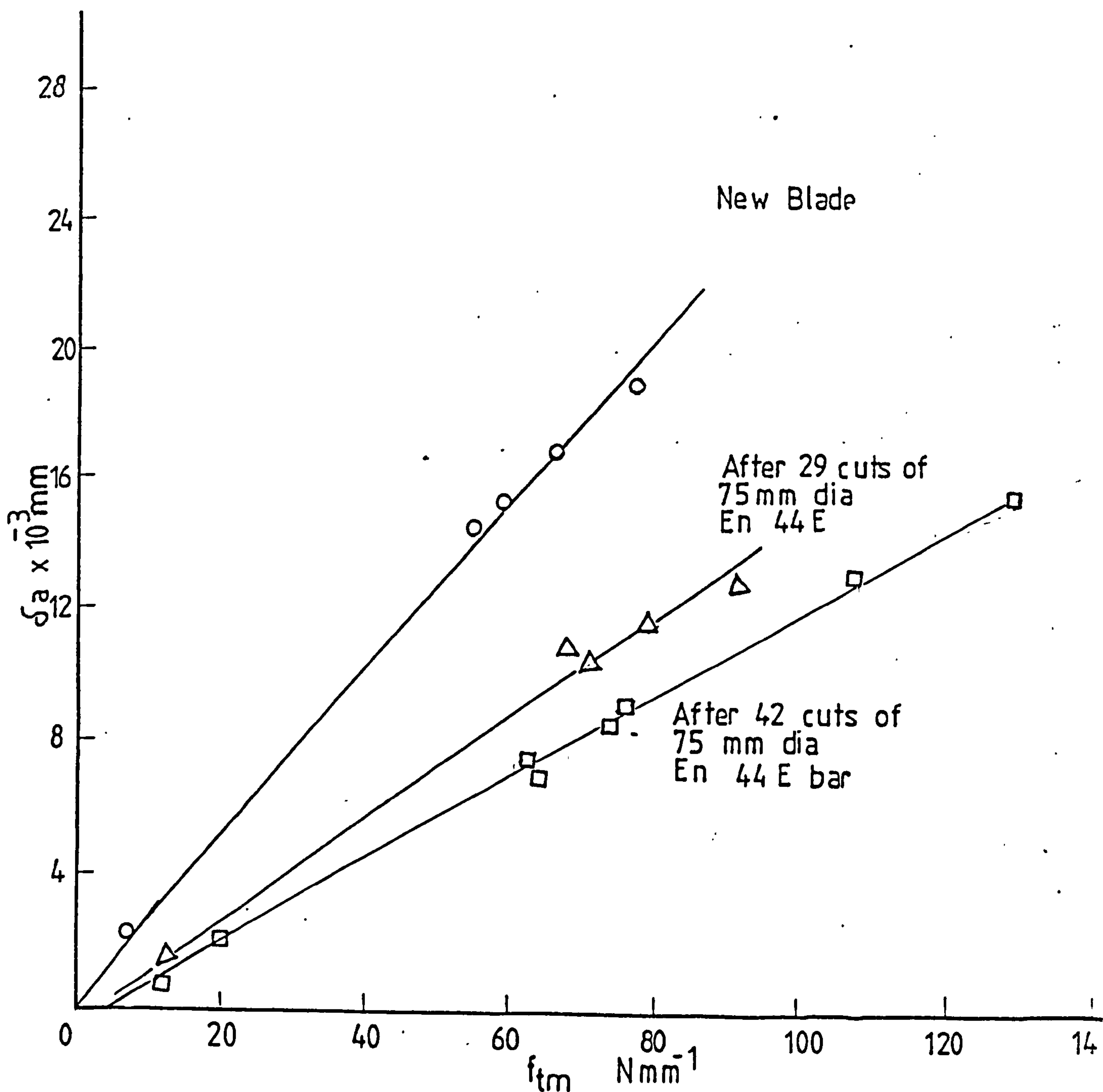


Fig.41

FIG. 42: The effect of blade wear on its cutting performance

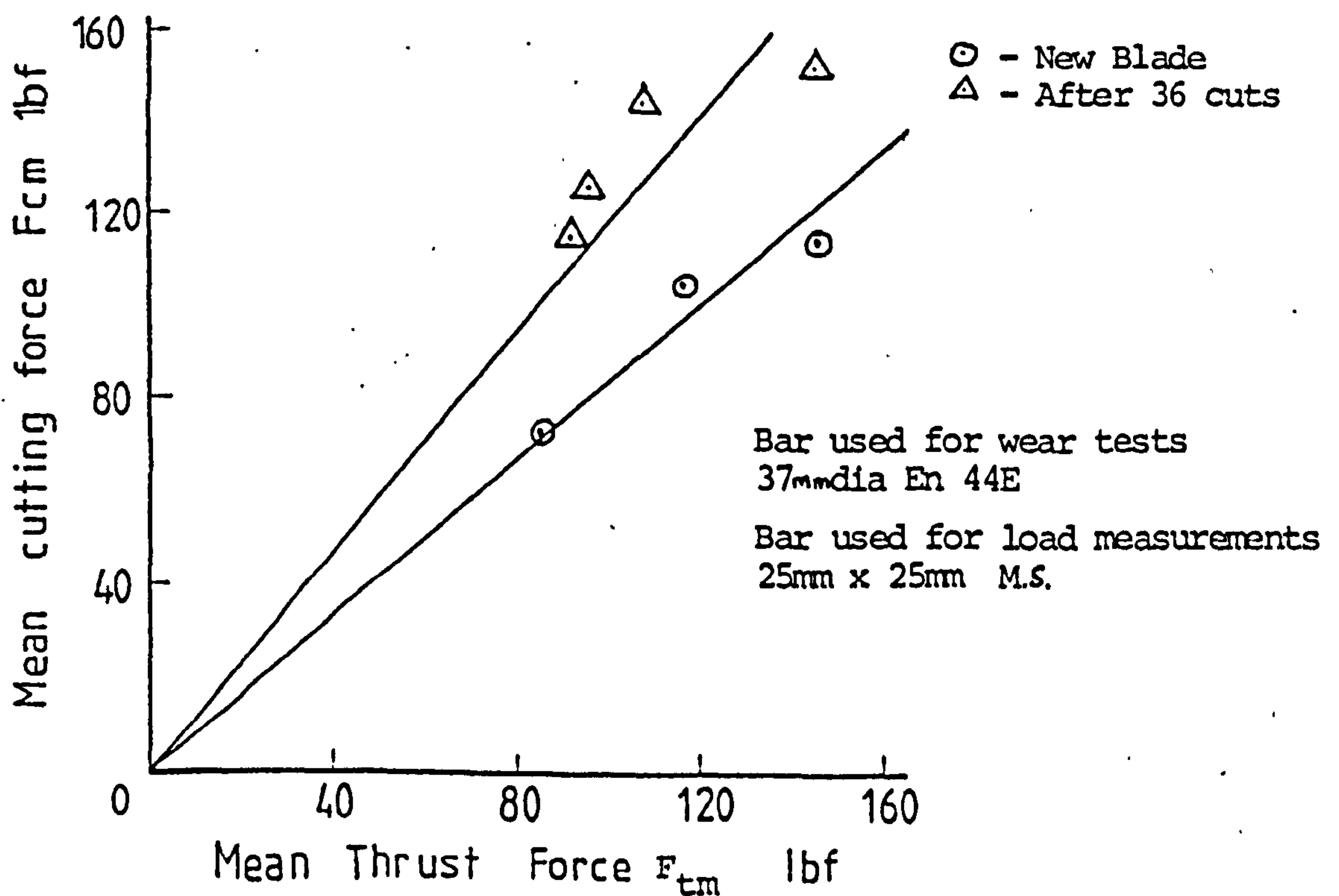
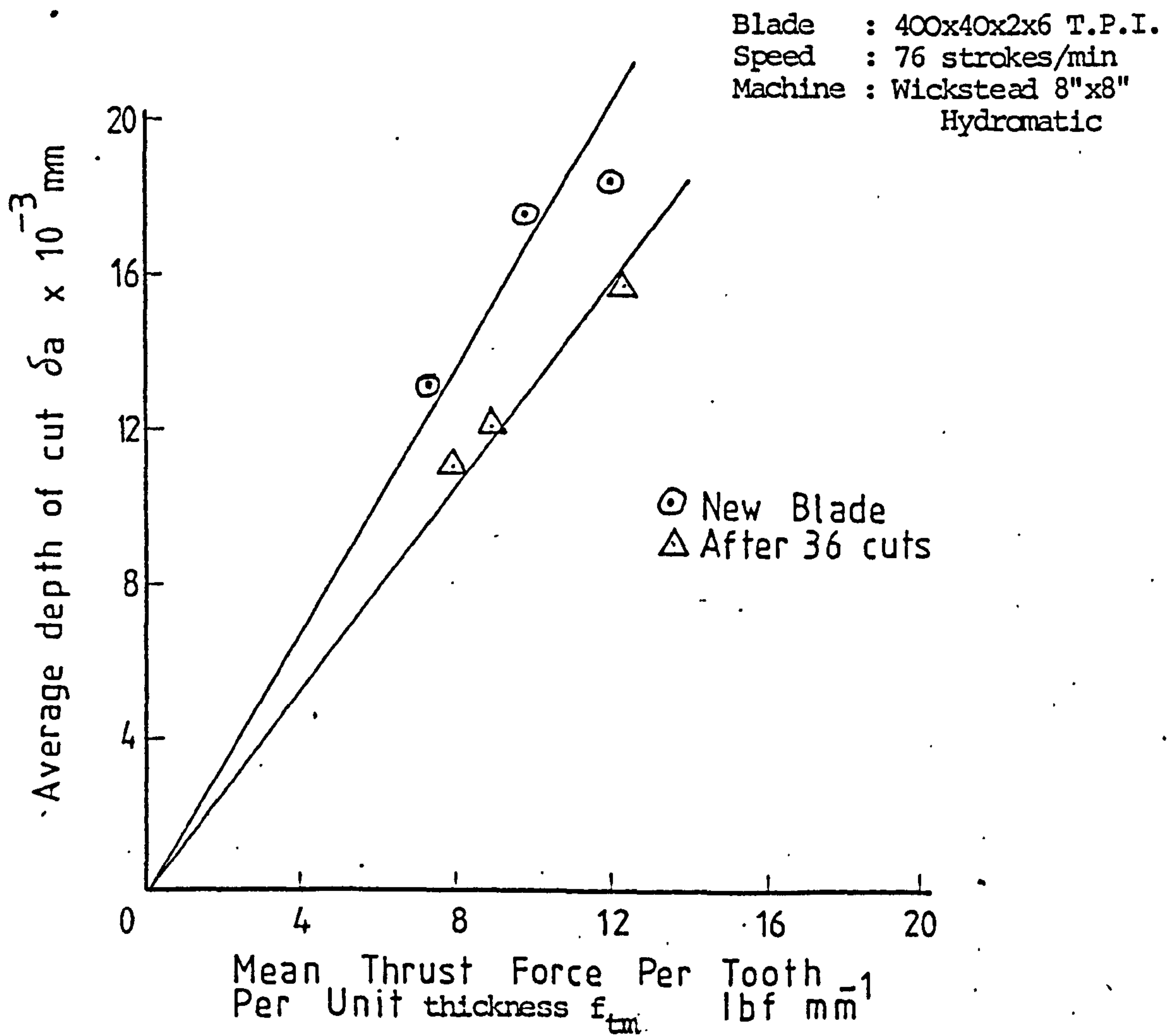
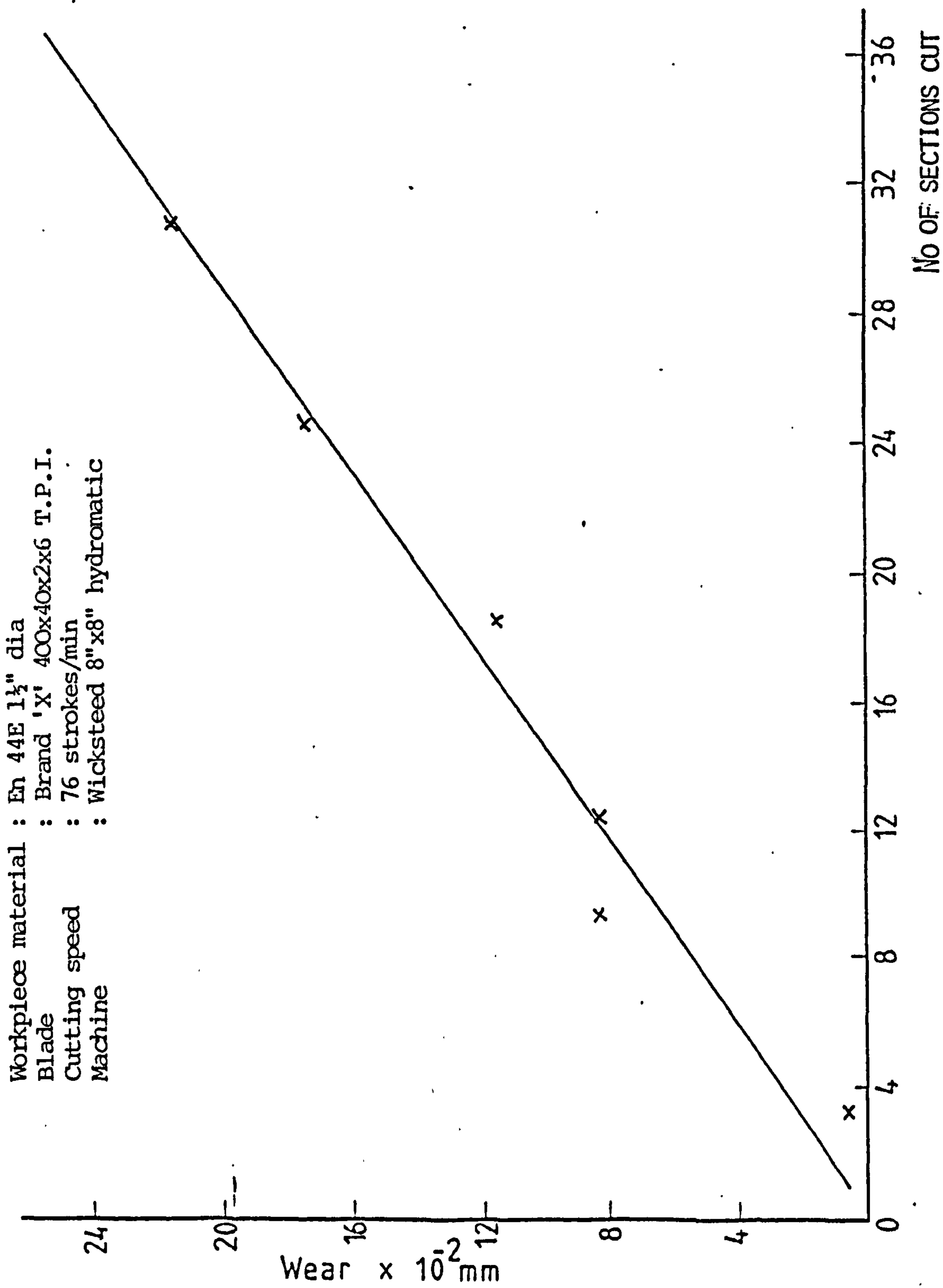


FIG. 43: Loss in tooth height against number of sections cut



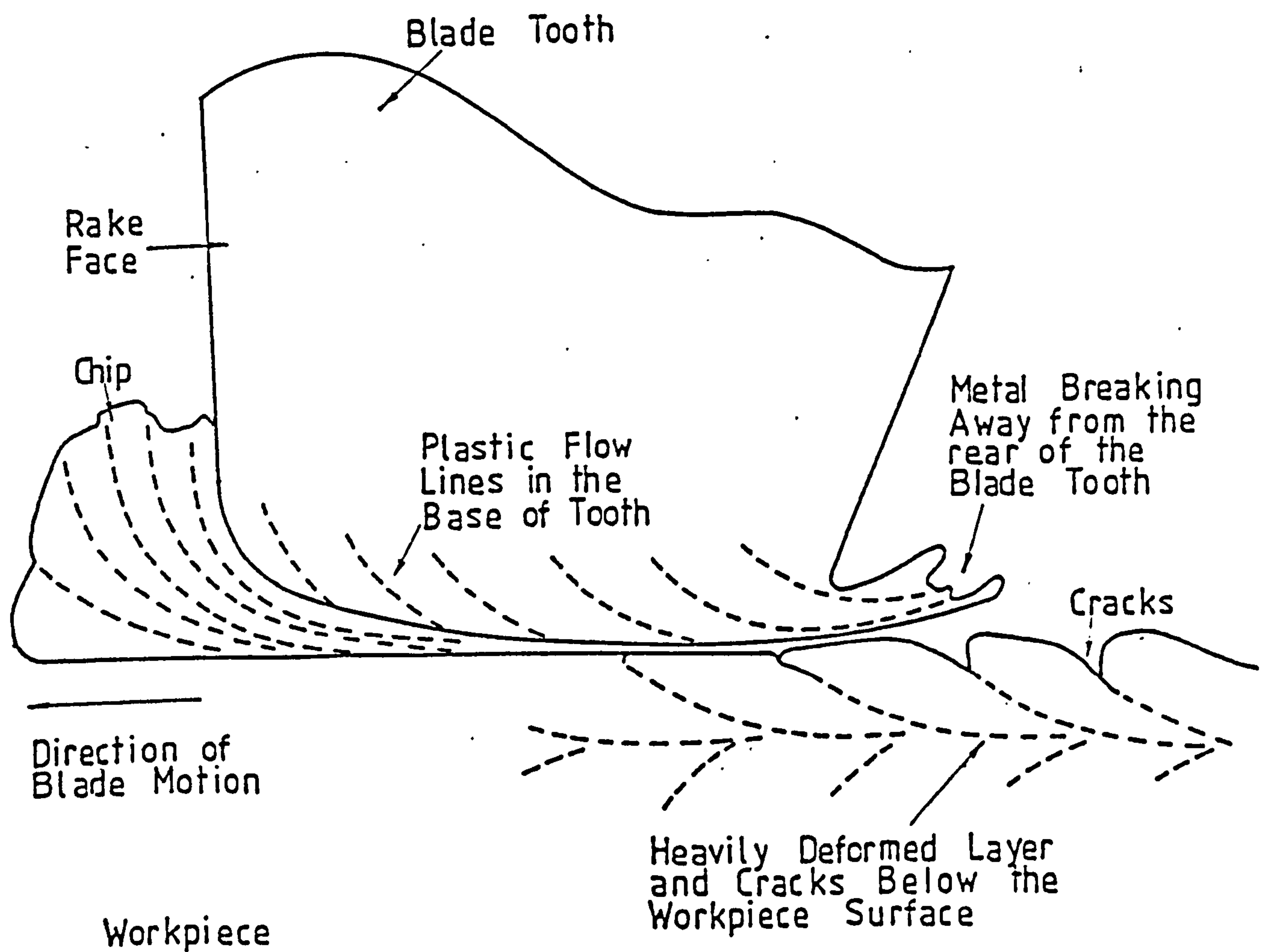


FIG.44 DEFORMATION OCCURRING IN BOTH THE BLADE AND WORKPIECE
COMPILED FROM MICROSCOPIC OBSERVATIONS DURING WEAR
TESTS ON EN44E (25)

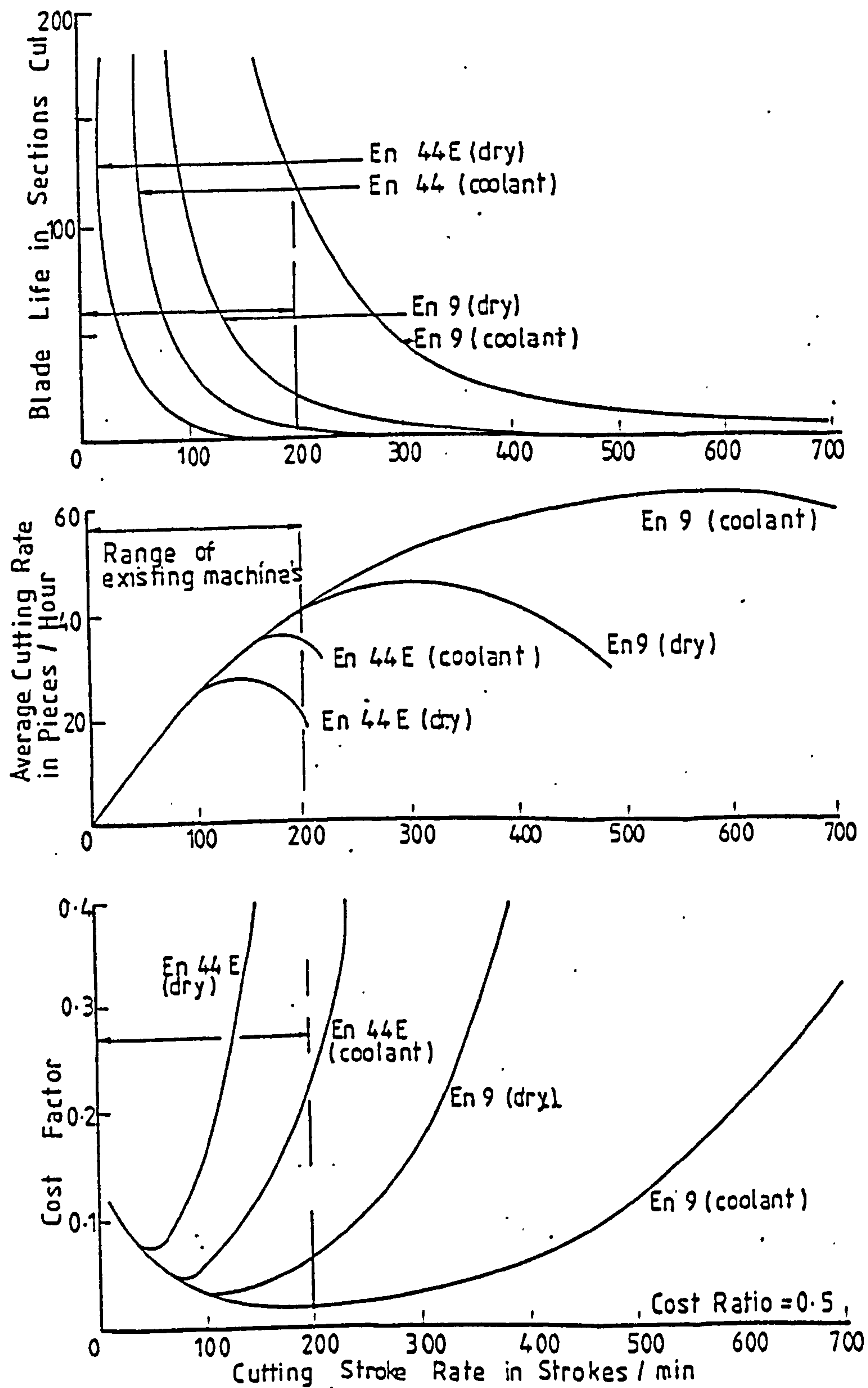


FIG. 45: The effects of the cutting stroke rate on blade life, average cutting rate and the cost factor (27)

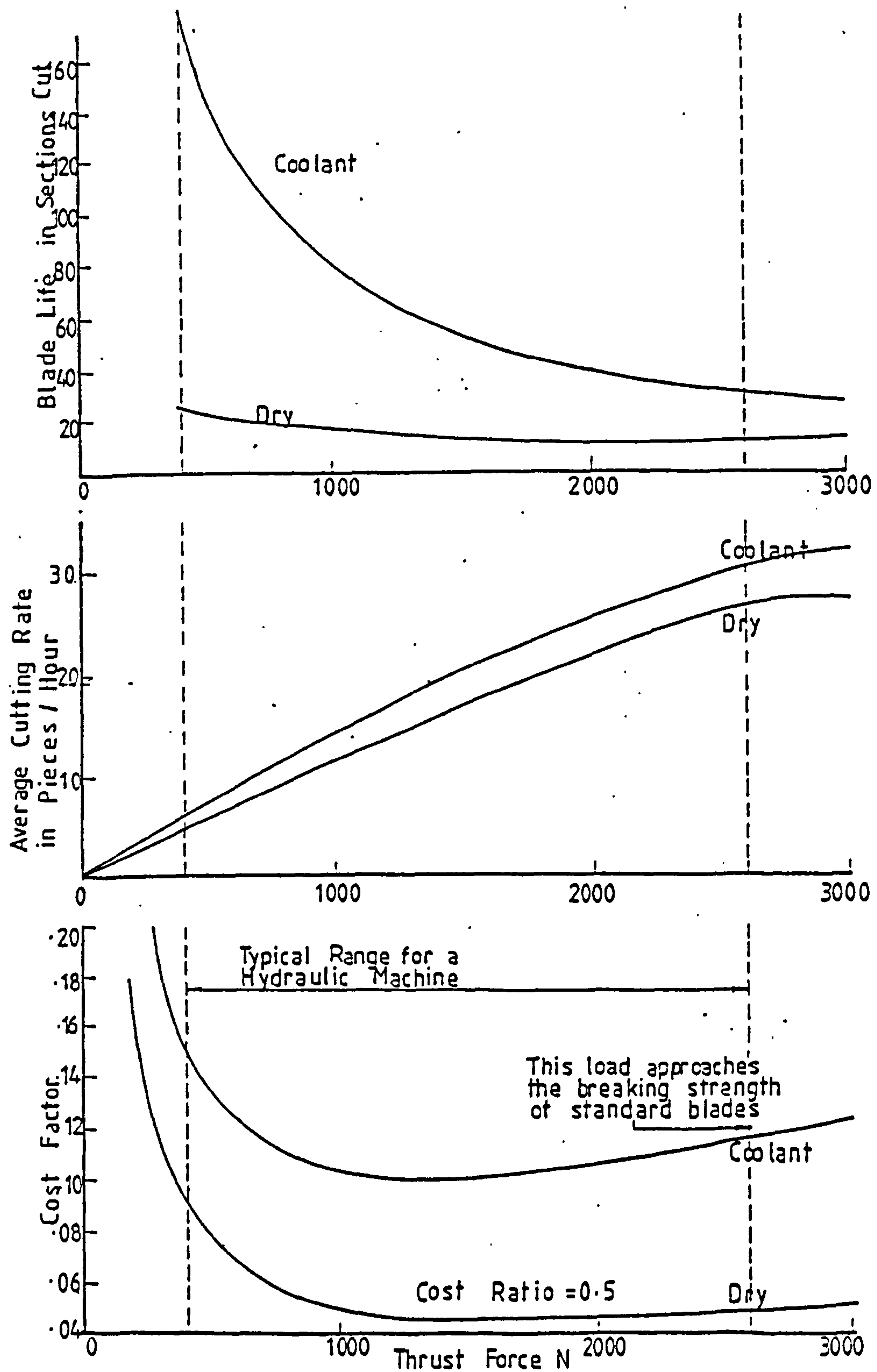


FIG. 46: The effects of the thrust load on the blade life, the average cutting rate and the cost factor (27)

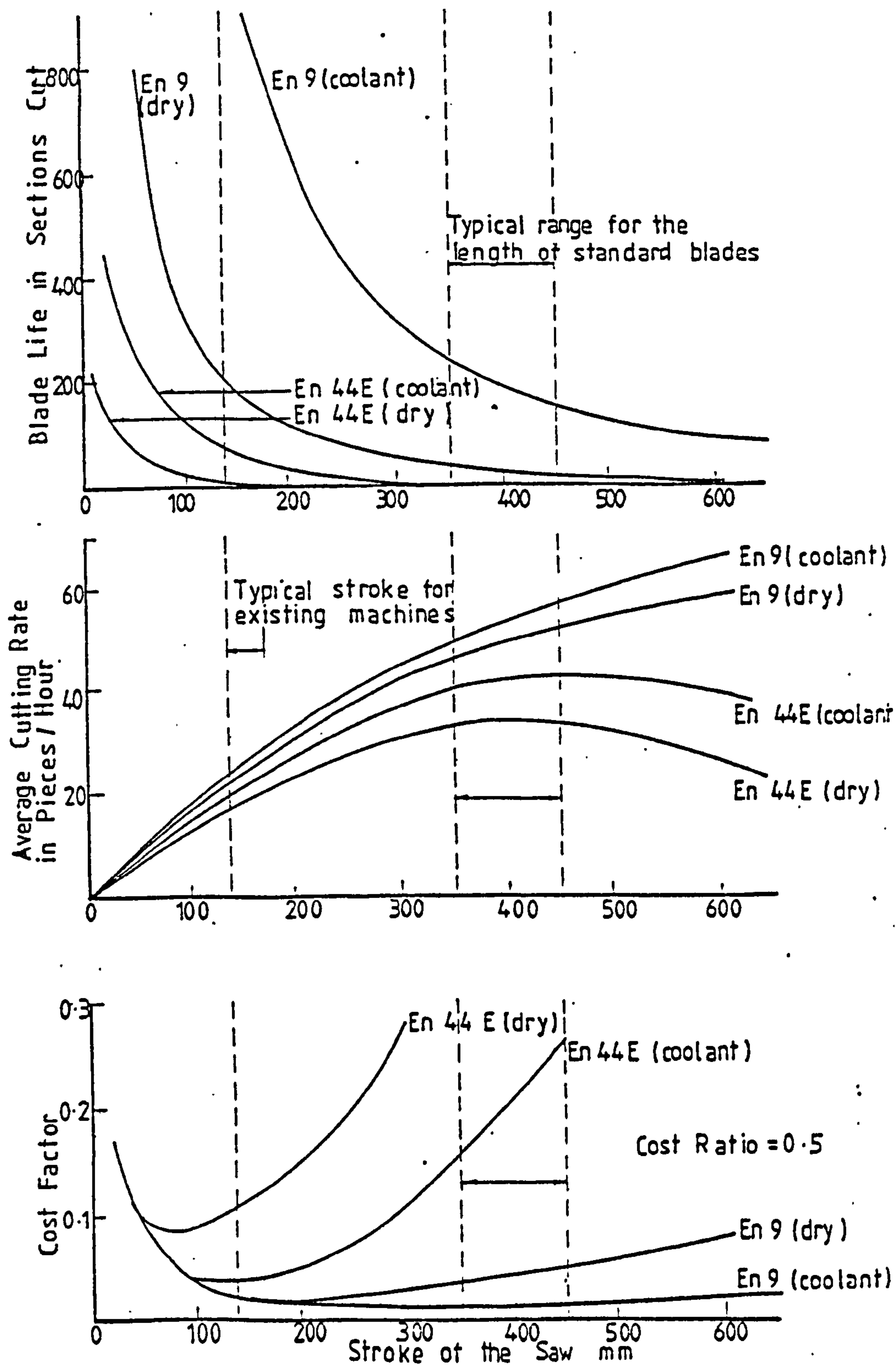


FIG. 47: The effects of the stroke of the saw on the blade life, the average cutting rate and the cost factor (27)

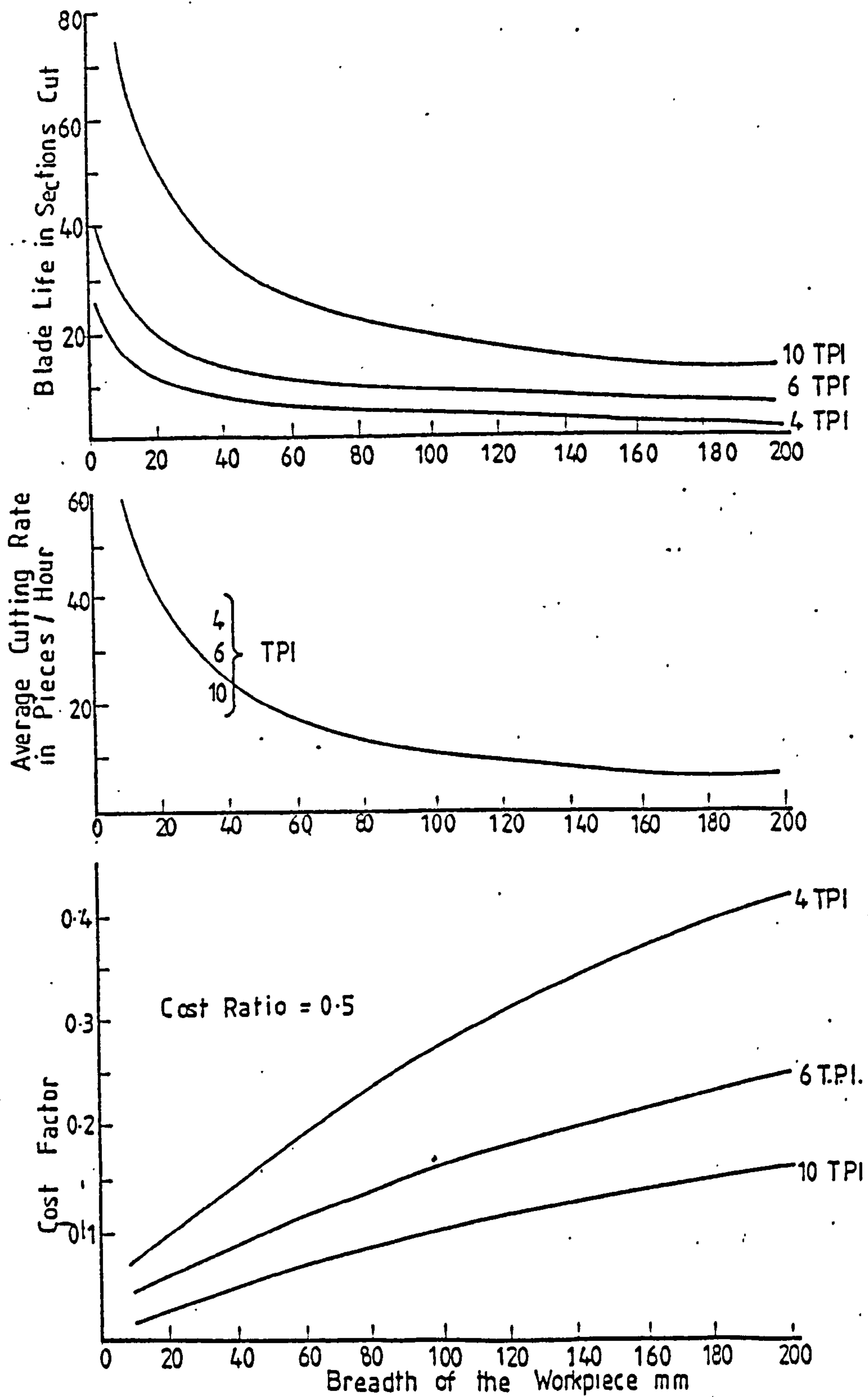
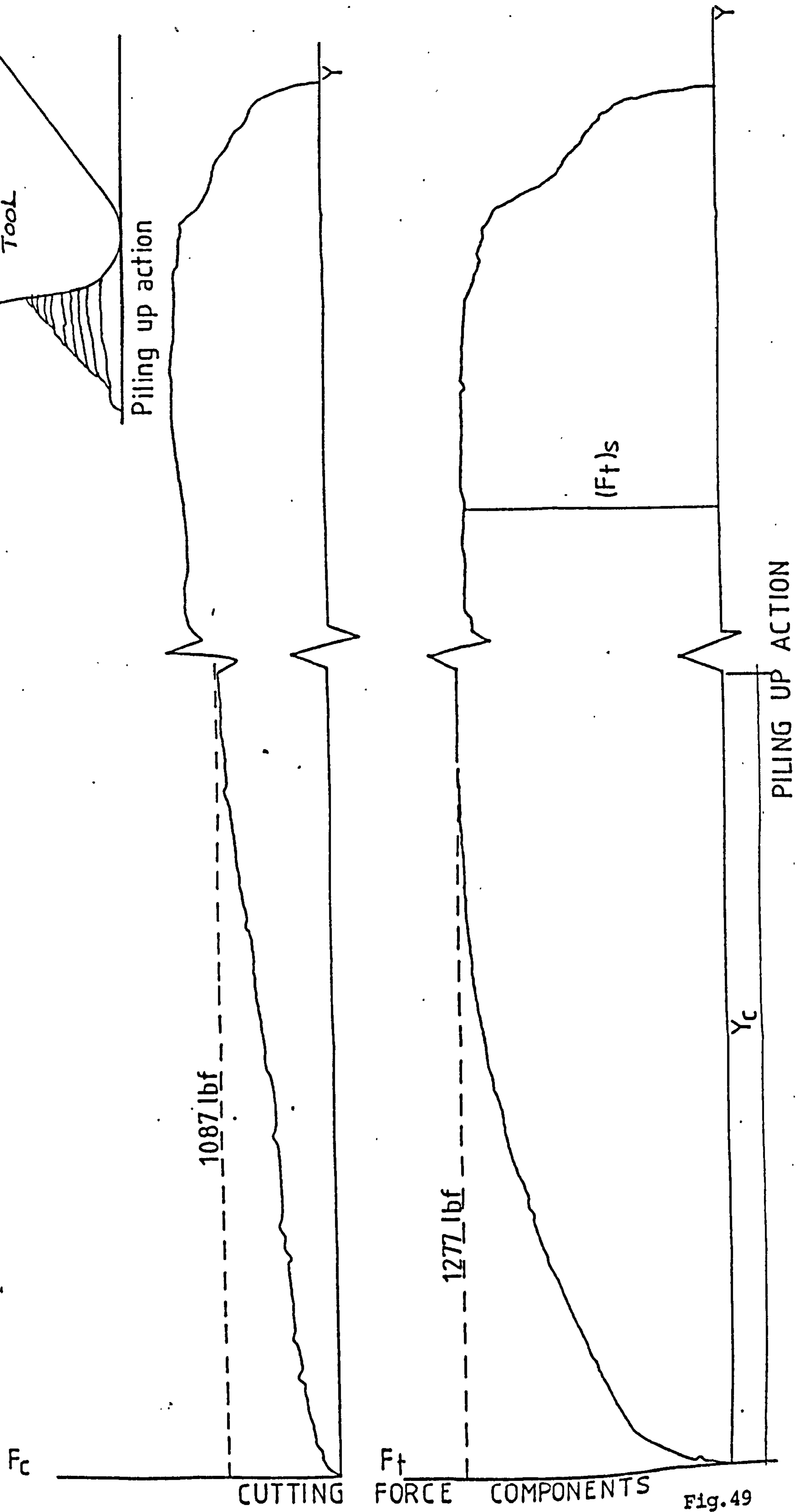


FIG. 48: The effects of blade teeth pitch and breadth of workpiece on the blade life, the average cutting rate and the cost factor (27)

FIG. 49: Variation of the cutting force components with increase in the length of cut

Workpiece : Copper
 Length of specimen : 153 mm
 Table speed : 3.34m/min
 Depth of cut : 0.12mm



(a)

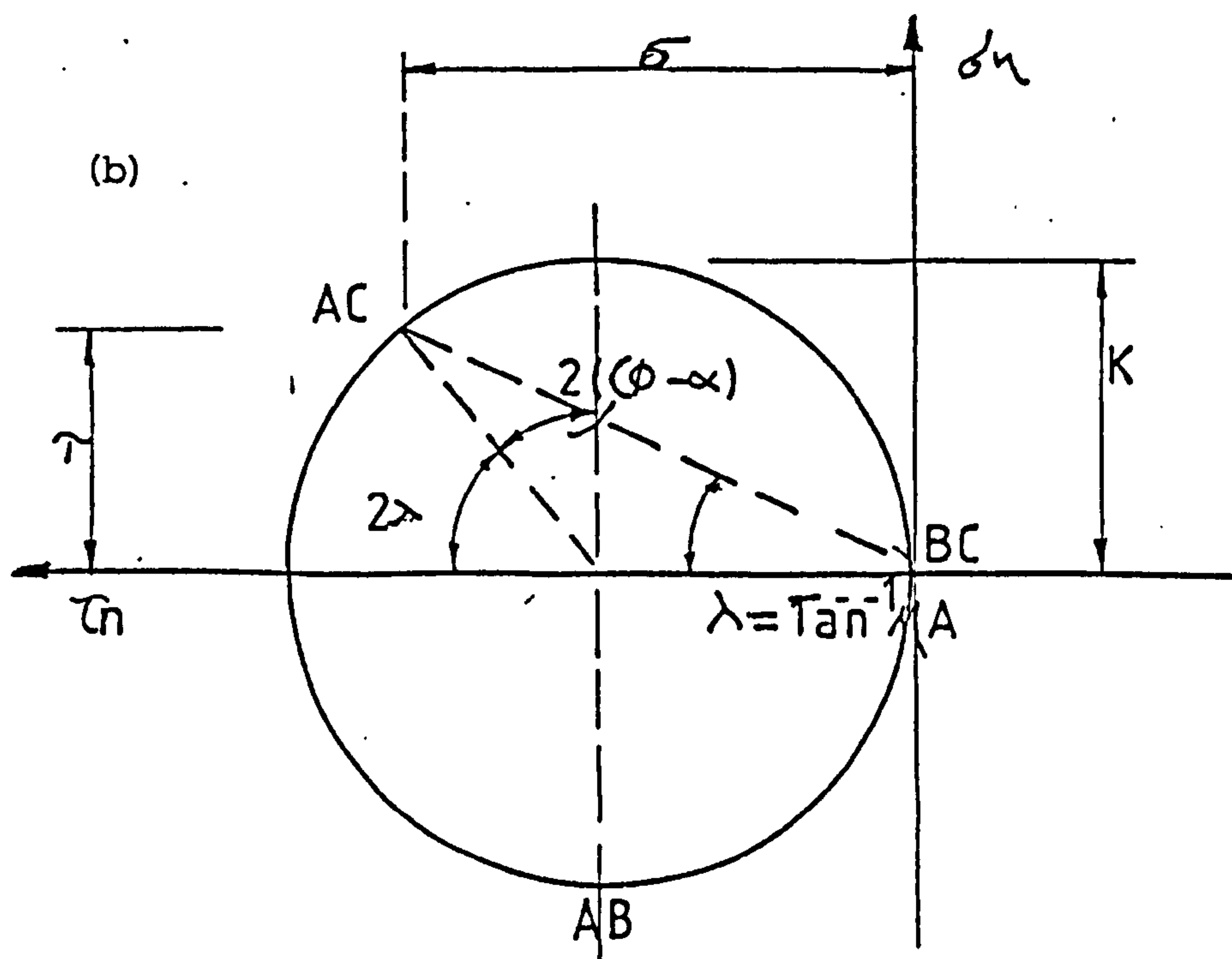
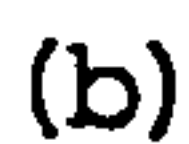


FIG. 51: Predicted variation in the cutting constant
against the apparent coefficient of friction
for a fully developed deformation zone

Material : En 1a ($k = 461.87 \text{ Nmm}^{-2}$)
Rake angle : -4 degrees

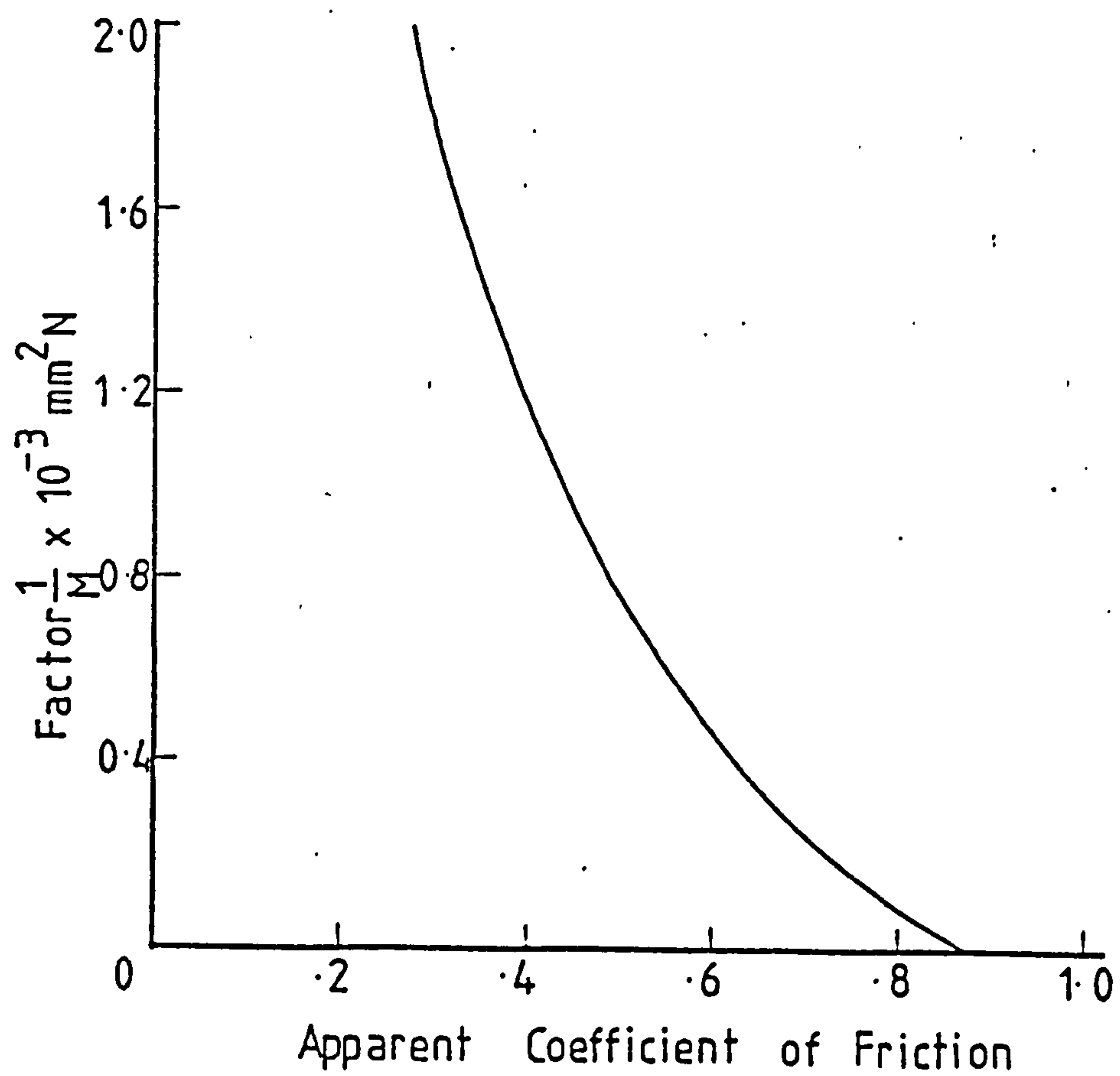
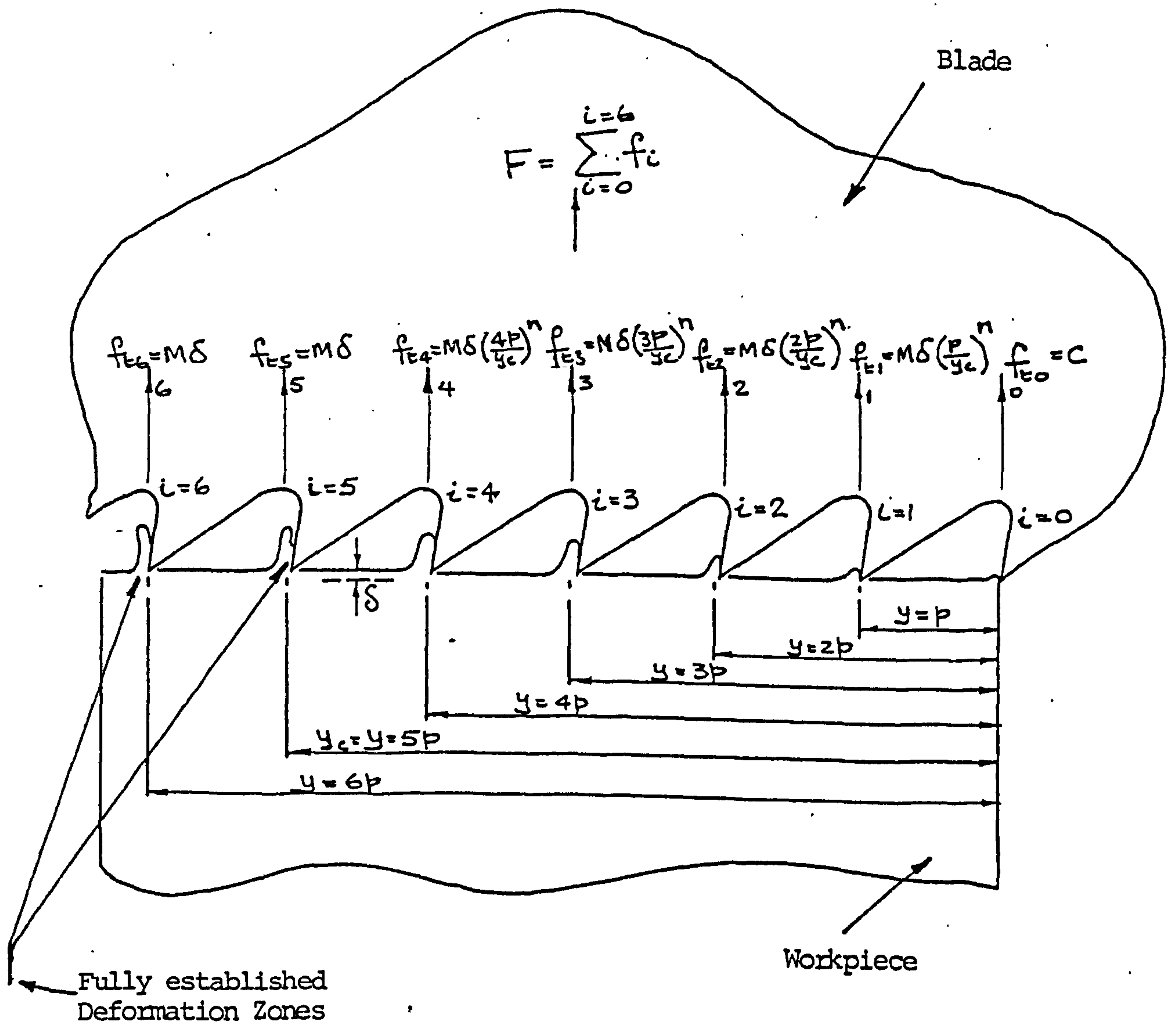


FIG. 52: Thrust loads acting on the teeth (24)



Note: δ is constant for all teeth

FIG. 53: Comparison between the computed values of the reciprocal of the chip factor for various values of the cutting force index and experimental values

(24)

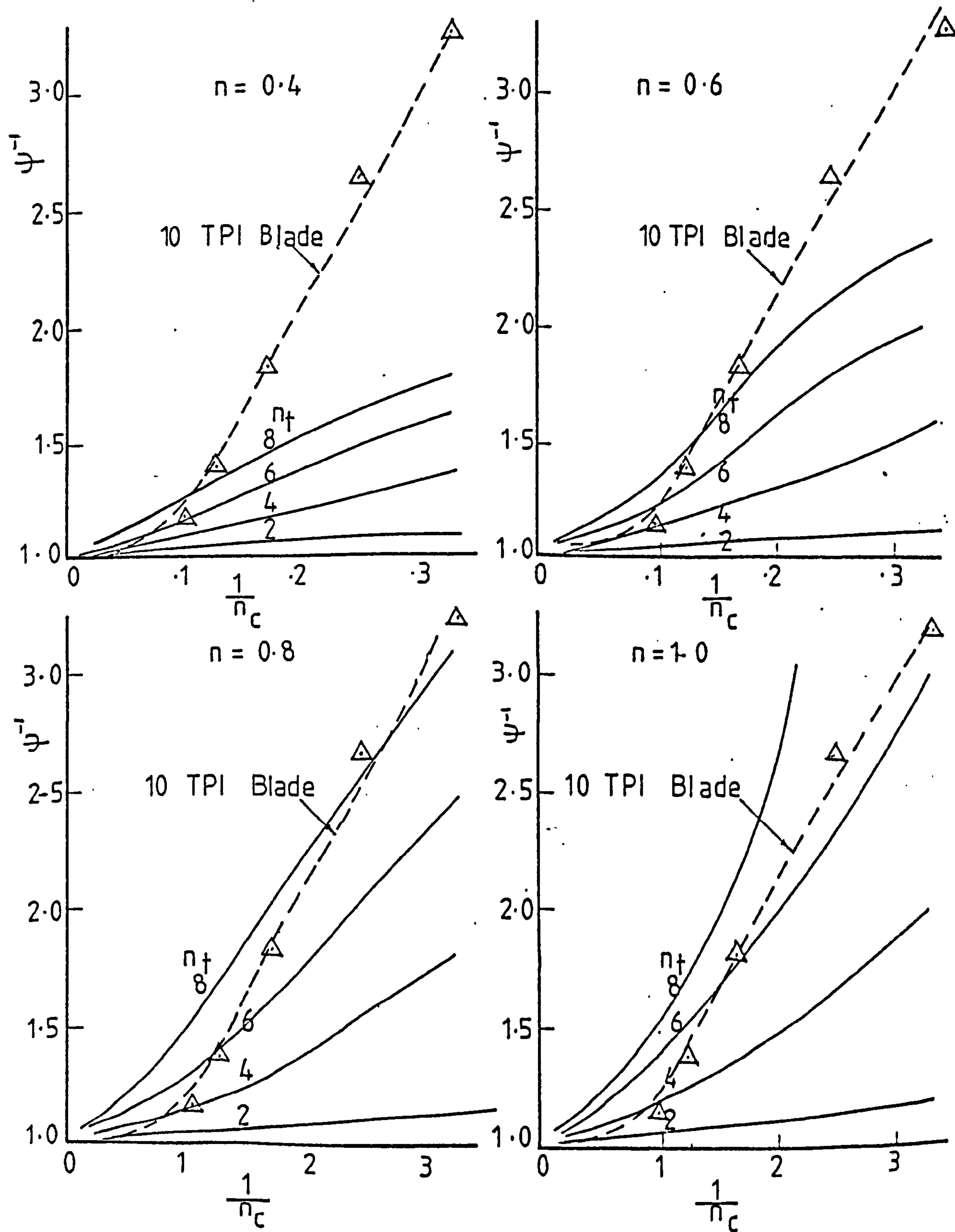


FIG. 54: Comparison between the computed values of the reciprocal of the chip factor for cutting force index of 1 and experimental data obtained with blades of various pitch

(24)

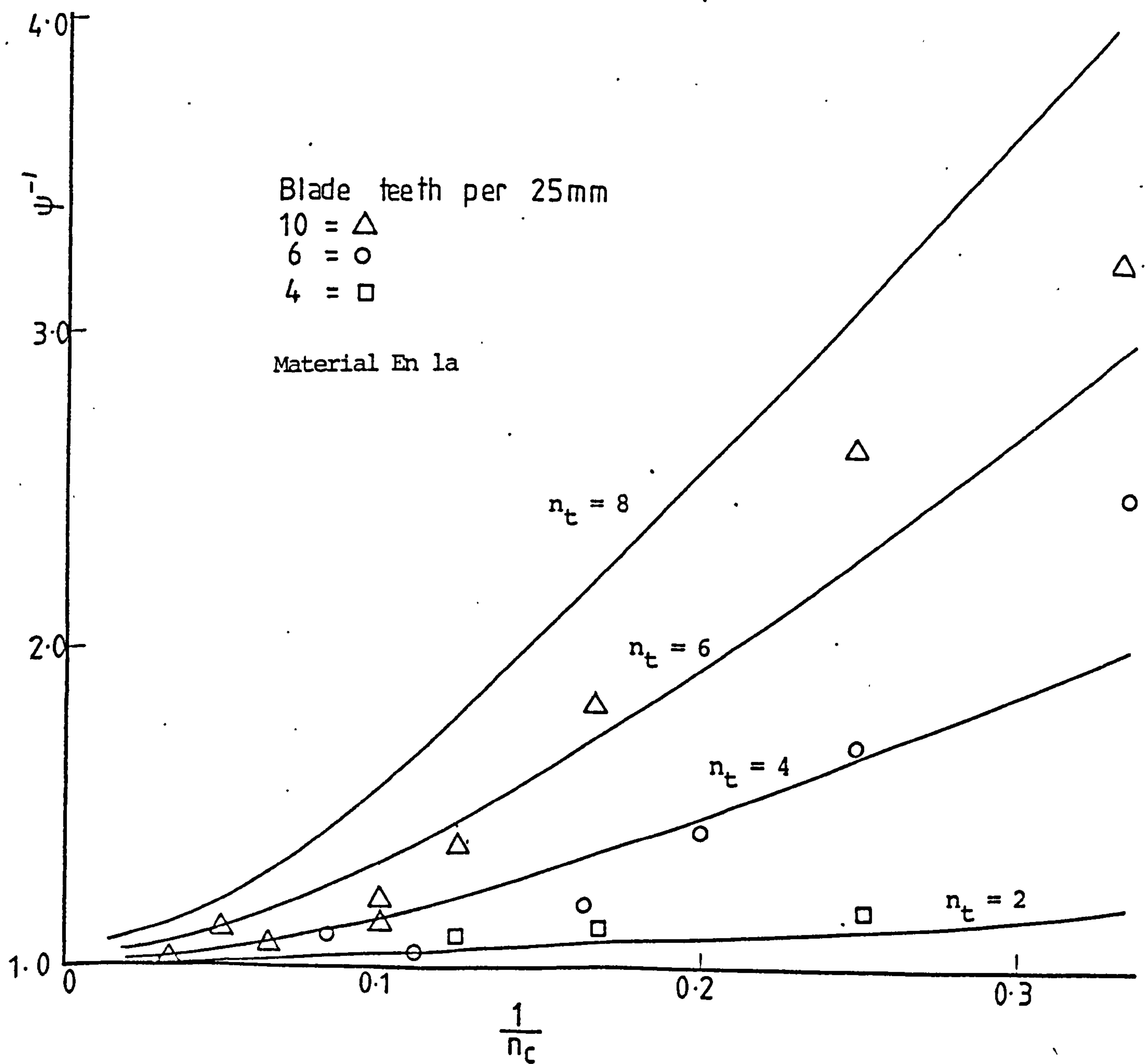


Fig. a.

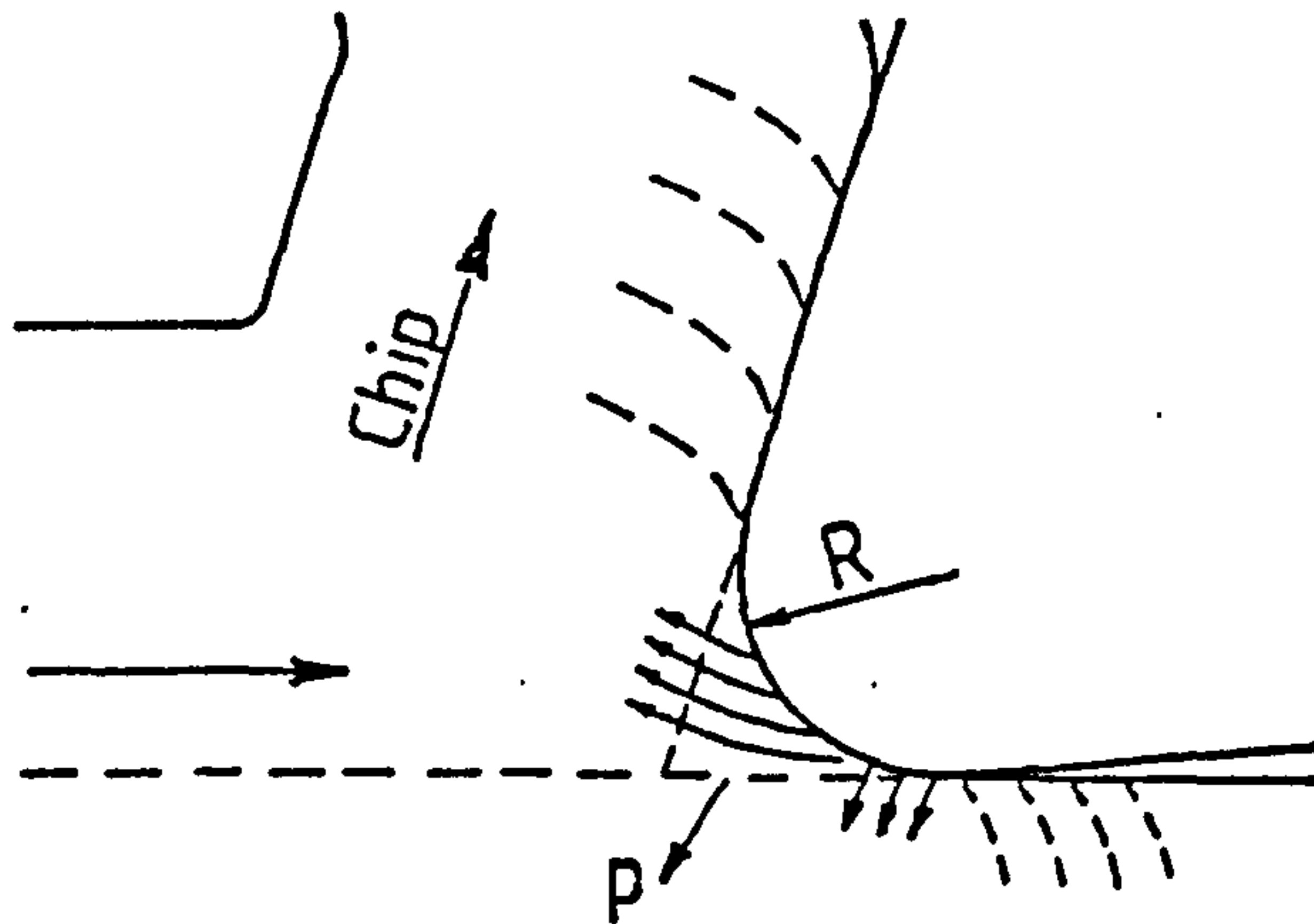


Fig. b.

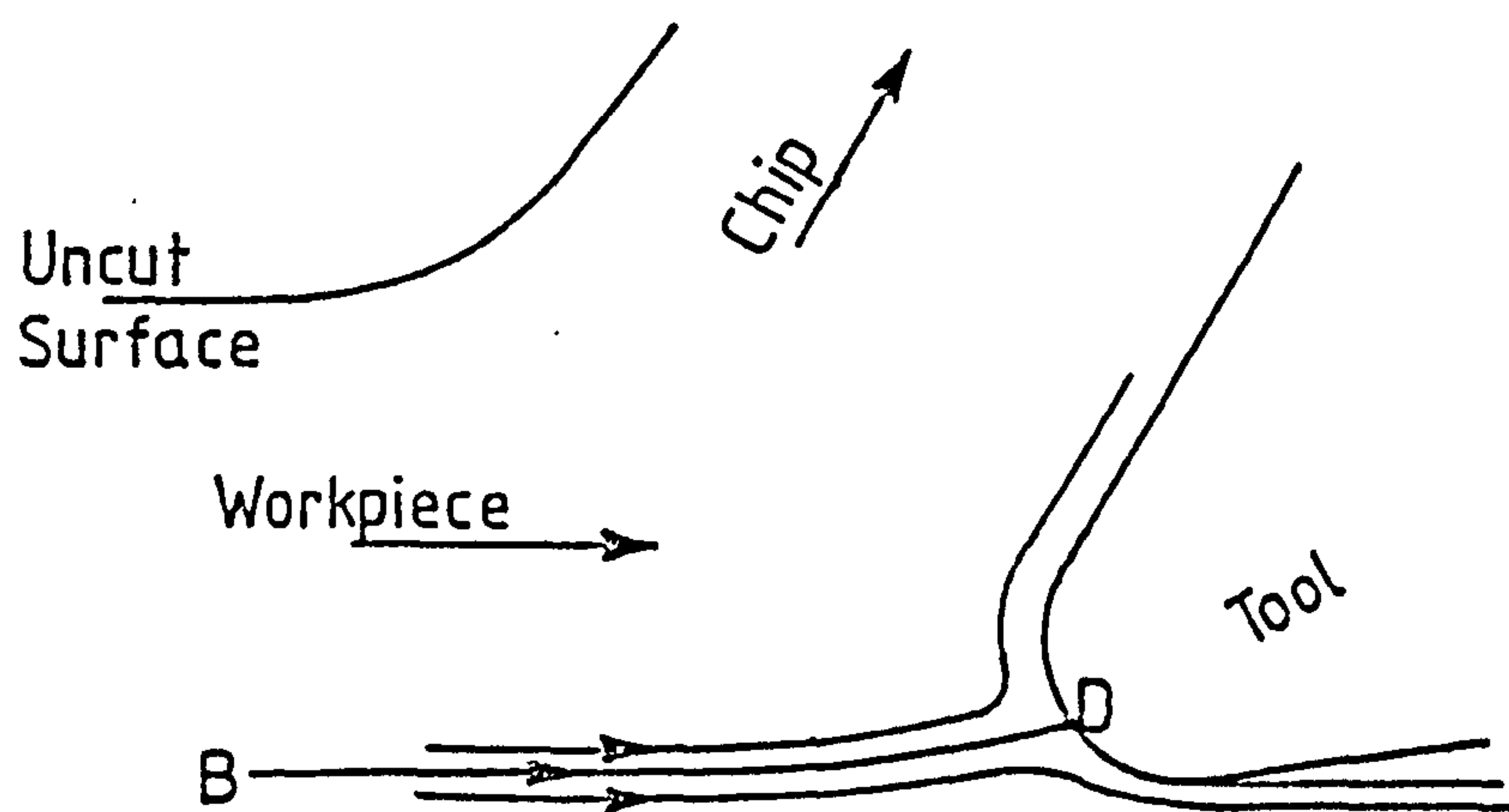


Fig. C.

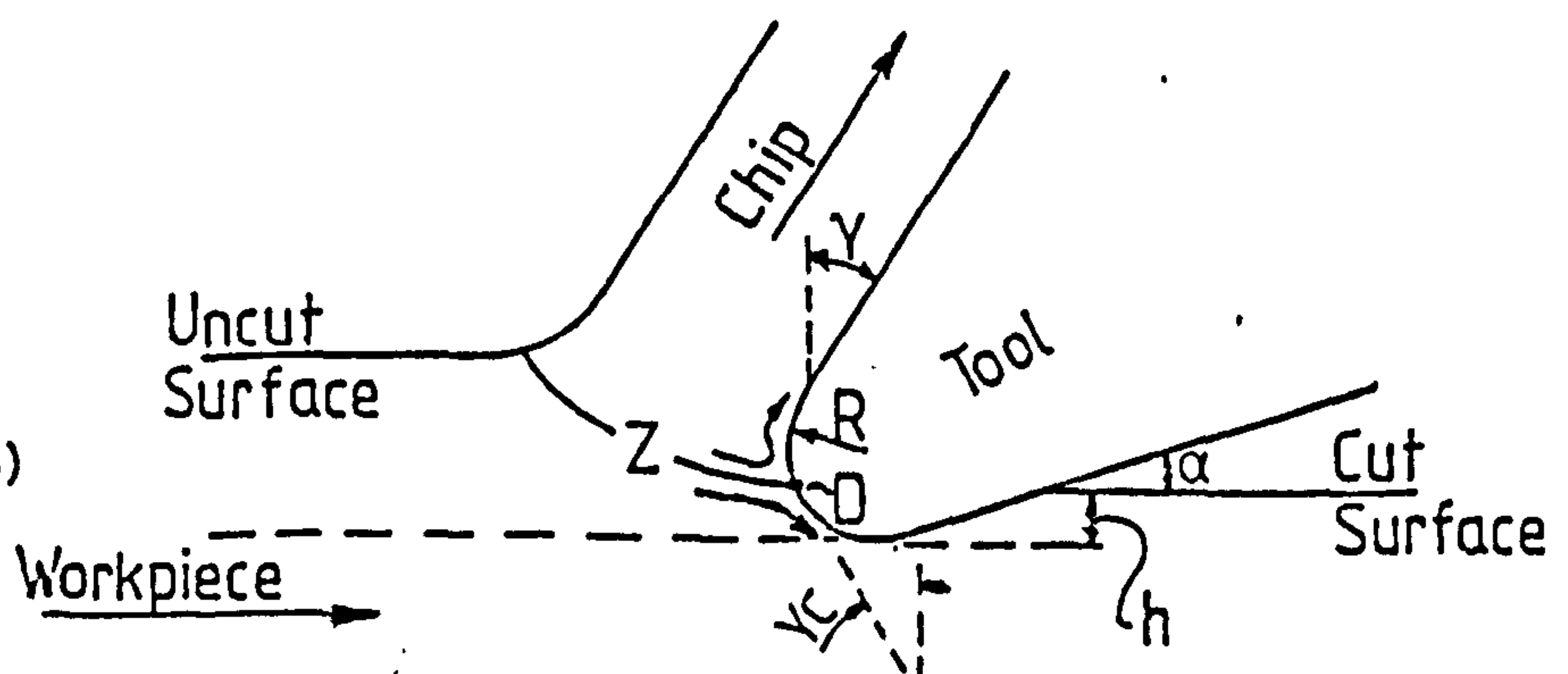


FIG. 55: Diagrammatic representation of the cutting process with a tool having an extreme cutting edge radius

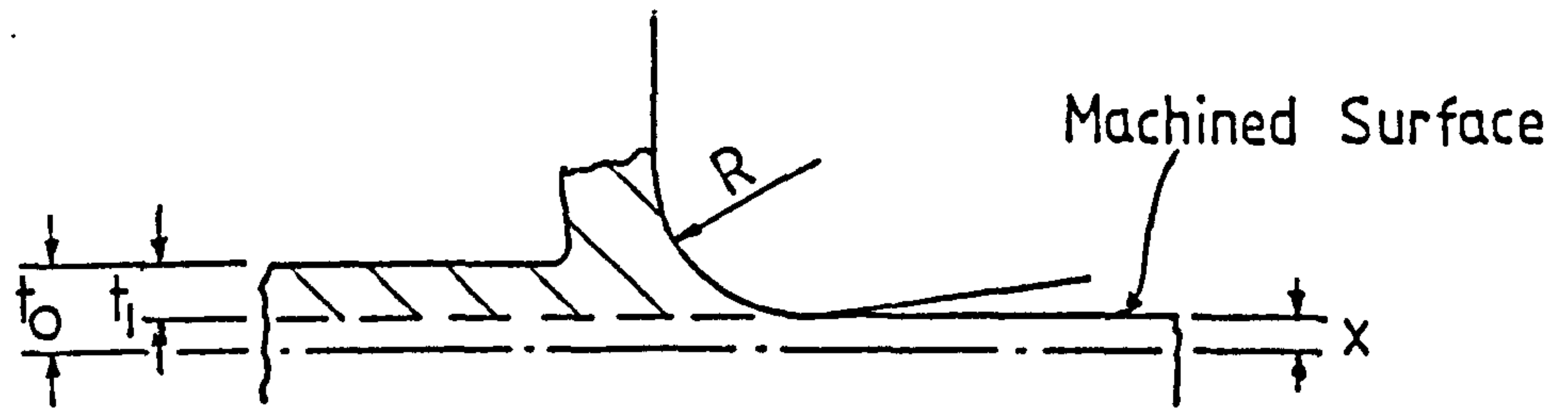
h = Material Recovery.

x = Machine Deflection.

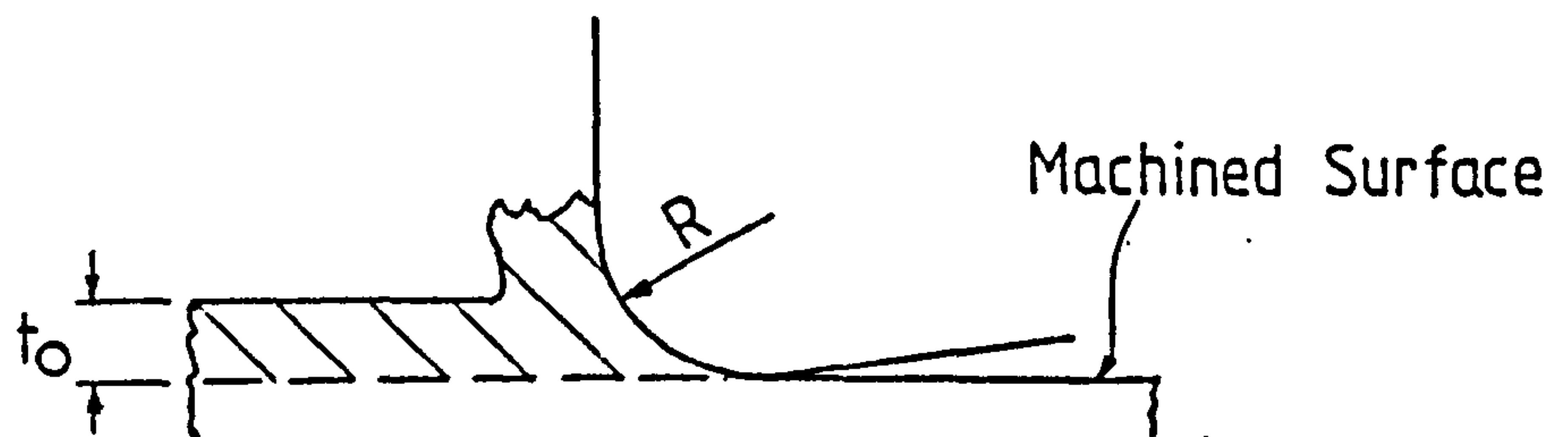
t_o = Nominal Set Depth.

t_i = Layer Removed.

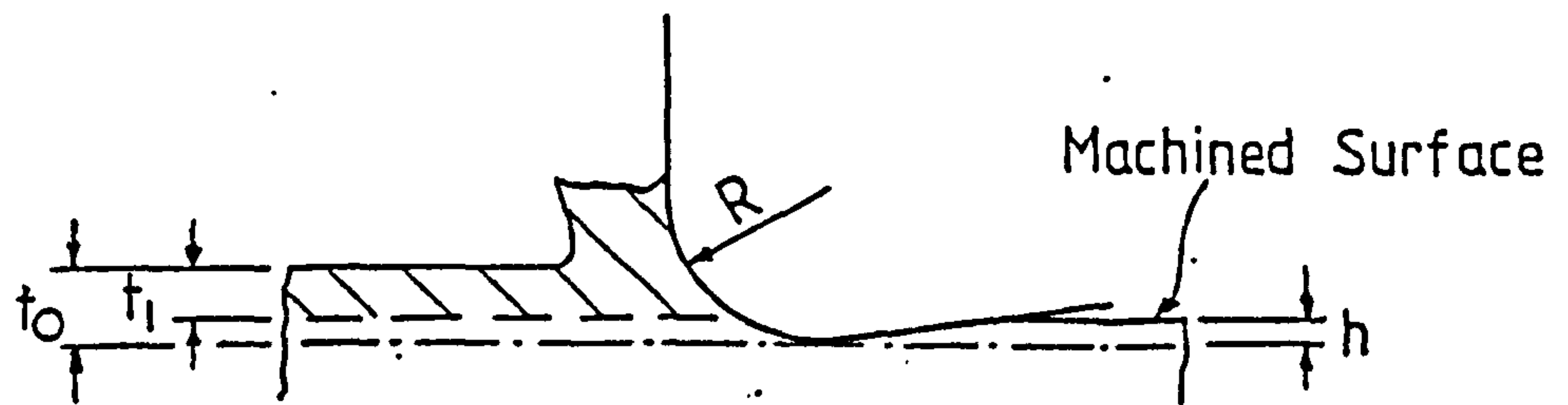
(a) $t_o > t_i$



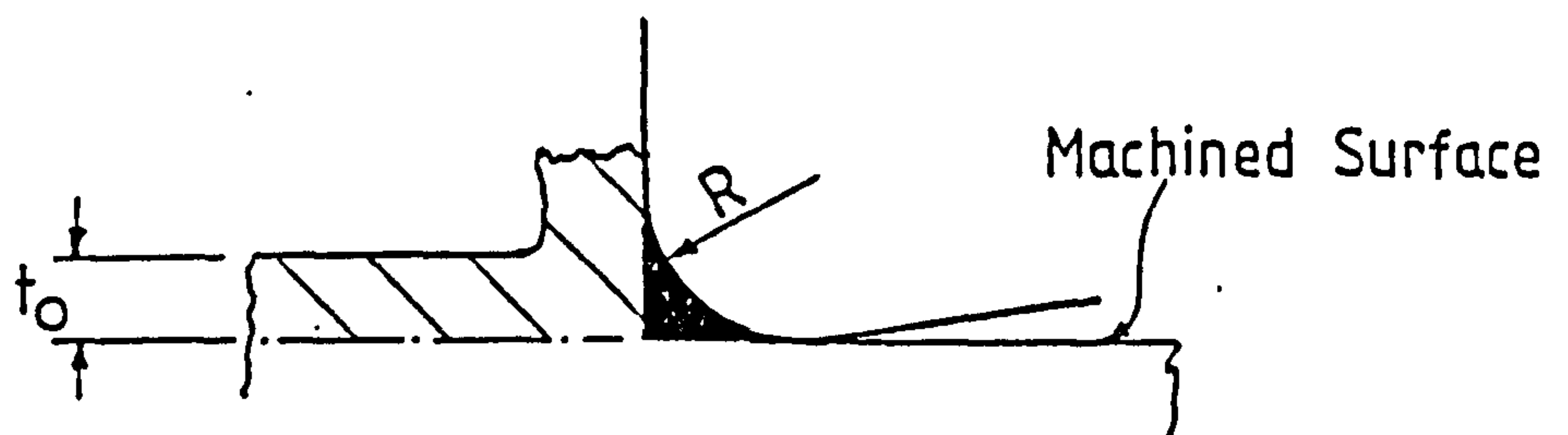
(b) $t_o = t_i$



(c) $t_o > t_i$



(d) $t_o = t_i$



(e) $t_o < t_i$

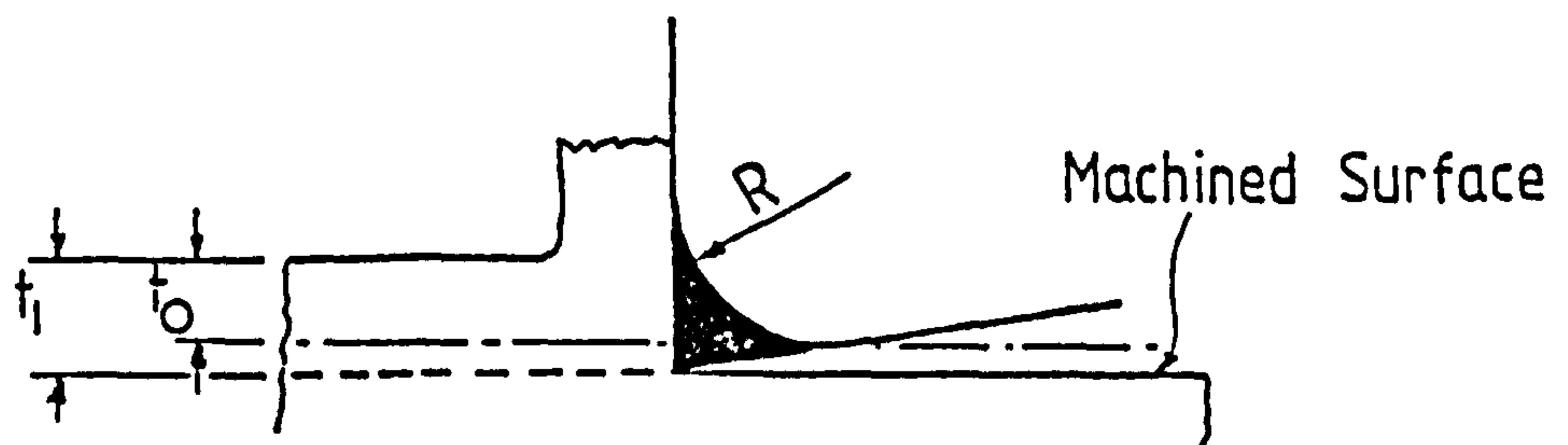


FIG. 56: Diagrammatic representation of the relationship between the set depth, layer of material removed and the machined surface

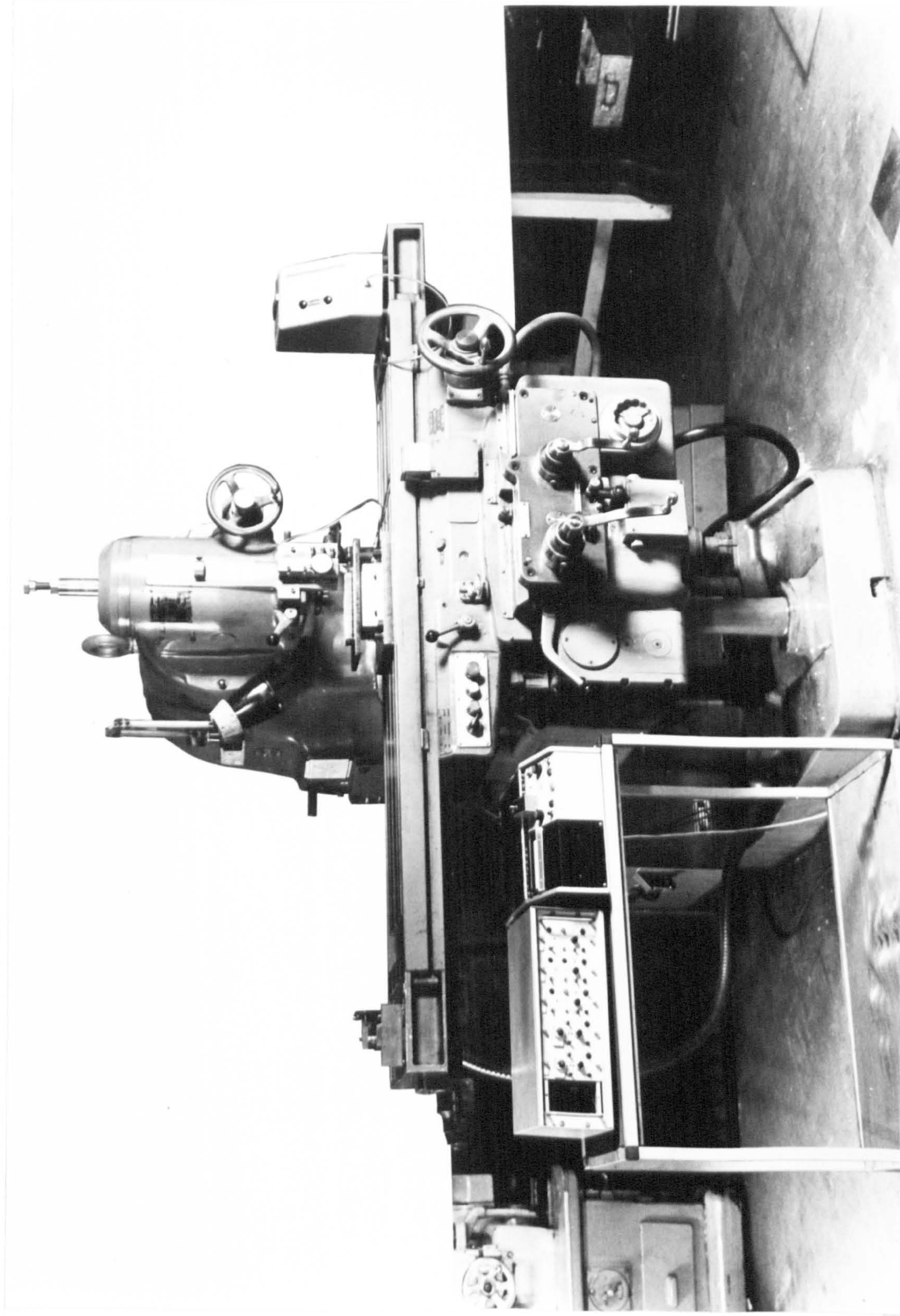


FIG.57 MACHINE TOOL AND ASSOCIATED EQUIPMENT USED FOR SIMULATION TESTS

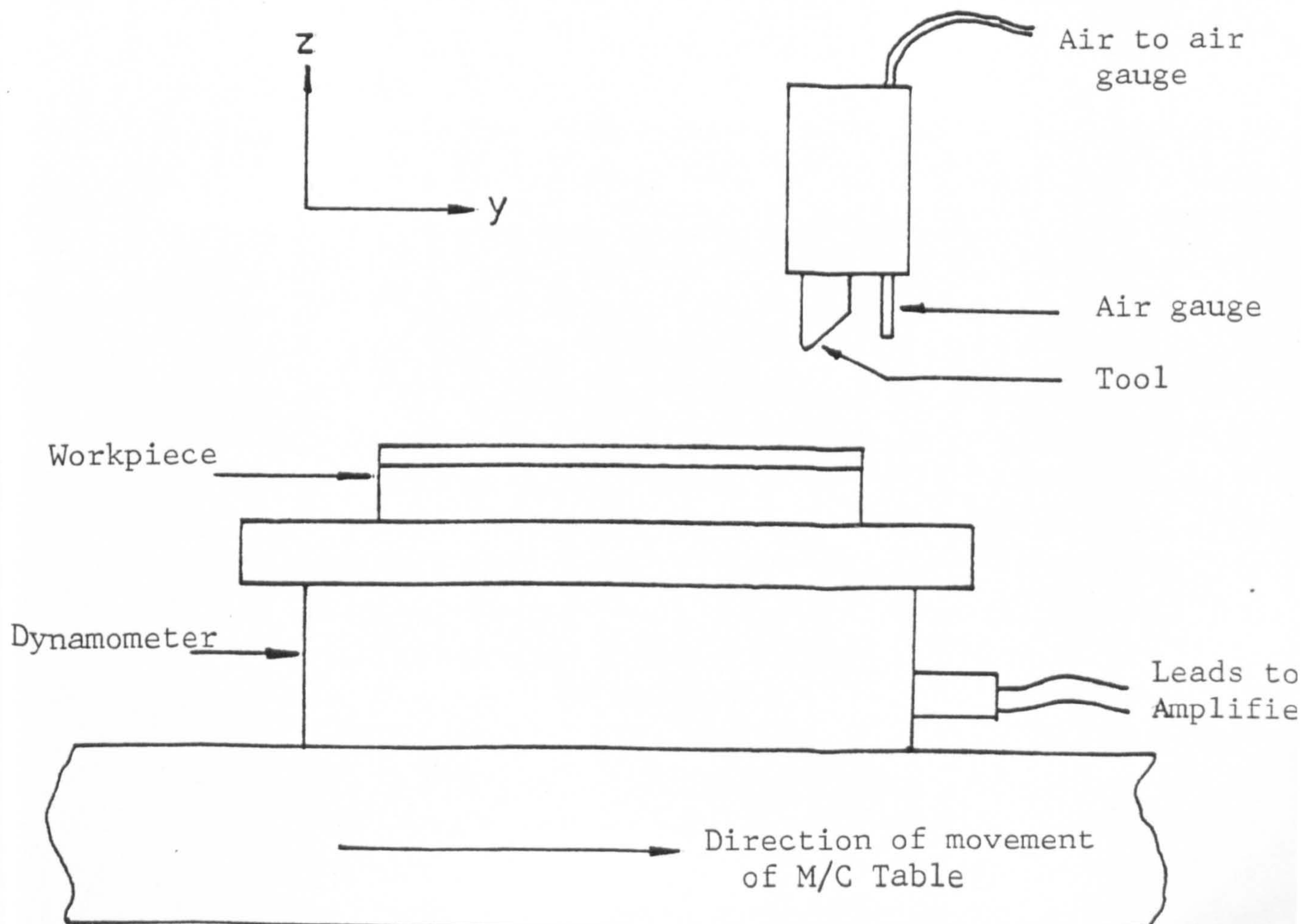
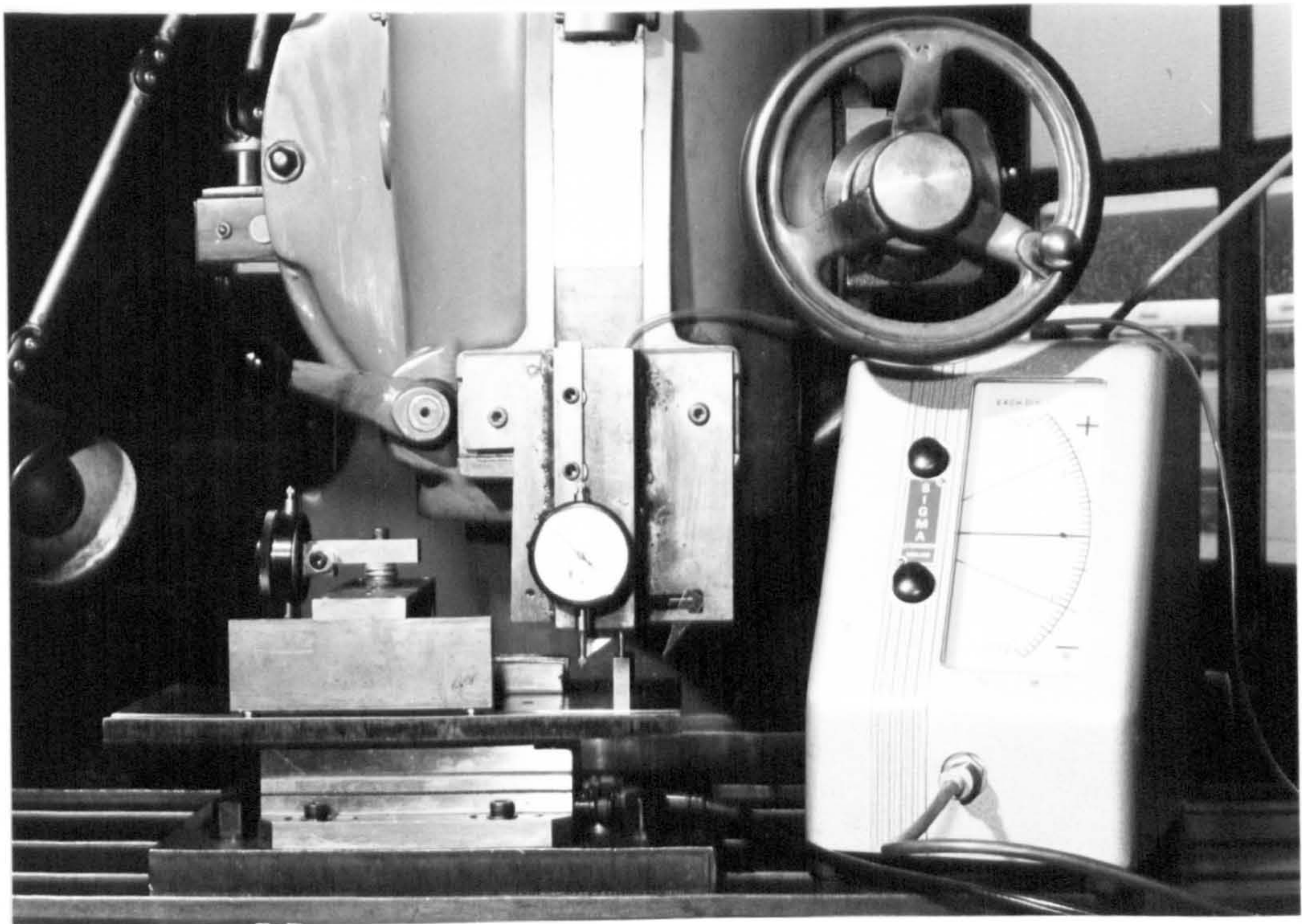
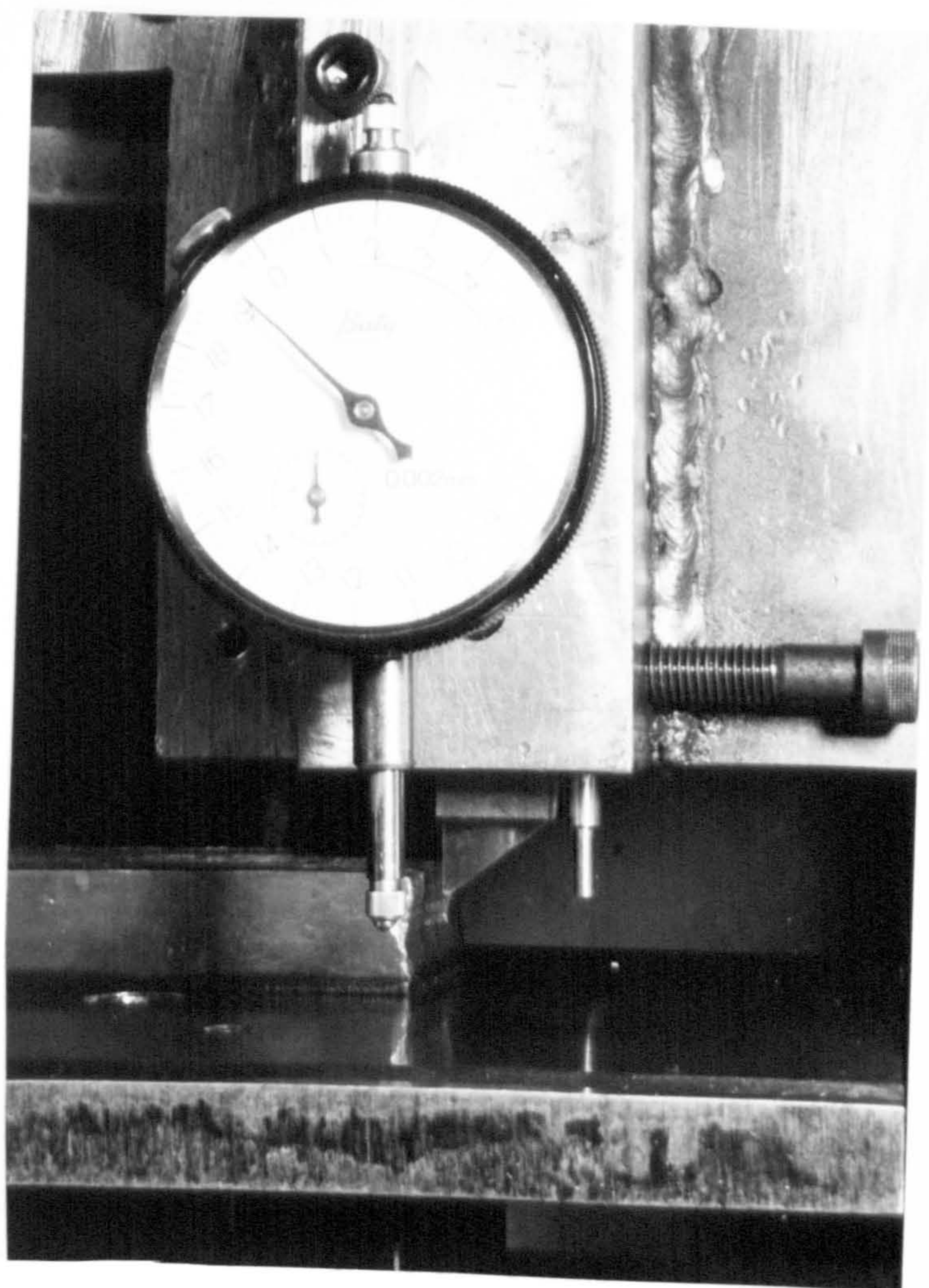


FIG.58 VIEW OF THE CUTTING TOOL-WORKPIECE SET-UP FOR SIMULATION TESTS

(A)



(B)

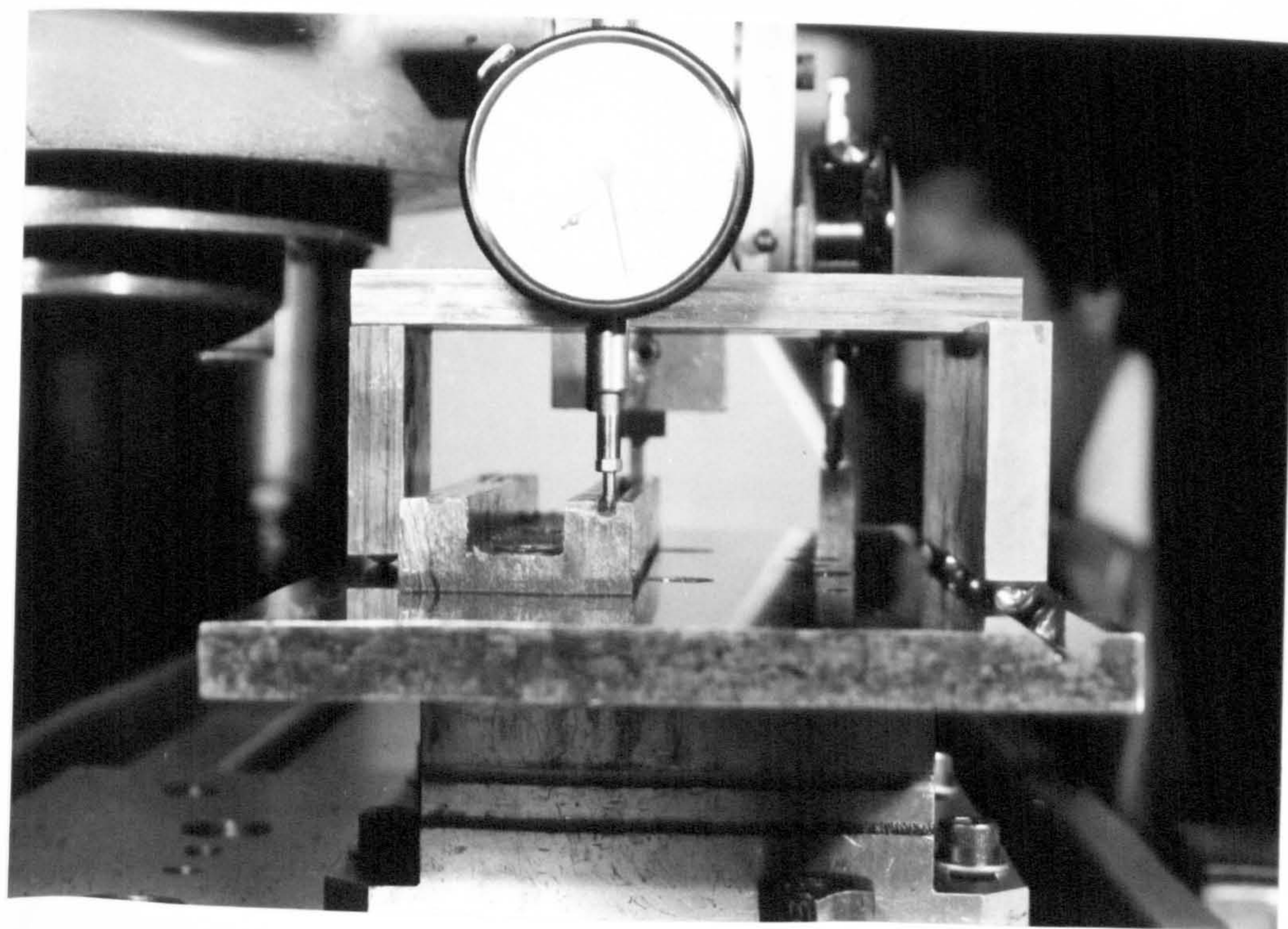
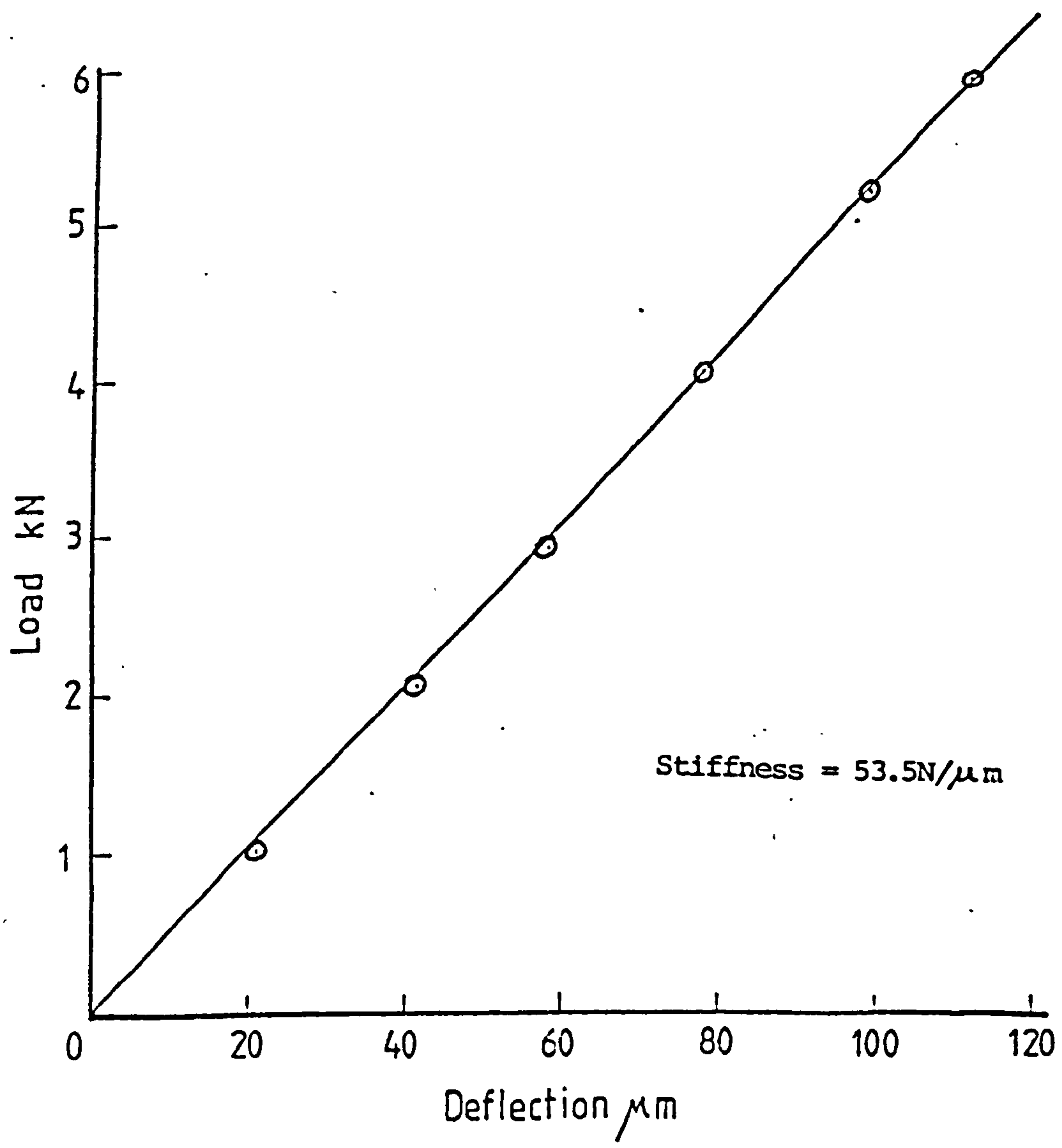


FIG.59 CLOSE-UP OF THE BRIDGE DIAL GAUGE ARRANGEMENTS

FIG. 60: Stiffness measurements at position of tool holder
(Parkson Miller)



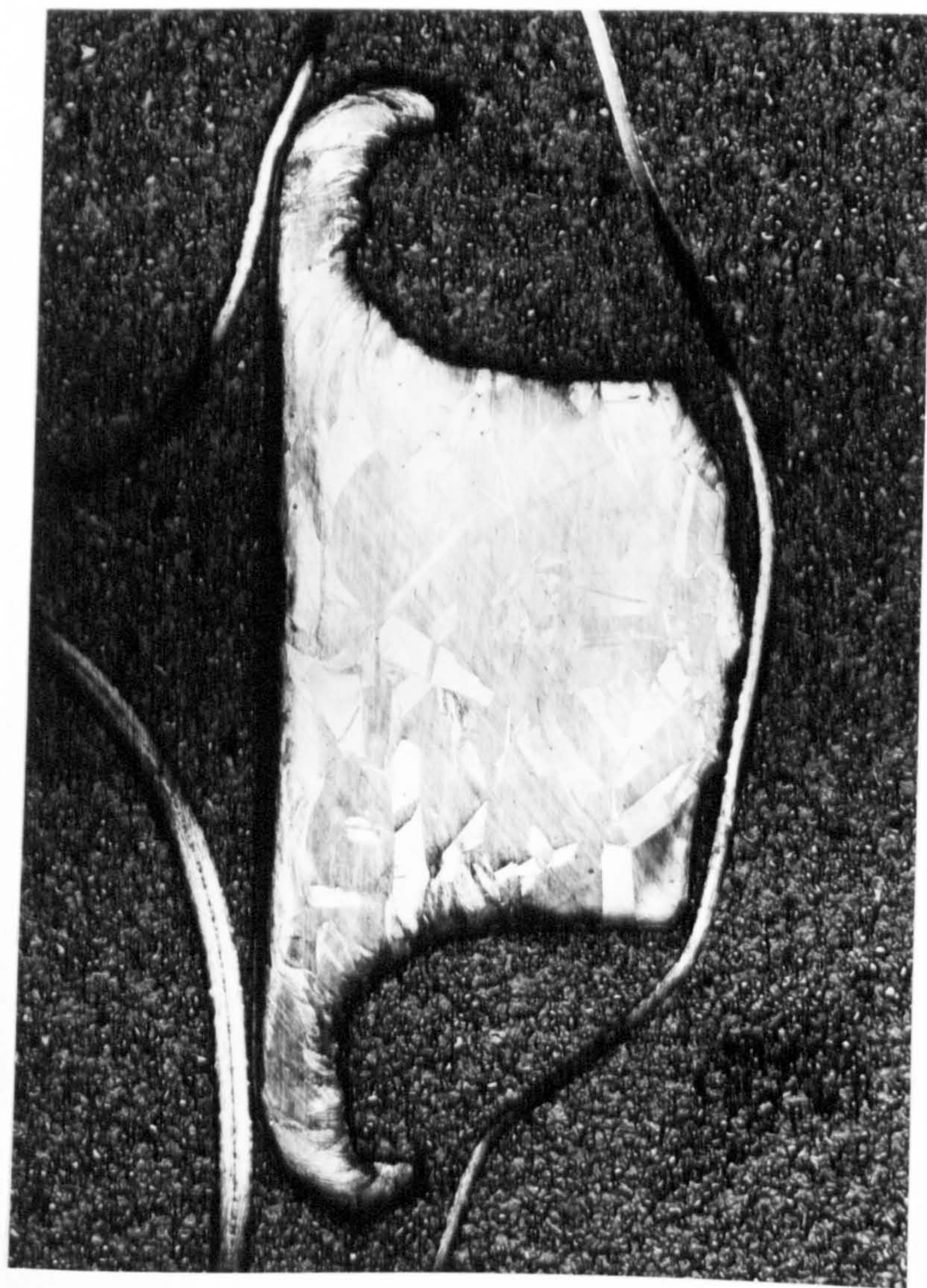


FIG.61 CROSS-SECTION OF AN INITIALLY 3.55 MM WIDE COPPER SPECIMEN AFTER MACHINING, SHOWING
SIDE SPREAD

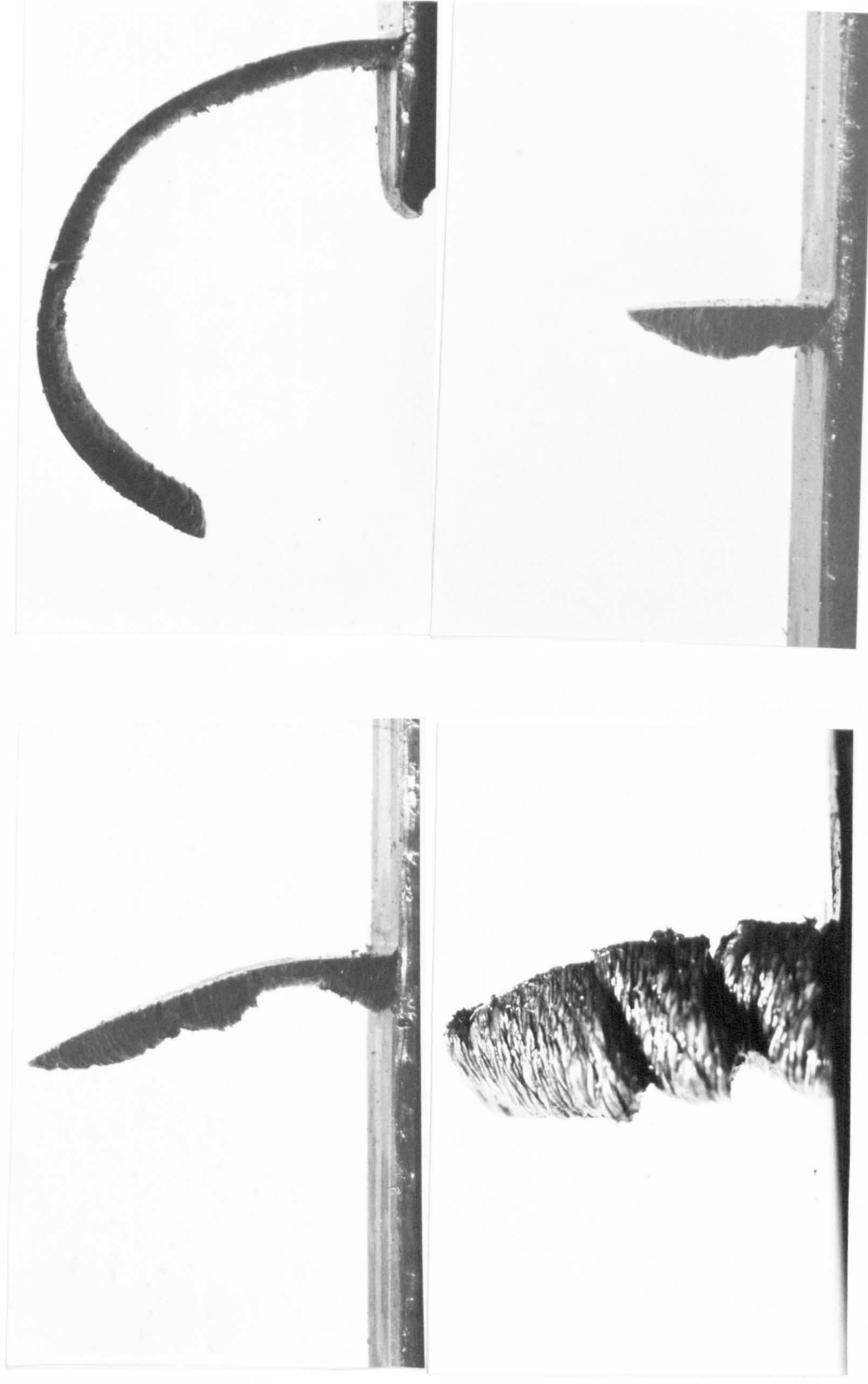


FIG.62 CHIPS OF VARYING GEOMETRY PRODUCED WHEN MACHINING COPPER WITH A BLUNT TOOL
(0.56 MM RADIUS) (DEPTH OF CUT : 0.25 MM, 95 MM/MIN)

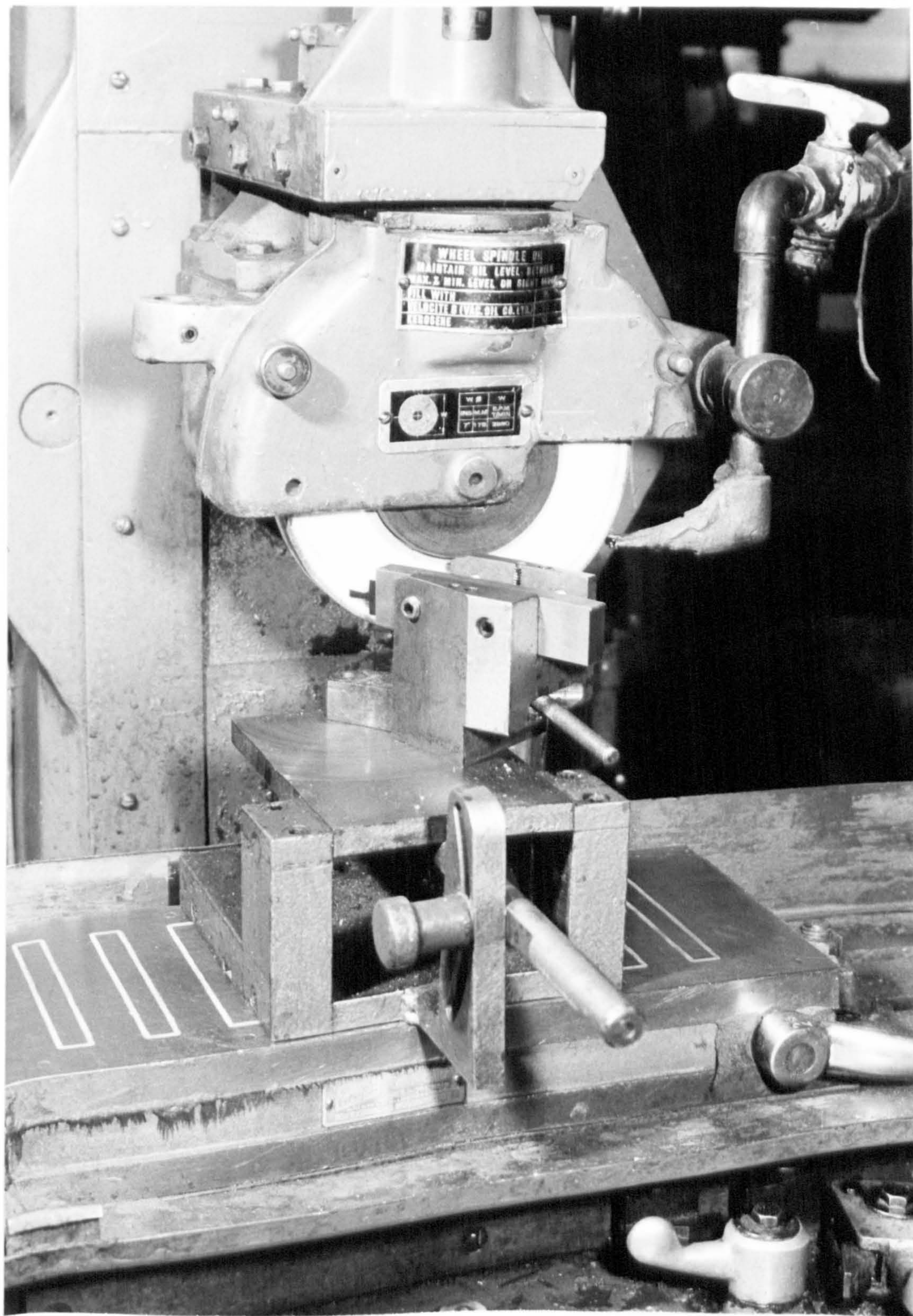


FIG.63(A) TOOL EDGE RADIUS GRINDING JIG SET-UP ON THE SURFACE GRINDING MACHINE

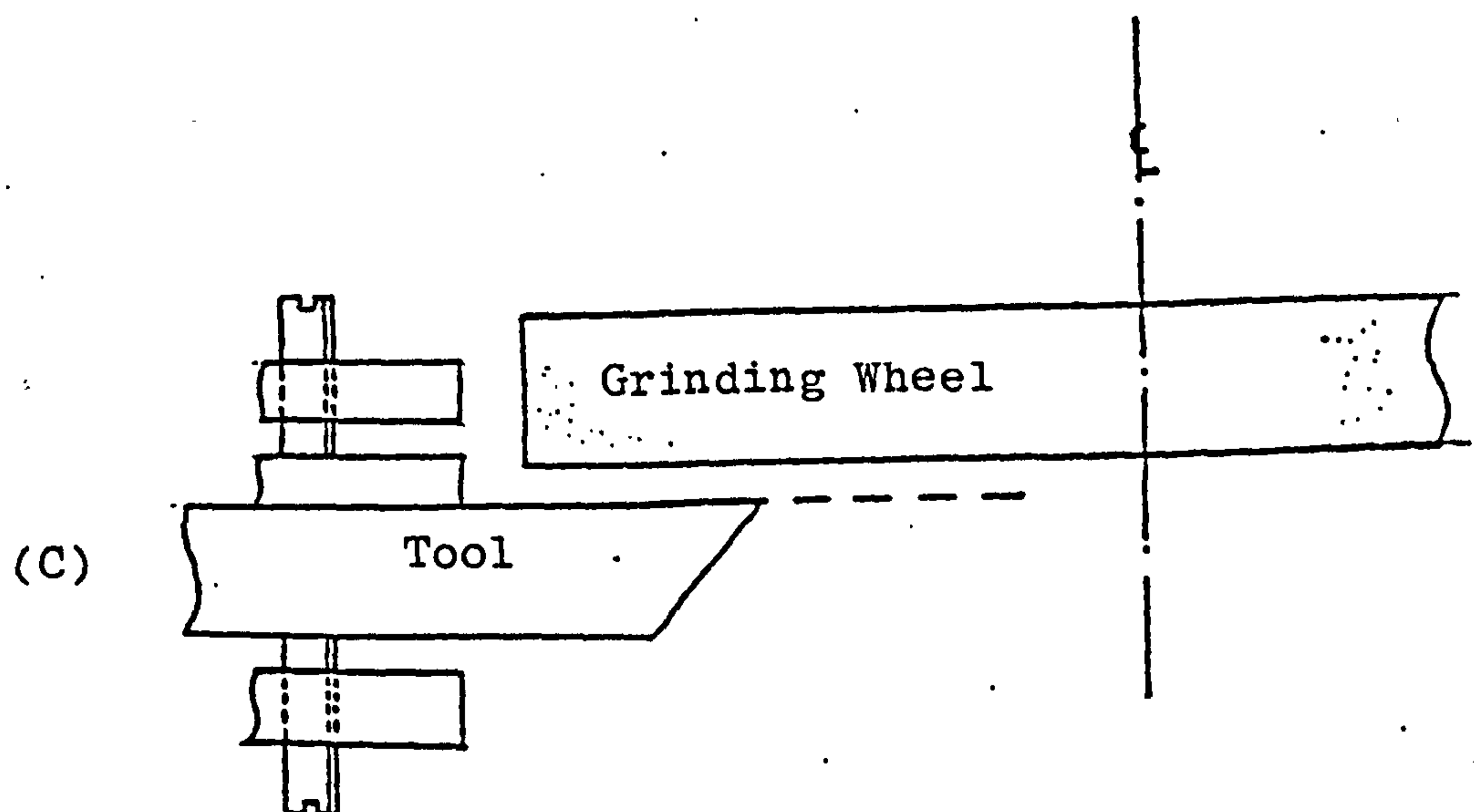
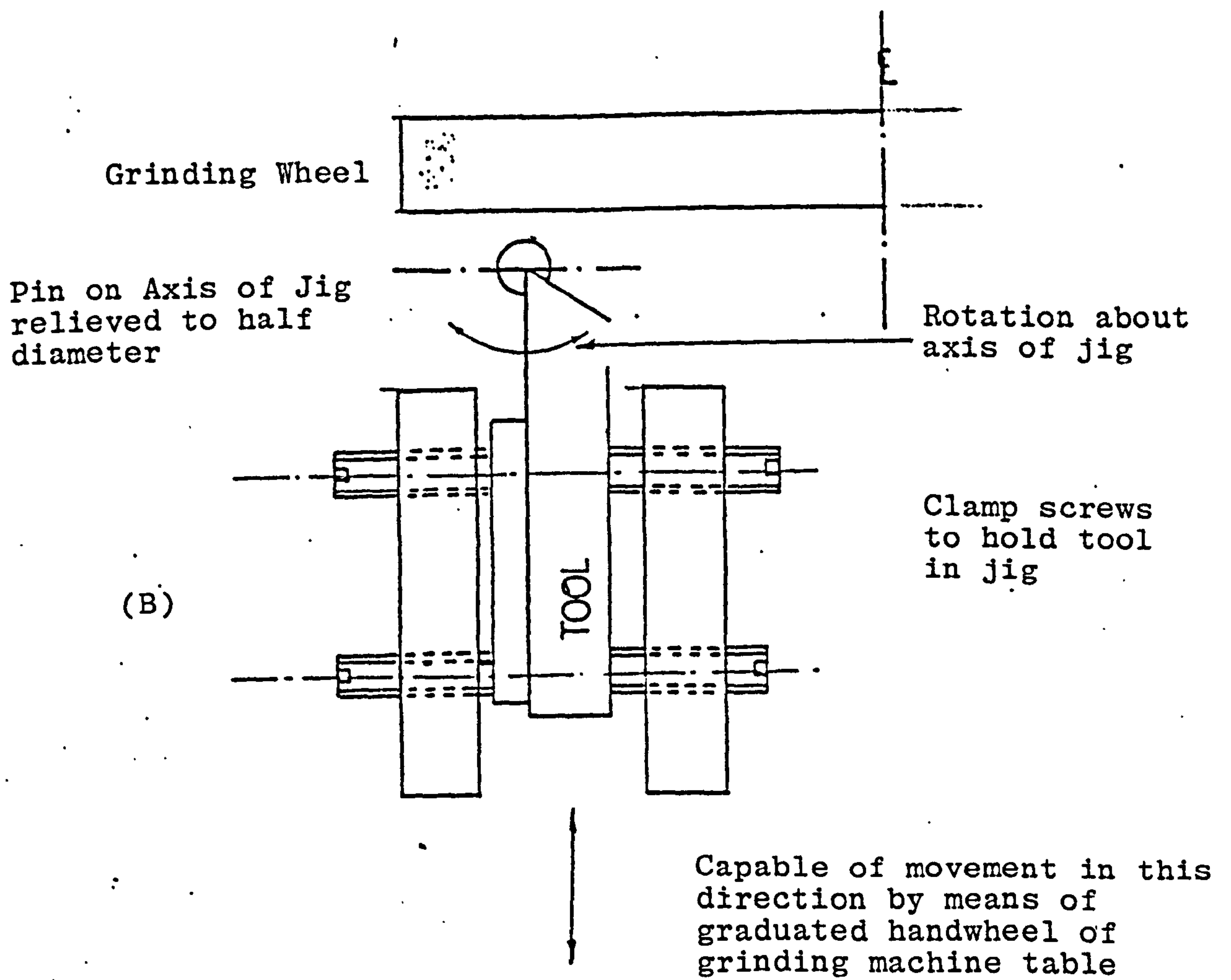
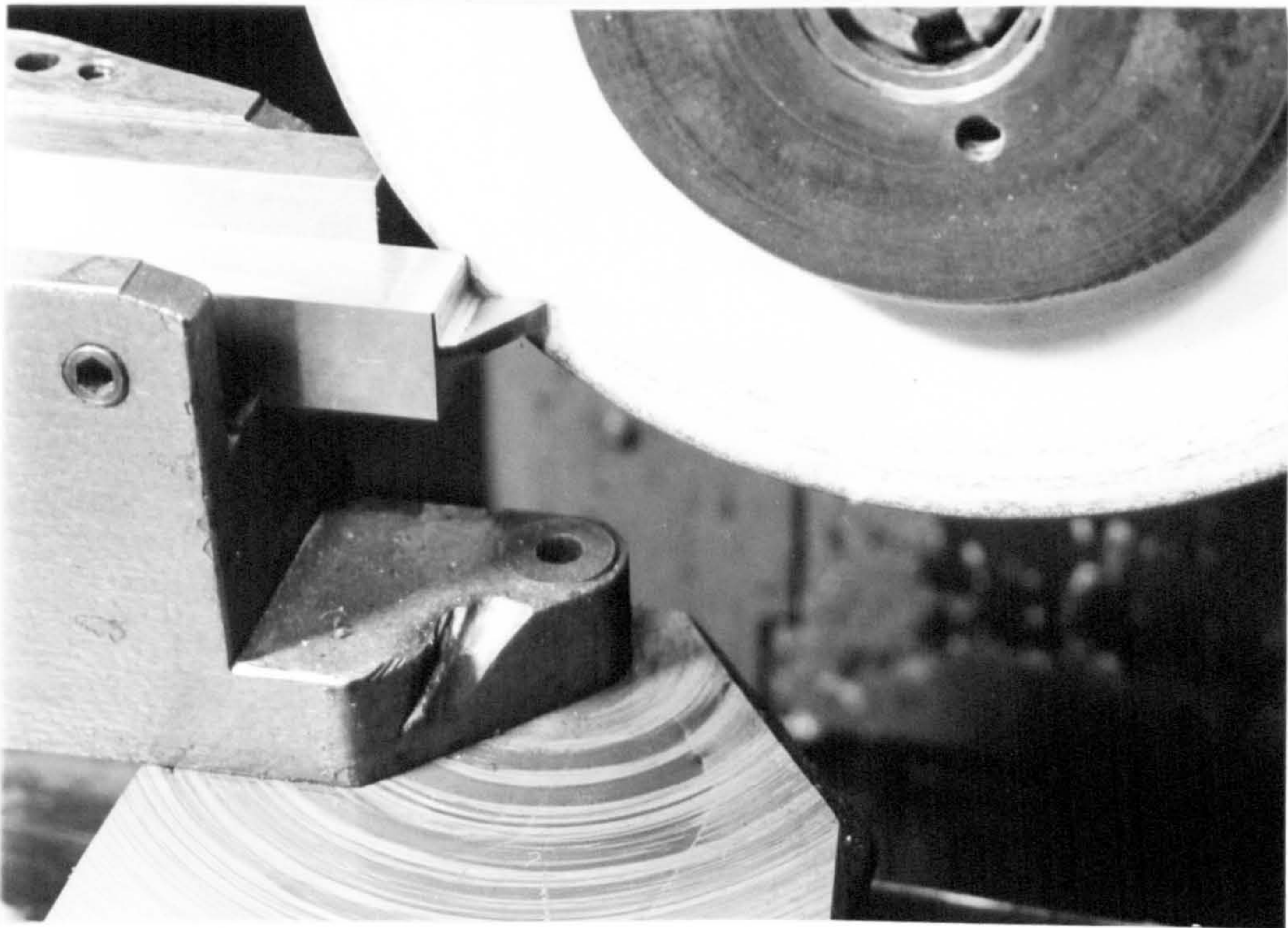


FIG.63 ESSENTIAL FEATURES OF RADIUS GRINDING JIG

(A)



(B)

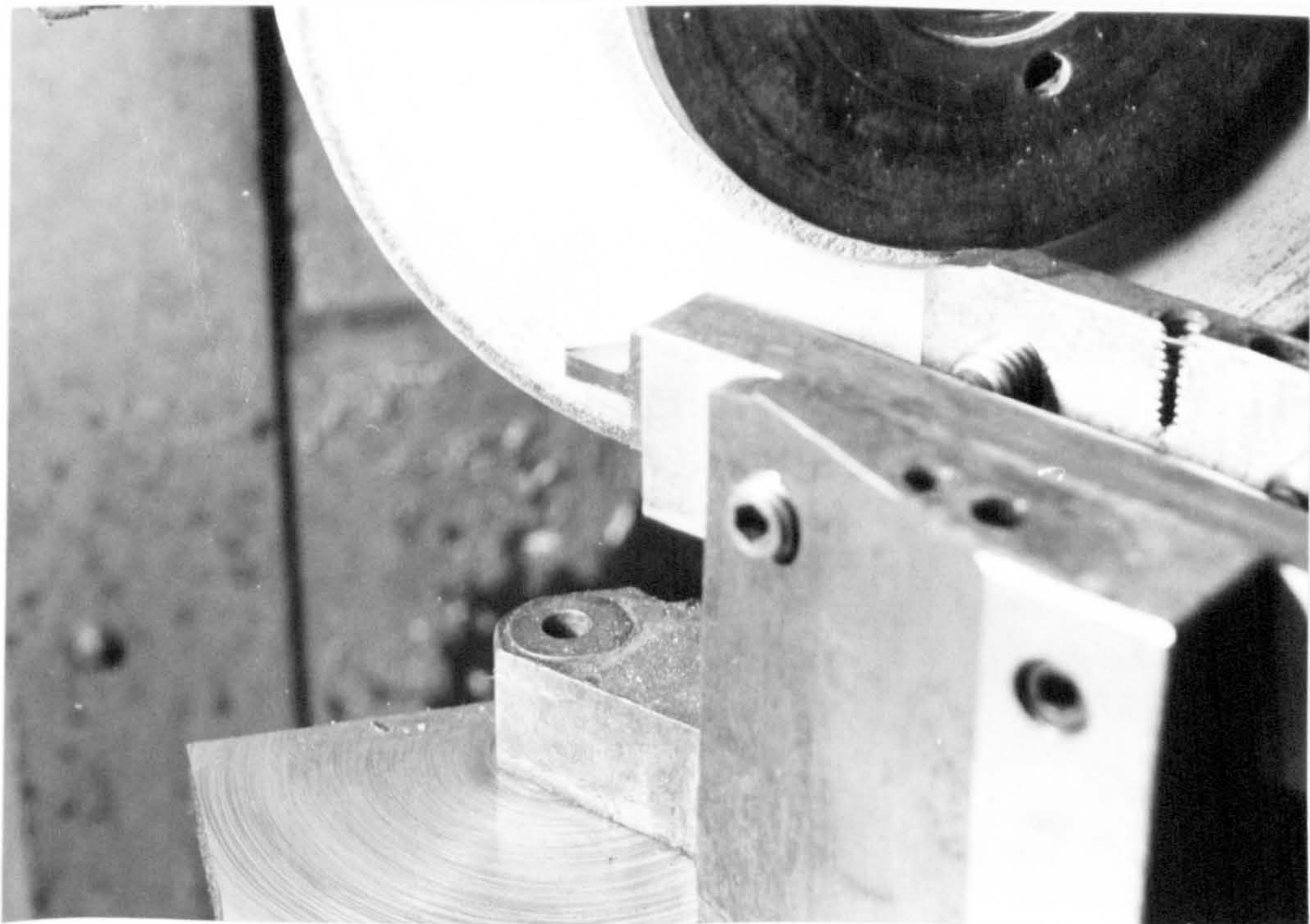
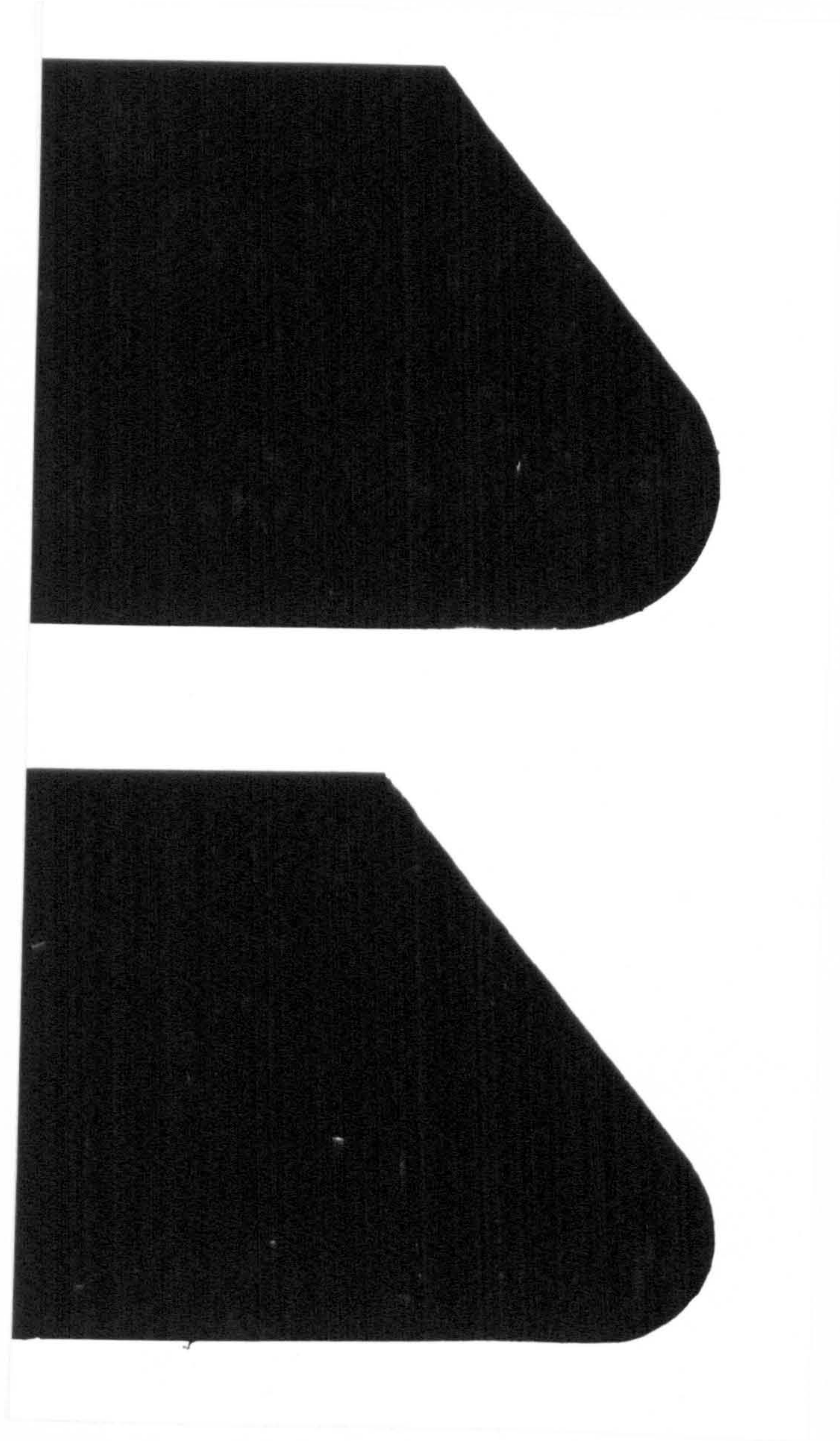


FIG.64 CLOSE-UP VIEWS WHEN GRINDING THE FACE AND FLANK OF THE TOOL



(A)

(B)

FIG. 65 SHADOGRAPHS OF TOOL PROFILES (A) 0.56 MM EDGE RADIUS
(B) 0.81 MM EDGE RADIUS

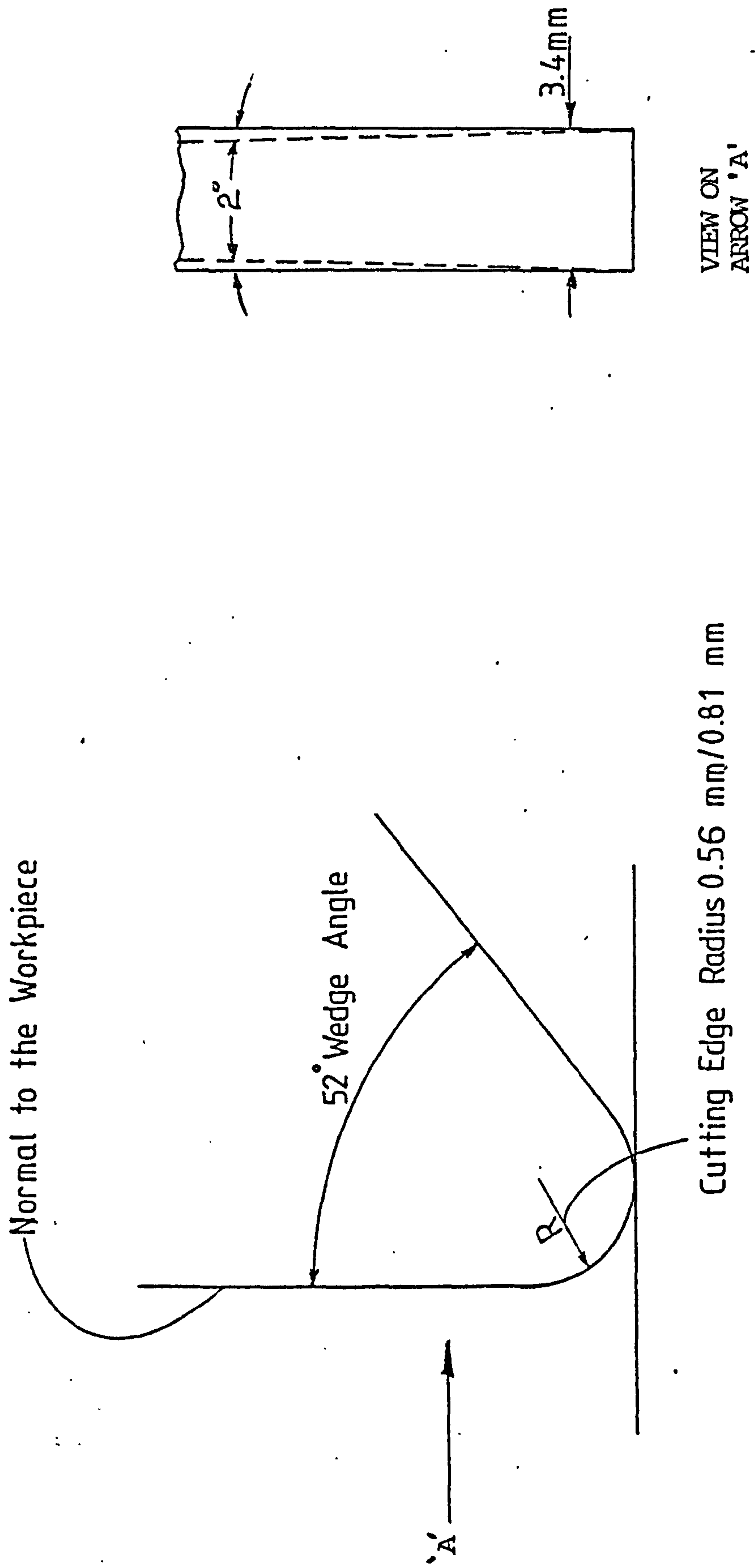


FIG. 65(c): Tool cutting edge geometry

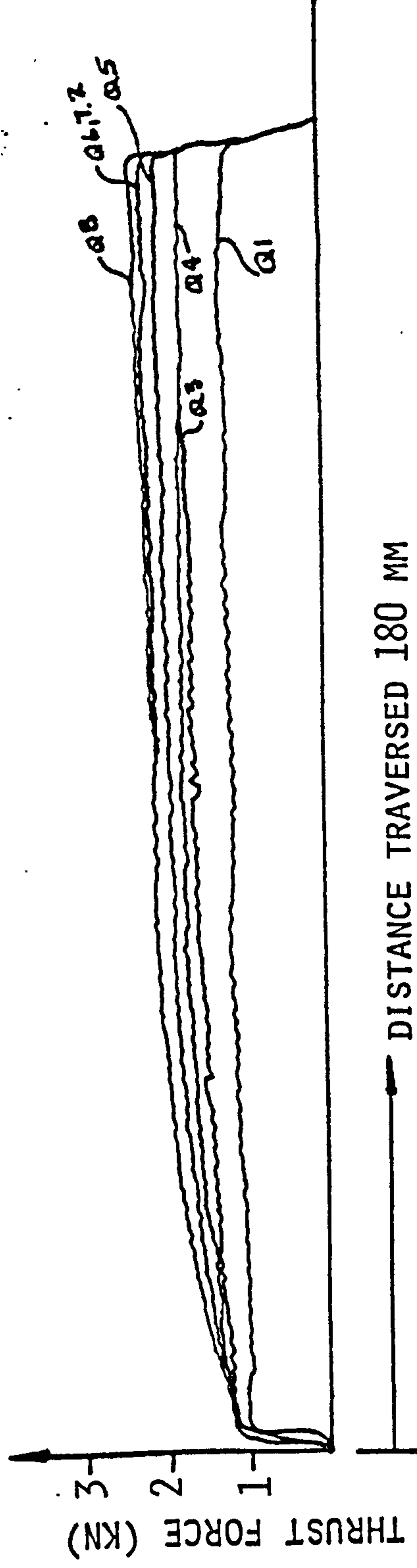
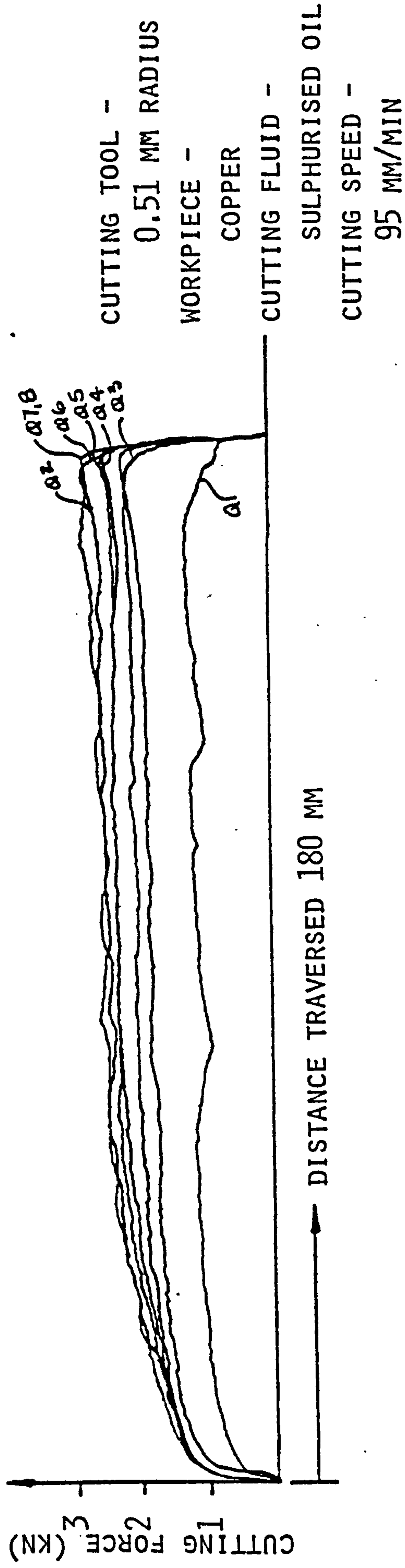
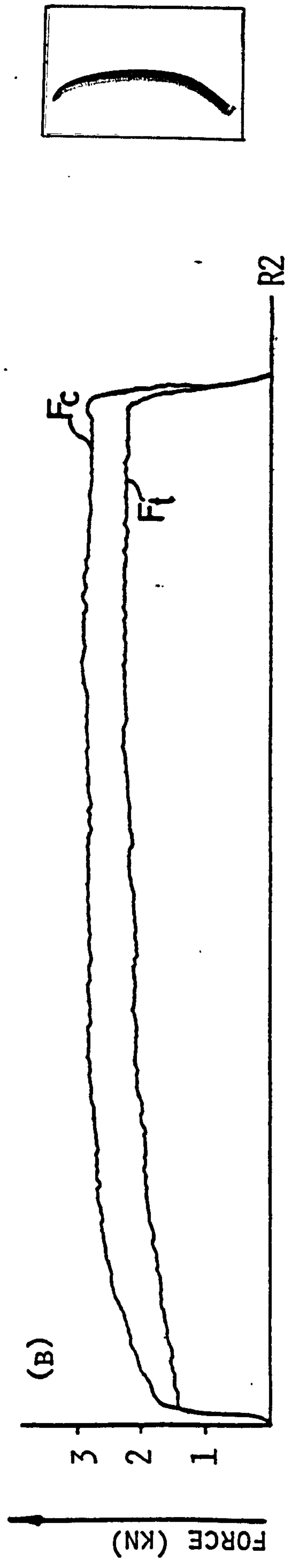
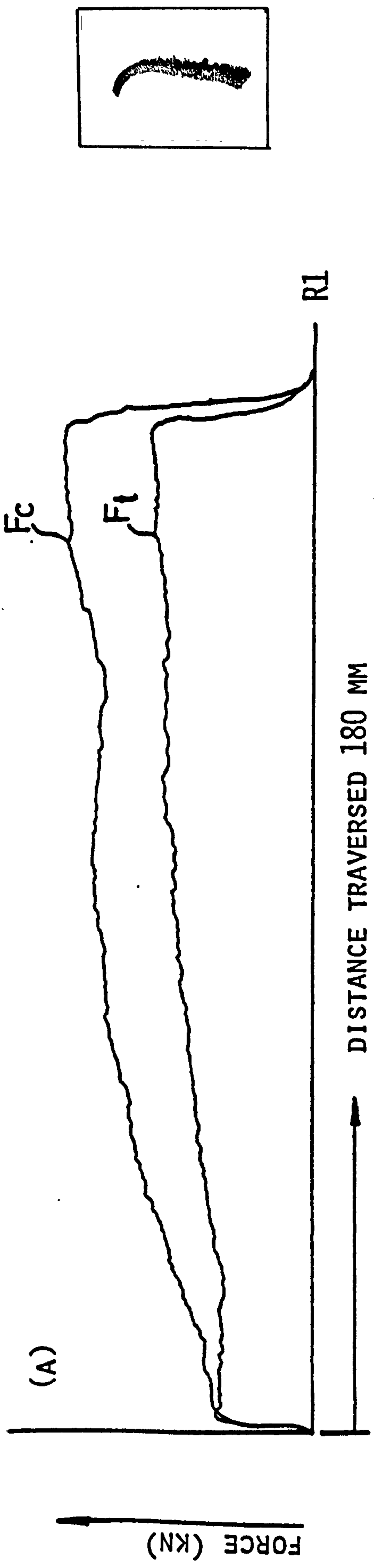


FIG.66 FORCES OBTAINED DURING GROOVE CUTTING FOR A CONSTANT NOMINAL DEPTH OF CUT (0.1 MM) USING A BLUNT TOOL



WORKPIECE:- COPPER
 CUTTING FLUID:- SULPHURISED OIL
 CUTTING TOOL:- 0.51 mm RADIUS

FIG.67 FORCES OBTAINED DURING GROOVE CUTTING FOR A CONSTANT NOMINAL DEPTH OF CUT (0.25 mm) USING A BLUNT TOOL

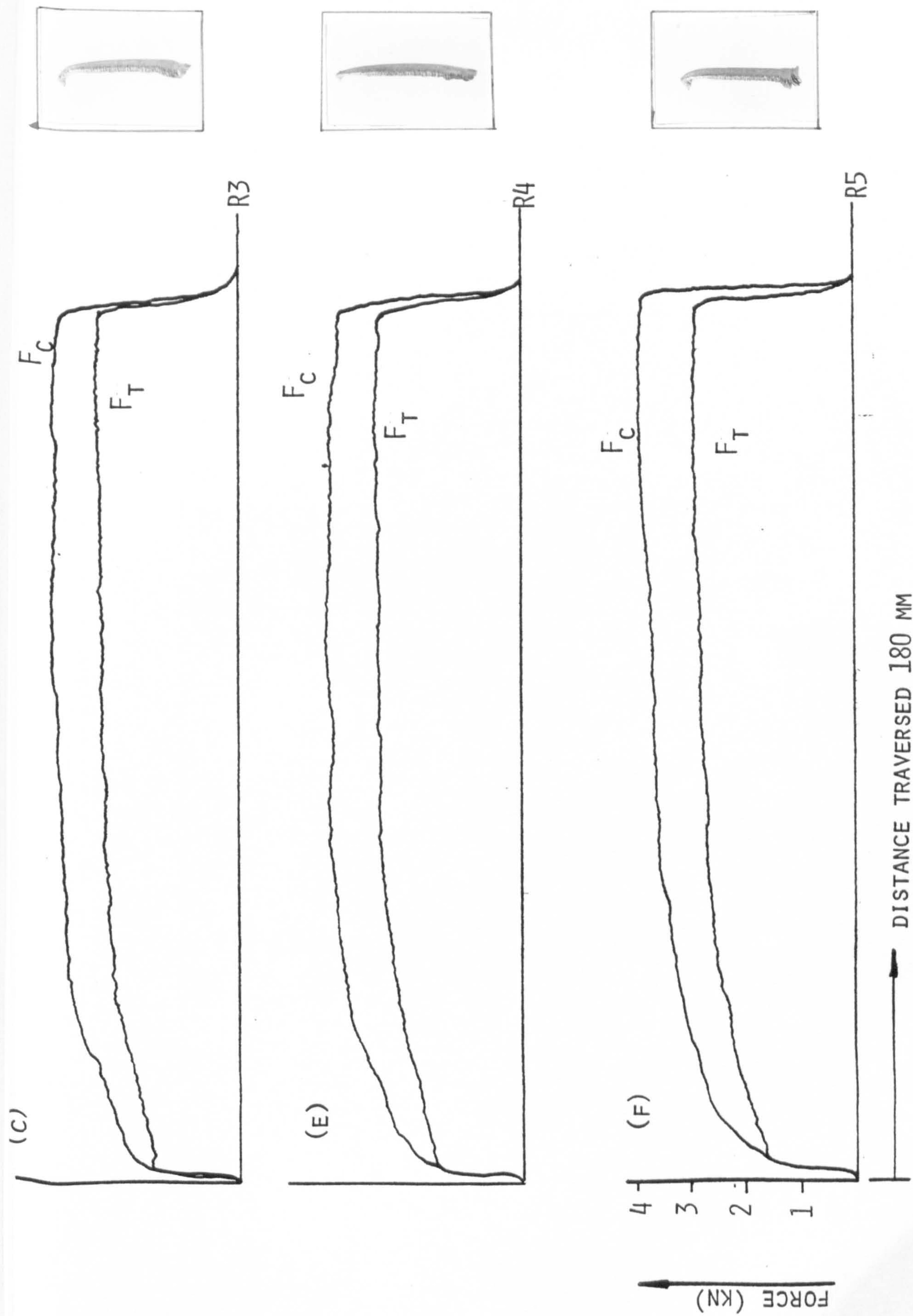


Fig.67

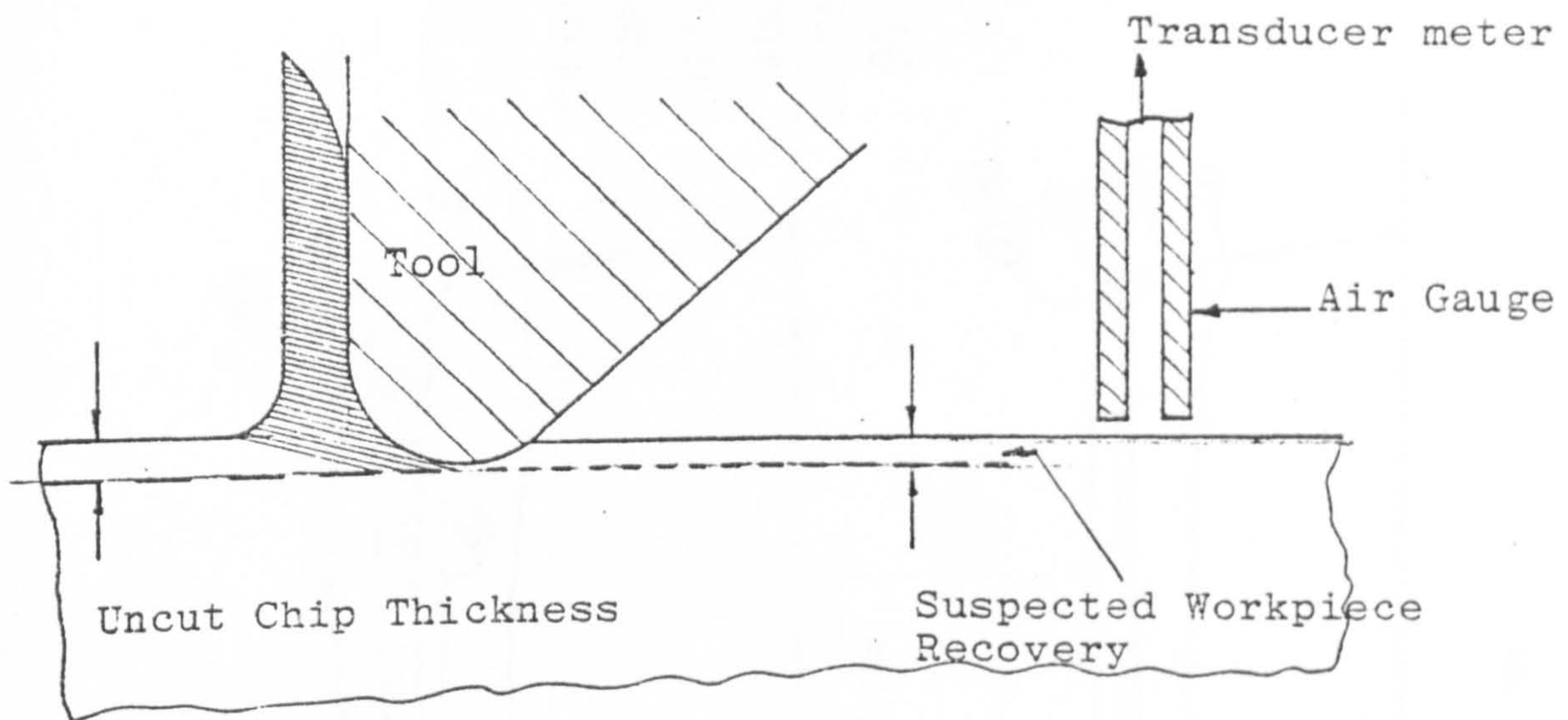


FIG.68(A) MEASUREMENT OF WORKPIECE RECOVERY

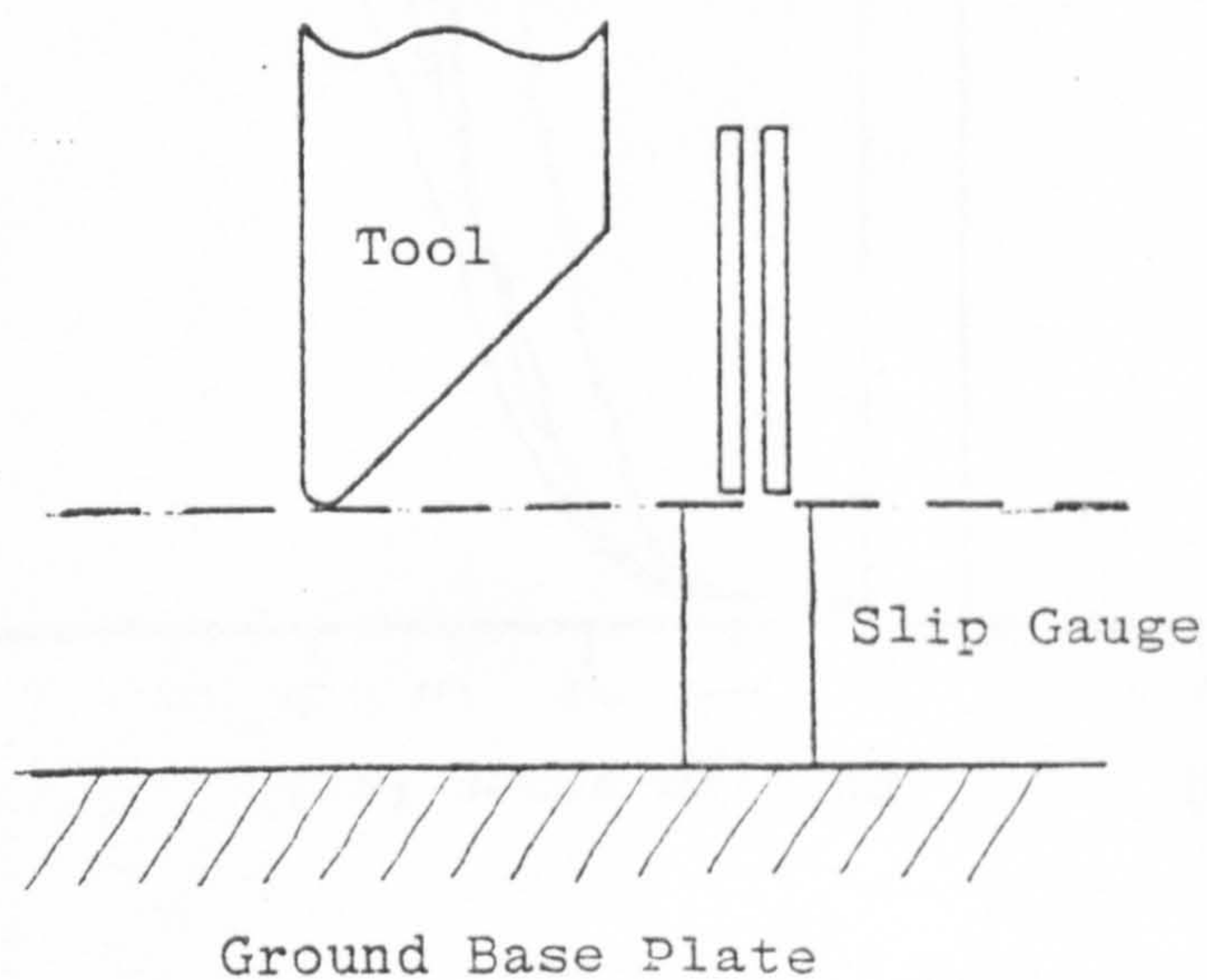


FIG.68(B) INITIAL SETTING-UP OF TOOL AND AIR GAUGE

0 - DENOTES TEST SEQUENCE

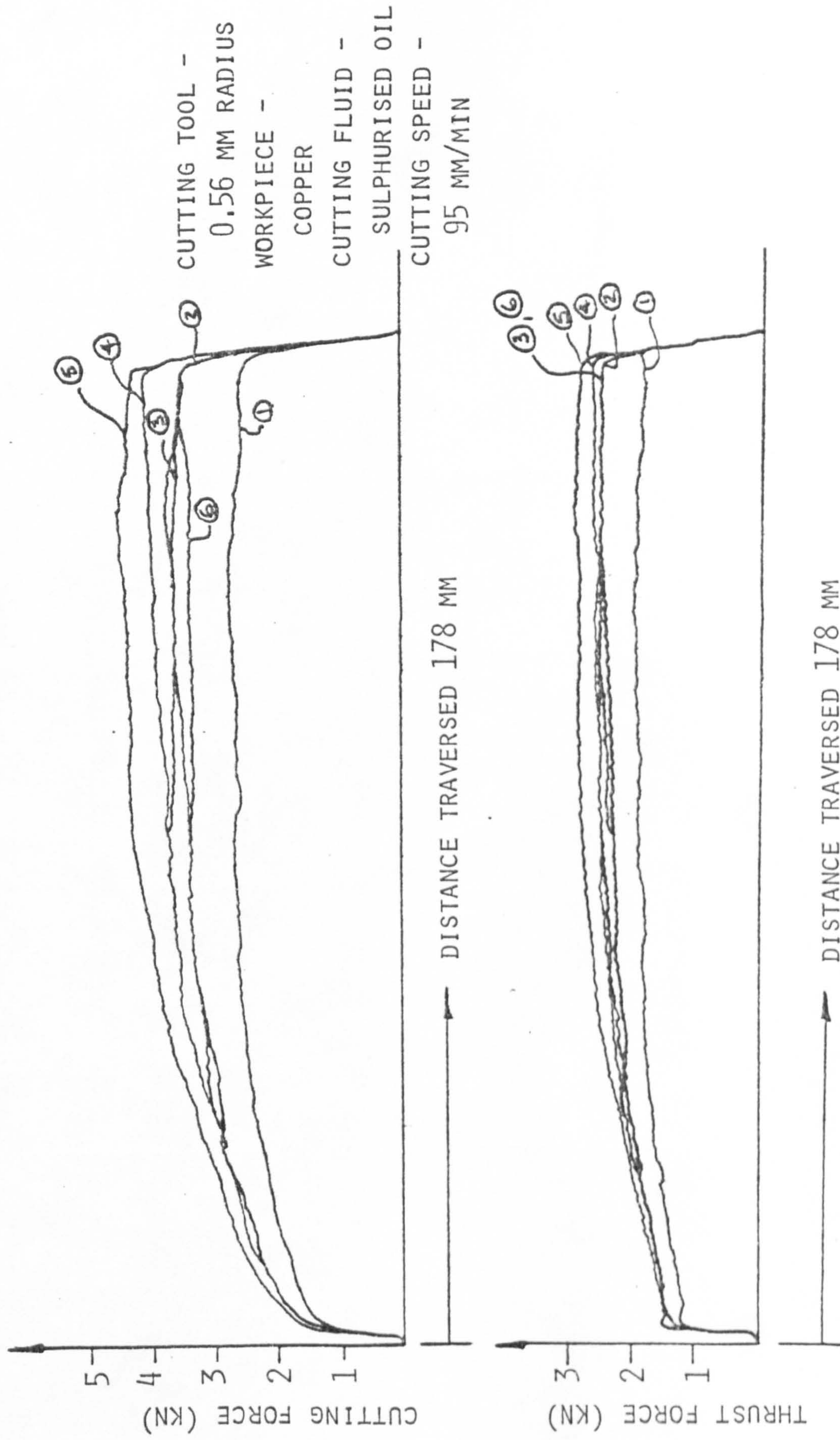


Fig.69(A) FORCES OBTAINED DURING GROOVE CUTTING FOR A CONSTANT NOMINAL DEPTH OF CUT (0.2 MM) USING A BLUNT TOOL



①



②



③



④



⑤



⑥

FIG.69(B) PHOTOGRAPHS OF CHIPS RELATING TO FIG.69(A) INDICATED BY ○

FIG. 70(a): Variation of chip-tool contact length with increased depth of cut for two different types of chip

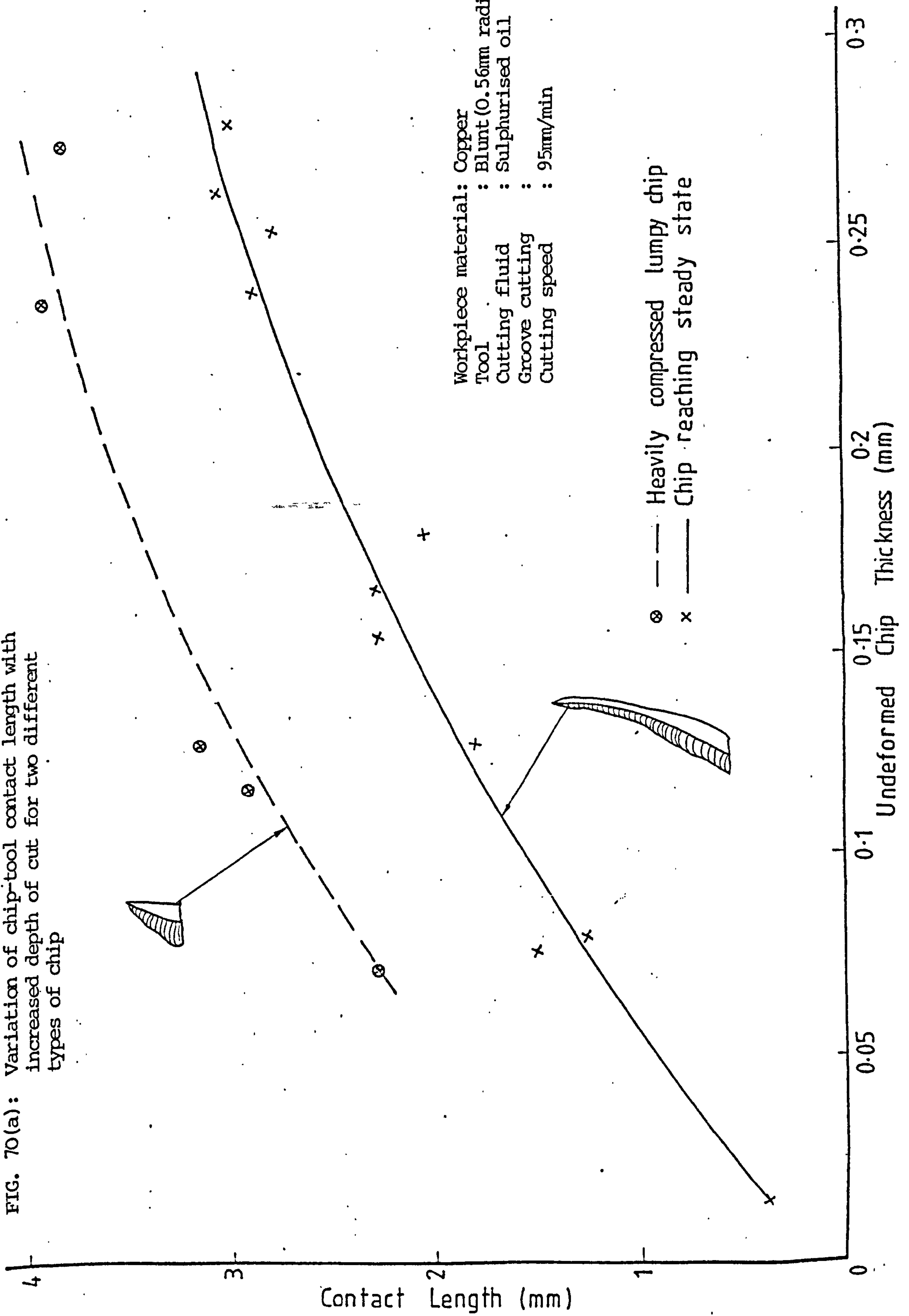


Fig.70(a)

FIG. 70(b): Variation of chip-tooth contact length with increased depth of cut

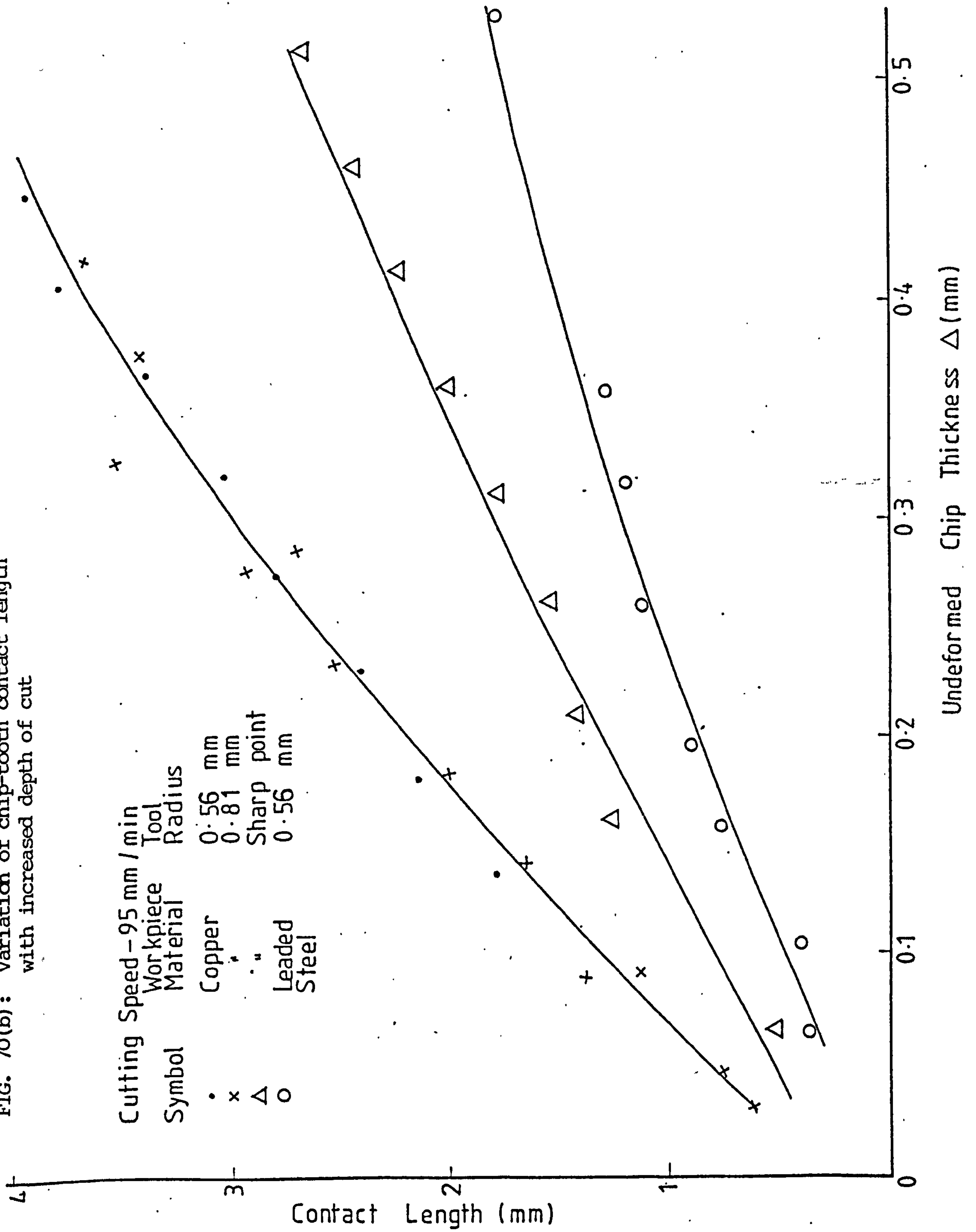


Fig. 70(b)

CUTTING SPEED : 95 mm / MIN
 WORKPIECE MATERIAL : LEADED STEEL
 TOOL BLUNT + - 0.56 mm EDGE RADIUS
 O - 0.81 mm EDGE RADIUS
 GROOVE CUTTING:
 CUTTING FLUID : SULPHURISED OIL

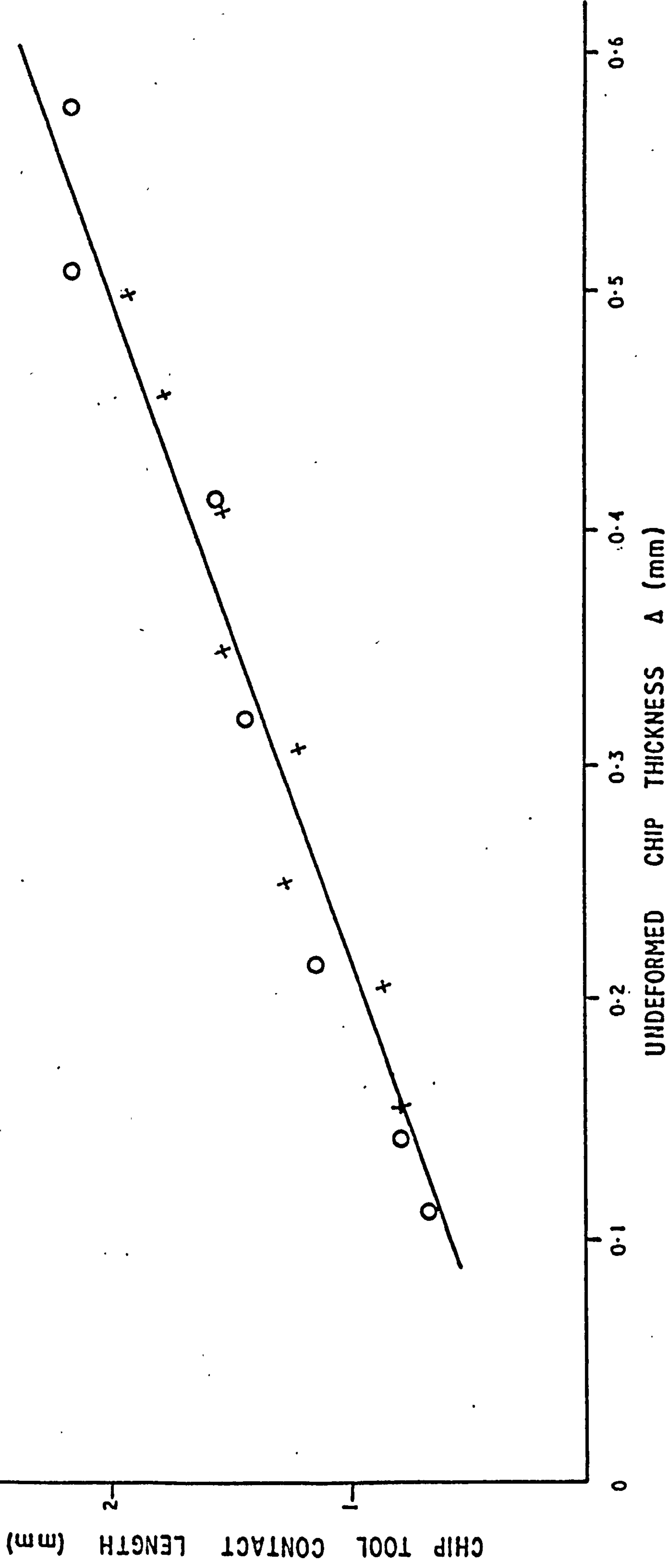
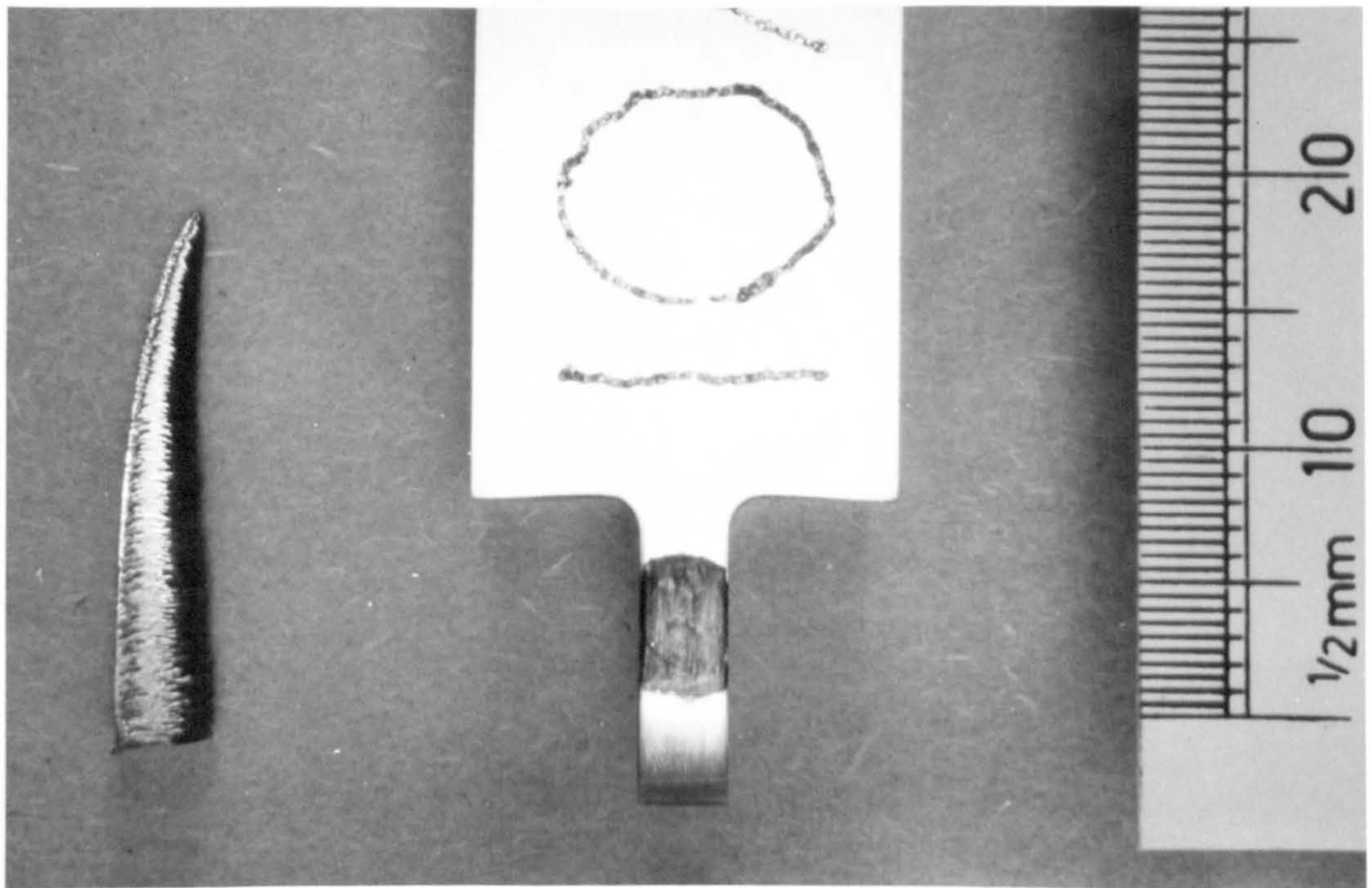


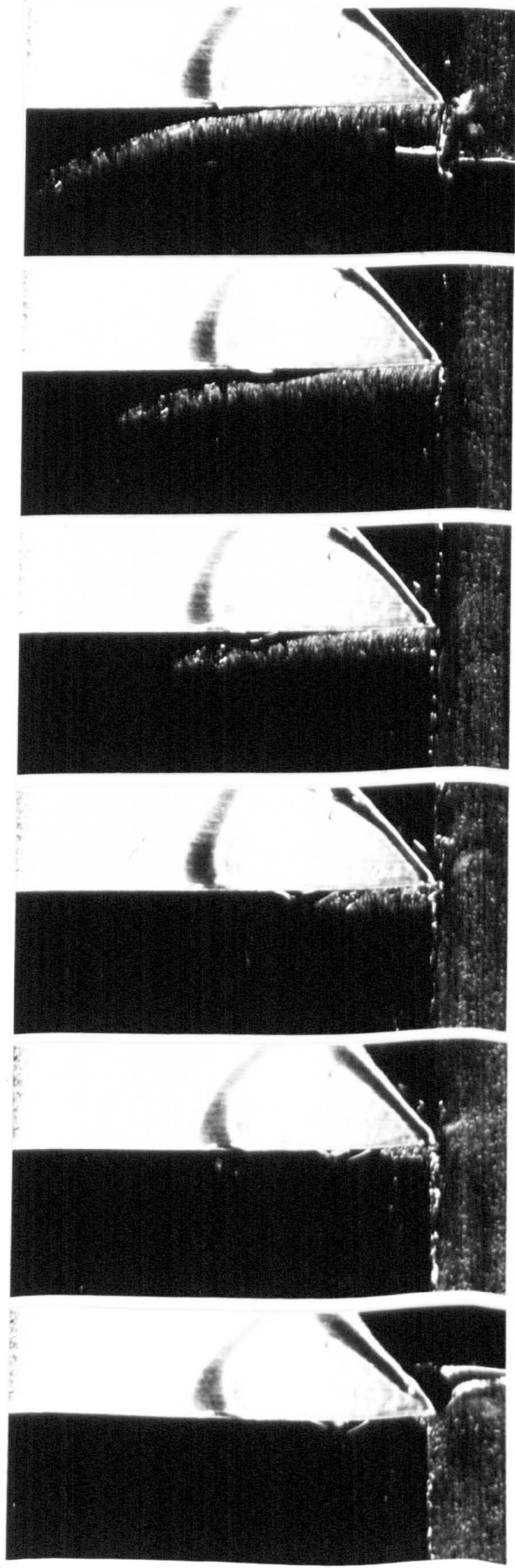
FIG. 70 (c) INFLUENCE OF CUTTING EDGE RADIUS ON THE CHIP TOOL CONTACT LENGTH.



NOMINAL DEPTH OF CUT: 0.5 mm
CUTTING EDGE RADIUS: 0.81 mm
CONTACT LENGTH: 3.81 mm
WORKPIECE MATERIAL: COPPER
CUTTING SPEED: 95 mm/min

FIG.70(d) TOOL-CHIP CONTACT LENGTH AND THE APPROPRIATE CHIP

(A)
SHARP
TOOL



(B)
BLUNT
TOOL

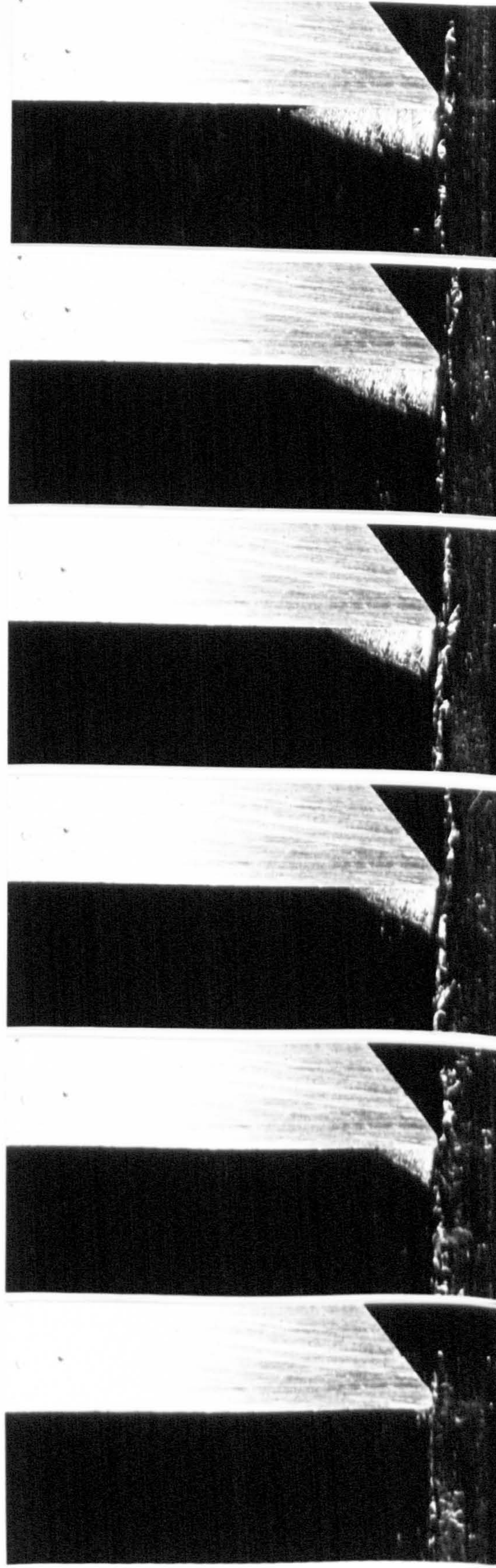


FIG.71 THE CHIP FORMATION AT VARIOUS POSITIONS ALONG THE LENGTH OF CUT



FIG.71(c) CHIP PRODUCED WHEN MACHINING
COPPER WITH A SHARP TOOL.
NOMINAL SET DEPTH: 0.1 MM
CUTTING FLUID: SULPHURISED OIL
CUTTING SPEED: 95 MM/MIN

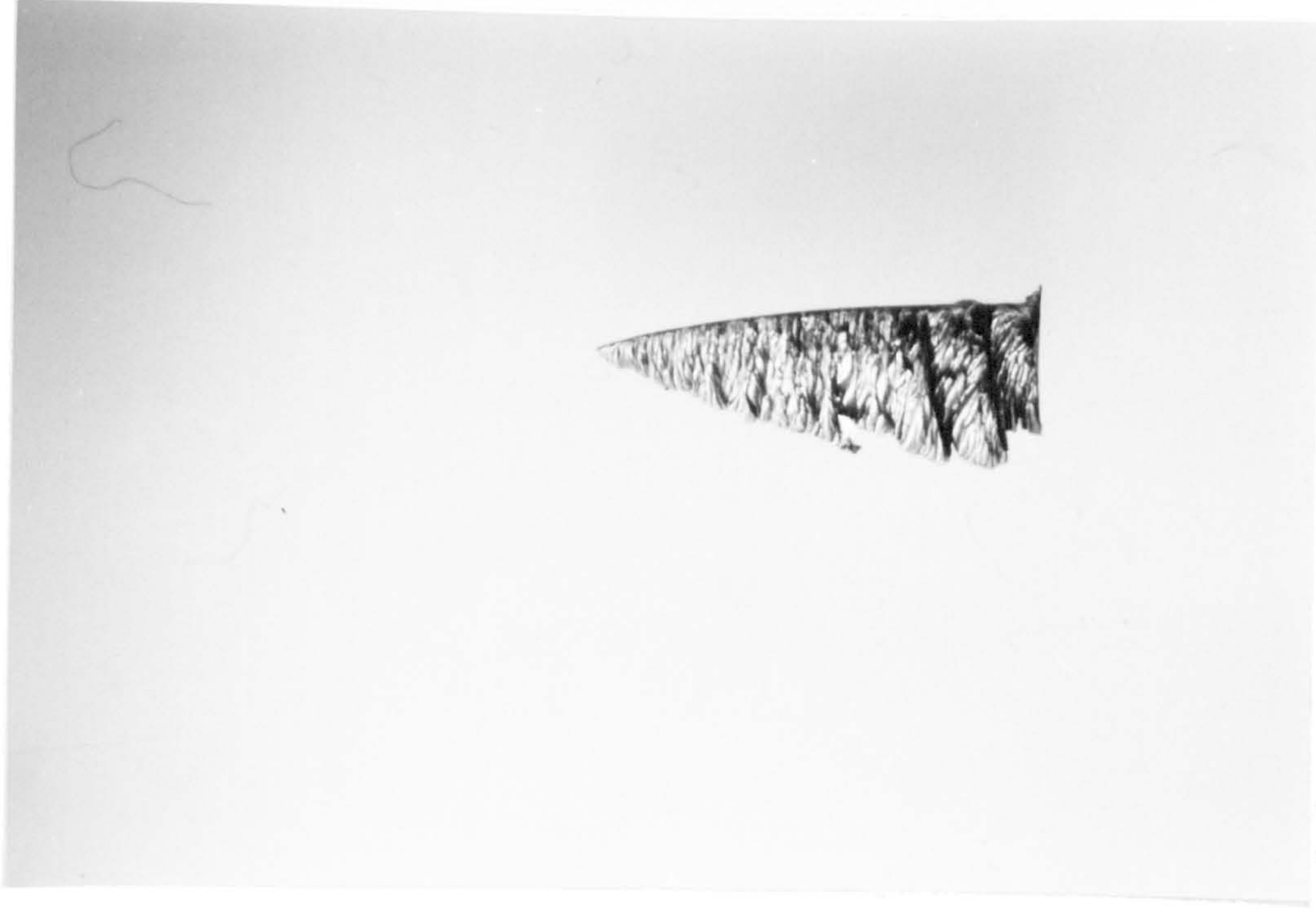
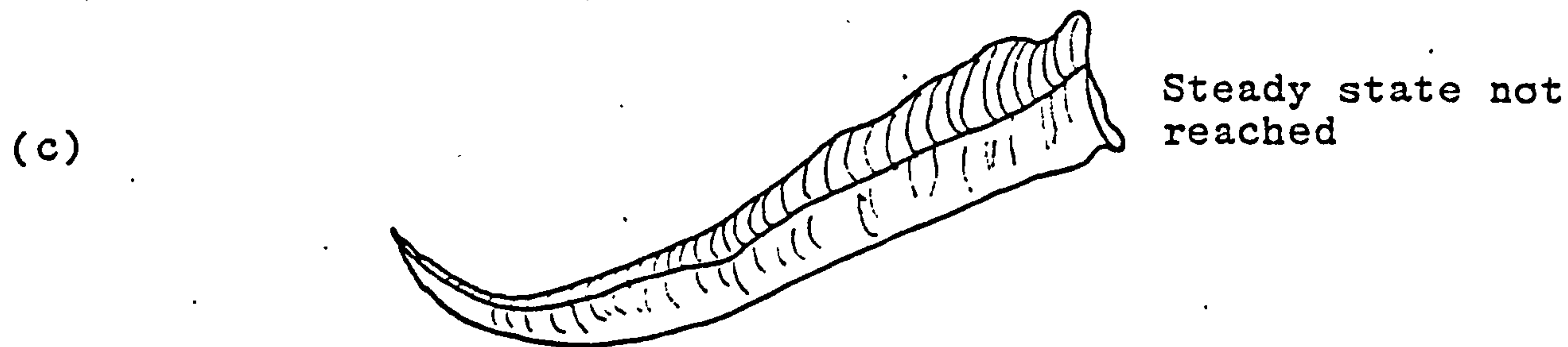
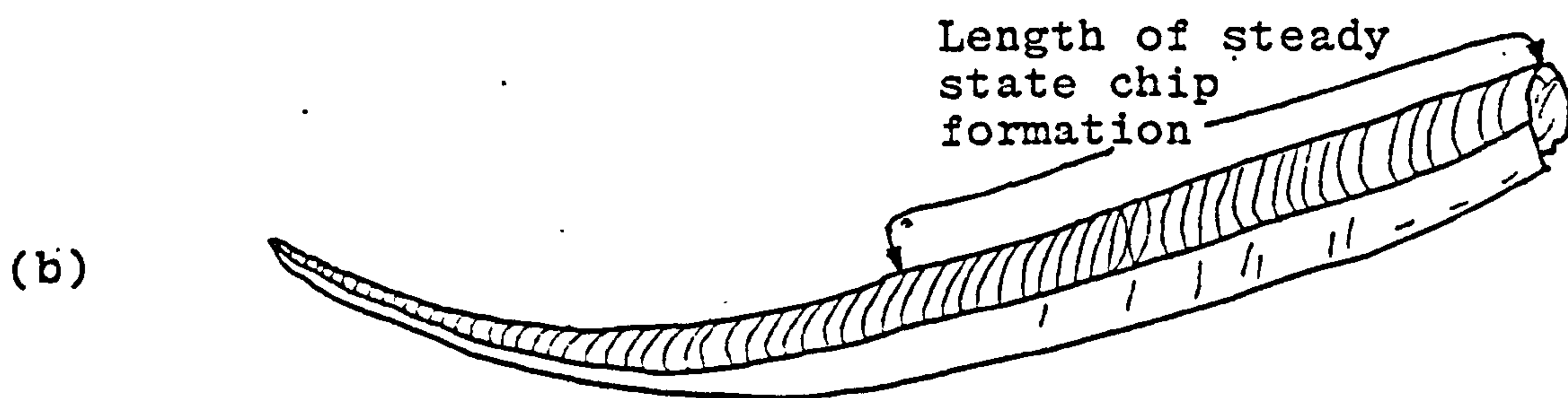
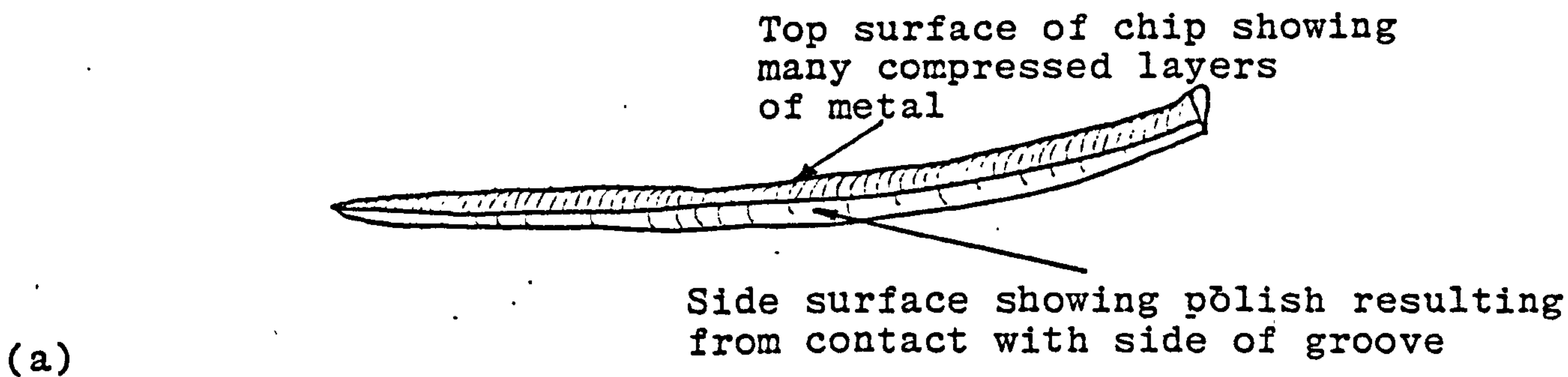


FIG.71(d) CHIP PRODUCED WHEN MACHINING
COPPER WITH A BLUNT TOOL. (0.56 MM
RADIUS)
CUTTING FLUID: SULPHURISED OIL
CUTTING SPEED: 95 MM/MIN



(d) Cross-section of chips

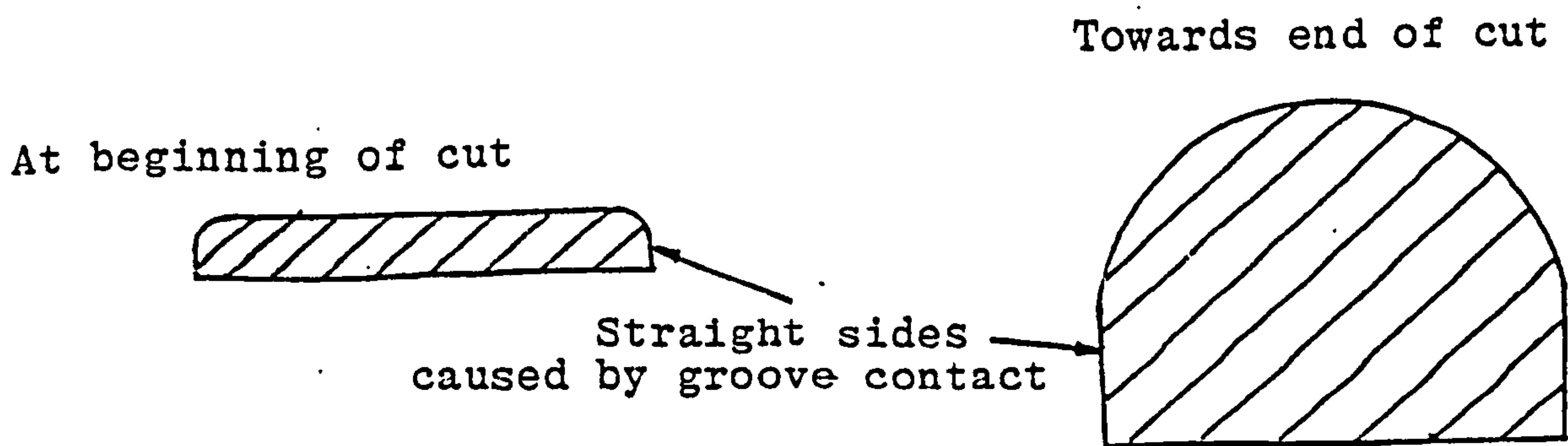


FIG.72 SOME FEATURES OF COPPER CHIPS PRODUCED DURING GROOVE CUTTING

TOOL

CHIP

CAP

WORKPIECE

TOOL

CHIP

RAKE
FACE



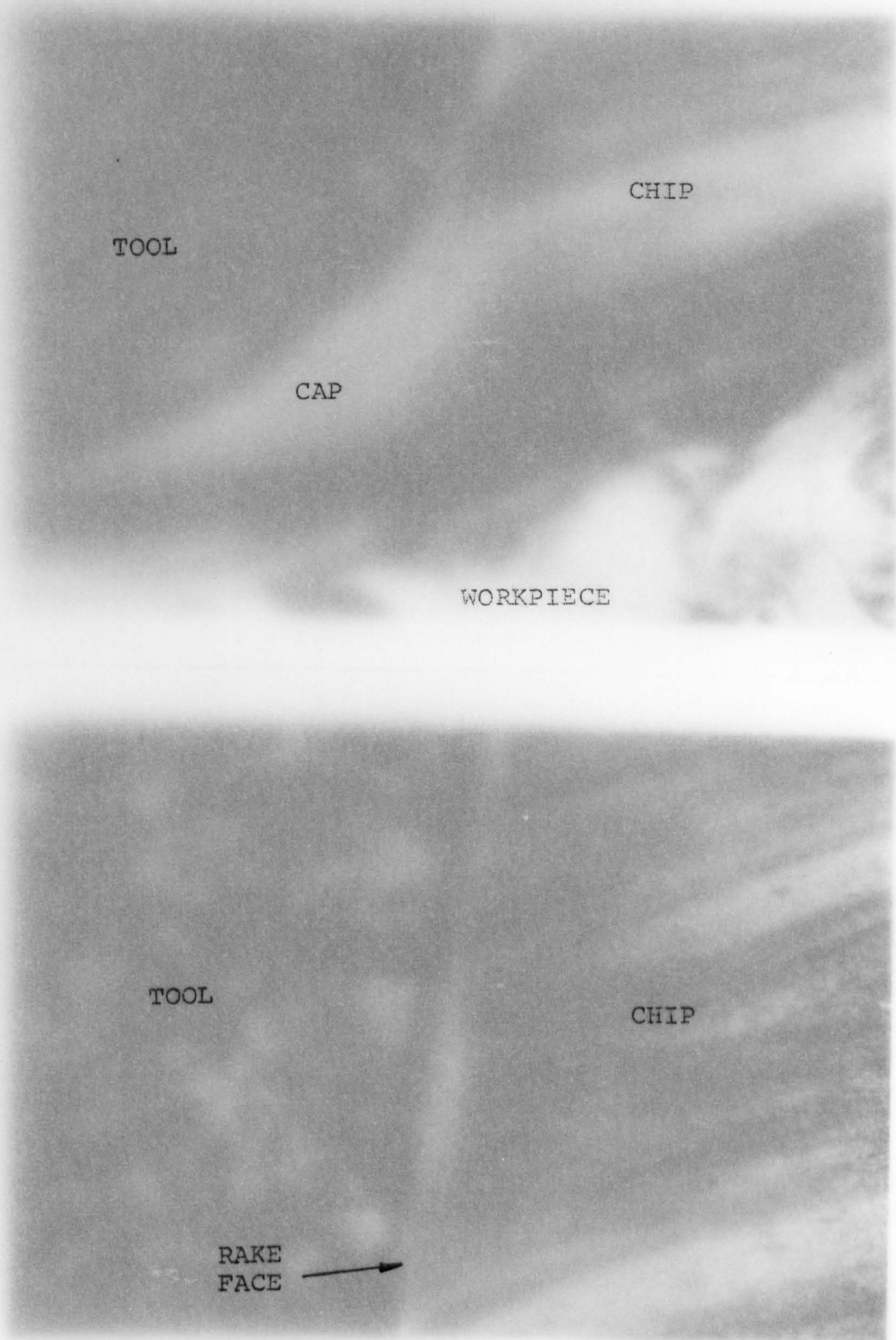


FIG. 73 PHOTOMICROGRAPHS OF QUICK STOPS (MAGNIFICATION X 16)
COPPER WORKPIECE, NOMINAL DEPTH: 0.25 MM
CUTTING FLUID: SULPHURISED OIL
CUTTING TOOL: 0.56 MM RADIUS

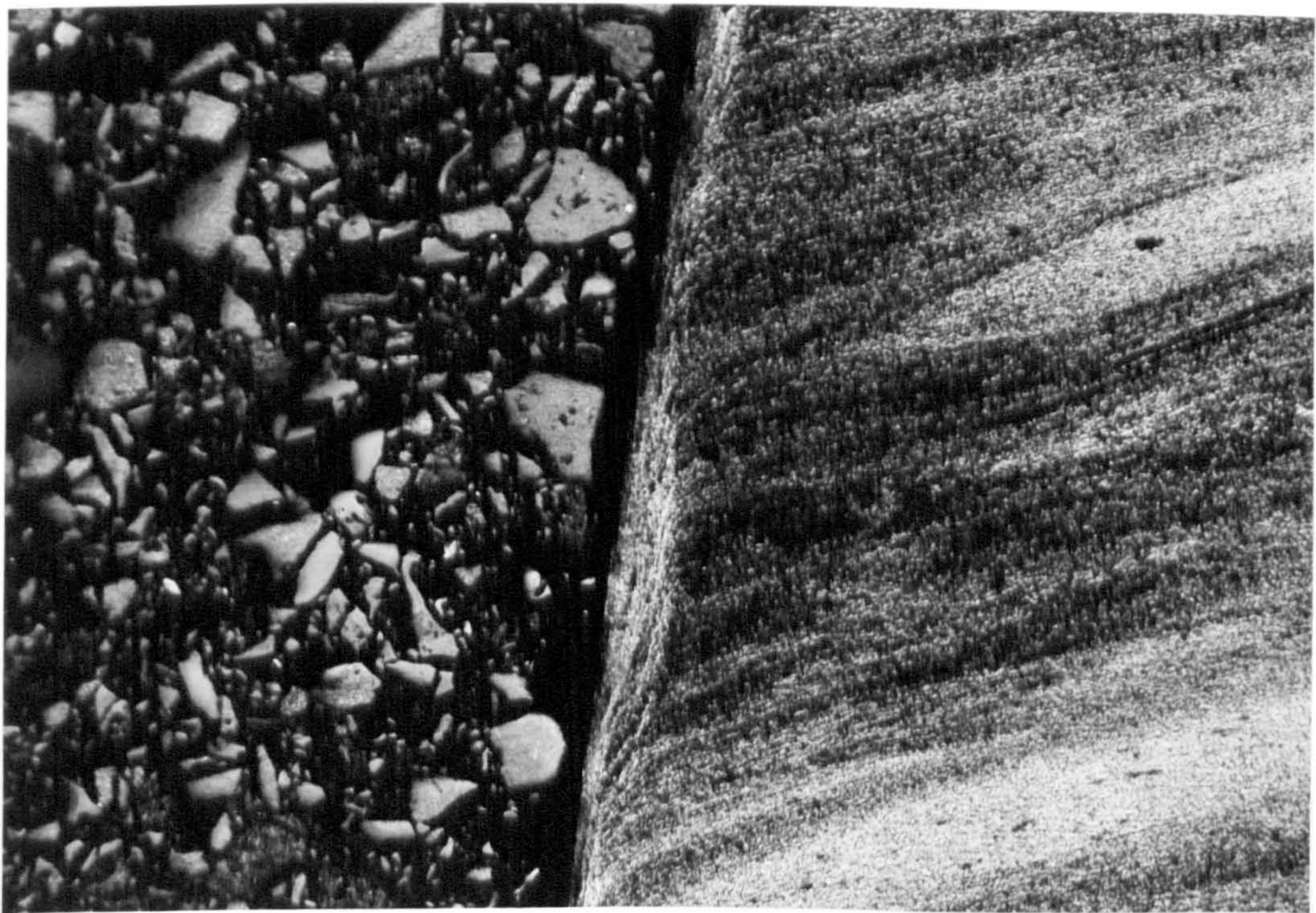
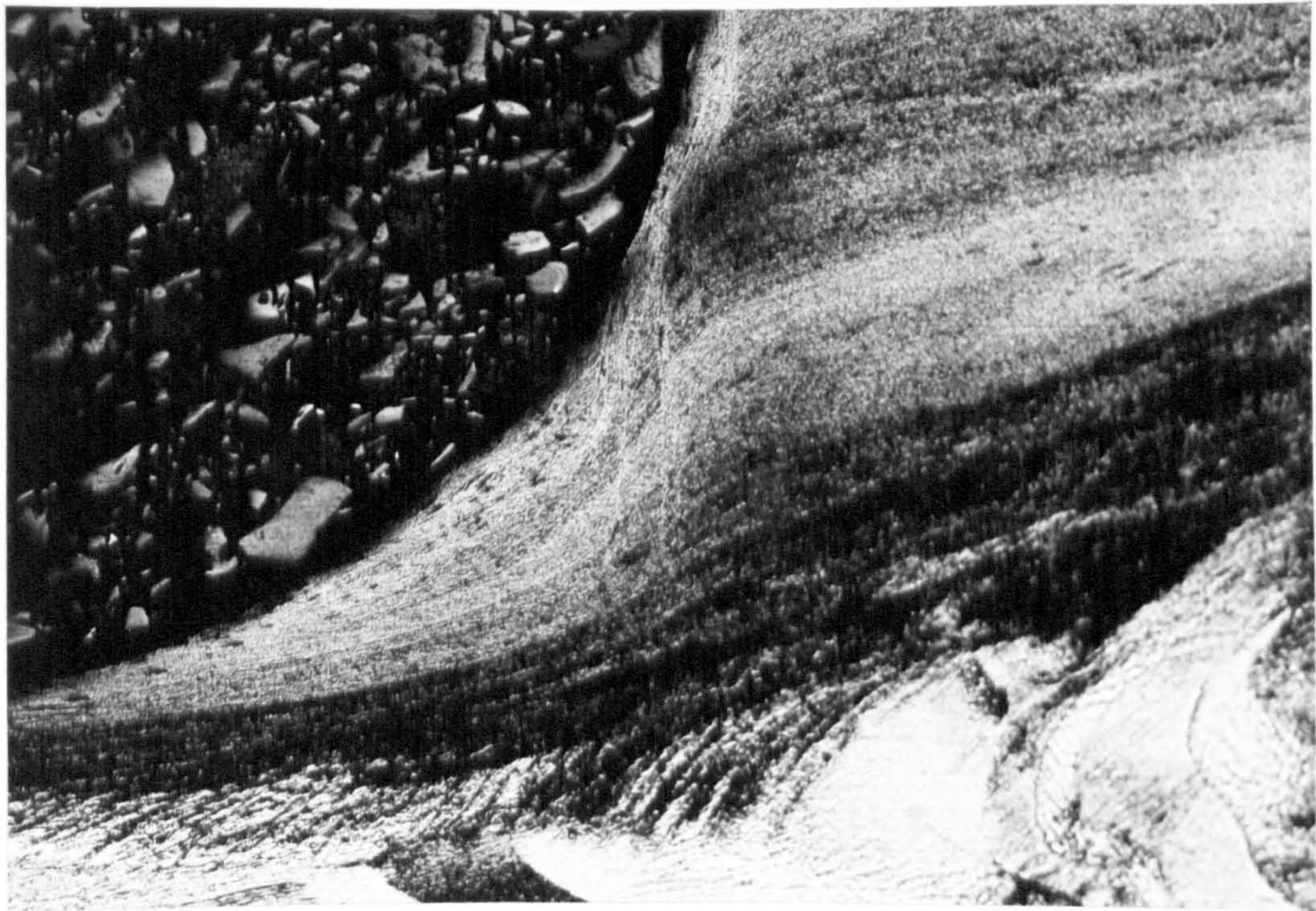
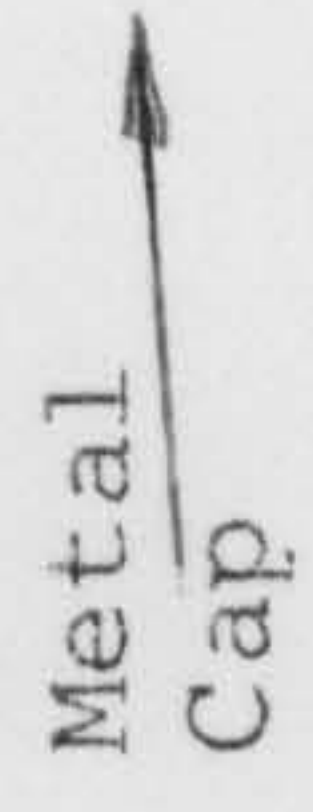


FIG.73 PHOTOMICROGRAPHS OF QUICK STOPS (MAGNIFICATION X 16)
COPPER WORKPIECE, NOMINAL DEPTH: 0.25 MM
CUTTING FLUID: SULPHURISED OIL
CUTTING TOOL: 0.56 MM RADIUS

Chip

Tool

Metal
Cap

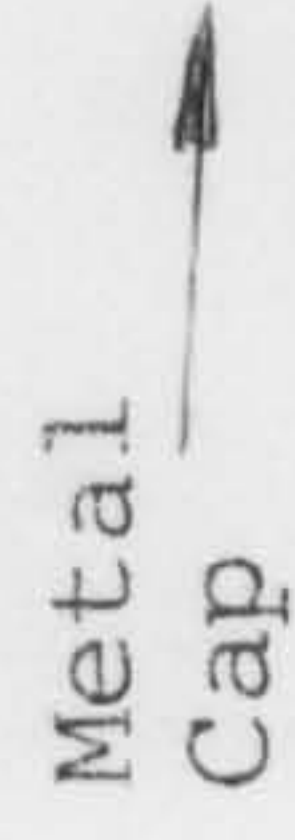


A horizontal line with an arrow pointing to the right, representing the direction of chip removal. The text 'Metal' is above the line and 'Cap' is below it.

Workpiece

Tool

Metal
Cap



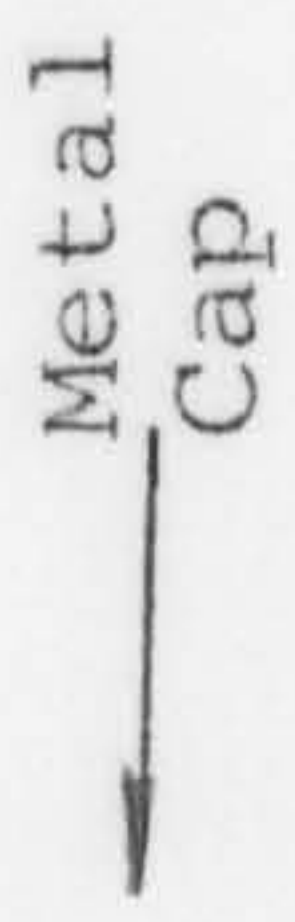
A horizontal line with an arrow pointing to the right, representing the direction of chip removal. The text 'Metal' is above the line and 'Cap' is below it.

Workpiece

Chip

Tool

Metal
Cap



A horizontal line with an arrow pointing to the right, representing the direction of chip removal. The text 'Metal' is above the line and 'Cap' is below it.

Workpiece

Tool

Metal
Cap

Workpiece

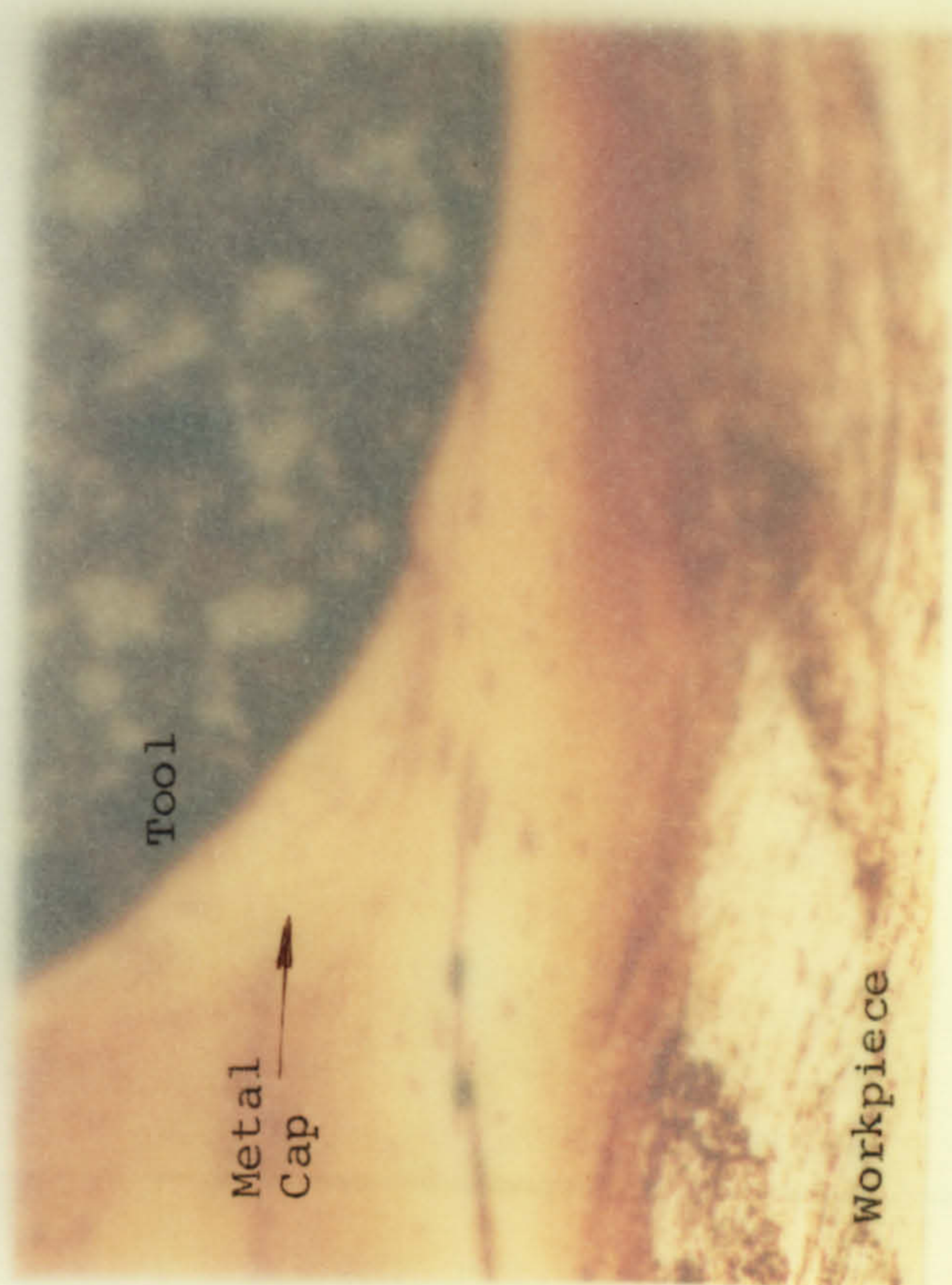
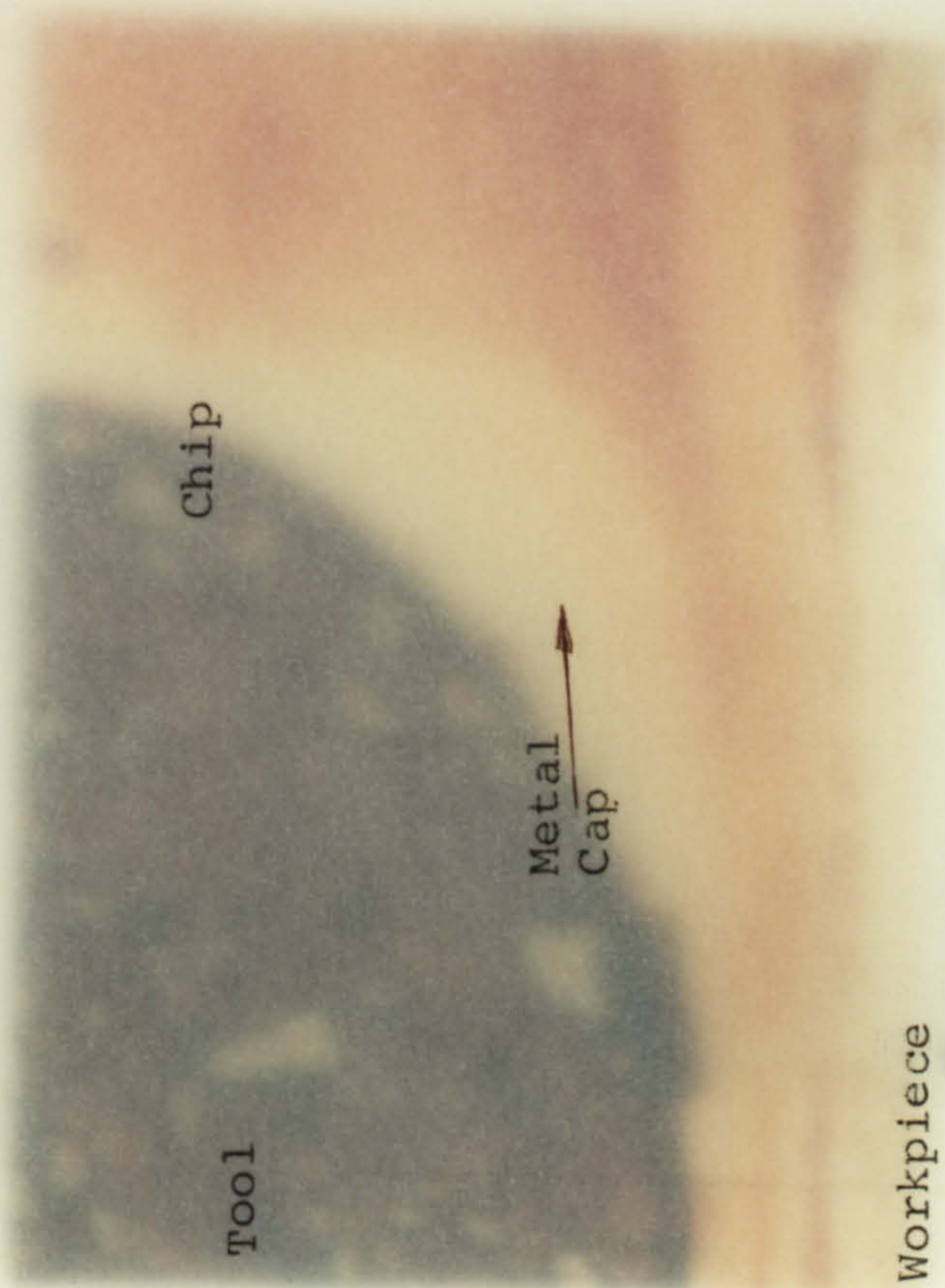
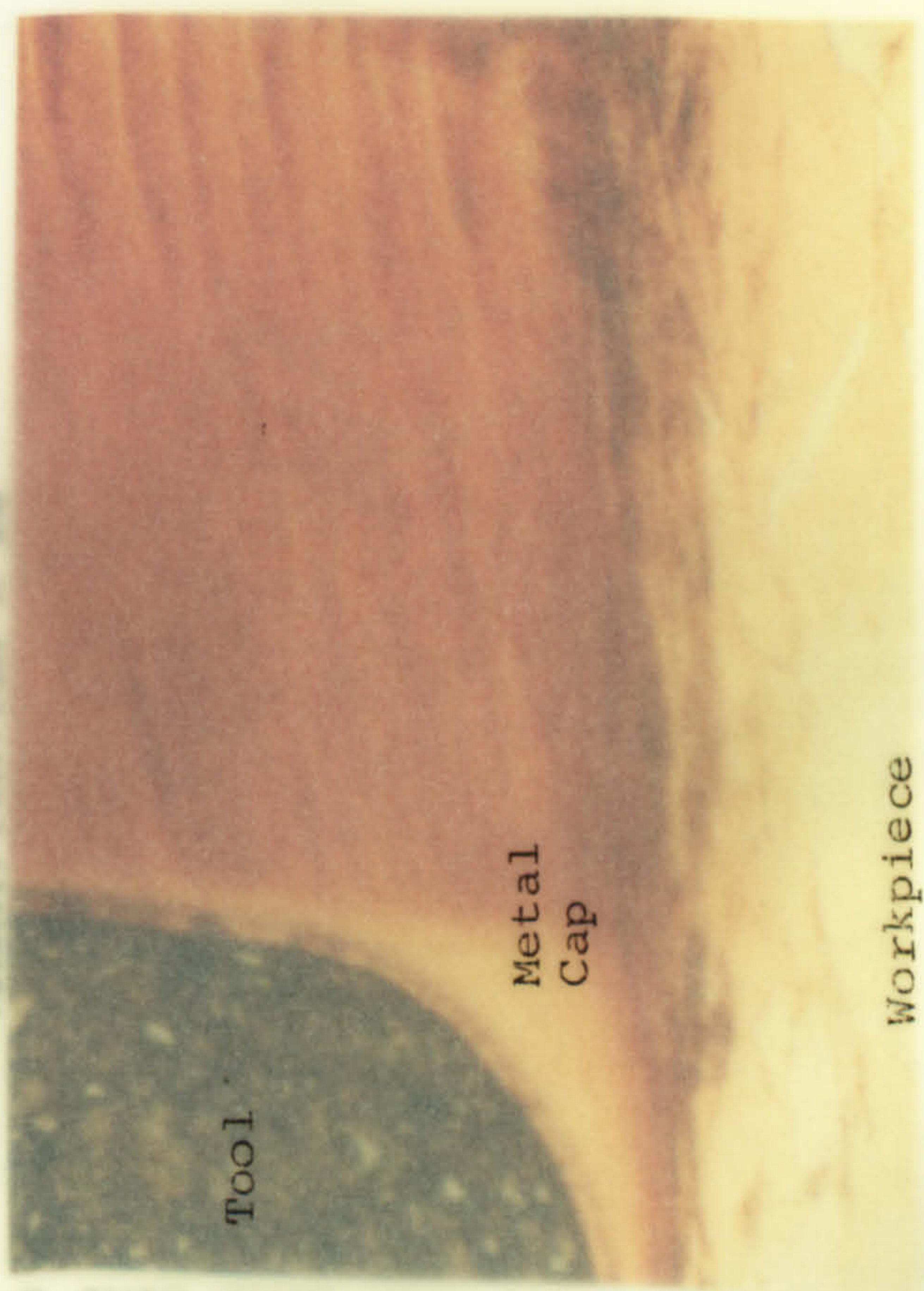
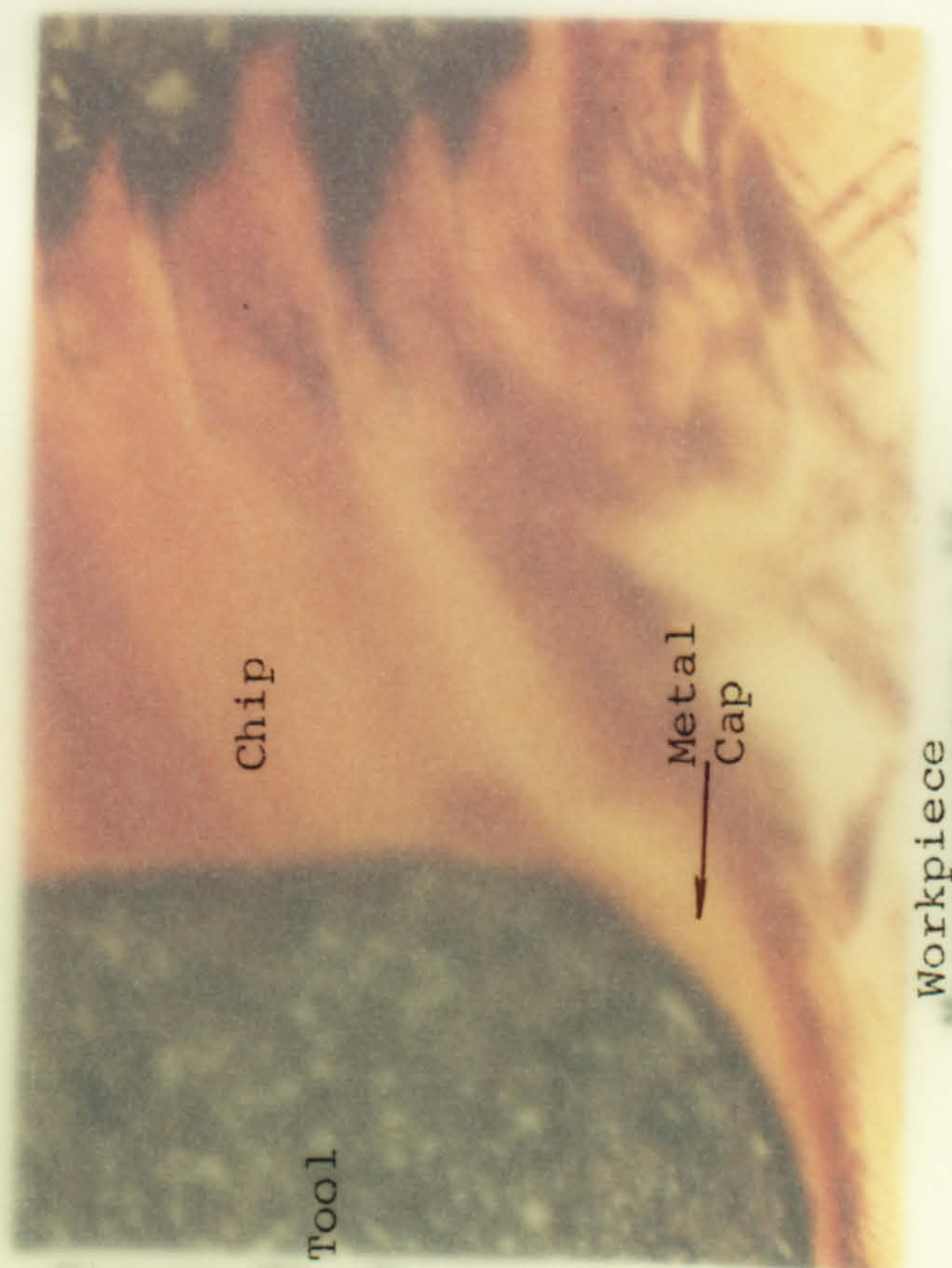
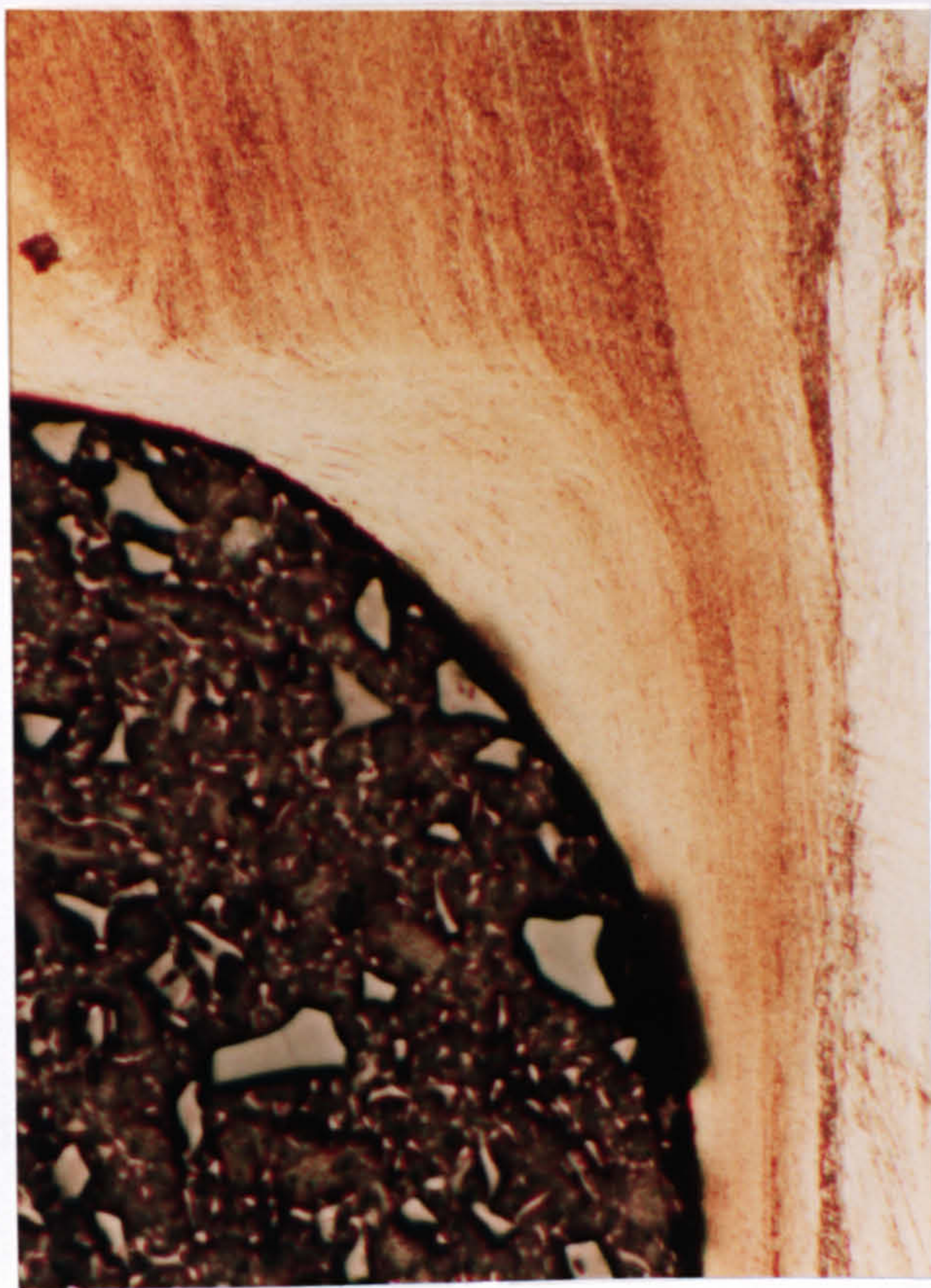
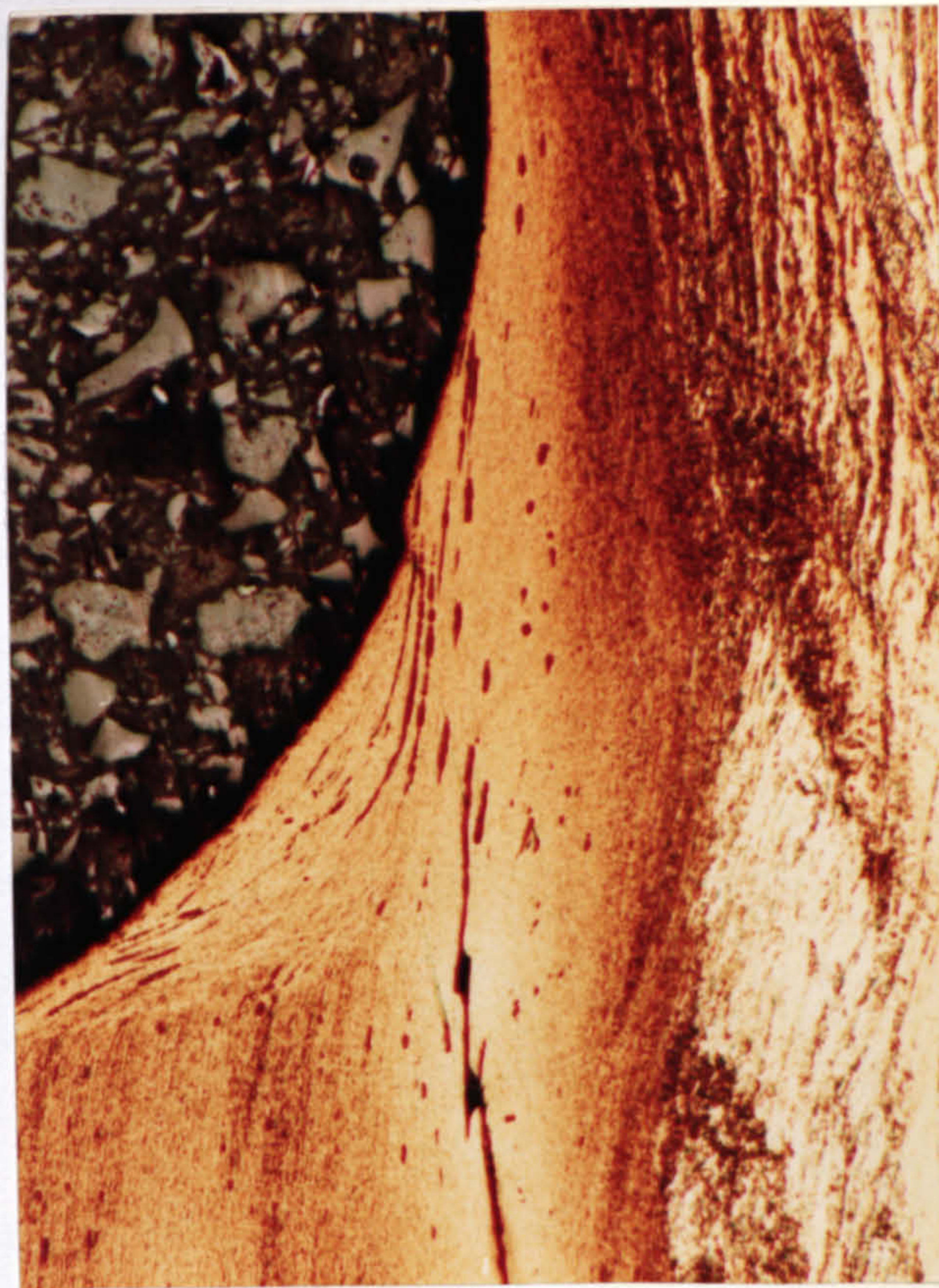


FIGURE 74 PHOTOMICROGRAPHS OF THE CHIP ROOT AREA WHEN CUTTING COPPER WITH BLUNT TOOLS (0.56 MM RADIUS) (NOMINAL SET DEPTH - 0.25 MM)



MAGNIFICATION X 32



MAGNIFICATION X 16



FIGURE 74 PHOTOMICROGRAPHS OF THE CHIP ROOT AREA WHEN CUTTING COPPER WITH BLUNT TOOLS (0.56 MM RADIUS) (NOMINAL SET DEPTH - 0.25 MM)

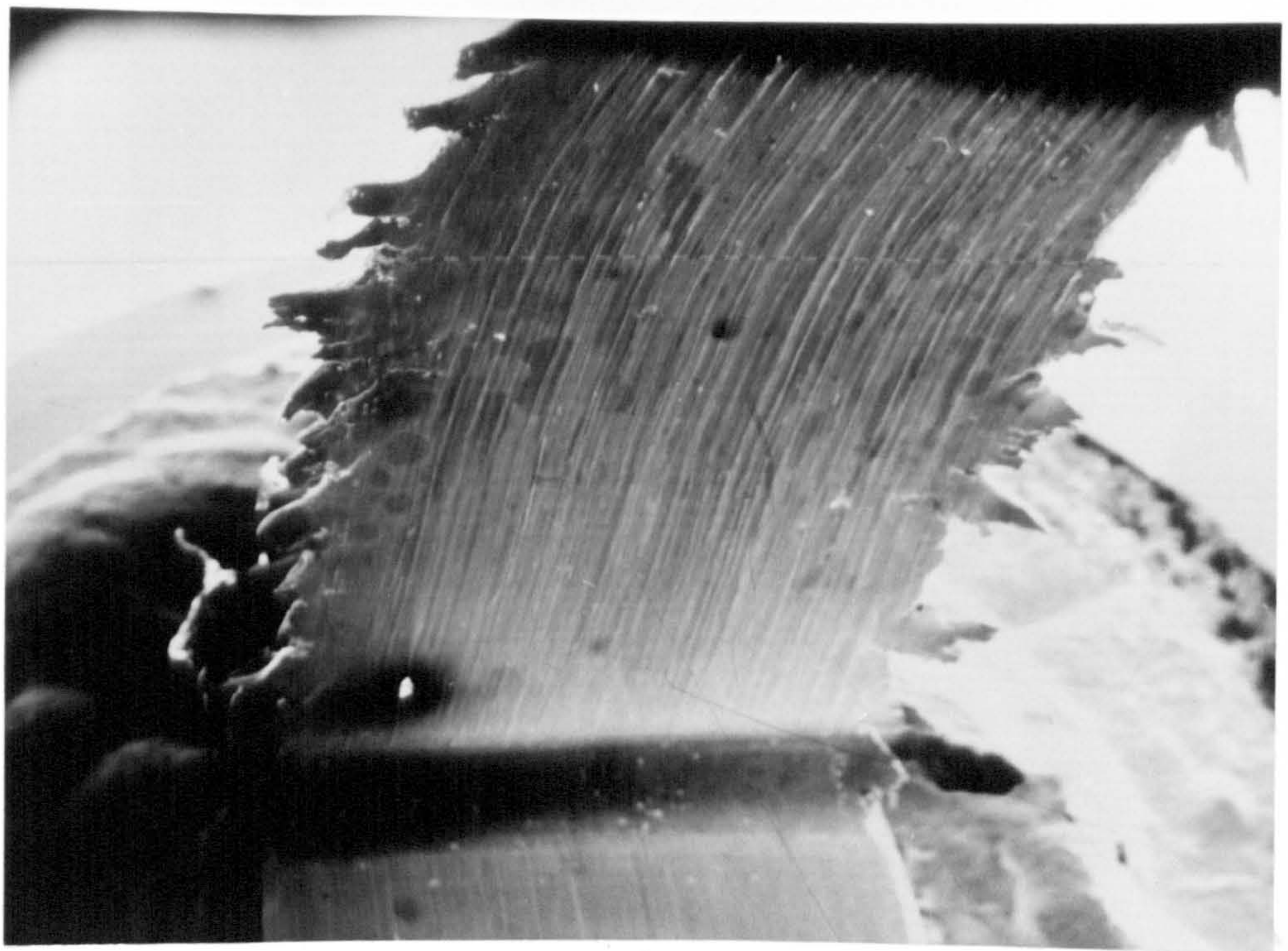


FIG.75 ELECTRON-MICROSCOPE PICTURE OF THE CHIP ROOT AREA

WORK PIECE MATERIAL: COPPER
 NOMINAL SET DEPTH: 0.25 MM
 CUTTING TOOL: 0.56 MM RADII
 CUTTING FLUID: SULPHURISED OIL
 TOOL WIDER THAN WORKPIECE

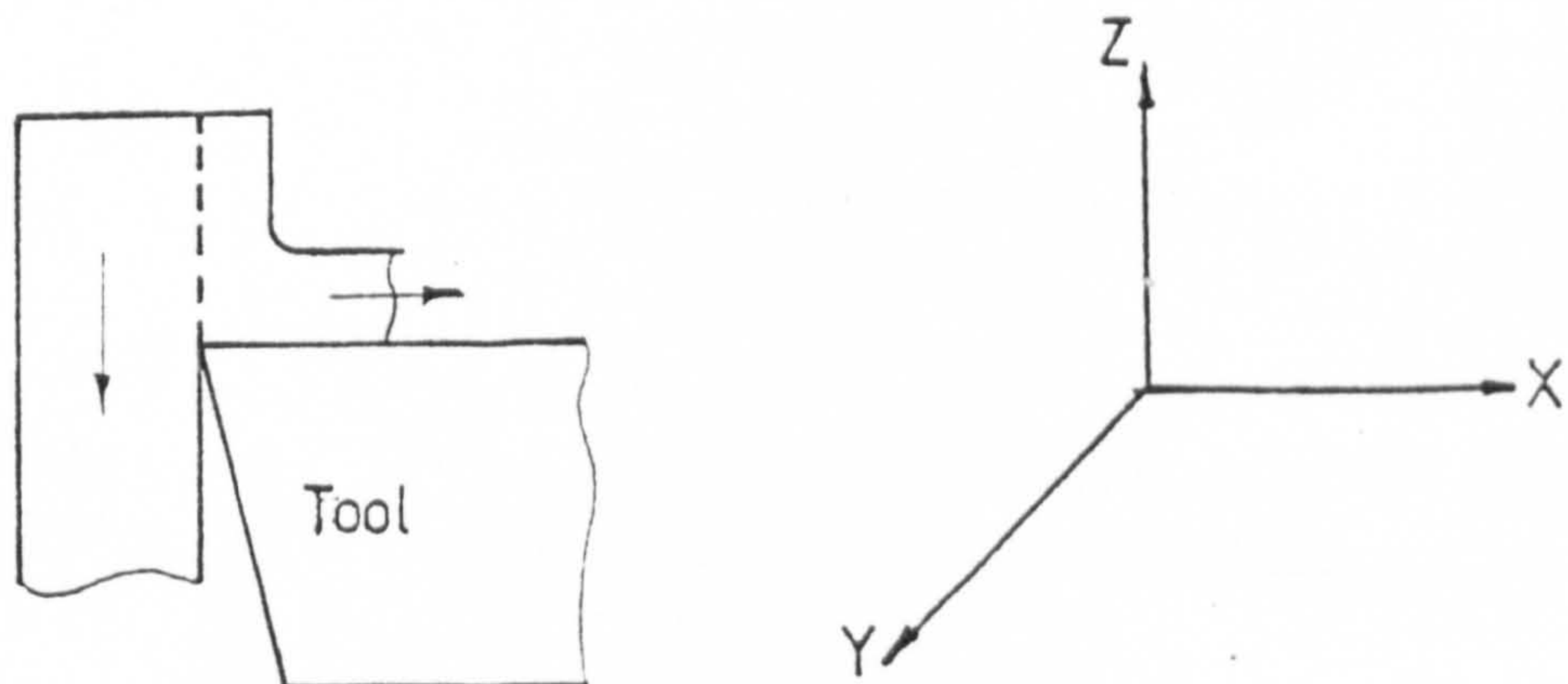


FIG.76 MATERIAL BEHAVIOUR AT THE CENTRE OF THE WORKPIECE

WORKPIECE MATERIAL: COPPER
GROOVE CUTTING
BLUNT TOOL: 0.56 MM RADIUS
TOOL WIDTH: 3.4 MM
CUTTING SPEED: 95 MM/MIN
CUTTING FLUID: SULPHURISED OIL
NOMINAL DEPTH OF CUT; 0.15 MM

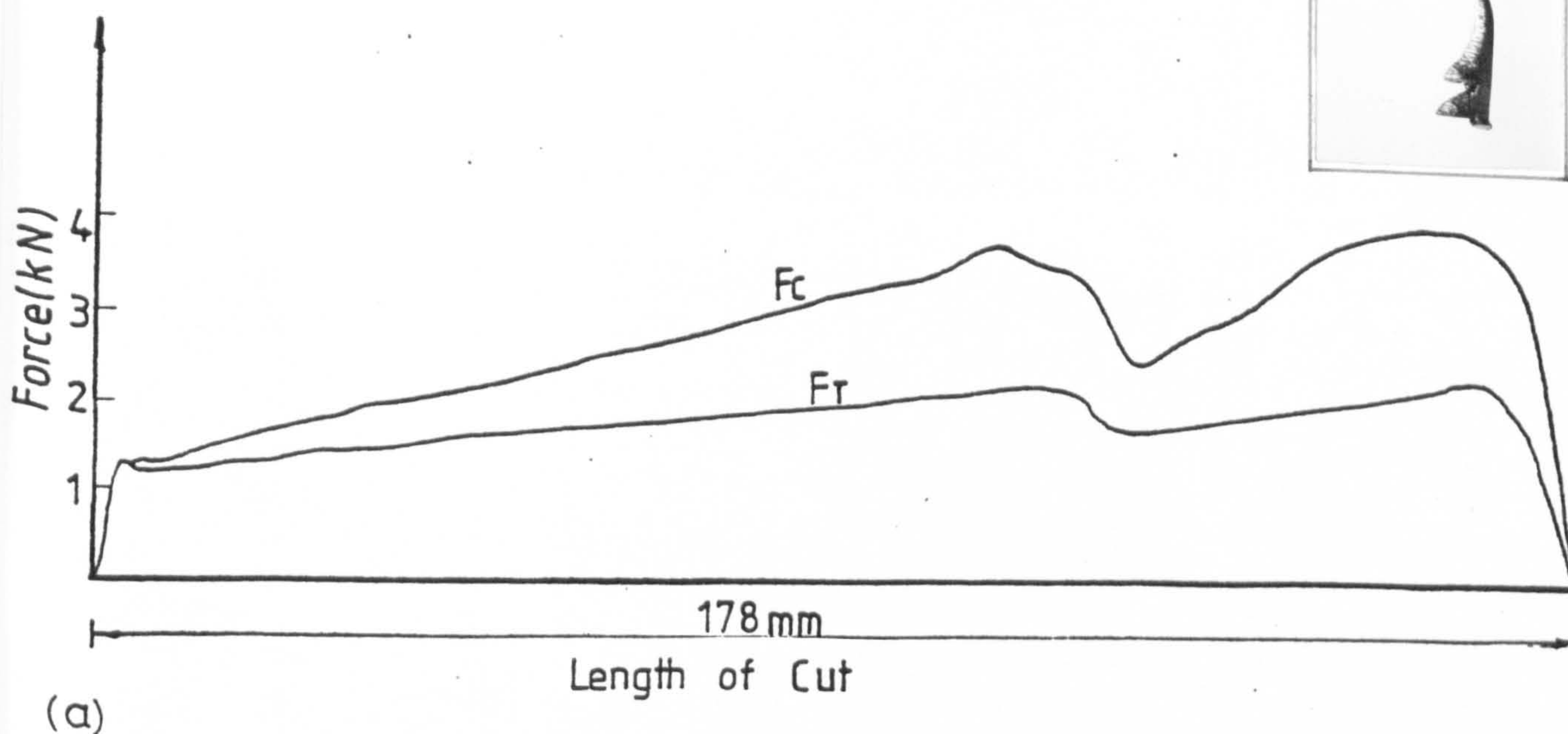


FIG.77 VARIATION OF CUTTING FORCES DURING GROOVE CUTTING WITH A BLUNT TOOL AND THE APPROPRIATE CHIP PRODUCED

WORKPIECE MATERIAL: COPPER
 GROOVE CUTTING
 BLUNT TOOL: 0.56 MM RADII
 TOOL WIDTH: 3.4 MM
 CUTTING SPEED: 95 MM/MIN
 NOMINAL DEPTH OF CUT: 0.1 MM
 CUTTING FLUID: SULPHURISED OIL

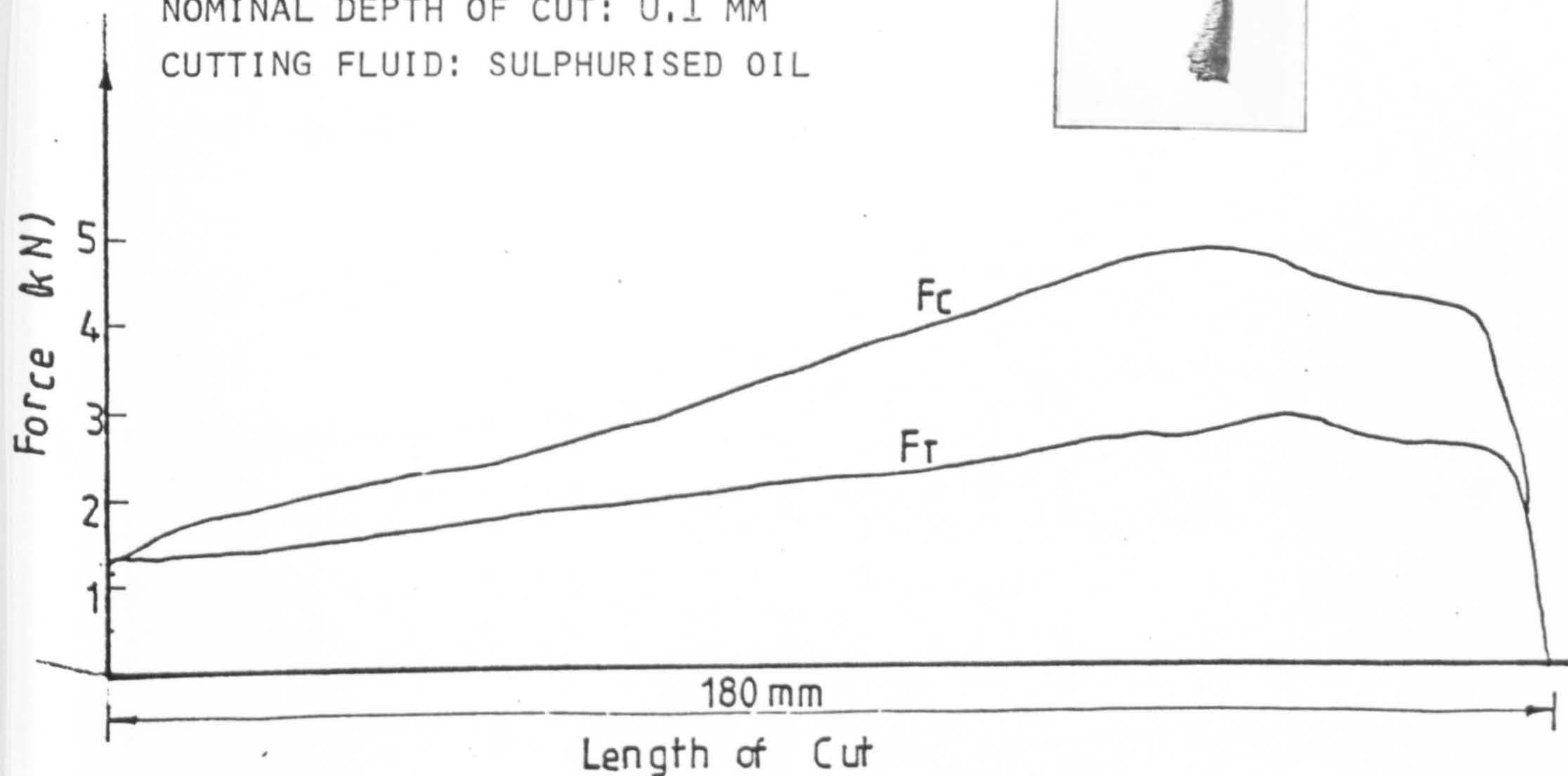


Fig 77(b)

CUTTING CONDITIONS: AS ABOVE

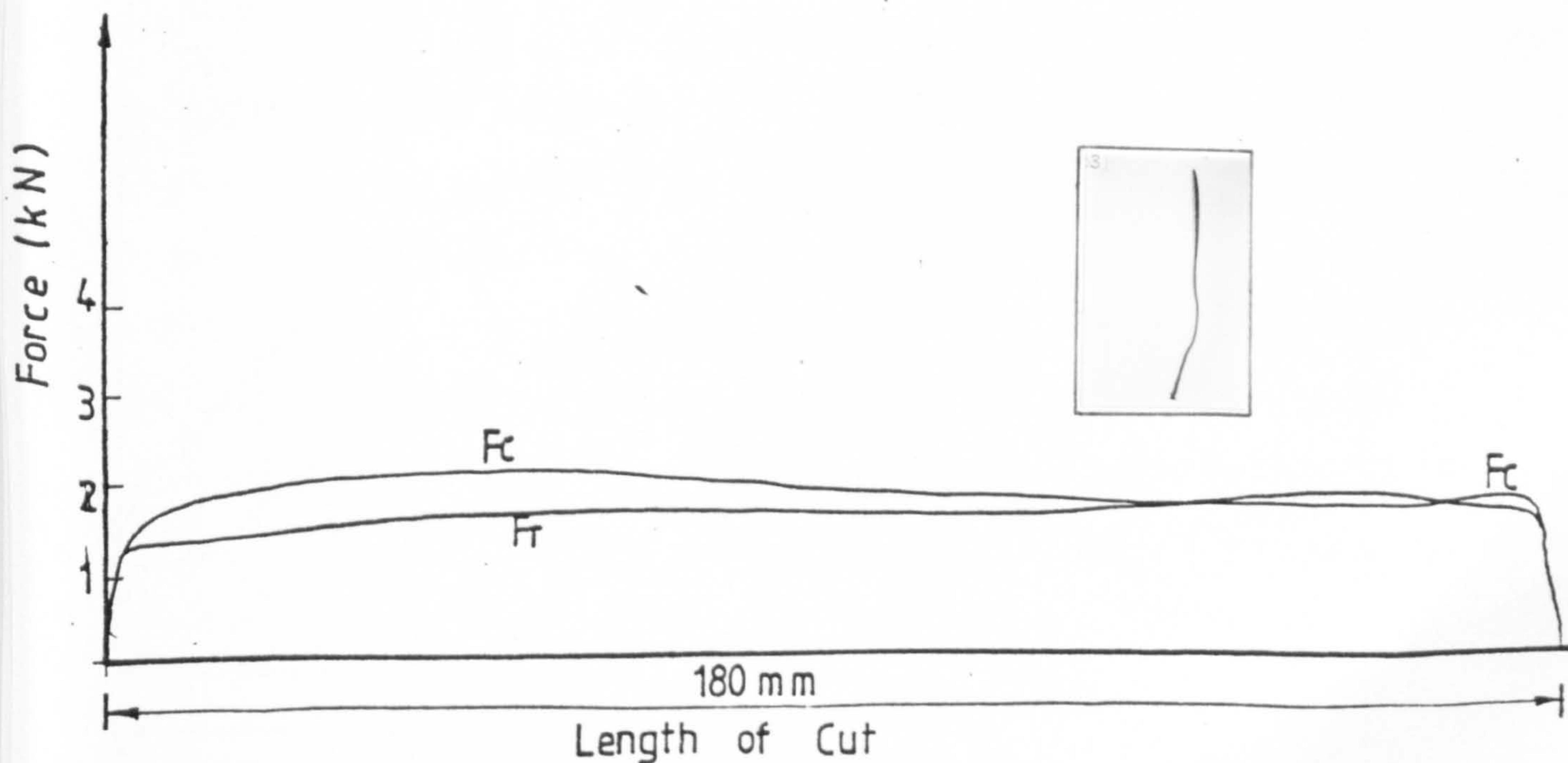


Fig 77 (c)

WORKPIECE MATERIAL: COPPER
 GROOVE CUTTING
 BLUNT TOOL: 0.56 MM RADII
 TOOL WIDTH: 3.4 MM
 CUTTING SPEED: 95 MM/MIN
 CUTTING FLUID: SULPHURISED OIL
 NOMINAL DEPTH: 0.15 MM

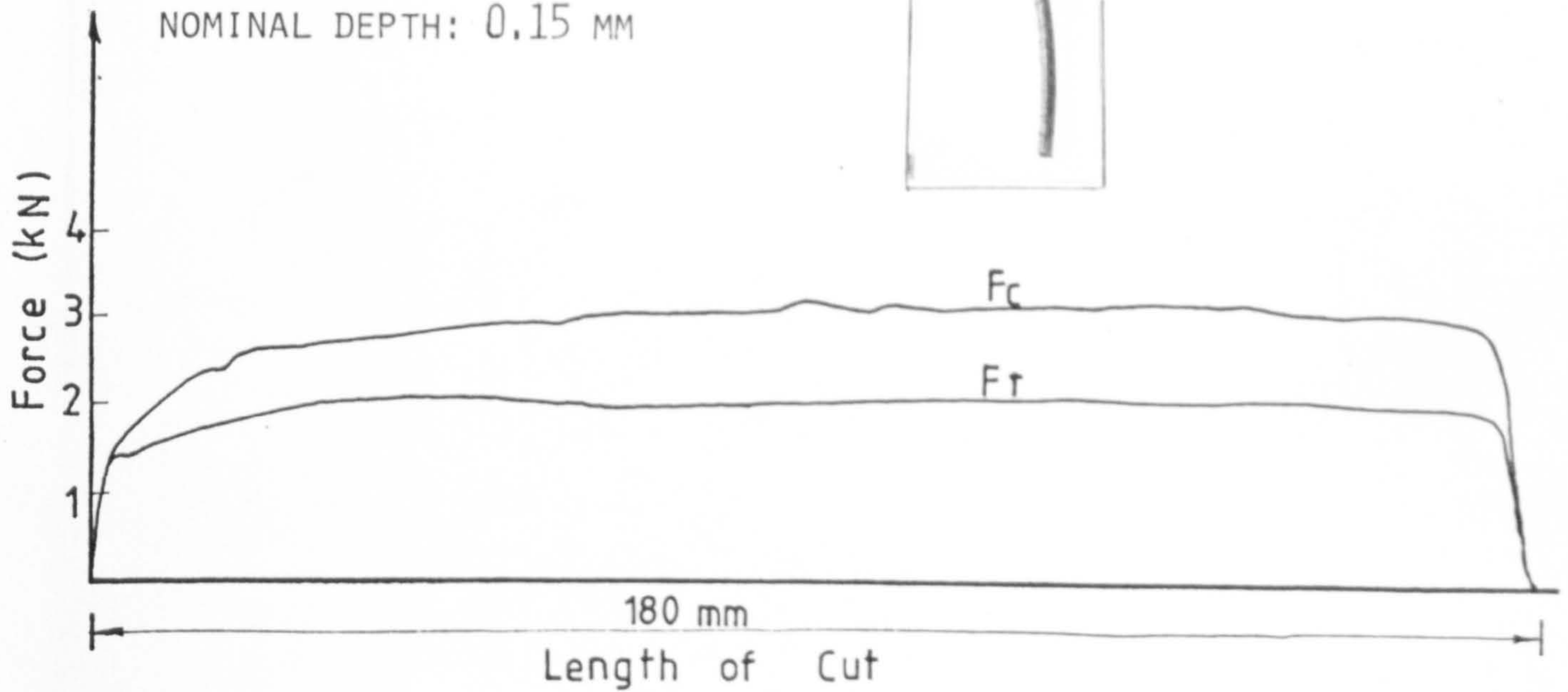


Fig 77 (d)

WORKPIECE MATERIAL: COPPER
 GROOVE CUTTING
 BLUNT TOOL: 0.56 MM RADII
 TOOL WIDTH: 3.4 MM
 CUTTING SPEED: 95 MM/MIN

CUTTING FLUID: SULPHURISED OIL
 NOMINAL DEPTH: 0.5 MM

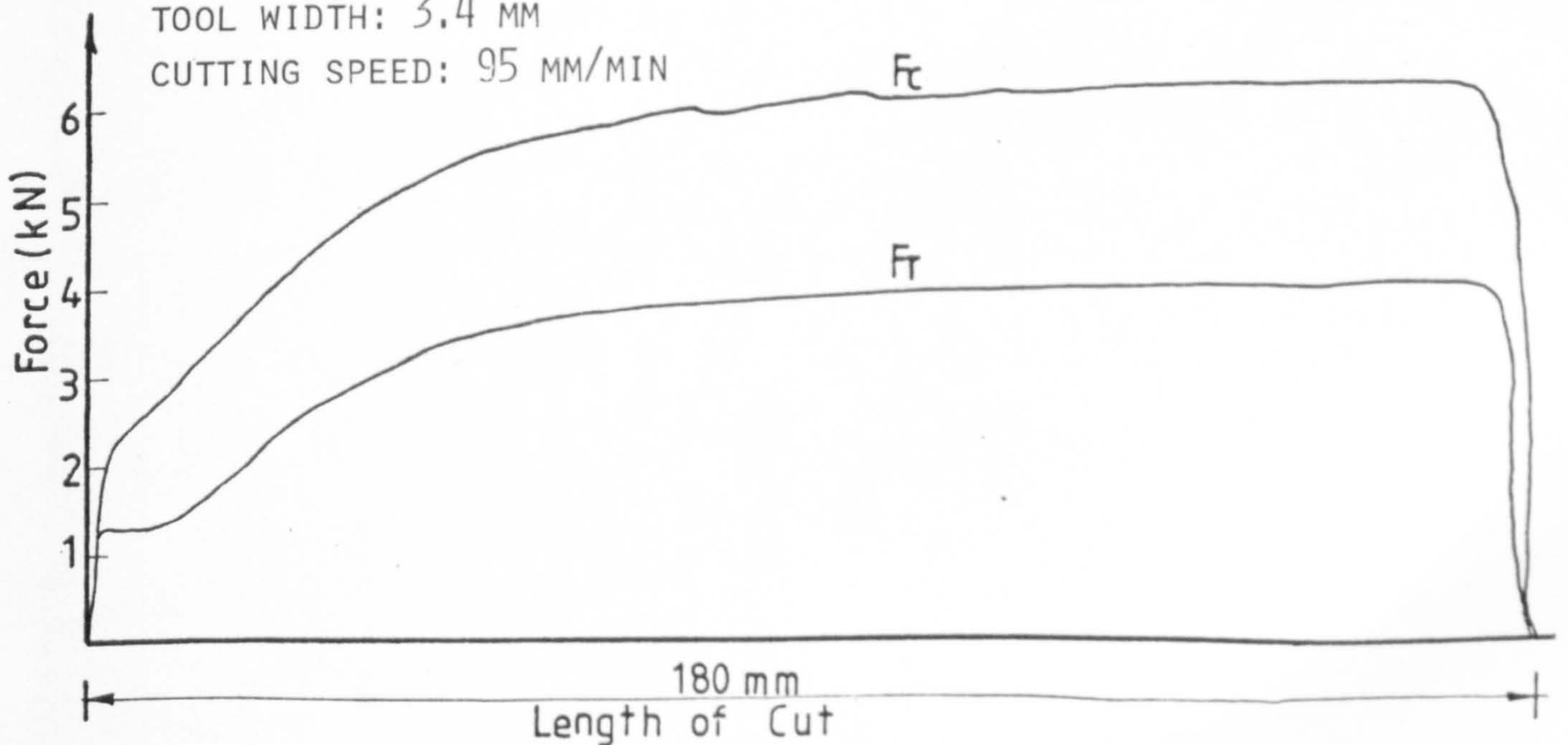


Fig 77 (e)

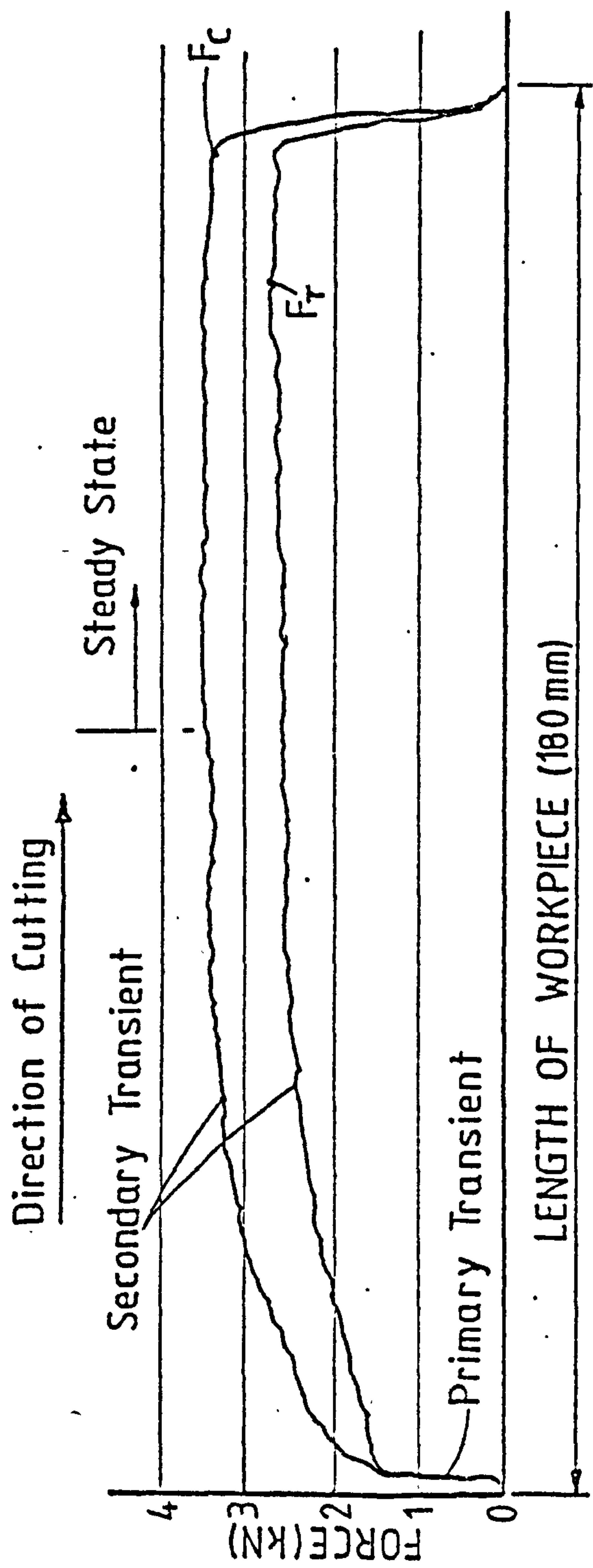


FIG. 78: Variation of cutting forces during groove cutting showing primary, secondary and steady state force regions

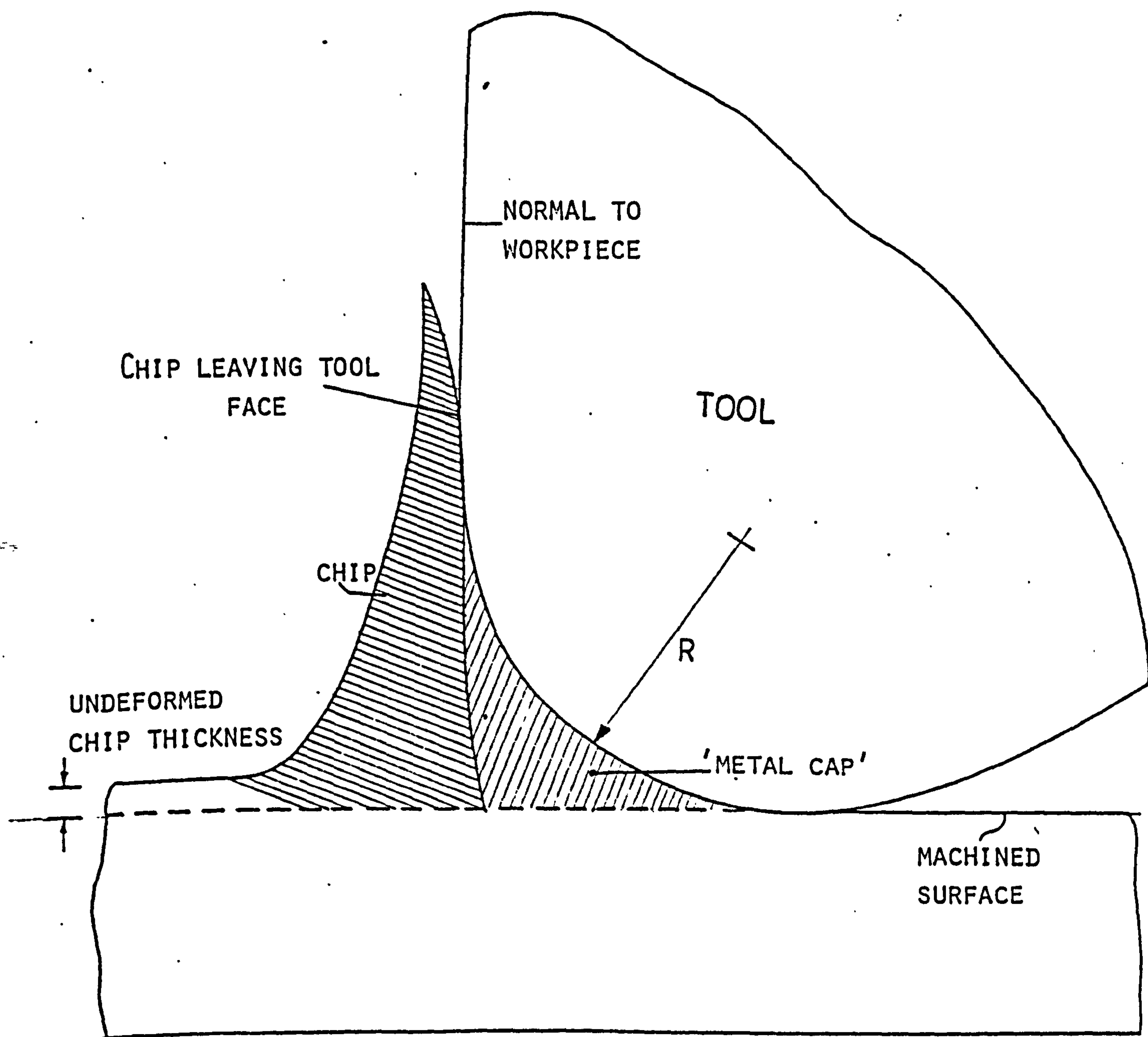


FIG.79(A) SCHEMATIC DIAGRAM OF THE CHIP FORMATION WHEN MACHINING WITH A BLUNT TOOL

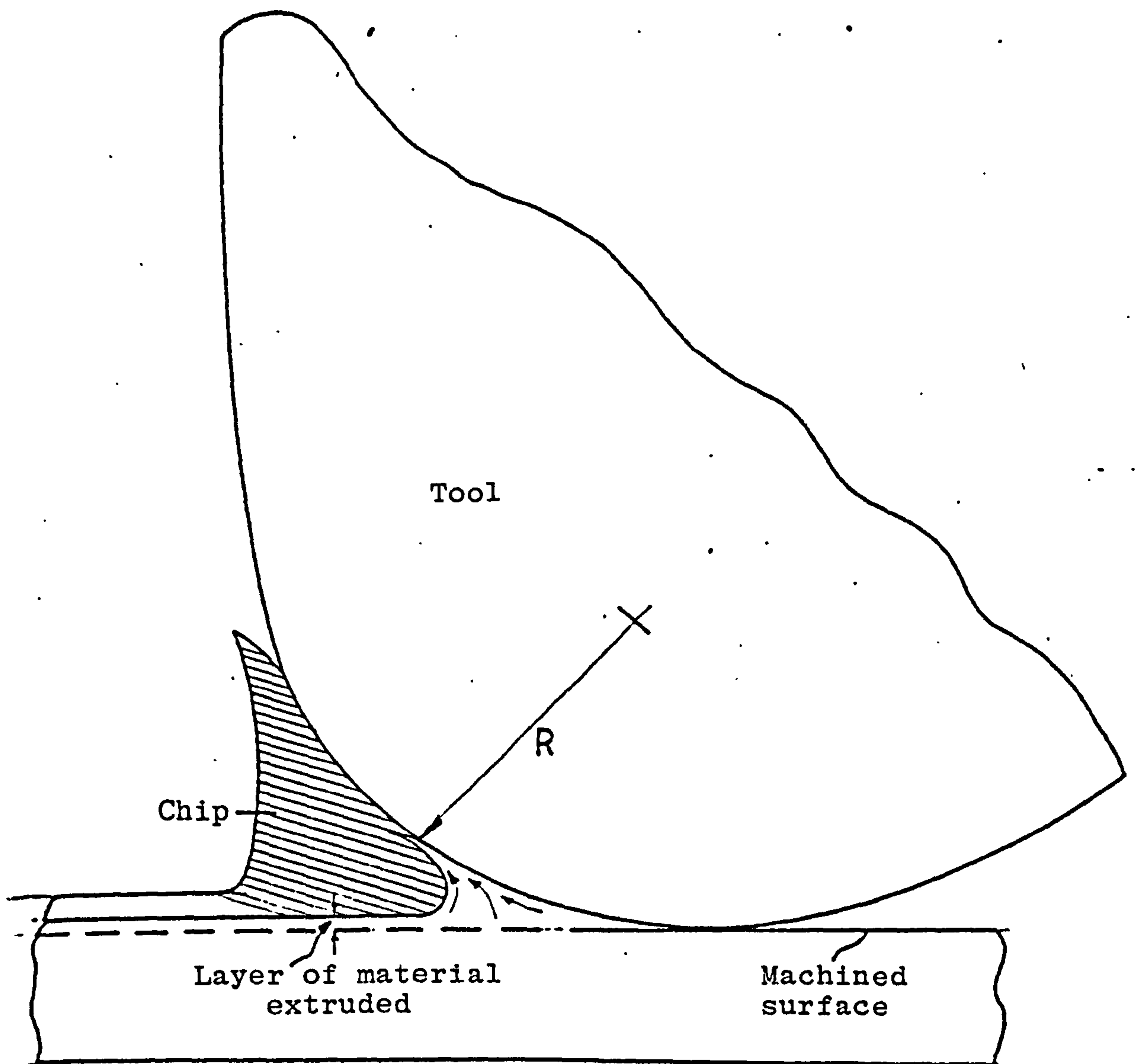


FIG.79(B) SCHEMATIC DIAGRAM, SHOWING LAYER OF MATERIAL BEING EXTRUDED AROUND THE CHIP ROOT AREA

FIG. 80: Variation of forces and chip tool contact length with increase in depth of cut

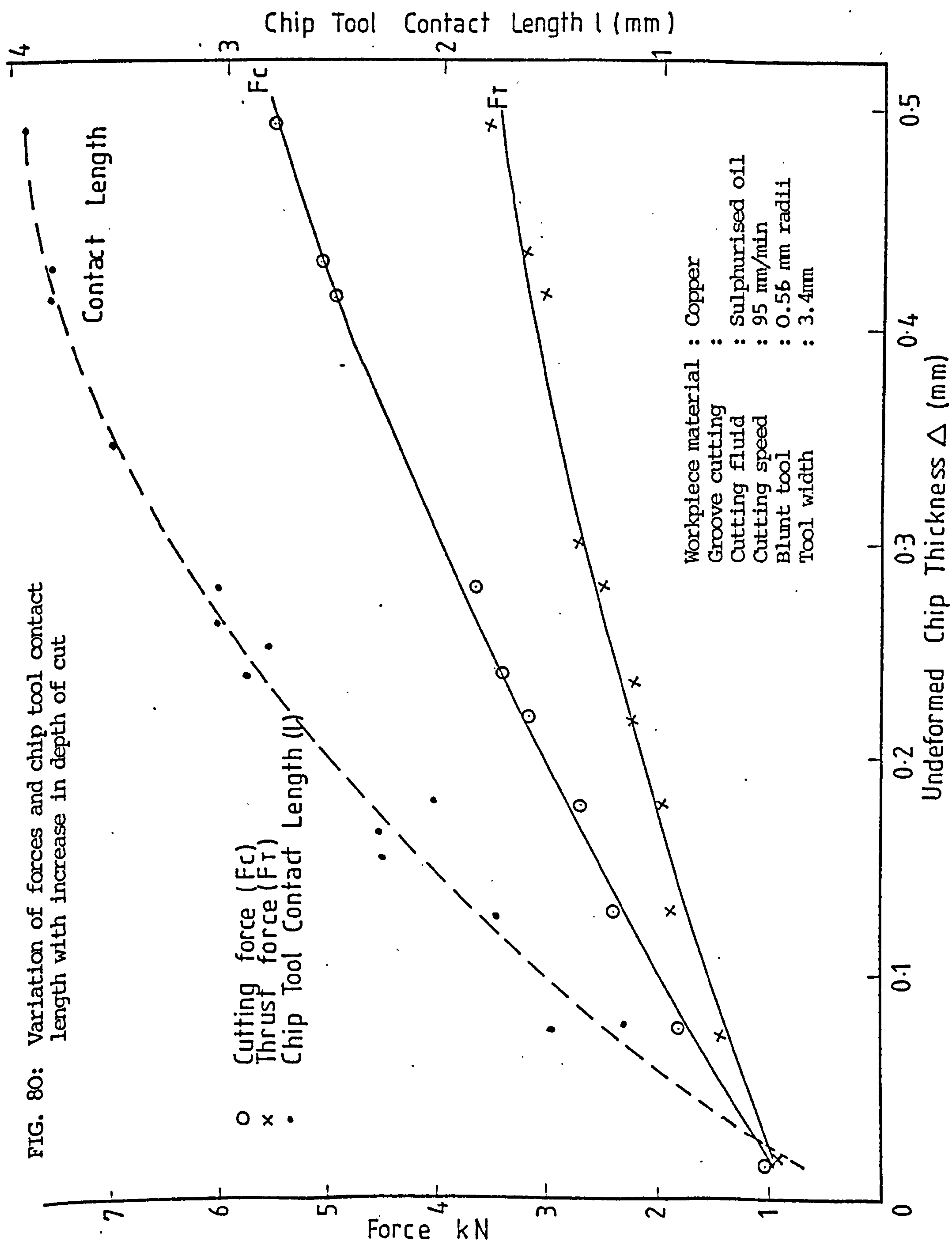


FIG. 81: Variation of forces and chip tool contact length with increase in depth of cut

Workpiece material : Copper
 Groove cutting : Sulphurised oil
 Cutting fluid : 95 mm/min
 Cutting speed : 0.81 mm radii

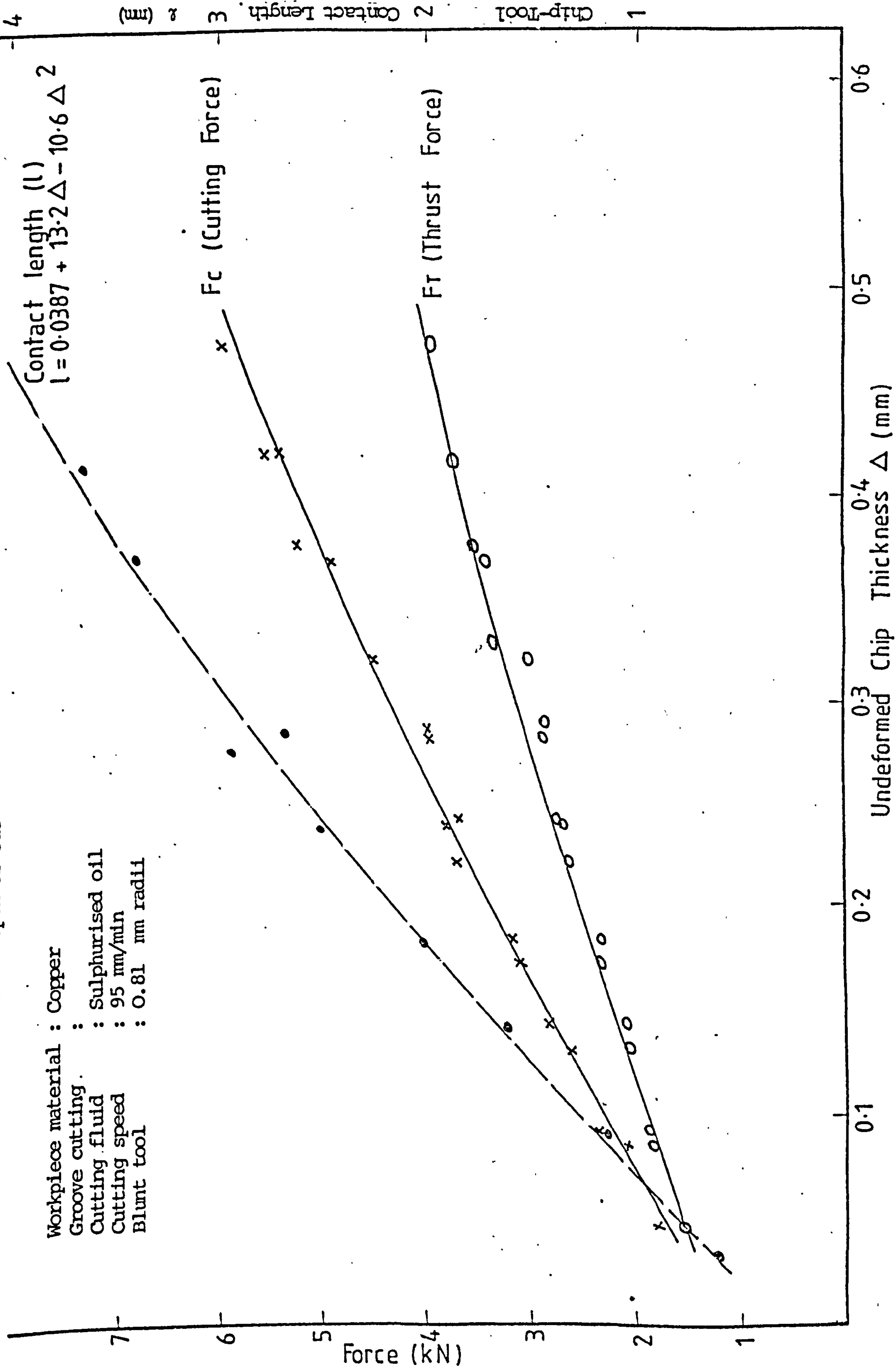


FIG. 82: Variation of forces and chip tool contact length with increase in depth of cut

Workpiece material: Lead steel
 Groove cutting :
 Cutting fluid : Soluble oil + water
 Cutting speed : 95 mm/min
 Tool width : 3.4mm
 Blunt tool : 0.56mm radii

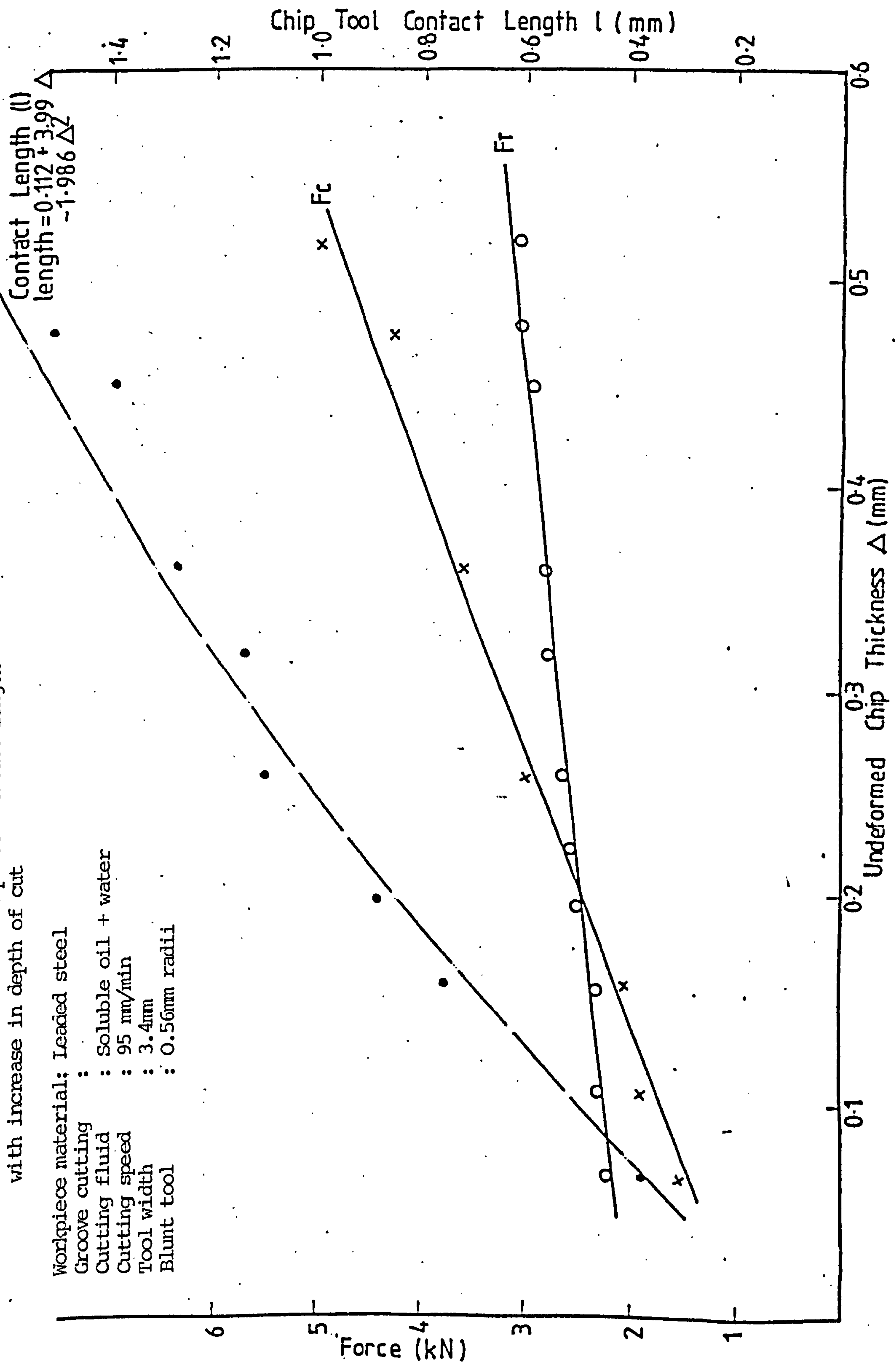


FIG. 82

FIG. 83: Comparison of thrust forces, blunt and sharp tools

Workpiece material : Copper
 Groove cutting :
 Cutting fluid : Sulphurised oil
 Cutting speed : 95mm/min
 Tool width : 3.4mm

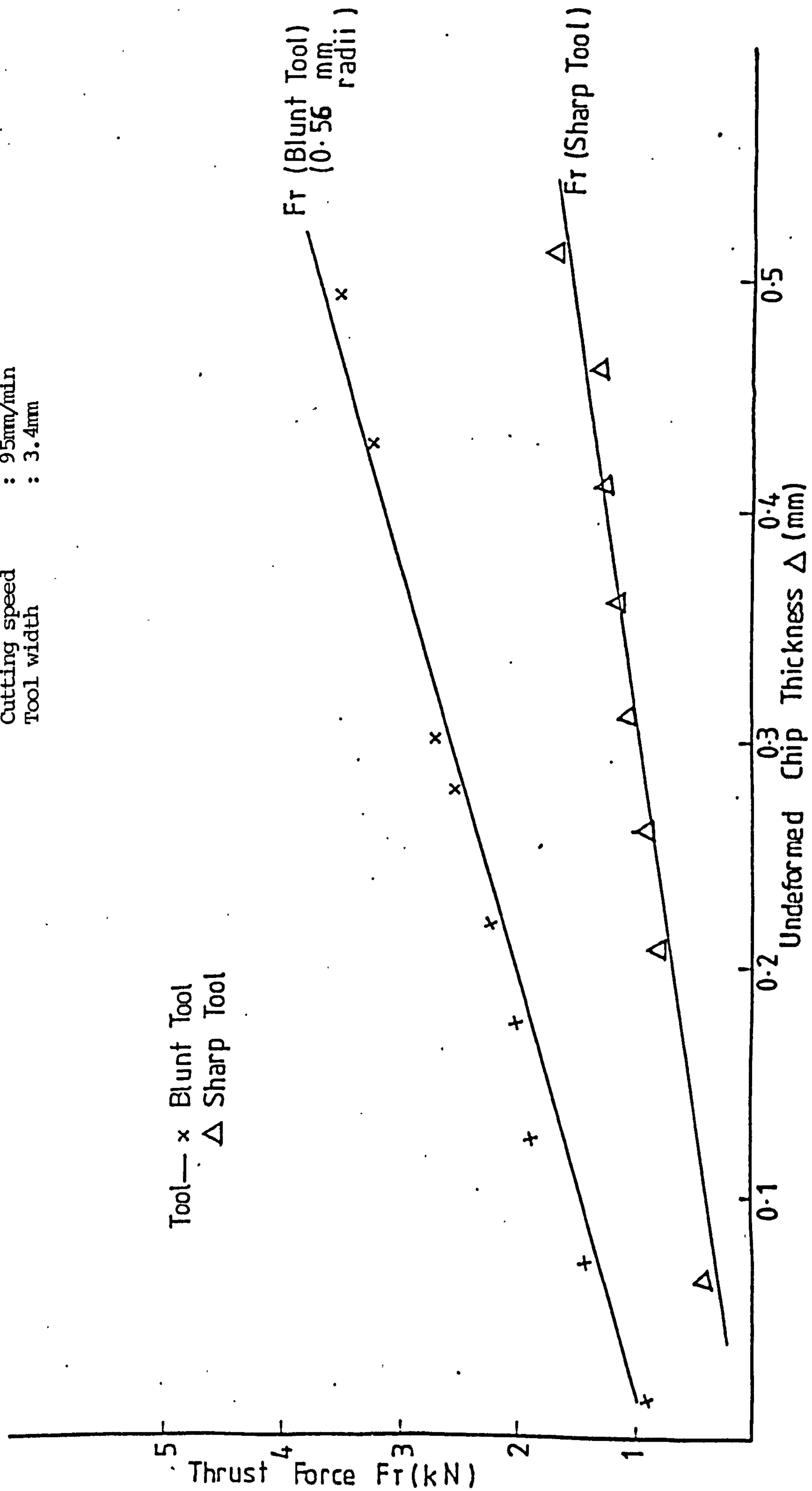


FIG. 84: Variation of Specific Cutting Energy with increase in depth of cut using blunt and sharp tools

Workpiece material : Copper
 Groove cutting : 95mm/min
 Cutting fluid : Sulphurised oil

Δ : -Blunt Tool: 0.5b mm radii
 x -Sharp Tool: 0.02mm radii

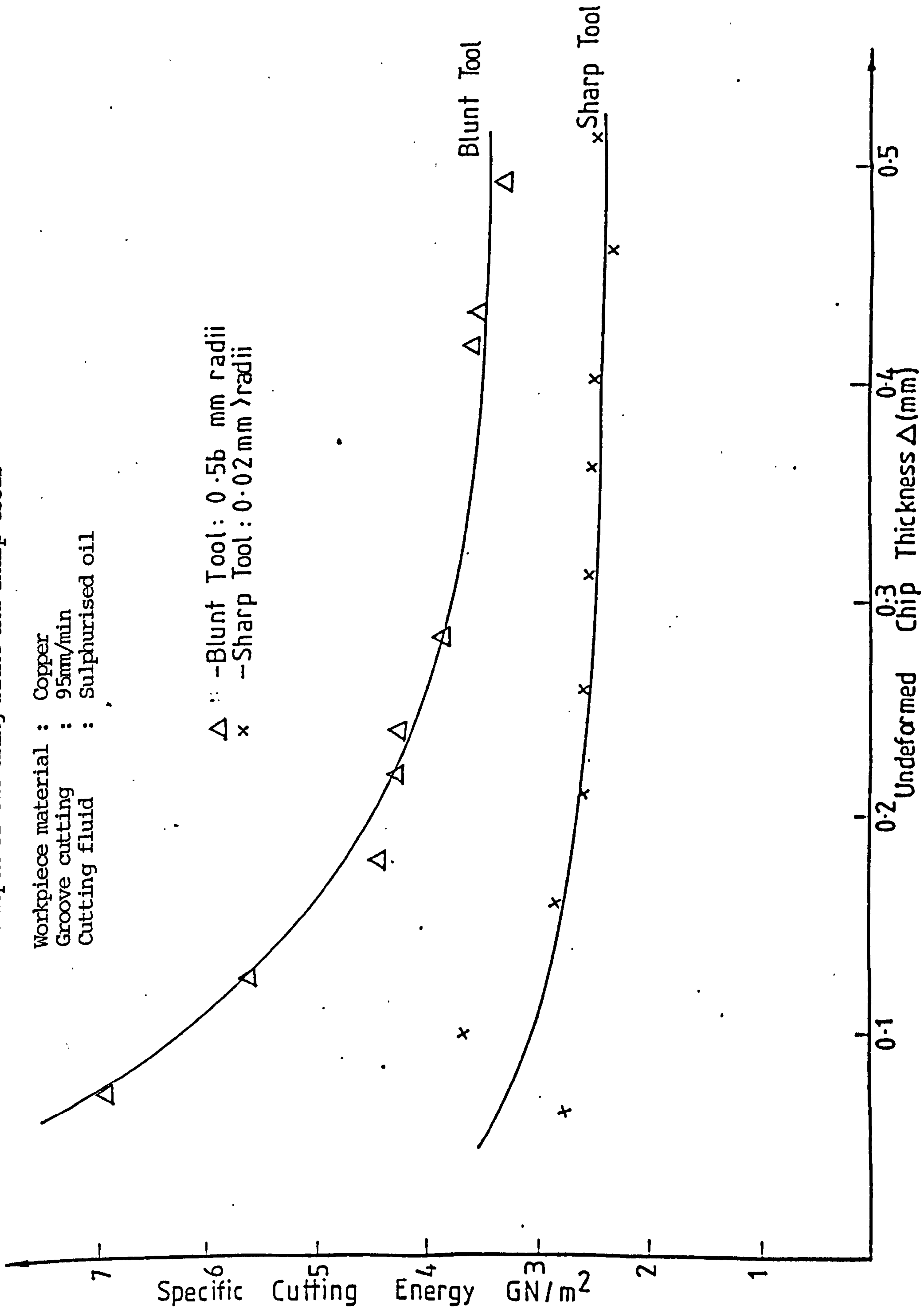
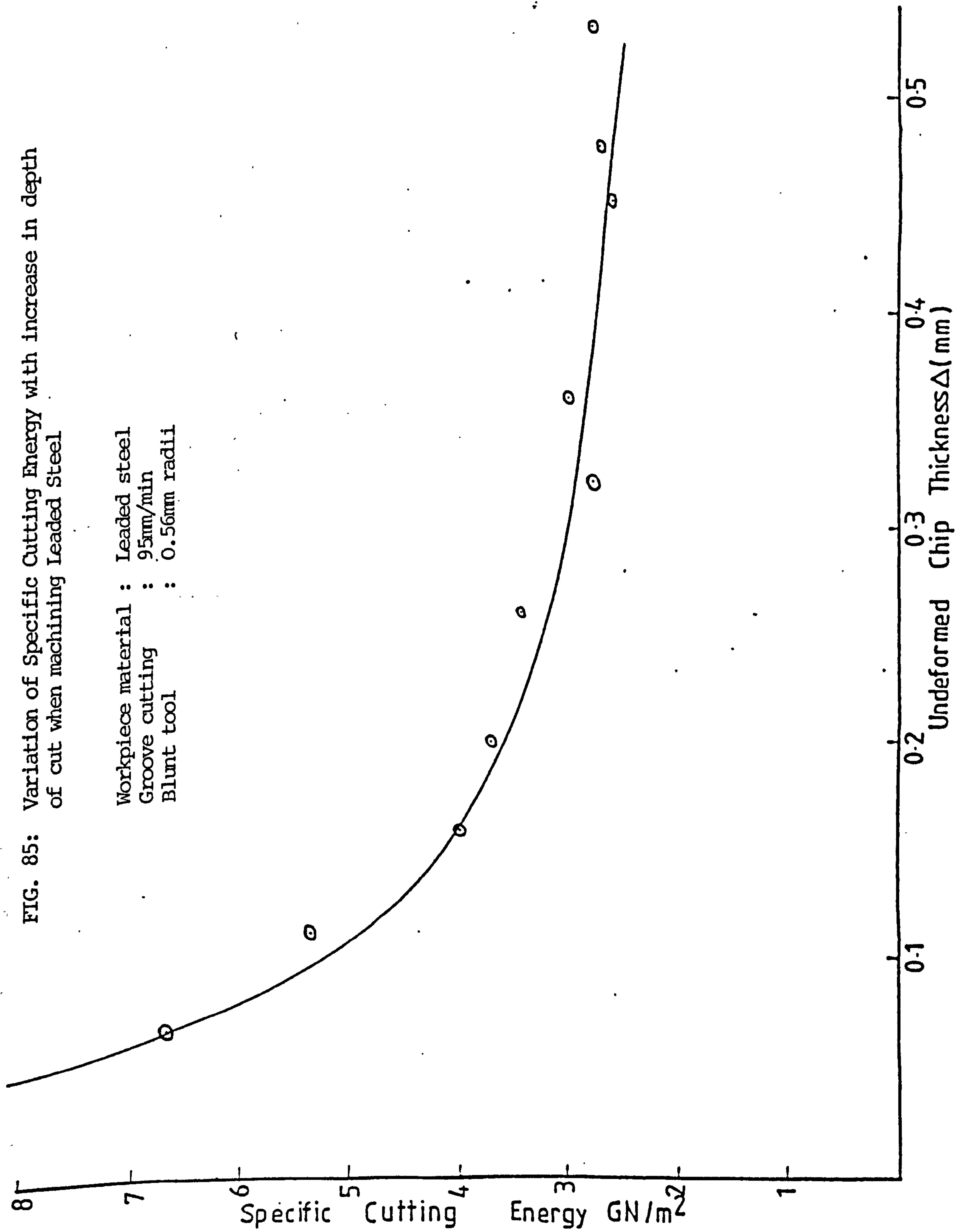


FIG. 85: Variation of Specific Cutting Energy with increase in depth of cut when machining Lead Steel

Workpiece material : Lead steel
 Groove cutting : 95mm/min
 Blunt tool : 0.56mm radii



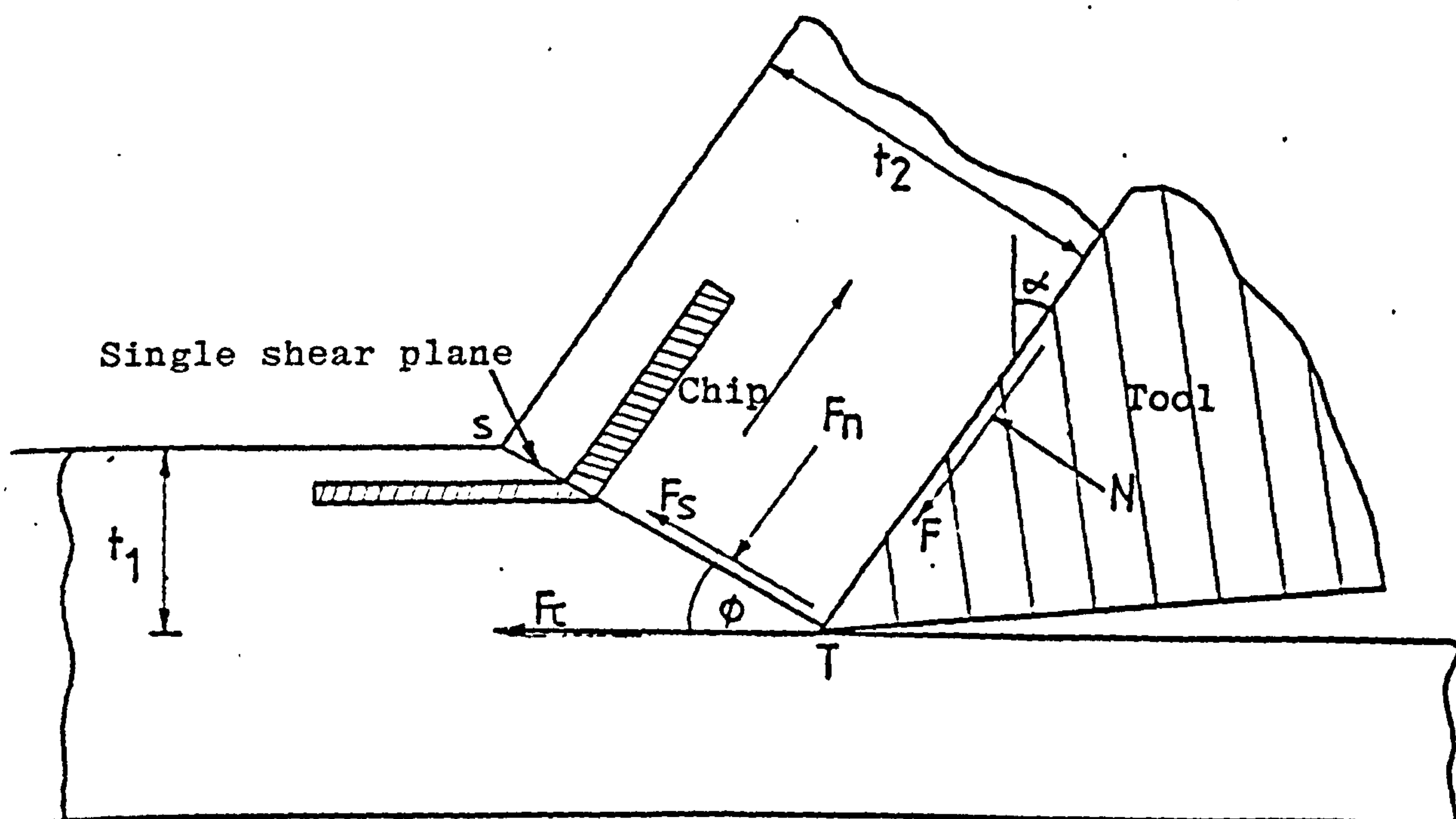
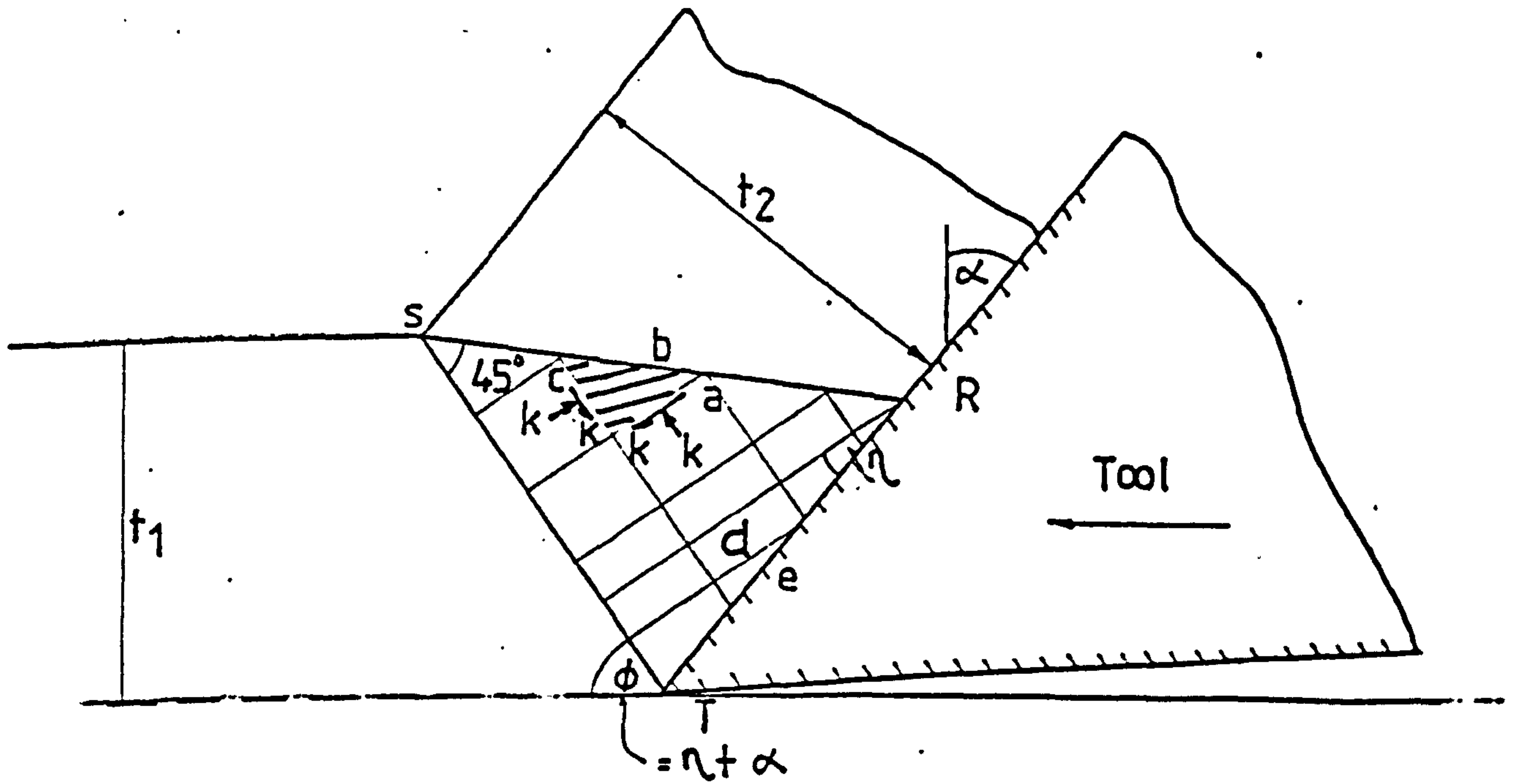


FIG.85 SINGLE SHEAR PLANE MODEL (70)

(a) Slip line field



(b) Mohr circle for stress field

$$\eta = \frac{\pi}{4} - \lambda$$

$$\phi = \frac{\pi}{4} + \alpha - \lambda$$

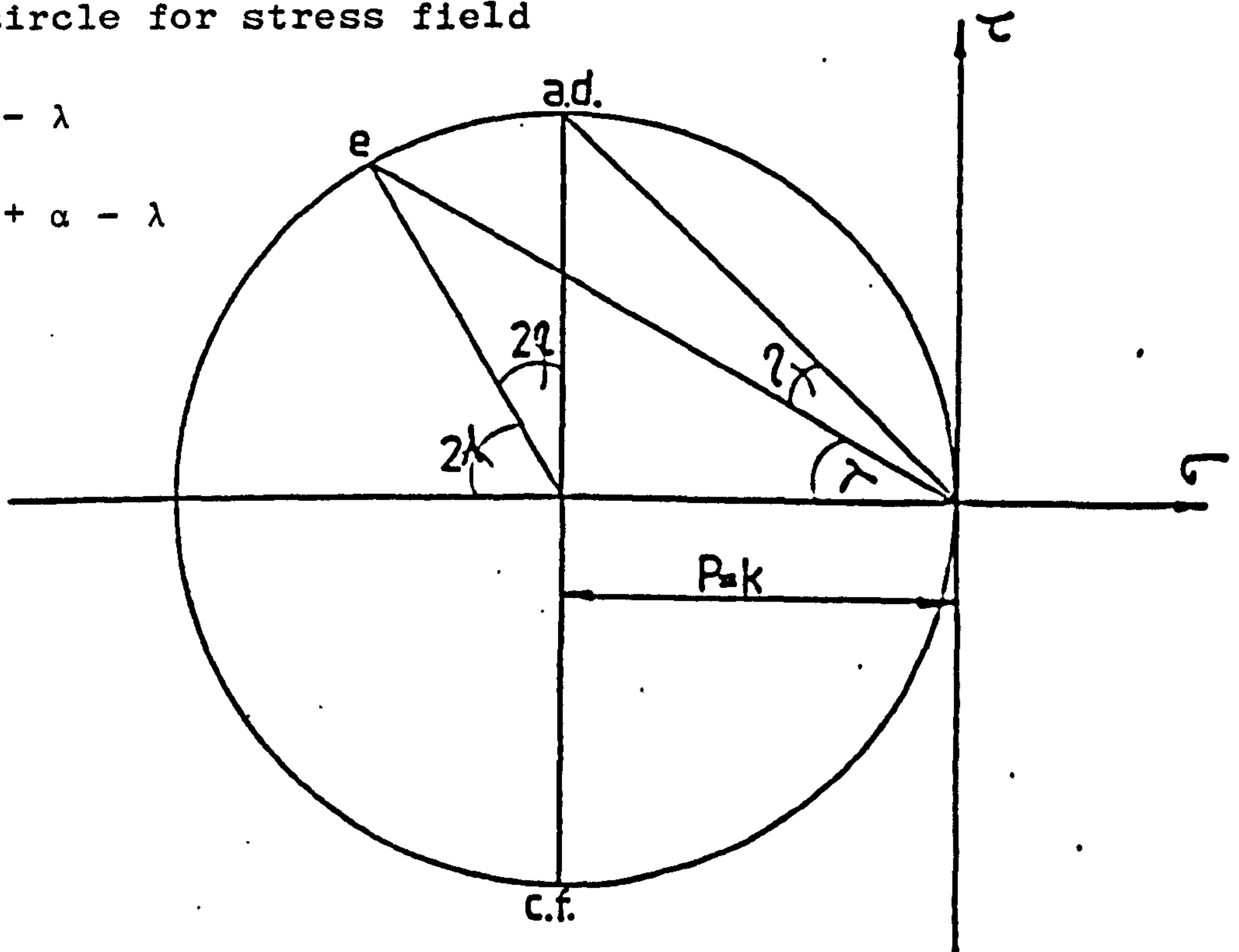


FIG. 87 LEE AND SCHAFFER'S SLIP LINE FIELD SOLUTION FOR A SINGLE SHEAR PLANE (59)

FIG. 88: Slip-line field and hodograph for built-up nose after Lee and Shaffer (60)

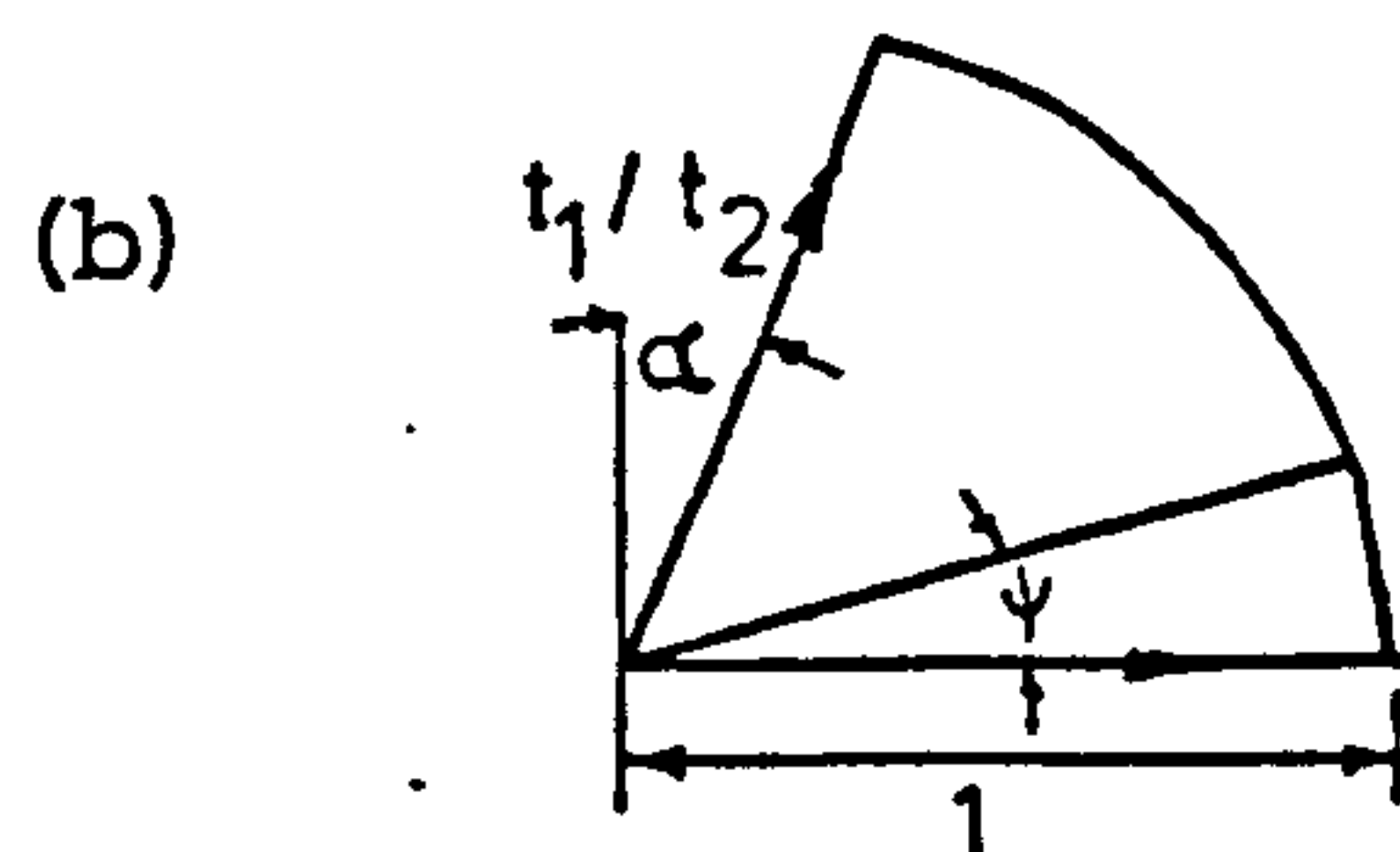
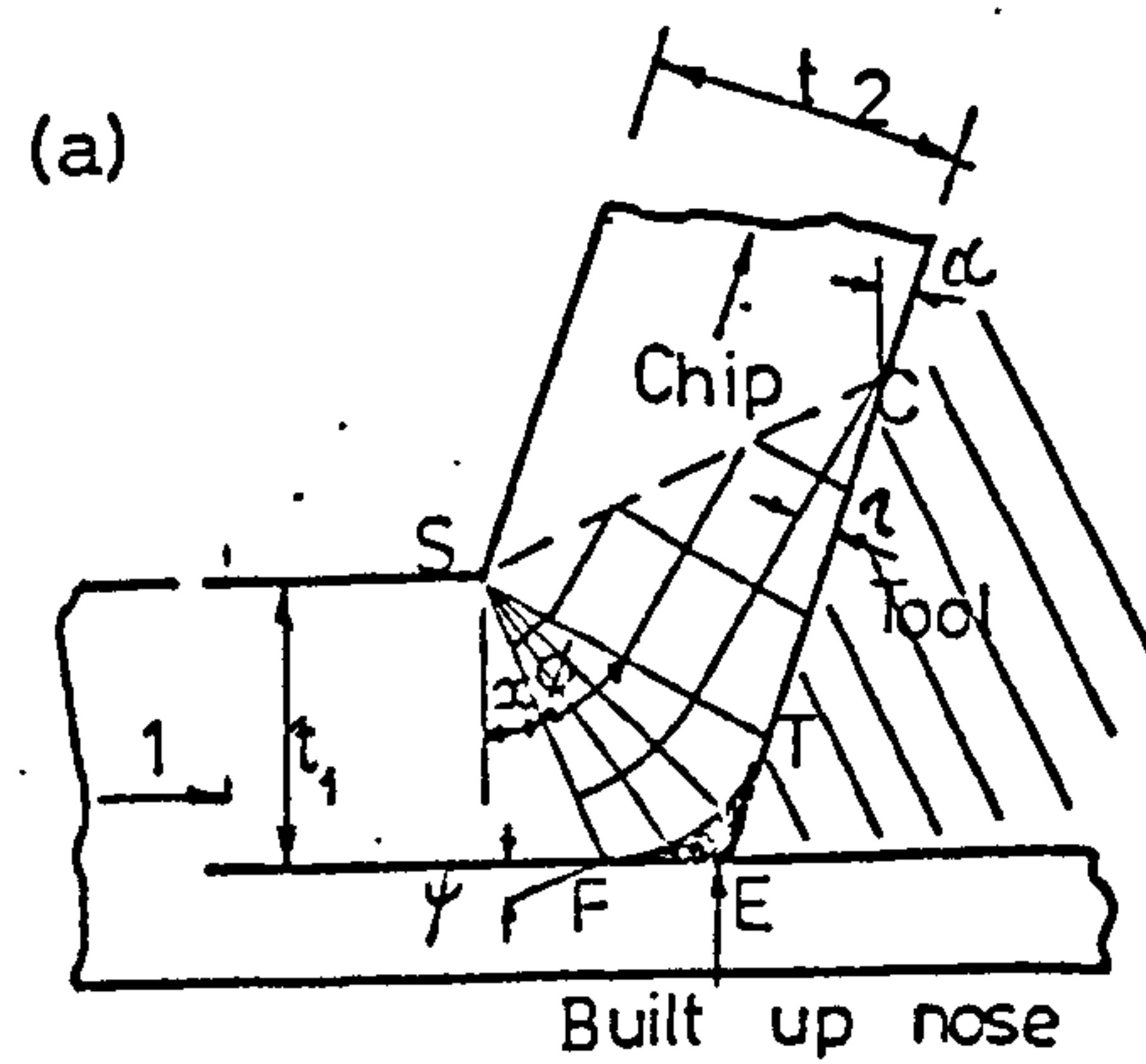


FIG. 89: Diagrammatic sketch of suggested cutting process (74,75)

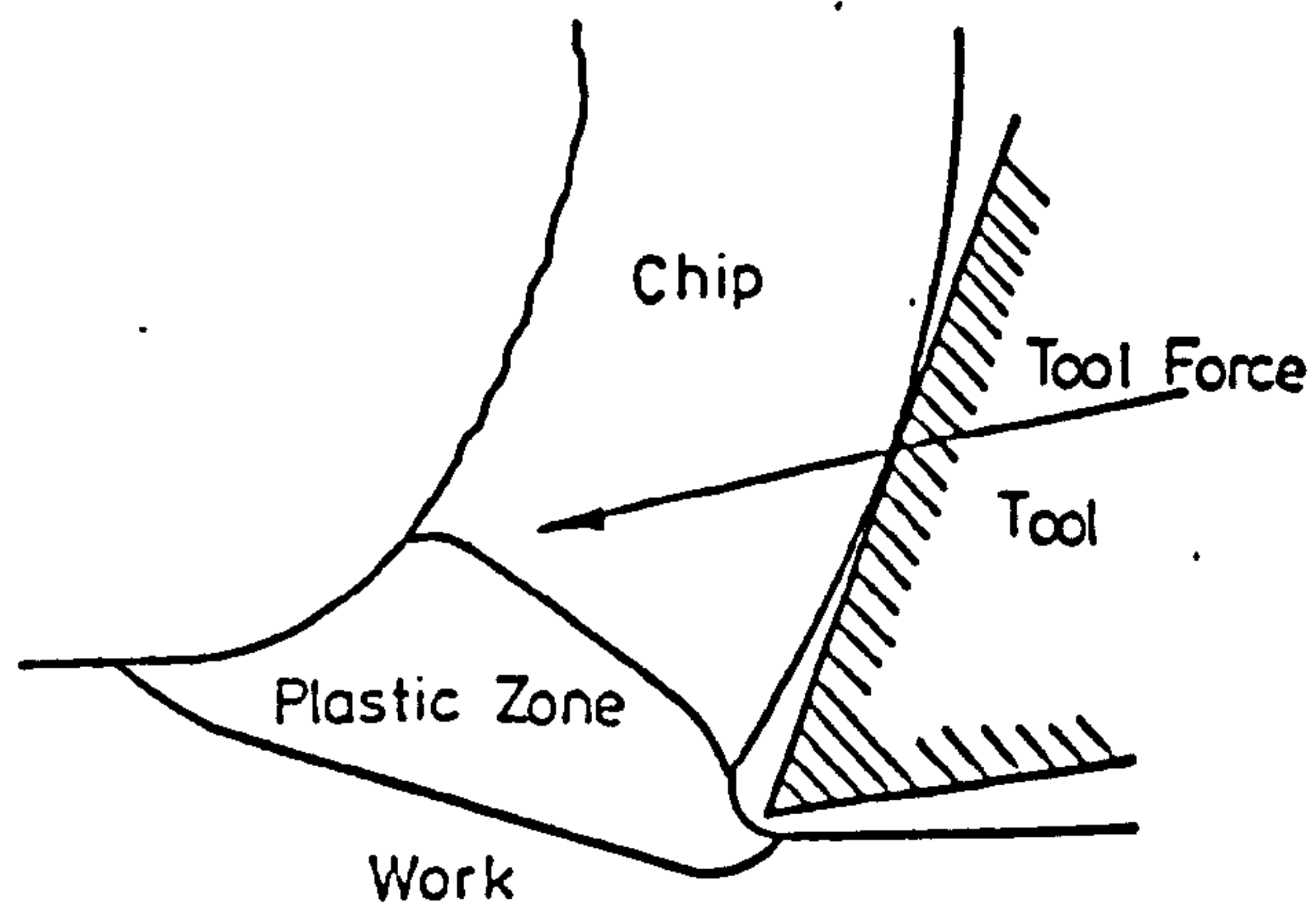
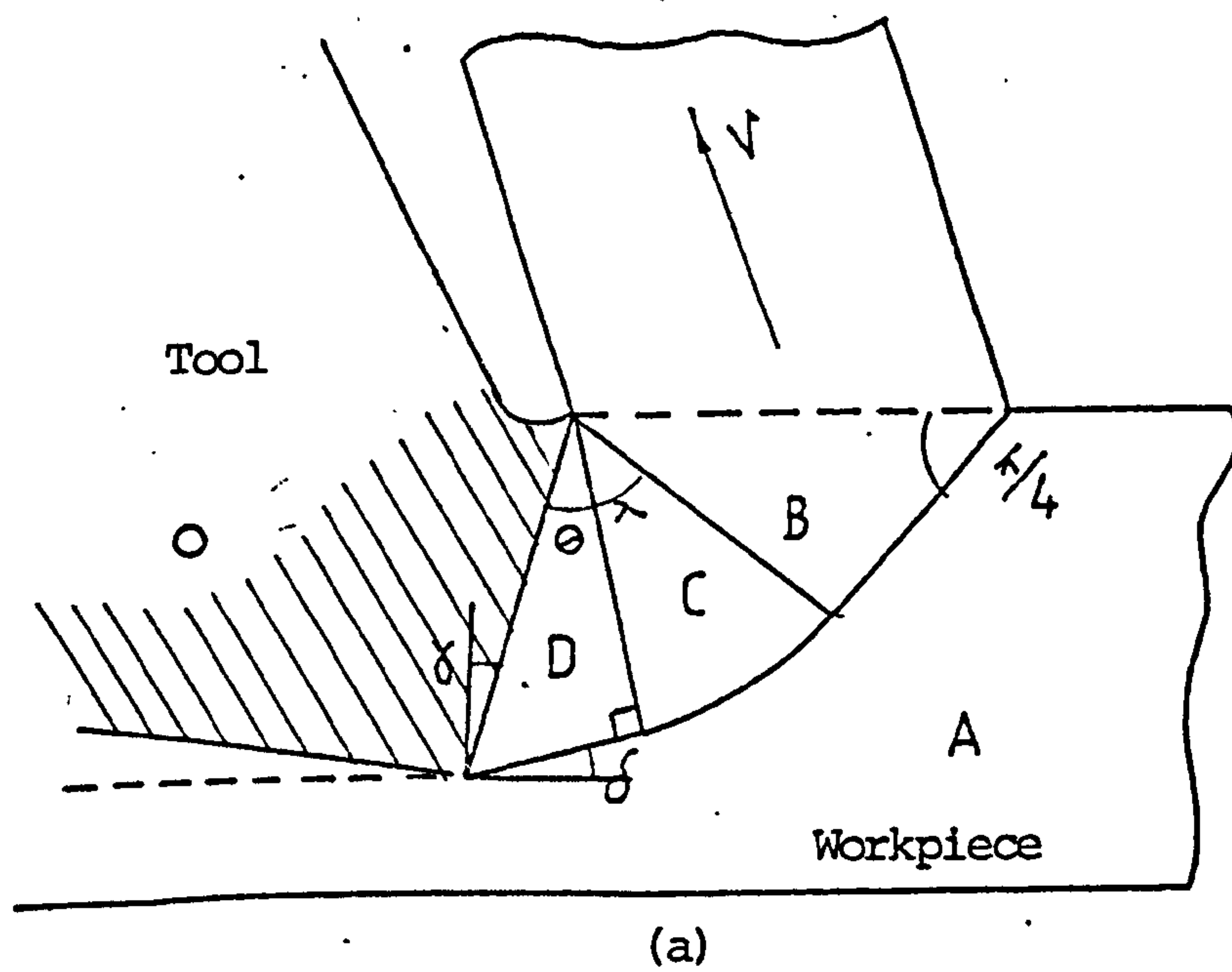
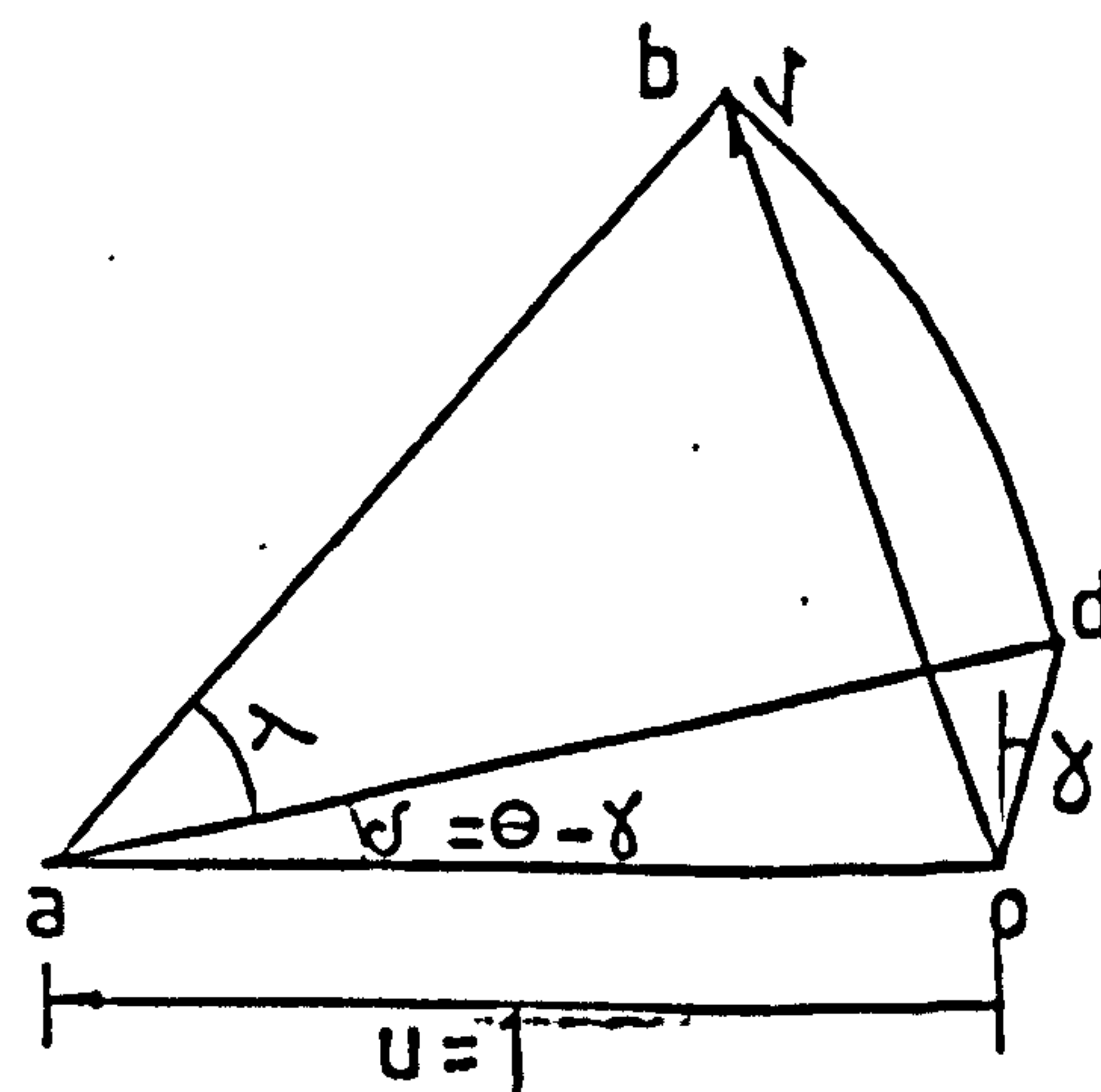


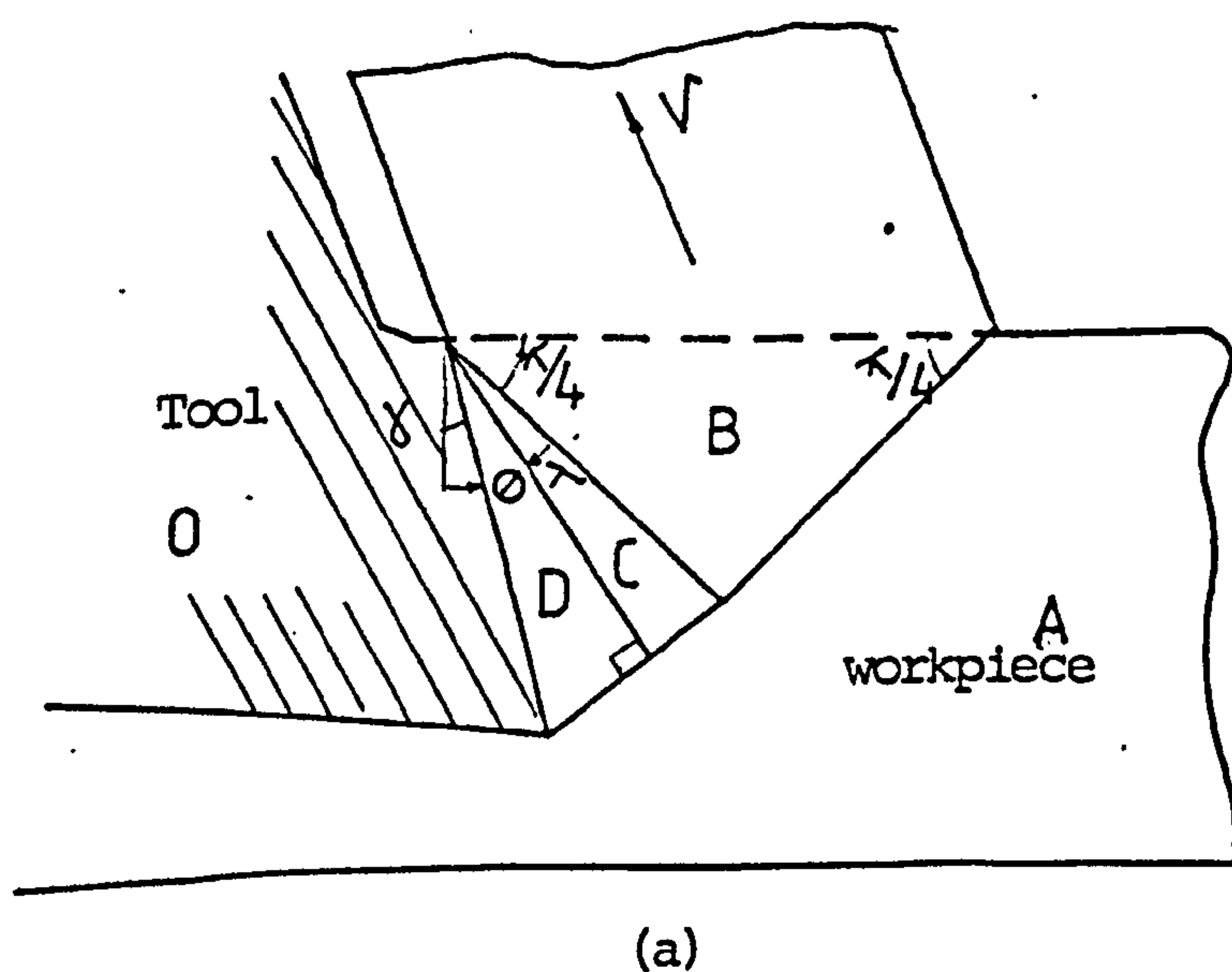
FIG. 90: Slip-line fields solutions and hodographs for restricted tool contact (77)



(a) Slip-line field - Negative Rake

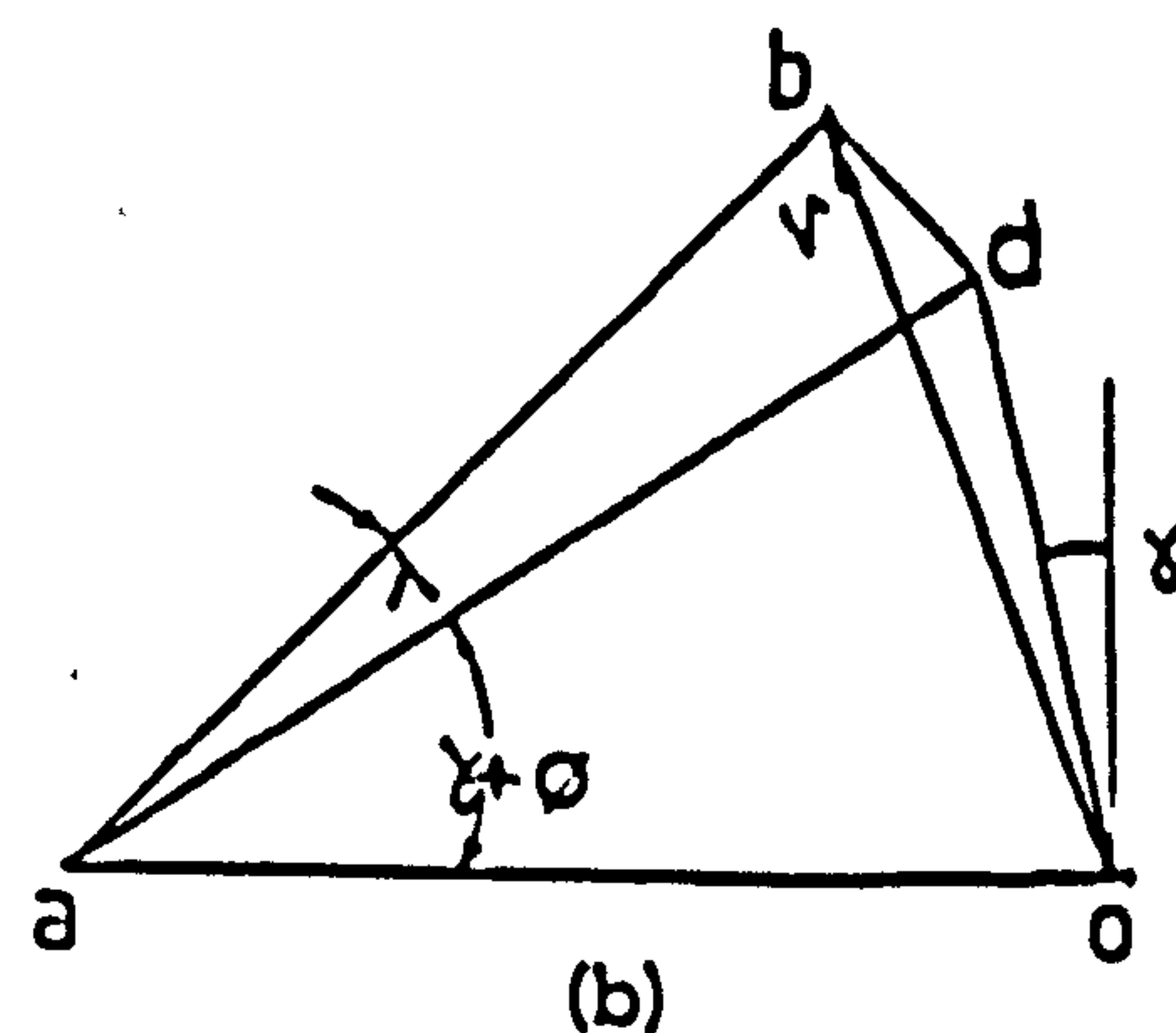


(b) Hodograph - negative rake tool (-ve)



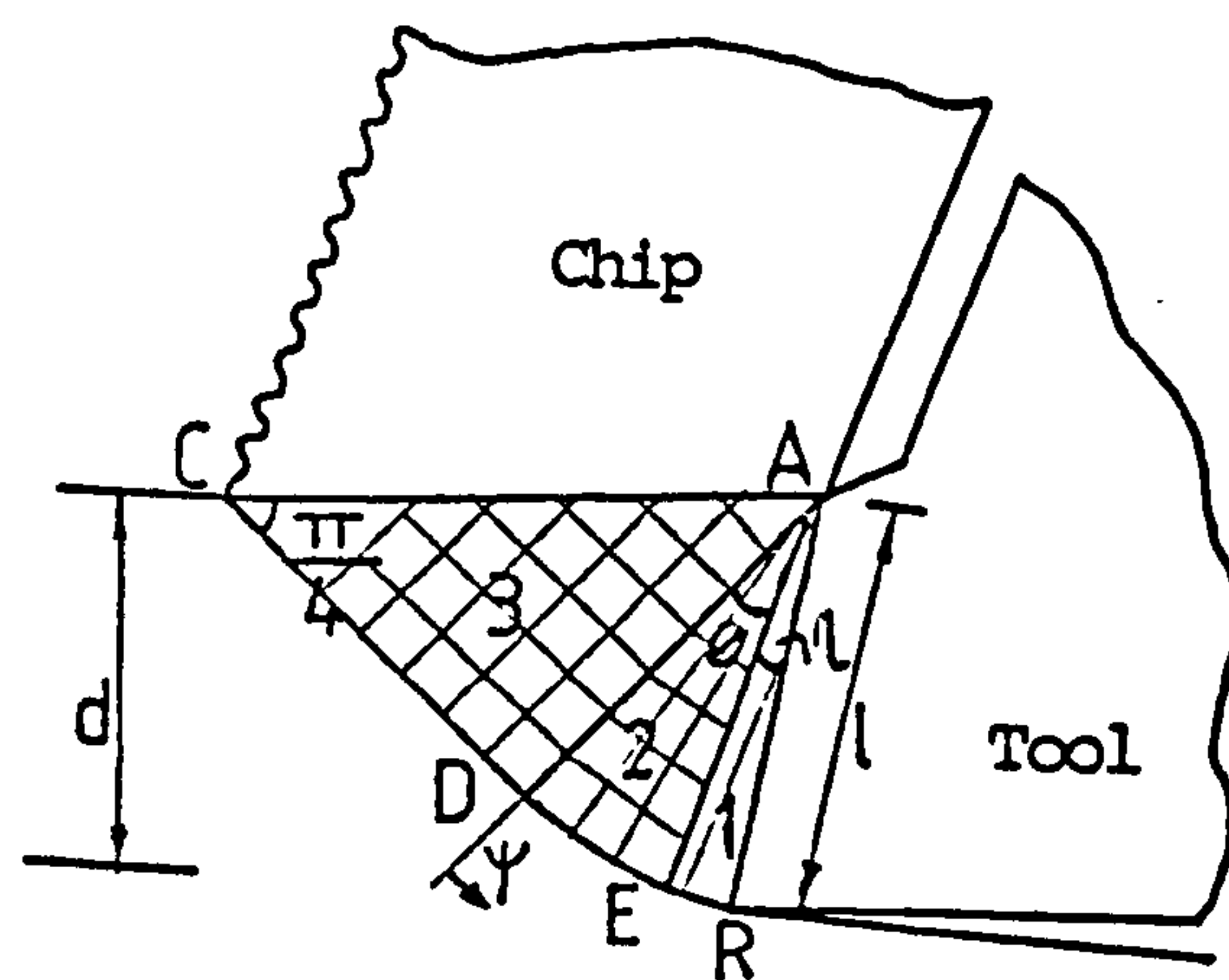
(a) slip-line field

Positive Rake



(b) Hodograph - positive rake tool (+ve)

FIG. 91: Slip-line field in machining with cut-away tool (81)



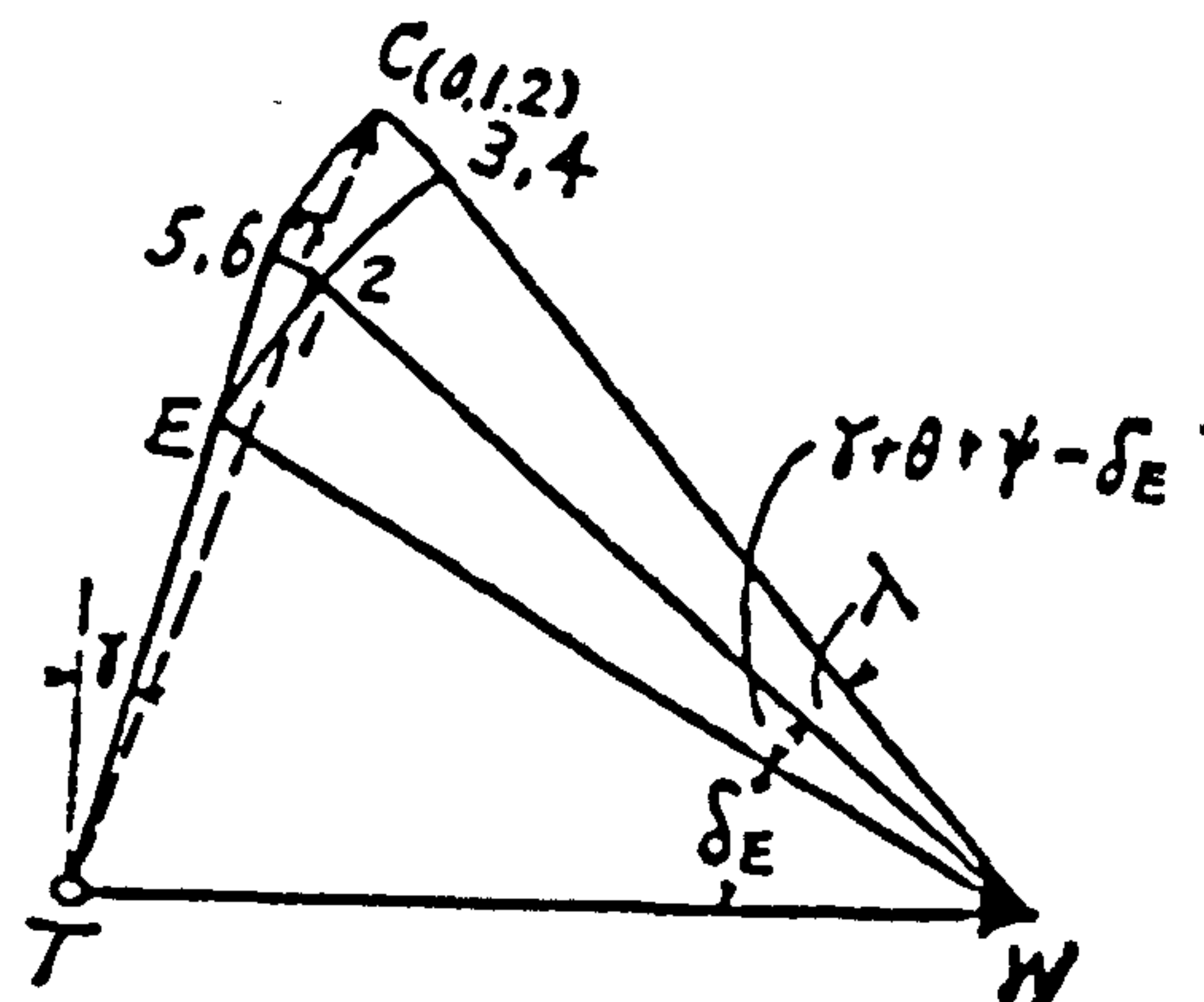
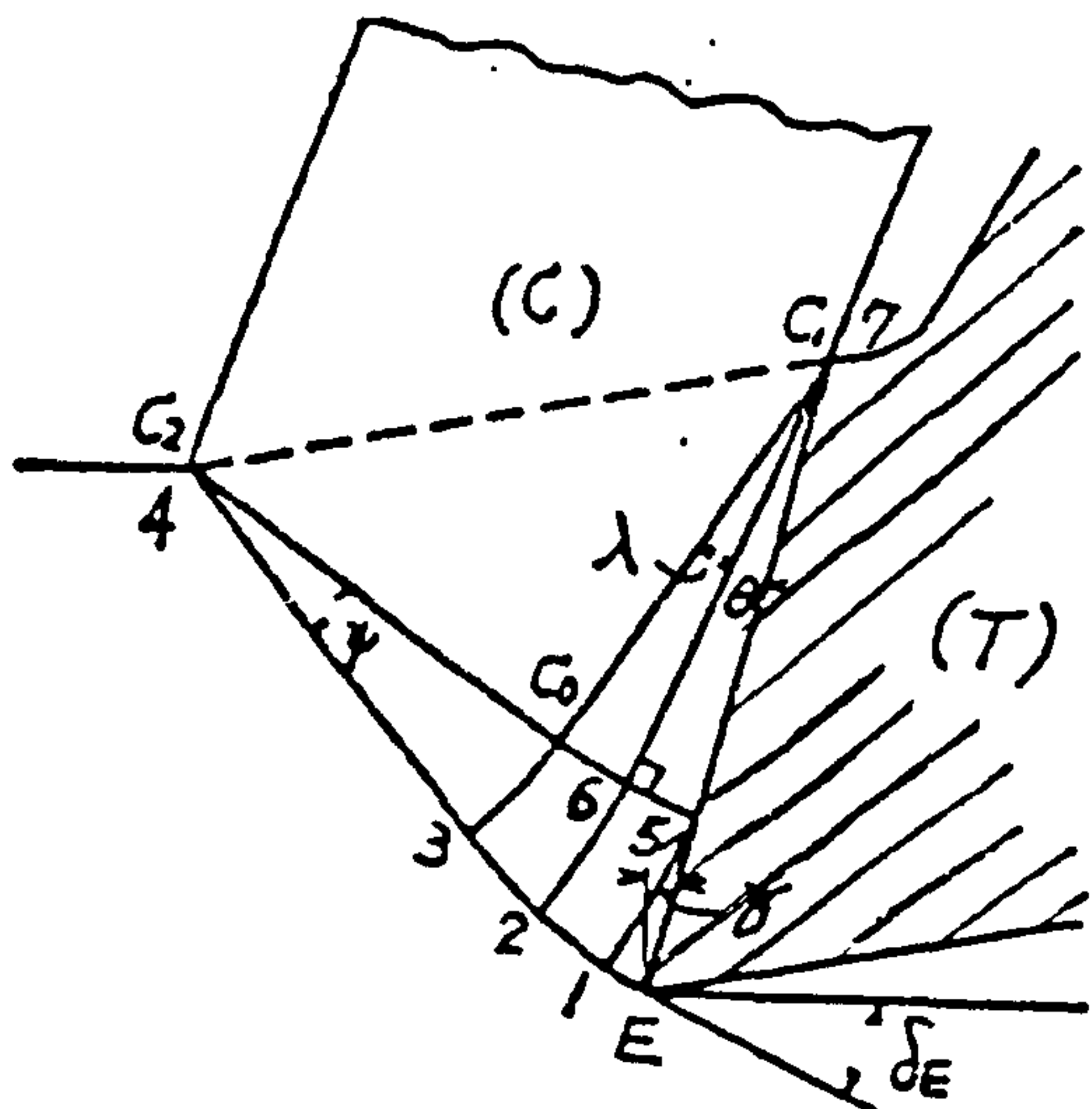


FIG.92 MODIFIED JOHNSON-USUI SOLUTION FOR RESTRICTED TOOL FACE. (A) SLIP LINE FIELD (B) HODOGRAPH (82)

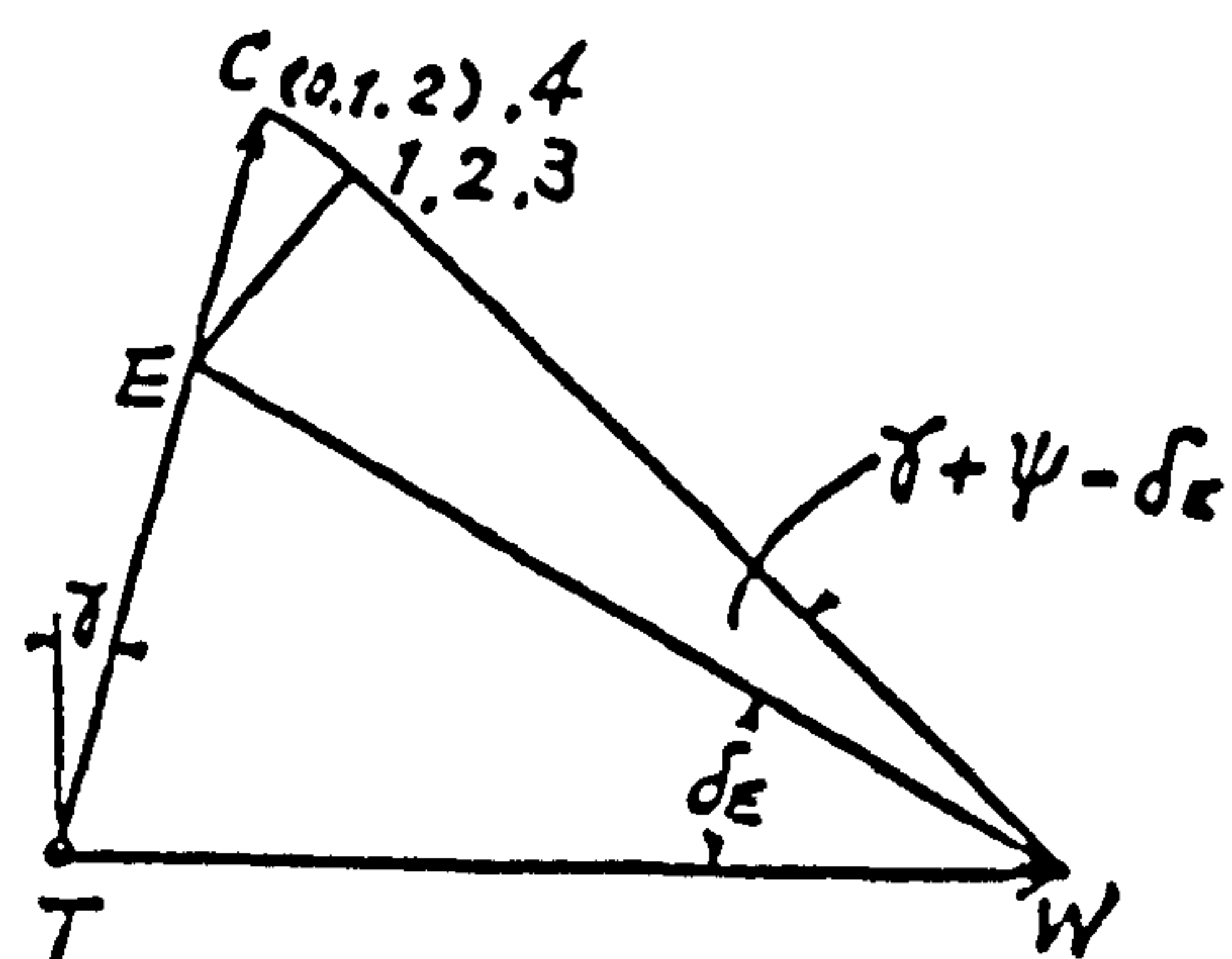
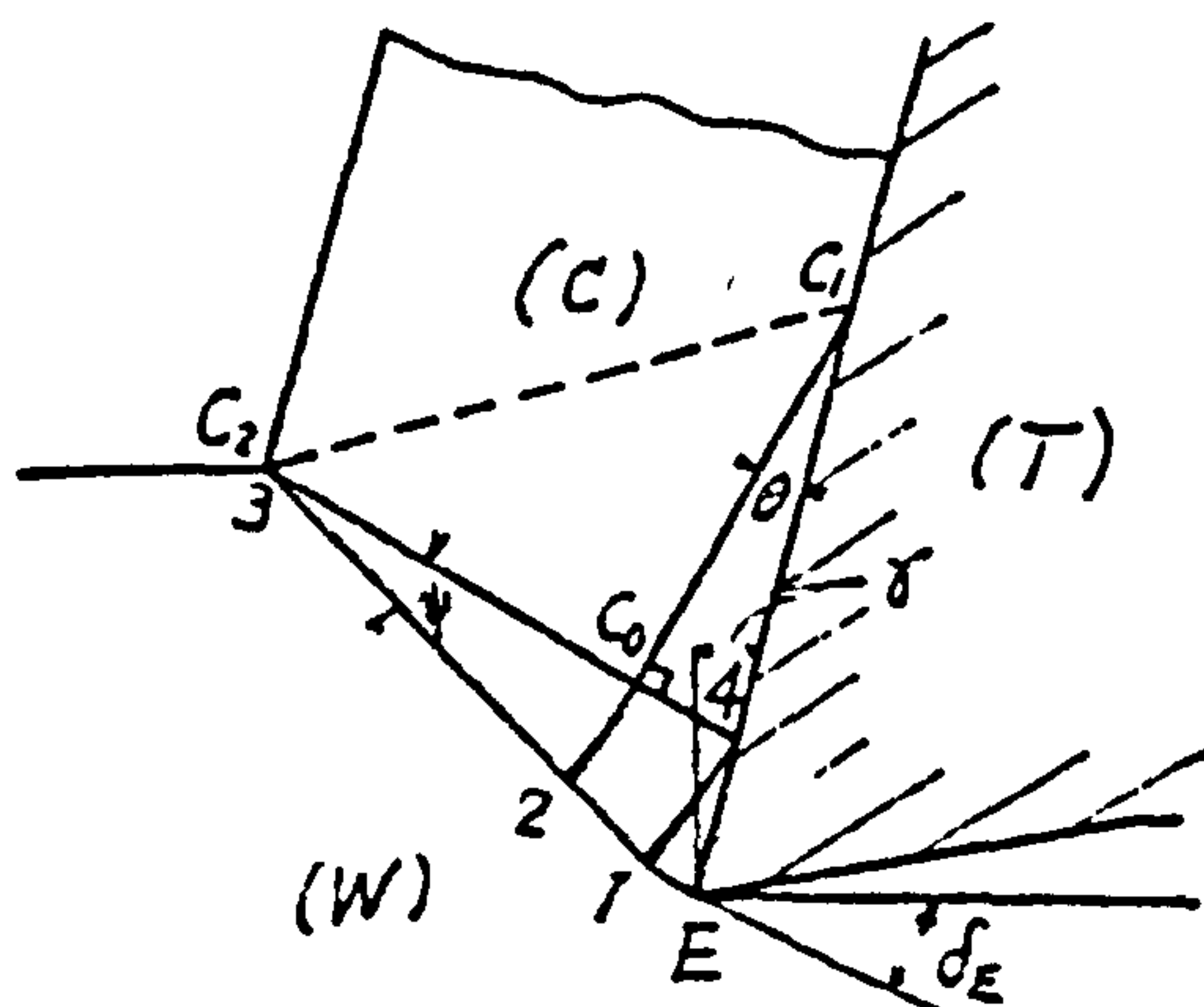
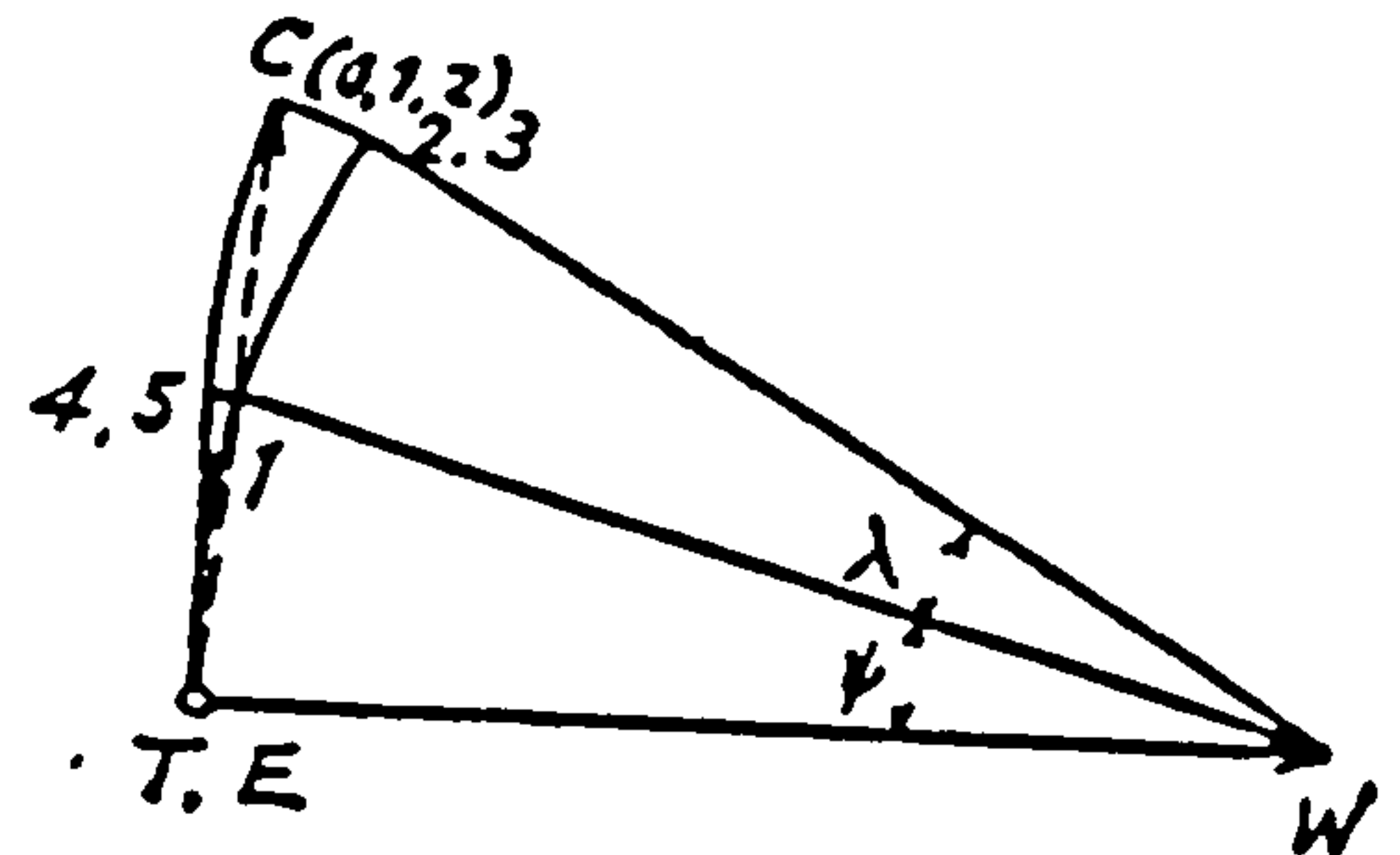
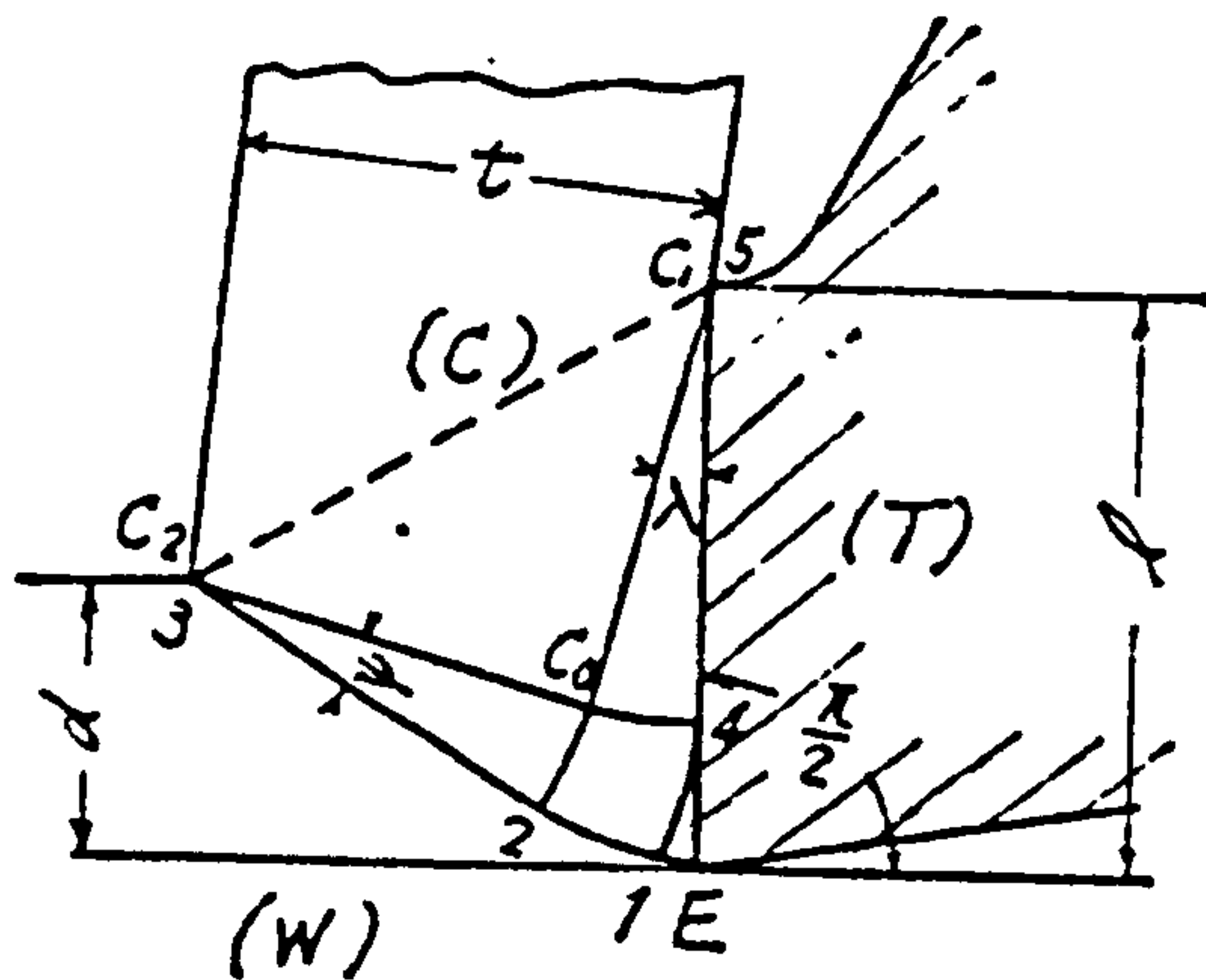
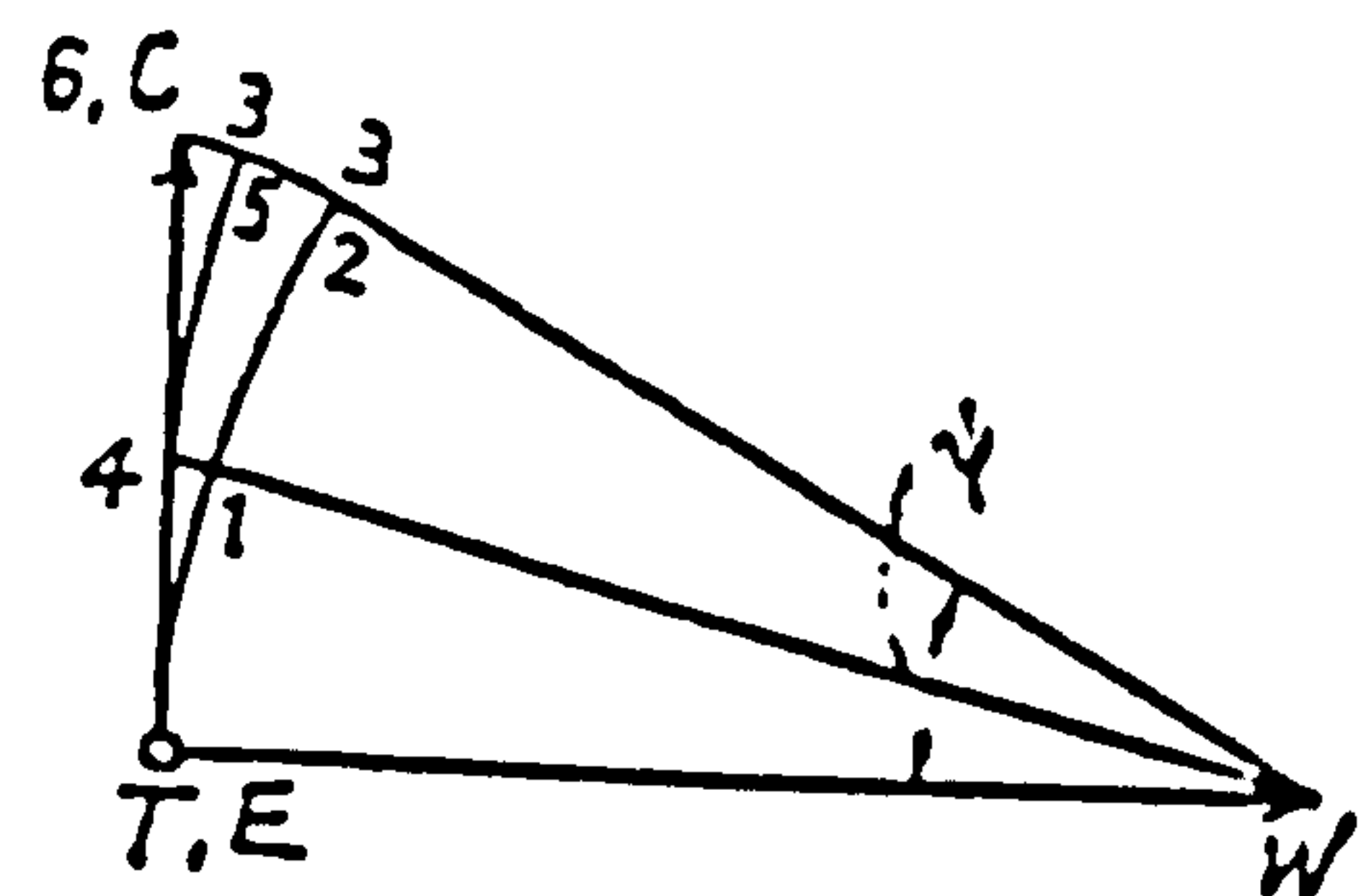
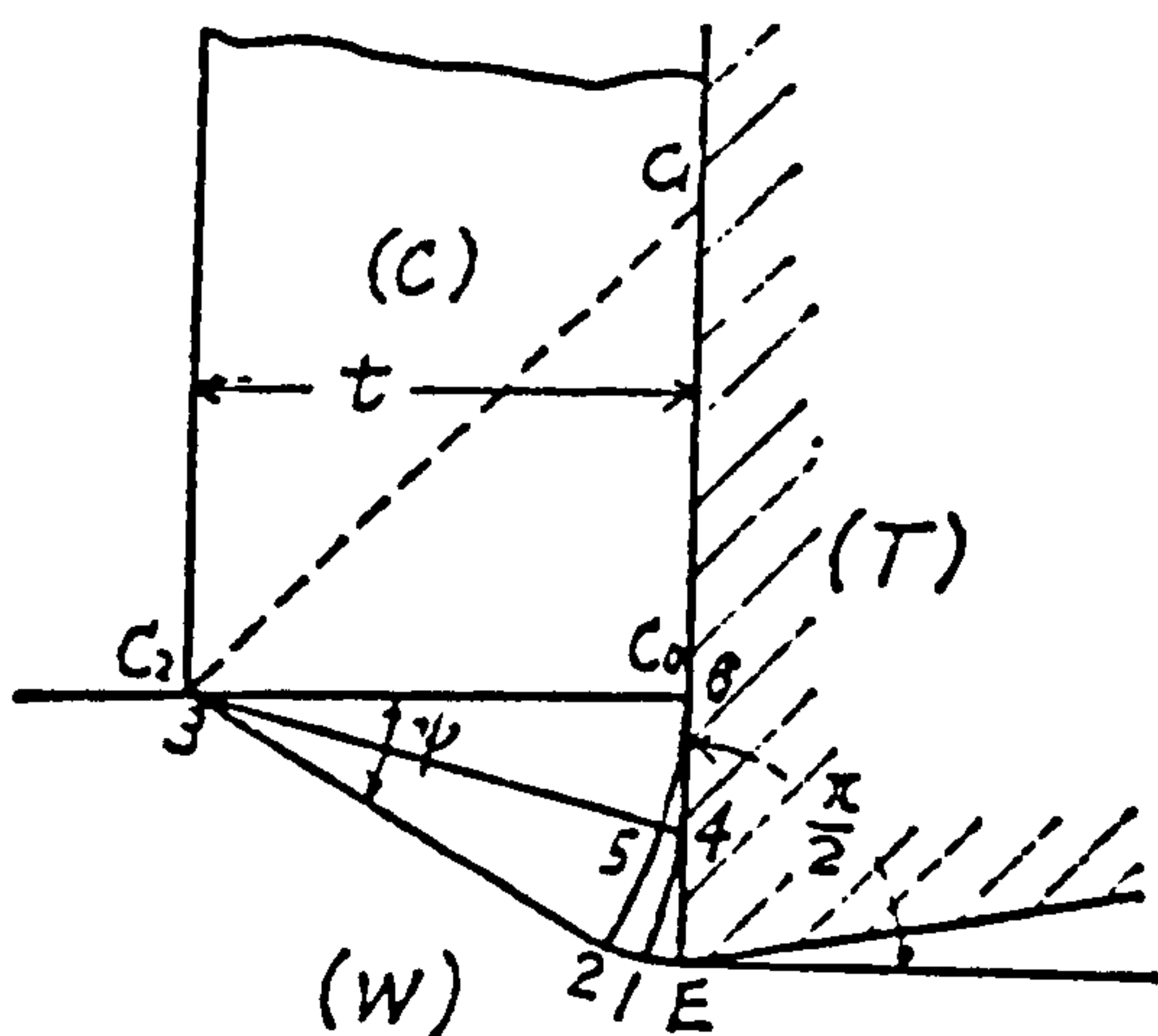


FIG.93 MODIFICATION OF FIG.92 FOR UNRESTRICTED TOOL FACE. (A) SLIP LINE FIELD (B) HODOGRAPH (82)



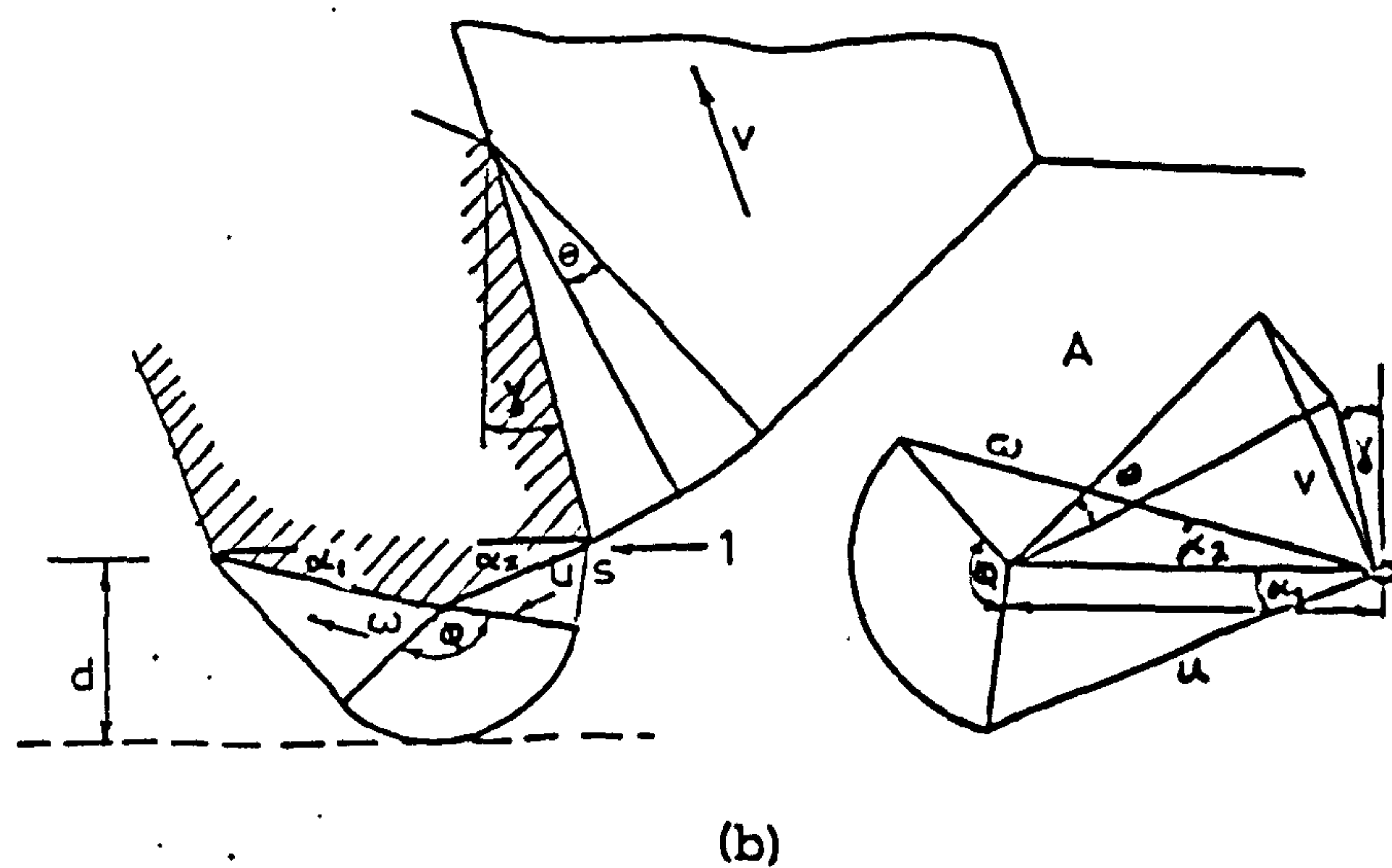
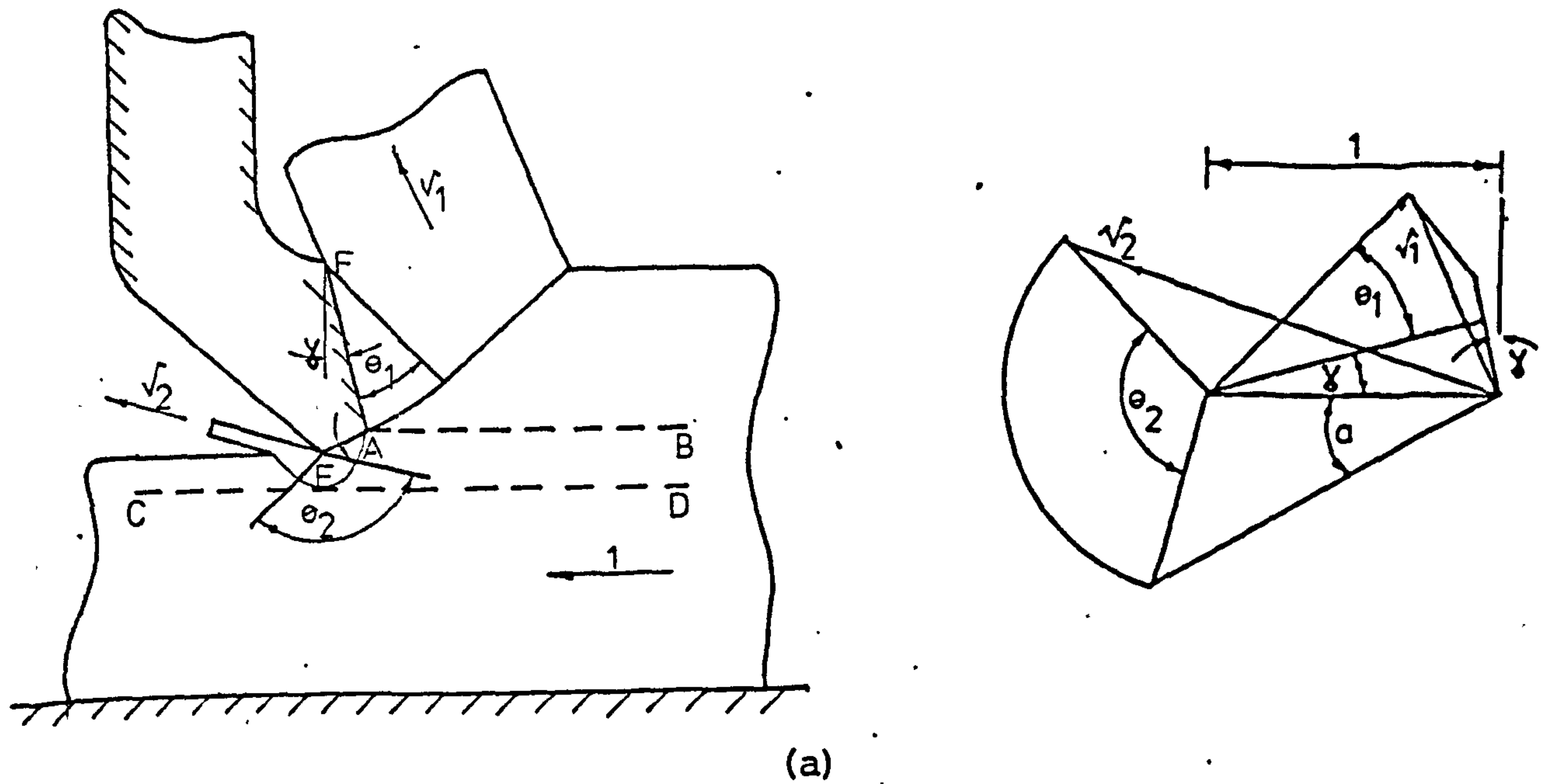
(A) MODIFICATION OF FIG. 92 FOR ZERO RAKE ANGLE AND STICKING FRICTION, SLIP LINE FIELD AND HODOGRAPH, (82)



(B) MODIFICATION OF FIG. 93 FOR ZERO RAKE ANGLE AND STICKING FRICTION, SLIP LINE FIELD AND HODOGRAPH (82)

FIG. 94 SLIP-LINE FIELD SOLUTIONS FOR RESTRICTED AND UNRESTRICTED CHIP-TOOL CONTACT, (82)

FIG. 95: Slip-line field and hodograph for restricted tool contact, where cutting edge radius is approximated by straight edges (79)



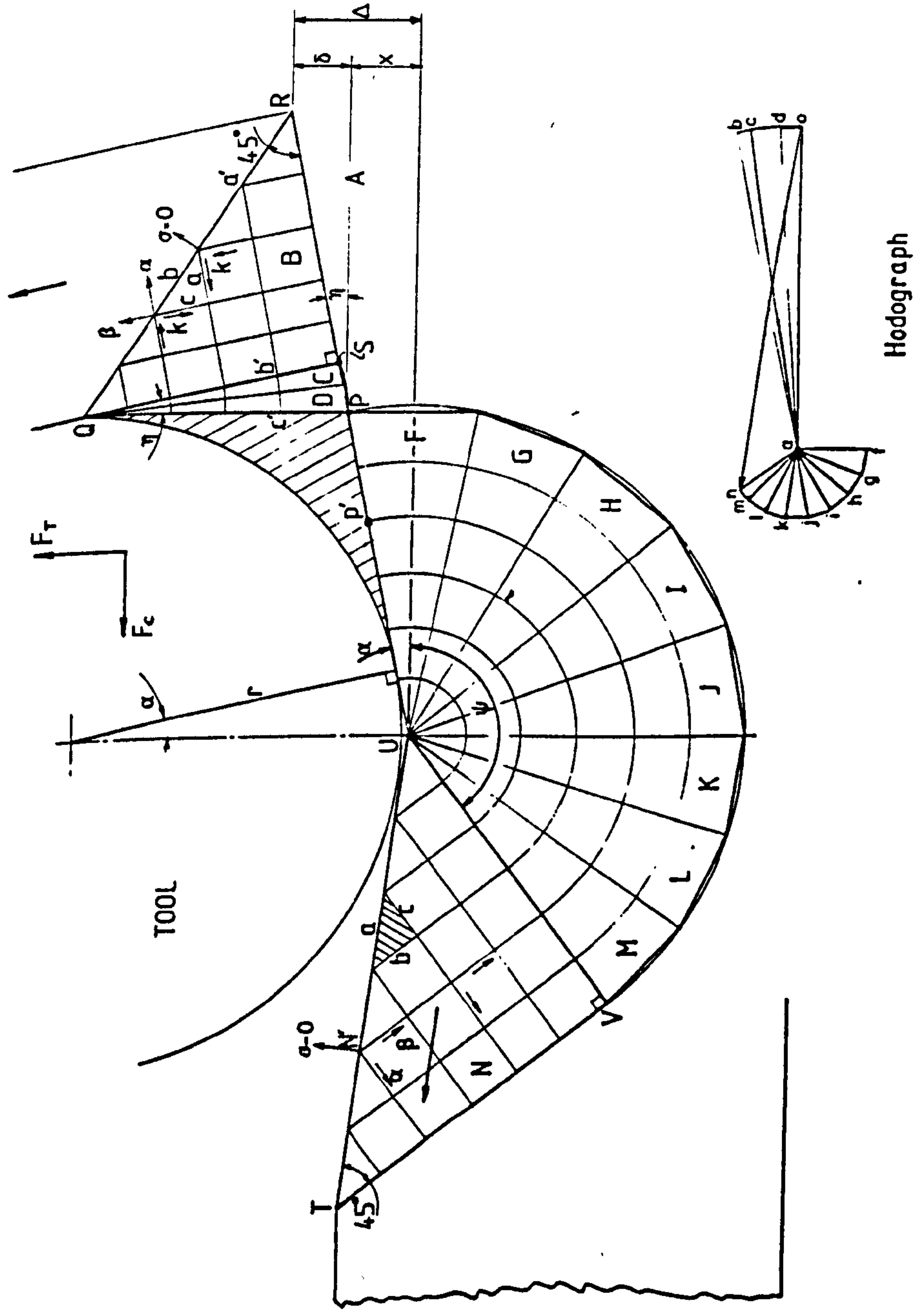


FIG.96 SLIP-LINE FIELD (INVALID), WHERE MATERIAL IS ASSUMED TO FLOW BENEATH THE TOOL, WHEN MACHINING WITH A BLUNT TOOL.

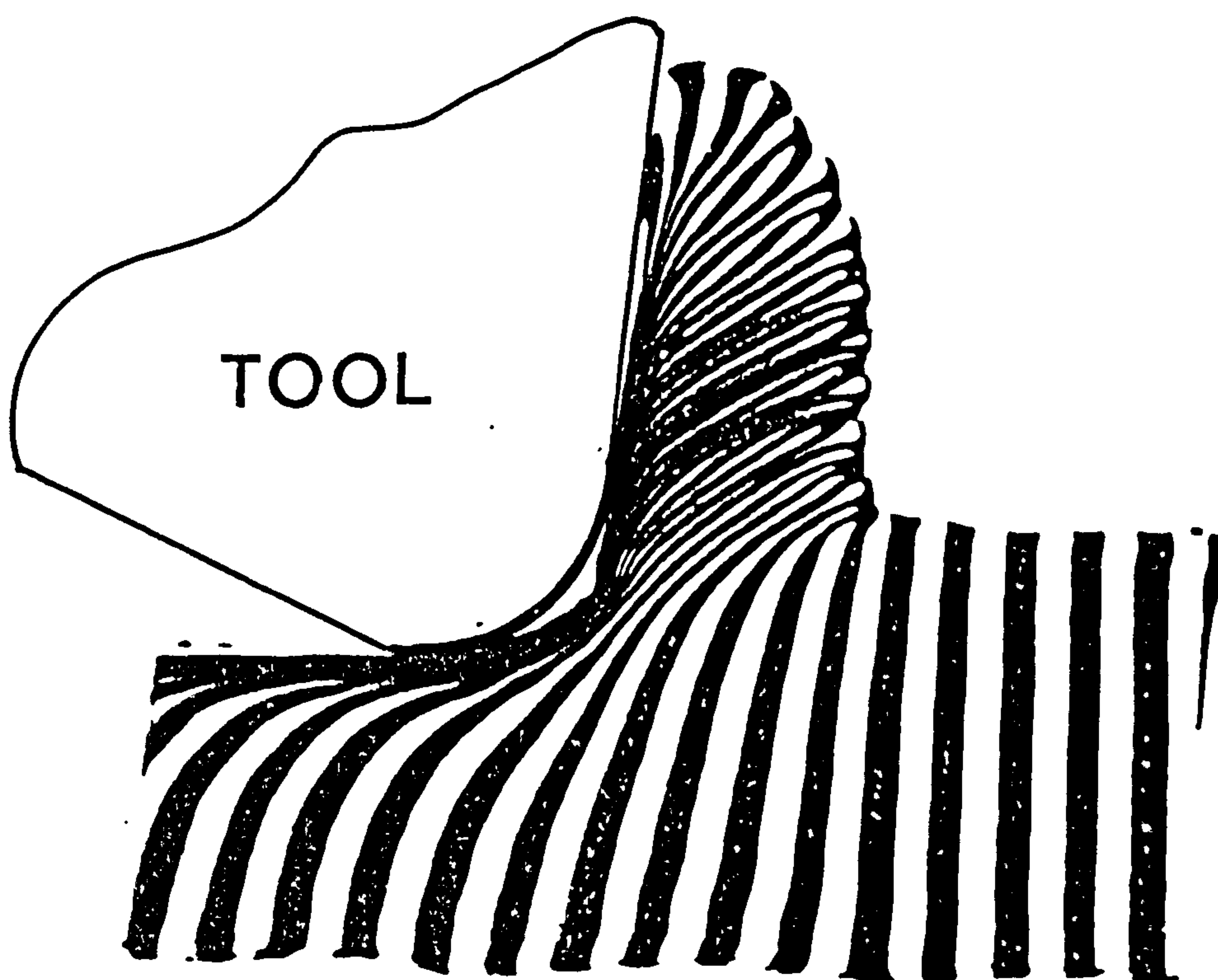
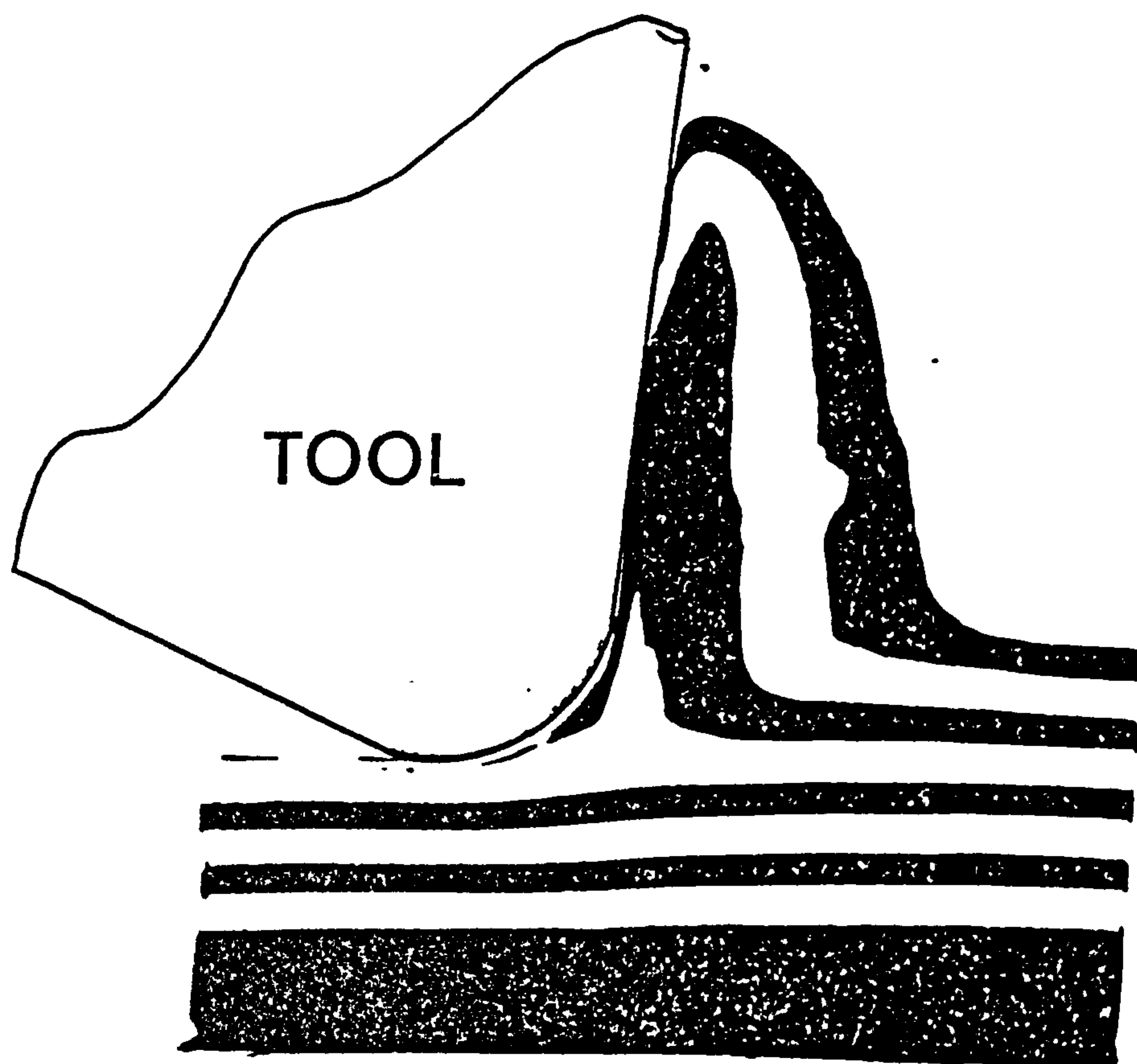
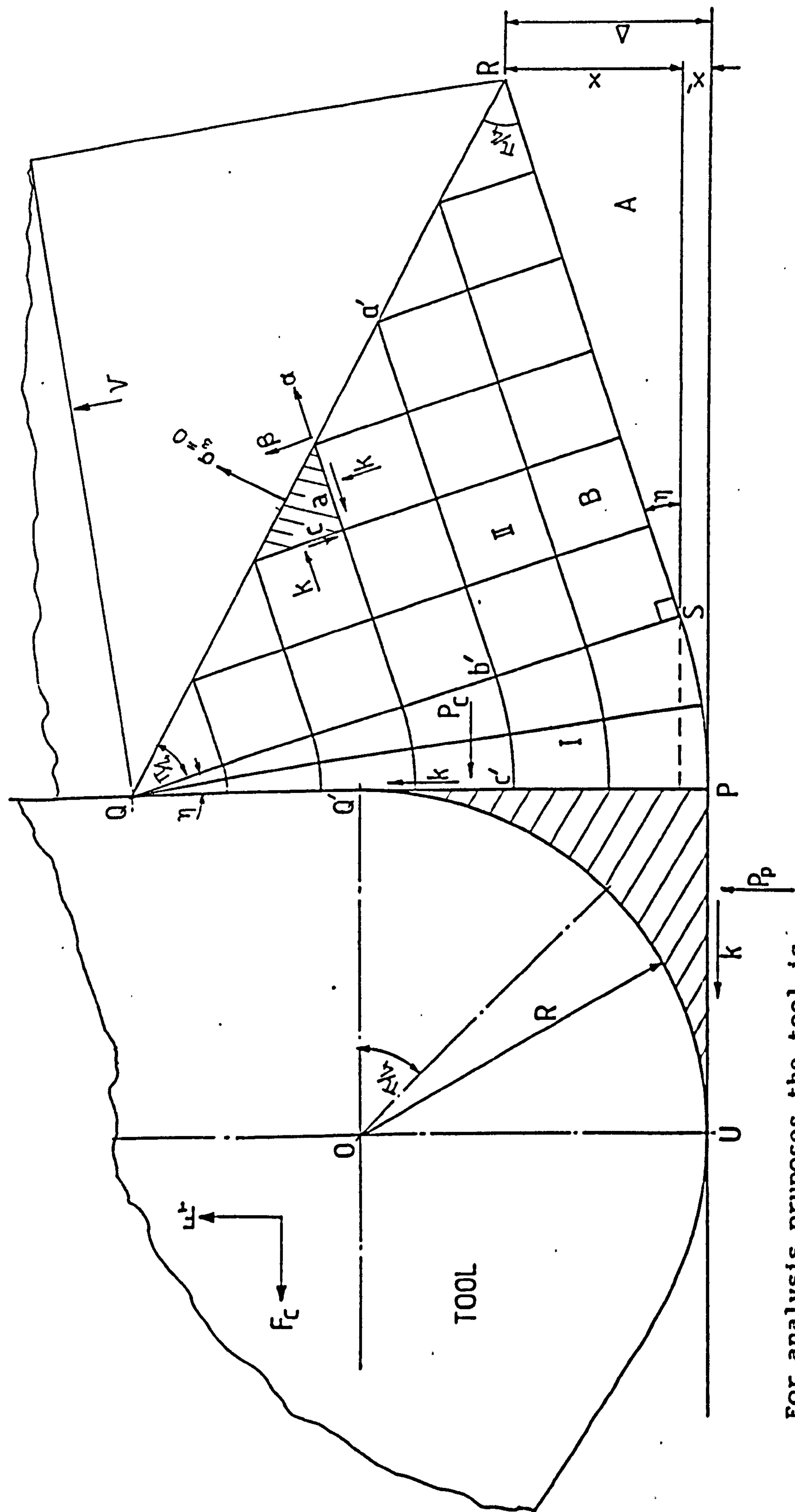
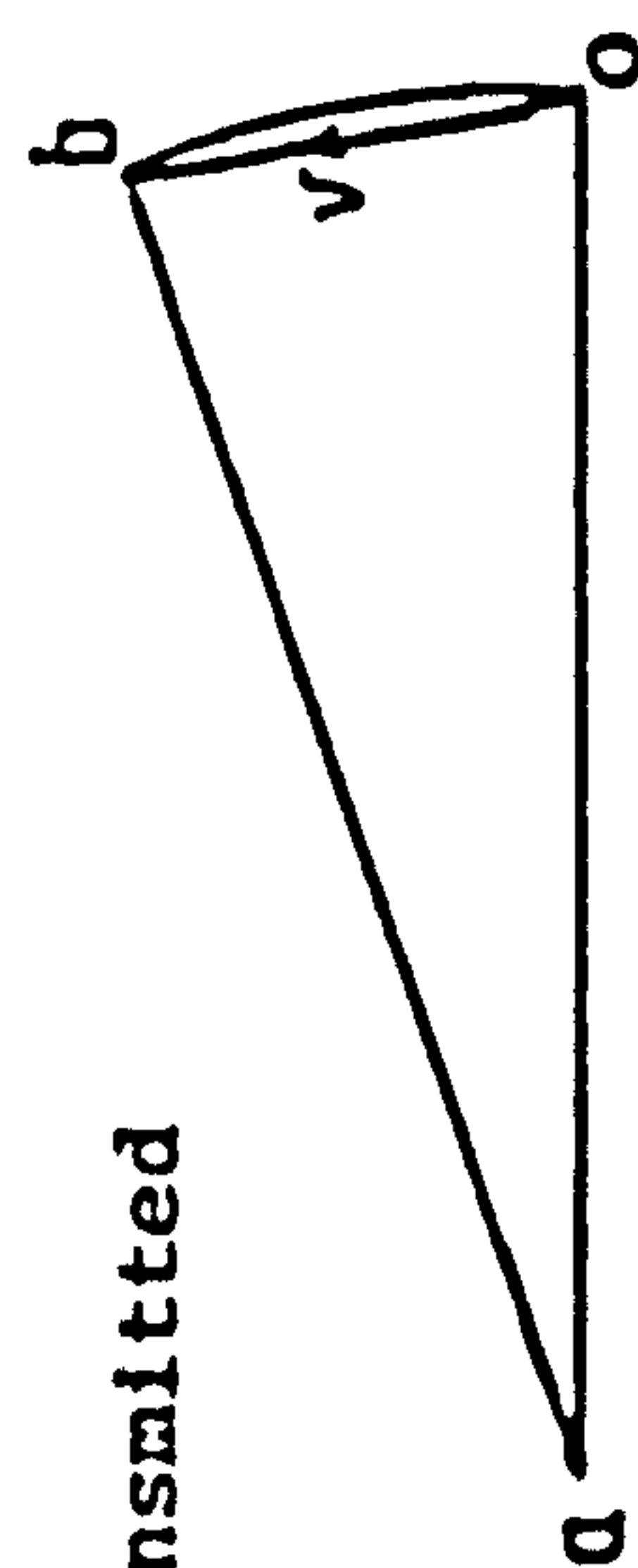


FIG. 97 DEFORMATION PATTERNS PRODUCED IN HORIZONTAL AND VERTICAL LAYERS OF PLASTICINE, WHEN SIMULATING THE CUTTING ACTION OF BLUNT TOOLS, USING A PERSPEX MODEL TOOL.



For analysis proposes the tool is considered to be of restricted contact design up to the point Q . No stress is transmitted across QR .

FIG. 98: Slip-line field in machining with a blunt tool and the corresponding hodograph



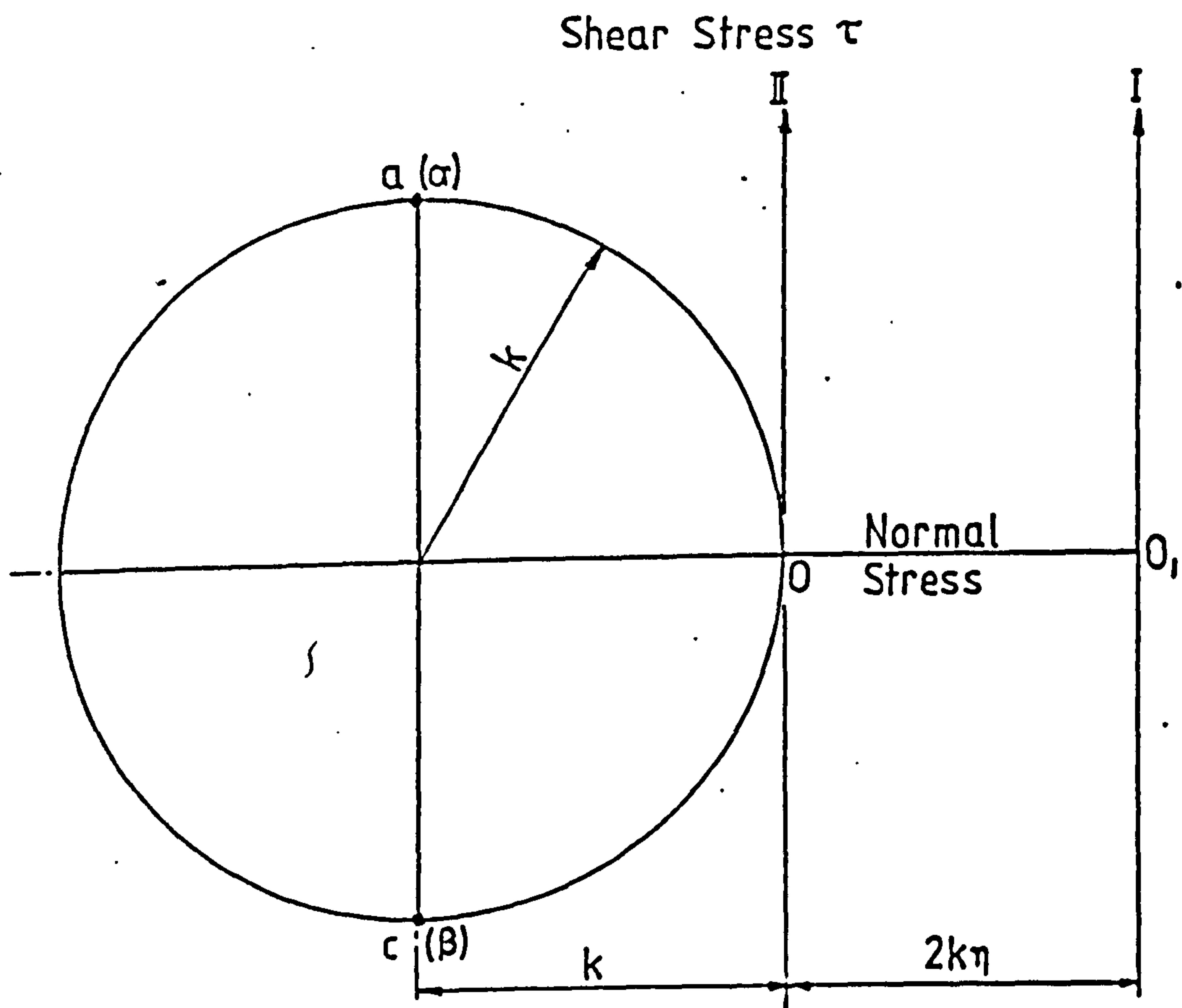


FIG. 99(a): Mohr's stress circle for slip-line field in Fig. 98

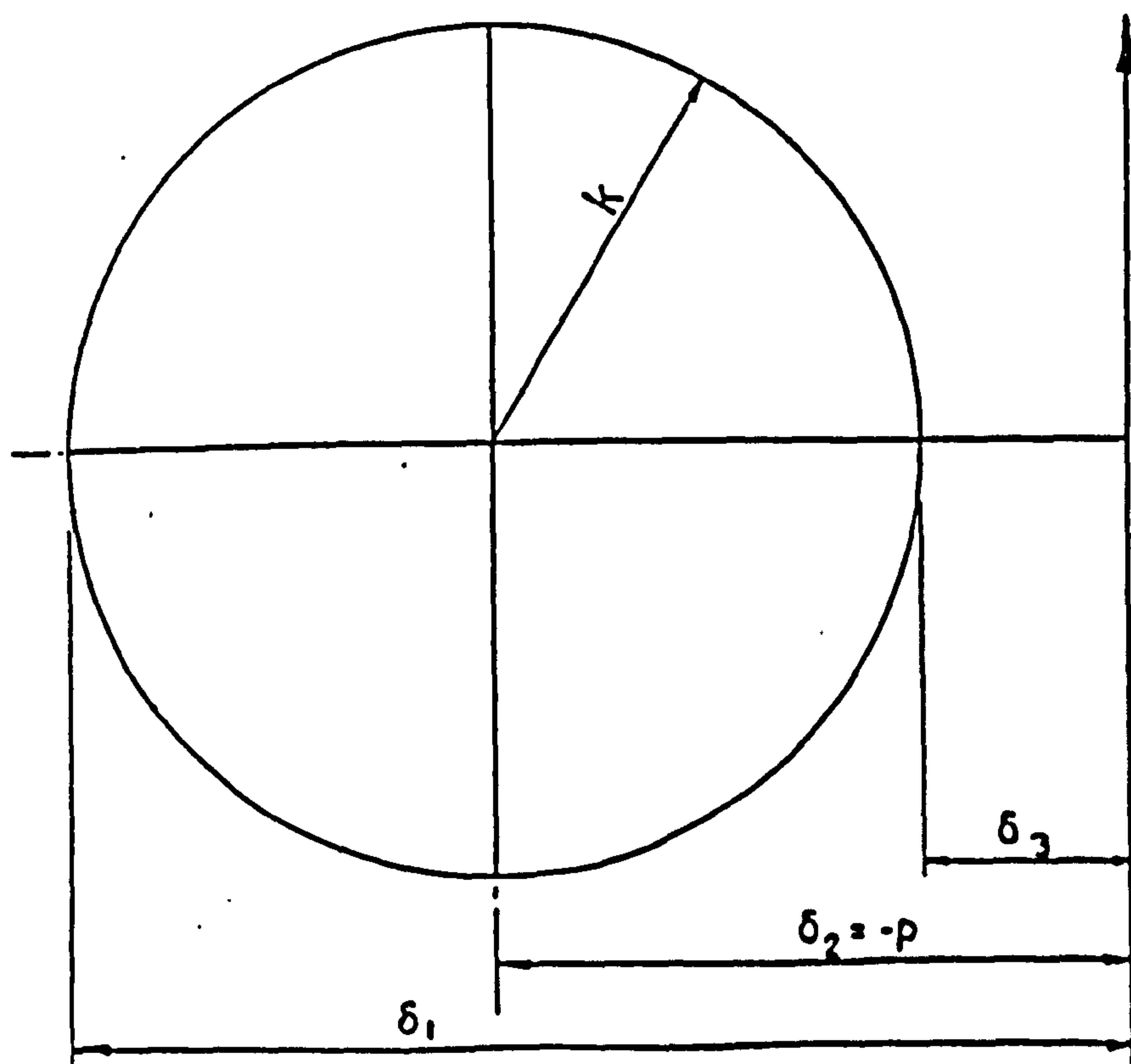


FIG. 99(b): Mohr's stress circle

Uni-axial compression tests
carried out in accordance to
standard procedures (89).

x Copper Specimen no 1
o Copper Specimen no 2

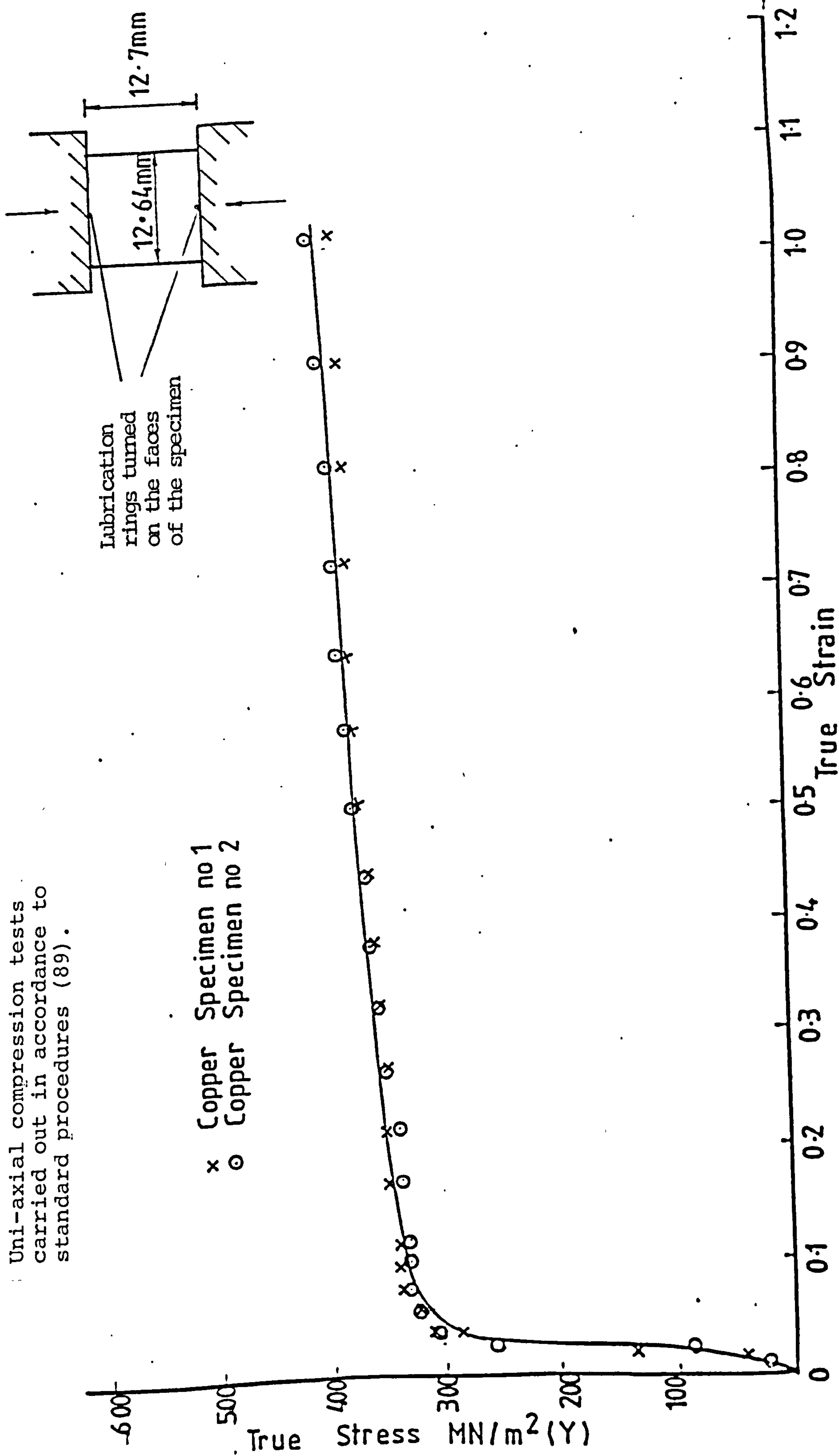
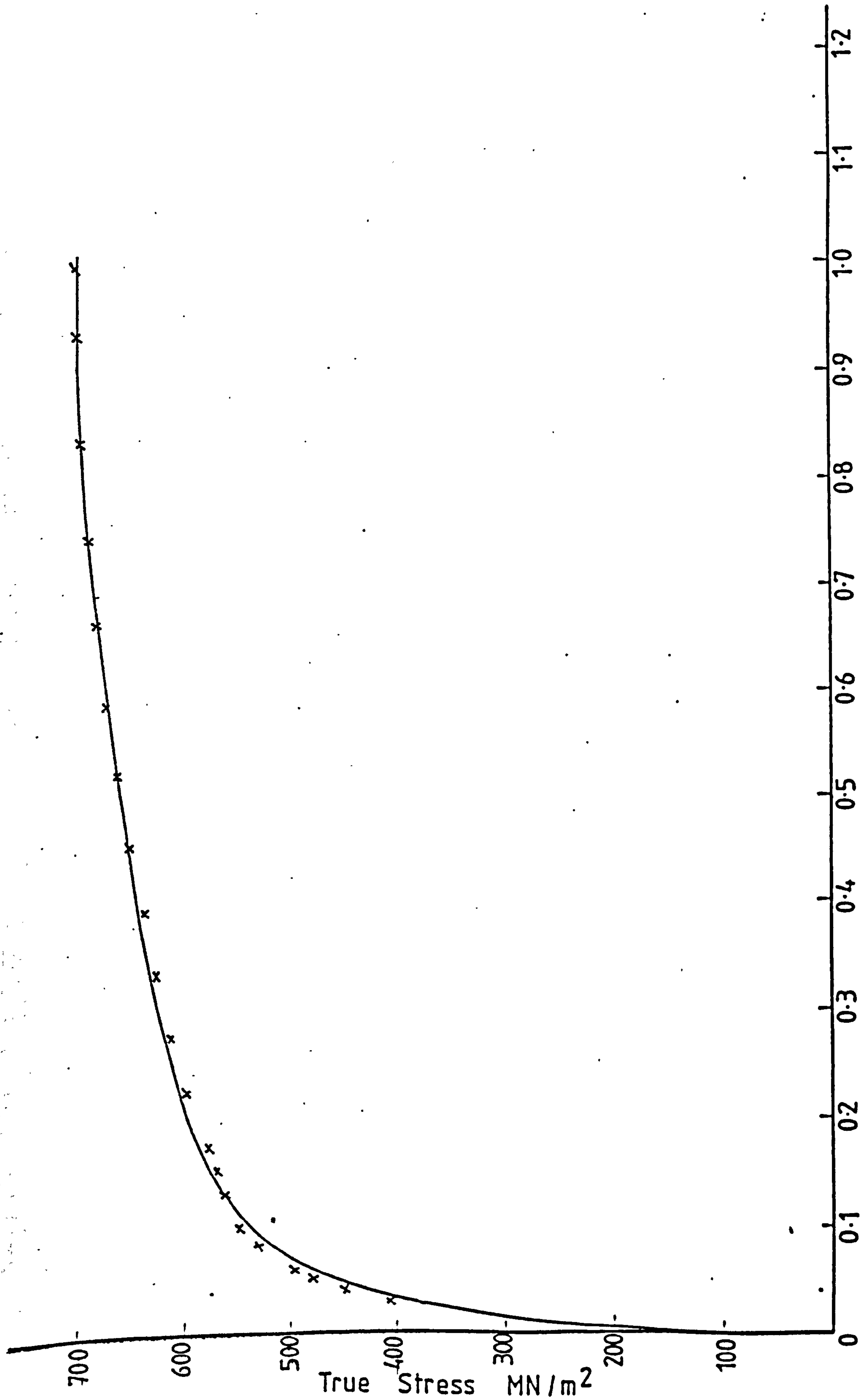


FIG.100(A) STRESS-STRAIN CURVE FOR COPPER WORKPIECE FROM COMPRESSION TEST RESULTS



True Strain

FIG.100(B) STRESS-STRAIN CURVE FOR LEADED STEEL FROM COMPRESSION TEST RESULTS

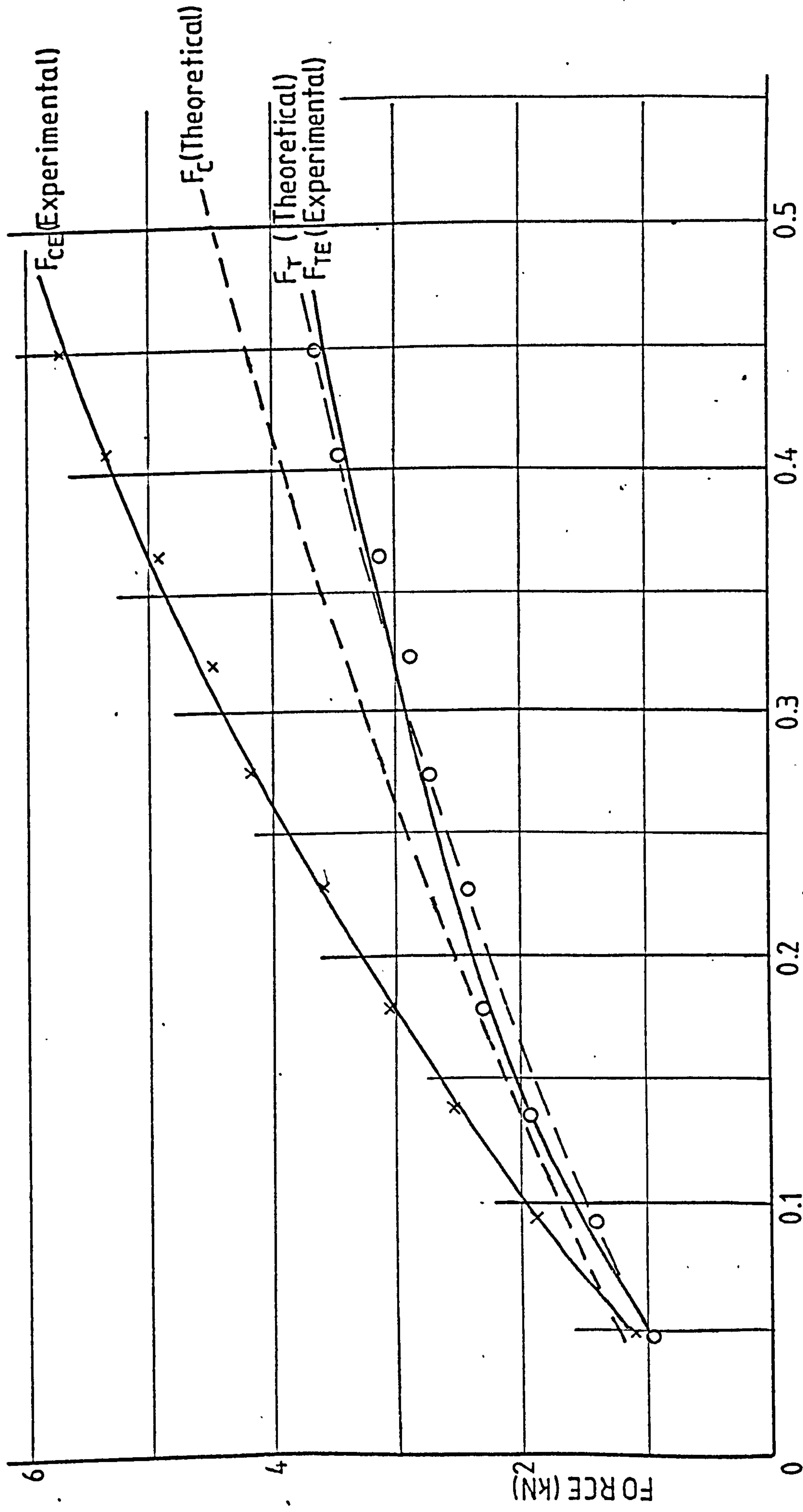
Workpiece Specimen:-Copper.

Cutting Tool:-0.56 mm radius.

Groove Cutting.

Lubricant:-Sulphurised Oil.

Cutting Speed:-95mm/min.



UNDEFORMED CHIP THICKNESS Δ (mm)

FIG.101 (a): Experimental and theoretical forces with variation in the depth of cut.

Workpiece Specimen:--Copper.

Cutting Tool:--0.81 mm radius.

Groove Cutting.

Contact Length $L=0.038+13.21\Delta-10.6\Delta^2$

Lubricant :-- Sulphurised Oil.

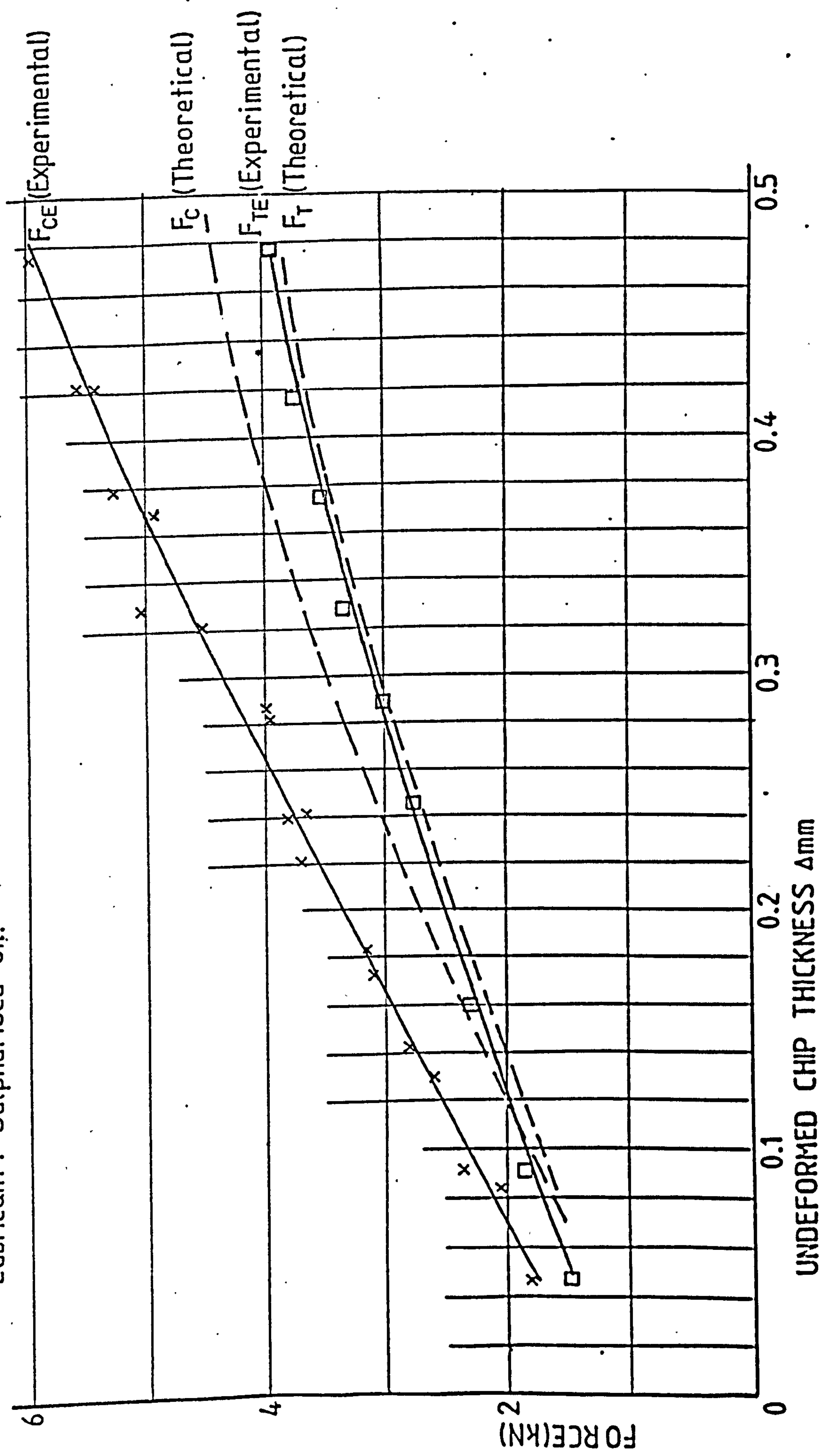


FIG. 101(b): Experimental and theoretical forces with variation in the depth of cut

Workpiece Specimen:-Copper.

Cutting Speed:-95mm/min.

Groove Cutting.

Lubricant:-Sulphurised Oil.

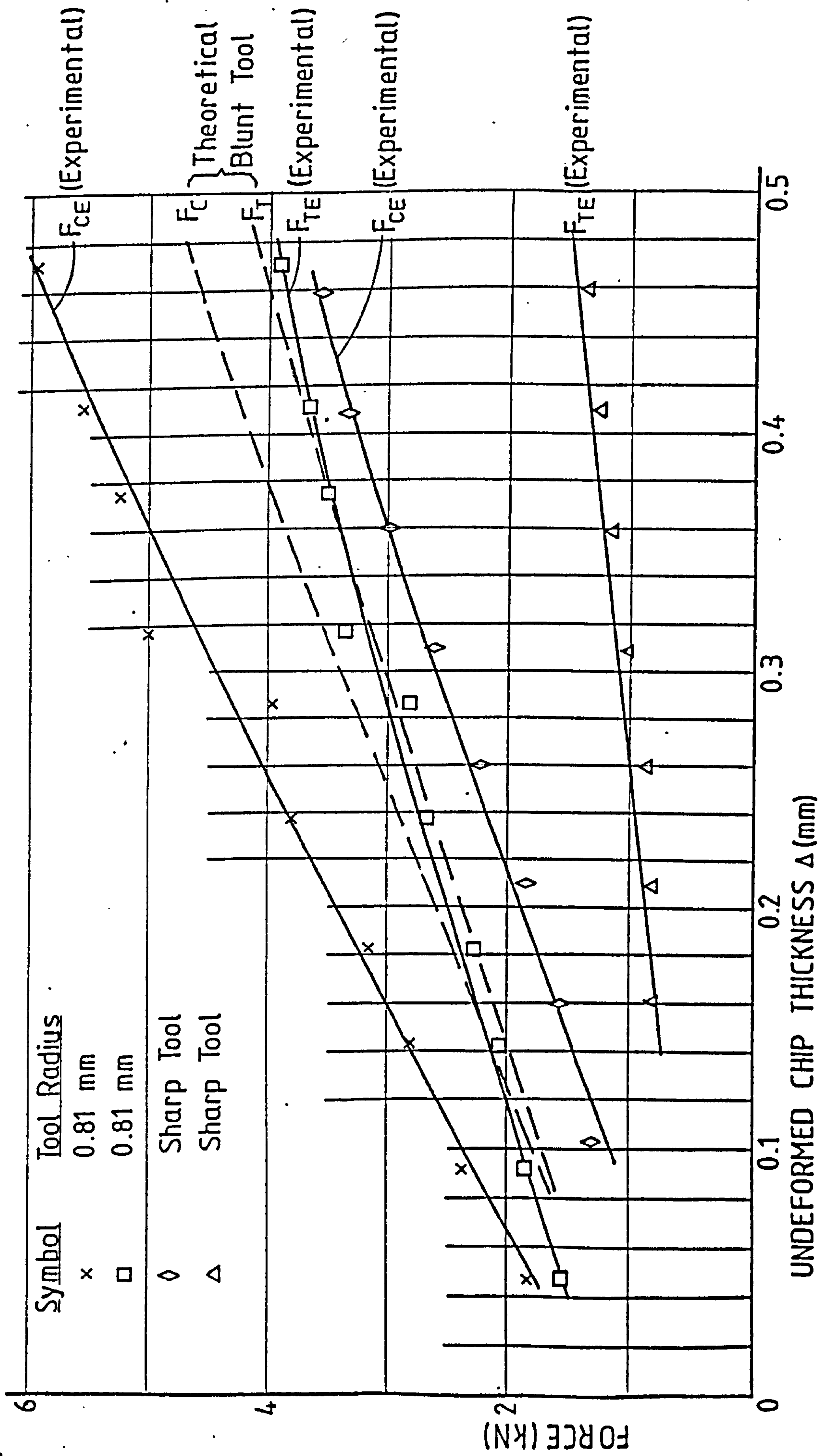


FIG. 102: Comparison of experimental and theoretical forces for sharp and blunt tools

Workpiece Specimen:-Lead Steel.

Cutting Tool:-0.56 mm radius.

Groove Cutting.

Chip Tool Contact Length= $0.112+3.95 \Delta -1.986 \Delta^2$

Cutting Speed:-95mm/min.

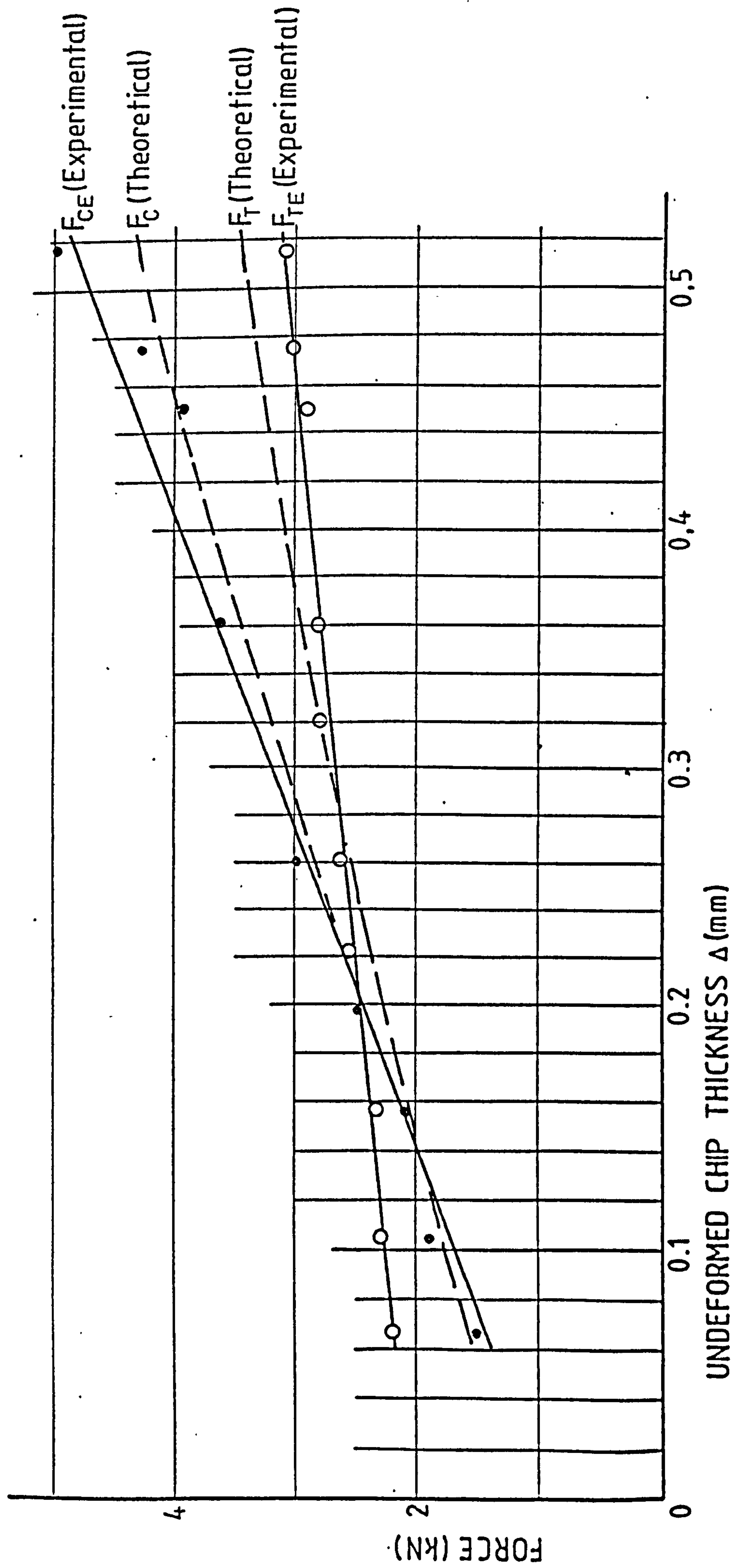


FIG. 103: Variation of forces with depth of cut when machining lead steel

ivob

CHIP

25

02

Tool:

145

A

 $\Delta=0.25\text{mm}$ 

FIG. 104 SLIP LINE FIELD TO SCALE FOR CUTTING CONDITIONS STATED

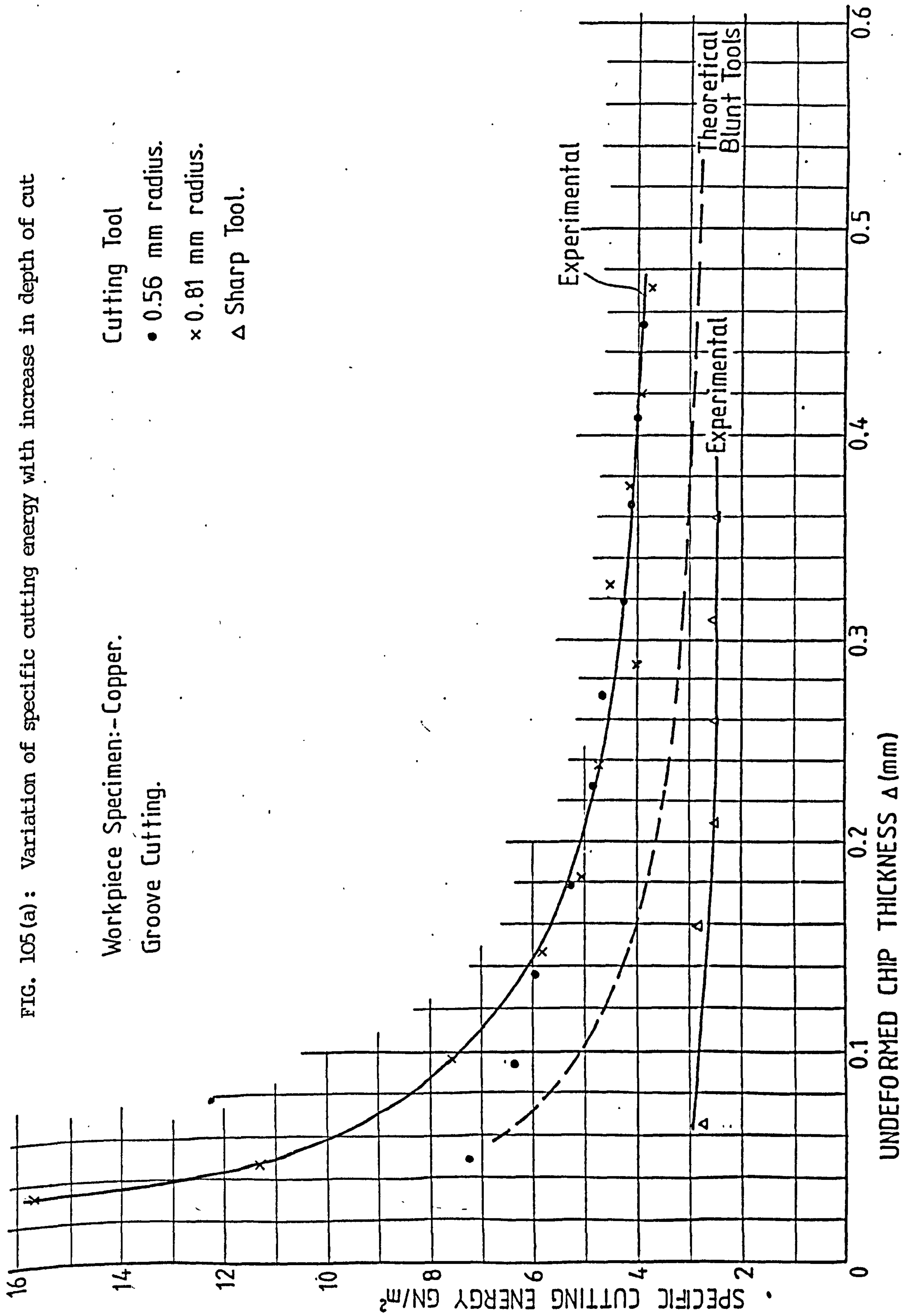


Fig.105(a)

FIG. 105(b): Variation in specific cutting energy with increase in depth of cut

Workpiece Specimen:-Lead Steel.

○-Experimental.

Groove Cutting.

●-Theoretical.

Cutting Tool:-0.56 mm radius.

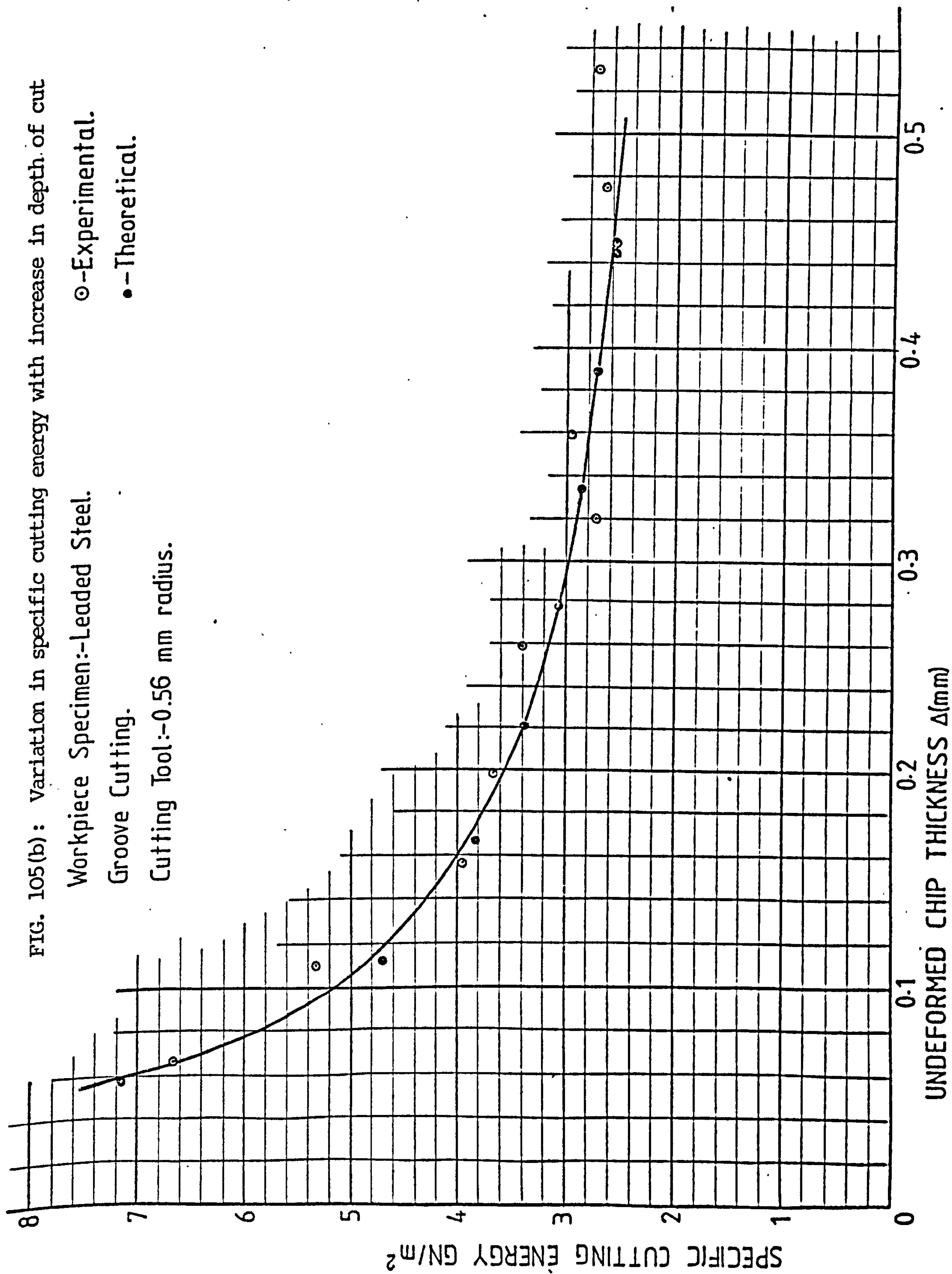


Fig.105(b)

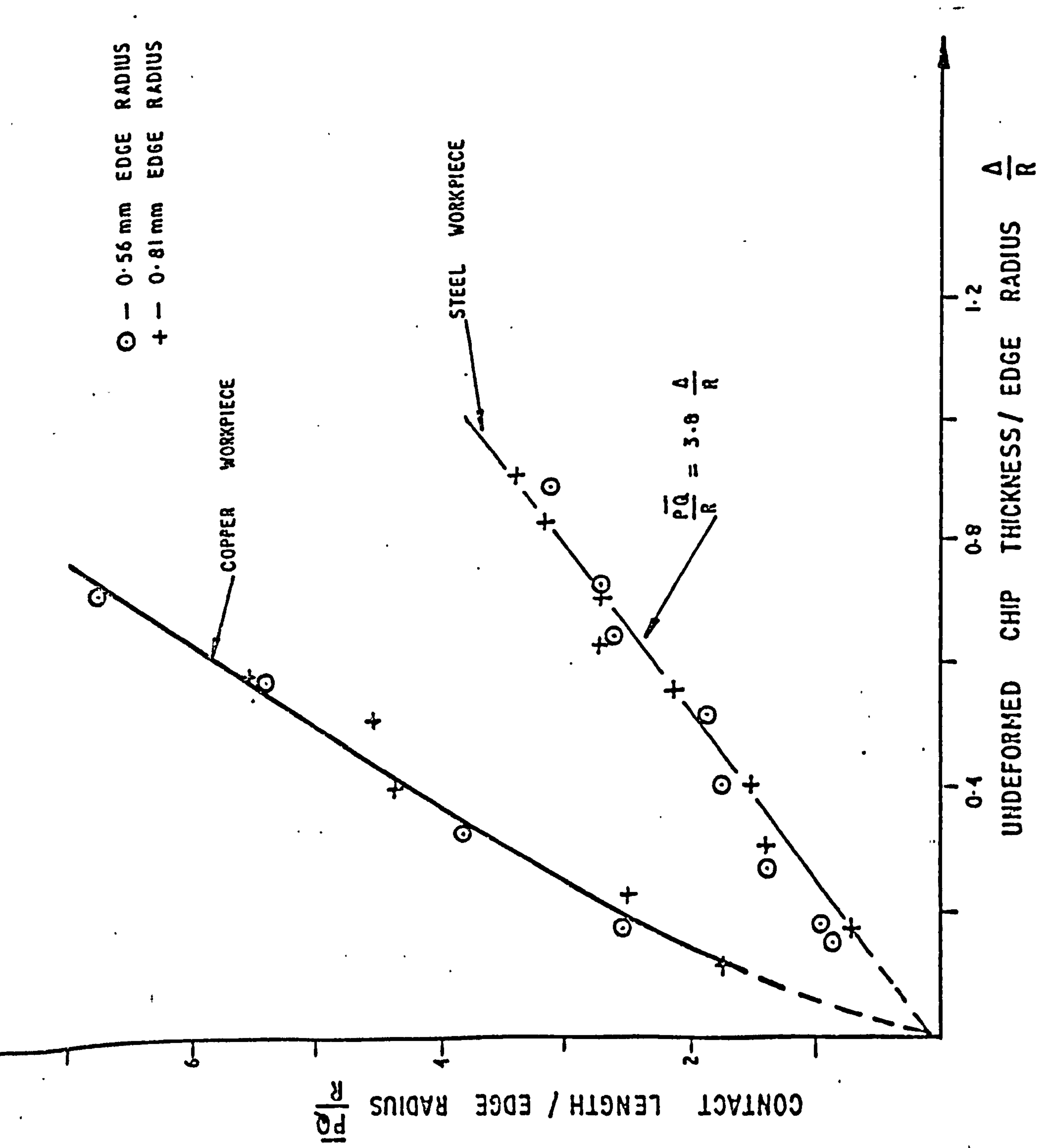


FIG. 106 CHIP TOOL CONTACT LENGTH/EDGE RADIUS VS UNDEFORMED CHIP THICKNESS/ EDGE RADIUS DERIVED FROM SIMULATION TESTS.

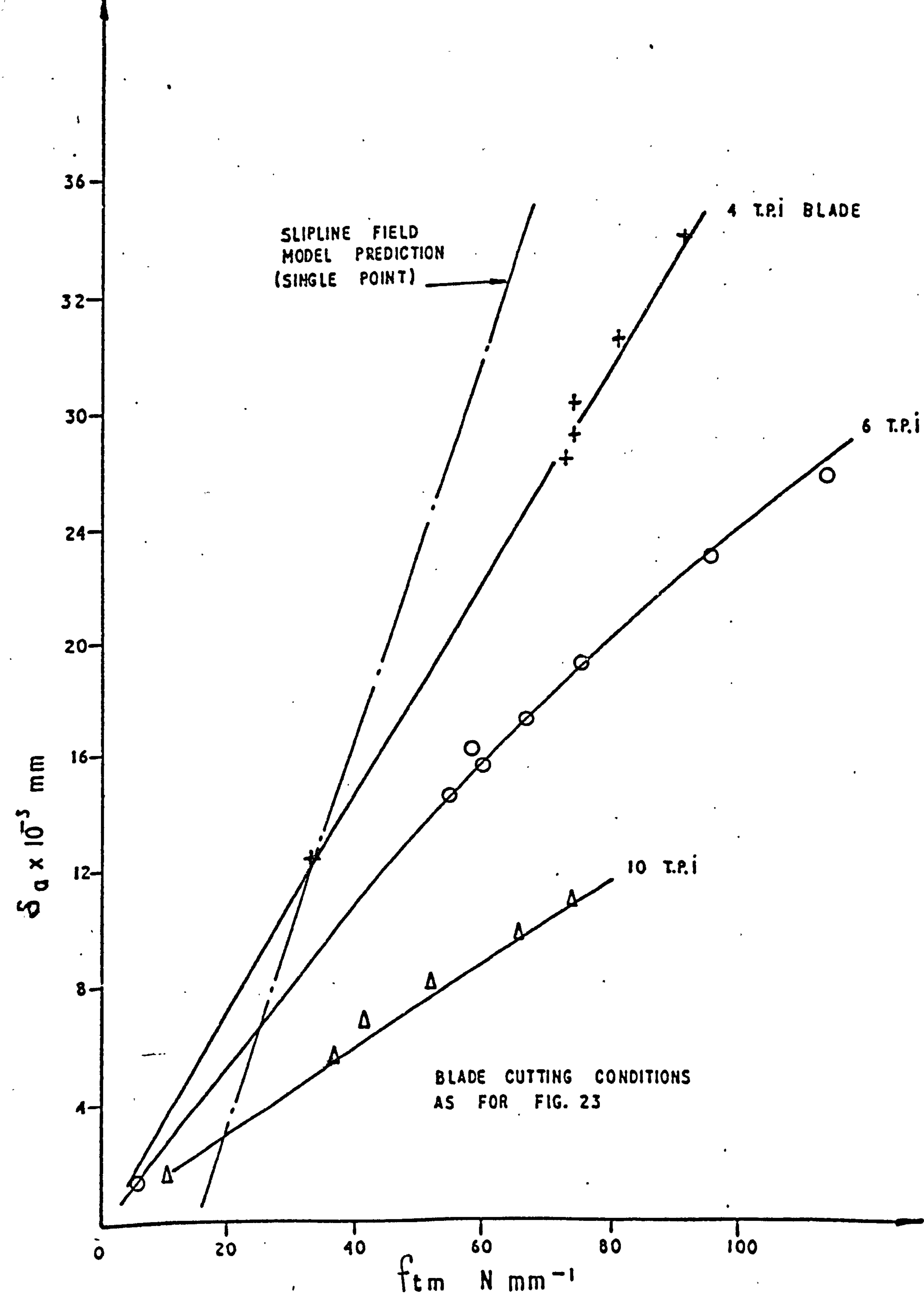


FIG. 107

COMPARISON OF SINGLE POINT PERFORMANCE
(FROM THE MODEL) AND BLADES OF DIFFERENT
PITCH.

Standard Blades (Raker Set)

400 x 40 x 2 x 4 T.P.I.)
 400 x 40 x 2 x 6 T.P.I.) Brand 'X'
 400 x 32 x 1.6 x 10 T.P.I.)

Steel workpiece (Enla)

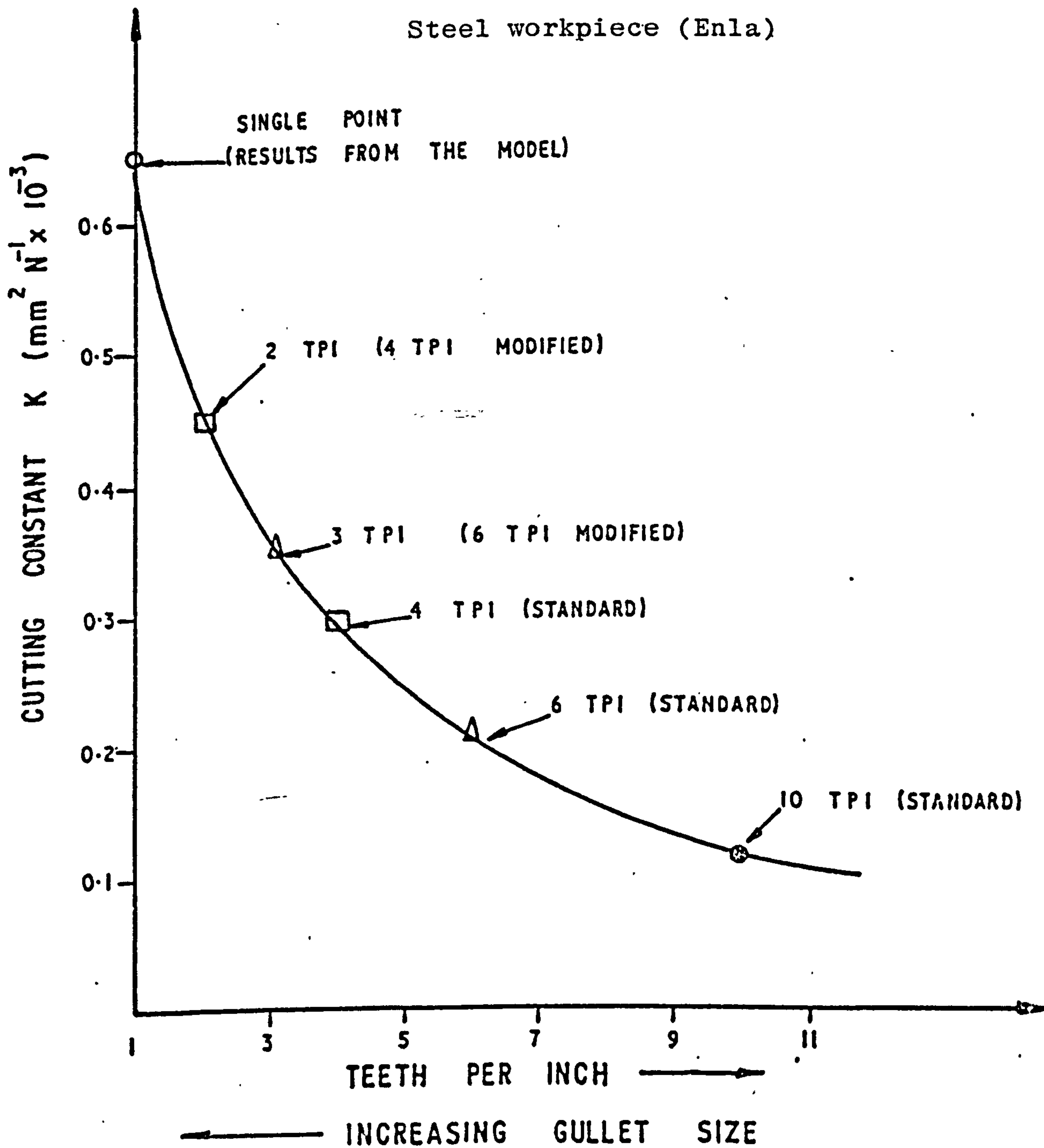


FIG. 108 COMPARISON OF THE PERFORMANCE OF NEW AND MODIFIED BLADES OF DIFFERENT PITCH.

WORKPIECE: MILD STEEL; 50 mm BREADTH x 25 mm DEPTH
 BLADE: 400 x 40 x 2 x 4 T.P.I. BRAND 'X'
 HYDRAULIC SAW MACHINE
 76 STROKES / MIN
 CUTTING FLUID: AIR

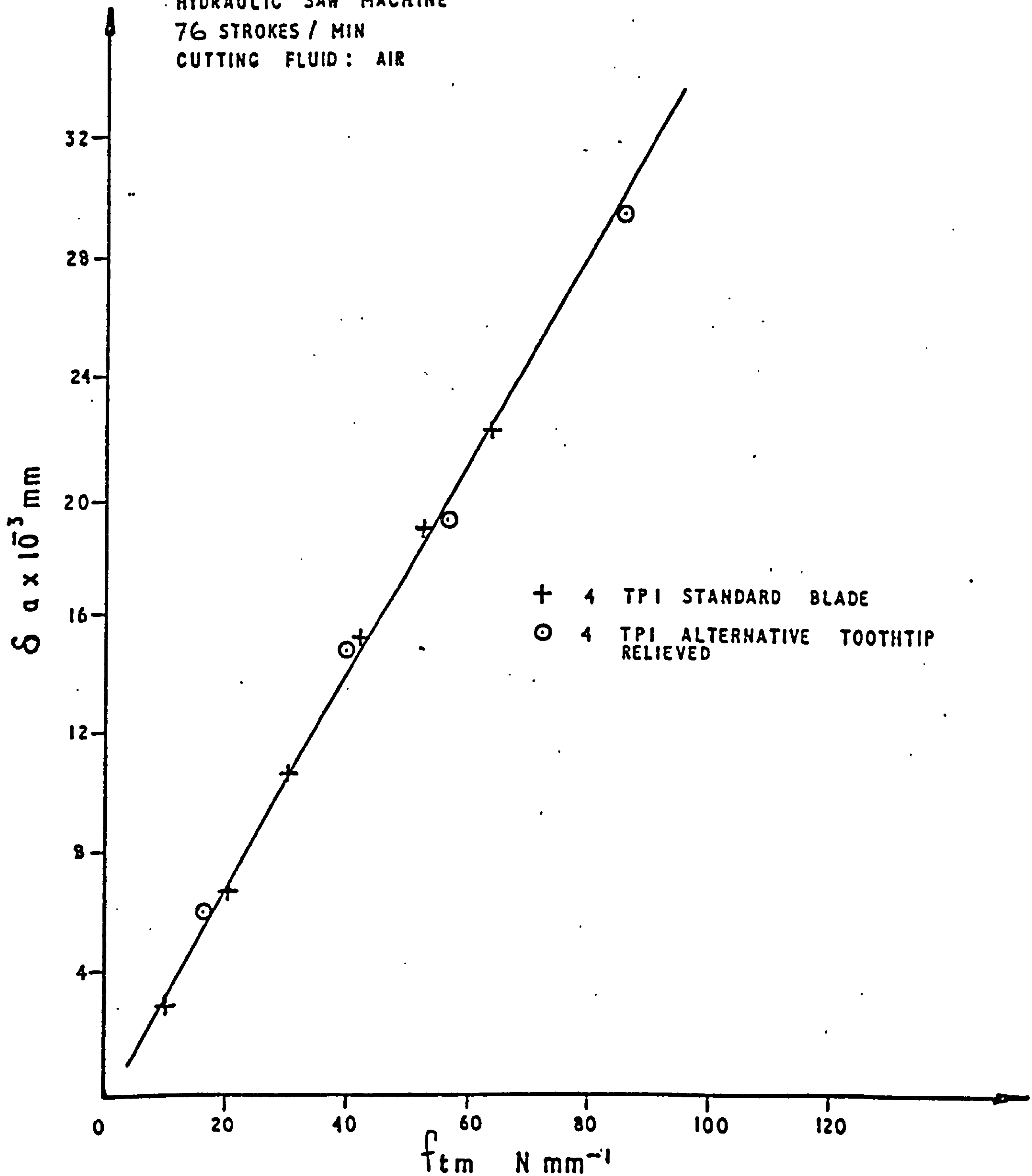


FIG. 109

COMPARISON OF THE PERFORMANCE OF A STANDARD
 AND MODIFIED 4 T.P.I. BLADE.

WORKPIECE: MILD STEEL 50 mm BREADTH x 25 mm DEPTH
 BLADE: BRAND 'X' (400 x 40 x 2 mm)
 HYDRAULIC SAW MACHINE
 76 STROKES / MIN
 CUTTING FLUID: AIR

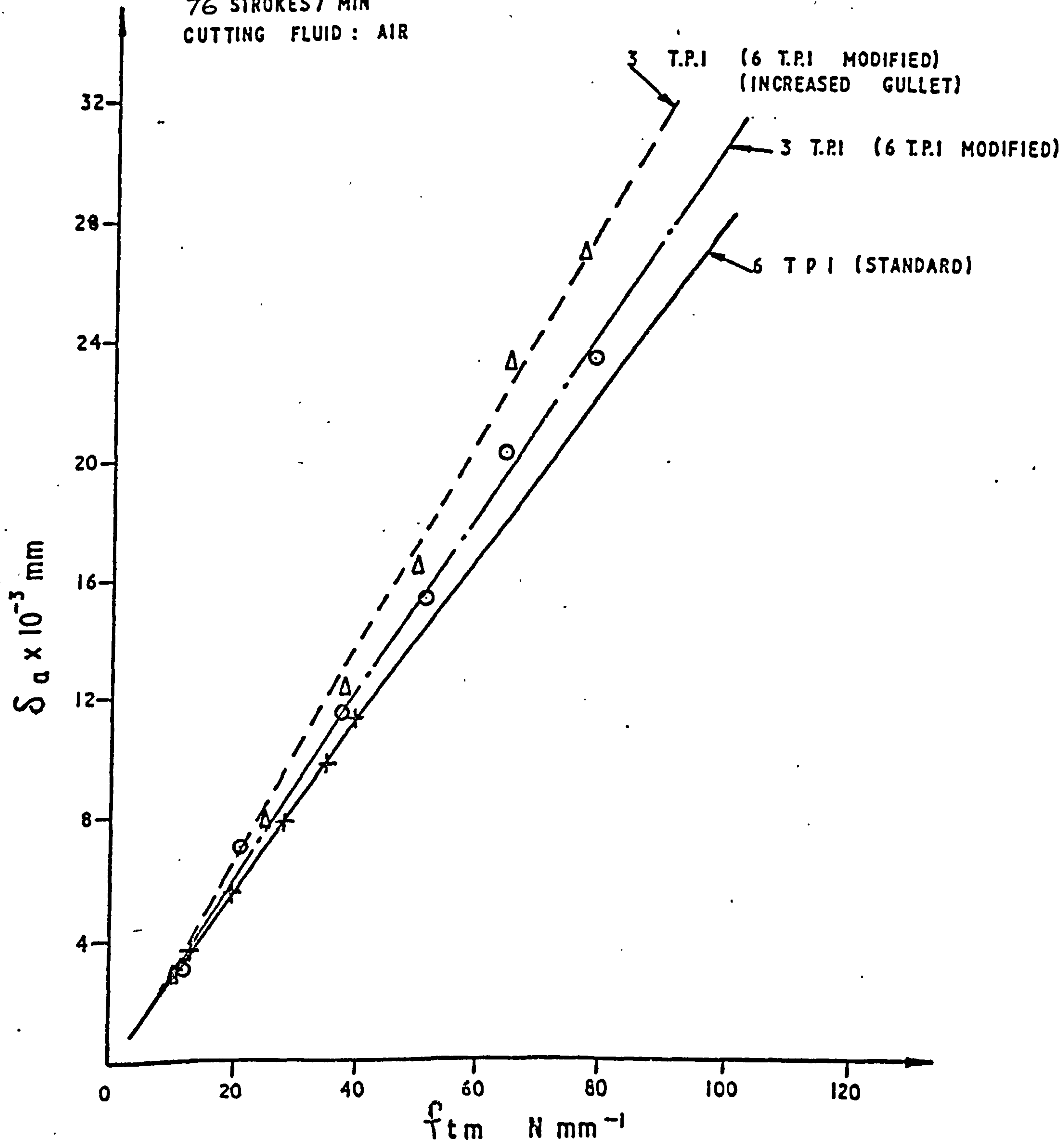


FIG. 110 (a) COMPARISON OF THE PERFORMANCE OF 'STANDARD' AND MODIFIED BLADES (6 T.P.I — 3 T.P.I)

WORKPIECE: MILD STEEL 50mm BREADTH x 25 mm DEPTH
 BLADE: BRAND 'X' (400 x 40 x 2 mm)
 HYDRAULIC SAW MACHINE
 76 STROKES / MIN
 CUTTING FLUID : AIR

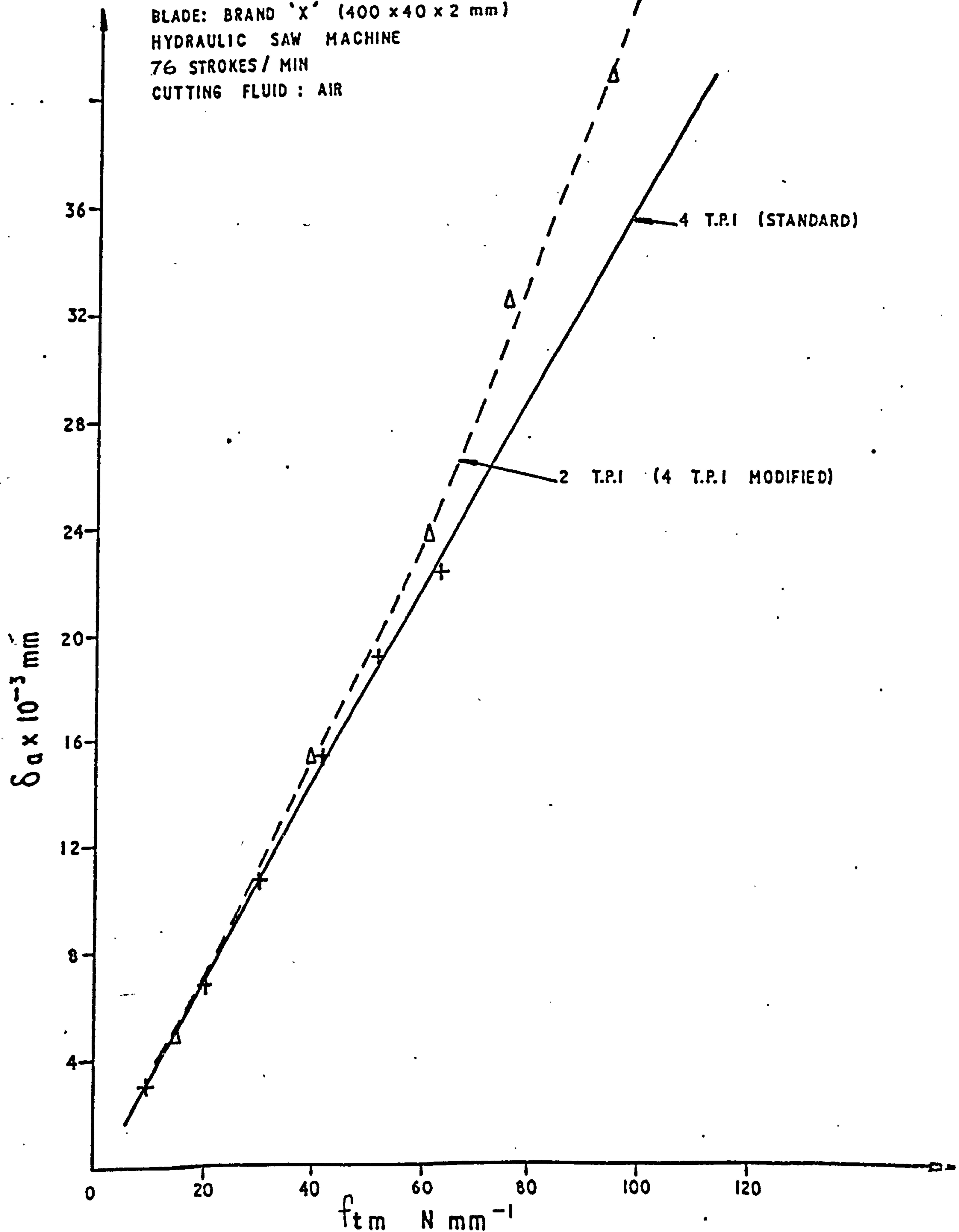
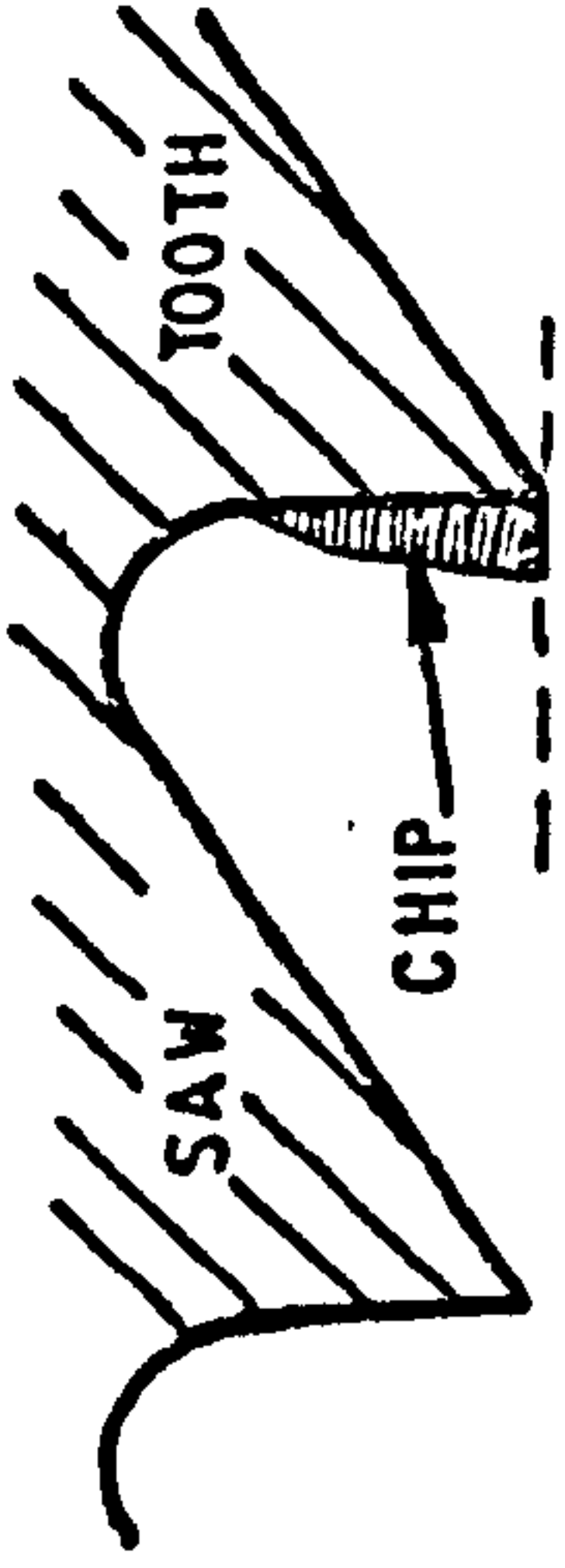
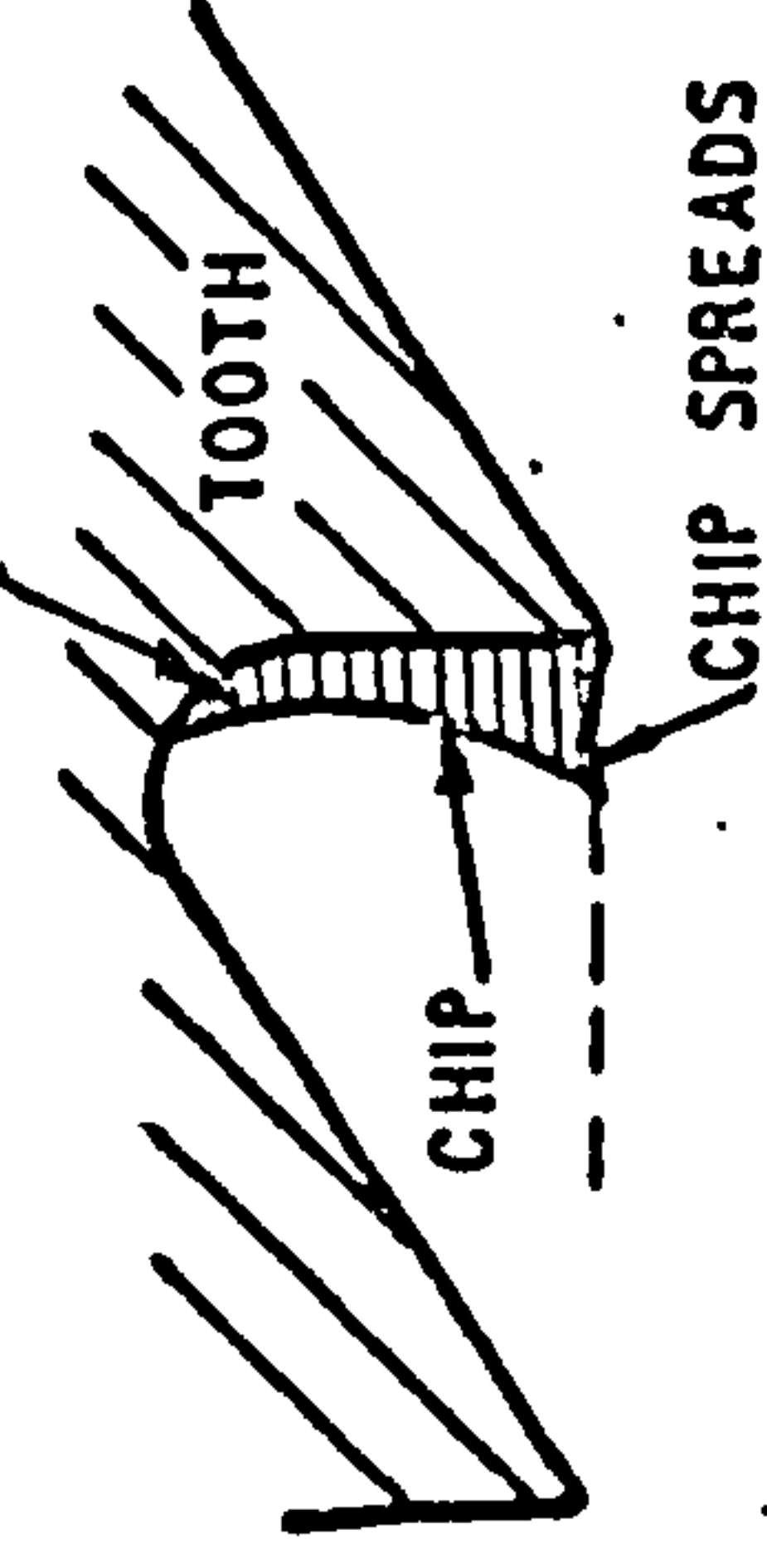


FIG. 110 (b) COMPARISON OF THE PERFORMANCE OF 'STANDARD' AND MODIFIED BLADES (4 TPI → 2 TPI)



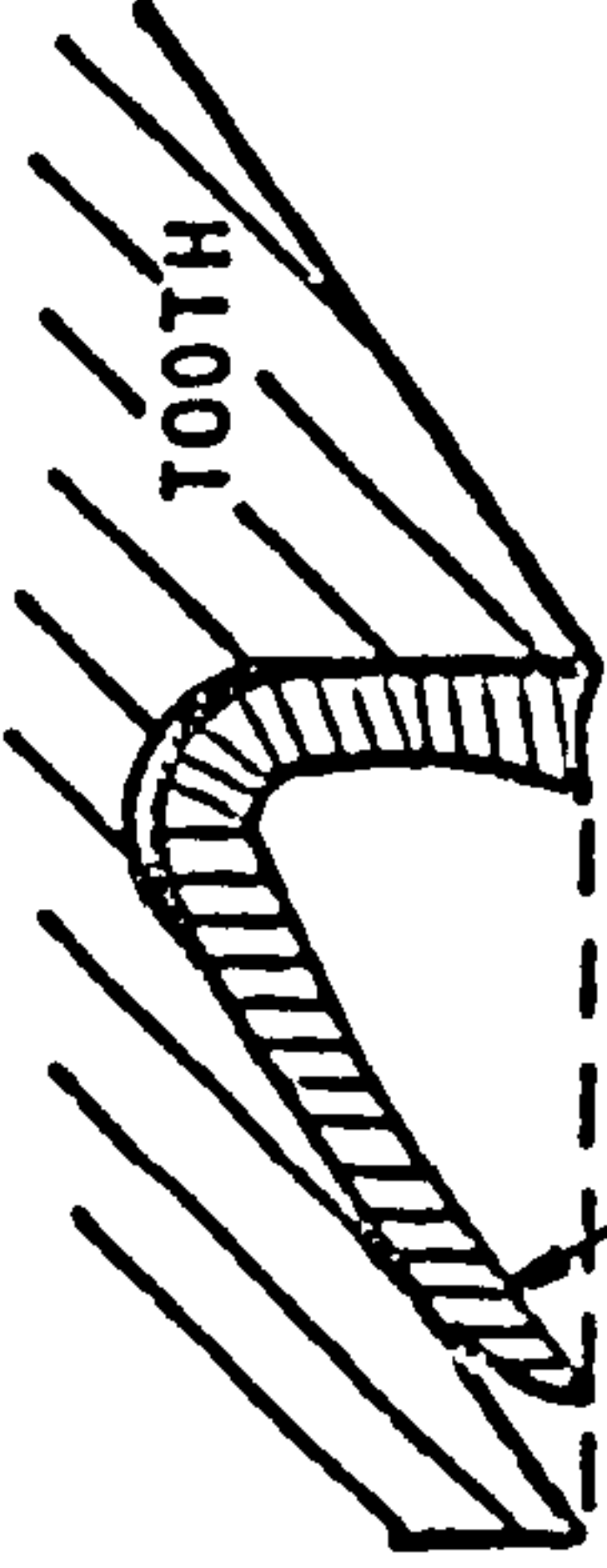
CONDITION I.

CHIP HITS THE ROOT

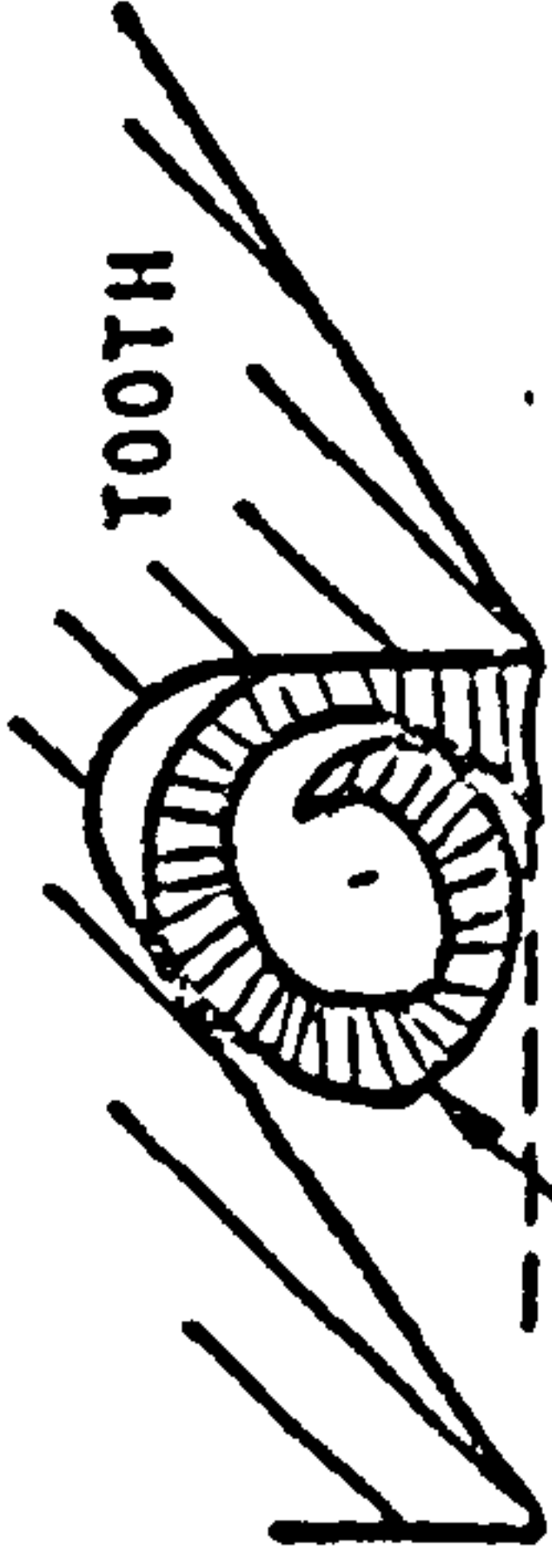


CONDITION II

CHIP SPREADS AT THE BASE



CONDITION III



CONDITION IV.

CHIP TRAPPED IN GULLET

CURLY CHIP

FIG. 111 SCHEMATIC DIAGRAMS SHOWING CHIP FORMATION IN THE GULLET FOR VARIOUS SITUATIONS IN HACKSAWING.

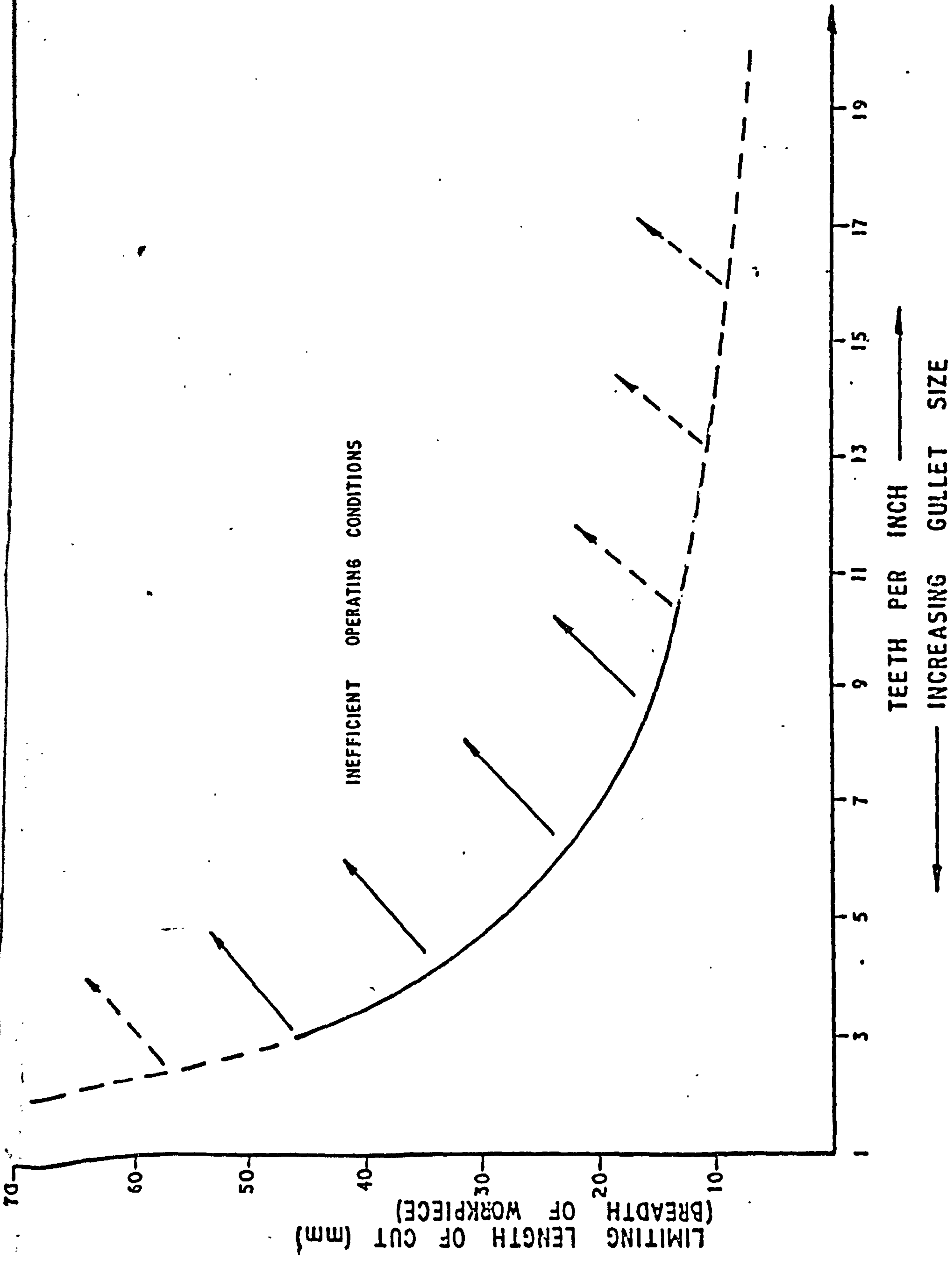


FIG. 112. INFLUENCE OF BLADE PITCH ON THE LIMITING LENGTH OF CUT (STEEL WORKPIECE) (GULLET PERIMETER B_2 AS THE LIMITING FACTOR)

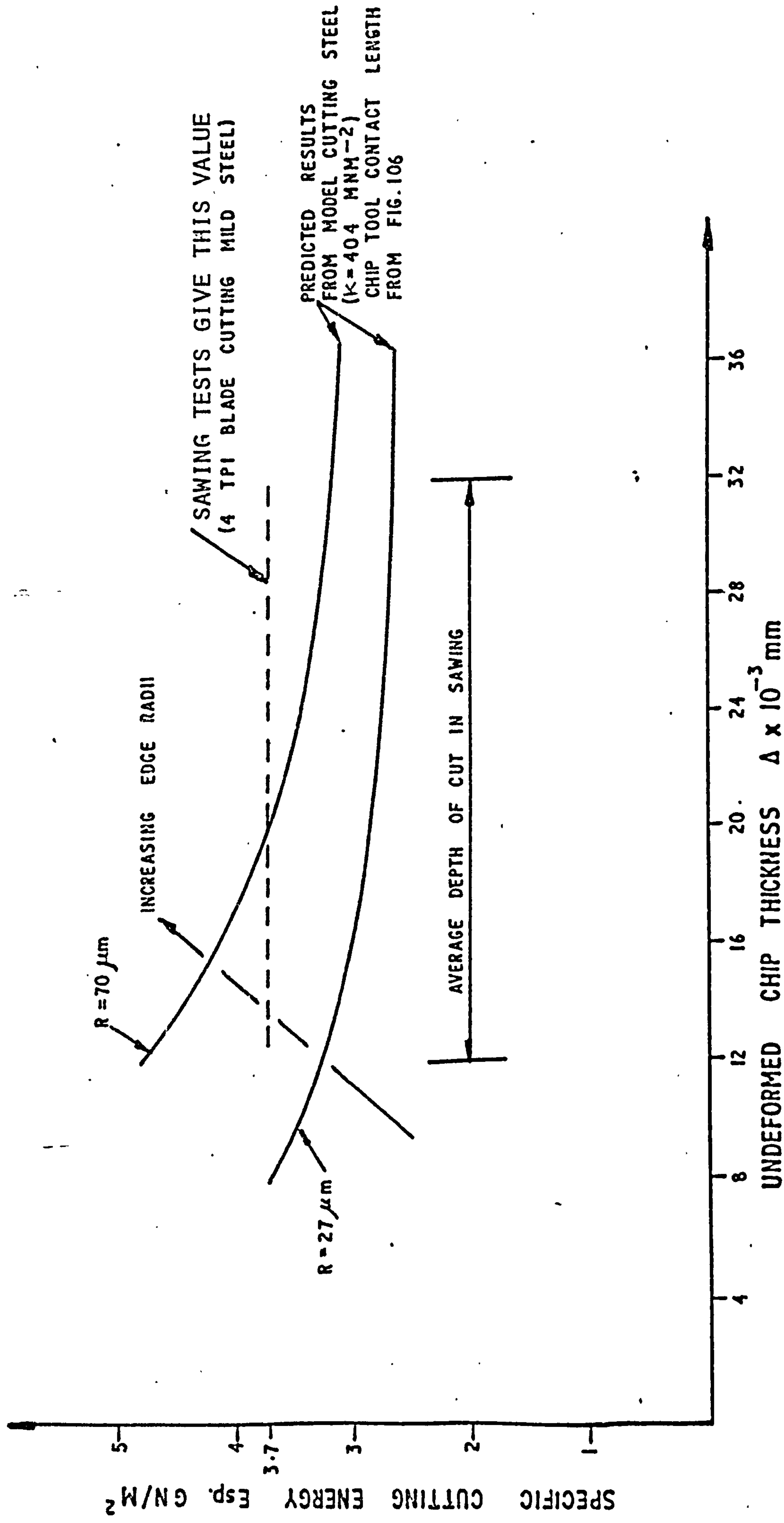


FIG. 113. VARIATION IN Esp Vs Δ USING THE SLIP-LINE FIELD MODEL FOR A 4 T.P.I. SAW BLADE, EDGE RADIUS $27 \mu\text{m}$, AND THE EFFECT OF INCREASING THE RADIUS TO $70 \mu\text{m}$.

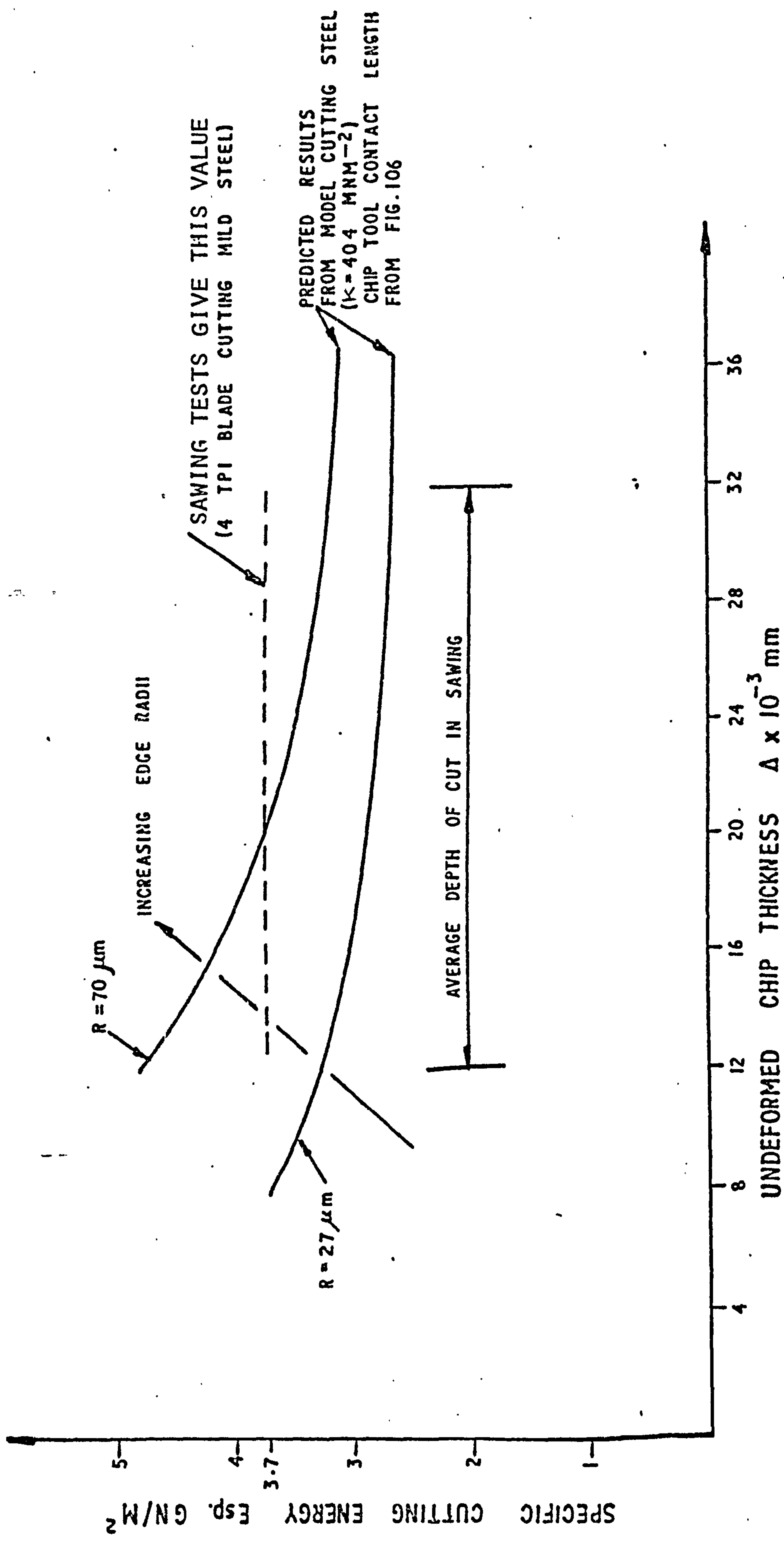


FIG. 113. VARIATION IN ESP VS Δ USING THE SLIP-LINE FIELD MODEL FOR A 4 T.P.I. SAW BLADE, EDGE RADIUS $27 \mu\text{m}$, AND THE EFFECT OF INCREASING THE RADIUS TO $70 \mu\text{m}$.